OLIGOMERIC AND POLYMERIC BIBENZIMIDAZOLE BASED METAL COMPLEXES AND CROSSLINKED POLYETHYLENIMINE BASED FLAME RETARDANTS

by

JUN YIN

Presented to the Faculty of the Graduate School of

The University of Texas at Arlington in Partial Fulfillment

of the Requirements

for the Degree of

DOCTOR OF PHILOSOPHY

THE UNIVERSITY OF TEXAS AT ARLINGTON

December 2005

ACKNOWLEDGEMENTS

I would like to express my most sincere appreciation to my research and dissertation advisor, Professor Ronald L. Elsenbaumer, for his generous support, technical guidance and encouragement throughout the course of my graduate study at UTA. Grateful acknowledgement is expressed to the members of my Ph.D. advisory committee members: Professors Frederick MacDonnell, Martin Pomerantz, Dmitry Rudkevich, Zoltan Schelly, and Richard Timmons for their valuable contributions during the course of this dissertation work. I am also indebted to Professor Carl Lovely for his encouragement and enlightening discussion on various subjects related to this study, to Professor Rasika Dias for his technical assistance in the preliminary X-ray analysis.

The helpful discussions and various degrees of technical assistance from the members of the Elsenbaumer's research group: Xin Chen, Dr. Mahn-Jong Kim, Dr. Meser M. Ali, and Jateen Gandhi are greatly appreciated.

I would like to extend my special thanks to Professor Fred MacDonnell for providing technical assistance in the chemistry of the ruthenium complexes, to Professor Norma Tacconi for her enlightening discussion pertaining to electrochemistry, to Professor MacDonnell's research group for including me in their group activities, in which I enjoyed and was enlightened through the discussions with Kelly Wouters,

Thamara Janaratne. I also thank Russ Emerick for his invaluable training in operation and repair of various experimental instruments, and thank Charles Savage for his technical support in various aspects.

I acknowledge the special and timely X-ray crystallographic analysis of my crystal samples created in this dissertation research performed by Dr. Douglas Ogrin (Rice University) and Dr. Simon Bott (University of Houston). The financial assistance provide by UTA throughout my Ph.D. study program in the form of Teaching Assistantship and Research Assistantship from the Robert A. Welch Foundation, and the assistance from Spartech Polycom Corporation, Arlington, TX, for the investigation of the flame retardants. I wish to thank the Department of Chemistry and Biochemistry at UTA for providing the friendly working and research environment and excellent administrative assistance during my entire stay at UTA: Ruth Handley, Marilyn Hagan, Jackie Vinson, Erin Hampe, Barbara Douglas, Rita Anderson, Elizabeth Woodlee, Jeanmarie Bryant, Jeffrey Bryson, James Garner and Gill Howard.

I thank Phyllis Harris and Carol Brown for all the help.

Finally, I sincerely thank my parents and sisters for their love and constant encouragement and support, especially thank my husband, Dr. Yong He, for many of his advice and discussions on this dissertation research project, and for his endless love, patience and understanding over the past five years, without which all of this would not have been possible.

November 7, 2005

ABSTRACT

OLIGOMERIC AND POLYMERIC BIBENZIMIDAZOLE BASED METAL COMPLEXES AND CROSSLINKED POLYETHYLENIMINE BASED FLAME RETARDANTS

Publication No. _____

Jun Yin, Ph.D.

The University of Texas at Arlington, 2005

Supervising Professor: Ronald L. Elsenbaumer

In Part I, a simple and mild condensation route for the synthesis of novel bibenzimidazole oligomers and polymers is described using methyl 2,2,2-trichloroacetimidate as a key starting material. The dimer, trimer, tetramer, and polymers of bibenzimidazole were synthesized as a new series of potential conjugated chelating ligands for the metallopolymer studies. The polymers show the maximum absorption at around 400 nm. The optical band gap of the polymer is estimated to be 2.68 eV.

In Part II, a series of multinuclear Ru complexes containing di-, tetra-, and octa-Ru^{II} centers based on the oligomeric bibenzimidazoles were synthesized and characterized. The species with high nuclearity exhibit extended, one-dimensional structures. They show very intense ligand-centered (LC) absorptions (ε up to 3.6×10^5 $M^{-1}\cdot cm^{-1}$) and moderately intense metal-to-ligand charge transfer bands in the visible region (ε up to 6.6×10^4 $M^{-1}\cdot cm^{-1}$). The interactions between the Ru metal centers across the bidentate bibenzimidazole ligands, and along the oligomeric bibenzimidazole ligands are relatively weak, which is not expected.

In Part III, the homochiral multinuclear Ru complexes of the oligomeric bibenzimidazoles were synthesized stereospecifically using Λ-$[Ru(bpy)_2(py)_2]$[(−)-*O*,*O*′-dibenzoyl-L-tartrate]$\cdot 12H_2O$ as the enantiomerically pure chiral building block. The complexation of bibenzimidazole and the chiral building block proceeds with the complete retention of configuration. The tetra-Ru complex has an estimate size of $2.1 \times 1.1 \times 1.0$ nm^3. They were characterized by means of circular dichroism, NMR spectroscopy, and mass spectrometry.

In Part IV, a new intumescent flame retardant system for use in olefinic polymers was discovered by crosslinking polyethylenimine ("Lupasol") with pyromellitic dianhydride, and then further treating with phosphoric acid to make the phosphate salts. The LOI of the phosphate salts can be greater than 70.0, and the char yield at 800 °C reaches 37.6%, which indicates that they could be non-halogenated, enviromental friendly, low smoke level, and cost effective intumescent flame retardants for polyolefins.

TABLE OF CONTENTS

LIST OF FIGURES

LIST OF TABLES

LIST OF ABBREVIATIONS

$BiBzImH_2$: 2,2′-bibenzimidazole

Bpy: 2,2′-bipyridine

Bpm: 2,2′-bipyrimidine

DMAC: *N*,*N*-dimethylacetamide

DMF: *N*,*N*-dimethylformamide

DMSO: dimethylsulfoxide

NMP: 1-methyl-2-pyrrolidinone

R.T.: room temperature

CV: cyclic voltammogram

CD: circular dichroism

PART I

EFFICIENT SYNTHESIS AND CHARACTERIZATION OF NOVEL BIBENZIMIDAZOLE OLIGOMERS AND POLYMERS AS POTENTIAL CONJUGATED CHELATING LIGANDS

CHAPTER 1

INTRODUCTION

1.1 Metal Containing Conductive Polymers

Metal complexed conjugated polymers have attracted significant attention in recent years.[1-4] The incorporation of transition metals has the potential to greatly expand the function and ultimate applications of conducting polymer systems. More specifically, there is a steady and growing effort to incorporate redox-active metal centers into conducting polymer structures to create highly efficient redox modulated conductivity for sensory (i.e., anions and small molecules), catalytic, photochemical, and photoelectronic applications. In conducting metallopolymers, an understanding of the interactive roles that the metal centers and the organic polymer backbone play is in its early stages.

A variety of π conjugated heteroaromatic polymers which serve as electrically conducting, rigid chelating ligands have been prepared and their metal complexes have been investigated.[5-11] Yamamoto and co-workers have reported that complexes of $RuCl_3$ with polypyridine and polybipyridine (**1**) (Chart 1.1) exhibit notable photocatalytic cleavage of water to H_2.[8] Swager and co-workers have developed a series of polymetallorotaxanes for sensory[9] and molecular electronic applications.[10]

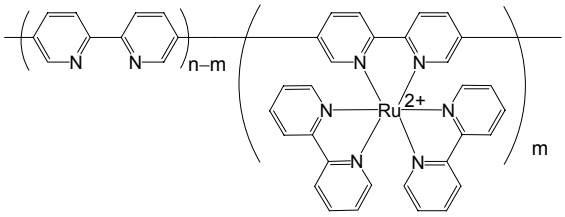

Ru Complexed Poly(bipyridine)

1

Chart 1.1

1.2 Mechanisms of Conductivity in Metallopolymers

Electron transport in redox polymers has been shown to occur by at least three mechanisms — outer sphere, superexchange and mediated, as illustrated schematically in Figure 1.1. The outer sphere mechanism is distinguished by the lack of mixing the respective metal orbitals. In contrast, in unsaturated systems, and particularly in highly conjugated systems, the electron transport can also occur through the polymer backbone by mediated and/or superexchange mechanisms. These are distinguished by the availability of redox states of suitable energy on the polymer to mediate electron transport. If such states are available, the electrons can hop between a localized metal-based redox site, a polymer-based site, and a second metal site in two steps (mediated mechanism). If such states are not available, then electron transfer through the backbone must result from a mixing of appropriate orbitals of both metals with the HOMO and/or LUMO of the polymer backbone (superexchange). It is important to note that the rate of electron transfer by this mechanism is highly dependent on the nature of the bridging ligand and its orbital overlap with the two metal centers.[11]

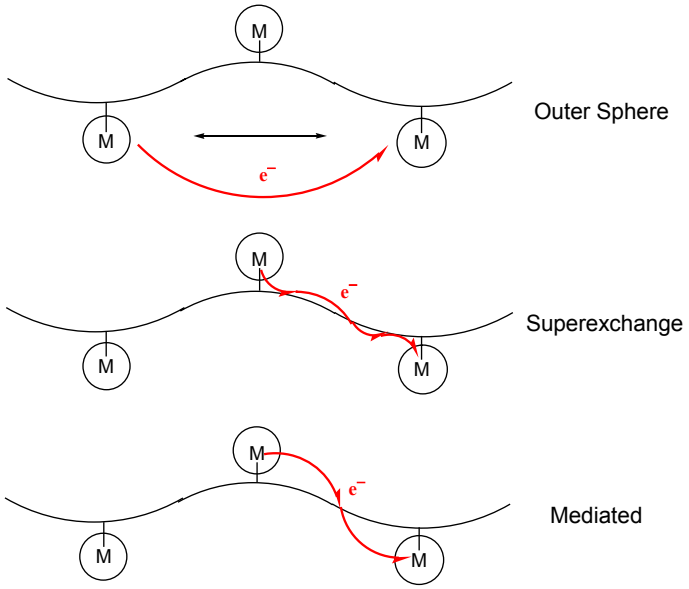

Figure 1.1 Mechanisms for Electron Transfer Between Metal Sites in a Metallopolymer

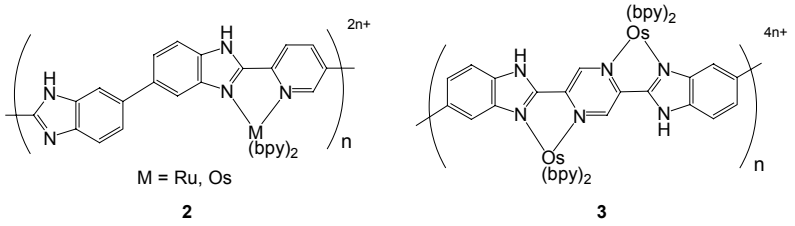

Chart 1.2

1.3 Examples of Metal Complexed Poly(benzimidazoles)

It has been demonstrated by Pickup and co-workers that the existence of superexchange interactions between metal centers coordinated to conjugated polymer backbones enhanced the rate of electron transport through the polymer in a series of Ru- and Os-complexed polybenzimidazoles based on benzimidazole-pyridine or benzimidazole-pyrazine as the repeat units. For example, $Ru(bpy)_2$ or $Os(bpy)_2$

complexed poly(6,6′-bibenzimidazole-2,2′-diyl)-2,5-pyridine (**2**) and $Os(bpy)_2$ complexed poly(6,6′-bibenzimidazole-2,2′-diyl)-2,5-pyrazine (**3**) (Chart 1.2).[7,11,12] It was predicted that higher rates of electron transport could be achieved by better matching of orbital energies between the metal based $d\pi$ orbitals and the polymer π or π^* orbitals.

1.4 Our Project: Synthesis of Poly(bibenzimidazoles) and Their Metal Complexes

To probe the orbital interactions between metals and conjugated polymers, poly(bibenzimidazoles) (**4**) with 2,2′-bibenzimidazole (**5**) as the repeat unit were chosen in our research as the π conjugated backbones. It appears that polybenzimidazoles are attractive choices for a number of reasons.[4] They tend to be very robust and remain stable under considerable thermal and chemical stress.[13] The studies of binuclear benzimidazole complexes have shown that they possess significant electronic coupling between the two metals.[14-16] In addition, the removal of the imidazole proton allows pH control of the electron density on the conjugated ligands.[17-24]

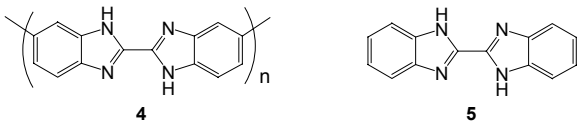

4 **5**

Chart 1.3

Polybenzimidazoles are generally synthesized via melt polymerization of aromatic bis(*o*-diamine)s with dicarboxylic acid derivatives.[25-27] Another common

method is solution polymerization performed in poly(phosphoric acid).[28] However, the drawbacks with these protocols often include high temperatures, long reaction times and strongly acidic conditions. In addition, the structures and the molecular weights of the obtained polymers are difficult to determine. Our initial attempts for the synthesis of poly(bibenzimidazole) started with the condensation reaction between 3,3′-diaminobenzidine (**6**) and oxamide (**7**) or oxalic acid in polyphosphoric acid in the presence of phosphorus pentoxide, but both of the polymer products met with limited success when using them for further metal complexation.

In this regard, the synthesis and investigation of a discrete set of oligomers with precise lengths has been an exciting approach to provide specific information for interpreting structural and conformational properties of the corresponding polymers.[29] This is because oligomers serve as excellent models for the solution, electronic, photonic, thermal, and morphological properties of their corresponding polymers.[29] In addition, the metal complexes of the oligomers would also provide further information about the metallopolymers. However, the synthesis of well-defined bibenzimidazole oligomers has not been reported.

In chapter 2, a concise and mild route for the first synthesis of bibenzimidazole oligomers and polymers using methyl 2,2,2-trichloroacetimidate (**8**) as the key starting material will be described.[30,31] From a retrosynthetic standpoint, a bibenzimidazole unit is constructed via a ring-closure reaction of *o*-phenylenediamine (**9**) with 2-trichloromethylbenzimidazole (**10**) or its derivative. This methodology does not involve

tedious precursor synthesis and metal-catalyzed aryl–aryl bond formation, which is commonly used for heterocyclic aromatic oligomer and polymer synthesis.[32]

CHAPTER 2

RESULTS AND DISCUSSION

2.1 Synthesis of Bibenzimidazole Monomer

Initial attempts for the synthesis of 2,2′-bibenzimidazole monomer (**5**) followed the most commonly used method in the literature via a condensation reaction of *o*-phenylenediamine (**9**) and oxamide (**7**) in ethylene glycol at reflux, which was reported by Fieselmann et al. in 1978 (Scheme 2.1).[33] However, the drawbacks of this approach are the high reaction temperature (around 196 °C), low product yield, and difficulties in the purification of the desired product due to the formation of an isomeric byproduct fluoflavin **11** (ca. 10%).[34] Interestingly, the formation of **11** in this reaction was never reported in the literature. Due to the similar solubility to that of 2,2′-bibenzimidazole, fluoflavin **11** was very difficult to be separated from the monomer **5**. Furthermore, this method cannot be extended to the synthesis of either bibenzimidazole oligomers or polymers due to the nature of the reaction and the formation of the mixed products.

Scheme 2.1 Formation of 2,2′-Bibenzimidazole **5** and Byproduct Fluoflavin **11**

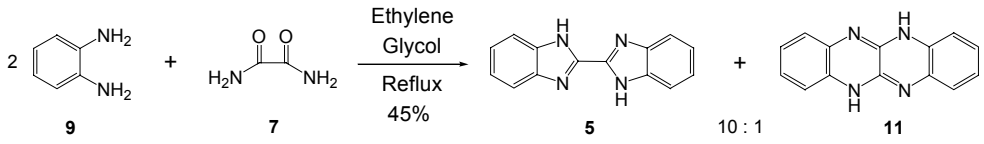

Therefore, an alternative and more efficient approach is required. In an older report, in 1967, Holan and coworkers published a series of papers describing their studies on the synthesis and reactions of 2-trichloromethylbenzimidazole (**10**).[35-38] A mild and efficient synthesis of 2,2′-bibenzimidazole (**5**) was also reported by simply reacting *o*-phenylenediamine (**9**) with methyl 2,2,2-trichloroacetimidate (**8**) in methanol at room temperature (Scheme 2.2). The pure product **5** was obtained in an excellent 90% yield after a simple filtration. The advantages of this method are obvious: the reaction occurred at the room temperature; the desired product precipitated out from the reaction mixture, which allowed easy separation and purification; no byproduct formed and recrystallization was not necessary. Surprisingly, despite the practical convenience, high yields, simple product purification and mild reaction conditions, this approach for the synthesis of bibenzimidazole has been largely overlooked in the literature.

Scheme 2.2 Holan's Synthesis of 2,2′-Bibenzimidazole

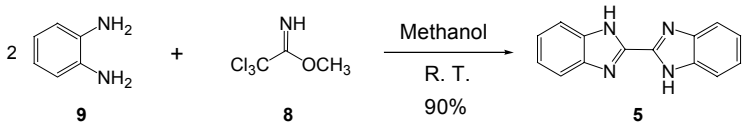

Intrigued by these advantages, we explored the synthesis of bibenzimidazole oligomers by utilizing similar methodology for the construction of the bibenzimidazole unit. The successful extension of this efficient method for the synthesis of bibenzimidazole oligomers (n = 2–4, n is the number of the repeat unit in the oligomers)

and the applications for the synthesis of bibenzimidazole polymers are described in this chapter.

2.2 Synthesis of Bibenzimidazole Dimer

Following Holan's procedures,[35] the key intermediate 2-trichloromethyl-benzimidazole (**10**) for the synthesis of the oligomers was prepared by reacting *o*-phenylenediamine (**9**) with methyl 2,2,2-trichloroacetimidate (**8**) in acetic acid. The use of a weak acid, e.g., acetic acid, was the key to the successful suppression of the formation of bibenzimidazole (**5**) and isolation of the relatively stable trichloride **10**. Holan and co-workers have demonstrated that **10** can react with a variety of *o*-bifunctional nucleophiles **12** to generate heterocyclic ring systems **13** (Scheme 2.3).[38]

Scheme 2.3 Holan's Synthesis and Reactions of Trichloride **10**

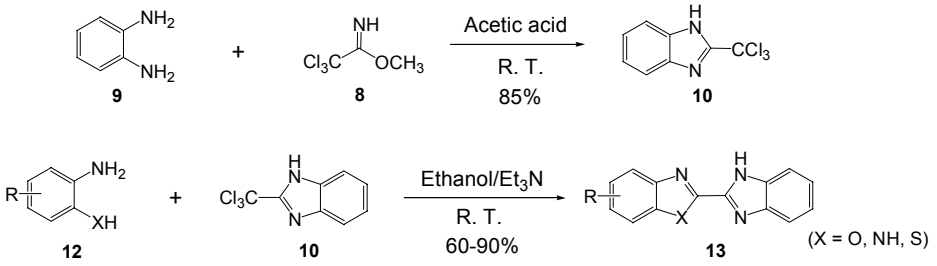

We have found that when 3,3′-diaminobenzidine (**6**) was employed as a bis-*o*-bifunctional nucleophile and treated with two equivalents of trichloride **10** under similar reaction conditions at reflux, the desired bibenzimidazole dimer **14** was obtained in 70% yield (Scheme 2.4).

The X-ray structure determination reveals that it is a rigid coplanar structure and this will be discussed in detail (Figure 2.2).

Scheme 2.4 Synthesis of Bibenzimidazole Dimer **14**

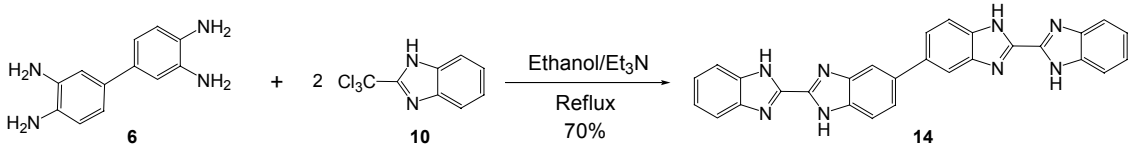

2.3 Synthesis of [(4-(2-(1*H*-Benzo[*d*]imidazol-2-yl)-1*H*-benzo[*d*]imidazol-5-yl) benzene-1,2-diamine)] (15)

The key nonsymmetric building block for the synthesis of bibenzimidazole trimer and the tetramer is the 4-bibenzimidazole substituted *o*-phenylenediamine derivative **15** (Scheme 2.5). It possesses one bibenzimidazole unit with an *o*-phenylenediamino functionality, which could further participate in a similar cyclization process with either imidate **8** or trichloride **10** as *o*-phenylenediamine (**9**) does (Schemes 2.2 and 2.3) to generate more bibenzimidazole units.

To synthesize the compound **15**, the cyclization of 3,3′-diaminobenzidine **6** with trichloride **10** has to occur on one side of 3,3′-diaminobenzidine, which could be achieved by controlling the stoichiometry. Therefore, when the trichloride **10** was treated with an excess of 3,3′-diaminobenzidine in DMF at room temperature for several hours and then heated at 130 °C for 44 h, the desired amine **15** was obtained in 51% yield, along with 6% of the dimer **14**. A third byproduct was also isolated in 30% yield (entry 1, Table 1), for which ^{1}H NMR spectroscopy showed a singlet proton at

9.25 ppm. In accordance with the spectroscopy data, the structure of the byproduct was assigned as 2-(1*H*-benzo[*d*]imidazol-2-yl)-5-(1*H*-benzo[*d*]imidazol-5-yl)-1*H*-benzo[*d*]imidazole (**16**), presumably produced by the cyclization of the diamine **15** with DMF.

Subsequent control experiments provided supportive evidence for the formation of the byproduct **16**. For example, when diamine **15** was heated in DMF in the presence or absence of Et_3N, **16** was formed exclusively in ca. 76% yield. It is interesting to note that the formation of benzimidazole derivative by the cyclization of aromatic diamine with DMF without an appropriate activating agent has not been reported in the literature.[39]

Scheme 2.5 Synthesis of Diamino Compound **15**

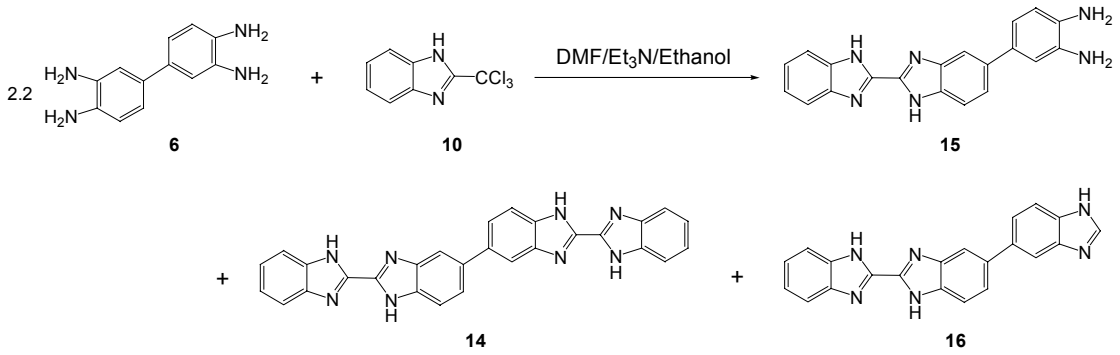

Table 2.1 Comparisons of the Reactions at Different Temperatures in Scheme 2.5

entry	reaction conditions	diamine **15**	dimer **14**	byproduct **16**
1	RT 5 h, then 130 °C 44 h	51%	6%	30%
2	RT 5 h, then 75 °C 7–10 h	63%	10%	0%

To prevent the further cyclization of diamine **15** with DMF, the reaction of trichloride **10** with 3,3′-diaminobenzidine (**6**) was performed at a relatively low temperature: room temperature for several hours, then at 75–80 °C for 7–10 h. Under these conditions, the formation of the byproduct **16** was completely suppressed and the desired diamine **15** was obtained in a satisfactory 63% yield, along with a small amount of the dimer **14** (ca. 10%) (entry 2, Table 2.1), which was readily separated from **15** by fractional precipitation.

Scheme 2.6 Synthesis of Bibenzimidazole Trimer **17** and Tetramer **19**

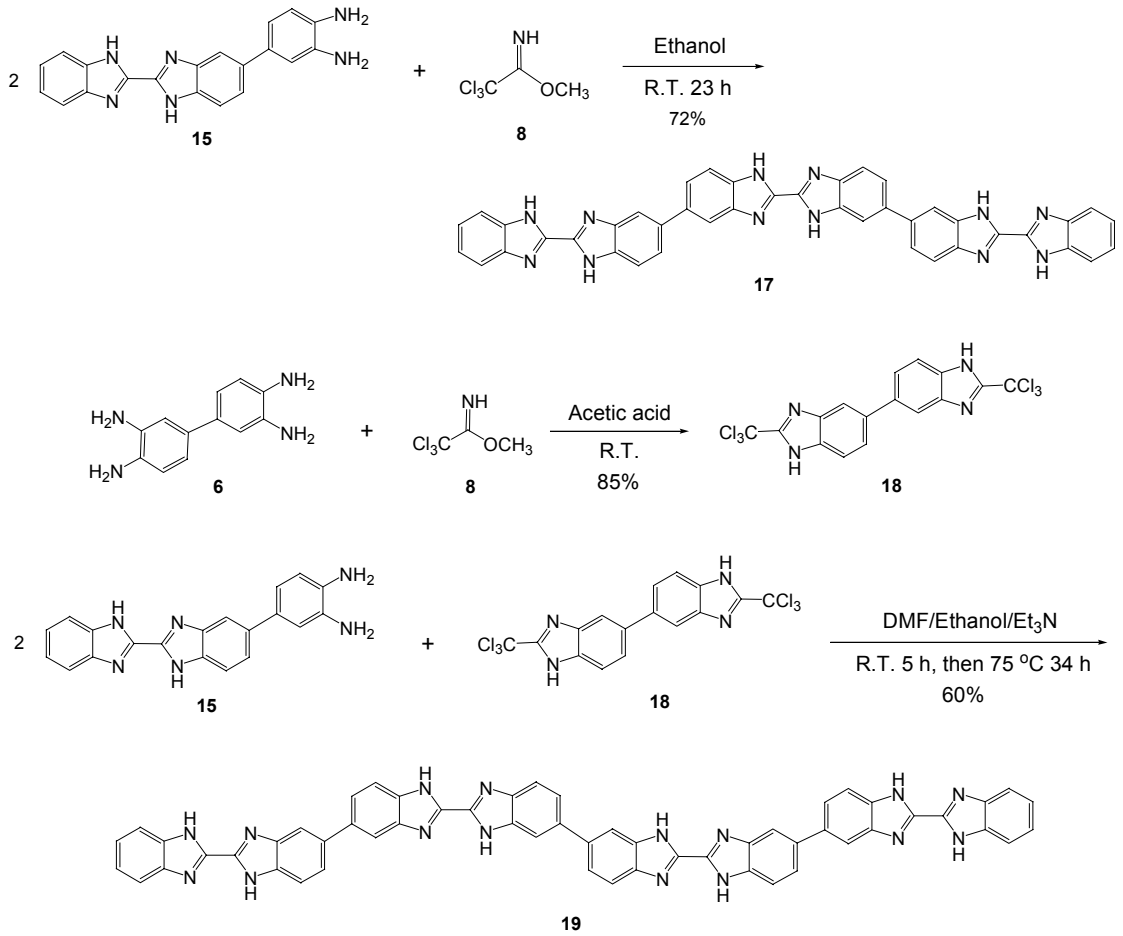

2.4 Synthesis of Bibenzimidazole Trimer and Tetramer

With **15** in hand, the synthesis of the trimer **17** was readily achieved by condensation of two equivalents of **15** with imidate **8** at room temperature in 72% yield, following the same strategy used for the synthesis of 2,2′-bibenzimidazole (**5**) from *o*-phenylenediamine (Scheme 2.6).

Another important symmetric difunctional building block for the synthesis of the tetramer, bis(trichloride) (**18**), was prepared using the same strategy as that used for 2-trichloromethylbenzimidazole (**10**). 3,3′-Diaminobenzidine (**6**) was treated with 2.2 equivalents of imidate **8** in acetic acid providing the desired bis(trichloride) **18**, which precipitated out from the reaction medium and was isolated in an excellent 85% yield after a simple filtration.

With both diamine **15** and bis(trichloride) **18** accessible, the tetramer **19** was synthesized by condensation of two equivalents of **15** with one equivalent of **18** using the previous diamine-trichloride cyclization conditions (Scheme 2.6). The product **19** precipitated from the reaction medium and was isolated in 60% yield. A small amount of DMF cyclization byproduct **16** was also formed under the reaction conditions and was removed by trituration of the crude product in DMF under heating (around 130 °C).

The melting point of the monomer bibenzimidazole **5** was greater than 300 °C.[34] The melting points of the oligomers (**14**, **17**, **19**) were not measured due to the high temperature. The thermal properties of polybenzimidazoles have been widely investigated.[13] The polybenzimidazoles have T_g's greater than 430 °C.[13] The thermal properties are discussed in the following section.

The dimer, trimer and tetramer are all brownish yellow powders and are soluble in concentrated sulfuric acid and methanesulfonic acid. The dimer is soluble in DMAC, DMF, DMSO, CF_3COOH, and HCOOH. The trimer and tetramer are partially soluble in DMAC and HCOOH, and sparingly soluble in DMF, DMSO, NMP, and CF_3COOH.

2.5 Synthesis of Bibenzimidazole Polymers

Poly(bibenzimidazoles) (**4**) were synthesized by two methods (Scheme 2.7). One method is the polycondensation reaction between 3,3′-diaminobenzidine (**6**) and methyl 2,2,2-trichloroacetimidate (**8**) in different solvents. For the polymer **4a**, the interfacial polycondensation of equal amounts of 3,3′-diaminobenzidine (**6**) and methyl 2,2,2-trichloroacetimidate (**8**) was carried out in a nonsolvent ethanol. The reaction was initiated at room temperature and then heated to reflux for 82 h to ensure that the cyclization went to completion. The brown polymer **4a** was obtained by simple filtration in 70% yield. The number average molecular weight (M_n) was around 19000 based on the viscosity determination (discussed in the viscosity section).

The synthesis of polymer **4b** was carried out in a homogeneous solution using DMF as the solvent in the presence of ethanol. The brown polymer **4b** precipitated out from the solution in 60% yield with a number average molecular weight (M_n) around 15000.

The comparison of these two reaction conditions indicates that the interfacial polymerization gave a higher molecular weight polymer (**4a**) than the solution polymerization, which produces the polymer **4b**. On the basis of Holan's study of the

reaction between the diaminocompound and methyl 2,2,2-trichloroacetimidate (**8**),[35] the reactions need to be initiated at room temperature for at least several hours and then heated to around 70 °C to ensure that the cyclization goes to completion. If the reaction is heated directly to 70 °C without being stirred at room temperature, it would not provide the polymer with the expected structure.

Scheme 2.7 Synthesis of Poly(bibenzimidazole)s **4a**–**d**[a]

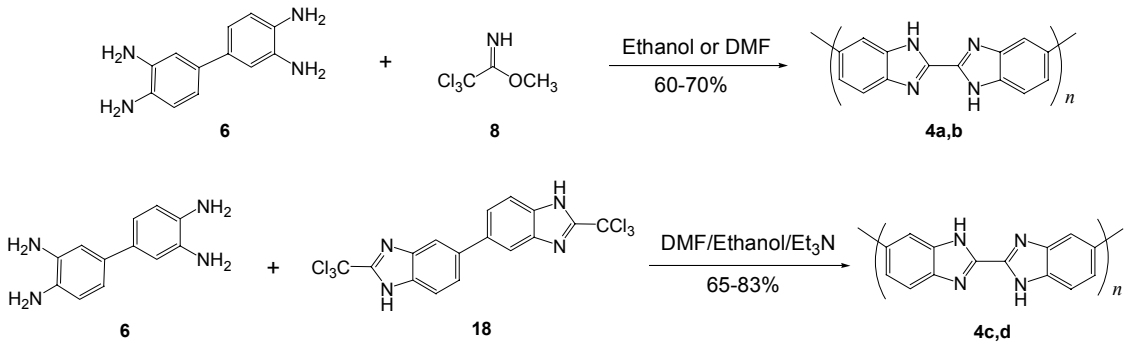

[a]**4a**: In ethanol, RT, then reflux. **4b**: In DMF in the presence of ethanol, RT, then 75 °C. **4c**: RT, then 75–80 °C. **4d**: RT, then 75 °C, then 120–130 °C, and then 150 °C.

The other method of synthesizing poly(bibenzimidazole) (**4c**–**d**) is the polycondensation reaction between diaminobenzidine **6** and bis(trichloride) **18** in DMF under different conditions. The direct polycondensation of equal amounts of 3,3′-diaminobenzidine (**6**) and bis(trichloride) **18** was carried out in a homogeneous DMF solution in the presence of Et_3N and ethanol. For the polymer **4c**, the reaction was initiated at room temperature for 5 h, then heated to 75 °C, and kept at 75–80 °C for 72 h. The orange-colored polymer was obtained by addition of water to the reaction mixture and precipitate out in 83% yield.

For the polymer **4d**, the reaction was initiated at room temperature for 5 h, then heated to 75 °C, then to 120–130 °C, and eventually to a maximum of 150 °C. The greenish yellow polymer **4d** precipitated out from the reaction mixture and was isolated in 65% yield.

Polymer **4c** has a higher molecular weight (M_n = 9600) than does polymer **4d** (M_n = 6400). Keeping the reaction temperature at 75 °C leads to the formation of the higher molecular weight polymer **4c**. For the polymer **4d**, the temperature was eventually increased to 150 °C, which might lead to the cyclization of the diamino groups with DMF and therefore terminate the chain growth.

Polymers **4a**,**b** are partially soluble in concentrated sulfuric acid, methanesulfonic acid, and HCOOH; but are not soluble in CF_3COOH, DMAC, DMF, DMSO, and NMP. Polymer **4c** is soluble in all the above solvents. Polymer **4d** is soluble in concentrated sulfuric acid and methanesulfonic acid; partially soluble in HCOOH and CF_3COOH; not soluble in DMAC, DMF, DMSO, and NMP. The solubility of polymer **4c** is different from those of polymers **4a, b** and **d**, probably because the reaction temperature of 75 °C is not high enough for the complete cyclization in the polymer chains.

2.6 NMR Studies of Bibenzimidazole Oligomers

^{1}H NMR spectra of the oligomers (**5**, **14**, **17**, and **19**) are shown in Figure 2.1. In order to clarify the NMR spectra by removing the tautomer effect,[40] CF_3COOD was used as the solvent as well as forming the trifluoroacetate salts of the oligomers. The

crystal structure of the dimer **14** shows that the rings are coplanar and the molecule is centrosymmetric. In the aromatic region of the ^{1}H NMR spectrum, the dimer shows five groups of peaks (H_1, H_2, H_3, $H_{4/4'}$ and $H_{5/5'}$). The singlet (H_1) is at 8.43 ppm; there are two double doublets at 8.28 and 8.26 ppm, which represent the protons H_2 and H_3 in the repeat unit; there are two double doublets at 8.12 and 7.93 ppm, which represent the protons $H_{4/4'}$ and $H_{5/5'}$ on both sides of the end groups. The NMR spectrum of trimer **17** and dimer **14** are very similar, which indicates that the trimer might have the coplanar structure. But the spectrum of the tetramer **19** is a little different from those of the dimer and the trimer. There are three singlets representing H_1, $H_{1'}$, and $H_{1''}$ respectively, instead of one singlet in the dimer and trimer; $H_{2/2'/2''}$ and $H_{3/3'/3''}$ show multiplets instead of the two double doublets in the dimer and the trimer. This indicates that H_1, $H_{1'}$, $H_{1''}$ are different, as well as H_2, $H_{2'}$, $H_{2''}$ and H_3, $H_{3'}$, $H_{3''}$. The tetramer may not have the coplanar structure that the dimer does. This noncentrosymmetric nature may lead to the nonequivalence of the protons in the repeat units.

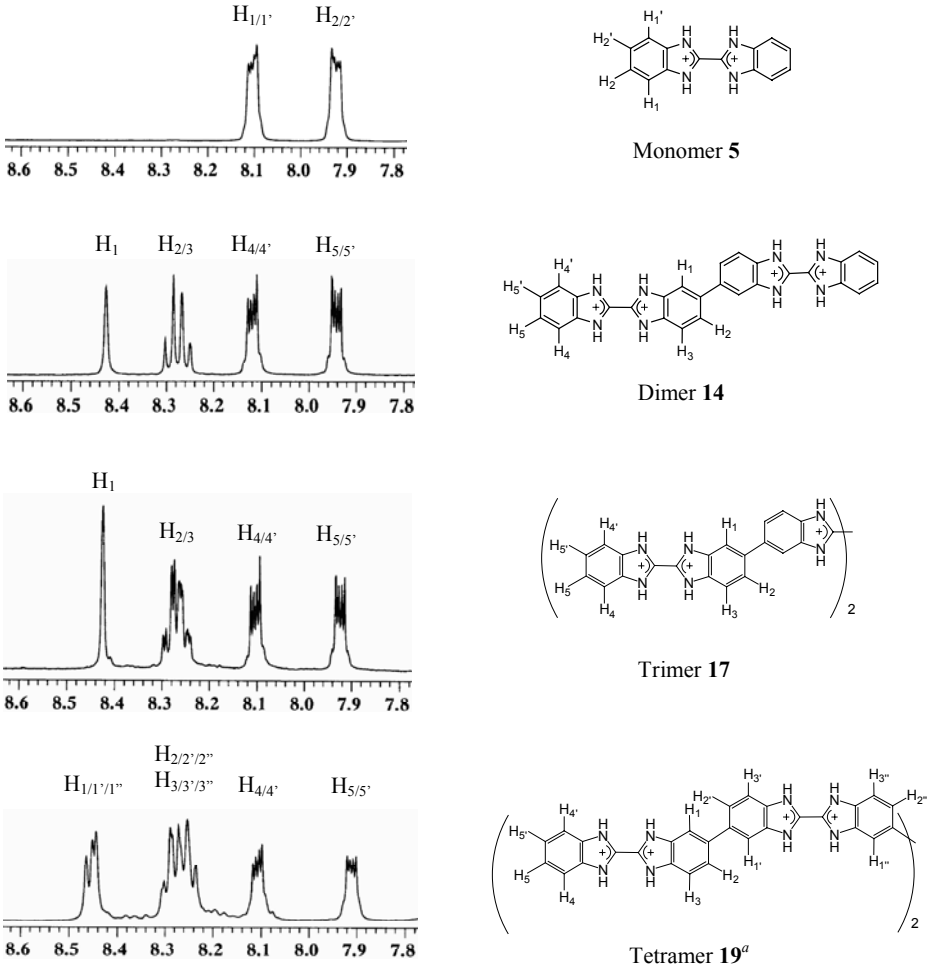

Figure 2.1 ^{1}H NMR Spectra of Bibenzimidazole Oligomers in CF_3COOD. The CF_3COO^- counter ions were omitted from the structures for clarity; "*a*" indicates that the NMR of the tetramer was in CF_3COOD/D_2O to improve the solubility.

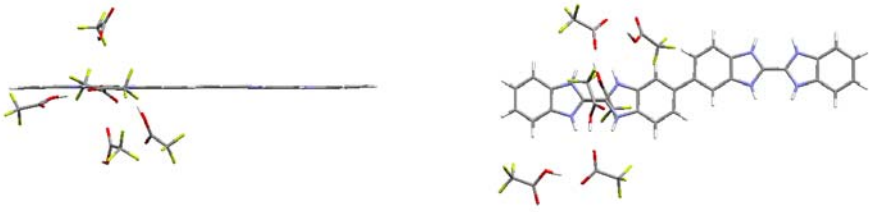

(a)

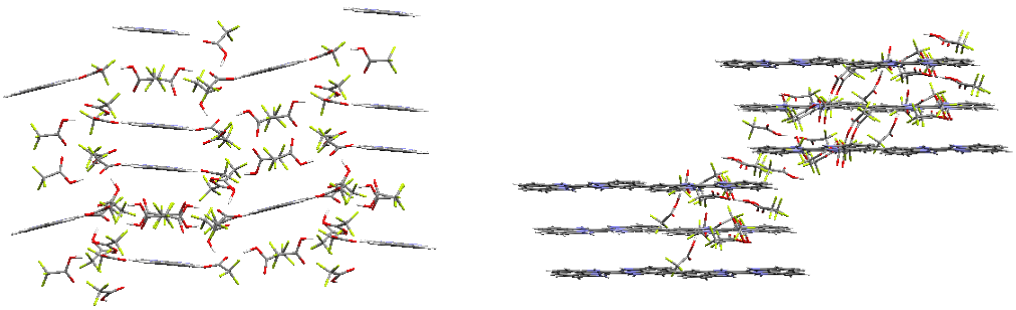

(b)

Figure 2.2 Crystal Structure and Packing Pattern of
$[Bis(bibenzimidazole)]_2(CF_3COOH)_{12}$
(a): Coplanar structure. (b): Zigzag pattern and alternating stacking column

2.7 X-ray Structure of Bibenzimidazole Dimer

Yellow block single crystals of the CF_3COOH salt of the dimer **14** were grown by slow evaporation of a CF_3COOH solution at room temperature [monoclinic space group $P2_1/C$ (Figure 2.2)]. The X-ray crystal structure analysis reveals the almost coplanar structure of the dimer. One dimer of bibenzimidazole was protonated with four CF_3COOH molecules, and the rest of the CF_3COOH molecules are in the lattice to support the crystals by intermolecular H-bonding interactions. The protonated

bis(bibenzimidazole) formed a zigzag pattern with alternating stacking columns. The structure indicates an efficient π-stacking in the solid state with an intermolecular spacing of 7.90 Å.

Table 2.2 Photophysical Properties of Bibenzimidazole Oligomers and Polymers

compound	MW	λ_{max}^{abs} (nm)	ε (10^4, $M^{-1}\cdot cm^{-1}$)	E_g (eV)	λ_{max}^{em} (nm)	stokes shift (nm)
monomer **5**	234.28	340	4.22	-	414	74
dimer **14**	466.54	373	9.21	2.89	495	122
trimer **17**	698.74	382	14.82	2.81	495	113
tetramer **19**	930.98	389	20.72	2.78	490	101
polymer **4a**	19000	400	-	2.68	498	98
polymer **4b**	15000	400	-	2.65	495	95
polymer **4c**	9600	388	-	2.70	505	117
polymer **4d**	6400	397	-	2.75	495	98

2.8 UV–vis Properties of Bibenzimidazole Oligomers and Polymers

The UV–vis properties of the oligomers and the polymers were investigated in the protonated forms in methanesulfonic acid (Figures 2.3–2.6, Table 2.2). The bibenzimidazole monomer **5** has a maximum absorption at 340 nm, which represents the π–π* transition. The X-ray crystal analysis of the dimer **14** shows the coplanar structure. Its λ_{max} (π–π* transition) is at 373 nm, which indicates the extension of the conjugation. The λ_{max} of the trimer **17** is at 382 nm, which indicates further extension of

conjugation, but not as much as from the monomer to the dimer. The tetramer **19** only red-shifted 7 nm to 389 nm compared to that of the trimer, which indicates the large chain length extension does not produce the expected further decrease of the HOMO–LUMO gap. This phenomenon indicates that the structure of the tetramer might not be coplanar.

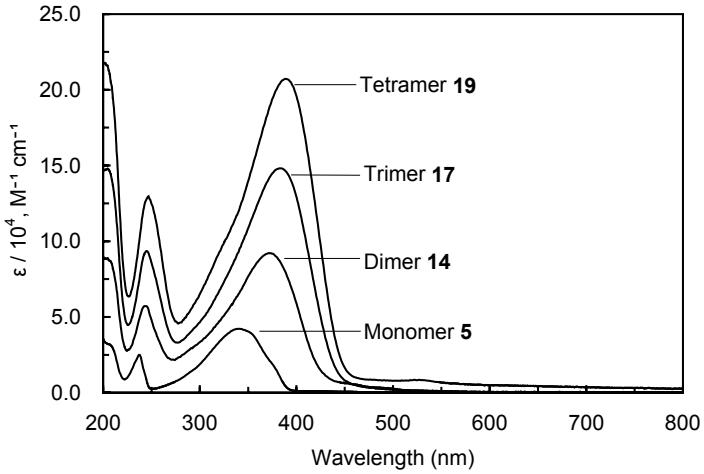

Figure 2.3 UV–vis Spectra of Bibenzimidazole Oligomers in Methanesulfonic Acid (10^{-6} M)

Figure 2.4 shows the linear relationship between the extinction coefficient and the number of the repeat unit in the oligomers. The solid line, a, is the experimental data; the dotted line, b, is the theoretical data assuming that there is no interaction between the repeat units. The slope of the solid line a (5.51×10^4) is larger than that of the dotted line b (4.22×10^4), which indicates that there are some interactions between the repeat units due to the π orbital overlap. The extinction coefficients ε ($M^{-1} \cdot cm^{-1}$) per repeat unit were found to be 4.22×10^4 in the monomer, 4.61×10^4 in the dimer, $4.94 \times$

10^4 in the trimer, and 5.18×10^4 in the tetramer. This suggests that in the tetramer, one repeat unit absorbs 1.2 times more light than one repeat unit in the monomer. The extinction coefficients of the trimer and the tetramer are larger than 140000 $M^{-1} \cdot cm^{-1}$, which is unusually large for the short chain oligomers.

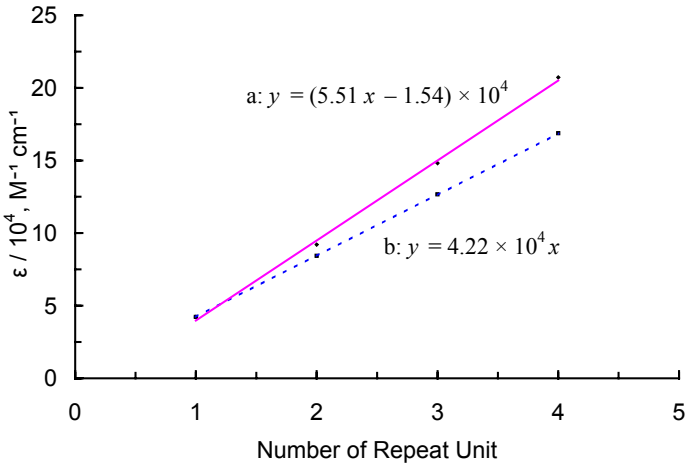

Figure 2.4 Extinction Coefficient vs the Number of Repeat Unit
in Bibenzimidazole Oligomers
(a, Solid line): Experimental value; (b, dotted line): Theoretical values,
assuming the repeat units are isolated with no interactions.

The λ_{max} values of the polymers **4(a–d)** are at 388–400 nm, which are very similar to that of the tetramer (Figures 2.5 and 2.6). From the onset of the absorptions, the band gap of polymer **4a** in methanesulfonic acid is estimated at 2.68 eV. An optical saturation or near saturation occurred at around 400 nm. **4a** shows a narrow absorption band centering at 400 nm, while **4b** shows a broad absorption band centering at around 350 nm with a shoulder at 400 nm. This indicates that the interfacial polycondensation reaction in ethanol gives polymer **4a** with a uniform molecular weight distribution,

while the solution polymerization in DMF gives polymer **4b** with a broad molecular weight distribution.

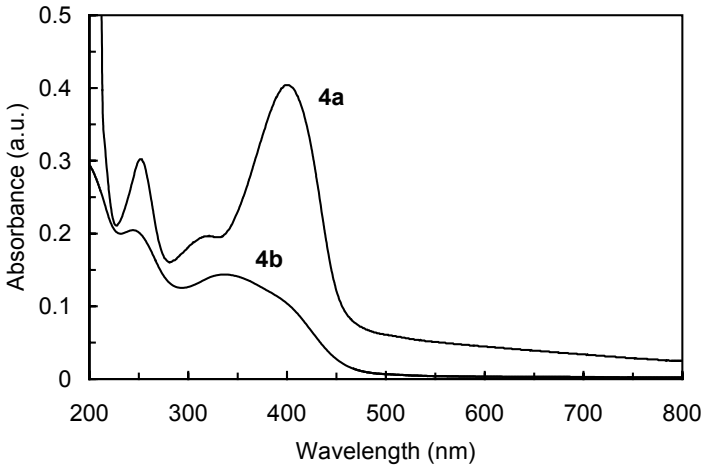

Figure 2.5 UV–vis Spectra of Poly(bibenzimidazole)s **4a**,**b** in Methanesulfonic Acid (10^{-6} M)

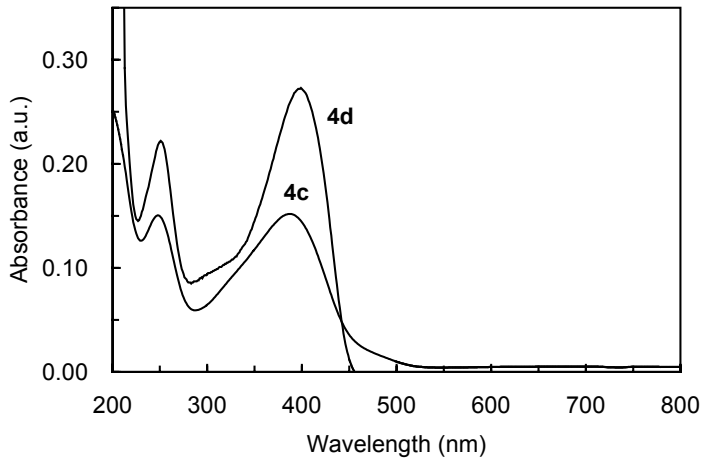

Figure 2.6 UV–vis Spectra of Poly(bibenzimidazole)s **4c**,**d** in Methanesulfonic Acid (10^{-6} M)

2.9 Photoluminescence Properties of Bibenzimidazole Oligomers and Polymers

The photoluminescence spectra of the oligomers and the polymers in the diluted solution of methanesulfonic acid are shown in Figures 2.7–2.9. All the oligomers and the polymers have similar emission bands with the maxima at 490–505 nm. These results indicate that there is little effect of the chain length on the solution luminescence of the protonated oligomers and the polymers. Large excitation and emission energy differences were observed for the oligomers and polymers in the solution. From the dimer to the polymer, the Stokes shifts between the excitation and emission decreased from 122 to 95 nm (Table 2.2).

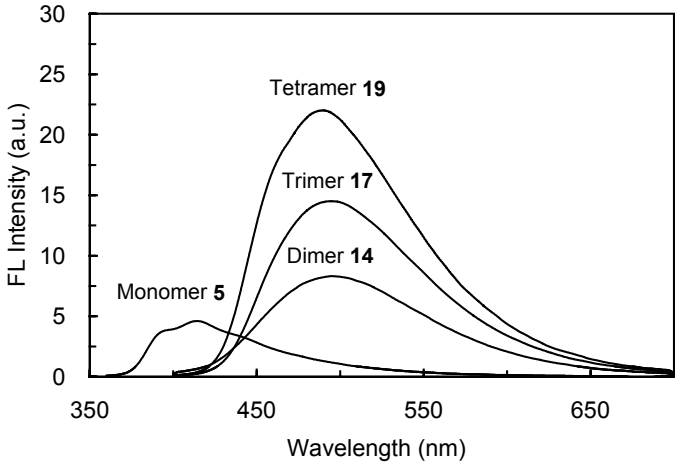

Figure 2.7 Photoluminescence Spectra of Bibenzimidazole Oligomers in Methanesulfonic Acid Based on the Same Molar Concentration (5.7×10^{-8} mol/L) (The excitation wavelength was 340 nm for the monomer **5**, 373 nm for the dimer **14**, 382 nm for the trimer **17**, 389 nm for the tetramer **19**.)

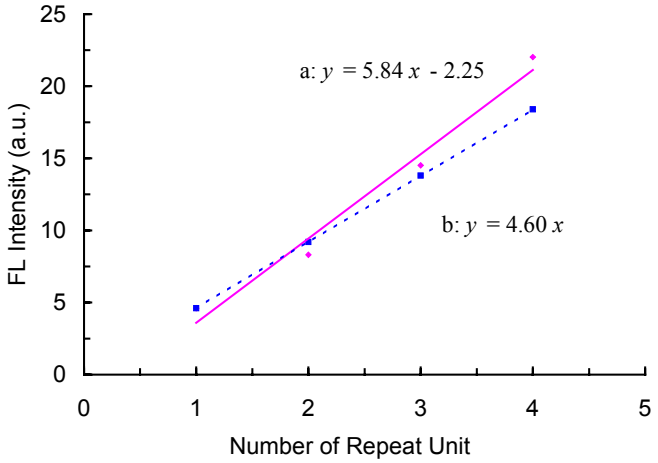

Figure 2.8 Photoluminescent Intensity at λ_{max}^{em} vs the Number of Repeat Unit in Bibenzimidazole Oligomers
(a, Solid line): Experimental value; (b, dotted line): Theoretical values, assuming the repeat units are isolated with no interactions.

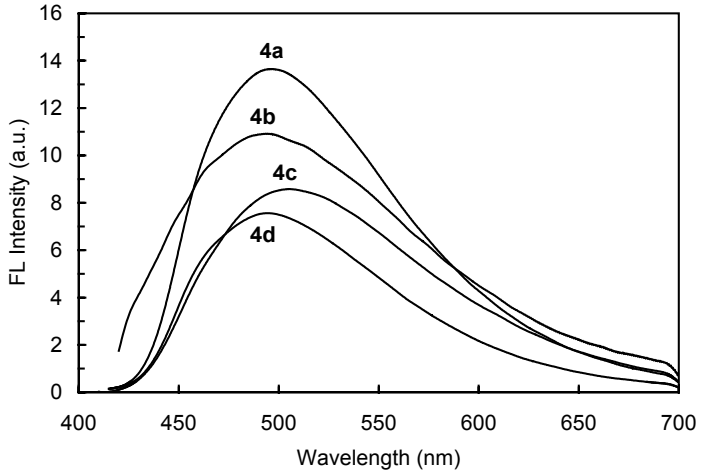

Figure 2.9 Photoluminescence Spectra of Poly(bibenzimidazole)s **4a–d** in Methanesulfonic Acid (The excitation wavelength was 400 nm for the polymer **4a**,**b**, 388 nm for the polymer **4c**, 397 nm for the polymer **4d**.)

Figure 2.8 shows the linear relationship between photoluminescent intensity at λ_{max}^{em} and the number of the repeat units in the oligomers. The solid line, a, is the

experimental value; the dotted line, b, is the theoretical value assuming that there is no interaction between the repeat units. The slope of the solid line a (5.84) is larger than that of the dotted line b (4.60), which indicates that there are some interactions between the repeat units due to the π orbital overlap. This suggests that in the tetramer, one repeat unit emits 1.27 times more light than one repeat unit in the monomer, which is consistent with the UV−vis properties shown in Figure 2.4, that in the tetramer, one repeat unit absorbs 1.2 times more light than one repeat unit in the monomer.

2.10 Viscosity and Molecular Weight of Poly(bibenzimidazole)s 4a–d

The viscosities of the poly(bibenzimidazole) (**4a–d**) were determined in methanesulfonic acid at 30.00 °C (Figure 2.10, Table 2.3). (The plots of **4b–d** are similar to the plot of **4a** shown in Figure 2.10). The inherent viscosity η_{inh} is 0.705 and 0.553 dL/g at a concentration of 0.400 g/dL for **4a** and **4b**, respectively. The intrinsic viscosity [η] of **4a** is 0.720 dL/g, and [η] of **4b** is 0.521 dL/g obtained by extrapolating to zero concentration.[41] The number average molecular weight (M_n) of **4a** can be roughly estimated to be around 19000, and the M_n of **4b** is around 15000 based on the molecular weight-inherent viscosity relationship established for poly[2,2′-(*m*-phenylene)-5,5′-bibenzimidazole].[13] The inherent viscosity η_{inh} is 0.425 and 0.287 dL/g at a concentration of 0.400 g/dL for **4c** and **4d**, respectively. The intrinsic viscosity [η] of **4c** is 0.387 dL/g, and [η] of **4d** is 0.344 dL/g obtained by extrapolating to zero

concentration. The number average molecular weight (M_n) of **4c** can be roughly estimated to be around 9600, and the M_n of **4d** is around 6400.

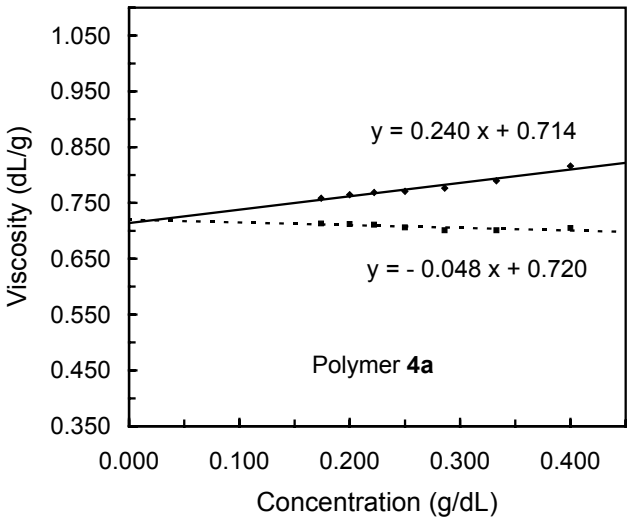

Figure 2.10 Plots of Inherent Viscosity η_{inh} and Reduced Specific Viscosity η_{sp}/c vs Concentration of Poly(bibenzimidazole) (**4a**) at 30.00 °C in Methanesulfonic Acid Solid line: $\eta_{red} = \eta_{sp}/c$. Dotted line: $\eta_{inh} = (\ln\eta_r)/c$

Table 2.3 Viscosities of Poly(bibenzimidazole)s **4a–d** in Methanesulfonic Acid

entry	η_{inh} (dL/g) at 0.400 g/dL	[η] (dL/g)	M_n
polymer **4a**	0.705	0.720	19000
polymer **4b**	0.553	0.521	15000
polymer **4c**	0.425	0.387	9600
polymer **4d**	0.287	0.344	6400

2.11 Infrared Analysis of Poly(bibenzimidazole)s 4a–d

The infrared spectra of a variety of polybenzimidazoles have been discussed previously.[28,42,43] The characteristic infrared peaks of the benzimidazoles are observed in the bibenzimidazole oligomers (**5**, **14**, **17**, **19**) and polymer series (**4a–d**). In the spectral region between 3500 and 2500 cm^{-1}, a very broad peak was observed. A relatively sharp peak at 3403 cm^{-1} was attributed to the stretching absorption of isolated, non-hydrogen bonded N-H groups. The very broad, asymmetric absorption, approximately centered at 3145 cm^{-1}, was assigned to hydrogen bonded N–H groups. The low intensity peak at 3053 cm^{-1} was attributed to the stretching modes of the aromatic C–H groups.

The region at 1660–1480 cm^{-1} is very characteristic of benzimidazoles. The C=C/C=N stretching vibrations (1622 cm^{-1}) are observed in this region, as well as ring modes which are characteristic of the conjugation between the benzene and the imidazole rings (1585 cm^{-1}). Strong absorptions due to in-plane ring modes are found at 1422 and 1397 cm^{-1}. An imidazole ring-breathing mode gives rise to a peak at 1280 cm^{-1}. The in-plane C–H bending bands, characteristic of substituted benzimidazoles, are found at 1230–1090 cm^{-1}. For the benzene C–H out-of-plane bending modes, typically the tri-substituted benzene ring modes are observed in the range 950–675 cm^{-1}, especially at 947 and 802 cm^{-1}.

Polymers **4c,d** made by the reaction of 3,3′-diaminobenzidine (**6**) and bis-trichloride **18** show the characteristic IR peaks described above. In addition, they show

weak absorption at around 1670 cm^{-1}, which might be due to the formation of the amide functionality in the polymer chain or at the end groups by hydrolysis in the presence of base and ethanol.[35]

Table 2.4 Thermostability of Bibenzimidazole Oligomers and Polymers under N_2

entry	onset decomposition temp (T_d, °C)	residue at 800 °C (%)
dimer **14**	516	17.44
trimer **17**	561	52.78
tetramer **19**	572	59.30
polymer **4a**	656	47.39
polymer **4b**	646	50.80
polymer **4c**	639	54.90
polymer **4d**	662	68.98

2.12 Thermostability of Bibenzimidazole Oligomers and Polymers

The oligomers and the polymers are thermally stable (Table 2.4). The TGA graph of the dimer **14**, trimer **17**, tetramer **19**, and polymer **4a** under N_2 are shown in Figures 2.11 and 2.12. The onset decomposition temperatures (T_d) from the trimer to the polymers are all higher than 500 °C. With the extension of the chain length, the T_d increases. The smooth curve in Figure 2.12 indicates a uniform polymer structure.

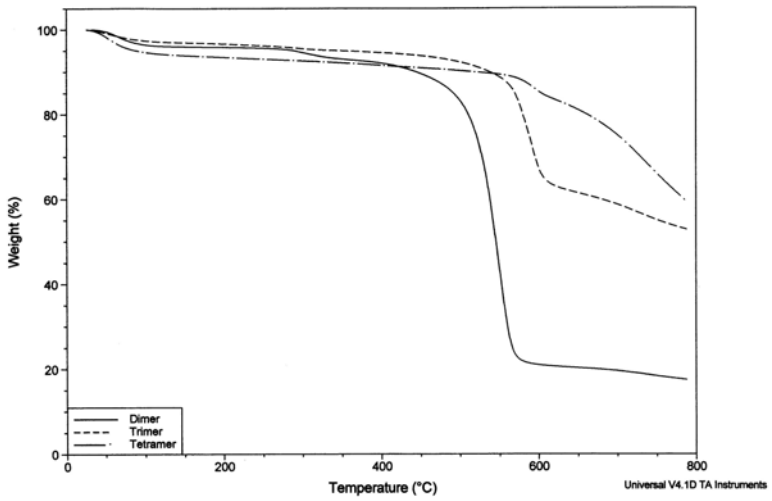

Figure 2.11 TGA Curves of Bibenzimidazole Dimer, Trimer and Tetramer under N_2 at a Heating Rate of 10 °C / min
Solid line: dimer **14**. Dashed line: trimer **17**.
Dashed dotted line: tetramer **19**.

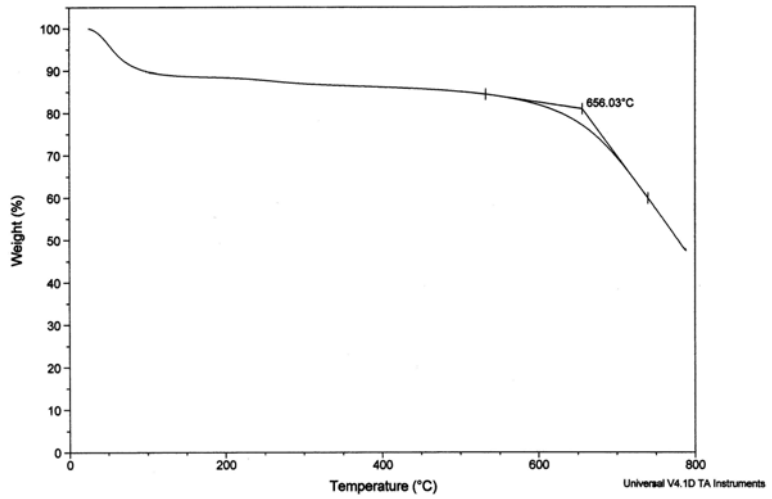

Figure 2.12 TGA Curves of Poly(bibenzimidazole) **4a** under N_2 at a Heating Rate of 10 °C / min

2.13 Conclusions

The oligomers of bibenzimidazole (dimer, trimer and tetramer) were first synthesized using a concise and efficient synthetic strategy. This methodology is very practical overall, requires few synthetic steps, and is suitable for the synthesis of the bibenzimidazole polymers. The X-ray structure of the dimer shows that it is coplanar and centrosymmetric. This series of oligomers provides useful information for the analysis of the poly(2,2′-bibenzimidazole)s. The UV–vis spectra show that the chain extension results in a decrease of the HOMO–LUMO gap, and the maximum absorption saturates at around 400 nm. The optical band gap of the polymer is estimated to be 2.68 eV.

The synthesis and properties of the metal complexes of the oligomers will be discussed in Part II and Part III.

CHAPTER 3

EXPERIMENTAL DETAILS

3.1 General

3.1.1 Reagents and Materials

All reagents were used without further purification. 1,2-Phenylenediamine (98%), 3,3′-diaminobenzidine (99%), methyl 2,2,2-trichloroacetimidate (98%), and methanesulfonic acid (99.5%) were purchased from Aldrich. Ethanol and DMF (EMD) were used as received without further purification.

3.1.2 Measurements

^{1}H NMR (500 MHz) and ^{13}C NMR (125 MHz) spectra were obtained on a JEOL Eclipse+ 500 MHz spectrometer. Chemical shifts (δ values) were given in parts per million with tetramethylsilane as an internal standard. UV−vis spectra were measured using a Varian Cary 500 UV−vis−NIR spectrophotometer. The photoluminescence (PL) emission spectra were obtained with a Jobin−Yvon Horiba Spex Fluoromax−3 Fluorimeter. Elemental analysis was performed by Quantitative Technologies Inc. (QTI) (Whitehouse, NJ). Mass analysis was performed by Scripps Research Institute (La Jolla, CA). ESI-MS spectra were obtained on a Waters−Micromass LCT. X-ray crystal structure of the dimer (**14**) was solved by Dr.

Douglas Ogrin at the Texas Center for Crystallography at Rice University and Dr. Simon Bott at University of Houston. FTIR spectra were recorded on a Bruker Vector 22 FTIR spectrometer with KBr pellets. Intrinsic viscosity [η] of the polybibenzimidazoles was determined at 30.00 ± 0.05 °C in methanesulfonic acid using a Cannon–Ubbelohde dilution viscometer (Size 150).[28,44]

3.2 Synthesis

2-Trichloromethylbenzimidazole (10). This is a known compound,[35] but NMR data was not reported. To a cooled suspension of the *o*-phenylenediamine (**9**) (5.41 g, 0.05 mol) and glacial acetic acid (100 mL), methyl 2,2,2-trichloroacetimidate (**8**) (8.82 g, 6.19 mL, 0.05 mol) was added slowly. When the resultant exothermic reaction subsided, the reaction mixture was kept at the room temperature for 10 h. A white powdered 2-trichloromethylbenzimidazole (**10**) precipitated and was collected by filtration, washed with a small amount of water, and vacuum-dried at 50 °C for 15 h. Yield: 85%. ^{1}H NMR (500 MHz, CF_3COOD): 7.94 (dd, J = 6.6, 3.3 Hz, 2H), 7.85 (dd, J = 6.6, 3.3 Hz, 2H); ^{13}C NMR (125 MHz, CF_3COOD): δ = 149.6, 132.4, 131.8, 116.7, 83.6. ESI-MS (*m*/*z*): 234 $[M - H]^+$. FTIR (KBr pellet, cm^{-1}): 3500–2500 broad (3061, 2983, 2908, 2829, 2724, 2658, 2603, 2478), 1620, 1590, 1448, 1428, 1309, 1278, 1228, 1043, 892, 816, 741, 683, 501.

2,2′-Bibenzimidazole (5). (i) Following Holan's method:[35] *o*-Phenylenediamine (**9**) (5.52 g, 0.05 mol) and methyl 2,2,2-trichloroacetimidate (**8**) (4.40 g, 3.10 mL, 0.025

mol) were kept stirring in methanol (50 mL) at room temperature for 24 h. After the aqueous quenching, the yellow-colored precipitate was filtered, rinsed with water, and vacuum-dried to afford the pure 2,2′-bibenzimidazole (10.5 g, 90%). It melts generally above 360 °C. ^{1}H NMR (500 MHz, CF_3COOD): 8.10 (dd, J = 6.3, 3.3 Hz, 4H), 7.92 (dd, J = 6.3, 3.3 Hz, 4H). ^{13}C NMR (125 MHz, CF_3COOD): δ = 133.9, 133.8, 132.4, 117.0. FTIR (KBr pellet, cm^{-1}): 3500–2500 broad (3029, 2949, 2870, 2798, 2750, 2673, 2585), 1616, 1586, 1500, 1397, 1343, 1271, 1235, 1183, 1143, 949, 742.

(ii) Following Fieselmann's method:[33] *o*-Phenylenediamine (**9**) (22 g, 0.20 mol) and oxamide (**7**) (8.81 g, 0.10 mol) were mixed in 20 mL of ethylene glycol, and refluxed with stirring for 24 h. After the solution was cooled, it was added to 400 mL of refluxing water and was filtered while hot to give 13 g. of water-insoluble yellow product. The crude product contained around 10 : 1 molar ratio of 2,2′-bibenzimidazole **5** and its isomer fluoflavin **11** on the basis of NMR spectrum of the crude. The crude mixture was heated in di(ethylene glycol) methyl ether at 140 °C, then filter while hot. The collected solid contained mainly fluoflavin **11** (still contaminated with 12% of 2,2′-bibenzimidazole**)**. The filtrate was set to recrystallize to provide the yellow powder which was mainly 2,2′-bibenzimidazole **5** (mixed with 2.7% of fluoflavin **11**). Fluoflavin **11** is soluble in concentrated H_3PO_4. The pure **11** was obtained by the addition of water into the concentrated H_3PO_4 solution to precipitate, and then neutralized with 5% NaOH solution. The NMR data of **11** is consistent with that of the literature reported.[34] ^{1}H NMR (500 MHz, CF_3COOD): 7.45 (dd, J = 6.1, 3.1 Hz, 4H),

7.37 (dd, J = 6.1, 3.1 Hz, 4H). ^{13}C NMR (125 MHz, CF_3COOD): δ = 144.0, 131.7, 127.1, 120.1.

Bis(2,2′-bibenzimidazole)·1.5H_2O (14). To a suspension of 3,3′-diaminobenzidine (**6**) (1.24 g, 5.8 mmol) and 2-trichloromethylbenzimidazole (**10**) (3.00 g, 12.7 mmol) in absolute ethanol (50 mL), triethylamine (5.86 g, 58 mmol) was added dropwise. The suspension was stirred at room temperature for 12 h and then refluxed under nitrogen for 36 h. The precipitated bis(2,2′-bibenzimidazole) ([bis($BiBzImH_2$)]) was collected by filtration and washed with hot glacial acetic acid. Then it was stirred in diluted ammonium hydroxide solution to neutralize the acid residue. The final product was a yellow powder. Yield: 70%. DMF can also be the solvent to replace ethanol. If DMF was used as the solvent, then 10 equiv of absolute ethanol was needed to facilitate the reaction. The reaction in DMF was stirred at room temperature under nitrogen for 5–10 h, and then heated at 75–80 °C for 24 h. The produced dimer was soluble in DMF and was precipitated by adding water dropwise to the DMF solution. The final product was collected by filtration. ^{1}H NMR (500 MHz, CF_3COOD): δ = 8.43 (s, 2H), 8.29 (d, J = 8.8 Hz, 2H), 8.26 (d, J = 8.8 Hz, 2H), 8.12 (dd, J = 6.6, 3.3 Hz, 4H), 7.94 (dd, J = 6.6, 3.3 Hz, 4H). ^{13}C NMR (125 MHz, CF_3COOD): δ = 144.0, 135.3, 134.8, 134.3, 134.1, 133.7, 132.5, 132.3, 118.2, 117.0, 116.1. ^{13}C NMR (125 MHz, D_2SO_4) (for comparison with the spectra of trimer, tetramer and polymers): δ = 143.1, 133.0, 132.6, 132.5, 132.3, 132.2, 130.5, 117.5, 116.4, 116.3, 115.3, 115.2. ESI-MS (*m*/*z*): 467.2 $[M + H]^+$. FTIR (KBr pellet, cm^{-1}): 3500–2500

broad (3350, 3203, 3052), 1650, 1619, 1586, 1560, 1520, 1447, 1315, 1276, 809, 740. Anal. Calcd for $C_{28}H_{18}N_8 \cdot 1.5H_2O$: C, 68.14; H, 4.29; N, 22.71. Found: C, 67.60; H, 3.79; N, 22.27.

[(4-(2-(1*H*-Benzo[*d*]imidazol-2-yl)-1*H*-benzo[*d*]imidazol-5-yl)benzene-1,2-diamine)] (15). 3,3′-Diaminobenzidine (**6**) (4.00 g, 19 mmol) was dissolved in 200 mL of DMF. 2-Trichloromethylbenzimidazole (**10**) (2.00 g, 8.6 mmol) was dissolved in 45 mL of DMF and added dropwise to the above solution, followed by addition of absolute ethanol (2.5 mL). Triethylamine (6 mL) was added dropwise to the above solution. The solution was stirred at room temperature for 5 h and heated at 75–80 °C under nitrogen for 7–10 h. The reaction mixture was cooled and filtered to remove the small amount of dark brown impurity. To the filtrate, 150 mL of water was added to precipitate the solid, which was bis(2,2′-bibenzimidazole) ([bis(BiBzImH_2)]) (**14**) (0.40 g, 0.857 mmol, yield 20%). Then to the filtrate of the above solution after **14** was removed by filtration, around 600 mL of water was added to precipitate the compound **15** (1.86 g, 5.46 mmol, yield 63%). In total, 7.17 mmol of 2-trichloromethylbenzimidazole (**10**) was consumed to form compounds **14** and **15**. The overall yield was 83% based on the consumed 2-trichloromethylbenzimidazole. Product **15** was further purified as follows: 100 mg of crude sample was dissolved in 15 mL of DMF, then 30 mL of water was added dropwise to precipitate the desired product. The collected solid was washed with 300 mL of water (3×) to remove DMF and dried in a vacuum oven for 20 h at 60 °C to afford the final pure product **15** as a yellow powder. ^{1}H NMR (500 MHz, CF_3COOD): δ

= 8.33 (s, 1H), 8.26 (d, J = 1.7 Hz, 1H), 8.24 (d, J = 8.8 Hz, 1H), 8.12 (dd, J = 8.8, 1.7 Hz, 1H), 8.09 (dd, J = 6.6, 3.3 Hz, 2H), 8.09 (d, J = 8.3 Hz, 1H), 8.02 (d, J = 8.3 Hz, 1H), 7.92 (dd, J = 6.6, 3.3 Hz, 2H). ^{13}C NMR (125 MHz, CF_3COOD): δ = 145.6, 142.0, 135.6, 134.9, 134.6, 134.0, 133.7, 132.9, 132.5, 131.4, 129.6, 127.9, 126.8, 126.0, 118.3, 117.0, 115.7. ESI-MS (*m*/*z*): 341 $[M + H]^+$. FTIR (KBr pellet, cm^{-1}): 3500–2500 broad (3345, 3177, 3058, 2970), 1621, 1587, 1524, 1424, 1399, 1337, 1274, 805, 766, 748, 738. Anal. Calcd for $C_{20}H_{16}N_6 \cdot H_2O$: C, 67.02; H, 5.06; N, 23.45. Found: C, 67.65; H, 4.75; N, 23.89.

2-(1H-benzo[d]imidazol-2-yl)-5-(1H-benzo[d]imidazol-5-yl)-1H-benzo[d]imidazole (16). The following is the procedure for the formation of the compound **16** as a byproduct. 3,3′-Diaminobenzidine (**6**) (4.00 g, 19 mmol) was dissolved in 150 mL of DMF. 2-Trichloromethylbenzimidazole (**10**) (1.76 g, 7.50 mmol) was dissolved in 20 mL of DMF and added dropwise to the above solution, followed by the addition of absolute ethanol (3 mL, around 6.8 equiv). Triethylamine (7 mL, around 6.7 equiv) was added dropwise to the above solution. The solution was stirred at room temperature for 6 h and heated at 130 °C under nitrogen for 44 h. The reaction mixture was cooled and filtered to remove the small amount of dark brown impurities. To the filtrate, 200 mL of water was added to precipitate the solid, which was the bis(2,2′-bibenzimidazole) (**14**) (0.300 g, 0.643 mmol). Then, to the filtrate of the above solution after **14** was removed by filtration, around 200 mL of water was added dropwise to precipitate the compound **16** (1.17 g, 3.34 mmol). Then, to the

filtrate of the above solution after **16** was removed by filtration, around 200 mL of water was added dropwise to precipitate the compound **15** (1.85 g, 5.43 mmol). In total, 6.73 mmol of 2-trichloromethylbenzimidazole (**10**) was consumed to form compounds **14**, **15** and **16**. The overall yield was 89% based on the consumed 2-trichloromethylbenzimidazole (**10**). Product **16** was further purified by dissolving 100 mg of the crude sample in 15 mL of DMF. Then 20 mL of water was added dropwise to precipitate the desired product. The product was washed with 300 mL of water (3×) to remove DMF and dried in a vacuum oven at 70 °C for 20 h. The final product **16** was a beige-colored powder. ^{1}H NMR (500 MHz, CF_3COOD): δ = 9.25 (s, 1H), 8.35 (s, 1H), 8.25 (d, *J* = 8.6 Hz, 1H), 8.24 (s, 1H), 8.20 (d, *J* = 8.6 Hz, 1H), 8.11 (dd, *J* = 6.1, 3.1 Hz, 2H), 8.10 (d, *J* not determined due to the overlap, 2H), 7.93 (dd, *J* = 6.1, 3.1 Hz, 2H). ^{13}C NMR (125 MHz, CF_3COOD): δ = 144.7, 142.0, 141.4, 141.3, 135.0, 134.7, 134.0, 133.9, 133.7, 132.7, 132.5, 132.4, 132.3, 132.2, 130.1, 117.3, 117.0, 115.8. ESI-MS (*m/z*): 351 $[M + H]^+$. FTIR (KBr pellet, cm^{-1}): 3500–2500 broad (3048, 2968, 2887, 2794), 1398, 1377, 1344, 1282, 948, 812, 738. Anal. Calcd for $C_{21}H_{14}N_6$: C, 71.99; H, 4.03; N, 23.99. Found: C, 71.38; H, 4.08; N, 23.60.

Tris(2,2′-bibenzimidazole) (17). Compound **15** (0.20 g, 0.588 mmol) was suspended in 20 mL of absolute ethanol and stirred at room temperature for 1 h. Methyl 2,2,2-tricholoacetimidate (**8**) (0.060 g, 0.294 mmol, 0.04 mL) was added by syringe dropwise. The above suspension was stirred at room temperature for 23 h and filtered to collect the solid. The crude product was purified by heating in 50 mL of ethylene glycol

at 145 °C for 24 h to remove the soluble impurity. After the suspension was cooled to room temperature, the brownish yellow trimer was collected by filtration, washed with water, and dried under vacuum at 60 °C for 40 h. Yield: 72%. ^{1}H NMR (500 MHz, CF_3COOD): δ = 8.43 (s, 4H), 8.29 (dd, *J* = 8.8 Hz, 3.3 Hz, 4H), 8.26 (dd, *J* = 8.8 Hz, 3.3 Hz, 4H), 8.11 (dd, *J* = 6.6, 3.3 Hz, 4H), 7.93 (dd, *J* = 6.6, 3.3 Hz, 4H). ^{13}C NMR (125 MHz, D_2SO_4; **17** dissolves well in D_2SO_4, but does not dissolve well in CF_3COOD, so the ^{13}C NMR spectrum was taken in D_2SO_4): δ = 143.2, 143.0, 133.1, 133.0, 132.5, 132.4, 132.3, 132.2, 131.8, 130.6, 117.4, 116.3, 115.3. ESI-MS (*m*/*z*): 699 $[M + H]^+$ (CF_3COOH as the solvent for ESI). FTIR (KBr pellet, cm^{-1}): 3500–2500 broad (3402, 3057, 2965, 2858, 2774), 1622, 1585, 1422, 1396, 1372, 1335, 1280, 947, 810, 783, 745. Anal. Calcd for $C_{42}H_{26}N_{12}\cdot 2H_2O$: C, 68.65; H, 4.12; N, 22.88. Found: C, 68.85; H, 3.88; N, 21.91.

Bis(2-trichloromethylbenzimidazole) (18). To a solution of 3,3′-diaminobenzidine (**6**) (2.14 g, 0.01 mol) in glacial acetic acid (50 mL), methyl 2,2,2-trichloroacetimidate (**8**) (4.41 g, 3.10 mL, 0.025 mol) was added dropwise. The reaction mixture was kept at the room temperature for around 15 h. The precipitated pale yellow product bis(trichloride) **18** was collected by filtration and washed with a small amount of water. Yield: 85%. ^{1}H NMR (500 MHz, DMSO-d_6): 7.93 (s, 2H), 7.78 (d, *J* = 8.7 Hz, 2H), 7.71 (d, *J* = 8.7 Hz, 2H). ^{13}C NMR (125 MHz, DMSO-d_6): δ = 151.2, 138.8, 137.8, 136.9, 123.7, 116.9, 114.2, 88.7. ^{13}C NMR (125 MHz, CF_3COOD): δ = 150.8, 143.5, 133.3, 132.5, 131.6, 117.8, 116.1, 83.5. ESI-MS (*m*/*z*): 431 $[M - Cl + H]^+$. FTIR

(KBr pellet, cm^{-1}): 3500–2500 broad (3427, 3075, 2916, 2823), 1626, 1584, 1419, 1293, 1206, 1028, 876, 815, 776, 679, 514. Anal. Calcd for $C_{16}H_8Cl_6N_4$: C, 40.98; H, 1.72; N, 11.95. Found: C, 40.62; H, 1.62; N, 11.82.

Tetra(2,2′-bibenzimidazole)·2.5H_2O (19). To a suspension of compound **15** (0.700 g, 2.05 mmol) in 40 mL of DMF, bis(trichloride) **18** (0.385 g, 0.82 mmol) and absolute ethanol (0.50 mL) were added, followed by the dropwise addition of triethylamine (0.83 g, 8.20 mmol, 1.15 mL). The suspension was stirred at room temperature for 10 h and then heated at 75 °C under nitrogen for 34 h. The precipitated yellow tetra(2,2′-bibenzimidazole) ([tetra(BiBzImH_2)]) (**19**) was collected by filtration and washed with water. Then it was heated in 90 mL of ethylene glycol or DMF at around 130 °C for 24 h to remove the soluble impurities. After the suspension was cooled to room temperature, the product was collected by filtration and washed with 300 mL of water (3×). The final product was a brownish yellow powder after vacuum-drying at 70 °C for 40 h. Yield: 60%. The NMR solvent was a combination of CF_3COOD/D_2O, since [tetra(BiBzImH_2)] does not dissolve well in CF_3COOD. ^1H NMR (500 MHz, CF_3COOD/D_2O): δ = 8.47 (s, 2H), 8.45 (s, 2H), 8.44 (s, 2H), 8.25 (multiplet, 12H), 8.11 (dd, *J* = 6.6, 3.3 Hz, 4H), 7.91 (dd, *J* = 6.6, 3.3 Hz, 4H). ^{13}C NMR (125 MHz, CF_3COOD/D_2O) (some peaks are overlapped and show multiplets, and some peaks are overlapped with CF_3COOD between δ 120–113 ppm): δ = 143.6, 135.2, 135.0, 134.9, 134.4, 134.3, 133.9, 133.7, 132.1, 131.8, 116.8. ^{13}C NMR (125 MHz, D_2SO_4, the tetramer dissolves well in D_2SO_4, but does not dissolve well in

CF_3COOD, so ^{13}C NMR spectrum was taken in D_2SO_4 for comparison): δ = 143.3, 143.2, 133.2, 133.1, 132.7, 132.6, 132.5, 132.4, 132.0, 130.6, 117.6, 116.5, 116.4, 115.5, 115.3. ESI-MS (*m*/*z*): 931 $[M + H]^+$ (CF_3COOH as solvent for ESI). FTIR (KBr pellet, cm^{-1}): 3500–2500 broad (3411, 3058, 2970, 2863, 2779), 1622, 1585, 1422, 1396, 1372, 1335, 1280, 947, 814, 783, 749. Anal. Calcd for $C_{56}H_{34}N_{16}·2.5H_2O$: C, 68.91; H, 4.03; N, 22.96. Found: C, 69.09; H, 3.69; N, 22.81.

Poly(2,2′-bibenzimidazole) (4a). 3,3′-Diaminobenzidine (**6**) was purified following the known procedures by making the tetrahydrochloride salt of it and regenerating it into the pure 3,3′-diaminobenzidine by using 5% NaOH solution.[27] The slightly pink of 3,3′-diaminobenzidine (**6**) (500 mg, 2.33 mmol) was suspended in 50 mL of absolute ethanol and the solution was degassed under nitrogen for 10 min. Methyl 2,2,2-trichloroacetimidate (**8**) (411 mg, 0.288 mL, 2.33 mmol) was added dropwise. The reaction suspension was stirred at room temperature for 26 h and then refluxed for 82 h. After the suspension was cooled to room temperature, the precipitated orange brown polymer was collected by filtration. Then it was stirred in 300 mL of deionized water (3×) for around 15 h each time to remove solvent ethanol. The final orange brown polymer was collected by filtration and dried under vacuum at 70 °C for 80 h. Yield: 70%. It is partially soluble in concentrated sulfuric acid, methanesulfonic acid, and HCOOH and not soluble in CF_3COOH, DMAC, DMF, DMSO, and NMP. The NMR spectra were taken in D_2SO_4, due to the low solubility in CF_3COOD. ^1H NMR (500 MHz, D_2SO_4): δ = 8.48 (s), 7.92 (s, br), 7.85−7.70 (multiplet), 7.58 (weak

multiplet). ^{13}C NMR (125 MHz, D_2SO_4, signals were relatively weak compared to those of the ^{13}C NMR of polymer **4d**, due to the lower solubility of **4a**): δ = 143.3 (br), 133.1, 132.5 (br), 131.8, 131.4, 131.0, 117.5 (br), 115.3 (br). FTIR (KBr pellet, cm^{-1}): 3500–2500 (broad), 1624, 1585, 1420, 1394, 1275, 947, 804. Anal. Calcd for $(C_{14}H_8N_4 \cdot H_2O)_n$: C, 67.19; H, 4.03; N, 22.39. Found: C, 66.53; H, 3.73; N, 21.95.

Poly(2,2′-bibenzimidazole) (4b). The slightly pink, purified 3,3′-diaminobenzidine (**6**) (700 mg, 3.27 mmol) was dissolved in 50 mL of DMF and the solution was degassed under nitrogen for 15 min. Methyl 2,2,2-trichloroacetimidate (**8**) (576 mg, 0.404 mL, 3.27 mmol) was added dropwise, followed by the addition of absolute ethanol (1.9 mL, 33 mmol). The deep orange brown reaction solution was stirred at room temperature for 54 h and then heated at 60–70 °C for 40 h. After the mixture was cooled to room temperature, the precipitated orange brown polymer was collected by filtration. Then it was stirred in 300 mL of deionized water (3×) for around 1 day each time to remove solvent DMF. The final orange brown polymer was collected by filtration, and dried under vacuum at 70 °C for 80 h. Yield: 60%. It is partially soluble in concentrated sulfuric acid, methanesulfonic acid, and HCOOH and not soluble in CF_3COOH, DMAC, DMF, DMSO and NMP. The NMR spectra were taken in D_2SO_4, due to the low solubility in CF_3COOD. ^{1}H NMR (500 MHz, D_2SO_4): δ = 8.46 (s), 7.92–7.57 (multiplet, br). ^{13}C NMR (125 MHz, D_2SO_4): not obtained due to the low solubility. FTIR (KBr pellet, cm^{-1}): 3500–2500 (broad), 1624, 1585, 1420,

1394, 1275, 947, 804. Anal. Calcd for $(C_{14}H_8N_4 \cdot 1.5H_2O)_n$: C, 64.86; H, 4.28; N, 21.61. Found: C, 64.48; H, 3.60; N, 21.11.

Poly(2,2′-bibenzimidazole) (4c). The slightly pink, purified 3,3′-diaminobenzidine (**6**) (365.5 mg, 1.706 mmol) was dissolved in 50 mL of DMF and the solution was degassed under nitrogen for 15 min, followed by the addition of absolute ethanol (2 mL, 34 mmol). Bis(trichloride) (**18**) (800.0 mg, 1.706 mmol) was added in one portion. Then triethylamine (4.75 mL, 34 mmol) was added dropwise to the above solution over 10 min. (After around 4 equiv of triethylamine was added, the reaction mixture became gel-like and difficult to stir, with the formation of precipitate.) The color of the mixture was brownish orange. The reaction mixture was stirred at room temperature for 8 h, then heated at 70–75 °C. The precipitate was almost completely dissolved after 8 h at 75 °C. The mixture was kept at 70–75 °C for totally 72 h and then cooled down. The orange polymer was precipitated out from the reaction mixture by the addition of deionized water, and collected by filtration. Then it was stirred in 300 mL of deionized water (3×) for around 1 day each time to remove DMF. The final orange powdered polymer was collected by filtration and dried under vacuum at 70 °C for 80 h. Yield 83%. It is soluble in concentrated sulfuric acid, methanesulfonic acid, HCOOH, CF_3COOH, DMAC, DMF, DMSO, and NMP. ^{1}H NMR (500 MHz, D_2SO_4): δ = 8.49 (s), 7.93–7.50 (multiplet, br). ^{13}C NMR (125 MHz, D_2SO_4): δ = 143.2, 140.2 (br, weak), 133.1, 132.6 (br), 132.4, 131.9, 131.4, 127.8, 117.6, 116.6, 115.3. FTIR (KBr pellet, cm^{-1}): 3500–2500 broad (3060), 1624, 1585, 1420, 1379, 1334, 1283, 946, 803.

Anal. Calcd for $(C_{14}H_8N_4 \cdot H_2O)_n$: C, 67.19; H, 4.03; N, 22.39. Found: C, 67.13; H, 3.62; N, 21.61.

Poly(2,2′-bibenzimidazole) (4d). The slightly pink, purified 3,3′-diaminobenzidine (**6**) (365.5 mg, 1.706 mmol) was dissolved in 50 mL of DMF and the solution was degassed under nitrogen for 15 min, followed by the addition of absolute ethanol (2 mL, 34 mmol). Bis(trichloride) (**18**) (800.0 mg, 1.706 mmol) was added in one portion. Then triethylamine (4.75 mL, 34 mmol) was added dropwise to the above solution over 10 min. (After around 4 equiv of triethylamine was added, the reaction mixture became gel-like and difficult to stir, with the formation of precipitate. The color of the mixture was brownish orange.) The reaction mixture was stirred at room temperature for 7 h and then heat at 75–80 °C, the precipitate was almost completely dissolved after 8 h at 78 °C. The reaction was maintained at 75–80 °C for 20 h, then heated at 120–130 °C. After around 20 h, a gray yellow precipitate formed. The mixture was heated at 120–130 °C for an additional 20 h, then heated at 145–50 °C for 46 h. After the mixture was cooled to room temperature, the precipitated greenish yellow polymer was obtained by filtration. Then it was stirred in 300 mL of water (3×) for around 1 day each time to remove DMF. The final yellow powdered polymer was collected by filtration and dried under vacuum at 70 °C for 80 h in 65% yield. It is soluble in concentrated sulfuric acid and methanesulfonic acid; partially soluble in CF_3COOH, and HCOOH and not soluble in DMAC, DMF, DMSO, and NMP. The NMR solvent was D_2SO_4, due to the low solubility in CF_3COOD. ^1H NMR (500 MHz,

D_2SO_4): δ = 8.48 (s), 7.93 (s, br), 7.85–7.70 (multiplet), 7.58 (weak multiplet). ^{13}C NMR (125 MHz, D_2SO_4): δ = 143.2 (br), 140.3 (br, weak), 133.1, 132.6 (br), 132.4, 131.9, 131.4, 131.0, 129.3, 117.6, 116.7, 115.3, 114.8. FTIR (KBr pellet, cm^{-1}): 3500–2500 broad (3060), 1624, 1585, 1420, 1379, 1334, 1283, 946, 803. Anal. Calcd for $(C_{14}H_8N_4 \cdot H_2O)_n$: C, 67.19; H, 4.03; N, 22.39. Found: C, 67.87; H, 3.54; N, 22.70.

The procedures for the initial attempts on the synthesis of poly(2,2′-bibenzimidazole)s using the condensation reactions between 3,3′-diaminobenzidine (**6**) and oxamide (**7**) or oxalic acid in polyphosphoric acid in the presence of phosphorus pentoxide are listed below for comparison. Both of the polymer products met with limited success when using them for further metal complexation. The possible reasons are: 1) The polymer **4e** is not soluble in the high boiling point solvents, rendering the difficulty in the metal complexation. This is probably due to the high molecular weight. The molecular weight was not determined due to the low solubility. 2) The polymerization reaction between 3,3′-diaminobenzidine (**6**) and oxalic acid provided a low molecular weight compound **4f** and the starting material 3,3′-diaminobenzidine (**6**). The polymer was not formed due to the decomposition of oxalic acid.

Poly(2,2′-bibenzimidazole) (4e). The slightly pink, purified 3,3′-diaminobenzidine (**6**) (3.00 g, 14.0 mmol), polyphosphoric acid (PPA) (83.3%, 29.56 g), oxamide (**7**) (1.23 g, 14.0 mmol) and P_2O_5 (4.80 g, 34 mmol) were added into a 3-

neck round bottom flask. The mixture was thoroughly degassed by repeated evacuations and flushes with N_2 for 1 h. Under a positive N_2 pressure, a mechanic stirrer was set up. The mixture was heated to 50 °C and kept at this temperature for 5 h. Then it was heated to 120 °C slowly in 2 h. The mixture turned dark brown. It was kept at this temperature for 12 h. The reaction temperature was increased to 220 °C slowly in 4 h and held at this temperature for 68 h. The mixture turned to very viscous dope, with orange red color, and eventually very deep red color. The polymerization dope in PPA was cooled, and precipitated in water. PPA was extracted with deionized water for 1 day, and then the mixture was filtered to collect the solid. The deep red crude polymer was treated with 1 liter of aqueous solution of 0.30 M NH_4OH (2x) for 2 days. The polymer turned black. Then the polymer was washed with a large amount of water to ensure that it was free of any residual acid PPA. The solid was dried under vacuum at 60 °C for 48 h to give a black solid in a yield of 100%. ^{1}H NMR (500 MHz, in D_2SO_4, very deep red solution): a broad peak in the region of δ = 6.5–8.0, centering at δ = 7.0. FTIR (KBr pellet, cm^{-1}): 3500–2500 broad (3325, 3198, 3042), 1608, 1581, 1443, 1397, 1271, 1115, 869, 806. Anal. Calcd for $(C_{14}H_8N_4 \cdot H_2O)_n$: C, 67.18; H, 4.03; N, 22.39. Found: C, 68.65; H, 3.33; N, 22.81. UV–vis (in methanesulfonic acid): λ_{max} at 535 nm, with a shoulder at 496 nm; in the UV region: 274 nm.

Poly(2,2′-bibenzimidazole) (4f). The slightly pink, purified 3,3′-diaminobenzidine (**6**) (8.00 g, 37.3 mmol), and polyphosphoric acid (PPA) (83.3%, 55.79 g) were added to a three-neck round bottom flask, and thoroughly degassed by

repeated evacuations and flushes with N_2 for 1 h. Under a positive N_2 pressure, a mechanic stirrer was set up, and oxalic acid (3.36 g, 37.3 mmol) was added. Then the mixture was slowly heated to 114 °C and kept at this temperature for 3 h. The light gray-brown mixture foamed up, probably due to the decomposition of oxalic acid. Then it was cooled down to 95 °C, and P_2O_5 (23 g, 162 mmol) was added under a positive N_2 pressure to compensate the water released from the condensation reaction. Then the mixture was heated to 124 °C, and kept at this temperature for 12 h; then heated to 144 °C, and held at this temperature for 11 h. The reaction temperature was eventually raised to 200 °C and was allowed to proceed at this temperature for 49 h. The mixture turned to very viscous dope, with bright orange red color. The polymerization dope in PPA was cooled, and precipitated in water. PPA was extracted with water for 3 days, and then the mixture was filtered to collect the solid. The bright orange red polymer was treated with 1 liter of aqueous solution of 0.30 M NH_4OH (2x) for 2 days. The polymer turned greenish black color. Then the polymer was washed with a large amount of water to ensure that it was free of any residual acid PPA. The polymer was dried under vacuum at 60 °C for 40 h to give a greenish black solid in 25% yield. ^{1}H NMR (500 MHz, in D_2SO_4, dark brown solution): δ = 7.00–7.60 (sharp multiplet). FTIR (KBr pellet, cm^{-1}): 3500–2500 broad (3342), 1615, 1584, 1475, 1397, 1281, 1123, 806, 747. Anal. Calcd for $(C_{14}H_8N_4 \cdot 2.5H_2O)_n$: C, 60.63; H, 4.73; N, 20.21. Found: C, 60.88; H, 4.60; N, 19.85. UV–vis (in methanesulfonic acid): λ_{max} at 461 nm, with two shoulders at 430 and 495 nm; in the UV region: 270 nm.

The NMR data of 3,3′-diaminobenzidine (**6**) in D_2SO_4 is listed here for comparison. ^{1}H NMR (500 MHz, in D_2SO_4): δ = 7.53 (d, *J* = 8.3 Hz, 2H), 7.48 (s, 2H), 7.43 (d, *J* = 8.3 Hz, 2H). FTIR (KBr pellet, cm^{-1}): 3388, 3357, 3302, 3182, 1634, 1575, 1499, 1410, 1276, 1251, 1164, 1088, 939, 876, 823, 762, 719.

PART II

MULTINUCLEAR RU COMPLEXES OF BIBENZIMIDAZOLE OLIGOMERS

CHAPTER 4

INTRODUCTION

Polynuclear metal complexes based on ruthenium(II) and/or osmium(II) polypyridine building blocks constitute a class of compounds which has attracted the attention of many researchers in the last decade and continue to be subject to an ever increasing research effort.[45,46] Primarily this is because the building blocks exhibit an unusual combination of properties rarely found simultaneously in other compounds.

Ru(II) and Os(II) form low-spin octahedral complexes with strong-field ligands such as bipyridine and phenanthroline. The stability of these complexes is presumably enhanced by the symmetrical t_{2g}^6 configuration.[47] The relevant properties of Ru(II) polypyridine complexes are: (i) good stability of the ground as well as the excited and redox states; (ii) absorption in the visible region, due to intense spin-allowed metal-to-ligand charge transfer (MLCT) bands; (iii) relatively long-lived (typically in the microsecond time range) and luminescent excited states; (iv) reversible metal-centered oxidation and ligand-centered reduction processes at accessible potentials; (v) tunability of all the properties.[48] This unique combination of photophysical and redox properties has allowed Ru(II) polypyridine complexes to be perfect candidates for the synthesis of new redox active metallopolymers.[1,4]

In this part, the synthesis and characterization of the multinuclear Ru complexes based on the oligomeric bibenzimidazoles using $[Ru(bpy)_2]^{2+}$ as the building block are discussed. The following molecular orbital approximation is discussed first to understand the properties of the Ru complexes.

4.1 Localized Molecular Orbital Approximation

The spectroscopic, redox, and kinetic properties of transition metal complexes are usually discussed with the assumption that the ground state, the excited states, and the redox species can be described in a sufficiently approximate way by localized molecular orbital configurations.[45,47,49-55] To better understand this point, it is convenient to make reference to schematic molecular orbital (MO) diagrams shown in Figure 4.1, which represents the case of an octahedral complex. In this very simplified diagram, each MO is labeled as metal (M) or ligand (L) according to its predominant localization. Thus, for example, the low-energy σ-bonding MO's, which result from the combination of metal and ligand orbitals of appropriate symmetry, are labeled L since they receive the greatest contribution from the ligand orbitals. In the ground electronic configuration of transition metal complexes in their usual oxidation states, the σ_L and π_L orbitals are completely filled, the π_M orbitals are either partially or completely filled, and the higher orbitals are usually empty. Light absorption and redox processes change the orbital population, and each excited or redox state is assumed to be described by a single MO configuration.

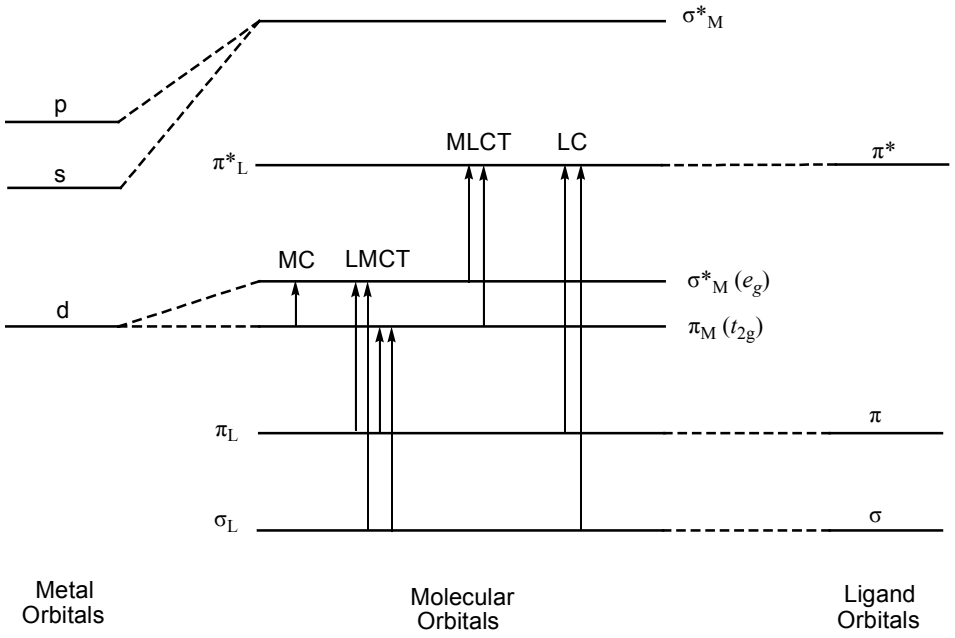

Figure 4.1 Schematic Energy-Level Diagram for an Octahedral Transition Metal Complex[45]
The various kind of electronic transitions are also indicated.

4.2 Classification of the Excited States in Mononuclear Ru Complexes

The assignment of the various bands which appear in the absorption spectra of transition metal complexes is often a very difficult problem because the absorption spectra reflect the complexity of the electronic structure of these molecules. By using a diagram shown in Figure 4.1, it is possible to make a classification of the various electronic transitions according to the localization of the MO's involved. Specifically, we may identify three fundamental types of electronic transitions:[45,47,53-55]

(i) Transitions between MO's predominantly localized on the central metal, usually called *metal-centered* (MC), ligand-field, or *d–d* transitions. For example, promotion of an electron from t_{2g} to e_g orbitals gives rise to a weak (Laporte forbidden)

absorption band (ε = ca. 100 $M^{-1}\cdot cm^{-1}$); (ii) transitions between MO's predominantly localized on the ligands, usually called *ligand-centered* (LC) or intraligand transitions. For example, the transitions within the ligand π-bonding orbital to the π^*-antibonding orbital, labeled $\pi\rightarrow\pi^*$ transitions, usually lie at high energies and are substantially ligand in character; (iii) transitions between MO's of different localization, which cause the displacement of the electronic charge from the ligands to the metal or *vice versa*. These transitions are called *charge-transfer* (CT) transitions and, more specifically, can be distinguished into *ligand-to-metal charge-transfer* (LMCT) and *metal-to-ligand charge-transfer* (MLCT) transitions. For example, excitation of a metal t_{2g} electron to π^*-antibonding orbital on the ligand gives rise to $d\rightarrow\pi^*$ states. These transitions have significant absorptions in the visible region (ε = ca. 20,000–25,000 $M^{-1}\cdot cm^{-1}$).[53]

Less frequently encountered types of transitions (not shown in Figure 4.1) are those from a metal-centered orbital to a solvent orbital (*charge-transfer to solvent,* CTTS), or between two orbitals predominantly localized on different ligands of the same metal center (*ligand-to-ligand charge-transfer*, LLCT).

It should also be noticed that the energy ordering of the various orbitals may be different from that shown in Figure 4.1. For example, in the case of $[Ru(bpy)_3]^{2+}$ the π^*_L orbital is thought to be lower in energy than the σ^*_M orbital.

4.3 Redox Behavior of Mononuclear Ru Complexes

In the localized MO approximation, oxidation and reduction processes are viewed as metal or ligand centered.[51,56,57] The highest energy occupied molecular orbital

(HOMO) is most usually metal centered, whereas the lowest unoccupied molecular orbital (LUMO) is either metal or ligand centered, depending on the relative energy ordering. When the ligand field is sufficiently strong and/or the ligands can be easily reduced, reduction takes place on the ligand. When the ligand field is weak and/or the ligands cannot be easily reduced, the lowest empty orbital can be metal centered.

Typical examples of well-behaved compounds are the Ru^{II}-polypyridine complexes. Their oxidation is metal centered and leads to Ru(III) compounds (low-spin $\pi_M(t_{2g})^5$ configuration) which are inert to ligand substitution:

$$[Ru^{II}(L)_3]^{2+} \longrightarrow [Ru^{III}(L)_3]^{3+} + e^- \qquad \text{(eq. 4.1)}$$

Reduction of the Ru^{II}-polypyridine complexes takes place on a π^* orbital of the polypyridine ligands. Therefore the reduced form, keeping the low-spin $\pi_M(t_{2g})^6$ configuration, is usually inert and the reduction process is reversible:

$$[Ru^{II}(L)_3]^{2+} + e^- \longrightarrow [Ru^{II}(L)_2(L^-)]^+ \qquad \text{(eq. 4.2)}$$

The added electron is localized on a single ligand.[51,58,59] Several reduction steps can often be observed in the accessible potential range. For example, in DMF at –54 °C, up to six CV waves can be observed for $[Ru(bpy)_3]^{2+}$ in the potential range between –1.33 and –2.85 V (vs SCE), which are assigned to successive first and second reduction of the three bpy ligands yielding a complex that can be formulated as $[Ru^{2+}(bpy^{2-})_3]^{4-}$.[60]

In Chapter 5, the synthesis and characterization of the multinuclear Ru complexes based on the oligomeric bibenzimidazoles will be discussed.

CHAPTER 5

RESULTS AND DISCUSSION

5.1 Bibenzimidazole-Based Ru Complexes $[Ru(bpy)_2(BiBzImH_2)](PF_6)_2$ (20), $[Ru(bpy)_2(BiBzIm)]$ (21) and $[Ru(bpy)_2(BiBzIm)Ru(bpy)_2](PF_6)_2$ (22)

*5.1.1 Synthesis of $[Ru(bpy)_2(BiBzImH_2)](PF_6)_2$ (**20**), $[Ru(bpy)_2(BiBzIm)]$ (**21**) and $[Ru(bpy)_2(BiBzIm)Ru(bpy)_2](PF_6)_2$ (**22**)*

Synthesis of the Ru complexes based on 2,2′-bibenzimidazole (**5**) are summarizes in Scheme 5.1 following the reported procedures.[16,20] The reaction of $Ru(bpy)_2Cl_2$ with 2,2′-bibenzimidazole (**5**) in ethanol/water (1:1 v/v) gave the desired mix-ligand complex $[Ru(bpy)_2(BiBzImH_2)](PF_6)_2$ (**20**). The acidity of the bibenzimidazole ligand increases upon the coordination with the ruthenium ion. This is consistent with the ease of deprotonation of the coordinating ligand. The pK_a values of $[Ru(bpy)_2(BiBzImH_2)]^{2+}$ in 50% acetonitrile/water mixture have been reported.[17,20] The pK_{a1} and pK_{a2} are 5.74 ± 0.05 and 10.51 ± 0.05 at 25 °C, respectively (equation 5.1).

$$[Ru(bpy)_2(BiBzImH_2)]^{2+} \underset{H^+}{\overset{pK_{a1}}{\rightleftharpoons}} [Ru(bpy)_2(BiBzImH)]^{+} \underset{H^+}{\overset{pK_{a2}}{\rightleftharpoons}} [Ru(bpy)_2(BiBzIm)] \qquad \text{(eq. 5.1)}$$

20 **20a** **21**

Deprotonation of the complex **20** in methanol with sodium methoxide gave rise to a purple suspension. The purple solid was isolated as the neutral complex $[Ru(bpy)_2(BiBzIm)]$ (**21**).

The fully deprotonated complex **21** may further act as a bidentate ligand. It was complexed with another equivalent of $Ru(bpy)_2Cl_2$ to give binuclear ruthenium complex $[Ru(bpy)_2(BiBzIm)Ru(bpy)_2](PF_6)_2$ (**22**).

Scheme 5.1 Synthesis of Ru Complexes **20**–**22**

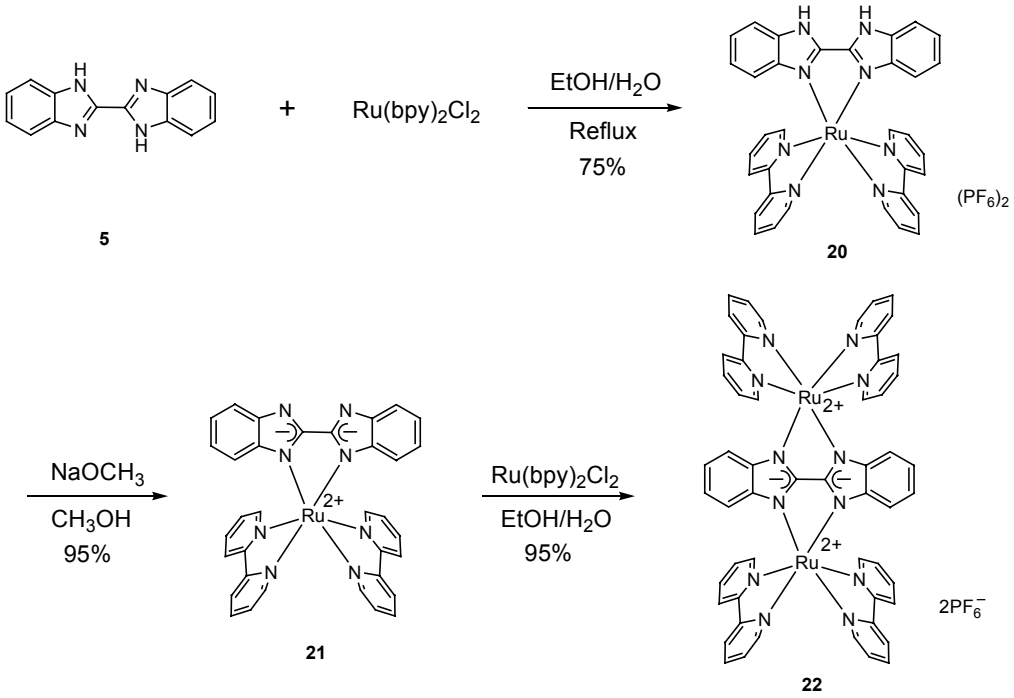

*5.1.2 UV–vis Properties of [Ru(bpy)$_2$(BiBzImH$_2$)](PF$_6$)$_2$ (**20**) and [Ru(bpy)$_2$(BiBzIm)] (**21**)*

The UV–vis spectral comparisons are illustrated in Figure 5.1, and the accumulated data are summarized in Table 5.1. The optical transitions have been separated into those related to metal-to-ligand charge transfer (MLCT) transitions ($d\pi$–π*) and those characteristic to intraligand π–π* transitions.[20,61] For the mix-ligand complex **20**, it is difficult to make assignments related to the specific ligand involved in the transition. The optical transitions are often the overlapping bands and difficult to deconvolute into their components. The low-energy maxima at 463 nm is more likely related to $d\pi$–π* (bpy) due to the fact that coordinated bpy rather than the coordinated BiBzImH$_2$ is reduced electrochemically. The transitions located at 328 and 347 nm are assigned as π–π* (BiBzImH$_2$) and the 290-nm band is assigned as π–π* (bpy). The far–UV bands appear to be related to transitions involving both ligands. Compared with the MLCT of $[Ru(bpy)_3]^{2+}$ at 452 nm, the MLCT transition energies of $[Ru(bpy)_2L]^{2+}$ decrease in the order of L = bpy > BiBzImH$_2$, which is consistent with the π-donor ability of the imidazole ligands. A stronger π-donor bibenzimidazole ligand increases the electron density on the metal, which results in the decrease of the MLCT band energies.

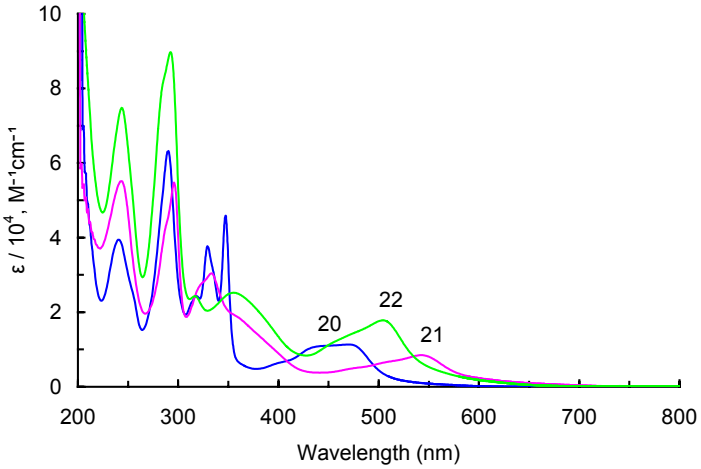

Figure 5.1 UV–vis Spectra of $[Ru(bpy)_2(BiBzImH_2)](PF_6)_2$ (**20**), $[Ru(bpy)_2(BiBzIm)]$ (**21**) and $[Ru(bpy)_2(BiBzIm)Ru(bpy)_2](PF_6)_2$ (**22**) in CH_3CN

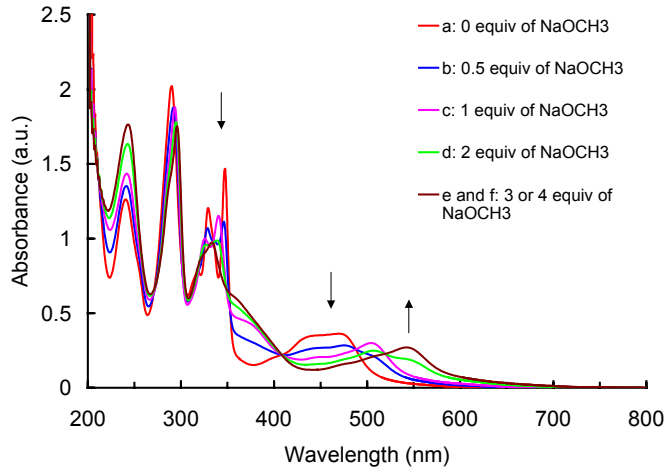

Figure 5.2 UV–vis Spectra of Stepwise Deprotonation of $[Ru(bpy)_2(BiBzImH_2)](PF_6)_2$ (**20**) in CH_3CN by Adding $NaOCH_3/CH_3OH$ Solution

The stepwise deprotonation of $[Ru(bpy)_2(BiBzImH_2)](PF_6)_2$ (**20**) at various pH's has been reported previously.[20] In our study, the complex **20** was deprotonated by the stoichiometric titration with $NaOCH_3$ as shown in Figure 5.2. After the addition of 0.5 and 1 equivalents of $NaOCH_3$, the MLCT transition red shifted to 500 nm and 506

nm, respectively. Two equivalents of $NaOCH_3$ make the MLCT transition red shifted to 512 nm, with the peak at 543 nm growing up. In total, four equivalents of $NaOCH_3$ was added to ensure the fully deprotonation of the complex. The results indicate that the dication of **20** in solution undergoes two successive deprotonations to exist as an equilibrium mixture with the monocation (**20a**) and neutral species (**21**) as shown in Scheme 5.2. Upon the fully deprotonation, the lowest energy MLCT of the complex $[Ru(bpy)_2(BiBzIm)]$ (**21**) red shifted to 543 nm, with the lower intensity.

Scheme 5.2 Stepwise Deprotonation of Ru Complex **20**

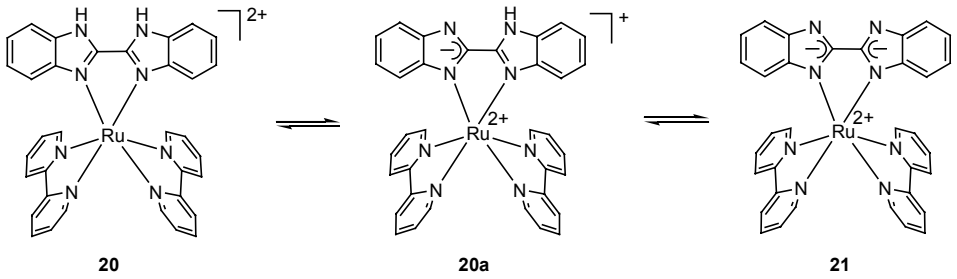

Table 5.1 UV–vis Absorption Spectral Data for Ru Complexes (**20–26**) Based on Bibenzimidazole Oligomers in CH_3CN at 298 K (λ, nm (ε, $M^{-1}\cdot cm^{-1}$))

Ru Complex	$\pi - \pi^*$ (bpy)		$\pi - \pi^*$ ($BiBzImH_2$)		$d\pi - \pi^*$ (bpy)
$[Ru(bpy)_2(BiBzImH_2)]^{2+}$ (**20**)[a,b]	240 (39375)	290 (63125)	328 (37500)	347 (45803)	469 (11334) 438 (sh)
$[Ru(bpy)_2(BiBzIm)]$ (**21**)[a]	243 (55125)	295 (54688)	333 (30425)		543 (8465)
$[(Ru(bpy)_2)_2(BiBzIm)]^{2+}$ (**22**)[b]	245 (74700)	294 (89700)	318 (24280)	355 (25200)	505 (17800)
$[(Ru(bpy)_2)_2$(bis-$BiBzImH_2)]^{4+}$ (**23**)	244 (66649)	290 (108108)	353 (sh)	367 (62594)	464 (22108)
$[(Ru(bpy)_2)_2$(bis-BiBzIm)] (**24**)	246 (80950)	295 (101397)	350 (57095)	392 (sh)	543 (13182)
$[(Ru(bpy)_2)_4$(bis-BiBzIm)]$^{4+}$ (**25**)	244 (138956)	293 (202045)	363 (71184)	398 (sh)	506 (37946)
$[(Ru(bpy)_2)_8$(tetra-BiBzIm)]$^{8+}$ (**26**)	245 (230670)	293 (357460)	368 (141650)	415 (sh) (114620)	506 (65300)

[a]Reference 20. [b] References 15 and 61.

*5.1.3 UV–vis Properties of $[(Ru(bpy)_2)_2(BiBzIm)](PF_6)_2$ (**22**)*

Spectral changes related to $BiBzIm^{2-}$-based bis-Ru complex $[(Ru(bpy)_2)_2(BiBzIm)]^{2+}$ (**22**) are illustrated in Figure 5.1. The following features are noted:[61] (1) The π–π^* ($BiBzImH_2$) transitions found in the $[Ru(bpy)_2(BiBzImH_2)]^{2+}$ complex (**20**) are lost. (2) The intensity of the low-energy transition (506 nm) appears to

be related to the number of $Ru(bpy)_2^{2+}$ units, suggesting that this transition arises from these components and, on the basis of the discussion above, can be assigned as dπ–π* (bpy). (3) The spectral activity in the 350 nm region consists of the overlapping metal-to-ligand charge transfer (MLCT) bands. (4) The absorption maximum at 294 nm has its primary origin π–π* (bpy) transitions. As of the stoichiometry of the complexes, the monometallic complex has two bipyridine ligands, the bimetallic complex has four. The relative intensity of the complex **22** is two times larger than that of the complex **21**. (5) The far UV transitions increase in a systematic manner as the number of heterocyclic ligands increases, and most likely are overlapping π–π* transitions associated with both bpy and $BiBzImH_2$ ligands.

*5.1.4 Electrochemical Studies of $[Ru(bpy)_2(BiBzImH_2)]Cl_2$ (**20**) and $[Ru(bpy)_2(BiBzIm)]$ (**21**)*

*5.1.4.1 Oxidation of $[Ru(bpy)_2(BiBzImH_2)]Cl_2$ (**20**) and $[Ru(bpy)_2(BiBzIm)]$ (**21**)*[17]

In accordance with Haga's report,[17] the cyclic voltammogram (CV) of the mono-ruthenium complex **20** shows one reversible oxidation couple and one irreversible oxidation wave at more positive potentials at pH 7.1 (Figure 5.3). For the Ru(II)/Ru(III) couple, the potentials are pH independent in the pH < 0.6 and > 10.4 regions. At these two regions, the major Ru(II) species are $[Ru(bpy)_2(BiBzImH_2)]^{2+}$ (**20**) and $[Ru(bpy)_2(BiBzIm)]$ (**21**) respectively. The electrode processes are defined as[17]

$$[Ru^{II}(bpy)_2(BiBzImH_2)]^{2+} \rightleftharpoons [Ru^{III}(bpy)_2(BiBzImH_2)]^{3+} + e^- \ (pH < 0.6) \qquad \text{(eq. 5.2)}$$

$$[Ru^{II}(bpy)_2(BiBzIm)] \rightleftharpoons [Ru^{III}(bpy)_2(BiBzIm)]^{+} + e^- \ (pH > 10.4) \qquad \text{(eq. 5.3)}$$

Over the range 0.6 < pH < 5 and 7 < pH < 10, plots of $E_{1/2}$ vs pH are linear with slopes of 53 mV, which are consistent with one-electron, one-proton processes as follows:[17]

$$[Ru^{II}(bpy)_2(BiBzImH_2)]^{2+} \rightleftharpoons [Ru^{III}(bpy)_2(BiBzImH)]^{2+} + H^+ + e^- \ (0.6 < pH < 5) \qquad \text{(eq. 5.4)}$$

$$[Ru^{II}(bpy)_2(BiBzImH)]^{+} \rightleftharpoons [Ru^{III}(bpy)_2(BiBzIm)]^{+} + H^+ + e^- \ (7 < pH < 10) \qquad \text{(eq. 5.5)}$$

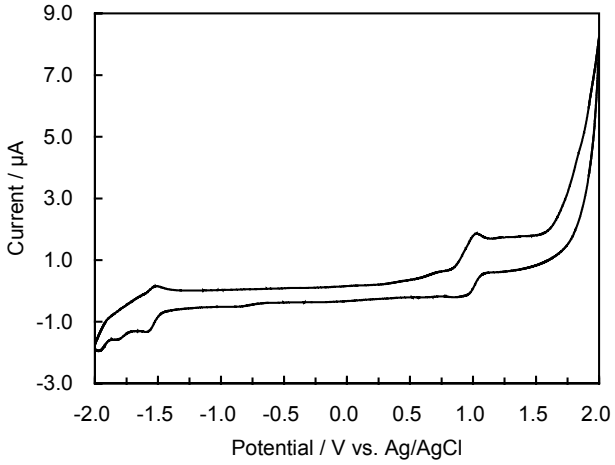

Figure 5.3 Cyclic Voltammogram of $[Ru(bpy)_2(BiBzImH_2)]Cl_2$ (**20**) in 0.10 M Bu_4NPF_6/CH_3CN Solution at a Scan Rate of 50 mv/s
The concentration of the Ru complex is around 2.11×10^{-4} M.

Deprotonation of $[Ru(bpy)_2(BiBzImH_2)]Cl_2$ (**20**) to give $[Ru(bpy)_2(BiBzIm)]$ (**21**) shifts the $Ru^{3+/2+}$ potential from 1.12 to 0.43 V vs SSCE. This effect is electrostatic in nature, leaving a net –2 charge on each BiBzIm ligand, which suggests the stronger π donation of the deprotonated BiBzIm to metal stabilizes the higher oxidation states. The $d\pi$ orbitals respond to this perturbation by increasing their energy.

*5.1.4.2 Reduction of $[Ru(bpy)_2(BiBzImH_2)]Cl_2$ (**20**)*

By analogy to $[Ru(bpy)_3]^{2+}$, the reductions can be assigned to the reduction of the coordinated bipyridine ligands.[62] The two reductions of $[Ru^{II}(bpy)_2(BiBzImH_2)]^{2+}$ (**20**) are illustrated in equations 5.6 and 5.7:

$$[Ru^{II}(bpy)_2(BiBzImH_2)]^{2+} + e^- \rightleftharpoons [Ru^{II}(bpy)(bpy^-)(BiBzImH_2)]^+ \quad \text{(eq. 5.6)}$$

$$[Ru^{II}(bpy)(bpy^-)(BiBzImH_2)]^+ + e^- \rightleftharpoons [Ru^{II}(bpy^-)(bpy^-)(BiBzImH_2)] \quad \text{(eq. 5.7)}$$

*5.1.5 Electrochemical Properties of $[(Ru(bpy)_2)_2(BiBzIm)](PF_6)_2$ (**22**)*

*5.1.5.1 Oxidation of $[(Ru(bpy)_2)_2(BiBzIm)](PF_6)_2$ (**22**)*

For the bisnuclear Ru complex $[(Ru(bpy)_2)_2(BiBzIm)]^{2+}$ (**22**), two successive electrode oxidation couples are observed at +0.75 V and +1.04 V (Figure 5.4). The electrode processes are shown in equations 5.8 and 5.9. The separations in peak potentials, ($\Delta E_p = E_{pa} - E_{pc}$), are about 60 mV, and the ratios of oxidation to reduction peak height are 1.0 ± 0.1, which indicates that the electrode oxidation processes are quasireversible. When the oxidation potentials of the binuclear complex is compared with that of mononuclear one, it is found that the first oxidation potential of binuclear

complex is 0.3 V lower than that of the mononuclear complex $[Ru(bpy)_2(BiBzImH_2)]^{2+}$ (**20**). This suggests that the BiBzIm bridging ligand in binuclear complex has an electron-donor property.

$$[Ru^{II}(bpy)_2(BiBzIm)Ru^{II}(bpy)_2]^{2+} \rightleftharpoons [Ru^{II}(bpy)_2(BiBzIm)Ru^{III}(bpy)_2]^{3+} + e^- \quad \text{(eq. 5.8)}$$

$$[Ru^{II}(bpy)_2(BiBzIm)Ru^{III}(bpy)_2]^{3+} \rightleftharpoons [Ru^{III}(bpy)_2(BiBzIm)Ru^{III}(bpy)_2]^{4+} + e^- \quad \text{(eq. 5.9)}$$

It has been shown that when the Ru(II/III) oxidation potential is regarded as a function of the metal ion in the second $Ru(bpy)_2$ site, the oxidation potential depends only on the charge of the second metal ion; i.e., the observed Ru(II/III) oxidation potentials are +0.78 and +1.0 V vs SCE for +2 and +3 charged second metal ions, respectively.[15] These results suggest that the electronic delocalization through BiBzIm is relatively small and the electrostatic interaction becomes an important factor for determining the oxidation potential in the present system.[14,15,61]

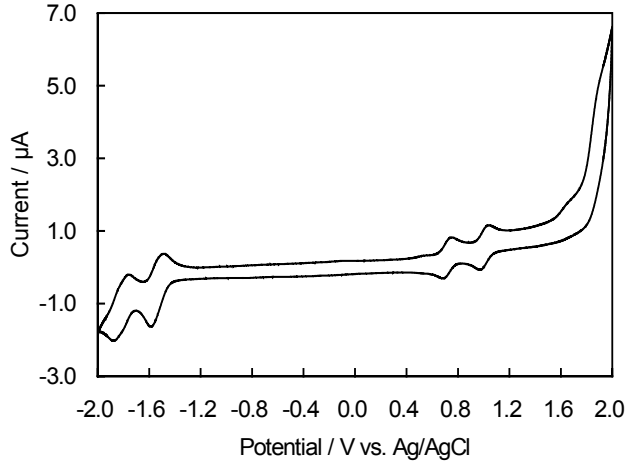

Figure 5.4 Cyclic Voltammogram of $[(Ru(bpy)_2)_2(BiBzIm)](PF_6)_2$ (**22**) in 0.10 M Bu_4NPF_6/CH_3CN Solution at a Scan Rate of 50 mv/s
The concentration of the Ru complex is around 2.11×10^{-4} M.

*5.1.5.2 Reduction of [(Ru(bpy)$_2$)$_2$(BiBzIm)](PF$_6$)$_2$ (**22**)*

Two chemically reversible reduction waves at –1.54 and –1.82 V are observed for the bis-ruthenium complex **22**. They are both resolved into two closely spaced one-electron reduction processes with similar half-wave potentials rather than a single two-electron process: the peak-to-peak separation of both processes in cyclic voltammogram is around 100 mV, which is considerably larger than the theoretically predicted value of 28 mV for a reversible two-electron-reduction process. It has been reported that they are ligand-based.[14] Since the BiBzIm ligand acts as a π donor, the π^* orbitals associated with BiBzIm are at much higher energies than those of bpy. Therefore, bpy can be regarded as the electroactive ligand. Furthermore, the monomeric complex, $[Ru(bpy)_2(BiBzImH_2)]^{2+}$, has been reported to exhibit two bpy ligand-based processes at –1.60 and –1.90 V.[61] Thus, it can be concluded that four one-electron reduction processes based on the bpy ligand are observed in the dinuclear complex.[14]

The existence of four substituted bpy ligands in the present symmetrical dinuclear complex are expected to show a maximum of eight reduction steps. However, only four reduction processes are observed within the accessible potential range. Since two $Ru(bpy)_2$ moieties are separated by a BiBzIm bridge, the interactions of the bpy ligand between the different moieties are relatively small. Thus, the first electron added to the dinuclear complex are predicted to be localized in a bpy ligand on one $Ru(bpy)_2$ moiety (equation 5.10). Further electrons may be accepted by the other bpy ligands on each $Ru(bpy)_2$ moiety at a more negative potential. Thus, the reduction processes can be summarized by equations 5.10–5.13. The separation of the reduction potential between

the first and second processes (equations 5.10 and 5.11) is smaller than that between the third and fourth ones (equations 5.12 and 5.13), which can be attributed to the electronic repulsion energy as pointed out by Vlcek, et al.[57]

$$[Ru(bpy)_2(BiBzIm)Ru(bpy)_2]^{2+} + e^- \rightleftharpoons [Ru(bpy)_2(BiBzIm)Ru(bpy)(bpy^-)]^+ \quad \text{(eq. 5.10)}$$

$$[Ru(bpy)_2(BiBzIm)Ru(bpy)(bpy^-)]^+ + e^- \rightleftharpoons [Ru(bpy)(bpy^-)(BiBzIm)Ru(bpy)(bpy^-)] \quad \text{(eq. 5.11)}$$

$$[Ru(bpy)(bpy^-)(BiBzIm)Ru(bpy)(bpy^-)] + e^- \rightleftharpoons [Ru(bpy)(bpy^-)(BiBzIm)Ru(bpy^-)_2]^- \quad \text{(eq. 5.12)}$$

$$[Ru(bpy)(bpy^-)(BiBzIm)Ru(bpy^-)_2]^- + e^- \rightleftharpoons [Ru(bpy^-)_2(BiBzIm)Ru(bpy^-)_2]^{2-} \quad \text{(eq. 5.13)}$$

Table 5.2 Cyclic Voltammogram Data for Ru Complexes (**20–26**) Based on Bibenzimidazole Oligomers [a]

complex	oxidation		reduction	
	$E_{1/2}$ (1), (V)	$E_{1/2}$ (2), (V)	$E_{1/2}'$ (1), (V)	$E_{1/2}'$ (2), (V)
$[Ru(bpy)_2(BiBzImH_2)]^{2+}$ [b] (**20**)	1.12 (70)		–1.60 (80)	–1.90 (80)
$[Ru(bpy)_2(BiBzIm)]$ [b] (**21**)	0.43 (68)		–1.58 (60)	–1.87 (60)
$[(Ru(bpy)_2)_2(BiBzIm)]^{2+}$ [b,c] (**22**)	0.76 (60)	1.04 (64)	–1.54 (100) [d]	–1.82 (120) [d]
$[(Ru(bpy)_2)_2(bis\text{-}BiBzImH_2)]^{4+}$ (**23**)	1.09 (94)		–1.41 (140)	–1.64 (484)
$[(Ru(bpy)_2)_2(bis\text{-}BiBzIm)]$ (**24**)	0.39 (72)		–1.64 (70)	–1.93 (80)
$[(Ru(bpy)_2)_4(bis\text{-}BiBzIm)]^{4+}$ (**25**)	0.75 (81)	1.04 (72)	–1.47 (124)	–1.64 (443)
$[(Ru(bpy)_2)_8(tetra\text{-}BiBzIm)]^{8+}$ (**26**)	0.71 (78)	1.00 (69)	–1.51 (55)	–1.72 (473)

[a] Solutions were 0.1 M $TBNPF_6$ in acetonitrile. The potentials $E_{1/2}$ were calculated from the equation $(E_{pa} + E_{pc}) / 2$ where E_{pa} and E_{pc} are anodic and cathodic peak potentials respectively. The values in parentheses are peak-to-peak separations, $\Delta E_p = E_{pa} - E_{pc}$. [b]Reference 20. [c]Reference 15 and 61. [d]This work.

Scheme 5.3 Synthesis of Ru Complexes **23–25**

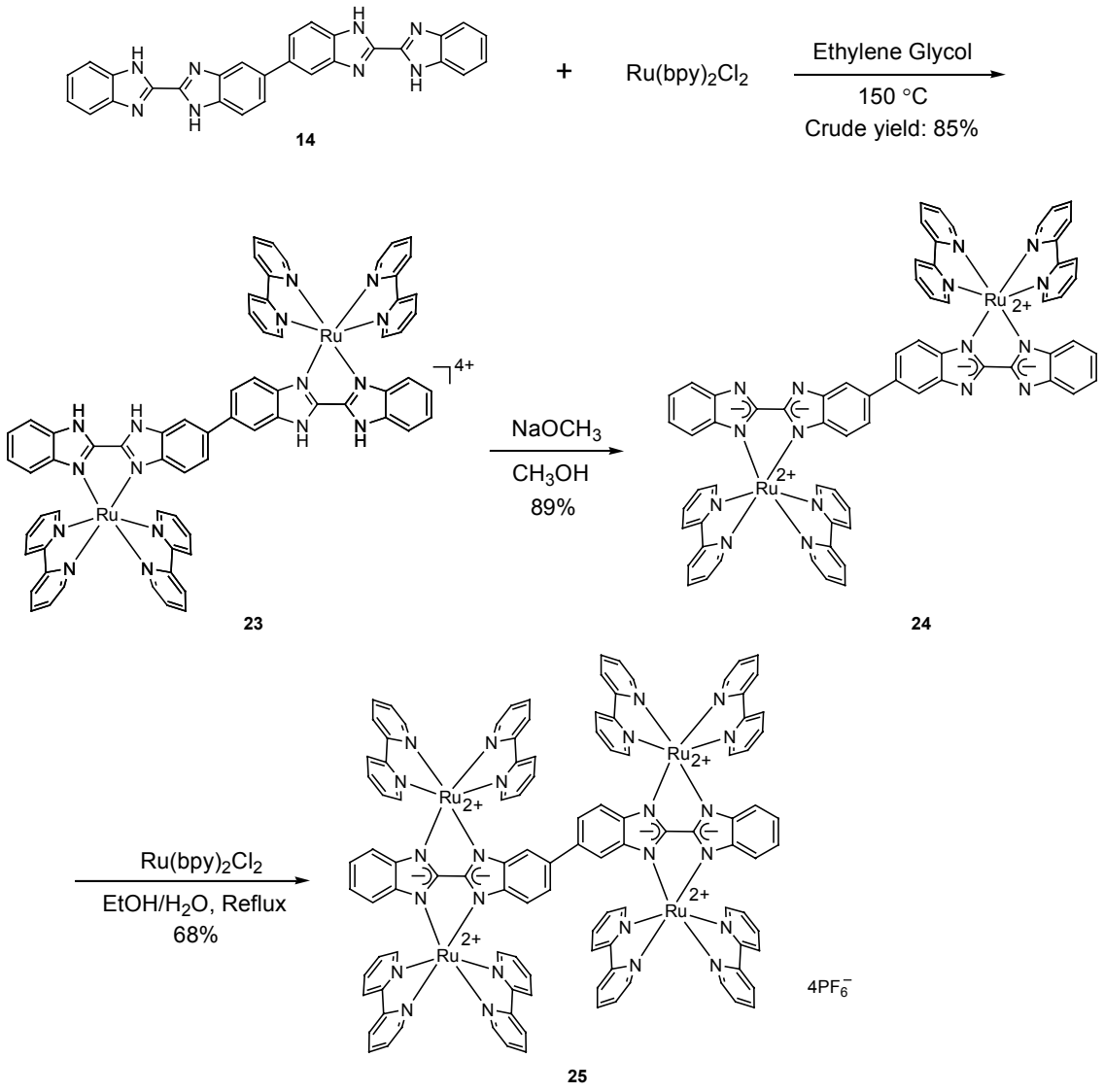

5.2 Bis(bibenzimidazole)-Based Ru Complexes $[(Ru(bpy)_2)_2(bis(BiBzImH_2))]Cl_4$ (**23**), $[(Ru(bpy)_2)_2(bis(BiBzIm))]$ (**24**) and $[(Ru(bpy)_2)_4(bis(BiBzIm))](PF_6)_4$ (**25**)[63]

*5.2.1 Synthesis of $[(Ru(bpy)_2)_2(bis(BiBzImH_2))]Cl_4$ (**23**), $[(Ru(bpy)_2)_2(bis(BiBzIm))]$ (**24**) and $[(Ru(bpy)_2)_4(bis(BiBzIm))](PF_6)_4$ (**25**)*

The multinuclear Ru complexes **23**–**25** based on the dimer of bibenzimidazole [bis(bibenzimidazle)] (**14**) were prepared following the procedures of making the complexes **20**–**22**. One equivalent of the bis(bibenzimidazole) (**14**) was complexed with two equivalents of $Ru(bpy)_2Cl_2$ to give the bis-Ru complex **23** (Scheme 5.3).

It should be noticed that after the complexation, the protons on the bis($BiBzImH_2$) ligand (**14**) in the complex $[(Ru(bpy)_2)_2(bis(BiBzImH_2))]^{4+}$ (**23**) become acidic and tend to be partially deprotonated in the reaction media, providing a mixture of protonated and partially deprotonated species. The deprotonation also occurs during the purification of **23** with Al_2O_3 (neutral) column. In order to circumvent this problem, the crude complex **23** was completely deprotonated first by $NaOCH_3$ in CH_3OH at reflux to provide the neutral complex $[(Ru(bpy)_2)_2(bis(BiBzIm))]$ (**24**), which could be easily purified due to the insolubility in acetone. Then **24** was protonated back by HCl to give the pure complex **23**. The tetranuclear Ru complex **25** was synthesized by the complexation of the neutral complex **24** with two equivalents of $Ru(bpy)_2Cl_2$.

The formation of the tetra-Ru complex **25** was confirmed by MALDI-TOF analysis (Figure 5.5) and the satisfactory elemental analysis. The mass spectrum clearly shows the parent ion complex minus $1PF_6^-$, $2PF_6^-$, $3PF_6^-$, and $4PF_6^-$ fragments.

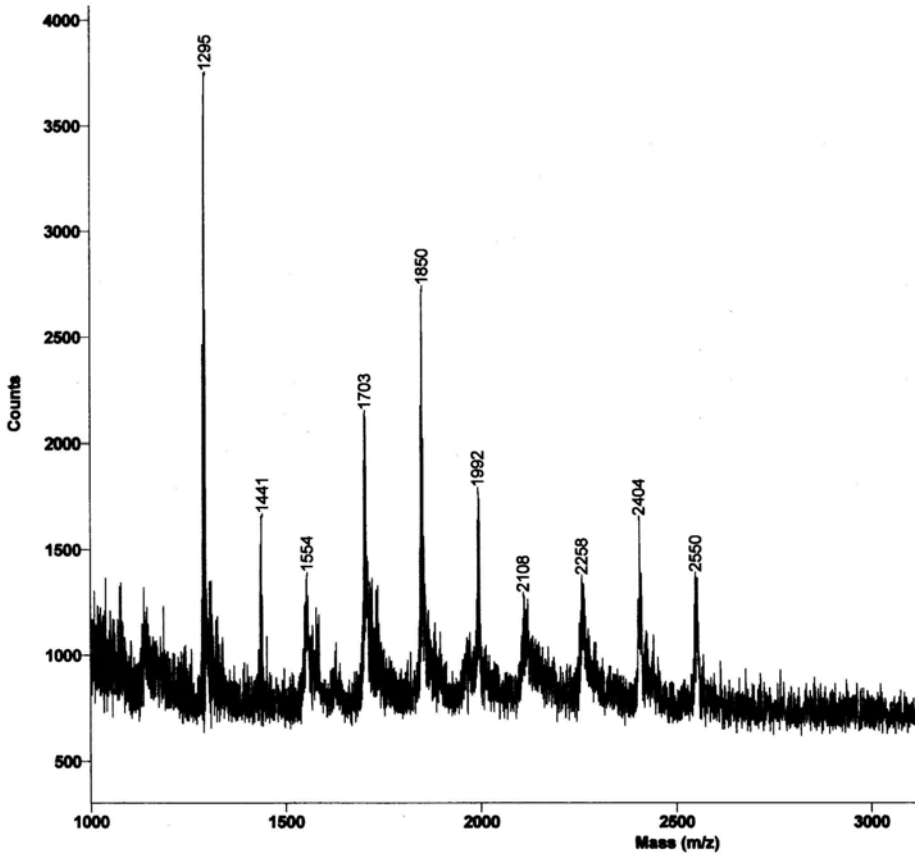

Figure 5.5 MALDI-TOF Spectra of $[(Ru(bpy)_2)_4(bis(BiBzIm))](PF_6)_4$ (**25**)
2550 $[M - 1PF_6]^+$, 2404 $[M - 2PF_6]^+$,
2258 $[M - 3PF_6]^+$, 2108 $[M - 4PF_6]^+$.

*5.2.2 UV–vis Properties of $[(Ru(bpy)_2)_2(bis(BiBzImH_2))]Cl_4$ (**23**), $[(Ru(bpy)_2)_2(bis(BiBzIm))]$ (**24**) and $[(Ru(bpy)_2)_4(bis(BiBzIm))](PF_6)_4$ (**25**)*

The spectroscopic properties of the complexes **23**–**25** are shown in Figure 5.6 and 5.7. For $[(Ru(bpy)_2)_2(bis(BiBzImH_2))](PF_6)_4$ (**23**), the extended conjugation of the bibenzimidazole ligand resulted in the appearance of a bis($BiBzImH_2$) π–π* band at 367 nm. The lowest energy MLCT transition remains at 464 nm. Compared to the mononuclear complex $[Ru(bpy)_2(BiBzImH_2)]](PF_6)_2$ (**20**), the lowest energy MLCT transition remains nearly constant, while the extinction coefficient doubles upon the

complexation of two $Ru(bpy)_2$ components. After the deprotonation, the lowest energy MLCT band of the neutral $[(Ru(bpy)_2)_2(Bis(BiBzIm))]$ (**24**) red shifts to 543 nm. The lowest energy MLCT band is still the $d\pi$–π^* (bpy) in nature. This is identical to the deprotonated mono-Ru complex **21**.

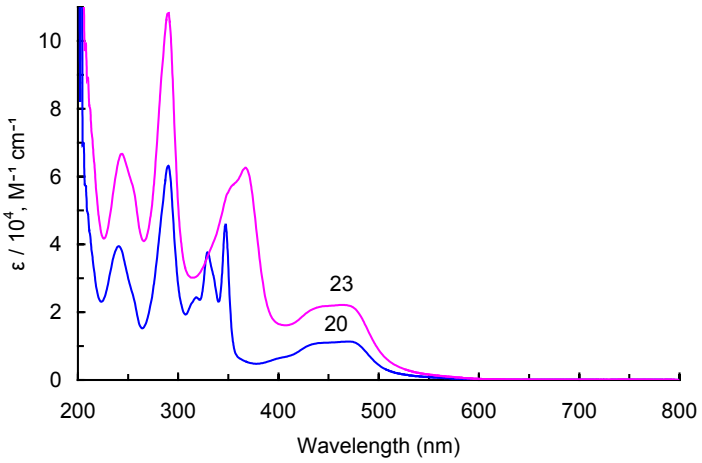

Figure 5.6 UV–vis Spectra of $[(Ru(bpy)_2)_2(bis(BiBzImH_2))]Cl_4$ (**23**) and $[Ru(bpy)_2(BiBzImH_2)]Cl_2$ (**20**) in CH_3CN

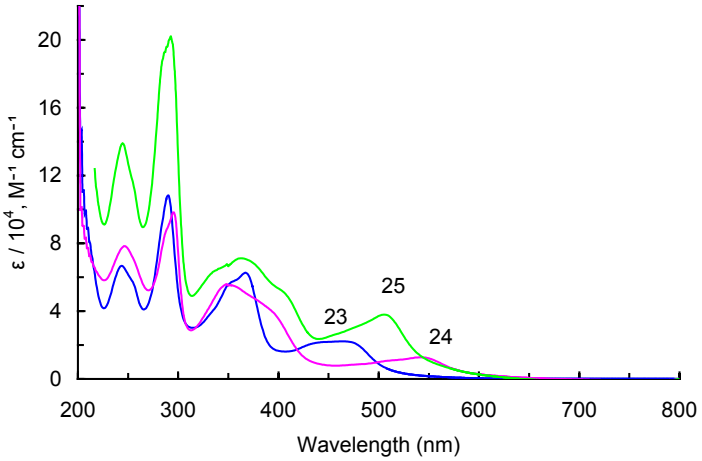

Figure 5.7 UV–vis Spectra of $[(Ru(bpy)_2)_2(bis(BiBzImH_2))]Cl_4$ (**23**), $[(Ru(bpy)_2)_2(bis(BiBzIm))]$ (**24**), and $[(Ru(bpy)_2)_4(bis(BiBzIm))](PF_6)_4$ (**25**) in CH_3CN

For the tetranuclear complex $[(Ru(bpy)_2)_4(bis(BiBzIm))](PF_6)_4$ (**25**), the band at 363 nm was broader than the 367-nm band of dinuclear complex **23**. This region consists of bis(BiBzIm) based π–π* transition overlapped with the multiple MLCT bands. The broadening of the band is probably due to the presence of the multinuclear effect. The lowest energy MLCT absorption is at the same position as the MLCT of the dinuclear complex **22** (506 nm). The extension of the bridging ligand from the monomer (**5**) to the dimer of bibenzimidazole (**14**) does not change the position of the lowest energy MLCT transition, which is still $d\pi$–π* (bpy) in nature.

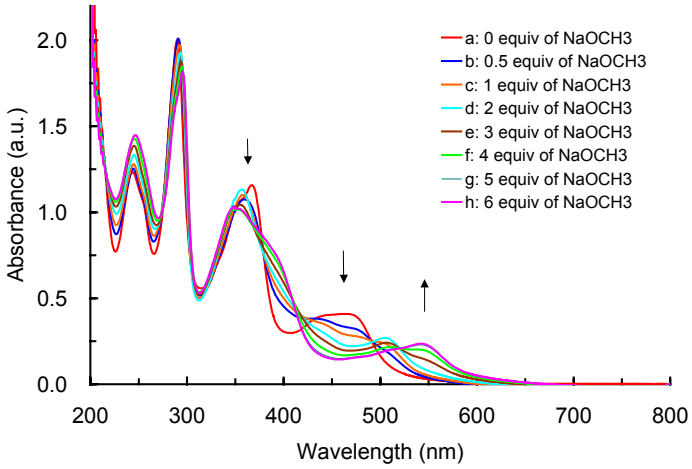

Figure 5.8 UV–vis Spectra of Stepwise Deprotonation of $[(Ru(bpy)_2)_2(bis(BiBzImH_2))]Cl_4$ (**23**) in CH_3CN by Adding $NaOCH_3/CH_3OH$ Solution

5.2.3 Proton-Induced Tuning of the Chemical Properties

The stepwise deprotonation of $[(Ru(bpy)_2)_2(bis(BiBzImH_2))]Cl_4$ (**23**) in CH_3CN by $NaOCH_3/CH_3OH$ is shown in Figure 5.8. There are four dissociable protons in this

complex. During the deprotonation process, the intensity at 440 nm and 464 nm decreases, and the lowest energy MLCT transition progressively shifts to the lower energy. After the addition of the 1st and the 2nd equivalents of $NaOCH_3$, the lowest energy MLCT transition red-shifts to 500 nm and 506 nm, respectively. The addition of the 3rd equivalent of $NaOCH_3$ makes the lowest energy MLCT transition red shifted to 512 nm, with the peak at 543 nm growing up. After the addition of the 4th equivalent of $NaOCH_3$, the peak at 543 nm grows up to be the major peak. In total, six equivalents of $NaOCH_3$ was added to ensure the fully deprotonation of the complex. This is similar to the stepwise deprotonation of the mono-Ru complex $[Ru(bpy)_2(BiBzImH_2)]](PF_6)_2$ (**20**) shown in Figure 5.2. The isosbestic points are at 491 nm and 520 nm, which indicate that the dinuclear Ru complex **23** in solution undergoes two successive deprotonations to exist as an equilibrium mixture with the monocation and neutral species. This result also indicates that the interaction between the two Ru centers is weak, which is consistent with the electrochemistry results.

*5.2.4 Electrochemical Properties of $[(Ru(bpy)_2)_2(bis(BiBzImH_2))]Cl_4$ (**23**), $[(Ru(bpy)_2)_2(bis(BiBzIm))]$ (**24**) and $[(Ru(bpy)_2)_4(bis(BiBzIm))](PF_6)_4$ (**25**)*

5.2.4.1 Oxidation Processes

The cyclic voltammogram of the dinuclear Ru complex **23** (Figure 5.9) shows the oxidation potential at +1.09 V. No difference is observed in the oxidation between the dinuclear complex **23** and the mononuclear complex **20**, which indicates that the electronic communication between the two Ru centers along the conjugated ligand bis(2,2′-bibenzimidazole) (**14**) is weak.

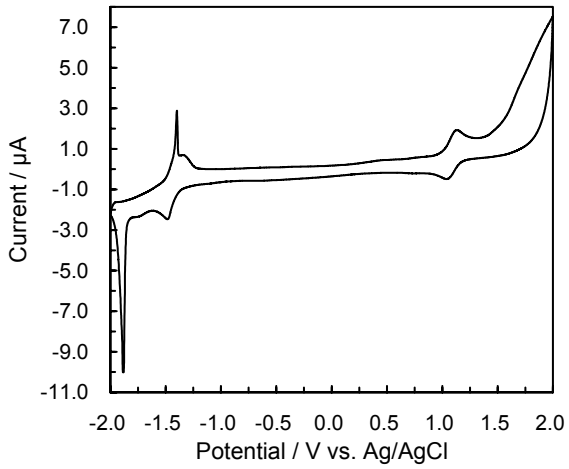

Figure 5.9 Cyclic Voltammogram of $[(Ru(bpy)_2)_2(bis(BiBzImH_2))](PF_6)_4$ (**23**) in 0.10 M Bu_4NPF_6/CH_3CN Solution at a Scan Rate of 50 mv/s
The concentration of the Ru complex is around 2.11×10^{-4} M.

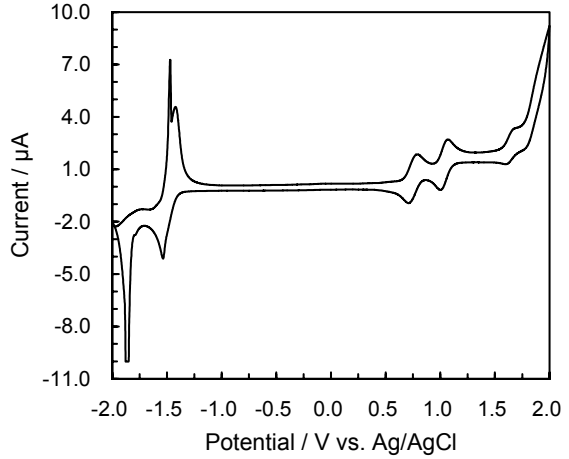

Figure 5.10 Cyclic Voltammogram of $[(Ru(bpy)_2)_4(bis(BiBzIm))](PF_6)_4$ (**25**) in 0.10 M Bu_4NPF_6/CH_3CN Solution at a Scan Rate of 50 mv/s
The concentration of the Ru complex is around 2.11×10^{-4} M.

The cyclic voltammogram (CV) of the tetranuclear Ru complex (**25**) is shown in Figure 5.9. It exhibits two oxidation waves at +0.75 V and +1.04 V. They are close to the oxidation potentials +0.77 V and +1.06 V of the dinuclear complex **22**. The

separations between the anodic and cathodic peak potentials ΔE_p are 81 mv and 72 mv, respectively; the ratios of the oxidation to the reduction peak heights are 1.0 V, which indicate that the oxidation processes are quasireversible. Four one-electron steps are involved in these two oxidation processes. The electronic interaction between the Ru metals along the conjugated bis(2,2′-bibenzimidazole) (**14**) is weak.

It has been shown that the first oxidation potential of the dinuclear Ru complex **22** was 0.3 V lower than those of the mononuclear complex **20**, which indicates that the BiBzIm bridging ligand in the dinuclear complex **22** has an electron donor property. The oxidation potentials of the tetranuclear complex **25** has the same oxidation behavior as the dinuclear complex **22** does, which suggests that the dimer of BiBzIm (**14**) also has an electron donor property. The Ru-Ru electrostatic interactions across the bridging ligand bis(BiBzIm) is similar to the Ru-Ru interaction in the dinuclear complex **22**.

5.2.4.2 Reduction Processes

The dinuclear complex **23** exhibits the reduction potentials at −1.41 V and −1.64 V. The tetranuclear complex **25** exhibits the reduction potentials at −1.47 V and −1.64 V. The sharp spikes might be due to the adsorption on the electrode. They may be the bpy ligand-based processes according to the previous results. The ΔE_p spacings (140 mV and 484 mV) and the increased currents suggest that more than one single electron transfer step occurs at each wave. This is reasonable given the presence of more than one $Ru(bpy)_2^{2+}$ unit.

Scheme 5.4 Synthesis of Octa-Ru Complex **26**

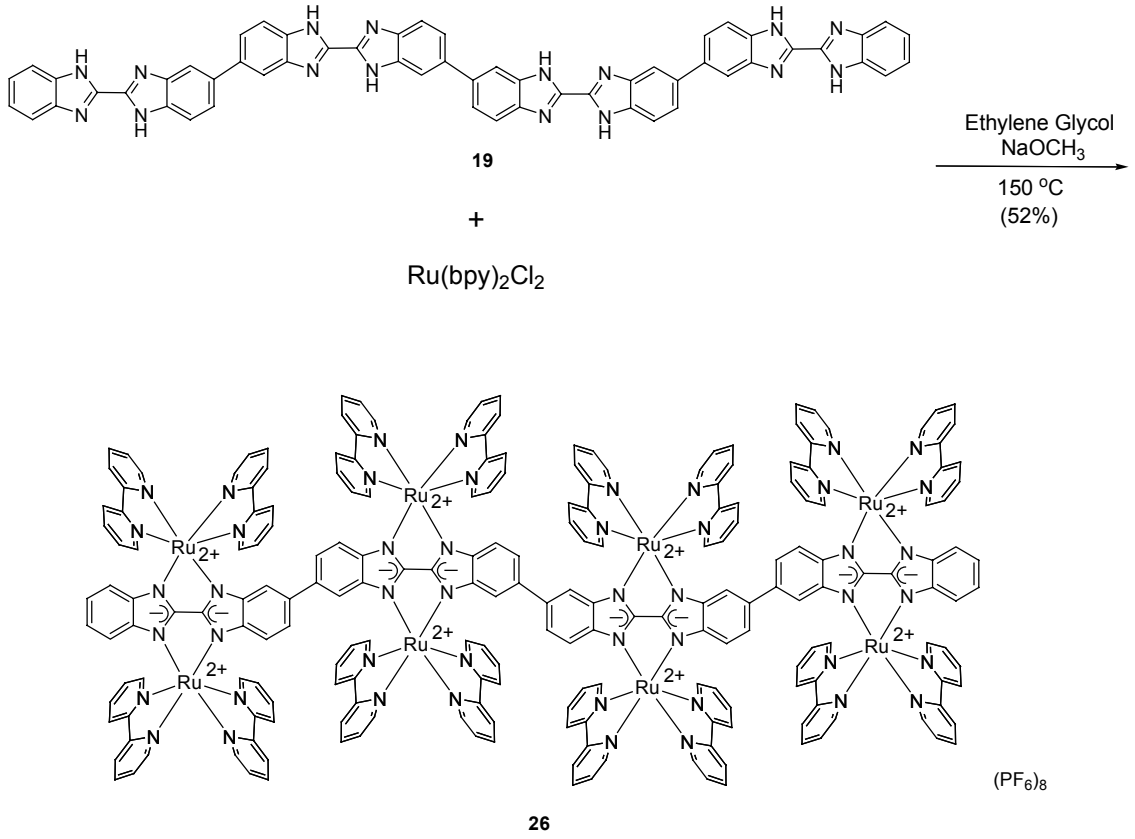

5.3 Tetra(bibenzimidazole)-Based Octa-Ru Complex $[(Ru(bpy)_2)_8(tetra(BiBzIm))](PF_6)_8$ (26)

*5.3.1 Synthesis of Octa-Ru Complex $[(Ru(bpy)_2)_8(tetra(BiBzIm))](PF_6)_8$ (**26**)*

The octa-Ru complex **26** was prepared in one pot as shown in Scheme 5.4. The tetramer of bibenzimidazole ligand **19** becomes acidic after being complexed with $Ru(bpy)_2Cl_2$, and tends to be partially deprotonated in the reaction media, providing a mixture of protonated and partially deprotonated species. To ensure that the tetramer bridging ligand is fully complexed with eight $Ru(bpy)_2Cl_2$, $NaOCH_3$ was added to fully

deprotonate the complex. Therefore, all the bidentate chelating sites on the tetramer bridging ligand were complexed with eight Ru metals.

The formation of the octa-Ru complex **26** was confirmed by the MALDI-TOF analysis (Figure 5.11). The spectra clearly shows the parent ion complex minus $1PF_6^-$, $2PF_6^-$, … , $7PF_6^-$, and $8PF_6^-$ fragments.

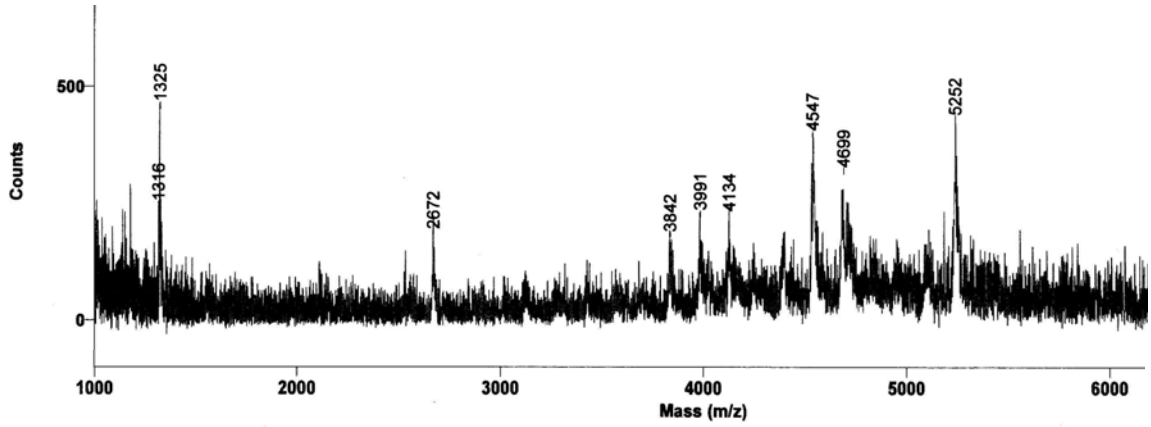

Figure 5.11 MALDI-TOF Spectra of $[(Ru(bpy)_2)_8(tetra(BiBzIm))](PF_6)_8$ (**26**)
5252 $[M - 1PF_6]^+$, 4699 $[M - 5PF_6]^+$, 4547 $[M - 6PF_6]^+$,
4375 $[M - 7PF_6]^+$, 4230 $[M - 8PF_6]^+$.

*5.3.2 UV−vis Properties of Octa-Ru Complex $[(Ru(bpy)_2)_8(tetra(BiBzIm))](PF_6)_8$ (**26**)*

For the octa-Ru complex **26**, the UV−vis spectra (Figure 5.12) is very similar to the tetra-Ru complex **25**. The extinction coefficient doubled compared to that of the tetra-Ru complex **25**. The lowest energy MLCT transition remains at 506 nm ($\varepsilon = 65300$ $M^{-1}\cdot cm^{-1}$), which is $d\pi$–π^* (bpy) in nature. The π^* of the bpy is lower than π^* of the tetra-$BiBzImH_2$, therefore, the lowest energy MLCT transition is $d\pi$–π^* (bpy). The progressive lowering of the π^* orbitals of the bridging ligands from the dimer to the

tetramer of bibenzimidazole does not change the position of the lowest energy MLCT transition. This indicates that the extension of the conjugated chain length of the bridging ligands does not provide the pathway for the electronic communication between the metal centers.

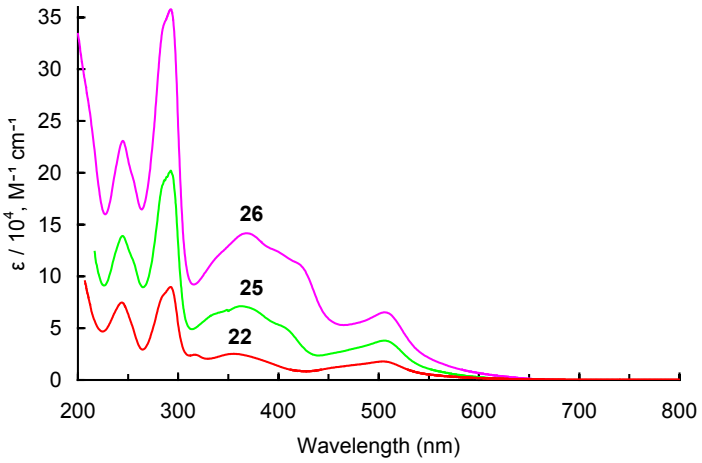

Figure 5.12 UV–vis Spectra of Bis-Ru Complex $[(Ru(bpy)_2)_2(BiBzIm)](PF_6)_2$ (**22**), Tetra-Ru Complex $[(Ru(bpy)_2)_4(bis(BiBzIm))](PF_6)_4$ (**25**), and Octa-Ru Complex $[(Ru(bpy)_2)_8(tetra(BiBzIm))](PF_6)_8$ (**26**) in CH_3CN

*5.3.3 Electrochemical Properties of Octa-Ru Complex $[(Ru(bpy)_2)_8(tetra(BiBzIm))](PF_6)_8$ (**26**)*

The cyclic voltammogram (CV) of the octa-nuclear Ru complex (**26**) is shown in Figure 5.13. It exhibits two oxidation waves at +0.71 V and +1.00 V. They are close to the two oxidation potentials +0.77 V and +1.06 V of the dinuclear complex **22**. The Ru complex **26** based on the tetramer of bibenzimidazoles **19** still undergoes the bpy-based reduction at –1.51 and –1.72 V. The Ru-Ru electrostatic interactions across the bridging ligand tetra(BiBzIm) is similar to the Ru-Ru interactions in the dinuclear and

tetranuclear complexes **22** and **25**. However, interactions along the tetramer of bibenzimidazole ligand are relatively weak.

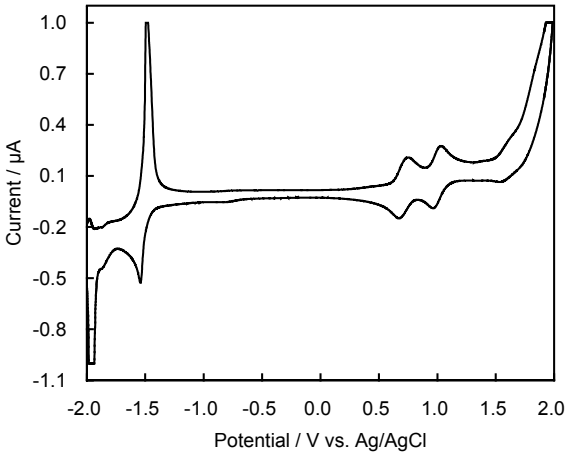

Figure 5.13 Cyclic Voltammogram of Octa-Ru Complex $[(Ru(bpy)_2)_8(tetra(BiBzIm))](PF_6)_8$ (**26**) in 0.10 M Bu_4NPF_6/CH_3CN Solution at a Scan Rate of 50 mv/s
The concentration of the Ru complex is around 2.11×10^{-4} M.

5.4 Conclusions

A series of multinuclear Ru complexes containing di-, tetra-, and octa-Ru^{II} centers based on the oligomeric bibenzimidazoles were synthesized and characterized. The species with high nuclearity exhibit extended one-dimensional structures. They show very intense ligand-centered (LC) absorptions (ε up to 3.6×10^5 $M^{-1}\cdot cm^{-1}$) and moderately intense metal-to-ligand charge transfer bands in the visible region (ε up to 6.6×10^4 $M^{-1}\cdot cm^{-1}$). The interactions between the Ru metal centers across the bidentate bibenzimidazole ligands, and along the oligomeric bibenzimidazole ligands are relatively weak, which is not expected.

CHAPTER 6

EXPERIMENTAL DETAILS

6.1 General

6.1.1 Reagents and Materials

All reagents were used without further purification. $RuCl_3 \cdot xH_2O$ (99.9%) was purchased from Alfa. 2,2′-Bipyridine (99%+) and ammonium hexafluorophosphate (95+%) were purchased from Aldrich. Acetonitrile was distilled over CaH_2 before use. Nylon membranes filter paper (pore size: 0.2 μm or 0.45 μm) for the filtration of the Ru complexes was purchased from Cole-Parmer Instrument Co.

6.1.2 Measurements

^1H NMR (500 MHz) and ^{13}C NMR (125 MHz) spectra were obtained on a JEOL Eclipse+ 500 MHz spectrometer. Chemical shifts (δ values) were given in parts per million with tetramethylsilane as an internal standard. UV−vis spectra were obtained using a Varian Cary 500 UV−vis−NIR spectrophotometer. Elemental analysis was performed by Quantitative Technologies Inc. (QTI) (Whitehouse, NJ). Mass analysis was performed by Scripps Research Institute (La Jolla, CA). ESI-MS spectra were obtained on a Waters−Micromass LCT mass spectrometer. MALDI-TOF spectra were obtained on Applied Biosystems Voyager−STR Mass spectrometer. Cyclic

Voltammogram experiments were performed at 20 °C using a PC-controlled potentiostat (CH Instruments, electroanalytical analyzer). The working electrode was a 1.5 mm glassy carbon electrode and the auxiliary electrode was a platinum wire. The reference electrode was a no leak Ag/AgCl reference electrode. They were purchased from Cypress Systems, Inc. (Lawrence, KS).

6.2 Synthesis

The synthesis of $Ru(bpy)_2Cl_2 \cdot 2H_2O$,[64,65] $[Ru(bpy)_2(BiBzImH_2)](PF_6)_2$, $[Ru(bpy)_2(BiBzIm)]$, and $[(Ru(bpy)_2)_2(BiBzIm)](PF_6)_2$ followed previously published procedures.[16,20]

$[(Ru(bpy)_2)_2(bis(BiBzImH_2))](PF_6)_4 \cdot H_2O$ (23). Bis($BiBzImH_2$) (**14**) (0.30 g, 0.64 mmol) was suspended in 80 mL of ethylene glycol. The mixture was degassed for 30 min under nitrogen, then heated at 120 °C for 3 h to dissolve bis($BiBzImH_2$). $Ru(bpy)_2Cl_2 \cdot 2H_2O$ (0.74 g, 1.42 mmol) was added to the above suspension, and heated at 150 °C for 16 h under nitrogen. The resulting deep brownish red solution was cooled, diluted with water, and filtered to remove the insoluble part. Then a saturated aqueous solution of NH_4PF_6 was added dropwise to precipitate the crude complex. The crude complex was directly used in the next deprotonation step without further purification. The pure product was obtained by protonation of the pure deprotonated complex **24** using HCl (6M), then reprecipitation with NH_4PF_6. MALDI-TOF (*m/z*): 1291 $[(M - 4HPF_6) + H]^+$. Anal. Calcd for $C_{68}H_{50}F_{24}N_{16}P_4Ru_2 \cdot H_2O$: C, 43.18; H, 2.77; N, 11.85. Found: C, 43.12; H, 2.70; N, 11.68.

[(Ru(bpy)$_2$)$_2$(bis(BiBzIm))] (24). The crude [(Ru(bpy)$_2$)$_2$-(bis(BiBzImH$_2$))](PF$_6$)$_4$ (**23**) (0.44 g, 0.23 mmol) was added to 50 mL of methanol and the suspension was degassed for 20 min under nitrogen. $NaOCH_3$ (0.20 g, 3.76 mmol) was added to the above mixture. The color of the solution turned from deep brownish red to purple. The solution was refluxed for 5 h under nitrogen and then cooled. The solvent was condensed to a half volume by rotary evaporation. The solid product was collected by filtration and purified by washing with acetone. Yield: 89%. Anal. Calcd for $C_{68}H_{46}N_{16}Ru_2 \cdot 8H_2O$: C, 56.97; H, 4.36; N, 15.63. Found: C, 56.88; H, 3.67; N, 14.95.

[(Ru(bpy)$_2$)$_4$(bis(BiBzIm))](PF$_6$)$_4$·4H$_2$O (25). [(Ru(bpy)$_2$)$_2$(bis(BiBzIm))] (**24**) (0.15 g, 0.12 mmol) and Ru(bpy)$_2$Cl$_2$·2H$_2$O (0.13 g, 0.26 mmol) were suspended in 24 mL of ethanol/water (1:1 v/v). Then it was degassed for 30 min and then refluxed under nitrogen for 15 h. The resulting deep brownish red solution was cooled and filtered to remove the insoluble part it may have. Ethanol was removed by rotary evaporation. Then a saturated aqueous solution of NH_4PF_6 was added dropwise to precipitate the complex. Around 250 mg of the solid crude product was collected by filtration. Half of the crude product (125 mg) was dissolved in a minimum of acetonitrile, and chromatographed over a neutral alumina column (21 cm in length, 17 mm in diameter). The first deep red broad band was collected. The eluate was concentrated to around 25 mL by rotary evaporation, and then diethyl ether was added dropwise to precipitate the desired complex. Overall yield: 68%. MALDI-TOF (*m/z*): 2551 [M – 1PF$_6$]$^+$, 2406 [M

– $2PF_6]^+$, 2261 [M – $3PF_6]^+$, 2116 [M – $4PF_6]^+$. Anal. Calcd for $C_{108}H_{78}F_{24}N_{24}P_4Ru_4 \cdot 4H_2O$: C, 46.86; H, 3.13; N, 12.14. Found: C, 46.37; H, 2.70; N, 11.85.

[(Ru(bpy)$_2$)$_8$(tetra(BiBzIm))](PF$_6$)$_8$ (26). Tetra(bibenzimidazole) (**19**) (0.050 g, 0.0537 mmol) was suspended in 25 mL of ethylene glycol. The mixture was degassed for 30 min under nitrogen, then heated at 160 °C for 8 h to partially dissolve the tetra(BiBzImH_2) ligand. Then the temperature was decreased to 110–120 °C, and Ru(bpy)$_2$Cl$_2$·2H_2O (0.234 g, 0.451 mmol, 8.4 equiv) was added to the above mixture. The mixture was heated at 150 °C for 2 h, then $NaOCH_3$ (0.058 g, 1.074 mmol, 20 equiv) was added to facilitate the deprotonation of all the tetramer ligand. The reaction was kept at 150 °C for 15 h. The resulting deep red-brown solution was cooled, diluted with water, and filtered to remove the insoluble part. Then a saturated aqueous solution of NH_4PF_6 was added dropwise to the filtrated to precipitate the complex. The crude solid was collected by filtration. It was dissolved in a minimum of acetonitrile, and chromatographed over a neutral alumina column (21 cm in length, 17 mm in diameter). First, acetonitrile was used as the eluent. The first bright orange band was the excess $[Ru(bpy)_3]^{2+}$. Then a saturated acetonitrile solution of NH_4PF_6 was used to elute the deep-red broad band from the top of the column. The eluate was concentrated to around 25 mL by rotary evaporation and then ether was added dropwise to precipitate the desired complex. The product was vacuum-dried at 60 °C for 15 h. Yield: 52%.

MALDI-TOF (*m/z*): 5252 $[M - 1PF_6]^+$, 4699 $[M - 5PF_6]^+$, 4547 $[M - 6PF_6]^+$, 4375 $[M - 7PF_6]^+$, 4230 $[M - 8PF_6]^+$. Anal. Calcd for $C_{216}H_{154}N_{48}P_8F_{48}Ru_8$: C, 48.13; H, 2.88; N, 12.47. Found: C, 47.29; H, 2.72; N, 12.13.

PART III

STEREOSPECIFIC SYNTHESIS OF MULTINUCLEAR RU COMPLEXES

CHAPTER 7

INTRODUCTION

7.1 Stereochemical Issues of Polynuclear Ru Complexes

Polymetallic assemblies which contains d_6 transition metal centers (*e.g.* Ru^{II}, Os^{II}), particularly coordinated to polypyridyl ligands, have been of great interest because of their favorable photophysical and redox characteristics.[56] Controlling the stereochemistry at the component octahedral metal centers should be of considerable importance as the spatial relationship of the components influences the nature of intramolecular electron and energy transfer processes within the assemblies. The polynuclear metal complexes without the stereocontrol of each octahedral center have generally been isomeric mixtures, and characterization using NMR technique has been extremely difficult, because the NMR spectra of the oligomeric assemblies are different for each stereoisomer (other than enantiomers) and thus complicated. In addition, crystals appropriate for X-ray structural studies of such assemblies, which could usually provide valuable information of the metal complexes, are very difficult to obtain.[66] This is particularly true when bidentate ligands are involved. Since these bidentate ligands are important as they extend the three-dimensionality of resultant polynuclear species, the stereospecific synthesis of the metal complexes is required.

Our research is focused on the investigation of the photochemical and electrochemical properties of the polynuclear metal complexes based on the conjugated oligomeric bibenzimidazoles. The stereospecific synthesis of multinuclear ruthenium complexes using an enantiomerically pure chiral building block Λ-$[Ru(bpy)_2(py)_2][(-)O,O'$-dibenzoyl-L-tartrate] (**27a**) is described in this Part.

7.2 Stereoisomers of Octahedral Multinuclear Complexes

7.2.1 Enantiomers of Tris-bidentate Mononuclear Ru Complexes

The D_3 symmetric tris-bidentate octahedral complex such as $[Ru(BiBzImH_2)_3]^{2+}$, as shown in Figure 7.1, has a helical structure in which the three bibenzimidazole ligands lie along the threads of a screw. It has no symmetry plane because its two halves are not mirror images, but it does have a threefold symmetry axis, which passes through the Ru(II) ion and is nearly perpendicular to the plane of the figure. Like a hand, it is chiral and can exist in two nonidentical mirror-image forms—a "right-handed" enantiomer (designated as Δ) in which the three bibenzimidazole ligands screw would advance into the the page as you rotate it to the right (clockwise) about the threefold axis, and a "left-handed" enantiomer (designated as Λ) in which the bibenzimidazole ligands screw would advance into the page as you rotate it to the left (counterclockwise) about the threefold axis. The direction of the spiral is indicated in Figure 7.1 by the red arrows.

The enantiomers have identical properties except for their reactions with other chiral substances and their effect on plane-polarized light. They are labeled (+) or (–),

depending on the direction of rotation of the plane of polarization. A 50:50 mixture of the (+) and (–) isomers, called a racemic mixture, produces no net optical rotation because the rotations produced by the individual enantiomers exactly cancel.

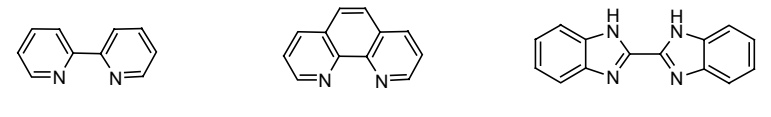

Chart 7.1

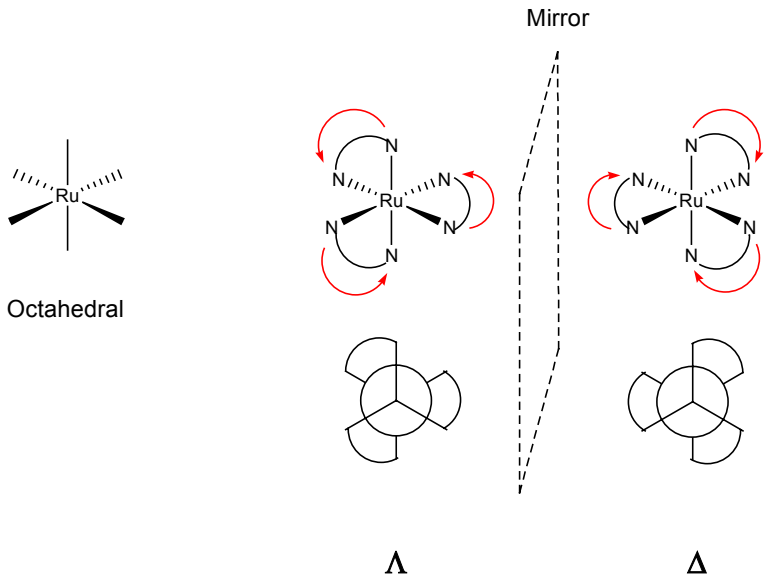

Figure 7.1 Enantiomers of D_3 Symmetric $[Ru(Bibenzimidazole)_3]^{2+}$

7.2.2 Stereoisomers of Dinuclear Ru Complexes

Ligand-bridged dinuclear Ru species represent the simplest examples of the multinuclear assemblies (Figure 7.2). The individual metal centers are tris(bidentate) in

nature, each may inherently possess right- or left-handed chirality (Δ and Λ respectively). In principle, a dinuclear species may therefore exist in two diastereoisomeric forms—ΔΔ/ΛΛ (a pair of enantiomers) or ΔΛ/ΛΔ (meso) where the bridge is relatively rigid. The stereoisomerism has a profound effect on shape and on the electronic interactions within the molecule.[66]

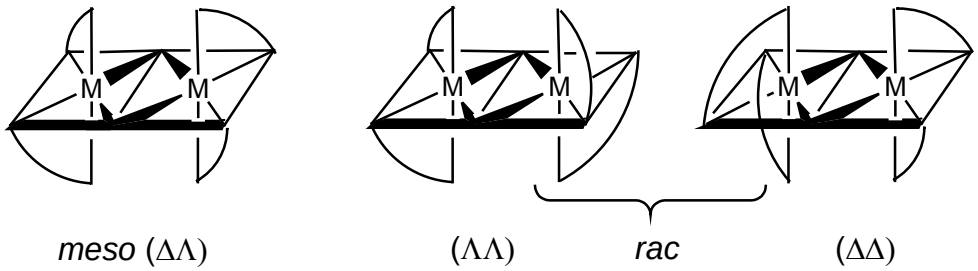

Figure 7.2 Stereoisomeric Forms of $[(Ru(pp)_2)_2(\mu\text{-BL})]^{n+}$

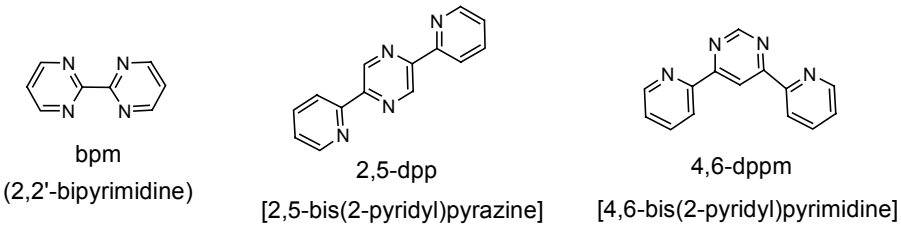

Chart 7.2

The most fundamental example of the dinuclear species is $[(Ru(pp)_2)_2(\mu\text{-BL})]^{n+}$ [where pp is a symmetrical bidentate ligand (C_{2v} point group symmetry) such as bpy, and BL is a symmetrical (C_{2v}) bridging ligand such as 2,2′-bipyrimidine (bpm) (Chart 7.2). In this case there are two diastereoisomers [*meso* (point group symmetry C_{2h}) and

racemic (point group symmetry D_2)], with the latter comprising two enantiomeric forms (ΔΔ/ΛΛ) (Figure 7.2).

Polynuclear and multifunctional species that are built from racemic unit yield up to 2^N isomers (where N is the number of chiral units involved), depending on the overall symmetry of the species, if a racemic starting material is used. If artificial, self-assembling structures are envisaged with a large number of centers, the number of isomers may therefore soon become very large.[67]

7.3 Stereospecific Synthesis of Multinuclear Ru Complexes

There are limited examples of complexes in the above categories where individual stereoisomers have actually been separated. Hua and von Zelewsky established the convenient resolution of *rac*-$[Ru(phen)_2(py)_2]^{2+}$ and *rac*-$[Ru(bpy)_2(py)_2]^{2+}$ by conventional diastereoisomer formation using the chiral arsenyl-(+)-tartrate and *O*,*O*′-dibenzoyltartrate anions, respectively.[67-71] This resolution method yields excellent chiral building blocks since the Δ- or Λ-$[Ru(phen)_2(py)_2]^{2+}$ or $[Ru(bpy)_2(py)_2]^{2+}$ undergo stereoretentive substitution of the two monodentate pyridine ligands. These chiral precursors were used to synthesize the dinuclear species$[(Ru(pp)_2)_2(\mu\text{-BL})]^{4+}$ [pp = bpy or phen; BL = bridging ligands 2,2′-bipyrimidine (bpm), 2,5-bis(2-pyridyl)pyrazine (2,5-dpp), or 4,6-bis(2-pyridyl)pyrimidine (4,6-dppm)] with predetermined stereochemistry (i.e. ΔΔ/ΛΛ or ΔΛ). The methodology has also been used for analogous dinuclear complexes involving the bridging ligands 2,3-

bis(2-pyridyl)-pyrazine (2,3-dpp) and its fused analogue pyrazino[2,3-*f*]-[4,7]phenanthroline (ppz).[72]

Keene and coworkers established the use of chiral $[Ru(pp)_2(CO)_2]^{2+}$ as a precursor for the synthesis of individual stereoisomers of the dinuclear complex $[(Ru(phen)_2)(Ru(Me_4bpy)_2)(\mu\text{-bpm})]^{4+}$,[73] and the use of cation exchange chromatographic methods to separate the diastereoisomers of the dinuclear species.[74,75] von Zelewsky and co-workers have reported the use of ligands ("chiragens") which impose a particular stereochemistry on the monomer precursors ("stereospecificity").[76,77] A number of studies have been reported utilizing condensation reactions of chiral monomers containing the 1,10-phenanthroline-5,6-dione ligand, e.g. $[Ru(phen)_2(1,10\text{-phenanthroline-5,6-dione})]^{2+}$,[78] as the precursor to form bridged complexes of predetermined stereochemistry.[79-81] Tor and coworkers have reported the use of the Hua and von Zelewsky precursor Δ/Λ-$[Ru(phen)_2(py)_2]^{2+}$ to produce the $\Lambda\Lambda\Lambda$ and $\Delta\Lambda\Delta$ diastereoisomers of alkyne-bridged trinuclear species.[82]

Given the high thermal stereochemical stability of the chiral building blocks developed by Hua and von Zelewsky, we applied this method for the synthesis of the homochiral multinuclear complexes of oligomeric bibenzimidazoles, using Λ-$[Ru(bpy)_2(py)_2]$[(−)*O*,*O′*-dibenzoyl-L-tartrate] (**27a**) as the enantiomerically pure chiral building block.

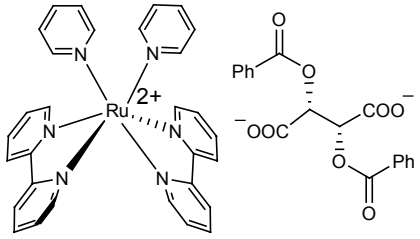

27a (Λ / *RR*)

Chart 7.3

Diastereomeric pure multinuclear complexes are usally characterized by the techniques such as NMR spectrometry, circular dichroism (CD) and mass spectrometry.

CHAPTER 8

RESULTS AND DISCUSSION

8.1 Enantiomerically Pure Chiral Building Block Λ-[Ru(bpy)$_2$(py)$_2$][(−)-*O*,*O*′-dibenzoyl-L-tartrate]·12H$_2$O (27a)

The resolution of *rac*-[Ru(bpy)$_2$(py)$_2$]$^{2+}$ (**27**) was achieved by the diastereoisomer formation with the chiral disodium [(−)-*O*,*O*′-dibenzoyl-L-tartrate] (**28**).[67,69-71] This resolution method yields excellent enantiomerically pure chiral building block Λ-[Ru(bpy)$_2$(py)$_2$][(−)-*O*,*O*′-dibenzoyl-L-tartrate]·12H$_2$O (**27a**). The two pyridine ligands in Λ-[Ru(bpy)$_2$(py)$_2$]$^{2+}$ can be easily substituted by other bidentate ligands under the complete retention of configuration.

8.1.1 Preparation of Chiral Building Block

The complex *cis*-[Ru(bpy)$_2$(py)$_2$]Cl$_2$ (**27**) (py = pyridine) was prepared from Ru(bpy)$_2$Cl$_2$·2H$_2$O with pyridine (**29**) as described previously.[83] The resolution of *cis*-[Ru(bpy)$_2$(py)$_2$]Cl$_2$ (py = pyridine) was achieved by the addition of an aqueous solution of disodium [(−)-*O*,*O*′-dibenzoyl-L-tartrate] (**28**) to an aqueous solution of *cis*-[Ru(bpy)$_2$(py)$_2$]Cl$_2$. Red crystals of Λ-[Ru(bpy)$_2$(py)$_2$][(−)-*O*,*O*′-dibenzoyl-L-tartrate]·12H$_2$O (**27a**) were obtained by the fractional recrystallization.[67,69,72]

Scheme 8.1 Preparation of the Ru Chiral Building Block

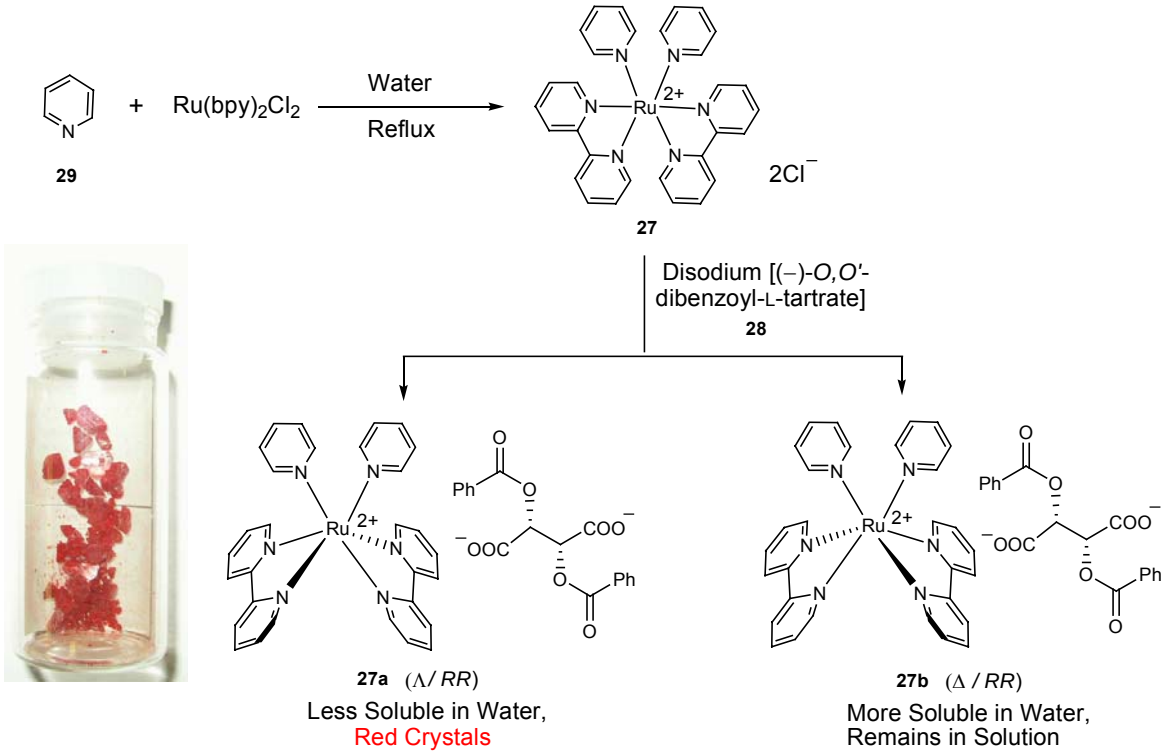

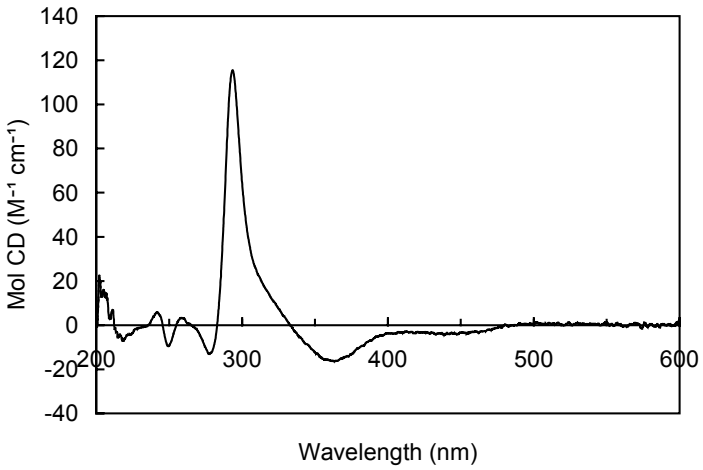

Figure 8.1 Circular Dichroism Spectra of Λ-$[Ru(bpy)_2(py)_2]Cl_2$ (**27c**) in Acetonitrile

8.1.2 Absolute Configuration of the Chiral Building Block

Assignment of the absolute configuration of the chiral building block Λ-[$Ru(bpy)_2(py)_2$][(−)-*O*,*O′*-dibenzoyl-L-tartrate]·$12H_2O$ (**27a**) and of the corresponding substituted products can be made by applying exciton theory;[84-86] i.e., in the regions of the long-axis-polarized transitions around 294 nm of the ligand bpy, the circular dichroism will appear strongly positive at lower energies and strongly negative at higher energies if the molecule has the absolute configuration related to (−)-$[Fe(phen)_3]^{2+}$ (Λ form). The circular dichroism (CD) spectra of the enantiomerically pure complexes exhibit typical excitonic interactions of the π–π* transitions[86] and the expected Cotton effects of the metal-to-ligand charge transfer bands in the visible region. Λ-[$Ru(bpy)_2(py)_2$][(−)-*O*,*O′*-dibenzoyl-L-tartrate]·$12H_2O$ (**27a**) was converted to the chloride salt Λ-$[Ru(bpy)_2(py)_2]Cl_2$ (**27c**), of which the CD spectra is shown in Figure 8.1. It is consistent with the Λ configuration.

8.1.3 Optical Purity of the Chiral Building Block

The determination of optical purity of the chiral building block is of basic importance. The retention or partial loss of optical purity in the course of a reaction often gives valuable information. Accurate knowledge of the optical purity is especially important in the area of polynuclear metal complex synthesis. Due to the multiplication effect, a relatively small amount of the other enantiomer will yield significant amount of isomerically mixed products, even if the reactions proceed with complete retention of configuration. For example, in the case of a dinuclear species, an 80%/20% mixture of a

chiral building block leads to 64% of the desired enantiomer, plus 4% of the other enantiomer, and 32% of the meso form.[67] Since we were interested in the use of the chiral building block for the synthesis of polynuclear ruthenium complexes, where the two pyridine ligands in general are replaced by the bidentate bibenzimidazole ligands, the determination of the optical purity of the obtained chiral building block is critical before it is used in the subsequent complexation.

A lower limit of the optical purity of the building blocks was determined by forming the diastereomers of $[Ru(bpy)_2(R,R\text{-dach})]^{2+}$ (**30**) through a substitution reaction with an optically active bidentate ligand (1*R*,2*R*)-(−)-1,2-diaminocyclohexane (**31**, *R*,*R*-dach) (Scheme 8.2).[67] The obtained diastereoisomers give different ^{1}H NMR chemical shifts (Figure 8.2). Spectrum (a) shows the ^{1}H NMR (aromatic region) of $[Ru(bpy)_2(R,R\text{-dach})]^{2+}$ (**30**) prepared from the racemic *cis*-$[Ru(bpy)_2(py)_2]^{2+}$ (**27**), clearly giving the signals of two diastereoisomers Λ-$[Ru(bpy)_2(R,R\text{-dach})]^{2+}$ (Λ/*RR*) and Δ-$[Ru(bpy)_2(R,R\text{-dach})]^{2+}$ (Δ/*RR*) in a 1:1 molar ratio. Since each diastereoisomer possesses a C_2 axis, the corresponding bpy protons in the complex are equivalent, giving a total of only eight nonequivalent protons. Spectrum (b) shows the ^{1}H NMR of Λ-$[Ru(bpy)_2(R,R\text{-dach})]^{2+}$ (Λ/*RR*) prepared from Λ-$[Ru(bpy)_2(py)_2]^{2+}$ (**27a**), clearly indicating the purity of the optically active chiral building block with the Λ/*RR* > 98% de.

Scheme 8.2 Synthesis of $[Ru(bpy)_2(R,R\text{-dach})]^{2+}$ and Λ-$[Ru(bpy)_2(R,R\text{-dach})]^{2+}$

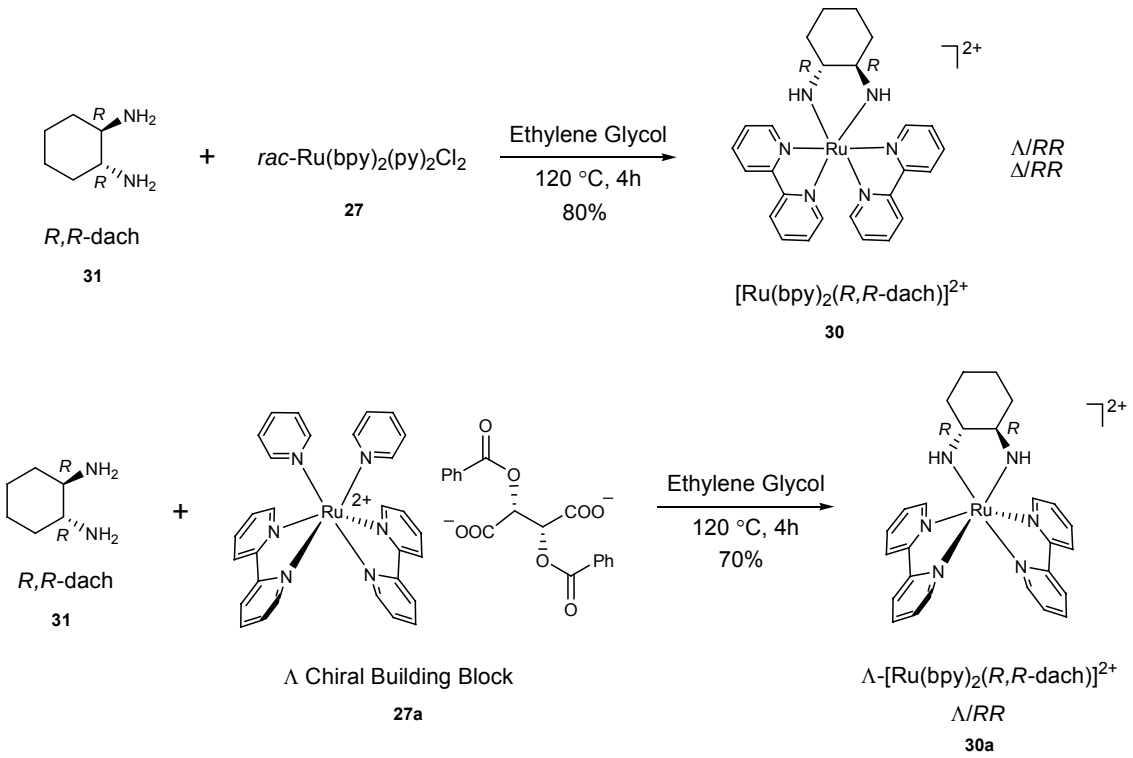

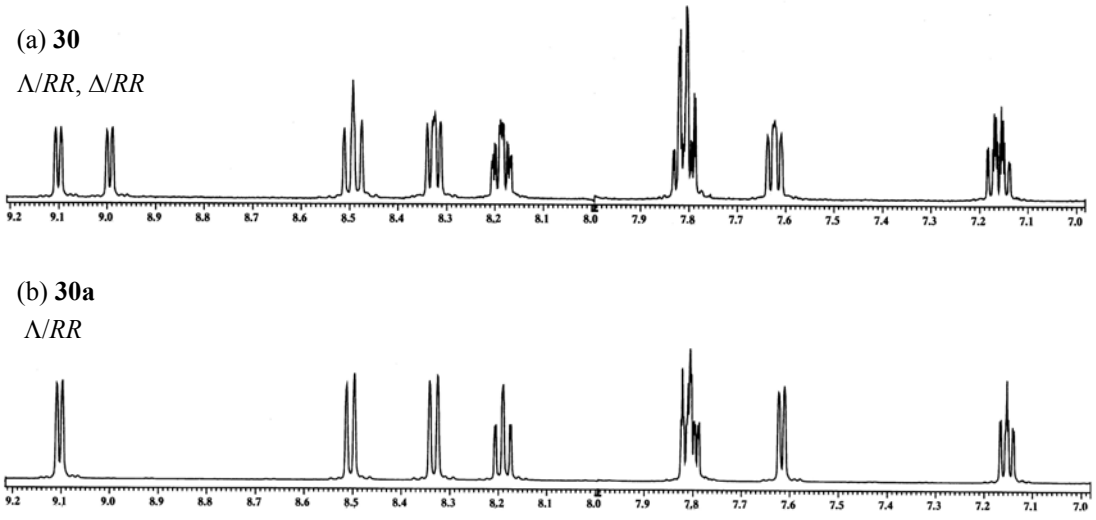

Figure 8.2 ^{1}H NMR Spectra (500 MHz) of (a) $[Ru(bpy)_2(R,R\text{-dach})](PF_6)_2$ (**30**) and (b) Λ-$[Ru(bpy)_2(R,R\text{-dach})](PF_6)_2$ (**30a**) in Acetonitrile-d_3

8.2 Synthesis of Diastereomerically Pure Ru Complexes Based on 2,2′-Bibenzimidazole

Mono- and di-nuclear Ru complexes represent the simplest examples of the polynuclear assemblies. The studies with the stereoselective synthesis of individual enantiomeric or diastereoisomeric forms, or the separation of these individual stereoisomeric forms from a mixture would provide useful information for the characterization of the higher nuclearity. Our study to probe the stereochemical control in the polynuclear assemblies of the oligomeric bibenzimidazoles started with the synthesis of the enantiomerically pure (ep) monomer Λ-**20** (Figure 8.3).

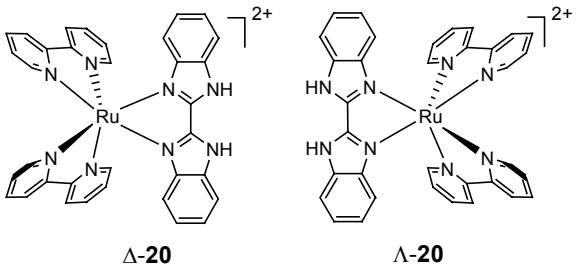

Figure 8.3 Enantiomers of $[Ru(bpy)_2(BiBzImH_2)](PF_6)_2$ (**20**)

*8.2.1 Synthesis of Λ-[Ru(bpy)$_2$(BiBzImH$_2$)](PF$_6$)$_2$ (Λ-**20**), Λ-[Ru(bpy)$_2$(BiBzIm)] (Λ-**21**) and ΛΛ-[Ru(bpy)$_2$(BiBzIm)Ru(bpy)$_2$](PF$_6$)$_2$ (ΛΛ-**22**)*

Λ-$[Ru(bpy)_2(py)_2]$[(−)-*O*,*O*′-dibenzoyl-L-tartrate]·$12H_2O$ (**27a**) was reacted with an excess of 2,2′-bibenzimidazole (**5**) in ethylene glycol at 120 °C. Interestingly, two complexes were obtained, which were proven to be the mono-deprotonated complex Λ-

20a and the bis-Ru complex ΛΛ-**22** (2.2 : 1), through the NMR spectroscopy and the further control experiment (Scheme 8.3 and Figure 8.4).

Scheme 8.3 Synthesis of Λ-$[Ru(bpy)_2(BiBzImH_2)](PF_6)_2$ (Λ-**20**)

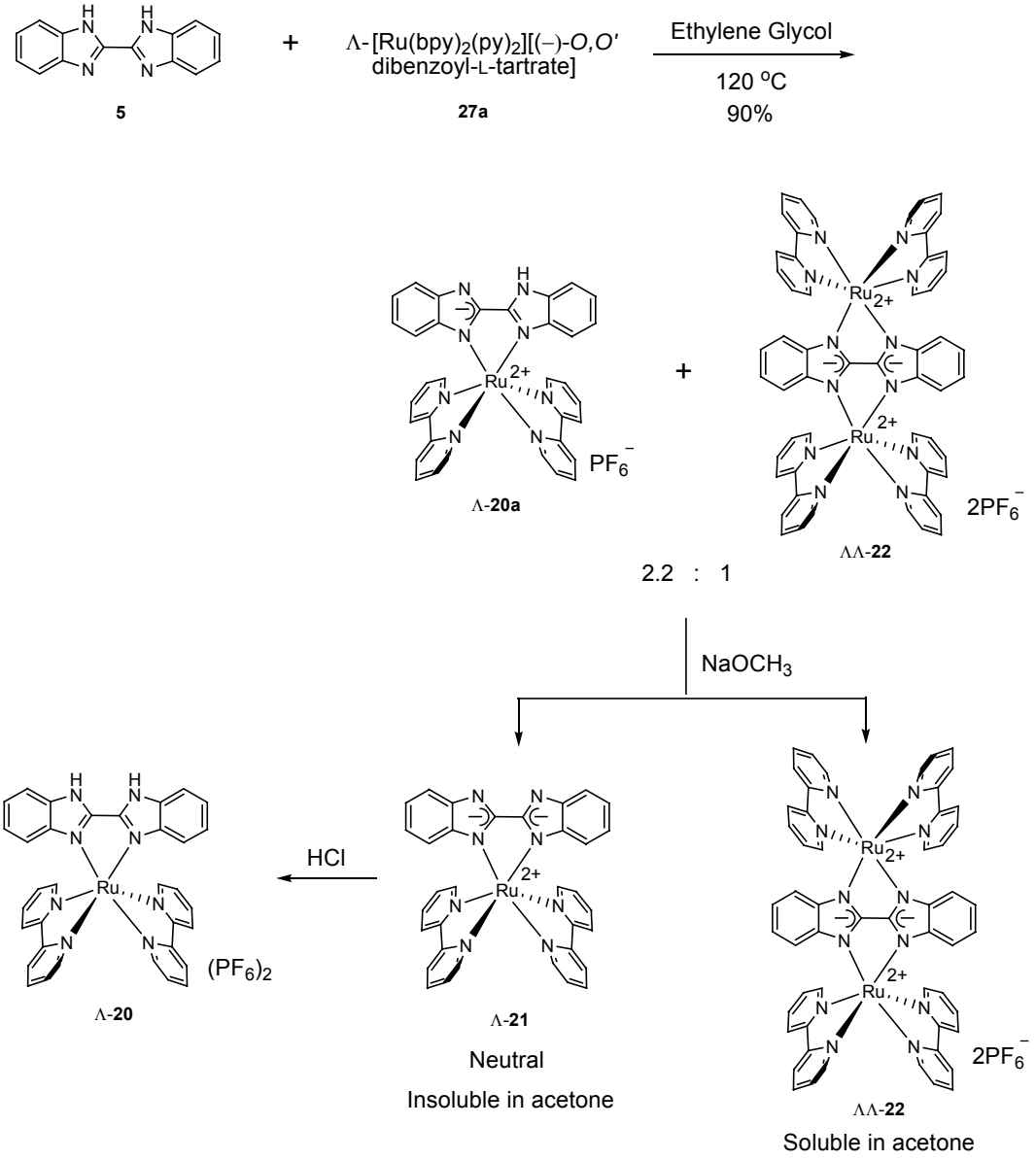

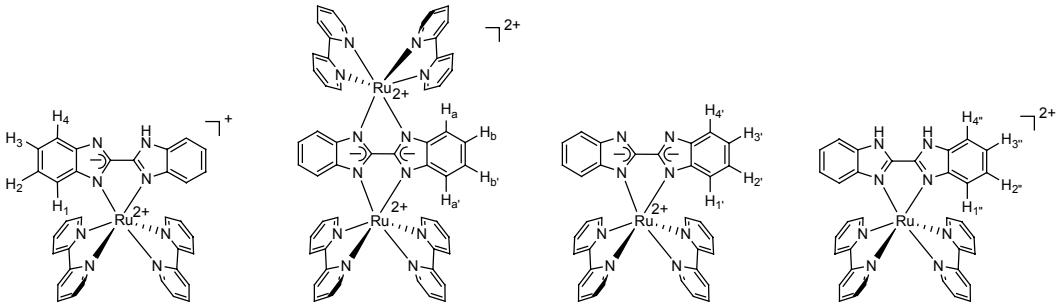

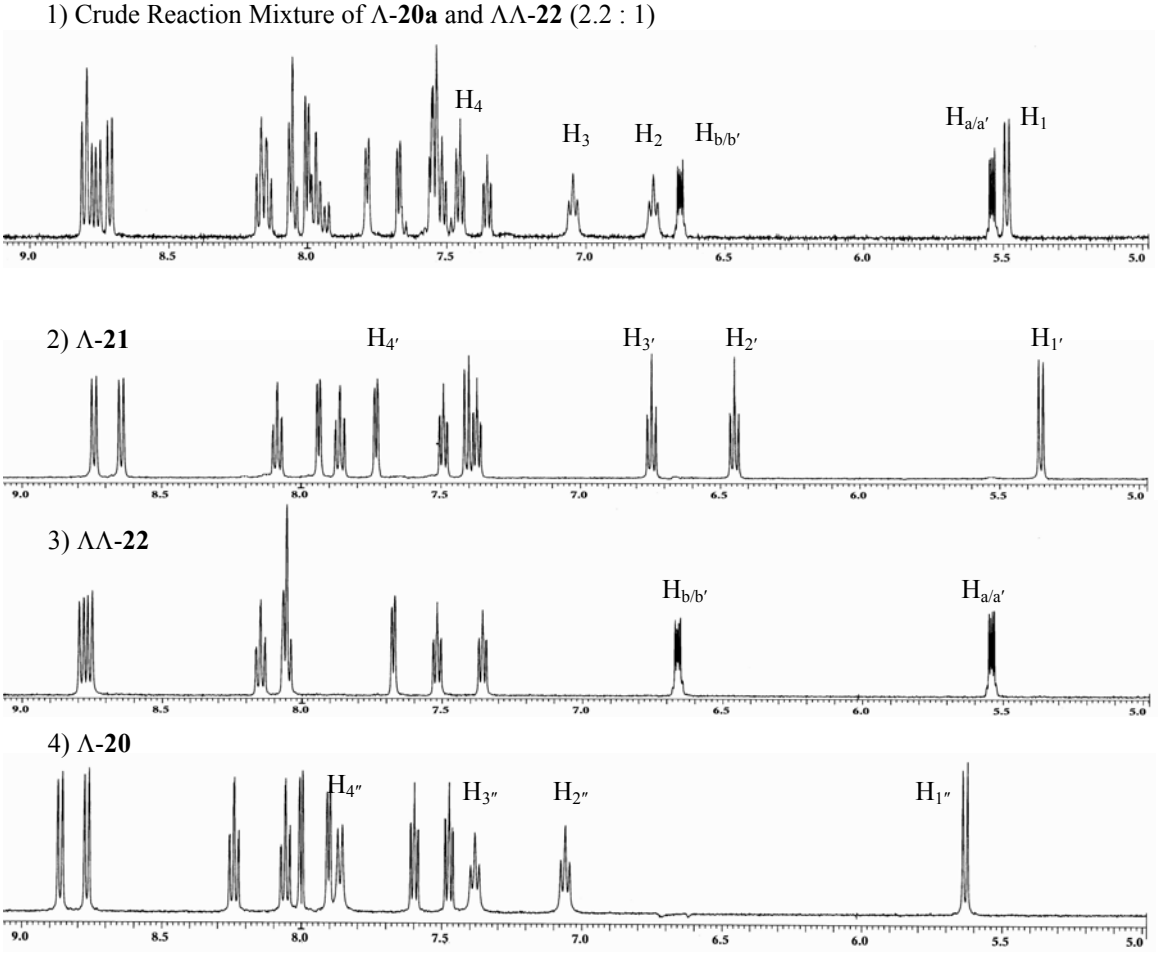

Figure 8.4 ^{1}H NMR Spectra of the Chiral Ru Complexes in Scheme 8.3
1) Crude product: Λ-**20a** and ΛΛ-**22** (2.2 : 1). 2) Λ-**21**, $H_{1'}$, $H_{2'}$, $H_{3'}$, $H_{4'}$ are upfield compared to H_1, H_2, H_3, H_4. 3) ΛΛ-**22**. $H_{a/a'}$, $H_{b/b'}$ remained unchanged after the base treatment. 4) Λ-**20**, $H_{1''}$, $H_{2''}$, $H_{3''}$, $H_{4''}$ are downfield compared to $H_{1'}$ $H_{2'}$, $H_{3'}$, $H_{4'}$.

The formation of Λ-**20a** is due to the deprotonation of Λ-**20** by pyridine released from the chiral building block **27a**. As being discussed in Chapter 5, the acidity of the bibenzimidazole ligand increases upon the coordination with the ruthenium ion, rendering the easy deprotonation of the complex Λ-**20**. The pK_a values of $[Ru(bpy)_2(BiBzImH_2)]^{2+}$ in 50% acetonitrile/water mixture have been reported: pK_{a1} and pK_{a2} are 5.74 ± 0.05 and 10.51 ± 0.05 at 25 °C, respectively.[17,20] The pKa of pyridinium ion is 5.25, which means that pyridine is basic enough to deprotonate the formed model complex Λ-**20**, rendering the formation of Λ-**20a** and the bis-Ru complex ΛΛ-**22**.

The mixture of the mono-deprotonated Λ-**20a** and the bis-Ru complex ΛΛ-**22** was separated by the treatment with $NaOCH_3$. Λ-**20a** was fully deprotonated to give the complex Λ-**21**, which was not soluble in acetone. The bis-Ru complex ΛΛ-**22** was stable, remaining unchanged under the basic condition, and its PF_6^- salt was soluble in acetone. Therefore, Λ-**21** was easily separated from ΛΛ-**22** by filtration. Then the pure deprotonated Λ-**21** was protonated by HCl to give the pure protonated model compound Λ-**20**. The structures of the products were proven by the NMR study (Figure 8.4). The protons $H_1/H_{1'}/H_{1''}$ and $H_a/H_{a'}$ are on the bibenzimidazole ligand, which are in the shielding zone of the benzene ring of the bpy, therefore they are strongly shielded (δ = 5–6 ppm). The structure of the bis-Ru complex ΛΛ-**22** was further confirmed by the experiment shown in the Scheme 8.4: the same bis-Ru complex was obtained by the

reaction of Λ-**21** with one equivalent of the chiral building block Λ-[Ru(bpy)$_2$(py)$_2$][(−)-*O*,*O*′-dibenzoyl-L-tartrate]·12H$_2$O (**27a**) (Scheme 8.4).

Scheme 8.4 Synthesis of ΛΛ-[Ru(bpy)$_2$(BiBzIm)Ru(bpy)$_2$](PF$_6$)$_2$ (ΛΛ-**22**)

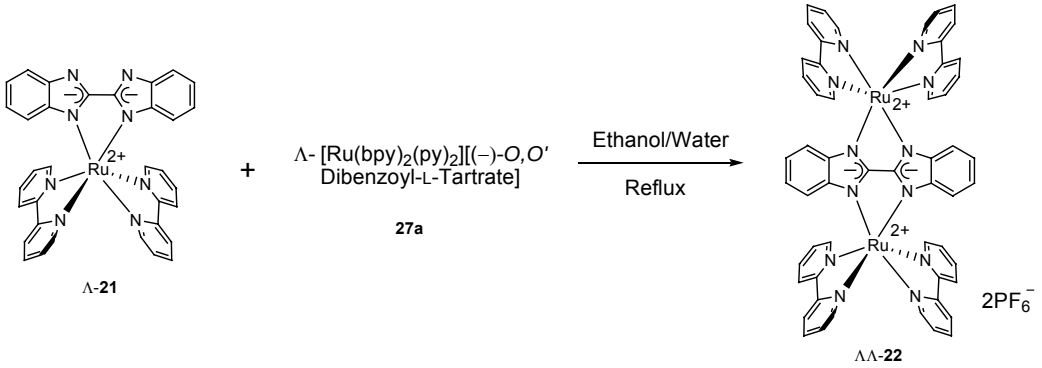

Scheme 8.5 Synthesis of Racemic [Ru(bpy)$_2$(BiBzImH$_2$)](PF$_6$)$_2$ (**20**)

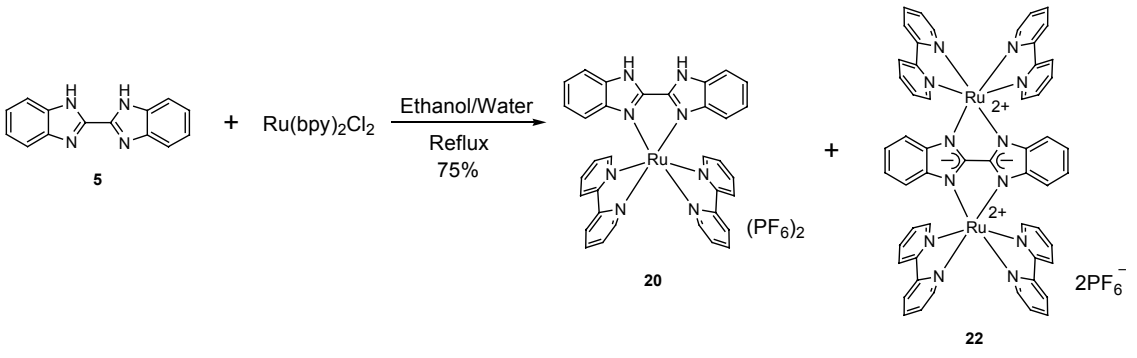

The single crystals of ΛΛ-[Ru(bpy)$_2$(BiBzIm)Ru(bpy)$_2$]Cl$_2$ (ΛΛ-**22**) were grown by the ether diffusion to the methanol solution of the complex ΛΛ-**22**. The crystals are of poor quality, crumbling easily and being extremely prone to solvent evaporation.

Although the refined structure was not completely solved, the preliminary X-ray crystal analysis showed the connectivity of the complex.

Compared with the stereospecific synthesis, the synthesis of the racemic mono-Ru complex **20** by complexing bibenzimidazole (**5**) with racemic $Ru(bpy)_2Cl_2$ gave the desired complex **20** without deprotonation, along with a small amount of the dinuclear complex **22** in a ratio of 19 : 1 (Scheme 8.5).

*8.2.2 Absolute Configuration of Λ-[Ru(bpy)$_2$(BiBzImH$_2$)](PF$_6$)$_2$ (Λ-**20**), Λ-[Ru(bpy)$_2$(BiBzIm)] (Λ-**21**) and ΛΛ-[Ru(bpy)$_2$(BiBzIm)Ru(bpy)$_2$]Cl$_2$ (ΛΛ-**22**)*

The circular dichroism (CD) spectra of Λ-$[Ru(bpy)_2(BiBzImH_2)](PF_6)_2$ (Λ-**20**), Λ-$[Ru(bpy)_2(BiBzIm)]$ (Λ-**21**) and ΛΛ-$[Ru(bpy)_2(BiBzIm)Ru(bpy)_2]Cl_2$ (ΛΛ-**22**) are shown in Figure 8.5 and 8.6. The Cotton effects are observed, which are in agreement with the expected Λ absolute configurations,[86] i.e., under the long-axis-polarized band around 294 nm, the circular dichroism is at low energies strongly positive, at higher energies negative, and positive at the lowest energy MLCT transition. Therefore the substitution of the pyridine ligands proceeds with the retention of configuration.

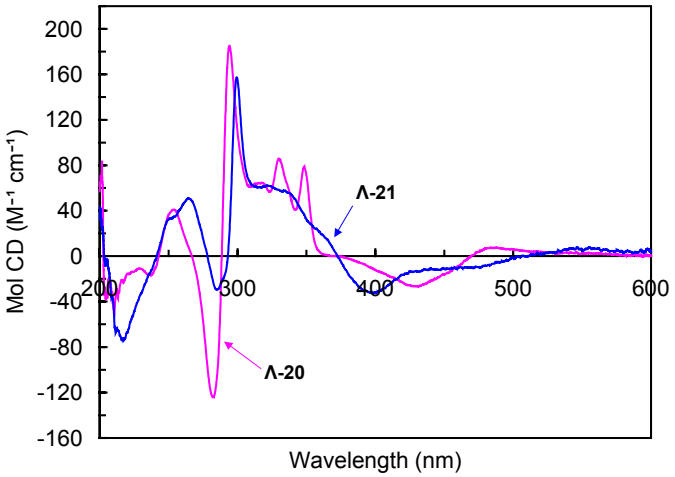

Figure 8.5 Circular Dichroism Spectra of Λ-[Ru(bpy)$_2$(BiBzImH$_2$)](PF$_6$)$_2$ (Λ-**20**) and Λ-[Ru(bpy)$_2$(BiBzIm)] (Λ-**21**) in Acetonitrile

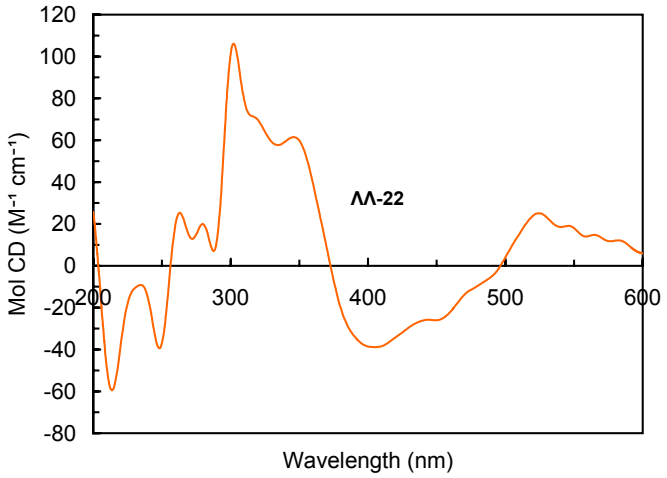

Figure 8.6 Circular Dichroism Spectra of ΛΛ-[Ru(bpy)$_2$(BiBzIm)$_2$Ru(bpy)$_2$]Cl$_2$ (ΛΛ-**22**) in Acetonitrile

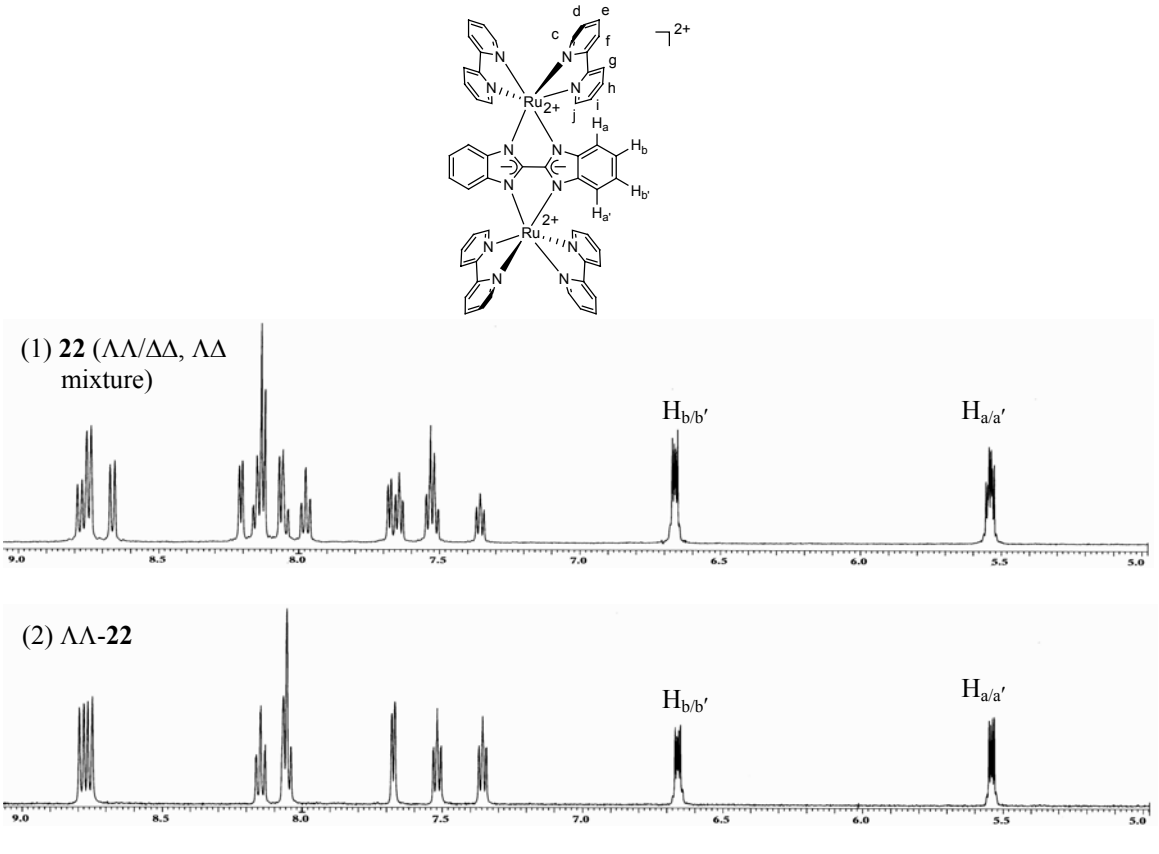

Figure 8.7 ^{1}H NMR Spectra of $[Ru(bpy)_2(BiBzIm)Ru(bpy)_2](PF_6)_2$
(1) **22** prepared from the racemic $Ru(bpy)_2Cl_2$. (2) ΛΛ-**22**.

*8.2.3 Optical Purity of ΛΛ-[Ru(bpy)$_2$(BiBzIm)Ru(bpy)$_2$](PF$_6$)$_2$ (ΛΛ-**22**)*

^{1}H NMR spectra of $[Ru(bpy)_2(BiBzIm)Ru(bpy)_2](PF_6)_2$ (**22**) prepared from the racemic $Ru(bpy)_2Cl_2$, and ΛΛ-**22** prepared from the chiral building block Λ-$[Ru(bpy)_2(py)_2]$[(−)-*O*,*O*′-dibenzoyl-L-tartrate]·$12H_2O$ (**27a**) are shown in Figure 8.7. With the use of the racemic $Ru(bpy)_2Cl_2$, the diastereoisomers (ΔΔ/ΛΛ and ΔΛ) were obtained (spectrum 1 in Figure 8.7). The relative abundance of the meso form and the enantiomeric pair is around 55 : 45, which is close to the statistical 50 : 50 value. The

D_2 symmetry of ΛΛ-[Ru(bpy)$_2$(BiBzIm)Ru(bpy)$_2$](PF$_6$)$_2$ (ΛΛ-**22**) requires the equivalence of the four bpy ligands. A total of 10 magnetically nonequivalent protons is therefore observed (spectrum 2 in Figure 8.7). $H_{a/a'}$ and $H_{b/b'}$ are the protons on the bibenzimidazole bridging ligand. $H_{a/a'}$ lie in the shielding zone of the adjacent bpy rings (δ = 5.5 ppm). The rest of eight protons (c–j) are on the bpy ligand. The ^{13}C NMR spectra of ΛΛ-[Ru(bpy)$_2$(BiBzIm)Ru(bpy)$_2$](PF$_6$)$_2$ gives 14 lines (10 lines from ligand bpy and 4 lines from BiBzIm). There is no sign of the formation of the other diastereoisomers compared with the spectrum 1 in Figure 8.7.

The use of a chiral building block almost entirely avoids the formation of the different isomers, with the ΛΛ > 98% de, which means that the complexation of the bibenzimidazole and the chiral building block is under the complete retention of configuration, without racemerization under the reaction condition. In the following complexations of the bibenzimidazole oligomers with the chiral building block under the similar reaction conditions, it is reasonable to believe that reactions will still proceed with the complete retention of configuration.

8.3 Synthesis and Properties of ΛΛ-[(Ru(bpy)$_2$)$_2$(bis(BiBzImH$_2$))](PF$_6$)$_4$ (ΛΛ-23)

As shown in Figure 8.8, there are two diastereoisomers in the bis-Ru complex ΛΛ-[(Ru(bpy)$_2$)$_2$(bis(BiBzImH$_2$))](PF$_6$)$_4$ (ΛΛ-**23**): ΛΛ/ΔΔ (racemic, a pair of enantiomers) and ΔΛ (meso). Due to the C_s symmetry of the dimer of bibenzimidazole (**14**), there is the possibility of forming the four regioisomers (Figure 8.9). This leads to

the complexity of the NMR spectra, rendering the difficulties in the purification and characterization.

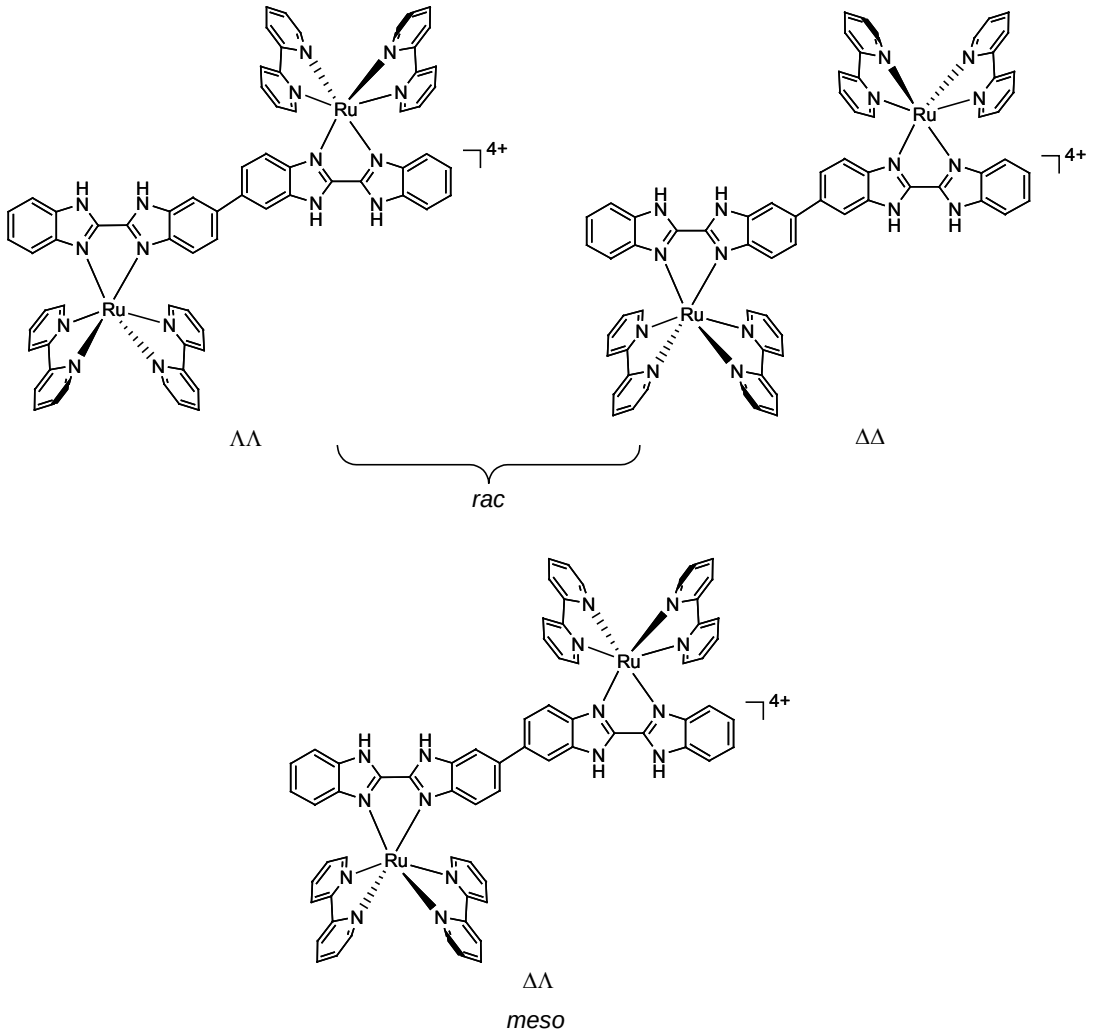

Figure 8.8 Diastereoisomers of $[(Ru(bpy)_2)_2(bis(BiBzImH_2))](PF_6)_4$ (**23**)
Two diastereisomers: *rac* (ΛΛ, ΔΔ) and *meso* (ΔΛ)

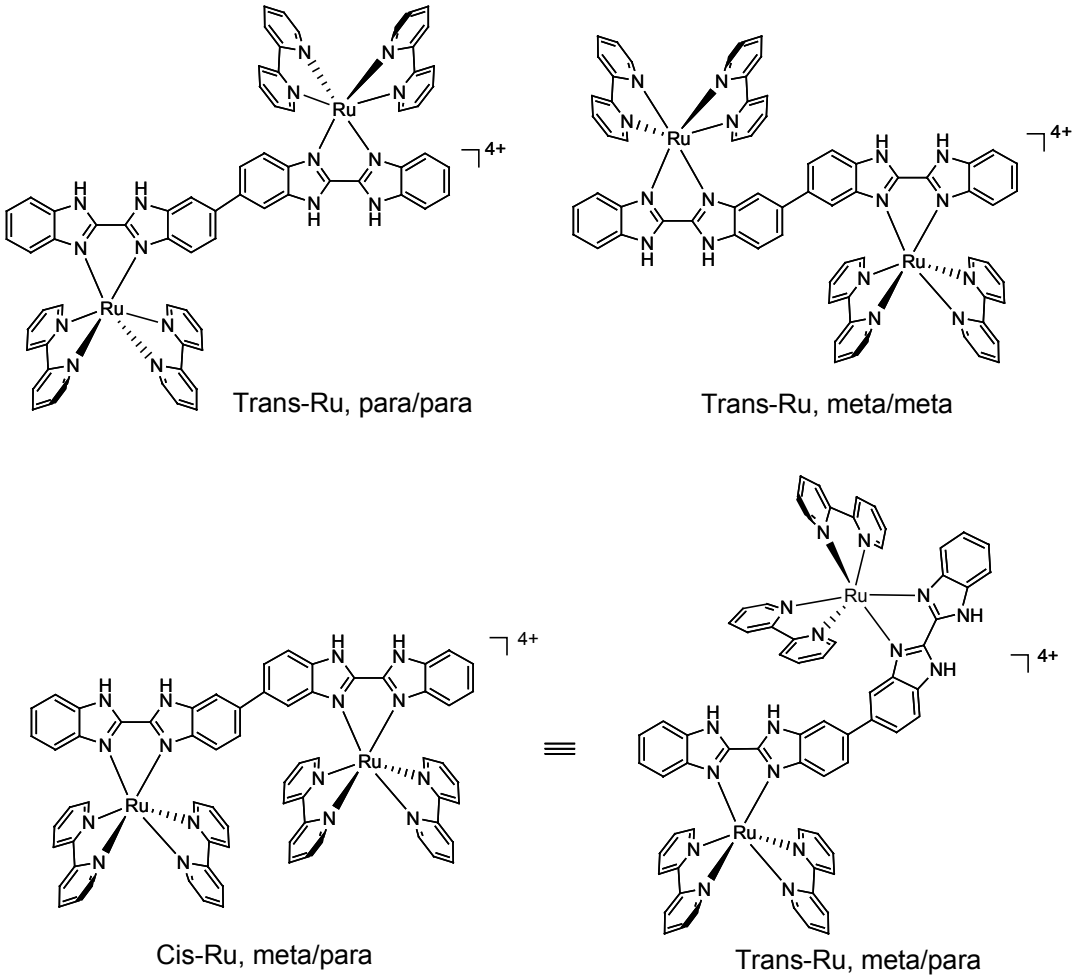

Figure 8.9 Regioisomers of ΛΛ-[(Ru(bpy)$_2$)$_2$(bis(BiBzImH$_2$))](PF$_6$)$_4$ (ΛΛ-**23**)
("Tran" means the two Ru(bpy)$_2$ are on the opposite side of C−C bond*.
"Cis" means the two Ru(bpy)$_2$ are on the same side of C−C bond.
"Para" means the Ru is connected to the nitrogen atom para to the C−C bond.
"Meta" means the Ru is connected to the nitrogen atom meta to the C−C bond.)
*C−C bond: the C−C bond between the two bibenzimidazole units.

Scheme 8.6 Synthesis of ΛΛ-[(Ru(bpy)$_2$)$_2$(bis(BiBzImH$_2$))](PF$_6$)$_4$ (ΛΛ-**23**)

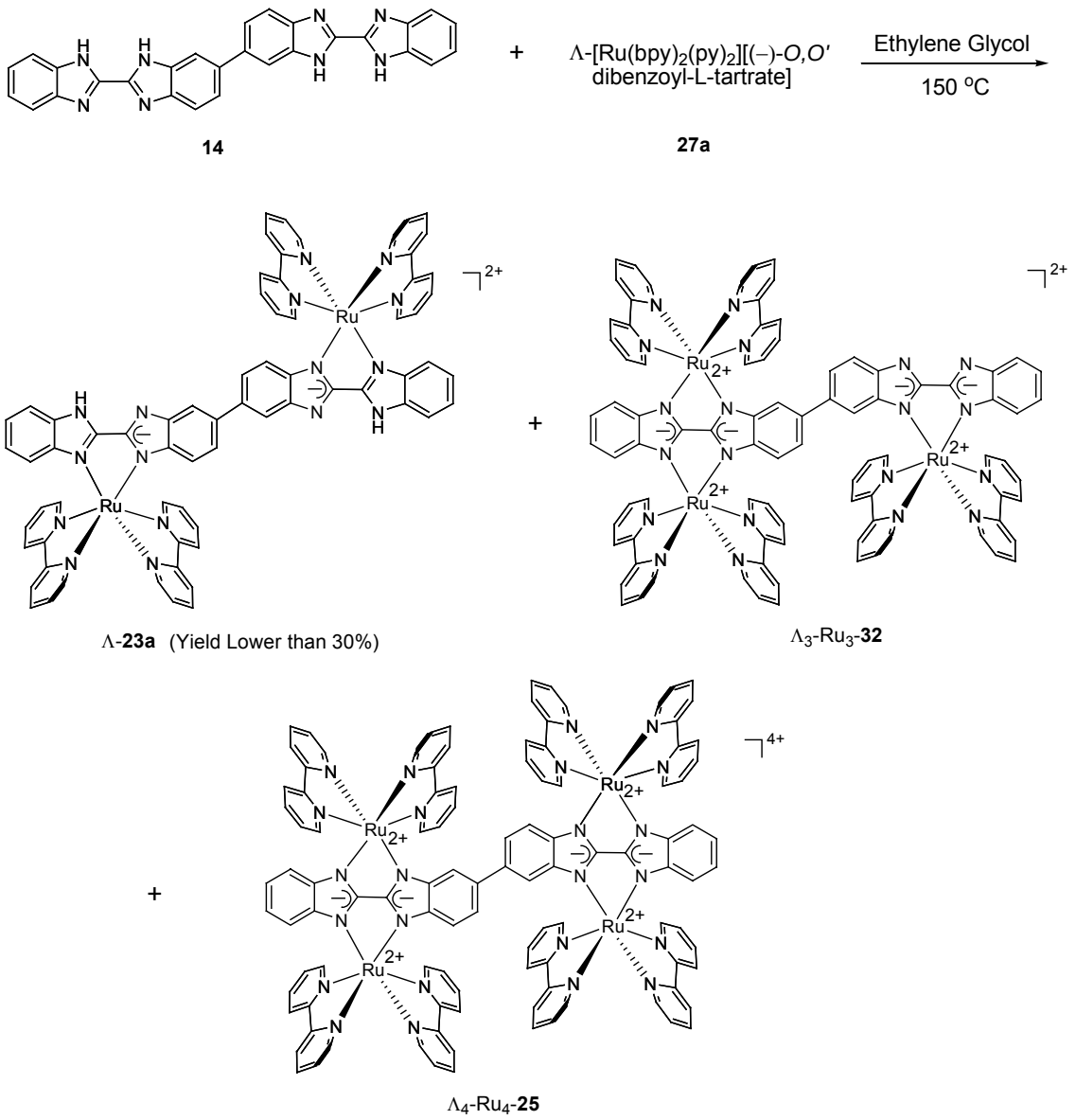

The stereospecific synthesis of the homochiral [(Ru(bpy)$_2$)$_2$(bis-(BiBzImH$_2$))](PF$_6$)$_4$ (ΛΛ-**23**) was attempted by the complexation of the dimer of bibenzimidazole (**14**) with the chiral building block (**27a**) following the same method

for the synthesis of Λ-**20**. However, the reaction provided a mixture with a very low yield of the possible product ΛΛ-**23** or its partially deprotonated form ΛΛ-**23a** (~30%). The possible reason for the formation of the complicated products is that the deprotonation by the pyridine released from the chiral building block during the reaction, and the over-complexation on both sides of the dimer of bibenzimidazole (**14**) to form the tris-Ru (Λ_3-Ru_3-**32**) or the tetra-Ru (Λ_4-Ru_4-**25**) complexes. No more studies were carried out to investigate the synthesis and structure of the stereoisomers of ΛΛ-**23** due to the above complexities.

8.4 Synthesis and Properties of Λ_4-[$(Ru(bpy)_2)_4$(bis(BiBzIm))]$(PF_6)_4$ (Λ_4-Ru_4-25)

To solve the above regioisomer and over-complexation issues, an easy way is to synthesize the homochiral tetra-Ru complex Λ_4-Ru_4-**25**. All the four bidentate sites of the dimer ligand **14** will be complexed by the Ru chiral building block **27a**, which excludes the formation of the regioisomers. Therefore, the homochiral tetra-Ru complex would be the major product in the reaction shown in Scheme 8.7, which simplifies the isolation and crystallization processes.

An excess of the chiral building block (i.e. 4.4 equiv) was added to ensure the fully complexation of the dimer **14**. The formation of the tetra-Ru complex Λ_4-Ru_4-**25** was confirmed by MALDI-TOF analysis (Figure 8.10) and the satisfactory elemental analysis. The mass spectrum clearly shows the parent ion complex minus $1PF_6^-$, $2PF_6^-$, $3PF_6^-$, and $4PF_6^-$ fragments.

Scheme 8.7 Synthesis of Λ_4-[(Ru(bpy)$_2$)$_4$(bis(BiBzIm))](PF$_6$)$_4$ (Λ_4-Ru$_4$-**25**)

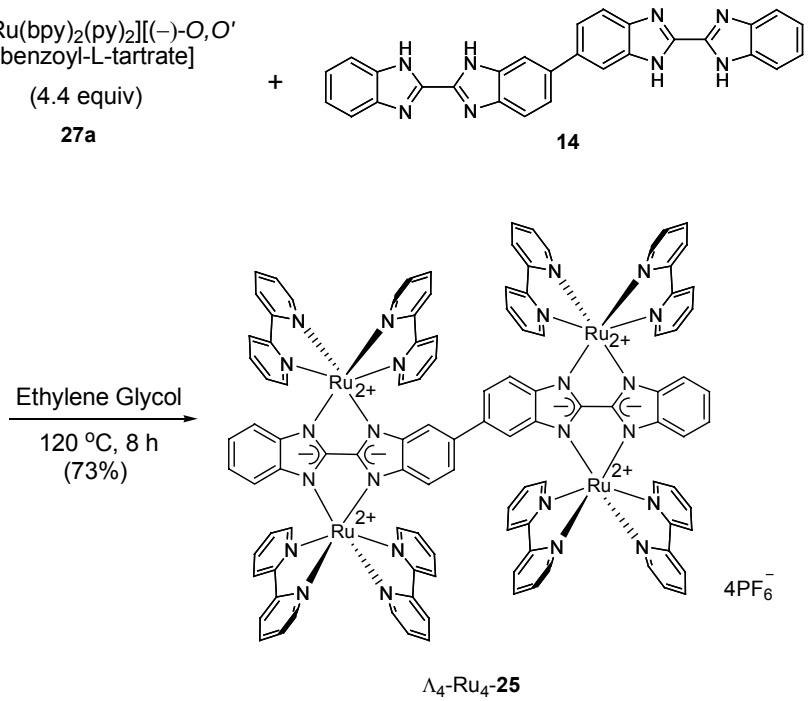

The single crystals of the PF_6^- salt of Λ_4-Ru$_4$-**25** were grown from the acetone/water mixture by the slow evaporation. The crystals are of poor quality, crumbling easily and being extremely prone to solvent evaporation. The refined structure was not completely solved. The preliminary X-ray crystal structure showed the connectivity of the complexes in Figure 8.11. The structure showed that the bridging ligand is close to be planar after being complexed with four Λ-$[Ru(bpy)_2]^{2+}$. The molecule has an estimate size of $2.1 \times 1.1 \times 1.0$ nm^3.

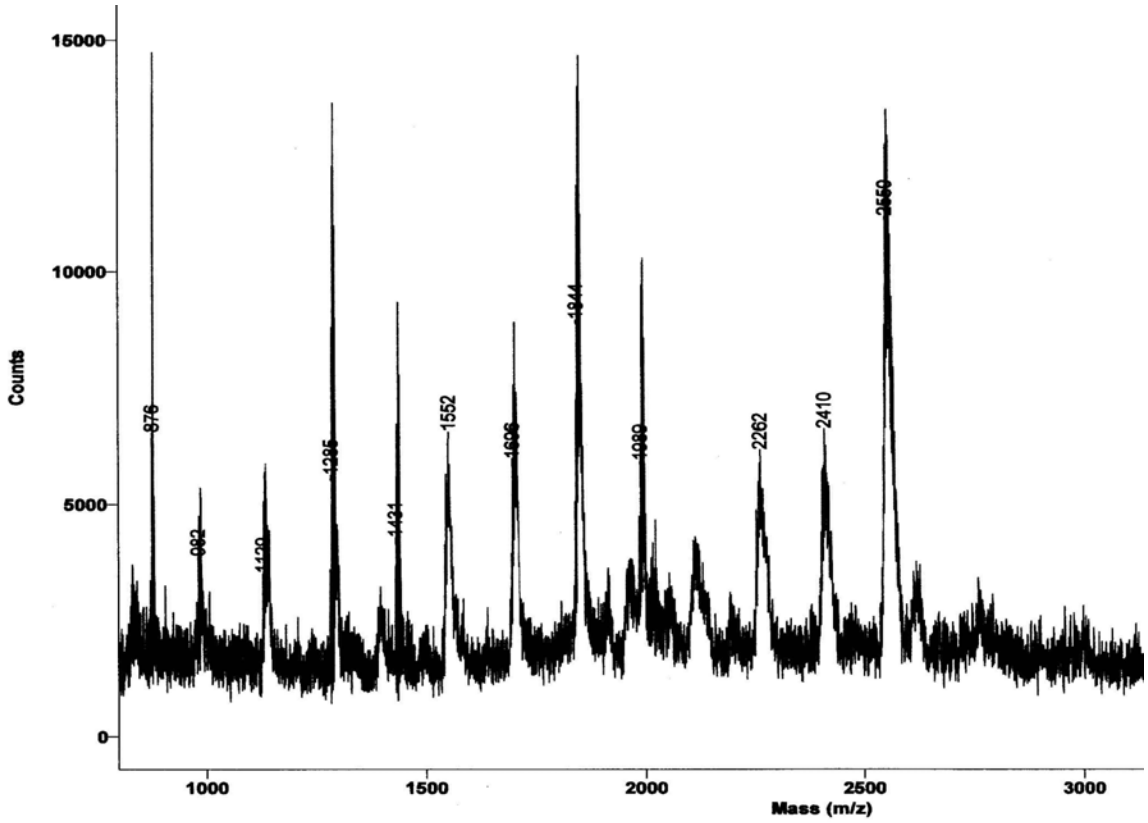

Figure 8.10 MALDI-TOF Spectra of Λ_4-[$(Ru(bpy)_2)_4$(bis(BiBzIm))]$(PF_6)_4$ (Λ_4-Ru_4-**25**)
2550 $[M - 1PF_6]^+$, 2410 $[M - 2PF_6]^+$,
2262 $[M - 3PF_6]^+$, 2116 $[M - 4PF_6]^+$.

(a)

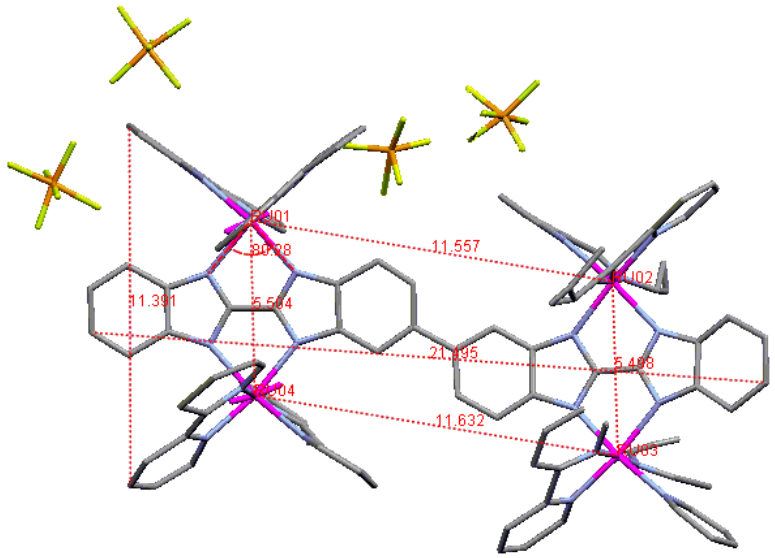

(b)

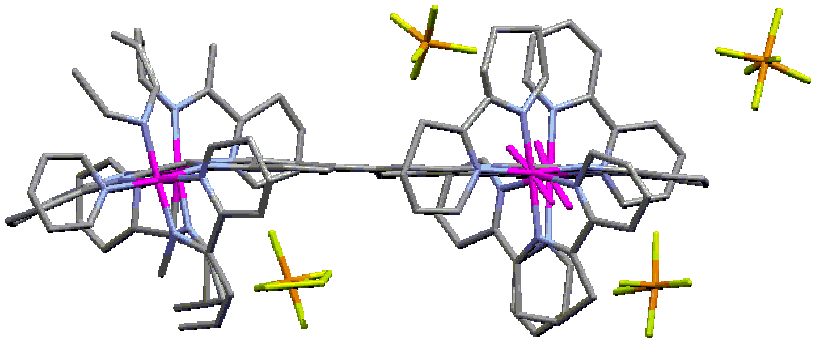

Figure 8.11 X-ray Crystal Structure of Λ_4-[$(Ru(bpy)_2)_4$(bis(BiBzIm))]$(PF_6)_4$ (Λ_4-Ru_4-**25**) (Incomplete refinement)
(a): A size of 2.1 × 1.1 × 1.0 nm^3
(b): The bridging ligand is close to be planar

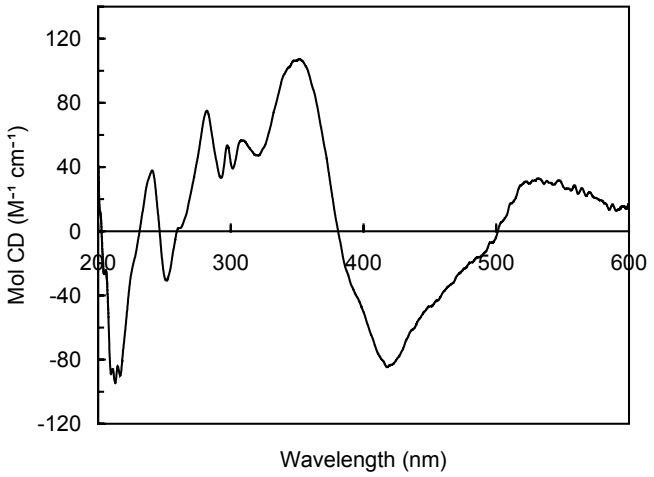

Figure 8.12 Circular Dichroism Spectra of Λ_4-[(Ru(bpy)$_2$)$_4$(bis(BiBzIm))](PF$_6$)$_4$ (Λ_4-Ru$_4$-**25**) in Acetonitrile

The CD spectra of Λ_4-Ru$_4$-**25** is shown in the Figure 8.12. The Cotton effects are observed, indicating the absolute configurations corresponding to the Λ configuration, i.e., under the long-axis-polarized band around 294 nm, the circular dichroism appears strongly positive at low energies, strongly negative at higher energies, and positive at the lowest energy MLCT absorption.

8.5 Synthesis and Properties of Λ_8-[(Ru(bpy)$_2$)$_8$(tetra(BiBzIm))](PF$_6$)$_8$ (Λ_8-Ru$_8$-26)

The same strategy was applied for the synthesis of the homochiral octa-Ru complex Λ_8-Ru$_8$-**26** of the tetramer of the bibenzimidazole (**19**) (Scheme 8.8). An excess of the chiral building block (**27a**) (8.4 equiv) and 20 equiv of $NaOCH_3$ were added to ensure the fully deprotonation and complexation of the tetramer ligand **19**. The formation of the octa-Ru complex Λ_8-Ru$_8$-**26** was confirmed by the MALDI-TOF

analysis (Figure 8.13). The spectra clearly shows the parent ion complex minus $1PF_6^-$, $2PF_6^-$, … , $7PF_6^-$, and $8PF_6^-$ fragments.

Scheme 8.8 Synthesis of Λ_8-[$(Ru(bpy)_2)_8$(tetra(BiBzIm))]$(PF_6)_8$ (Λ_8-Ru_8-**26**)

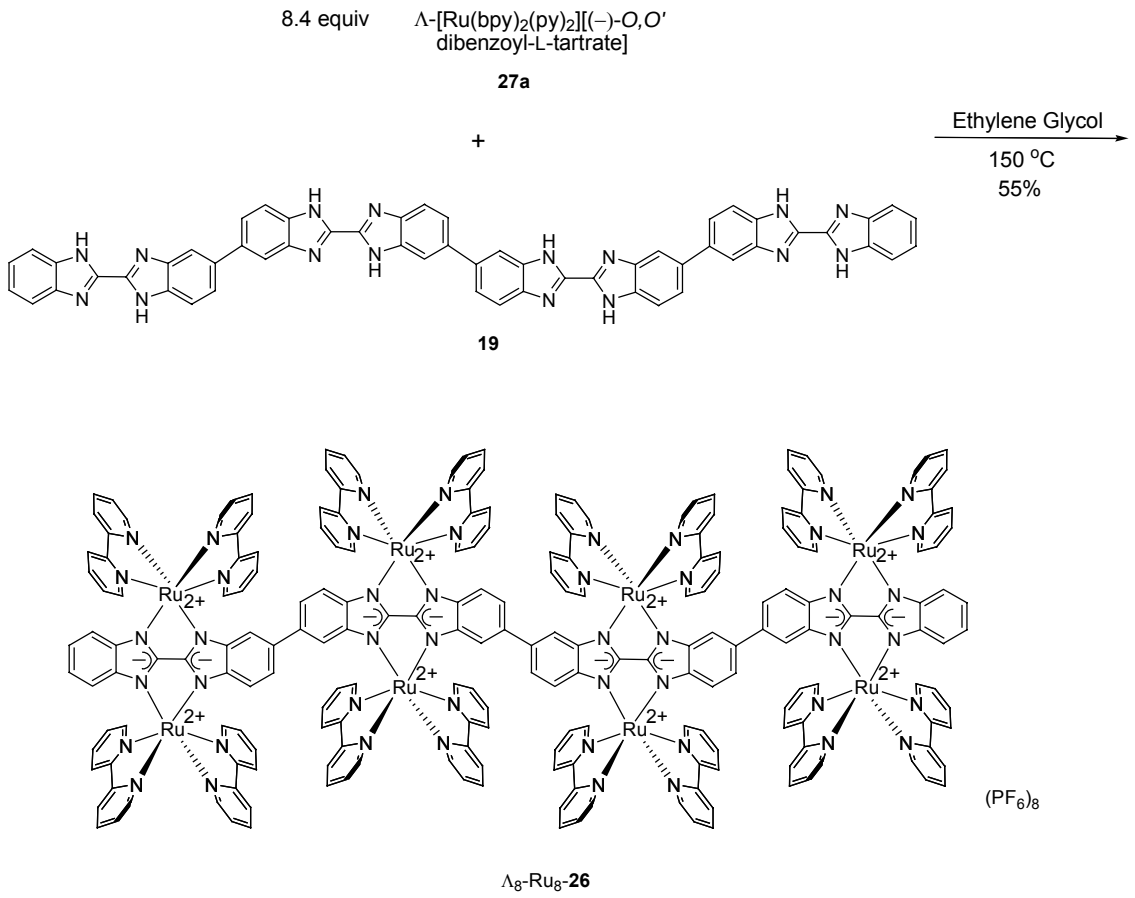

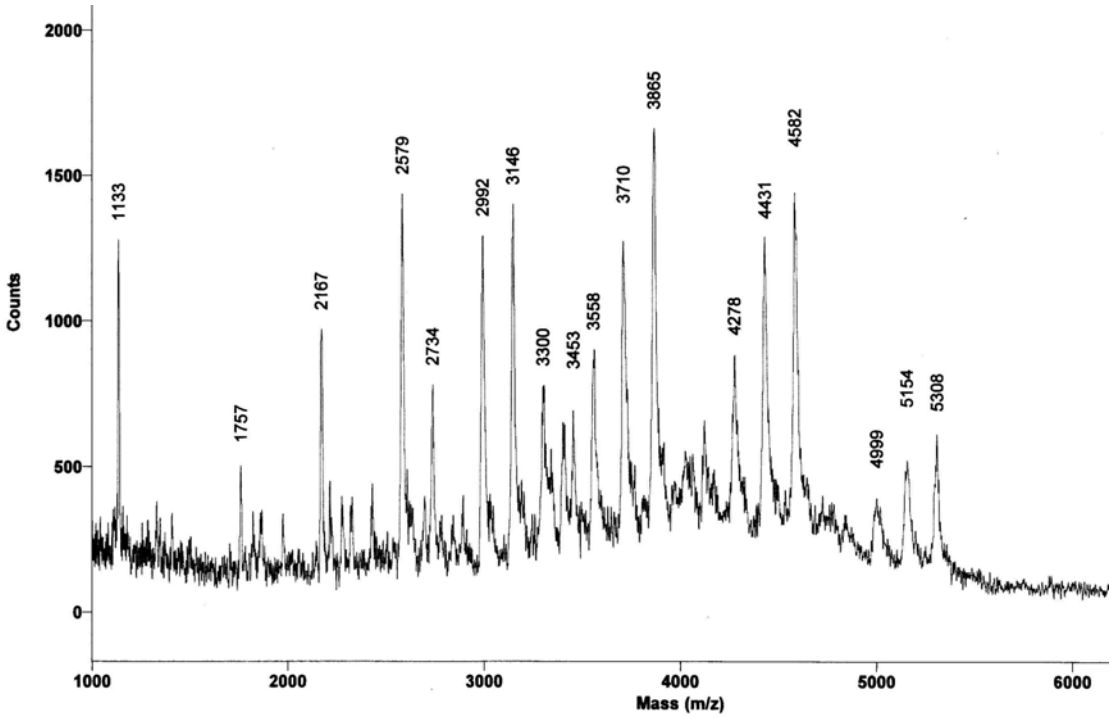

Figure 8.13 MALDI-TOF Spectra of Λ_8-[$(Ru(bpy)_2)_8$(tetra(BiBzIm))]$(PF_6)_8$ (Λ_8-Ru_8-**26**)
5308 $[M - 1PF_6]^+$, 5154 $[M - 2PF_6]^+$, 4999 $[M - 3PF_6]^+$,
4582 $[M - 6PF_6]^+$, 4431 $[M - 7PF_6]^+$, 4278 $[M - 8PF_6]^+$.

The CD spectra of Λ_8-Ru_8-**26** is shown in the Figure 8.14. The Cotton effects are observed, indicating the absolute configurations corresponding to the Λ configuration, i.e., under the long-axis-polarized band around 290 nm, the circular dichroism appear strongly positive at low energies, strongly negative at higher energies, and positive at the lowest energy MLCT absorption.

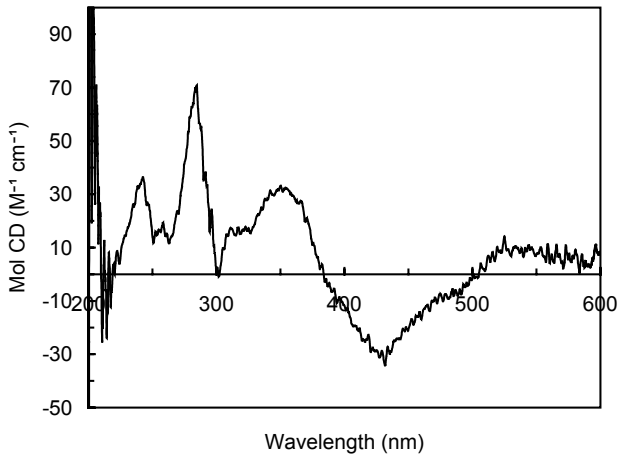

Figure 8.14 Circular Dichroism Spectra of Λ_8-[$(Ru(bpy)_2)_8$(tetra(BiBzIm))]$(PF_6)_8$ (Λ_8-Ru_8-**26**) in Acetonitrile

For the UV–vis and the electrochemical properties of the above homochiral Ru complexes, refer to the corresponding nonchiral complexes in Chapter 5.

8.6 Conclusions

The homochiral multinuclear Ru complexes of the oligomeric bibenzimidazoles were synthesized stereospecifically using Λ-[$Ru(bpy)_2(py)_2$][(−)-*O*,*O*′-dibenzoyl-L-tartrate]·$12H_2O$ as the enantiomerically pure chiral building block. The complexation of bibenzimidazole and the chiral building block proceeds with the complete retention of configuration. The tetra-Ru complex has an estimate size of $2.1 \times 1.1 \times 1.0$ nm^3.

CHAPTER 9

EXPERIMENTAL DETAILS

9.1 General

9.1.1 Reagents and Materials

All reagents were used without further purification. 2,2′-Bipyridine (99%), ammonium hexafluorophosphate (95+%) and $RuCl_3$ (98%) were purchased from Alfa. Dibenzoyl-L-tartaric acid (98%) and tetrabutylammonium chloride (98%) were purchased from Aldrich. Acetonitrile was distilled over CaH_2 before use. Nylon membranes filter paper (pore size: 0.2 μm or 0.45 μm) for the filtration of the Ru complexes was purchased from Cole-Parmer Instrument Co.

9.1.2 Measurements

NMR spectra were obtained on a JEOL Eclipse+ 500 MHz spectrometer. UV−vis spectra were measured using a Varian Cary 500 UV−vis−NIR spectrophotometer. Elemental analysis was performed by Quantitative Technologies Inc. (QTI) (Whitehouse, NJ). Mass analysis was performed by Scripps Research Institute (La Jolla, CA). MALDI-TOF spectra were obtained on Applied Biosystems Voyager STR mass spectrometer. Cyclic Voltammogram experiments were performed at 20 °C using a PC-controlled potentiostat (CH Instruments, electroanalytical

analyzer). The working electrode was a 1.5 mm glassy carbon electrode and the auxiliary electrode was a platinum wire. The reference electrode was a no leak Ag/AgCl reference electrode. They were purchased from Cypress Systems, Inc. (Lawrence, KS). Circular Dichroism spectra were recorded on a JASCO J–710 spectropolarimeter.

9.2 Synthesis

$[Ru(bpy)_2(py)_2]Cl_2$ (27). This material was prepared using a modification of a previously reported procedure.[72,83] A round bottom flask was charged with pyridine (23 mL), water (46 mL) and $Ru(bpy)_2Cl_2$ (2.00 g, 3.84 mmol). The reaction mixture was stirred while heating at reflux for 4 h, filtered while hot, and the solvent was evaporated under reduced pressure by the use of an oil pump. The deep red residue was dissolved in methanol (46 mL) and sufficient diethyl ether (around 170 mL) was added dropwise to result in the formation of a red precipitate. The mixture was allowed to stand at room temperature for 1 h, after which the precipitate was collected by suction filtration and the solids were washed with diethyl ether (2×50 mL). The recovered solid (2.30 g, yield: 93%) was identical in its properties to those previously reported for *rac*-$[Ru(bpy)_2(py)_2]Cl_2$. ^{1}H NMR (500 MHz, DMSO-d_6): δ = 9.02 (d, J = 5.4 Hz, 1H), 8.72 (d, J = 8.1 Hz, 1H), 8.64 (d, J = 8.1 Hz, 1H), 8.39 (d, J = 5.4, 2H), 8.25 (dd, J = 8.1 Hz, 8.1 Hz, 1H), 8.02 (dd, J = 8.1 Hz, 8.1 Hz, 1H), 7.94 (dd, J = 6.7, J = 6.7, 2H), 7.92 (d, J = 6.1, 1H), 7.89 (dd, J = 6.7 Hz, 6.7 Hz, 1H), 7.49 (dd, J = 6.7 Hz, 6.7 Hz, 1H), 7.40 (dd, J = 6.7 Hz, 6.7 Hz, 2H).

Resolution of $[Ru(bpy)_2(py)_2]^{2+}$ (27):[67,69,72]

Disodium (–)-*O,O′*-dibenzoyl-L-tartrate solution (0.5 M) (**28**): This solution was prepared using a modification of a previously reported procedure.[72] NaOH (14.0 g.) was dissolved in 50 mL of deionized water to make a NaOH solution (concentration = 7 mol/L). (–)-*O*,*O′*-dibenzoyl-L-tartaric acid (4.6 g, 12.2 mmol) was dissolved in 20 mL of H_2O to make a suspension. 4.3 mL of the above NaOH solution (concentration = 7 mol/L, 30.1 mmol, 2.47 equiv) was added dropwise to the above (–)-*O*,*O′*-dibenzoyl-L-tartaric acid solution. Keep stirring at room temperature for 2 h until the pH = 9.1. (pH around 9.1 is important for the formation of the red crystals described below.)

Λ-$[Ru(bpy)_2(py)_2]$[(–)-*O,O′*-dibenzoyl-L-tartrate] (27a). An aqueous solution of disodium (–)-*O*,*O′*-dibenzoyl-L-tartrate (**28**) (12 mL, 0.5 M, 6 mmol, 3.35 equiv) was added dropwise to a solution of *rac*-$[Ru(bpy)_2(py)_2]Cl_2$ (**27**) (1.15 g, 1.79 mmol) in 22 mL of water. The mixture was stirred for 10 min. In a dark room, the solvent was allowed to evaporate naturally. The red crystals formed the next day. After 8–10 days, the red crystals of Λ-$[Ru(bpy)_2(py)_2]$[(–)-*O*,*O′*-dibenzoyl-L-tartrate]·$12H_2O$ (**27a**) were collected by filtration, then rinsed with cold water and air-dried. Yield: 0.72 g, 35% (theory: 50%). ^{1}H NMR (500 MHz, DMSO-d_6): δ = 9.00 (d, *J* = 5.4 Hz, 1H), 8.67 (d, *J* = 8.1 Hz, 1H), 8.59 (d, *J* = 8.1 Hz, 1H), 8.38 (d, *J* = 5.4, 2H), 8.22 (dd, *J* = 8.1 Hz, *J* = 8.1 Hz, 1H), 8.00 (d, *J* = 6.7 Hz, 2H), 7.99 (dd, *J* = 8.1 Hz, 8.1 Hz, 1H), 7.92 (d, *J* = 7.4 Hz, 1H), 7.88 (dd, *J* = 6.7 Hz, 6.7 Hz, 2H), 7.59 (dd, *J* = 7.4 Hz, 7.4 Hz, 1H), 7.47 (dd, *J* = 7.4 Hz, 7.4 Hz, 3H), 7.39 (dd, *J* = 7.4 Hz, 7.4 Hz, 2H), 5.48 (s, 1H). ^{13}C NMR (125

MHz, DMSO-d_6): δ = 168.7, 165.4, 157.0, 156.8, 153.3, 152.5, 152.3, 138.0, 137.9, 137.7, 132.3, 131.8, 129.3, 128.2, 128.1, 127.7, 126.2, 124.0, 123.8, 76.9. The tartrate salt was dissolved in methanol, and was converted to Λ-$[Ru(bpy)_2(py)_2](PF_6)_2$ by precipitation with the addition of a saturated aqueous solution of NH_4PF_6. Then Λ-$[Ru(bpy)_2(py)_2](PF_6)_2$ was purified by metathesis with an acetone solution of tetrabutylammonium chloride to precipitate the chloride salt Λ-$[Ru(bpy)_2(py)_2]Cl_2$ **(27c)**. CD (CH_3CN, λ, nm, ($\Delta\varepsilon$, $M^{-1}\cdot cm^{-1}$)): 250 (–9.5), 278 (–13.1), 294 (+115.5), 364 (–16.3), 445 (–3.9), 502 (+1.4), 524 (+1.2).

Λ-$[Ru(bpy)_2(BiBzImH_2)](PF_6)_2$ (Λ-20). Bibenzimidazole (**5**) (0.11 g, 0.47 mmol, excess) was suspended in 20 mL of ethylene glycol and degassed for 15 min under nitrogen, then heated at 150 °C until it dissolved. Then the solution was cooled to 120 °C, and Λ-[$Ru(bpy)_2(py)_2$][(–)-*O*,*O*′-dibenzoyl-L-tartrate] (0.29 g, 0.25 mmol) was added. The mixture was heated at 120 °C for 8 h. The resulting deep red-brown solution was cooled, diluted with 30 mL of water, and filtered to remove the excess bibenzimidazole. A saturated aqueous solution of NH_4PF_6 was added dropwise to the above filtrate to precipitate the crude Ru complexes. The crude was collected by filtration and air-dried (0.17 g, crude yield: 90%). The crude product, which contained Λ-**20a** and ΛΛ-**22**, was deprotonated by $NaOCH_3$/methanol to get the mixture of Λ-**21** and ΛΛ-**22** (see the procedure of Λ-**21**). Λ-**21** was not soluble in acetone and was separated by filtration. ΛΛ-**22** remained in the acetone solution as the PF_6^- salt. Then the pure deprotonated complex Λ-**21** was suspended in methanol, and acidified by

adding concentrated HCl to get Λ-[Ru(bpy)$_2$(BiBzImH$_2$)]Cl$_2$ (Λ-**20**). Diethyl ether was added dropwise to precipitated out Λ-**20**. It was purified by dissolving in methanol and metathesis with a saturated aqueous solution of NH_4PF_6 to convert to the PF_6^- salt Λ-[Ru(bpy)$_2$(BiBzImH$_2$)](PF$_6$)$_2$. ^{1}H NMR (500 MHz, DMSO-*d*$_6$): δ = 8.88 (d, *J* = 8.1 Hz, 1H), 8.78 (d, *J* = 8.1 Hz, 1H), 8.25 (dd, *J* = 8.1 Hz, 8.1 Hz, 1H), 8.06 (dd, *J* = 8.1, 8.1 Hz, 1H), 8.01 (d, *J* = 6.1 Hz, 1H), 7.91 (d, *J* = 6.1 Hz, 1H), 7.86 (d, *J* = 8.1, 1H), 7.60 (dd, *J* = 6.1 Hz, 6.1 Hz, 1H), 7.48 (dd, *J* = 6.1 Hz, 6.1 Hz, 1H), 7.38 (dd, *J* = 8.1 Hz, 8.1 Hz, 1H), 7.06 (dd, *J* = 8.1 Hz, 8.1 Hz, 1H), 5.63 (d, *J* = 8.1 Hz, 1H). CD (CH_3CN, λ, nm, ($\Delta\varepsilon$, $M^{-1}\cdot cm^{-1}$)): 238 (−16.8), 254 (40.9), 282 (−124.0), 294 (+185.1), 314 (+64.1), 330 (+85.8), 348 (+78.9), 430 (−26.8), 482 (+7.2).

Λ-[Ru(bpy)$_2$(BiBzIm)] (Λ-21). The crude Ru complexes from the above reaction (0.17 g) were added to 20 mL of methanol, and the suspension was degassed for 15 min under nitrogen. $NaOCH_3$ (0.15 g, 2.77 mmol) was dissolved in 5 mL methanol and added to the above suspension dropwise. The color of the solution turned from deep red-brown to purple. The solution was refluxed for 3 h under nitrogen. After the resulting mixture was cooled, the solvent was condensed to a half volume by rotary evaporation. Then the mixture, which contained Λ-**21** and ΛΛ-**22**, was filtered and rinsed with acetone to provide the pure solid product Λ-**21**. Sometimes the solid was difficult to collect by filtration due to the small size, then the following method was applied: the mixture of Λ-**21** and ΛΛ-**22** was suspended in acetone. An acetone solution of tetrabutylammonium chloride was added dropwise to precipitate the chloride salt

ΛΛ-[(Ru(bpy)$_2$)$_2$(BiBzIm)]Cl$_2$ (ΛΛ-**22**) and Λ-**21**, which were collected by filtration. The solid obtained was suspended in water to dissolve ΛΛ-[(Ru(bpy)$_2$)$_2$(BiBzIm)]Cl$_2$ (ΛΛ-**22**). The deprotonated Λ-**21** was not soluble in water, and was separated by filtration. ^{1}H NMR (500 MHz, DMSO-d_6): δ = 8.75 (d, J = 8.1 Hz, 1H), 8.64 (d, J = 8.1 Hz, 1H), 8.09 (dd, J = 8.1 Hz, 8.1 Hz, 1H), 7.94 (d, J = 6.1 Hz, 1H), 7.86 (dd, J = 8.1, 8.1 Hz, 1H), 7.73 (d, J = 6.1 Hz, 1H), 7.49 (dd, J = 6.1 Hz, 6.1 Hz, 1H), 7.41 (d, J = 8.1, 1H), 7.37 (dd, J = 6.1 Hz, 6.1 Hz, 1H), 6.75 (dd, J = 8.1 Hz, 8.1 Hz, 1H), 6.45 (dd, J = 8.1 Hz, 8.1 Hz, 1H), 5.35 (d, J = 8.1 Hz, 1H). ^{13}C NMR (125 MHz, DMSO-d_6): δ = 158.8, 157.6, 157.2, 151.4, 150.8, 148.1, 145.0, 135.2, 134.5, 126.4, 126.3, 123.4, 123.0, 118.6, 118.0, 117.9, 111.1. CD (CH_3CN, λ, nm, (Δε, $M^{-1}\cdot cm^{-1}$)): 216 (–74.0), 249 (+31.5), 264 (50.8), 285 (–29.7), 299 (+157.3), 319 (+61.6), 322 (+62.5), 398 (–32.3), 467 (–10.1), 543 (+7.1).

ΛΛ-[(Ru(bpy)$_2$)$_2$(BiBzIm)](PF$_6$)$_2$ (ΛΛ-22). For the above deprotonation reaction, the product which was soluble in water is ΛΛ-[(Ru(bpy)$_2$)$_2$(BiBzIm)]Cl$_2$. It was precipitated by metathesis with a saturated aqueous solution of NH_4PF_6 to convert to the PF_6^- salt ΛΛ-[(Ru(bpy)$_2$)$_2$(BiBzIm)](PF$_6$)$_2$. ^{1}H NMR (500 MHz, DMSO-d_6): δ = 8.79 (d, J = 8.1 Hz, 1H), 8.76 (d, J = 8.1 Hz, 1H), 8.15 (dd, J = 8.1 Hz, 8.1 Hz, 1H), 8.06 (d, J = 8.1, 1H), 8.06 (dd, J = 8.1 Hz, 8.1 Hz, 1H), 7.68 (d, J = 6.1 Hz, 1H), 7.52 (dd, J = 6.1, 6.1 Hz, 1H), 7.36 (dd, J = 6.1, 6.1, 1H), 6.66 (dd, J = 6.1, 3.4 Hz, 1H), 5.54 (dd, J = 6.1, 3.4 Hz, 1H). ^{13}C NMR (125 MHz, DMSO-d_6): δ = 159.4, 157.8, 157.6, 152.9, 151.0, 144.9, 136.4, 136.2, 127.2, 126.6, 123.6, 123.5, 121.1, 113.7. MALDI-

TOF (*m/z*) (PF_6^- salt): 1367 $[M + H_2O]^+$, 1205 $[M - 1PF_6]^+$. CD (CH_3CN, λ, nm, ($\Delta\varepsilon$, $M^{-1}\cdot cm^{-1}$)): 214 (–59.4), 248 (–39.4), 302 (+106.2), 317 sh (+71.2), 346 (+61.5), 405 (–38.9), 449 (–26.0), 524 (+25.1).

Λ_4-[(Ru(bpy)$_2$)$_4$(bis(BiBzIm))](PF$_6$)$_4$ (Λ_4-Ru$_4$-25). Bis(bibenzimidazole) (**14**) (0.050 g, 0.11 mmol) was suspended in 10 mL of ethylene glycol (10% water), degassed for 20 min under nitrogen, and then heated at 150 °C for 2 h to dissolve bis($BiBzImH_2$) (**14**). Then the above solution was cooled to 120 °C, and Λ-[$Ru(bpy)_2(py)_2$] [(−)-*O*,*O*′-dibenzoyl-L-tartrate] (**27a**) (0.54 g, 0.47 mmol) was added. The reaction was heated at 120 °C for 8 h. The resulting deep red-brown solution was cooled, diluted with 10 mL water and filtered to remove the insoluble part which may have. Then a saturated aqueous solution of NH_4PF_6 was added dropwise to precipitate the complex. The crude solid was collected by filtration (320 mg). 160 mg of the crude product was dissolved in a minimum of acetonitrile, and chromatographed over a neutral alumina column (21 cm in length, 17 mm in diameter). The first deep red broad band was collected. The eluate was concentrated to around 25 mL by rotary evaporation, and then diethyl ether was added dropwise to precipitate the desired complex. Yield: 73%. MALDI-TOF (*m/z*): 2551 $[M - 1PF_6]^+$, 2406 $[M - 2PF_6]^+$, 2261 $[M - 3PF_6]^+$, 2116 $[M - 4PF_6]^+$. Anal. Calcd for $C_{108}H_{78}F_{24}N_{24}P_4Ru_4\cdot 4H_2O$: C, 46.86; H, 3.13; N, 12.14. Found: C, 46.66; H, 2.72; N, 12.17. CD (CH_3CN, λ, nm, ($\Delta\varepsilon$,

$M^{-1}\cdot cm^{-1}$)): 213 (–94.7), 240 (+37.9), 252 (–30.9), 282 (+75.1), 297 (+53.5), 309 sh (+56.7), 351 (+107.2), 417 (–84.7), 531 (+33.0).

Λ_8-[(Ru(bpy)$_2$)$_8$(tetra-BiBzIm)](PF$_6$)$_8$ (Λ_8-Ru$_8$-26). Tetra(bibenzimidazole) (**19**) (0.050 g, 0.054 mmol) was suspended in 25 mL of ethylene glycol, degassed for 20 min under nitrogen, and then heated at 170 °C for 8 h to dissolve the tetra($BiBzImH_2$) ligand. Eventually it was still partially dissolved due to the rigid structure of the ligand. Then the suspension was cooled to around 100 °C, Λ-[$Ru(bpy)_2(py)_2$] [(–)-*O*,*O*′-dibenzoyl-L-tartrate]·$12H_2O$ (**27a**) (0.516 g, 0.45 mmol) was added and heated at 150 °C for 2 h. $NaOCH_3$ (58 mg, 1.07 mmol) was added to facilitate the fully deprotonation. Then the solution was heated at 150 °C for another 14 h. The deep red-brown solution was cooled, diluted with around 20 mL water, and filtered to remove the insoluble part. A saturated aqueous solution of NH_4PF_6 was added dropwise to the filtrate to precipitate the complex. The solid crude product (300 mg) was collected by filtration. 150 mg of the crude product was dissolved in a minimum of acetonitrile, and purified by chromatography with a neutral alumina column (21 cm in length, 17 mm in diameter) using an acetonitrile solution of NH_4PF_6 as an eluent. The major portion stayed on the top of the column and was eluted slowly by a saturated acetonitrile solution of NH_4PF_6. The eluate was concentrated to around 10 mL by rotary evaporation and then ether was added dropwise to precipitate the desired complex. Yield: 55%. MALDI-TOF (*m/z*): 5308 $[M - 1PF_6]^+$, 5154 $[M - 2PF_6]^+$, 4999 $[M - 3PF_6]^+$, 4582 $[M - 6PF_6]^+$, 4431 [M –

$7PF_6]^+$, 4278 $[M - 8PF_6]^+$. Anal. Calcd for $C_{216}H_{154}N_{48}P_8F_{48}Ru_8$: C, 48.13; H, 2.88; N, 12.47. Found: C, 43.07; H, 2.68; N, 11.05. CD (CH_3CN, λ, nm, ($\Delta\varepsilon$, $M^{-1}\cdot cm^{-1}$)): 210 (–23.0), 242 (+35.5), 257 (+17.2), 284 (+70.9), 349 (+32.6), 432 (–34.2), 532 (+10.1).

[Ru(bpy)$_2$(*R,R*-dach)](PF$_6$)$_2$ (30).[67,69] *rac*-[Ru(bpy)$_2$(py)$_2$]Cl$_2$ (**27**) (100 mg, 0.16 mmol) and (1*R,2R*)-1,2-diaminocyclohexane (*R,R*-dach) (**31**) (50 mg, 0.44 mmol) were added to 4 mL of ethylene glycol (10% water). The solution was heated at 120 °C for 4 h, then cooled, diluted with 6 mL of H_2O, and filtered. A saturated aqueous solution of NH_4PF_6 was added dropwise to the filtrate until no more precipitate formed. The solid was collected by filtration, redissolved in acetonitrile, and reprecipitated by addition of diethyl ether. Yield: 80%.

Λ-[Ru(bpy)$_2$(*R,R*-dach)](PF$_6$)$_2$ (30a).[67,69] Λ-[Ru(bpy)$_2$(py)$_2$][(–)-*O,O′*-dibenzoyl-L-tartrate]·12H_2O (**27a**) (150 mg, 0.13 mmol) and *R,R*-dach (**31**) (50 mg, 0.44 mmol) were added to 4 mL of ethylene glycol (10% water). The solution was heated at 120 °C for 4 h, then cooled, diluted with 6 mL of H_2O and filtered. A saturated aqueous solution of NH_4PF_6 was added dropwise to the filtrate until no more precipitate formed. The solid was collected by filtration. Yield: 70%, Λ/*RR* > 98% de. ^{1}H NMR (500 MHz, acetonitrile-d_3, aromatic region): 9.10 (d, J = 6.1 Hz, 2H), 8.49 (d, J = 8.1 Hz, 2H), 8.32 (d, J = 8.1 Hz, 2H), 8.17 (ddd, J = 7.7 Hz, 7.7 Hz, 1.3 Hz, 2H), 7.83–7.78 (m, 4H), 7.62 (d, J = 6.1 Hz, 2H), 7.14 (ddd, J = 6.7 Hz, 6.7 Hz, 1.3 Hz, 2H).

PART IV

CROSSLINKED POLYETHYLENIMINE BASED FLAME RETARDANTS

CHAPTER 10

INTRODUCTION

10.1 Polymers and Flame Retardants

Polyethylene and polypropylene are the typical examples of polymers that undergo scission at random locations on the main chain to yield many smaller molecular fragments during burning. They melt, drip and decompose upon combustion and burn completely with very little char formation (carbonized polymer residue). The commercial use of this type of polymers requires that they exhibit selected degrees of flame retardancy. The potential markets for flame retarding polymers are very large. There are four major application areas. First is the electrical and electronic supplies, such as printed circuit boards, internal wires, cables, and the polymeric connectors for TV sets, etc. These materials must meet flammability standards. Second is the construction materials such as furniture cushions and carpets, etc. The third one is the transportation area. For example, polymer components of the interior of mass transit vehicles (airplane, buses, subways) must meet flammability standards. The fourth area is the fabrics and apparel such as workers' clothing in specific industries. The $2.1 billion global market for flame retardants is experiencing double-digit growth across nearly all applications in 2002.

The flame retardancy of polymers is usually achieved through the use of additives. There are several types of flame retardants: 1) fillers, for example adding clays to dilute polymers and reduce the flammability; 2) alumina trihydrate ($Al_2O_3 \cdot 3H_2O$) or magnesium hydroxide, which can decompose and produce water vapor as the incombustible gas to lower the oxygen concentration at the flame front and result in flame snuffing due to lack of oxygen; 3) halogenated compounds, forming highly active fragments during combustion, which enter gas or vapor phase to react with oxygen and therefore acts as potent flame retardants; 4) solid phase char formation flame retardants, such as phosphorus, boron, sulfur, silicon compounds, polynuclear aromatics and intumescence.[87]

Nonhalogenated, phosphorus-based flame retardant additives have been growing faster than traditional brominated formulations. The use of traditional halogenated flame retardants has been limited due to the formation of extremely toxic halogenated dioxins or dibenzofurans.[88,89] Environmentally friendly products, such as halogen-free flame retardants and organic heat stabilizers, are among the market niches that plastics additives producers are targeting for growth. Among alternative possibilities intumescent materials have gained considerable attention because they provide fire protection with minimum of overall health hazard. The term intumescent refers to the formation of a foamed char during burning of a polymer formulation.[90] Intumescent systems decompose on heating with formation of a large amount of thermally stable residue (“char”). This char should be able to act as a thermal shield for heat transmission from the flame to the polymer and as a physical barrier hindering

diffusion of volatiles towards the flame and of oxygen towards the polymer. “Intumescent” chars resulting from a combination of charring and foaming of the surface of the burning polymers may be able to produce an effectively insulating multicellular structure.

Typically, an intumescent system contains three main ingredients, a char former (carbonific, typically pentaerythritol), a blowing agent (spumific, typically melamine), and an acidic catalyst to catalyse the dehydration (phosphorus derivative, typically ammonium polyphosphate) to induce carbonization of the char former.[91] The fire retardant properties of small molecule organophosphorus compounds have been recognized and developed over a number of years and have thus found use as intumescent additives in a variety of polymer materials.[92] The commercially available examples are given in Figure 10.1. Ammonium polyphosphate (Exolit 422, Hoechst) is used as an intumescent fire retardant for thermoplastics such as polypropylene, as is the Great Lakes Chemicals product Char-Guard CN329.[92] Generally, organophosphorus fire retardants promote the formation of large amounts of char. However, typical systems require high loading of the three additives, which results in significantly diminished mechanical properties.[87] Moreover, the additives in many cases add cost and additional problems such as reduced processability. For example, polypropylene has been effectively flame retarded with intumescent systems, but at high loadings of 30 to 50 parts per 100 parts of polymer. It is highly desirable to design the three components into a single molecule. This approach has been the subject of extensive work over many years. For example, Halpern developed a series of pentaerythritol phosphates which are

char-forming, self-catalyzing and intumescent (e.g. Char-Guard CN 329).[89] They are phosphate dimelamine salt and melamine phosphate prepared from pentaerythritol, melamine, and $POCl_3$, which are sufficiently thermally stable for processing in thermoplastics. They are effective fire retardants for polypropylene at concentrations ≥ 20%, which are more efficient than conventional halogen-Sb retardants, and have a less adverse effect on physical properties.

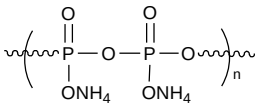

Exolit 422
(ammonium polyphosphate)
(Hoechst)

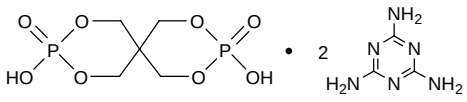

Char-Guard CN329
(Great Lakes Chemicals)

Figure 10.1 Examples of Commercially Available Organophosphorus Fire Retardants

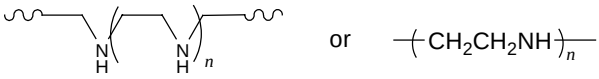

Polyethylenimine ("Lupasol")
33

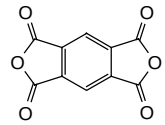

Pyromellitic dianhydride
(PMDA)
34

Chart 10.1

Our goal is to design a new series of intumescent flame retardant additives with low cost based on high molecular weight polyethylenimine (commercial name "Lupasol") (**33**). Using Lupasol as a flame retardant has not been reported, but it could be potentially a good flame retardant because of its high thermal stability. Also, it

contains a large mole fraction of nitrogen. It has been shown that nitrogen rich compounds perform better flame retardancy.[93] The disadvantage of Lupasol is that it is gooey liquid which is difficult to process. Our investigation is trying to change it into free flowing powder form by crosslinking reactions, at the same time, maintain the flame retardant property, so that it can be used as an additive to make flame retardant polymers.

Pyromellitic dianhydride (PMDA) (**34**) was chosen as one potential crosslinking agent. It is a very commonly used, inexpensive aromatic crosslinking agent for polymers. In this study, Lupasol was crosslinked by various amounts of PMDA. The crosslinked product was converted to phosphates and sulfates by reacting with phosphoric acid or sulfuric acid. These products were characterized by elemental analysis, FTIR and thermogravimetric analysis. Flammability was evaluated by measuring the limiting oxygen index (LOI). It turns out that they are non-halogenated, enviromental friendly, low smoke level and cost effective intumescent flame retardants for polyolefins.

10.2 Methods for the Measurement of Flame Retardancy and Thermal Stability

10.2.1 Limiting Oxygen Index Test (ASTM D-2863-97)

Limiting oxygen index method measures the minimum oxygen concentration to support candle-like flaming combustion of materials in a flowing mixture of oxygen and nitrogen. It describes the tendency of a material to sustain a flame, and is widely used as

a tool to investigate the flammability of polymers. It provides a convenient and reproducible means of determining a numerical measure of flammability.

The oxygen index apparatus (Figure 10.2) is designed to allow a candle-like burning of the specimen in a slowly rising mixture of oxygen and nitrogen.[94] In the test, a specimen is placed in the holder at the center of the base of the test column. The flow valves are adjusted to obtain the desired initial oxygen concentration and total flow rate. The oxygen and nitrogen flow into the dispersion chamber and through the glass bead bed. The gases thus are mixed and dispersed evenly over the cross section of the test column. The specimen is ignited so the entire top tip of the specimen is burning like a candle. A gas flame at the end of a tube with a small orifice is used to ignite the specimen.

For physically self-supporting plastic specimens (5” long, 1/4” wide and 1/8” thick), the oxygen concentration is above the oxygen index if the specimen burns for at least 3 minutes after the igniter is removed, or if the specimen burns down 50 mm. The concentration is below the oxygen index if the specimen stops flaming before the criteria (3 min. or 50 mm) are satisfied. The procedure is repeated with a new specimen and a higher or lower oxygen concentration until the lowest concentration of oxygen that will satisfy the criteria is determined. The concentration in percentage is reported as the oxygen index. ASTM Standard D 2863-97 specifies that the difference between oxygen concentrations that will and will not pass the criteria should be reduced to 0.2 percent or less. The entire procedure is repeated for three total gas flow rates between 3 and 5 cm per second. The average of the three results is usually reported. The

effectiveness of fire retardants is measured by the change in the critical oxygen concentration that they induce as a function of their concentration.

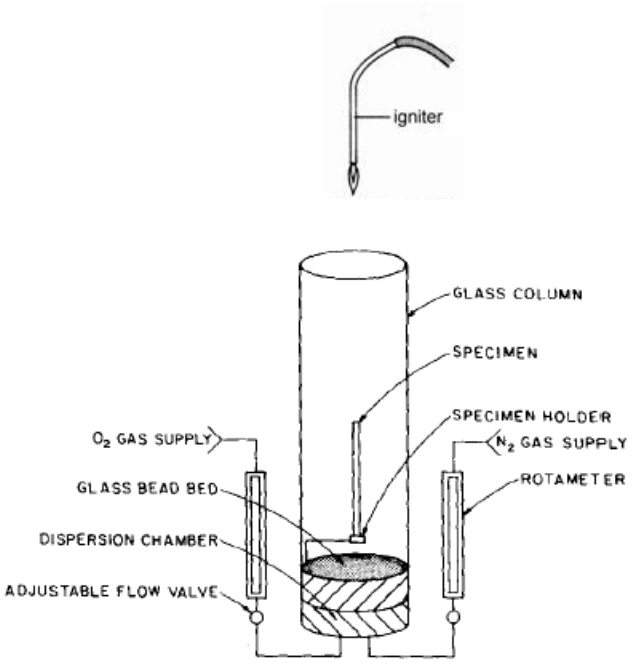

Figure 10.2 Diagram of the Limiting Oxygen Index Flammability Test Apparatus

The limiting oxygen index (LOI) or oxygen index (OI), is defined as:

$$\text{LOI} = \frac{100\ V_o}{V_o + V_N} \qquad \text{(equation 10.1)}$$

where LOI is the oxygen concentration, in percent by volumn; V_o and V_N are the minimum oxygen concentration in the inflow gases required to pass the "minimum burning length" criteria and the nitrogen concentration in the inflow gases respectively. Limiting oxygen index is more commonly reported as a percentage rather than fraction.

Since air comprises about 20.95% oxygen by volume, any material with a limiting oxygen index less than this will burn easily in air. Conversely, the burning behavior and tendency to propagate flame for a polymer with a limiting oxygen index greater than 20.95 will be reduced or even zero after removal of the igniting source. Self-sustaining combustion is not possible if LOI > 100, such values are not physically meaningful. Materials satisfying LOI < 20.95 are "flammable" and LOI > 100 are "intrinsically non-flammable" respectively. Materials with a LOI > 28 are generally self-extinguishing; with 20.95 < LOI < 28 are being "slow-burning".[95] Some typical LOI values of the commercially available polymers are listed in the Table 10.1.

Table 10.1 Oxygen Index of Polymer Systems[87]

Polymers	LOI
Polyolefins (polyethylene, polypropylene)	17.4
Flame-retarded polyolefins	24–28
Polystyrene	18.1
Flame-retarded polystyrene	27–30
Nylon 6,6	24–29
Polytetrafluoroethylene	95.0

10.2.2 Thermogravimetric Analysis (TGA)

The fire retardation of plastic materials is generally achieved by incorporating fire-retardant additives into the plastic during processing. Since processing requires that

the additives withstand temperatures up to above 200 °C, intumescent systems without sufficient thermal stability cannot be incorporated into a number of plastics. Thermogravimetric Analysis (TGA) was used as the major tool in this research to study the thermal stability of the flame retardants. TGA measures weight changes in a material as a function of temperature (or time) under a controlled atmosphere. Its principal usages include the measurement of a material's thermal stability and composition. TGA suspends a sample on a highly sensitive balance over a precisely controlled furnace. Usually the heating rates of 10–20°C/min are used to look for broad decomposition stages. In this study, a slower heating rate of 5°C/min is appropriate due to the intumescent properties of the flame retardants. They foam up upon heating, so the slow heating rate provides the smooth TGA curves. Sample sizes are usually kept as small as possible, within the limits of the apparatus this is usually around 10 mg per run. This reduces bulk effects and at higher heating rates avoids thermal gradients being set up within the sample. The instruments allow for temperatures up to 1000 °C. In this study, the weight loss of the flame retardants vs. the increase of the temperature under nitrogen atmosphere were recorded. The temperature at 5% weight loss and 50% weight loss, as well as the char yield at 800 °C were analyzed.

CHAPTER 11

RESULTS AND DISCUSSION

11.1 Synthesis of Pyromellitic Dianhydride Crosslinked Lupasol (35)

11.1.1 Determinination of the Degree of Crosslinking and Reaction Conditions

To crosslink Lupasol (**33**) into a free flowing powder, a different percentage of the crosslinking agent, pyromellitic dianhydride (PMDA (**34**)), was applied in the crosslinking reactions (Scheme 11.1, Table 11.1). The crosslinked product was represented by the empirical formula: $(C_2H_5N)_1(C_{10}H_4O_6)_x$ (**35**) on the basis of the elemental analysis. $(C_2H_5N)_1$ represents one mole of the repeat unit (CH_2CH_2NH) in the Lupasol long chain. $(C_{10}H_4O_6)_x$ represents the crosslinking agent PMDA (**34**). X is the molar ratio of the crosslinking agent PMDA compared to the mole of the repeat unit in Lupasol, which indicates the degree of crosslinking. A minimum of the PMDA is required to crosslink in order to keep the organic component to a lower limit, due to the high flammability of the organic compounds. The lowest amount of the PMDA studied was 3% (**35a**), but they are not enough to crosslink all the Lupasol, rendering the sticky property of the crude crosslinked product and difficulties in the separation from the solvent by filtration due to the hydrophilicity. The excess uncrosslinked Lupasol was washed away during the work up procedure. Then the actual degree of crosslinking was found to be 6.5%, which is higher than the theory.

Scheme 11.1 Synthesis of the Crosslinked Lupasol by PMDA (**35**)

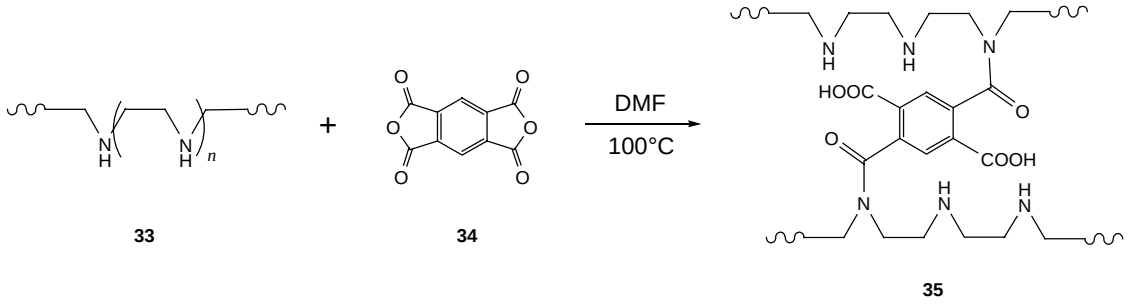

33 **34** **35**

Empirical Formula: $(C_2H_5N)_1(C_{10}H_4O_6)_x$

5% PMDA was applied for the crosslinking of Lupasol under different temperatures and times (**35b–d**). On the basis of the yield and the empirical formula, the products obtained from a low temperature (60 °C, product **35b**) and a short reaction time (7 h, product **35c**) showed higher degree of crosslinking in the empirical formulas than the theory, and the yield lower than 100%, indicating the incomplete crosslinking of all the Lupasol by PMDA. Therefore, the excess of uncrosslinked Lupasol was washed away during the work up procedure.

5% PMDA crosslinked Lupasol cured at 100–110 °C for around 24 h (**35d**) gave the product with a char yield of 22.5%, indicating the significant enhanced thermostability at 800 °C (Table 11.2). With the addition of 5% PMDA, the actual degree of crosslinking is around 8–10% (x is in the range of 0.080–0.090).

7.5% PMDA crosslinked Lupasol cured at 60–70 °C for around 24 h (**35e**) gave the product with no char left at 800 °C, indicating the incomplete crosslinking at 70 °C.

Table 11.1 Crosslink of Lupasol by PMDA

amount of crosslinking agent added	reaction temp, time and yield	crude product	empirical formula of the crosslinked product
3% PMDA (**35a**)	105 °C 20 h	Very sticky, difficult to work up due to the hydrophilicity, 10% H_2SO_4 solution help to separate	Sulfate obtained, $(C_2H_5N)_1(C_{10}H_4O_6)_{0.065}(H_2SO_4)_{0.44}$
5% PMDA (**35b**)	60 °C, 40 h, yield: 93%		$(C_2H_5N)_1(C_{10}H_4O_6)_{0.082}$
5% PMDA (**35c**)	100–130 °C, 7 h, yield: 74%	Not as sticky as 3% PMDA crosslinked product	$(C_2H_5N)_1(C_{10}H_4O_6)_{0.093}$
5% PMDA (**35d**)	90–105°C, 26 h, yield: 100%		$(C_2H_5N)_1(C_{10}H_4O_6)_{0.086}$
7.5% PMDA (**35e**)	60–70 °C, 24 h, yield: 88%	Not sticky, easy work up	$(C_2H_5N)_1(C_{10}H_4O_6)_{0.099}$
10% PMDA (**35f**)	105 °C, 26 h, yield: 100%	Not sticky, easy work up	$(C_2H_5N)_1(C_{10}H_4O_6)_{0.128}$

Table 11.2 Thermal Stability of Lupasol (**33**) and Crosslinked Lupasol (**35**)

sample	T (°C), at 5% Wt. Loss	T (°C), at 50% Wt. Loss	char yield, at 430 °C (%)	char yield, at 800 °C (%)
Lupasol (**33**)	288	387	0	–
$(C_2H_5N)_1(C_{10}H_4O_6)_{0.093}$ (**35c**)	140	364	40	25.1
$(C_2H_5N)_1(C_{10}H_4O_6)_{0.086}$ (**35d**)	154	336	30	22.5
$(C_2H_5N)_1(C_{10}H_4O_6)_{0.099}$ (**35e**)	199	466	53	0
$(C_2H_5N)_1(C_{10}H_4O_6)_{0.128}$ (**35f**)	153	366	41	28.6

10% PMDA crosslinked Lupasol cured at 100–110 °C for around 26 h (**35f**) gave the product with a char yield of 28.6%, which is more thermally stable than 5% PMDA crosslinked Lupasol (**35d**). But from the empirical formula, around 12.8% Lupasol was crosslinked by PMDA. The degree of crosslinking is too high, which introduced too much organic portion. Therefore, the addition of 10% PMDA is not appropriate.

In conclusion, the crosslinking reaction with 5% PMDA curing at 100–110 °C for around 24 h (**35d**) is appropriate to meet the requirement of low crosslinking agent and reach the improved thermostability.

*11.1.2 Characterization of the Crosslinked Lupasol (**35d**)*

The solid-state ^{13}C NMR (Figure 11.1) of the crosslinked Lupasol (**35d**) was performed to confirm the formation of the amide-linkage in the crosslinked Lupasol. The peaks centering at 49 ppm are the carbons on the Lupasol long chain. The peaks at 138 ppm are the carbons on the aromatic rings of PMDA. The peaks at around 170 ppm are the carbons on the carbonyl groups either as carboxylic acids or amides.

From the FTIR study, the band at 1653 cm^{-1} indicates the presence of the carbonyl groups (C=O) in the crosslinked Lupasol due to the formation of the amide and carboxylic acid functionality.

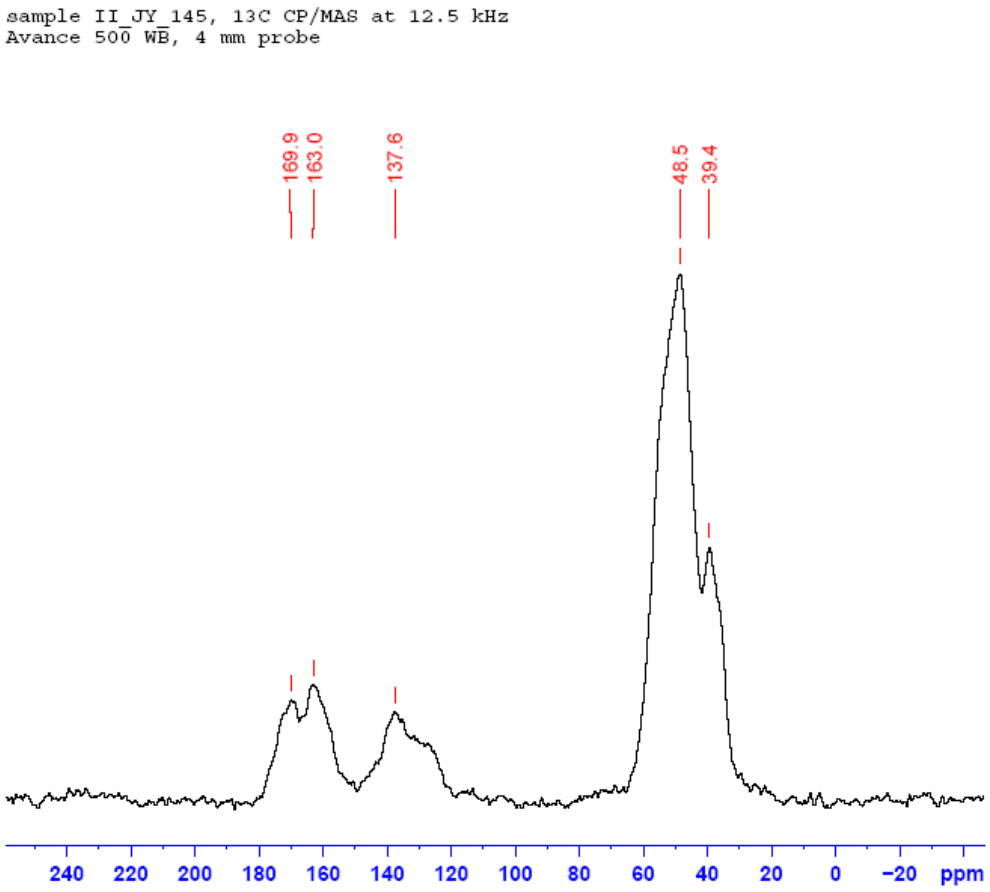

Figure 11.1 Solid State ^{13}C NMR Spectra of PMDA Crosslinked Lupasol $(C_2H_5N)_1(C_{10}H_4O_6)_{0.086}$ (**35d**)

*11.1.3 Thermostabilities of Lupasol (**33**) and Crosslinked Lupasol (**35**)*

The TGA of Lupasol shows that the polymer degraded completely to volatiles by 420 °C, leaving no char residue. However, after it was crosslinked with 5% PMDA, the char yield at 420 °C was 32% and at 800 °C was 22% (Figure 11.2). The LOI of PMDA crosslinked Lupasol was around 23 (Table 11.6). The thermostability at high temperature and the flame retardancy were greatly enhanced by the crosslinking with PMDA.

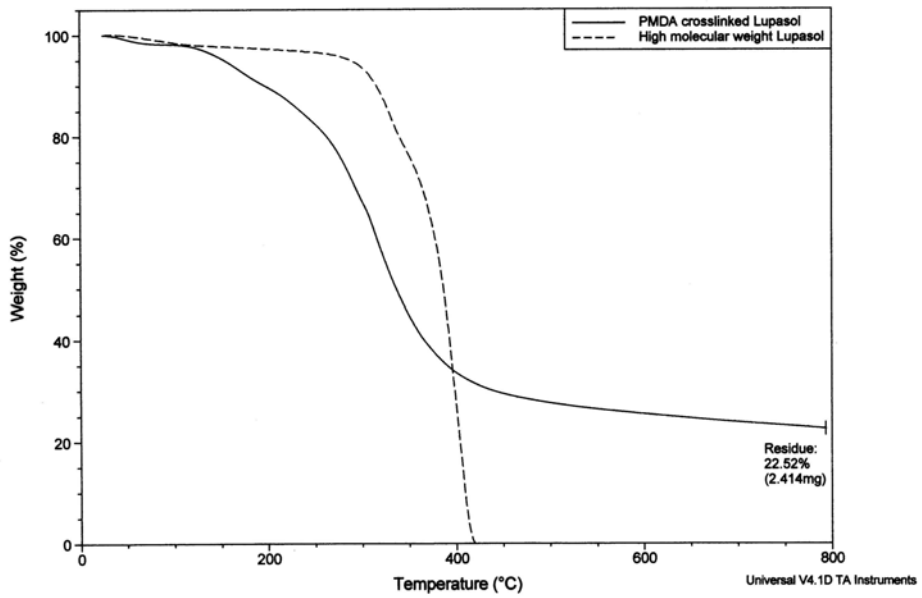

Figure 11.2 TGA Curves of Lupasol (**33**) and PMDA Crosslinked Lupasol (**35d**)
Solid line: **35d**. Dashed line: **33**

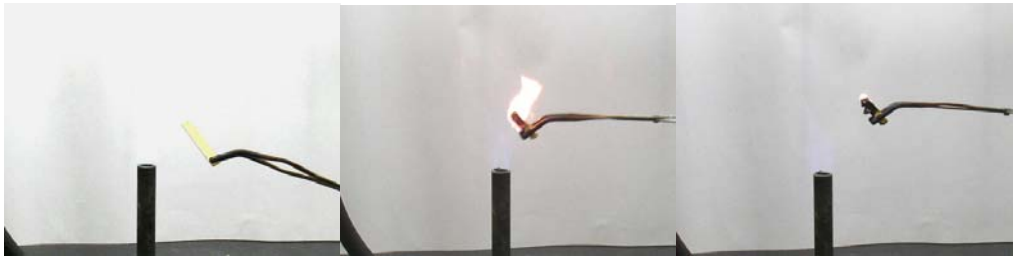

a b c

Figure 11.3 Burning Behavior of PMDA Crosslinked Lupasol (**35**)
a) Before applying the flame to the sample bar. b) During the burning on the flame. c) The char left after the removal of the flame.

However, this crosslinked Lupasol **35** is not satisfying for flame retarding polymers due to the relatively low LOI. The burning behavior of PMDA crosslinked Lupasol (**35**) is shown in Figure 11.3. The sample bar burned with large orange flame (Fig 11.3, b). On the removal of the flame, the bar was anti-glowing (Fig 11.3, c), self

extinguished within 1 minute, and the smoke was evolved. There was char foaming up around two times as large as the original sample, with no dripping.

11.2 Discovery of Sulfates with Improved Flame Retardancy

The Lupasol was a nitrogen rich polymer with quite amount of the free amino groups in the long chain. This structure feature leads to the hydrophilic properties of Lupasol itself and the PMDA crosslinked product (**35**). If the degree of crosslinking is too low (such as 3% PMDA), the crosslinked product was very difficult to be separated from the solvent such as methanol. 10% Sulfuric acid solution was mixed with the PMDA crosslinked product. It was gratifying to find that the acid treatment was not only helpful for the isolation of the crosslinked product, but also rendered improved flame retardancy of the isolated sulfate. It self-extinguished right on the removal of the flame with a low smoke level. From the elemental analysis, the empirical formula of the product was determined, which indicates the degree of crosslinking by the sulfuric acid due to the protonation of the amino groups on the Lupasol chain. This observation gave us some useful information—the formation of the sulfate of **35** would be a good way to make flame retardant. Thus, a series of sulfates were synthesized and their flame retardancies were tested.

*11.2.1 Synthesis of the Sulfates (**36**)*

The crosslinked product $(C_2H_5N)_1(C_{10}H_4O_6)_x$ (**35**) was treated with various concentrations of sulfuric acid to obtain a series of corresponding sulfates (**36**) as shown

in Scheme 11.2. The sulfates were represented by the empirical formula $(C_2H_5N)_1(C_{10}H_4O_6)_x(H_2SO_4)_y$ based on the elemental analysis. $(C_2H_5N)_1$ represents one mole of the repeat unit (CH_2CH_2NH) in the Lupasol long chain. $(C_{10}H_4O_6)_x$ represents the crosslinking agent PMDA. X represents the degree of crosslinking by mole ratio compared to the mole of the repeat unit in Lupasol. $(H_2SO_4)_y$ represents the degree of crosslinking of H_2SO_4 on the Lupasol long chain by mole ratio. Y is in the range of 0–0.50. The maximum of y is 0.50, since one mole of H_2SO_4 can protonate two nitrogen atoms on two repeat units.

Scheme 11.2 Synthesis of the Sulfates (**36**)

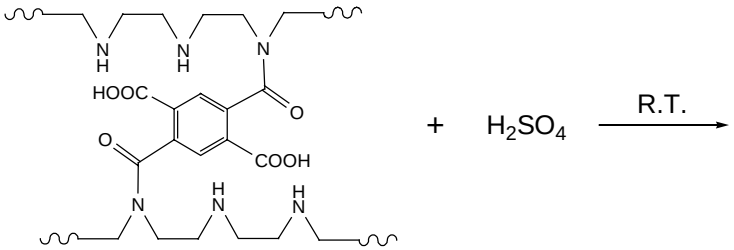

35

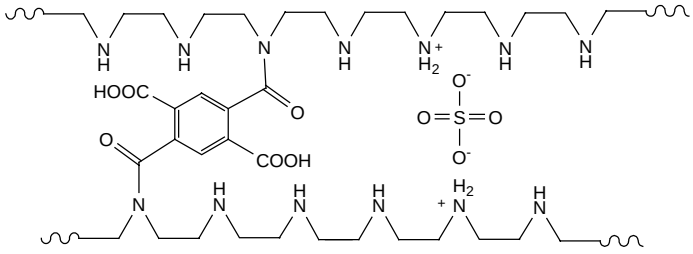

$(C_2H_5N)_1\ (C_{10}H_4O_6)_x\ (H_2SO_4)_y$

36

*11.2.2 Burning Behavior of the Sulfates (**36**)*

The burning behavior of the sulfates is shown in Figure 11.4. The sample was easily ignited, and burned with pale orange flame. On the removal of the flame, it was anti-glowing, self-extinguished immediately, a small amount of gray color smoke suppressed within 5 seconds, and the char foamed up two times than the original sample, with no dripping.

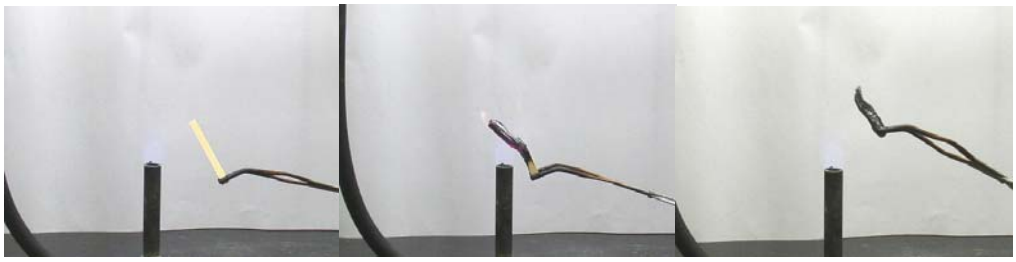

a b c

Figure 11.4 Burning Behavior of the Sulfates (**36**)
a) Before applying the flame to the sample bar. b) During the burning on the flame. c) Intumescent char left after the removal of the flame.

*11.2.3 Thermostability and Flammability of the Sulfates (**36**)*

Interestingly, the structure, the thermal stability and the flammability of the sulfates were related closely with the reaction time in the sulfuric acid solution (Scheme 11.3, Table 11.3). The calculated formulas based on the elemental analysis of the sulfates (Table 11.3) showed that with the extension of the reaction time in sulfuric acid, the degree of crosslinking with PMDA (x value in the formula) decreased, while the percentage of the sulfuric acid increased from 0.26–0.49 (y value in the formula). This is probably because the crosslinked amide bonds were hydrolyzed by the sulfuric acid with the extended reaction time.

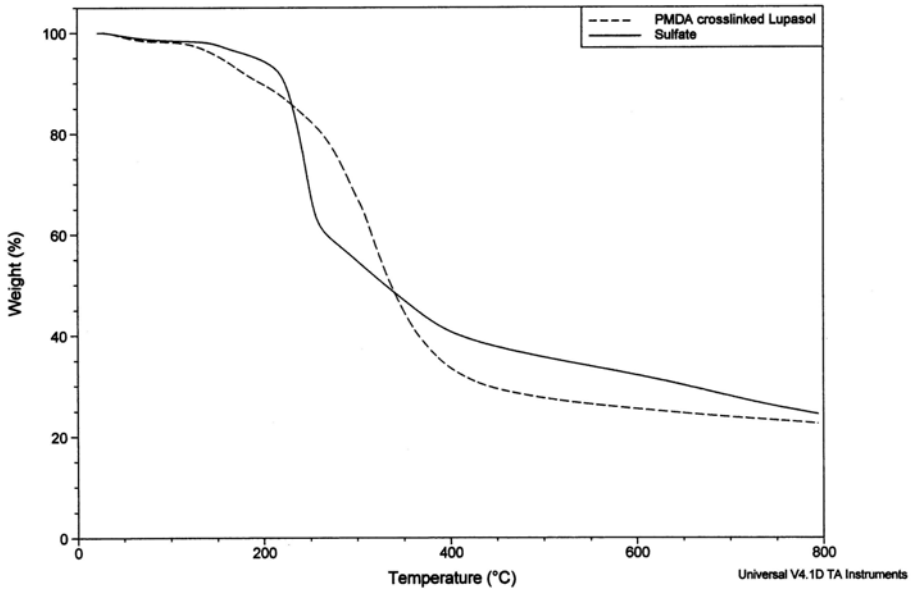

Figure 11.5 TGA Curves of PMDA Crosslinked Lupasol (**35**) and the Sulfate (**36b**)
Solid line: **36b**. Dashed line: **35**

Scheme 11.3 Formation of Sulfates under the Different Reaction Times

$(C_2H_5N)_1\ (C_{10}H_4O_6)_{0.093}$ (**35c**) + 0.77 equiv H_2SO_4 $\xrightarrow[\text{R.T.}]{\text{15 min}}$ $(C_2H_5N)_1\ (C_{10}H_4O_6)_{0.082}\ (H_2SO_4)_{0.26}$ (**36a**)

$(C_2H_5N)_1\ (C_{10}H_4O_6)_{0.086}$ (**35d**) + 0.42 equiv H_2SO_4 $\xrightarrow[\text{R.T.}]{\text{75 min}}$ $(C_2H_5N)_1\ (C_{10}H_4O_6)_{0.064}\ (H_2SO_4)_{0.36}$ (**36b**)

$(C_2H_5N)_1\ (C_{10}H_4O_6)_{0.128}$ (**35f**) + 1.17 equiv H_2SO_4 $\xrightarrow[\text{R.T.}]{\text{10.5 h}}$ $(C_2H_5N)_1\ (C_{10}H_4O_6)_{0.061}\ (H_2SO_4)_{0.49}$ (**36c**)

It is clear from the thermal analysis data that with the increase of the reaction time, the S/N ratio increased, the decomposition occurred at the lower temperature, and the less char left at 800 °C. This suggests that the sulfates formed under longer reaction

times are less thermally stable. Especially **36c,** which burned with no residue left at 800 °C, was formed by the reaction for 10.5 h in 10% sulfuric acid. It has the highest S/N ratio and lowest crosslinking by PMDA among the three samples. When it was burning in the LOI test chamber, there was a large amount of light brown smoke evolved, and eventually no char was left, which was not expected. The possible reason for the lower amount of char left for the higher S/N ratio product is that the sulfuric acid is too strong and breaks the crosslinked amide bonds either by acid catalyzed hydrolysis or by thermal pyrolysis during burning. Then there was no more crosslinking between the Lupasol long chains so that all the samples burned into low molecular weight volatile fragments.

Table 11.3 Thermal Stability and Flammability of the Sulfates (**36**)

formulation	S/N mole ratio	reaction time in 10% sulfuric acid solution	T, °C at 5% Wt. loss	T, °C at 50% Wt. loss	char yield at 800 °C (%)	LOI
$(C_2H_5N)_1(C_{10}H_4O_6)_{0.082}(H_2SO_4)_{0.26}$ (**36a**)	0.26	15 min	181	350	28.5	–
$(C_2H_5N)_1(C_{10}H_4O_6)_{0.064}(H_2SO_4)_{0.36}$ (**36b**)	0.36	75 min	192	330	24.3	46.0
$(C_2H_5N)_1(C_{10}H_4O_6)_{0.061}(H_2SO_4)_{0.49}$ (**36c**)	0.49	10.5 h	147	290	0	53.1

For the sulfates, the conclusions are: the crosslinking is very important to promote the char in order to have good flame retardancy; high S/N ratio will lead to the

break down of the crosslinked bonds when burning, which is not expected. This suggests that the reaction time of 10–15 minutes is enough to form the crosslinked sulfates with low S/N ratio.

Although the LOI of the sulfates is greater than 45%, which suggests that they could be the flame retardants, no further investigation on the sulfates was carried out because they may evolve sulfuric acid fragments during burning which are strongly acidic and corrosive. For the instrumental and environmental concerns, they are probably not suitable for being the useful flame retardants. Thus, a less corrosive, more environmental friendly acid, phosphoric acid, was chosen in the subsequent study. A series of phosphates of the PMDA crosslinked Lupasol were investigated.

11.3 Phosphates with Further Improved Flame Retardancy

*11.3.1 Synthesis of the Phosphates (**37**)*

The crosslinked product $(C_2H_5N)_1(C_{10}H_4O_6)_{0.086}$ (**35d**) was treated with various concentration of phosphoric acid to obtain a series of corresponding phosphates as shown in Scheme 11.4. The phosphates were represented by the empirical formula $(C_2H_5N)_1(C_{10}H_4O_6)_x(H_3PO_4)_z$ based on the elemental analysis. $(C_2H_5N)_1$ represents one mole of the repeat unit (CH_2CH_2NH) in the Lupasol long chain. $(C_{10}H_4O_6)_x$ represents the crosslinking agent PMDA. X represents the degree of the crosslinking by the mole ratio compared to the mole of the repeat unit in Lupasol. $(H_3PO_4)_z$ represents the amount of the H_3PO_4 crosslinked on the Lupasol long chain. Z is the mole ratio compared with the mole of the repeating unit of Lupasol. Z is in the range of 0–0.50.

The maximum of z is 0.50 theoretically, since one mole of H_3PO_4 can protonate two nitrogen atoms on two repeat units.

Scheme 11.4 Synthesis of the Phosphates (**37**)

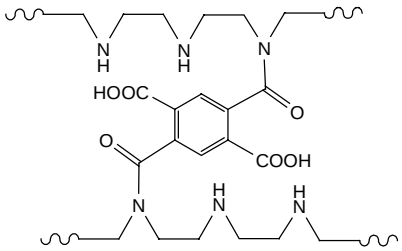

35

+ H_3PO_4 —R.T.→

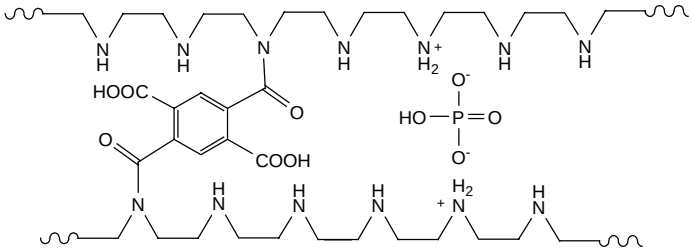

$(C_2H_5N)_1\ (C_{10}H_4O_6)_x\ (H_3PO_4)_z$

37

*11.3.2 Burning Behavior of the Phosphates (**37**)*

The burning behavior of the phosphates (**37**) is very exciting: after being ignited, it showed the light orange flame when burning (Figure 11.6). On the removal of the flame, it was antiglowing, self extinguished immediately, a small amount of smoke suppressed within 5–10 seconds, and the intumescent char foamed up 10 times larger than the original sample, with no dripping.

Due to the formation of the intumescent char, the good flame retardancy and the environmental friendly feature of the phosphorus compound, further detailed investigation were carried out.

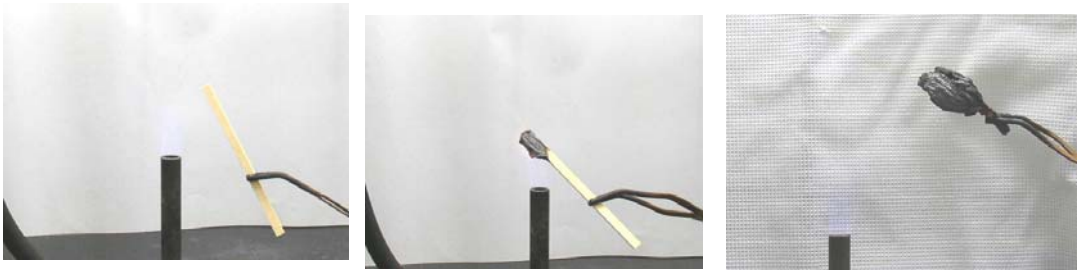

a b c

Figure 11.6 Burning Behavior of the Phosphates (**37**)
a) Before applying the flame to the sample bar. b) During the burning on the flame. c) After the removal of the flame—the intumescent char formed

11.3.3 Reaction Time Determination

The reaction time vs. the thermal stability and the flammability was investigated on the phosphates (**37**) (Scheme 11.5, Table 11.4).

It appears that an extension of the reaction time decreased the decomposition temperature at 5% weight loss, which means that the decomposition occurred at lower temperature (10–30 °C lower), but the tendency to form the char and the LOI were not changed very much. Phosphoric acid is not so strong to break all the crosslinked amide bonds. The conclusion is that it is necessary to limit the reaction time to 30 minutes to produce the phosphates with the enhanced thermal stability as well as the good flame retardancy.

Scheme 11.5 Formation of the Phosphates Series (**37**)

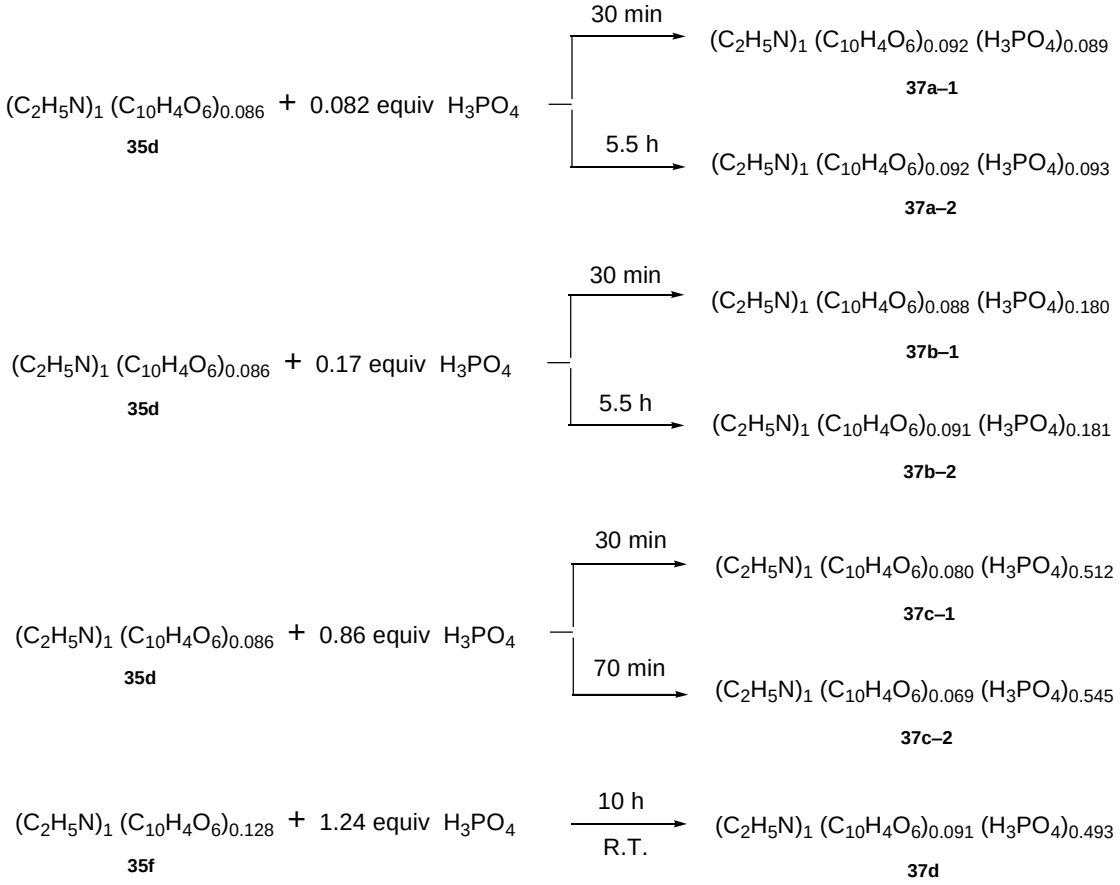

Table 11.4 Thermal Stability and Flammability of the Phosphates (**37**) vs Reaction Times

formulation	P/N mole ratio	reaction time in various concentration of phosphoric acid solution	T, °C at 5% wt. loss	T, °C at 50% wt. loss	char yield at 800 °C (%)	LOI
37a–1	0.089	30 min	163	477	15.2	50.0
37a–2	0.093	5.5 h	155	382	32.1	57.5
37b–1	0.179	30 min	166	439	34.0	> 70.0
37b–2	0.181	5.5 h	154	464	29.1	> 70.0
37c–1	0.512	30 min	191	527	32.8	> 70.0
37c–2	0.545	70 min	148	467	25.9	> 70.0
37d	0.493	10 h	178	537	29.6	> 70.0

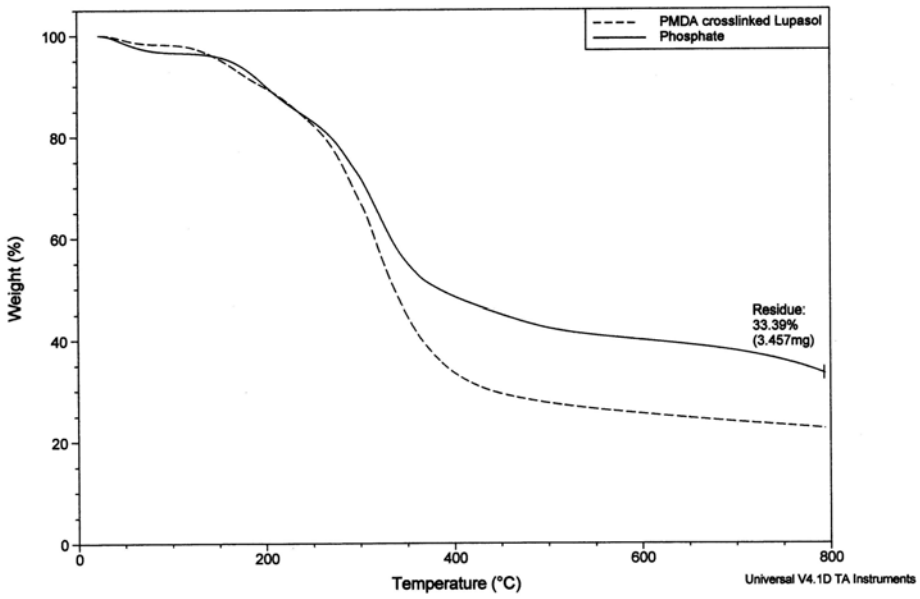

Figure 11.7 TGA Curves of PMDA Crosslinked Lupasol (**35**) and the Phosphate (**37f**) Solid line: **37f**. Dashed line: **35**

*11.3.4 Flame Retardancy of the Phosphates (**37**)*

The flame retardancy of a series of phosphates was evaluated in terms of the limiting oxygen index (LOI). The results are listed in Table 11.5, Figure 11.7 and 11.8. Some important conclusions may be obtained. (The following investigation was on the phosphates produced in various concentrations of the phosphoric acid for 30 minutes.)

Table 11.5 Flame Retardancy and Thermal Stability of the Phosphates (**37**)

formulation	P/N (mole ratio)	LOI	T (°C) at 5% wt. loss	T (°C) at 50% wt. loss	char yield at 800 °C (%)
$(C_2H_5N)_1(C_{10}H_4O_6)_{0.086}$ (**35d**)	0	23.0	154	336	22.5
$(C_2H_5N)_1(C_{10}H_4O_6)_{0.093}$ $(H_3PO_4)_{0.050}$ (**37e**)	0.050	36.0	163	399	22.6
$(C_2H_5N)_1(C_{10}H_4O_6)_{0.092}$ $(H_3PO_4)_{0.089}$ (**37f**)	0.089	50.0	163	383	33.3
$(C_2H_5N)_1(C_{10}H_4O_6)_{0.088}$ $(H_3PO_4)_{0.18}$ (**37g**)	0.179	> 70.0	166	439	34.0
$(C_2H_5N)_1(C_{10}H_4O_6)_{0.079}$ $(H_3PO_4)_{0.34}$ (**37h**)	0.340	> 70.0	182	495	35.3
$(C_2H_5N)_1(C_{10}H_4O_6)_{0.093}$ $(H_3PO_4)_{0.40}$ (**37i**)	0.397	> 70.0	182	547	37.6
$(C_2H_5N)_1(C_{10}H_4O_6)_{0.080}$ $(H_3PO_4)_{0.51}$ (**37j**)	0.512	> 70.0	190	527	32.8

Different degrees of flame retardancy were obtained by varying the P/N ratio of the phosphates. The P/N ratio can be tuned by controlling the stoichiometry between **35d** and H_3PO_4 using different concentrations of H_3PO_4 solution. With the increase of P/N ratio from 0 to 0.179, the LOI increase from 23 to 70. If the P/N ratio is greater than 0.179, the LOI is higher than 70%, which means that the phosphates self-extinguish on the removal of the flame, therefore they are potentially very effective flame retardants. The dotted line in Figure 11.8 shows the extrapolated trend which cannot be tested under the experimental condition: to reach 100% LOI, P/N ratio 0.30 would be estimated. This indicates that only 30% loading of the phosphorus content can give very high flame retardancy! Essentially the phosphates do not burn! (100% LOI could not be measured because it requires the burning in the pure oxygen, which is a very dangerous condition. For the safety concern, this measurement was not allowed at Spartech Polycom Corporation in Arlington, TX. So the highest oxygen level used was 70% for the phosphate LOI measurement).

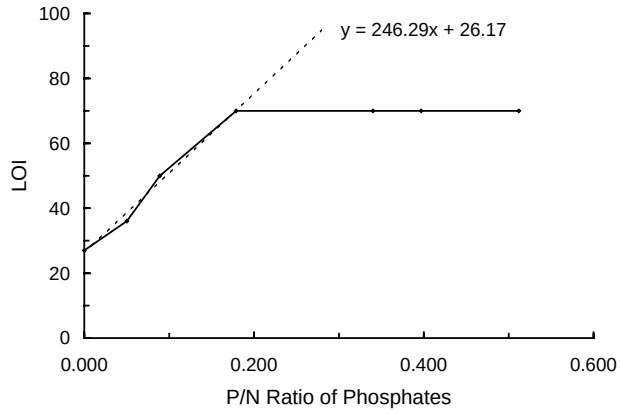

Figure 11.8 LOI of the Phosphates (**37**) as a Function of the P/N Ratio

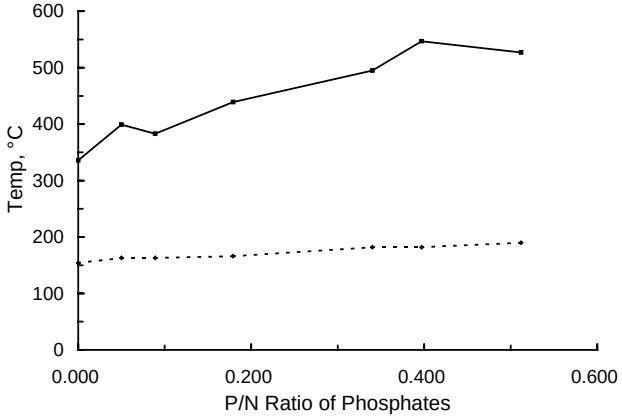

Figure 11.9 Temperatures at 5% and 50% Weight Loss
of the Phosphates (**37**) as a Function of the P/N Ratio
Dotted line: 5% weight loss. Solid line: 50% weight loss

The phosphates produced intumescent char during the burning test, which means that the char former, the blowing agent and the acidic catalyst are in one molecule. This is very exciting. When the phosphates are burning, they evolve very small amount of smoke, which is a very important character. When there is a fire, less smoke will prevent the people from suffocating and let them have more time to escape.

*11.3.5 Thermogravimetric Analysis of the Phosphates (**37**)*

The thermal analysis of the phosphates has been studied. The TGA data and graph of the phosphates are shown in Table 11.5 and Figure 11.9. The decomposition temperature at 5% and 50% weight loss and the char yields are increased with the increase of the P/N ratio. The char yield can reach 37.6%, which is high and is a very good character for the intumescent flame retardants. The formation of the phosphates of **35d** enhanced the thermal stability both at below 200°C and 800°C. But the temperature

at 5% weight loss is around 180°C. It will limit the usage of the phosphates to be processed only with polyethylene.

11.3.6 Flame Retardancy of Phosphate Blended Polyethylene

The LOI of the low density polyethylene (LDPE) is 17, which means it will continue to burn in the atmospheric conditions. The thermostability of the phosphate blended medium density polyethylene (MDPE) powder (**38**) was investigated, but the LOI values were not obtained, due to the busy production schedule of Spartech Polycom and the limit of time. The loading of the phosphates in the MDPE and the burning behavior are discussed here.

The MDPE and the phosphates were blended in an extruder. The MDPE was the powder from Aldrich, which is not suitable for the extrusion usage. But the LDPE was temporarily not available. The extruder was used for the small quantity fiber extrusion, which is not appropriate for this study. Several blending experiments with the phosphates were performed as the preliminary results. The thermoanalysis results showed that the MDPE burned with no char left at around 475 °C. The phosphate blended MDPE showed better thermostability. Two examples (**39a**,**b**) are shown in the Table 11.6 and Figure 11.10. 54% phosphate blended MDPE (**39a)** burned with around 16% char left at 800 °C. The sample burned with orange flame, and self-extinguished on the removal of the flame, with the low smoke level.

Table 11.6 Thermoanalysis of MDPE (**38**) and Phosphate Blended MDPE (**39a,b**) (P/N of the Phosphate is 0.545)

sample	T (°C), at 5% wt. loss	T (°C), at 50% wt. loss	char yield, at 800 °C (%)
MDPE powder **38**	330	440	0
54% phosphate blended MDPE **39a**	231	460	16.1
60% phosphate blended MDPE **39b**	231	463	20.8

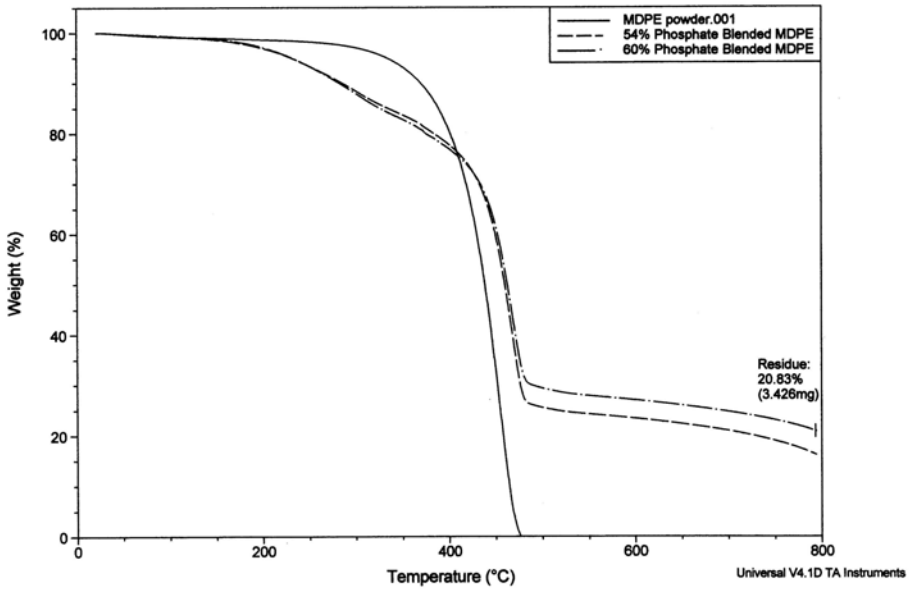

Figure 11.10 TGA Curves of MDPE (**38**) and Phosphate Blended MDPE (**39a,b**) Solid line: MDPE (**38**). Dashed line: 54% phosphate blended MDPE (**39a**). Dashed dot line: 60% phosphate blended MDPE (**39b**).

Jateen Gandhi in our research group continued this project. His investigation was on using toluene 2,4-diisocyanate as the crosslinking agent for Lupasol.[96] The crosslinking reaction condition was the same as the PMDA crosslinked Lupasol (curing at 100°C for 24 h). The crosslinked products were converted to the phosphates, then

blended with the LDPE to study the flame retardancy. The LDPE was from the Spartech Polycom and is suitable for the extrusion. According to his results, 40% phosphate blended LDPE gives the LOI of 26. 50% phosphate blended LDPE gives the LOI of 27. They both meet the flame retardant requirement for the commercial use.

11.4 Conclusions

A new intumescent flame retardant system for use in olefinic polymers was discovered by crosslinking polyethylenimine ("Lupasol") with pyromellitic dianhydride, and then further treating with phosphoric acid to make the phosphate salts. The LOI of the phosphate salts can be greater than 70.0, and the char yield at 800 °C reaches 37.6%, which indicates that they could be very potent flame retardants. The phosphates were blended with polyethylene to show the certain flame retardancy for the commercial use. It turns out that the crosslinking, the reaction time, and the phosphorus content are the three critical factors for the high intumescent flame retardancy.

CHAPTER 12

EXPERIMENTAL DETAILS

12.1 General

12.1.1 Reagents and Materials

Polyethylenimine (Aldrich, high molecular weight, M_w 25,000, M_n 10,000), pyromellitic dianhydride (Aldrich, 97%), polyethylene (Aldrich, powder, medium density, density 0.94 g/mL, mp 109–111 °C), *N*,*N*-dimethylformamide (EM Scientific, 99.8%), phosphoric acid (EM Scientific, 85.0%), sulfuric acid (EM Scientific, 95.0–98.0%) and dichloromethane (EM Scientific, 99.5%) were used as received.

12.1.2 Measurements

12.1.2.1 Elemental Analysis

The elemental analysis was performed at Quantitative Technologies Inc. (QTI) (Whitehouse, NJ). All the phosphates and the sulfates were analyzed under optimum combustion conditions. The solid state ^{13}C NMR was performed at Bruker BioSpin Corp. FTIR spectra were recorded on a Bruker Vector 22 FTIR spectrometer with KBr pellets.

12.1.2.2 Flammability test

The Limiting Oxygen Index (LOI) was determined by ASTM D-2863 using a Stanton Redcroft Flammability Unit (Rheometric Scientific) at SPARTEC Polycom Corporation in Arlington, TX. This test method describes a procedure for measuring the minimum concentration of oxygen that will just support flaming combustion in a flowing mixture of oxygen and nitrogen. A small test specimen (5" long, 1/4" wide and 1/8" thick) is supported vertically in a mixture of oxygen and nitrogen flowing upwards through a transparent chimney. The upper end of the specimen is ignited and subsequent burning behavior of the specimen is observed to compare the period for which burning continues. By testing a series of specimens in different oxygen concentrations, the minimum oxygen concentration is determined.

12.1.2.3 Thermostability Test

The thermogravimetric analysis (TGA) measurements were performed using a TA 2050 thermogravimetric analyzer (TA Instruments) at a heating rate of 5 °C/min under nitrogen.

12.2 Synthesis

*12.2.1 Synthesis of PMDA Crosslinked Lupasol (**35**)*

The reaction was carried out in a 3000 ml resin flask with neck opening of 4". The 3-neck head is a separated part and can be easily removed so that the final solid mass can be removed easily from the opening. To this flask equipped with a mechanical stirrer, was added a solution of Lupasol (393.82 g., 9.14 mol) in 600 ml DMF. While

this solution was stirred at 60 °C, a solution of PMDA (104.97 g., 0.48 mol) in 500 ml DMF was added dropwise. After the complete addition, the reaction mixture was cured for 26 h at 100 °C to give yellow solid mass. The solid mass was removed from the flask and transferred to a home use blender to reach 1/3 volume of the blender. Dichloromethane (around 1/3 of the total volume of the blender) was added to this blender to immerse the solid mass. Then the solid mass was pulverized in the blender and at the same time thoroughly washed with dichloromethane. The yellow crosslinking product was collected by filtration, dried to constant weight in a vacuum oven at 75 °C for at least 20 h. Grinding with mortar and pestle is necessary to make it powdered. The product is hygroscopic, so all the measurements were performed right after the product was taken out from the vacuum oven.

Table 12.1 Elemental Analysis of PMDA Crosslinked Lupasol (**35**)

$(C_2H_5N)_1(C_{10}H_4O_6)_x$	% C	% H	% N
35b	49.08	8.12	20.35
35c	53.11	7.89	21.12
35d	52.60	8.74	21.41
35e	51.97	8.45	20.33
35f	53.16	7.99	18.98

*12.2.2 Synthesis of the Sulfates of Crosslinked Lupasol (**36**)*

PMDA crosslinked Lupasol (**35**) was mixed with the sulfuric acid solutions at different concentrations and stirred at room temperature for various period. The light

brown sulfate powder was collected by filtration, washed once with water, and once with methanol. They were dried to constant weight in a vacuum oven at 75 °C for at least 20 h.

Table 12.2 Elemental Analysis of the Sulfates (**36**)

Sulfates	% C	% H	% N	% S
36a	38.36	6.27	15.85	9.34
36b	33.89	6.09	15.02	12.37
36c	30.19	5.80	13.43	15.12

*12.2.3 Synthesis of the Phosphates of Crosslinked Lupasol (**37**)*

PMDA crosslinked Lupasol (**35**) was mixed with the phosphoric acid solutions at different concentrations, and stirred at room temperature for a various period of times. The typical example is: PMDA crosslinked Lupasol (**35d**) (8.15 g. 0.131 mol repeat unit) was mixed with phosphoric acid (4.25%*, 50 mL, 0.0217 mol) and stirred at room temperature for 30 minutes. The light brown phosphate powder (**37g**) was collected by filtration, washed once with water, once with methanol, and dried to the constant weight in a vacuum oven at 75 °C for at least 20 h.

(*4.25% H_3PO_4 solution was prepared by taking 2.50 g. of 85% H_3PO_4 (concentrated) solution, and diluting to 50 mL with deionized water.)

Table 12.3 Elemental Analysis of the Phosphates (**37**)

Phosphates	% C	% H	% N	% P
37a-1	45.15	6.91	18.18	3.60
37a-2	44.91	9.04	17.92	3.70
37b-1	41.01	6.36	16.59	6.56
37b-2	41.23	8.55	16.52	6.59
37c-1	30.62	5.26	12.78	14.45
37c-2	28.43	5.77	12.37	14.88
37d	30.91	6.01	12.39	13.49
37e	48.18	9.53	19.20	2.11
37f	45.15	6.91	18.18	3.60
37g	41.01	6.36	16.59	6.56
37h	35.44	6.80	14.80	11.13
37i	34.73	5.73	13.83	12.13
37j	30.62	5.26	12.78	14.45

APPENDIX 1

^{1}H, ^{13}C NMR, AND FTIR SPECTRA OF

2,2′-Bibenzimidazole **5**

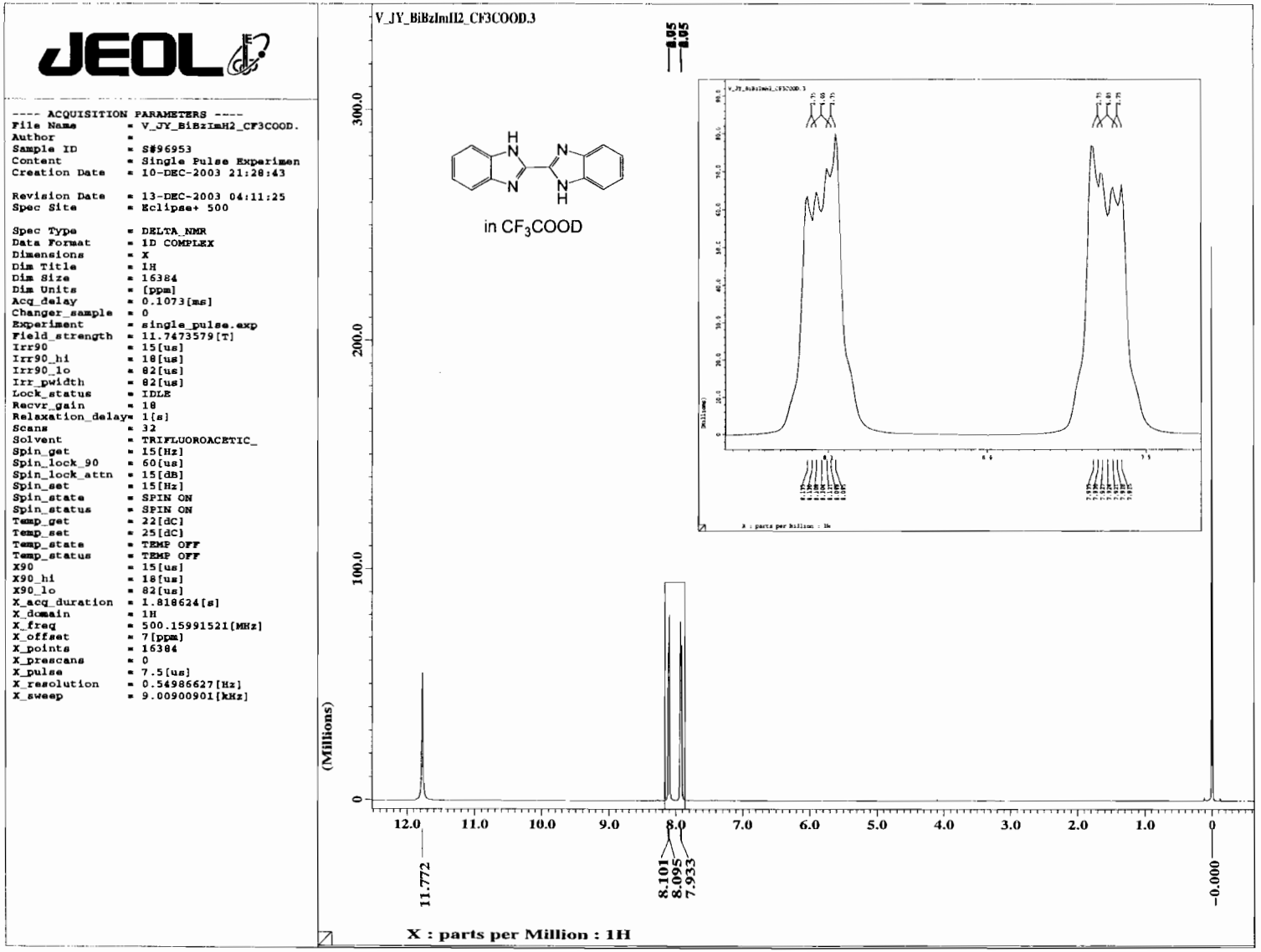
JEOL
---- ACQUISITION PARAMETERS ----
File Name = V_JY_BiBzImH2_CF3COOD.
Author =
Sample ID = S#96953
Content = Single Pulse Experimen
Creation Date = 10-DEC-2003 21:28:43
Revision Date = 13-DEC-2003 04:11:25
Spec Site = Eclipse+ 500
Spec Type = DELTA_NMR
Data Format = 1D COMPLEX
Dimensions = X
Dim Title = 1H
Dim Size = 16384
Dim Units = [ppm]
Acq_delay = 0.1073[ms]
Changer_sample = 0
Experiment = single_pulse.exp
Field_strength = 11.7473579[T]
Irr90 = 15[us]
Irr90_hi = 18[us]
Irr90_lo = 82[us]
Irr_pwidth = 82[us]
Lock_status = IDLE
Recvr_gain = 18
Relaxation_delay = 1[s]
Scans = 32
Solvent = TRIFLUOROACETIC_
Spin_get = 15[Hz]
Spin_lock_90 = 60[us]
Spin_lock_attn = 15[dB]
Spin_set = 15[Hz]
Spin_state = SPIN ON
Spin_status = SPIN ON
Temp_get = 22[dC]
Temp_set = 25[dC]
Temp_state = TEMP OFF
Temp_status = TEMP OFF
X90 = 15[us]
X90_hi = 18[us]
X90_lo = 82[us]
X_acq_duration = 1.818624[s]
X_domain = 1H
X_freq = 500.15991521[MHz]
X_offset = 7[ppm]
X_points = 16384
X_prescans = 0
X_pulse = 7.5[us]
X_resolution = 0.54986627[Hz]
X_sweep = 9.00900901[kHz]
V_JY_BiBzImH2_CF3COOD.3
8.05
8.05
in CF3COOD
(Millions)
300.0
200.0
100.0
0
12.0
11.0
10.0
9.0
8.0
7.0
6.0
5.0
4.0
3.0
2.0
1.0
0
11.772
8.101
8.095
7.933
-0.000
X : parts per Million : 1H

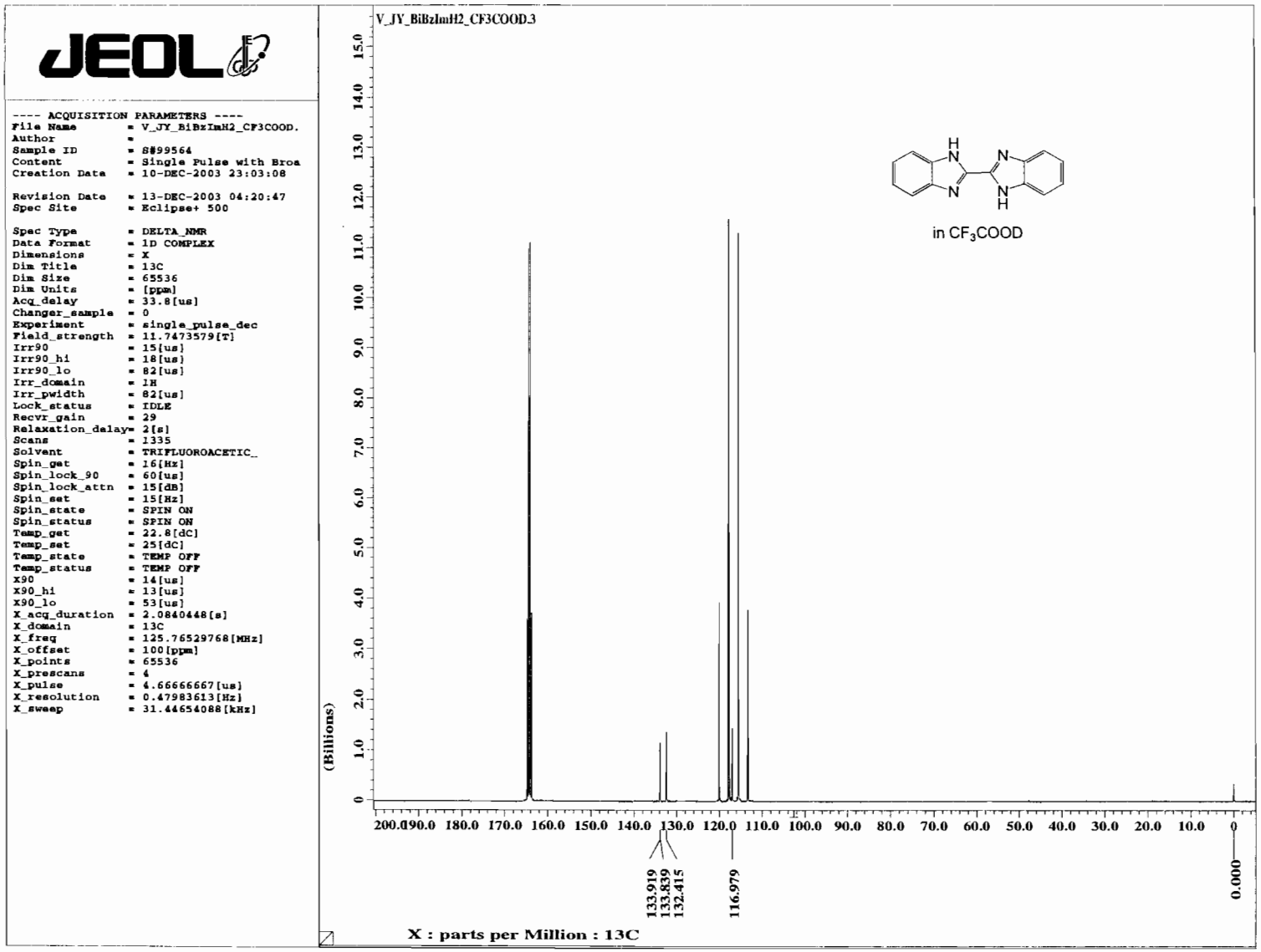
JEOL
---- ACQUISITION PARAMETERS ----
File Name = V_JY_BiBzImH2_CF3COOD.
Author =
Sample ID = S#99564
Content = Single Pulse with Broa
Creation Date = 10-DEC-2003 23:03:08
Revision Date = 13-DEC-2003 04:20:47
Spec Site = Eclipse+ 500
Spec Type = DELTA_NMR
Data Format = 1D COMPLEX
Dimensions = X
Dim Title = 13C
Dim Size = 65536
Dim Units = [ppm]
Acq_delay = 33.8[us]
Changer_sample = 0
Experiment = single_pulse_dec
Field_strength = 11.7473579[T]
Irr90 = 15[us]
Irr90_hi = 18[us]
Irr90_lo = 82[us]
Irr_domain = 1H
Irr_pwidth = 82[us]
Lock_status = IDLE
Recvr_gain = 29
Relaxation_delay= 2[s]
Scans = 1335
Solvent = TRIFLUOROACETIC_
Spin_get = 16[Hz]
Spin_lock_90 = 60[us]
Spin_lock_attn = 15[dB]
Spin_set = 15[Hz]
Spin_state = SPIN ON
Spin_status = SPIN ON
Temp_get = 22.8[dC]
Temp_set = 25[dC]
Temp_state = TEMP OFF
Temp_status = TEMP OFF
X90 = 14[us]
X90_hi = 13[us]
X90_lo = 53[us]
X_acq_duration = 2.0840448[s]
X_domain = 13C
X_freq = 125.76529768[MHz]
X_offset = 100[ppm]
X_points = 65536
X_prescans = 4
X_pulse = 4.66666667[us]
X_resolution = 0.47983613[Hz]
X_sweep = 31.44654088[kHz]
V_JY_BiBzImH2_CF3COOD.3
(Billions)
in CF3COOD
133.919
133.839
132.415
116.979
0.000
X : parts per Million : 13C

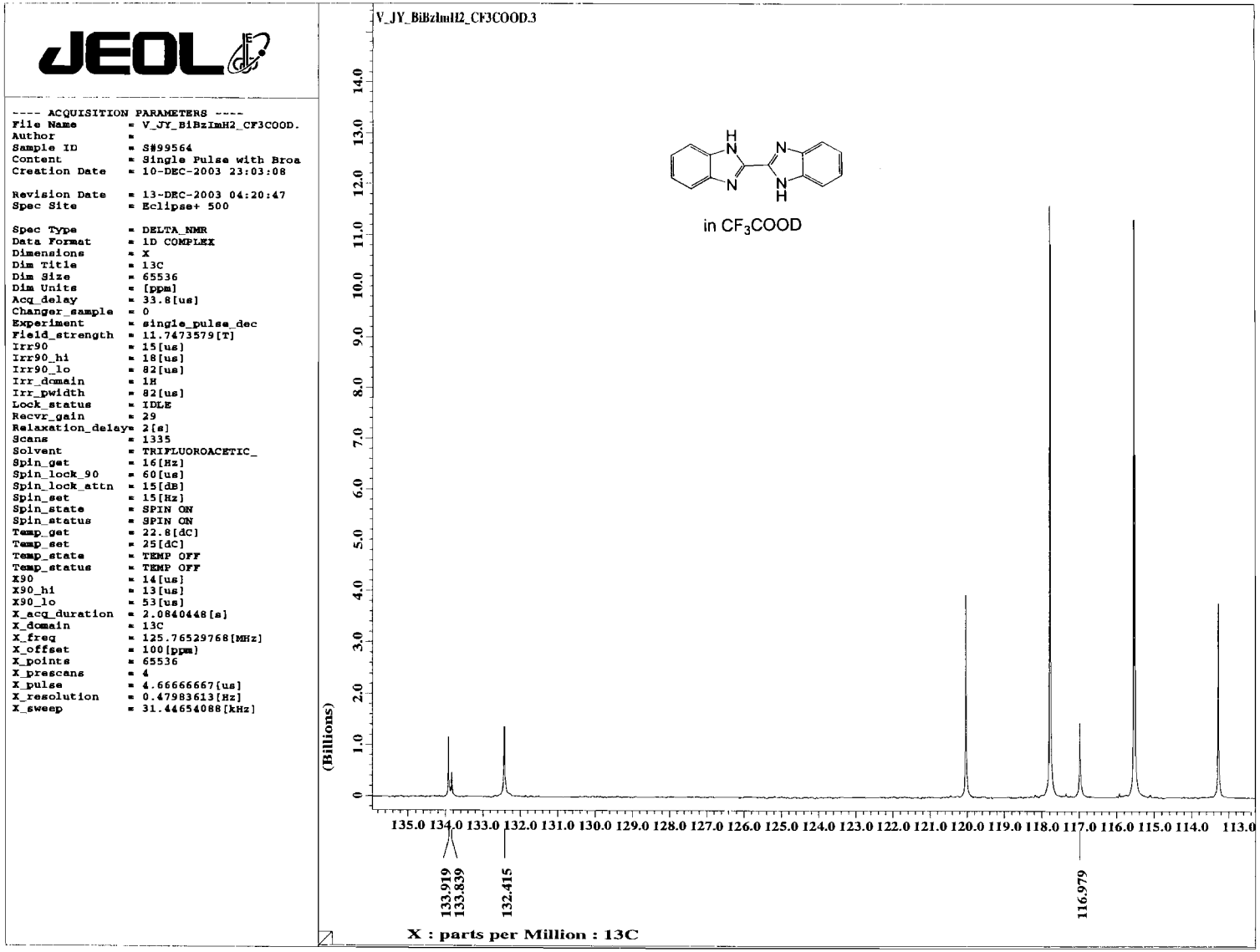
JEOL
---- ACQUISITION PARAMETERS ----
File Name = V_JY_BiBzImH2_CF3COOD.
Author =
Sample ID = S#99564
Content = Single Pulse with Broa
Creation Date = 10-DEC-2003 23:03:08
Revision Date = 13-DEC-2003 04:20:47
Spec Site = Eclipse+ 500
Spec Type = DELTA_NMR
Data Format = 1D COMPLEX
Dimensions = X
Dim Title = 13C
Dim Size = 65536
Dim Units = [ppm]
Acq_delay = 33.8[us]
Changer_sample = 0
Experiment = single_pulse_dec
Field_strength = 11.7473579[T]
Irr90 = 15[us]
Irr90_hi = 18[us]
Irr90_lo = 82[us]
Irr_domain = 1H
Irr_pwidth = 82[us]
Lock_status = IDLE
Recvr_gain = 29
Relaxation_delay= 2[s]
Scans = 1335
Solvent = TRIFLUOROACETIC_
Spin_get = 16[Hz]
Spin_lock_90 = 60[us]
Spin_lock_attn = 15[dB]
Spin_set = 15[Hz]
Spin_state = SPIN ON
Spin_status = SPIN ON
Temp_get = 22.8[dC]
Temp_set = 25[dC]
Temp_state = TEMP OFF
Temp_status = TEMP OFF
X90 = 14[us]
X90_hi = 13[us]
X90_lo = 53[us]
X_acq_duration = 2.0840448[s]
X_domain = 13C
X_freq = 125.76529768[MHz]
X_offset = 100[ppm]
X_points = 65536
X_prescans = 4
X_pulse = 4.66666667[us]
X_resolution = 0.47983613[Hz]
X_sweep = 31.44654088[kHz]
V_JY_BiBzImH2_CF3COOD.3
in CF3COOD
(Billions)
133.919
133.839
132.415
116.979
X : parts per Million : 13C

JEOL
---- ACQUISITION PARAMETERS ----
File Name = BiBzImH2_DMSO.9
Author =
Sample ID = S#762051
Content = Single Pulse Experiment
Creation Date = 15-OCT-2003 22:22:44
Revision Date = 10-DEC-2003 10:11:01
Spec Site = Eclipse+ 500
Spec Type = DELTA_NMR
Data Format = 1D COMPLEX
Dimensions = X
Dim Title = 1H
Dim Size = 16384
Dim Units = [ppm]
Acq_delay = 87.1[us]
Changer_sample = 0
Experiment = single_pulse.exp
Field_strength = 11.7473579[T]
Irr90 = 15[us]
Irr90_hi = 18[us]
Irr90_lo = 82[us]
Irr_pwidth = 82[us]
Lock_status = IDLE
Recvr_gain = 20
Relaxation_delay = 1[s]
Scans = 32
Solvent = DMSO-D6
Spin_gat = 15[Hz]
Spin_lock_90 = 60[us]
Spin_lock_attn = 15[dB]
Spin_set = 15[Hz]
Spin_state = SPIN ON
Spin_status = SPIN ON
Temp_gat = 22.2[dC]
Temp_set = 25[dC]
Temp_state = TEMP OFF
Temp_status = TEMP OFF
X90 = 15[us]
X90_hi = 18[us]
X90_lo = 82[us]
X_acq_duration = 1.48766672[s]
X_domain = 1H
X_freq = 500.15991521[MHz]
X_offset = 6[ppm]
X_points = 16384
X_prescans = 0
X_pulse = 7.5[us]
X_resolution = 0.67219335[Hz]
X_sweep = 11.01321586[kHz]
BiBzImH2_DMSO.9
in DMSO-d_6
2.0
4.0
4.0
4.0
13.578
7.669
7.300
3.376
0.000
(Millions)
X : parts per Million : 1H

JEOL

Filename	= BiBzImH2_Pure_DMSO-3.
Experiment	= single_pulse_dec
Sample_id	= S#774894
Solvent	= DMSO-D6
Creation_time	= 16-OCT-2003 07:10:42
Revision_time	= 26-MAY-2005 11:55:59
Current_time	= 26-MAY-2005 11:57:11
Content	= Single Pulse with Bro
Data_format	= 1D COMPLEX
Dim_size	= 32768
Dim_title	= 13C
Dim_units	= [ppm]
Dimensions	= X
Site	= Eclipse+ 500
Spectrometer	= DELTA_NMR
Field_strength	= 11.7473579[T] (500[MH
X_acq_duration	= 1.0420224[s]
X_domain	= 13C
X_freq	= 125.76529768[MHz]
X_offset	= 100[ppm]
X_points	= 32768
X_prescans	= 4
X_resolution	= 0.95967227[Hz]
X_sweep	= 31.44654088[kHz]
Irr_domain	= 1H
Irr_freq	= 500.15991521[MHz]
Irr_offset	= 5[ppm]
Mod_return	= 1
Scans	= 10000
X_90_width	= 14[us]
X_acq_time	= 1.0420224[s]
X_angle	= 30[deg]
X_pulse	= 4.66666667[us]
Initial_wait	= 1[s]
Phase_preset	= 3[us]
Recvr_gain	= 29
Relaxation_delay	= 2[s]
Temp_get	= 23[dC]
Unblank_time	= 2[us]

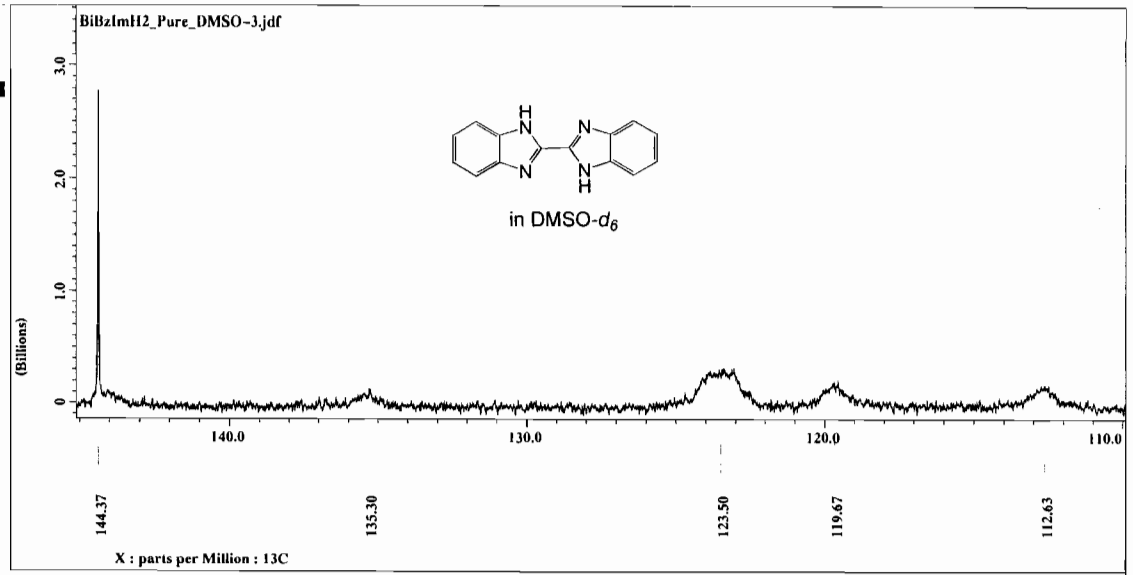

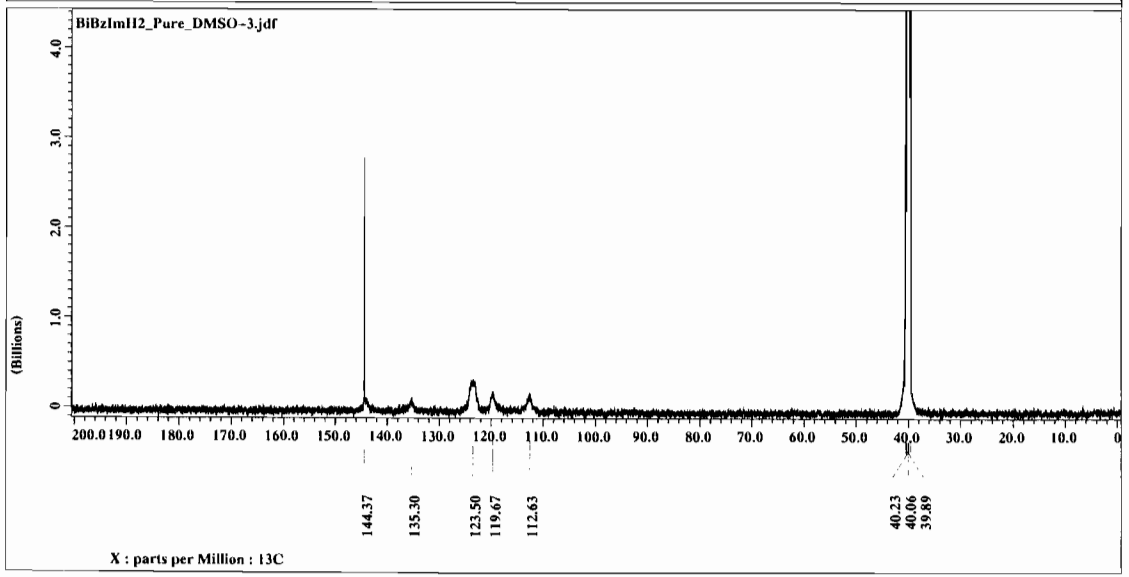

Transmittance [%]
0
20
40
60
80
100
4000
3500
3000
2500
2000
1500
1000
500
Wavenumber cm-1
3029.36
2949.01
2870.80
2798.67
2750.61
2673.93
2584.73
1616.65
1586.80
1500.22
1470.99
1397.64
1343.49
1271.28
1235.31
1183.52
1143.76
1011.33
949.00
844.41
777.58
742.29
662.25
618.11
542.30
D:\OPUS_NT\DATA\JunJun2\C P (Notebook IV, V)\Bibenzimidazole_2.0
Bibenzimidazole_2
Solid in KBr
07/10/2003

APPENDIX 2

^{1}H NMR AND FTIR SPECTRA OF

3,3′-Diaminobenzidine **6**

Filename	= VI_JY_Diaminobenzidin
Experiment	= single_pulse.exp
Sample_id	= S#757177
Solvent	= TRIFLUOROACETIC_
Creation_time	= 1-JUL-2004 17:32:25
Revision_time	= 31-MAY-2005 12:14:35
Current_time	= 31-MAY-2005 12:14:41
Content	= Single Pulse Experime
Data_format	= 1D COMPLEX
Dim_size	= 16384
Dim_title	= 1H
Dim_units	= [ppm]
Dimensions	= X
Site	= Eclipse+ 500
Spectrometer	= DELTA_NMR
Field_strength	= 11.7473579[T] {500[MH
X_acq_duration	= 1.818624[s]
X_domain	= 1H
X_freq	= 500.15991521[MHz]
X_offset	= 7[ppm]
X_points	= 16384
X_prescans	= 0
X_resolution	= 0.54986627[Hz]
X_sweep	= 9.00900901[kHz]
Mod_return	= 1
Scans	= 17
X_90_width	= 15[us]
X_acq_time	= 1.818624[s]
X_angle	= 45[deg]
X_pulse	= 7.5[us]
Initial_wait	= 1[s]
Phase_preset	= 3[us]
Recvr_gain	= 13
Relaxation_delay	= 1[s]
Temp_get	= 24.4[dC]
Unblank_time	= 2[us]

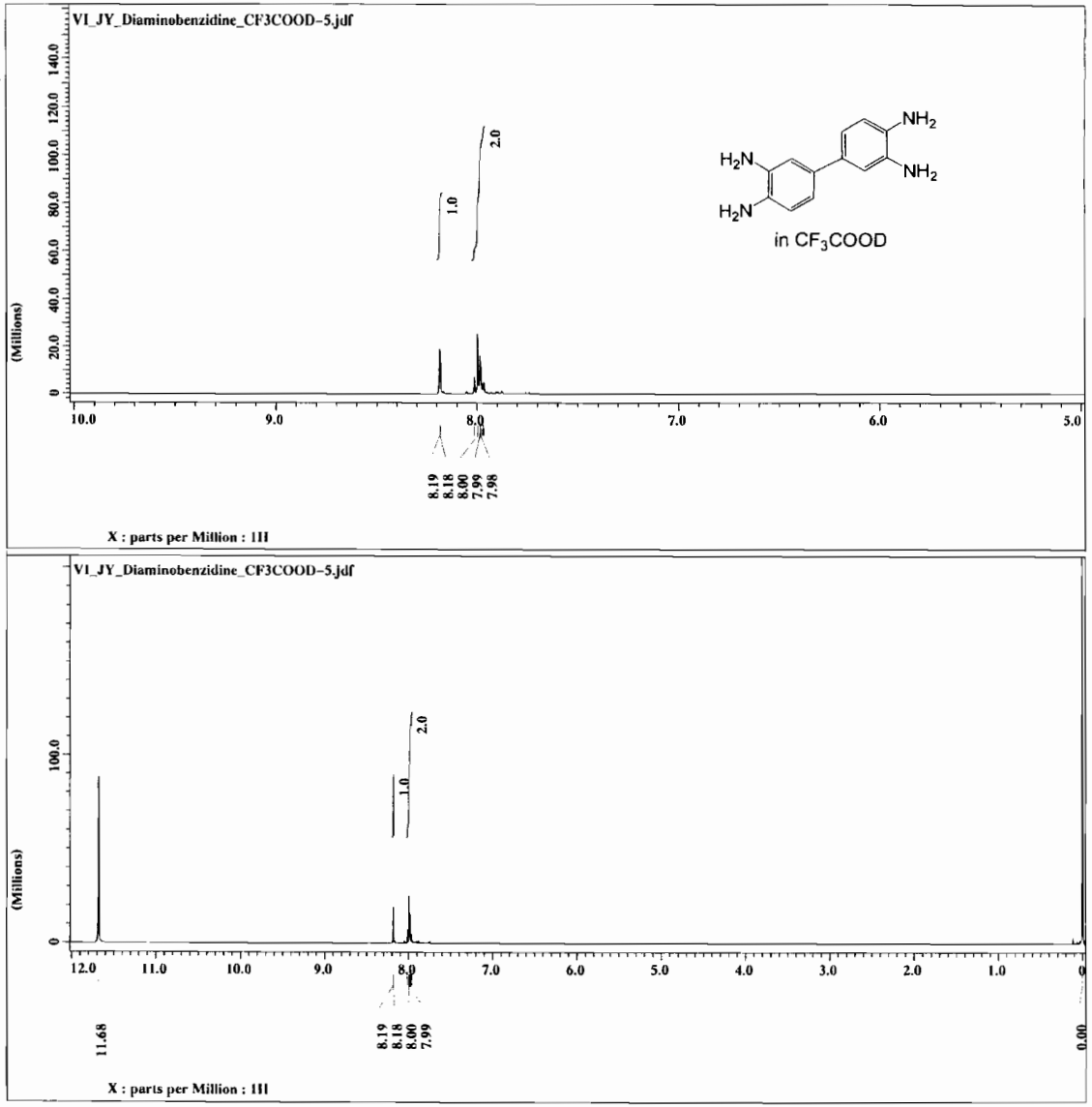

```
Filename          = IV_JY_diaminobenzidin
Experiment        = single_pulse.exp
Sample_id         = S#716861
Solvent           = TRIFLUOROACETIC_
Creation_time     = 22-SEP-2003 20:53:12
Revision_time     = 30-MAY-2005 20:37:36
Current_time      = 30-MAY-2005 20:44:20

Content           = Single Pulse Experime
Data_format       = 1D COMPLEX
Dim_size          = 16384
Dim_title         = 1H
Dim_units         = [ppm]
Dimensions        = X
Site              = Eclipse+ 500
Spectrometer      = DELTA_NMR

Field_strength    = 11.7473579[T] (500[MH
X_acq_duration    = 1.818624[s]
X_domain          = 1H
X_freq            = 500.15991521[MHz]
X_offset          = 5[ppm]
X_points          = 16384
X_prescans        = 0
X_resolution      = 0.54986627[Hz]
X_sweep           = 9.00900901[kHz]
Mod_return        = 1
Scans             = 37

X_90_width        = 15[us]
X_acq_time        = 1.818624[s]
X_angle           = 45[deg]
X_pulse           = 7.5[us]
Initial_wait      = 1[s]
Phase_preset      = 3[us]
Recvr_gain        = 18
Relaxation_delay  = 1[s]
Temp_get          = 22.6[dC]
Unblank_time      = 2[us]
```

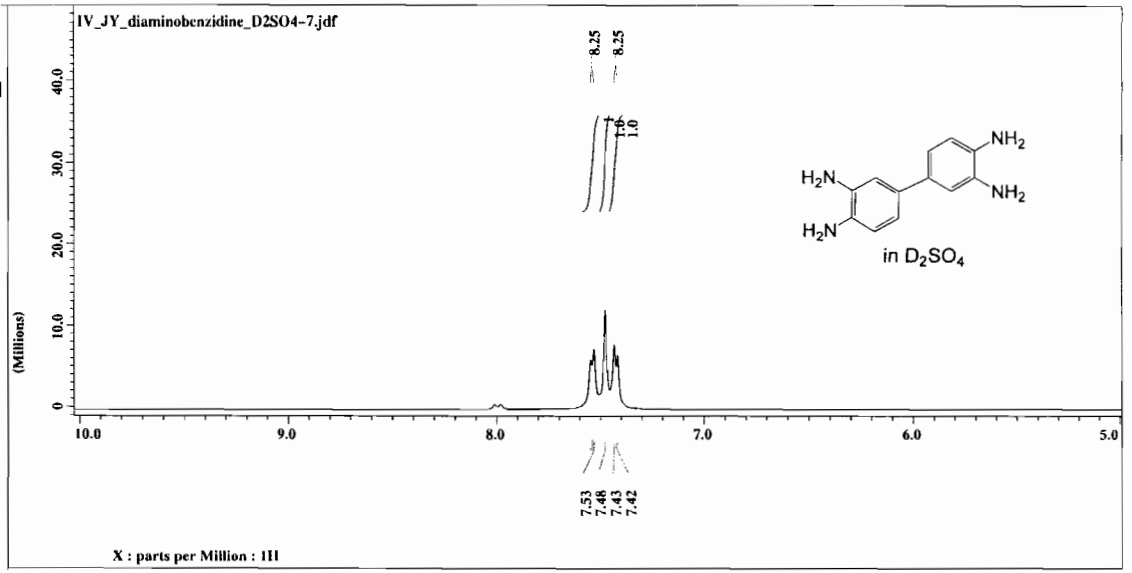

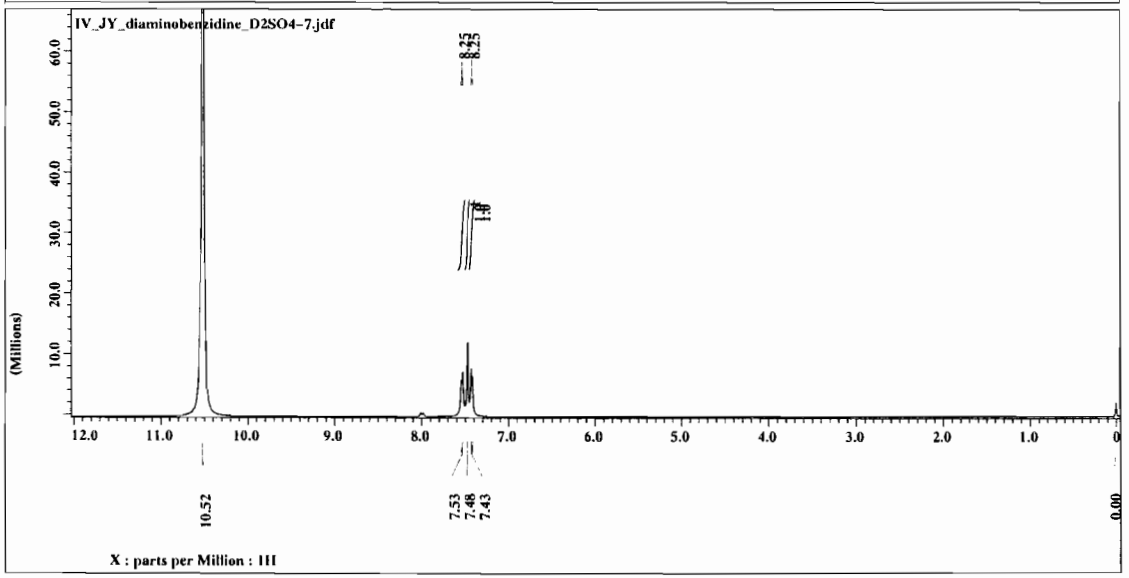

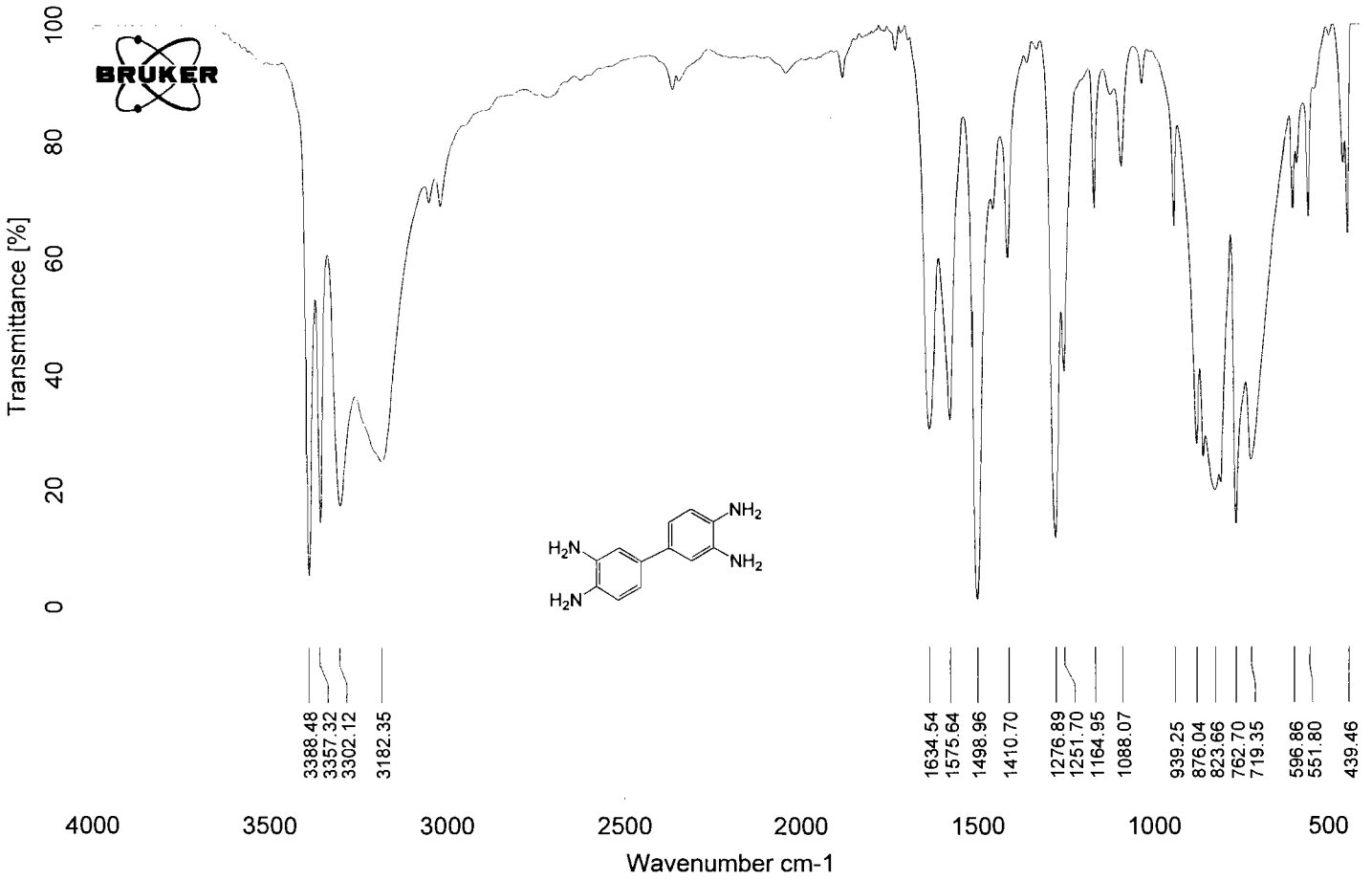

D:\OPUS_NT\DATA\Jun\Jun2\C P (Notebook IV, V)\V_JY_diaminobenzidine.0	V_JY_diaminobenzidine	Solid in KBr	23/09/2003

Page 1/1

APPENDIX 3

^{1}H, ^{13}C NMR, AND FTIR SPECTRA OF

2-Trichloromethylbenzimidazole **10**

Filename	= VI_JY_TriCl_BzImH2_CF
Experiment	= single_pulse.exp
Sample_id	= S#765954
Solvent	= TRIFLUOROACETIC_
Creation_time	= 1-JUL-2004 17:50:50
Revision_time	= 3-DEC-2005 21:26:23
Current_time	= 3-DEC-2005 21:26:47
Content	= Single Pulse Experime
Data_format	= 1D COMPLEX
Dim_size	= 16384
Dim_title	= 1H
Dim_units	= [ppm]
Dimensions	= X
Site	= Eclipse+ 500
Spectrometer	= DELTA_NMR
Field_strength	= 11.7473579[T] (500[MH
X_acq_duration	= 1.818624[s]
X_domain	= 1H
X_freq	= 500.15991521[MHz]
X_offset	= 7[ppm]
X_points	= 16384
X_prescans	= 0
X_resolution	= 0.54986627[Hz]
X_sweep	= 9.00900901[kHz]
Mod_return	= 1
Scans	= 96
X_90_width	= 15[us]
X_acq_time	= 1.818624[s]
X_angle	= 45[deg]
X_pulse	= 7.5[us]
Initial_wait	= 1[s]
Phase_preset	= 3[us]
Recvr_gain	= 13
Relaxation_delay	= 1[s]
Temp_get	= 24.4[dC]
Unblank_time	= 2[us]

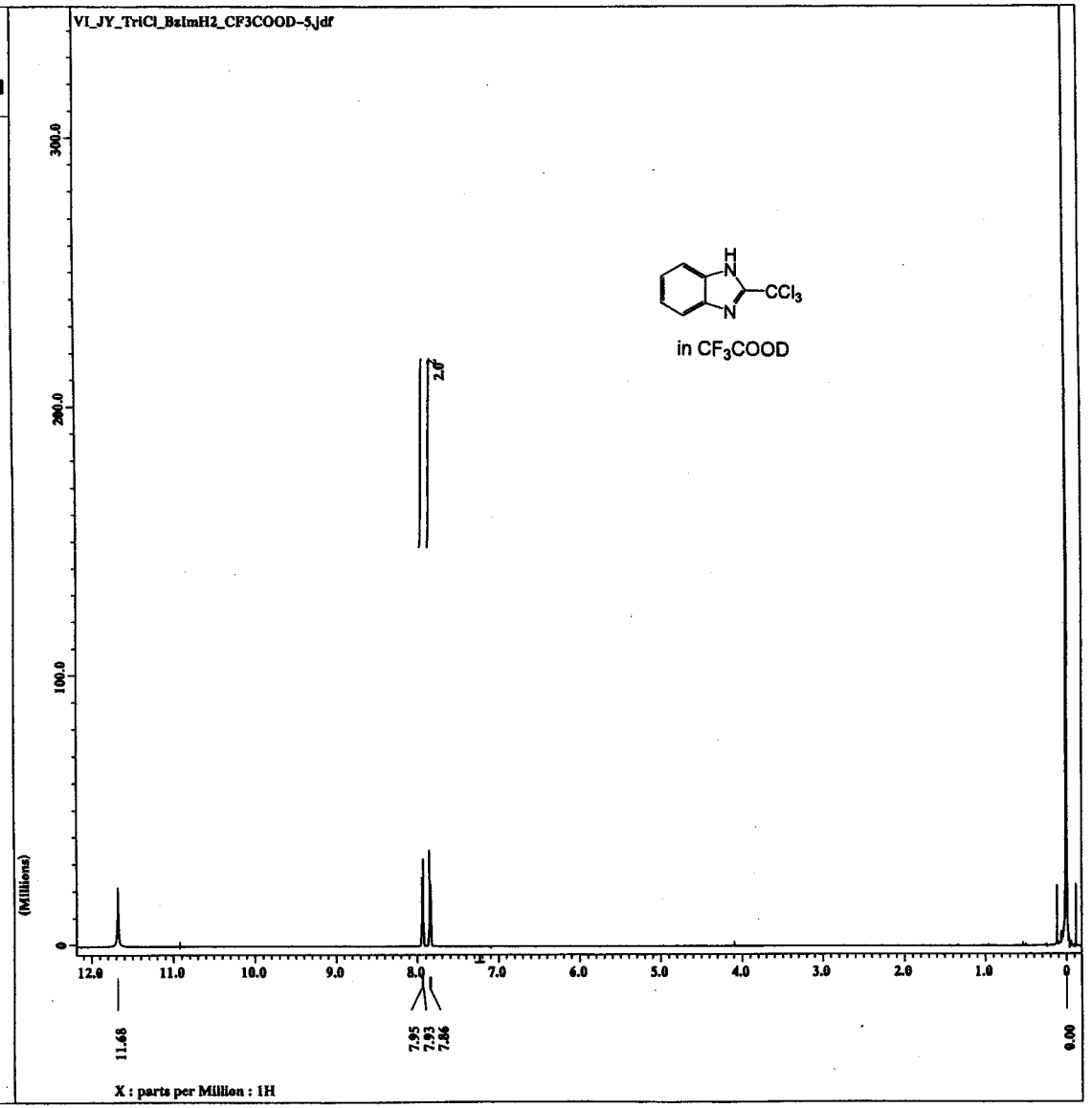

in CF_3COOD
V1_JY_TriCl_BzImH2_CF3COOD.5
X : parts per Million : 111
(Millions)
7.949
7.945
7.942
7.939
7.935
7.929
7.855
7.852
7.849
7.845
7.842
7.835
3.30
6.60
3.30
2.0
2

JEOL
---- ACQUISITION PARAMETERS ----
File Name = V1_JY_TriCl_BzImH2_TFA
Author =
Sample ID = S#229294
Content = Single Pulse with Broa
Creation Date = 13-SEP-2004 05:36:16
Revision Date = 20-SEP-2004 04:26:03
Spec Site = Eclipse+ 500
Spec Type = DELTA_NMR
Data Format = 1D COMPLEX
Dimensions = X
Dim Title = 13C
Dim Size = 65536
Dim Units = [ppm]
Acq_delay = 33.8[us]
Changer_sample = 0
Experiment = single_pulse_dec
Field_strength = 11.7473579[T]
Irr90 = 15[us]
Irr90_hl = 18[us]
Irr90_lo = 82[us]
Irr_domain = 1H
Irr_pWidth = 82[us]
Lock_status = IDLE
Recvr_gain = 29
Relaxation_delay = 2[s]
Scans = 1727
Solvent = TRIFLUOROACETIC_
Spin_pat = 14[Hz]
Spin_lock_90 = 60[us]
Spin_lock_attn = 15[dB]
Spin_set = 15[Hz]
Spin_state = SPIN ON
Spin_status = SPIN ON
Temp_pat = 25.6[dC]
Temp_set = 25.6[dC]
Temp_state = TEMP OFF
Temp_status = OFF
X90 = 14[us]
X90_hl = 13[us]
X90_lo = 53[us]
X_acq_duration = 2.0840448[s]
X_domain = 13C
X_freq = 125.76529768[MHz]
X_offset = 100[ppm]
X_points = 65536
X_prescans = 4
X_pulse = 4.66666667[us]
X_resolution = 0.4798363[Hz]
X_sweep = 31.44654088[kHz]
V1_JY_TriCl_BzImH2_TFA4
(Billions)
in CF_3COOD
164.292
163.945
163.598
149.561
132.427
131.778
119.992
117.741
116.688
115.486
113.235
83.621
0.000
X : parts per Million : 13C

JEOL
---- ACQUISITION PARAMETERS ----
File Name = VI_JV_TriCl_BzImH2_TFA
Author =
Sample ID = S#229294
Content = Single Pulse with Broa
Creation Date = 13-SEP-2004 05:36:16
Revision Date = 20-SEP-2004 04:26:03
Spec Site = Eclipse+ 500
Spec Type = DELTA_NMR
Data Format = 1D COMPLEX
Dimensions = X
Dim Title = 13C
Dim Size = 65536
Dim Units = [ppm]
Acq_delay = 33.8[us]
Changer_sample = 0
Experiment = single_pulse_dec
Field_strength = 11.7473579[T]
Irr90 = 15[us]
Irr90_hi = 18[us]
Irr90_lo = 82[us]
Irr_domain = 1H
Irr_pwidth = 82[us]
Lock_status = IDLE
Recvr_gain = 29
Relaxation_delay = 2[s]
Scans = 1727
Solvent = TRIFLUOROACETIC_
Spin_get = 14[Hz]
Spin_lock_90 = 60[us]
Spin_lock_attn = 15[dB]
Spin_set = 15[Hz]
Spin_state = SPIN ON
Spin_status = SPIN ON
Temp_get = 25.6[dC]
Temp_set = 25[dC]
Temp_state = TEMP OFF
Temp_status = TEMP OFF
X90 = 14[us]
X90_hi = 13[us]
X90_lo = 53[us]
X_acq_duration = 2.0840448[s]
X_domain = 13C
X_freq = 125.76529768[MHz]
X_offset = 100[ppm]
X_points = 65536
X_prescans = 4
X_pulse = 4.66666667[us]
X_resolution = 0.47983613[Hz]
X_sweep = 31.44654088[kHz]
VI_JV_TriCl_BzImH2_TFA.4
(Billions)
4.0
3.0
2.0
1.0
0
160.0
150.0
140.0
130.0
120.0
110.0
100.0
90.0
80.0
149.561
132.427
131.778
119.992
117.741
116.688
115.486
113.235
83.621
X : parts per Million : 13C

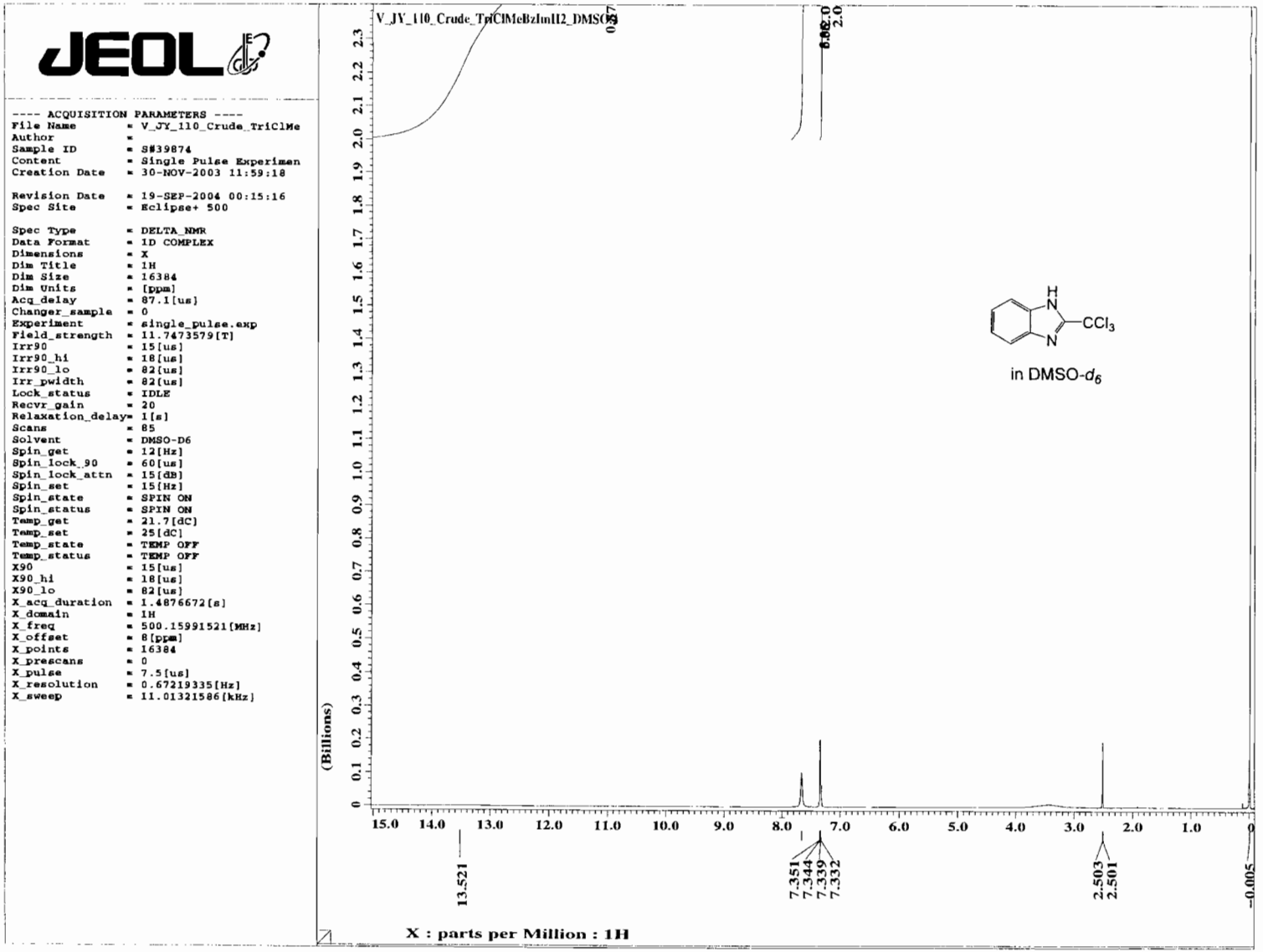
JEOL
---- ACQUISITION PARAMETERS ----
File Name = V_JY_110_Crude_TriClMe
Author =
Sample ID = S#39874
Content = Single Pulse Experimen
Creation Date = 30-NOV-2003 11:59:18
Revision Date = 19-SEP-2004 00:15:16
Spec Site = Eclipse+ 500
Spec Type = DELTA_NMR
Data Format = 1D COMPLEX
Dimensions = X
Dim Title = 1H
Dim Size = 16384
Dim Units = [ppm]
Acq_delay = 87.1[us]
Changer_sample = 0
Experiment = single_pulse.exp
Field_strength = 11.7473579[T]
Irr90 = 15[us]
Irr90_hi = 18[us]
Irr90_lo = 82[us]
Irr_pwidth = 82[us]
Lock_status = IDLE
Recvr_gain = 20
Relaxation_delay= 1[s]
Scans = 85
Solvent = DMSO-D6
Spin_get = 12[Hz]
Spin_lock_90 = 60[us]
Spin_lock_attn = 15[dB]
Spin_set = 15[Hz]
Spin_state = SPIN ON
Spin_status = SPIN ON
Temp_get = 21.7[dC]
Temp_set = 25[dC]
Temp_state = TEMP OFF
Temp_status = TEMP OFF
X90 = 15[us]
X90_hi = 18[us]
X90_lo = 82[us]
X_acq_duration = 1.4876672[s]
X_domain = 1H
X_freq = 500.15991521[MHz]
X_offset = 8[ppm]
X_points = 16384
X_prescans = 0
X_pulse = 7.5[us]
X_resolution = 0.67219335[Hz]
X_sweep = 11.01321586[kHz]
V_JY_110_Crude_TriClMeBzIm112_DMSO.1
(Billions)
13.521
7.351
7.344
7.339
7.332
2.503
2.501
-0.005
X : parts per Million : 1H
H
N
N
CCl3
in DMSO-d6

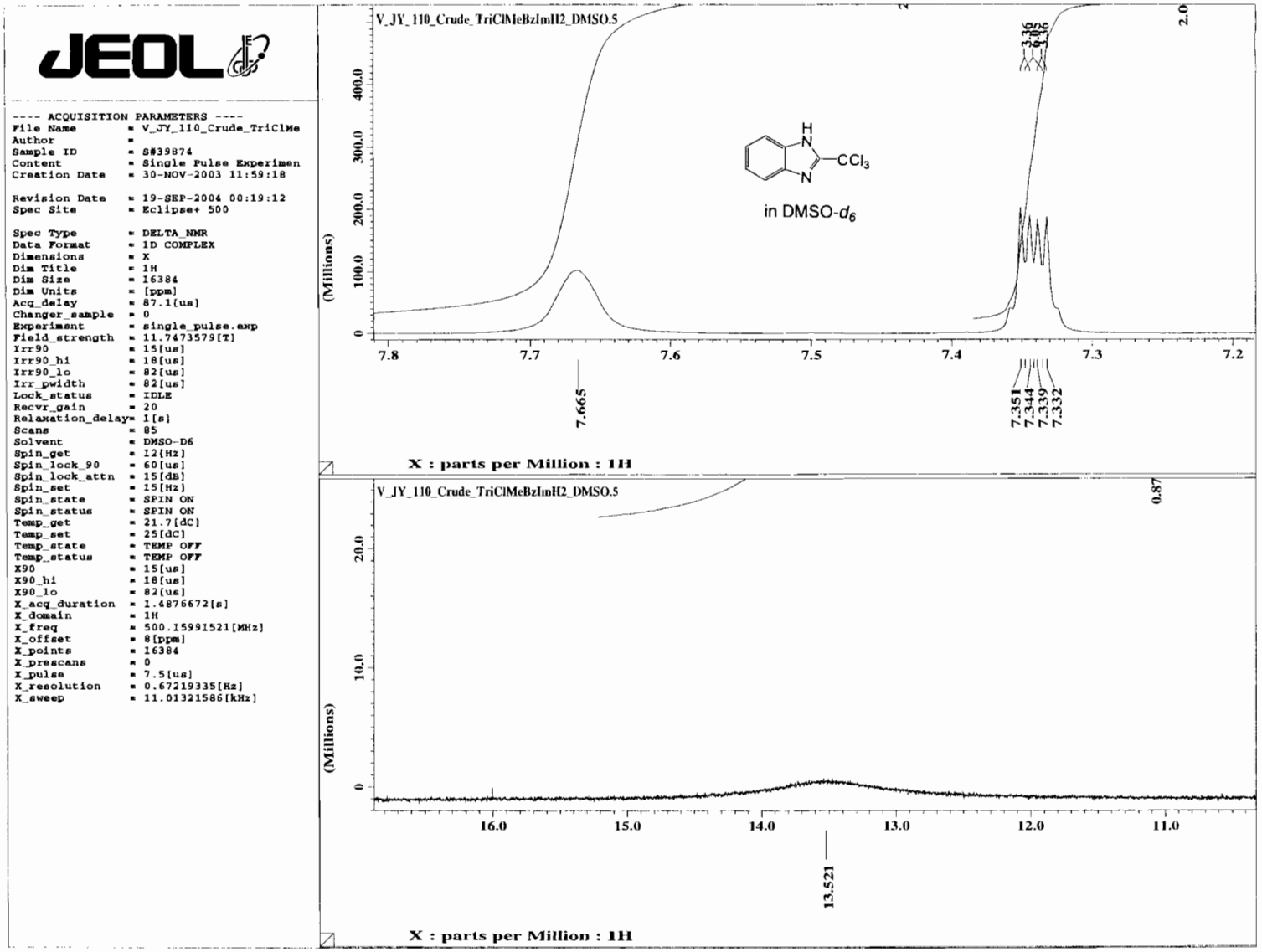
JEOL
---- ACQUISITION PARAMETERS ----
File Name = V_JY_110_Crude_TriClMe
Author =
Sample ID = S#39874
Content = Single Pulse Experimen
Creation Date = 30-NOV-2003 11:59:18
Revision Date = 19-SEP-2004 00:19:12
Spec Site = Eclipse+ 500
Spec Type = DELTA_NMR
Data Format = 1D COMPLEX
Dimensions = X
Dim Title = 1H
Dim Size = 16384
Dim Units = [ppm]
Acq_delay = 87.1[us]
Changer_sample = 0
Experiment = single_pulse.exp
Field_strength = 11.7473579[T]
Irr90 = 15[us]
Irr90_hi = 18[us]
Irr90_lo = 82[us]
Irr_pwidth = 82[us]
Lock_status = IDLE
Recvr_gain = 20
Relaxation_delay= 1[s]
Scans = 85
Solvent = DMSO-D6
Spin_get = 12[Hz]
Spin_lock_90 = 60[us]
Spin_lock_attn = 15[dB]
Spin_set = 15[Hz]
Spin_state = SPIN ON
Spin_status = SPIN ON
Temp_get = 21.7[dC]
Temp_set = 25[dC]
Temp_state = TEMP OFF
Temp_status = TEMP OFF
X90 = 15[us]
X90_hi = 18[us]
X90_lo = 82[us]
X_acq_duration = 1.4876672[s]
X_domain = 1H
X_freq = 500.15991521[MHz]
X_offset = 8[ppm]
X_points = 16384
X_prescans = 0
X_pulse = 7.5[us]
X_resolution = 0.67219335[Hz]
X_sweep = 11.01321586[kHz]
V_JY_110_Crude_TriClMeBzImH2_DMSO.5
(Millions)
400.0
300.0
200.0
100.0
0
7.8
7.7
7.6
7.5
7.4
7.3
7.2
7.665
7.351
7.344
7.339
7.332
3.36
6.06
4.16
2.0
in DMSO-d_6
X : parts per Million : 1H
V_JY_110_Crude_TriClMeBzImH2_DMSO.5
0.87
(Millions)
20.0
10.0
0
16.0
15.0
14.0
13.0
12.0
11.0
13.521
X : parts per Million : 1H

JEOL
---- ACQUISITION PARAMETERS ----
File Name = V_JY_110_Crude_TriClMe
Author =
Sample ID = S#51851
Content = Single Pulse with Broa
Creation Date = 30-NOV-2003 12:56:47
Revision Date = 19-SEP-2004 00:25:54
Spec Site = Eclipse+ 500
Spec Type = DELTA_NMR
Data Format = 1D COMPLEX
Dimensions = X
Dim Title = 13C
Dim Size = 32768
Dim Units = [ppm]
Acq_delay = 33.8[us]
Changer_sample = 0
Experiment = single_pulse_dec
Field_strength = 11.7473579[T]
Irr90 = 15[us]
Irr90_hi = 18[us]
Irr90_lo = 82[us]
Irr_domain = 1H
Irr_pwidth = 82[us]
Lock_status = IDLE
Recvr_gain = 30
Relaxation_delay= 1[s]
Scans = 1141
Solvent = DMSO-D6
Spin_get = 16[Hz]
Spin_lock_90 = 60[us]
Spin_lock_atn = 15[dB]
Spin_set = 15[Hz]
Spin_state = SPIN ON
Spin_status = SPIN ON
Temp_get = 22.2[dC]
Temp_set = 25[dC]
Temp_state = TEMP OFF
Temp_status = TEMP OFF
X90 = 14[us]
X90_hi = 13[us]
X90_lo = 53[us]
X_acq_duration = 1.0420224[s]
X_domain = 13C
X_freq = 125.76529768[MHz]
X_offset = 100[ppm]
X_points = 32768
X_prescans = 4
X_pulse = 4.66666667[us]
X_resolution = 0.95967227[Hz]
X_sweep = 31.4465408[kHz]
V_JY_110_Crude_TriClMeBzImH2_DMSO.6
in DMSO-d_6
(Billions)
X : parts per Million : 13C
150.553
137.977
123.754
116.230
88.782
39.542
39.374
39.206
-0.000

Transmittance [%]
0
20
40
60
80
100
4000
3500
3000
2500
2000
1500
1000
500
Wavenumber cm-1
2828.59
2723.19
1941.80
1780.79
1620.67
1589.83
1518.70
1486.27
1448.24
1428.37
1367.73
1309.41
1278.34
1228.37
1147.60
1043.61
1024.81
1000.10
935.04
911.96
892.55
816.10
788.40
765.85
742.82
682.93
618.40
561.28
501.47
BRUKER
D:\OPUS_NT\DATA\Juun\V_JY_TriClMe_BiBzImH2.0
V_JY_TriClMe_BiBzImH2
Solid in KBr
27/05/2005

APPENDIX 4

^{1}H, ^{13}C NMR SPECTRA OF

Fluoflavin **11**

JEOL

Filename	= VIII_JY_Fluoflavin_Pu
Author	= delta
Experiment	= single_pulse.exp
Sample_id	= S#747028
Solvent	= TRIFLUOROACETIC_
Creation_time	= 26-NOV-2005 22:20:41
Revision_time	= 29-NOV-2005 20:41:24
Current_time	= 29-NOV-2005 20:52:01
Content	= Single Pulse Experime
Data_format	= 1D COMPLEX
Dim_size	= 16384
Dim_title	= 1H
Dim_units	= [ppm]
Dimensions	= X
Site	= Eclipse+ 500
Spectrometer	= DELTA_NMR
Field_strength	= 11.7473579[T] (500[MH
X_acq_duration	= 1.6367616[s]
X_domain	= 1H
X_freq	= 500.15991521[MHz]
X_offset	= 8[ppm]
X_points	= 16384
X_prescans	= 0
X_resolution	= 0.61096253[Hz]
X_sweep	= 10.01001001[kHz]
Clipped	= FALSE
Mod_return	= 1
Scans	= 100
Total_scans	= 100
X_90_width	= 18.5[us]
X_acq_time	= 1.6367616[s]
X_angle	= 45[deg]
X_pulse	= 9.25[us]
Initial_wait	= 1[s]
Phase_preset	= 3[us]
Recvr_gain	= 12
Relaxation_delay	= 1[s]
Temp_get	= 25.3[dC]
Unblank_time	= 2[us]

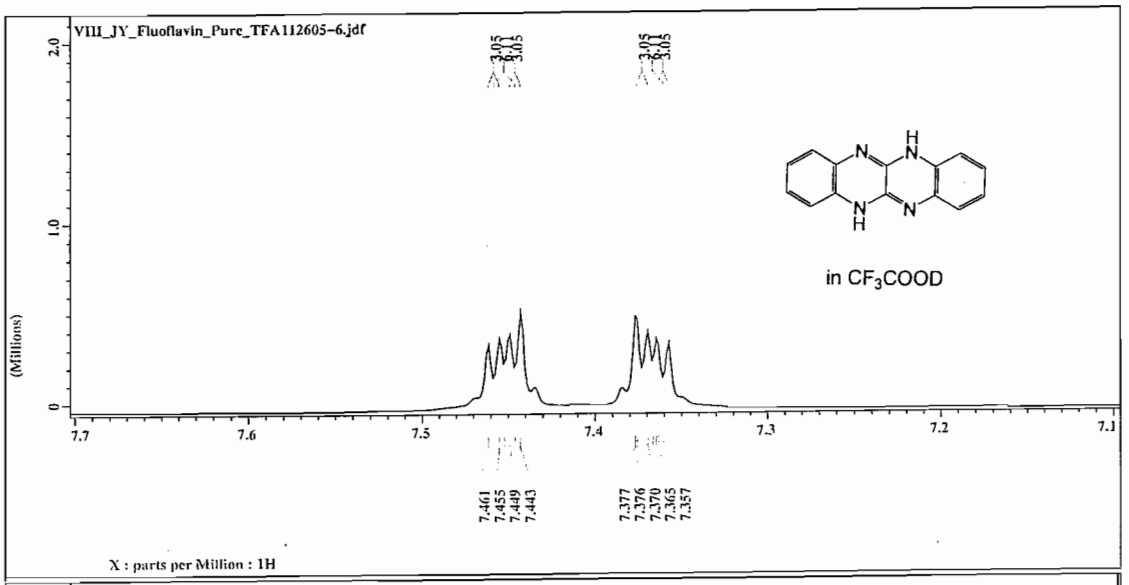

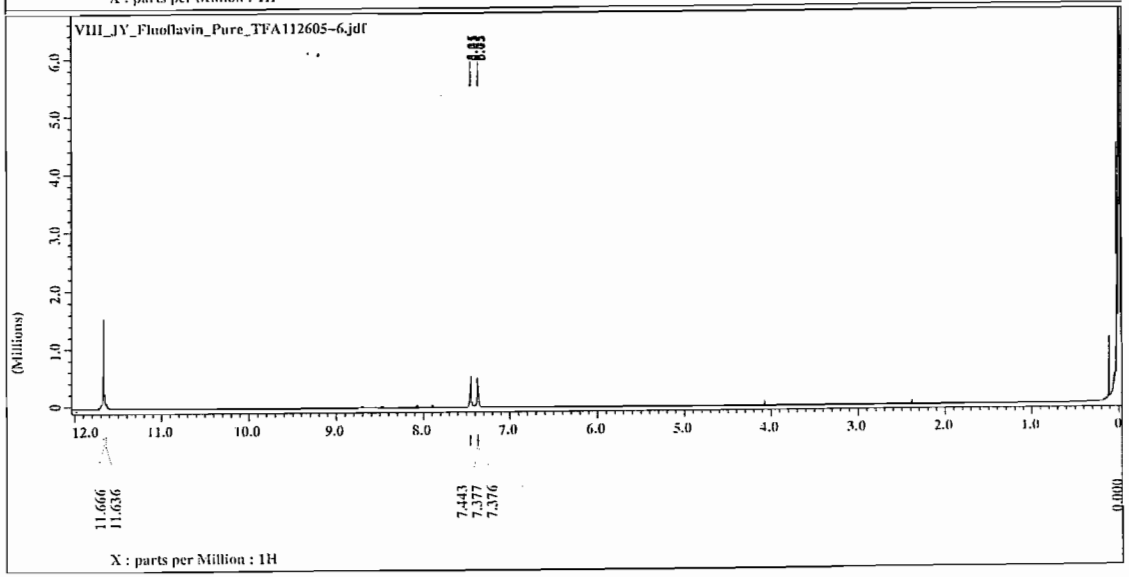

JEOL

```
Filename          = VIII_JY_Fluoflavin_TF
Author            = delta
Experiment        = single_pulse_dec
Sample_id         = S#750981
Solvent           = TRIFLUOROACETIC_
Creation_time     = 27-NOV-2005 01:03:47
Revision_time     = 29-NOV-2005 20:55:55
Current_time      = 29-NOV-2005 20:57:06

Content           = single pulse decouple
Data_format       = 1D COMPLEX
Dim_size          = 65536
Dim_title         = 13C
Dim_units         = [ppm]
Dimensions        = X
Site              = Eclipse+ 500
Spectrometer      = DELTA_NMR

Field_strength    = 11.7473579[T] (500[MH
X_acq_duration    = 2.0840448[s]
X_domain          = 13C
X_freq            = 125.76529768[MHz]
X_offset          = 100[ppm]
X_points          = 65536
X_prescans        = 4
X_resolution      = 0.47983613[Hz]
X_sweep           = 31.44654088[kHz]
Irr_domain        = 1H
Irr_freq          = 500.15991521[MHz]
Irr_offset        = 5[ppm]
Clipped           = FALSE
Mod_return        = 1
Scans             = 1885
Total_scans       = 1885

X_90_width        = 14.2[us]
X_acq_time        = 2.0840448[s]
X_angle           = 30[deg]
X_pulse           = 4.73333333[us]
Initial_wait      = 1[s]
Noe_time          = 1[s]
Phase_preset      = 3[us]
Recvr_gain        = 29
Relaxation_delay  = 2[s]
Temp_get          = 27.2[dC]
Unblank_time      = 2[us]
```

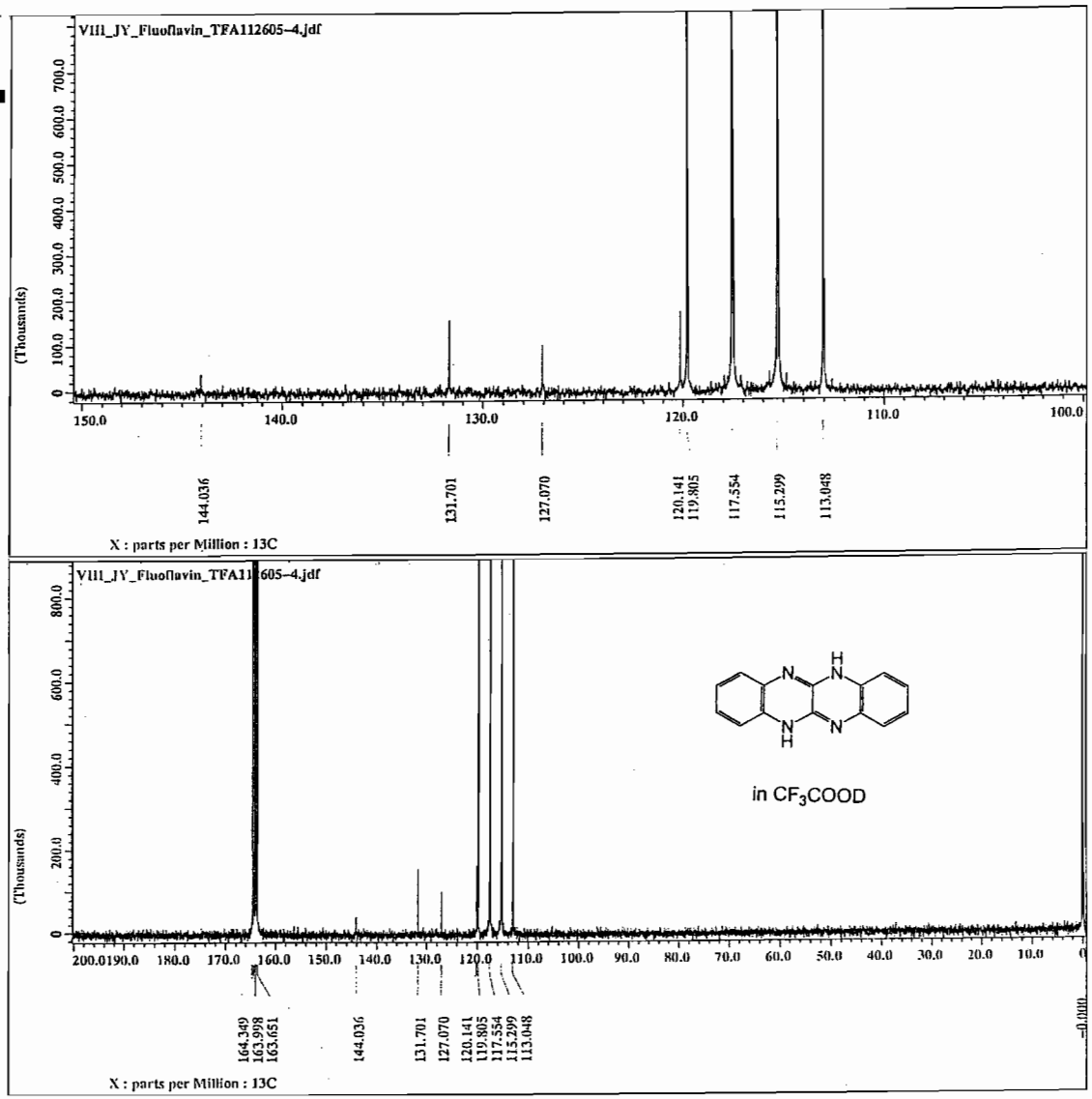

APPENDIX 5

^{1}H, ^{13}C, COSY NMR, ESI MASS, FTIR SPECTRA, AND X-RAY CRYSTALLOGRAPHY DATA OF Bis(2,2′-bibenzimidazole) **14**

```
Filename          = V_JY_130_Dimer_NH4OHW
Experiment        = single_pulse.exp
Sample_id         = S#855763
Solvent           = TRIFLUOROACETIC_
Creation_time     = 15-DEC-2003 18:37:34
Revision_time     = 25-MAY-2005 21:09:44
Current_time      = 25-MAY-2005 21:09:57

Content           = Single Pulse Experime
Data_format       = 1D COMPLEX
Dim_size          = 16384
Dim_title         = 1H
Dim_units         = [ppm]
Dimensions        = X
Site              = Eclipse+ 500
Spectrometer      = DELTA_NMR

Field_strength    = 11.7473579[T] (500[MH
X_acq_duration    = 1.818624[s]
X_domain          = 1H
X_freq            = 500.15991521[MHz]
X_offset          = 7[ppm]
X_points          = 16384
X_prescans        = 0
X_resolution      = 0.54986627[Hz]
X_sweep           = 9.00900901[kHz]
Mod_return        = 1
Scans             = 53

X_90_width        = 15[us]
X_acq_time        = 1.818624[s]
X_angle           = 45[deg]
X_pulse           = 7.5[us]
Initial_wait      = 1[s]
Phase_preset      = 3[us]
Recvr_gain        = 18
Relaxation_delay  = 1[s]
Temp_get          = 22.4[dC]
Unblank_time      = 2[us]
```

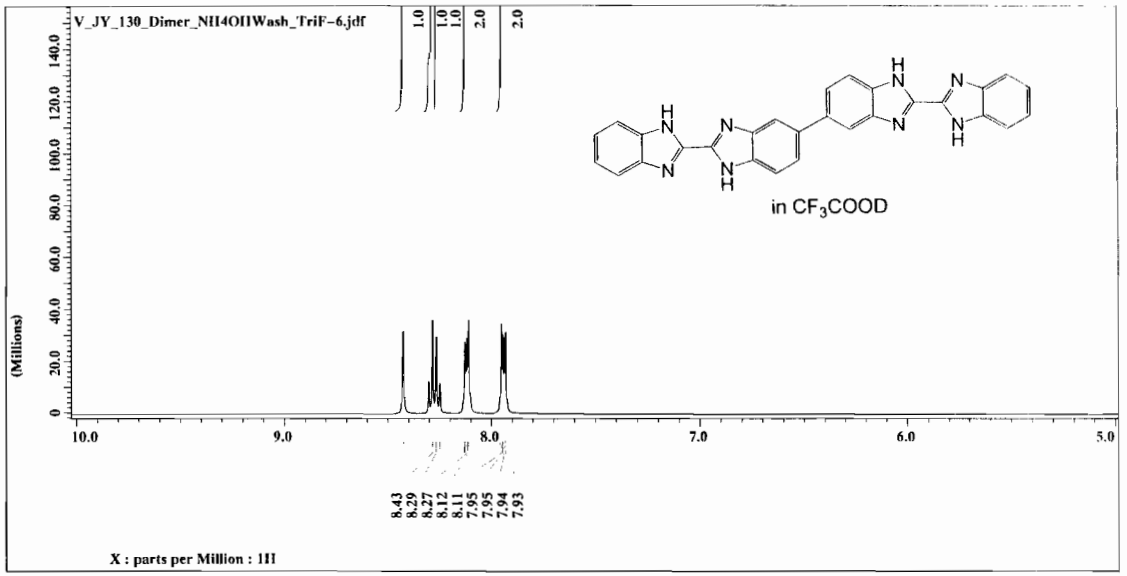

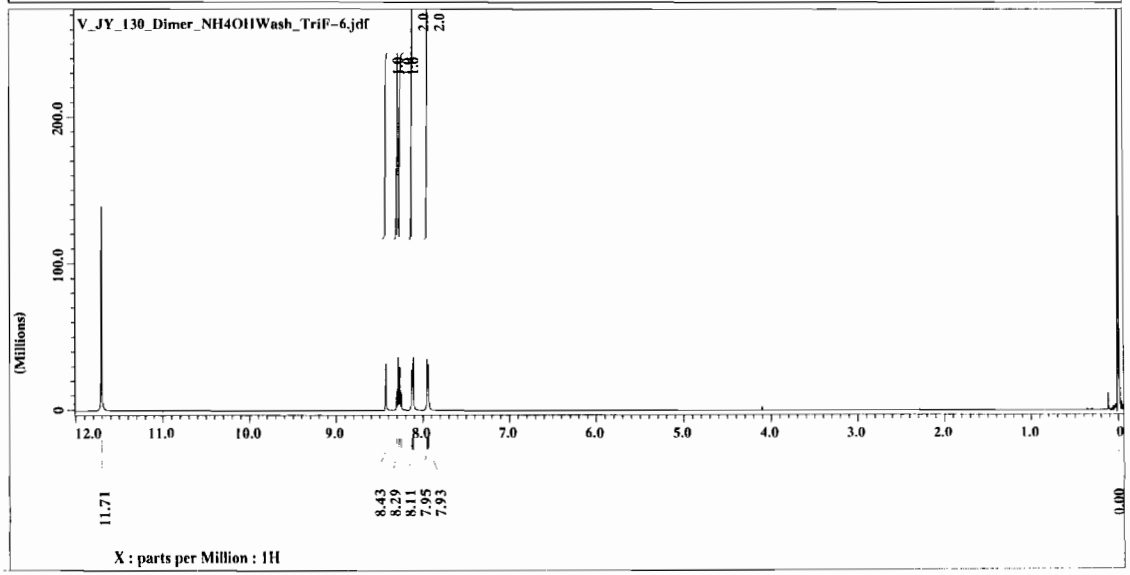

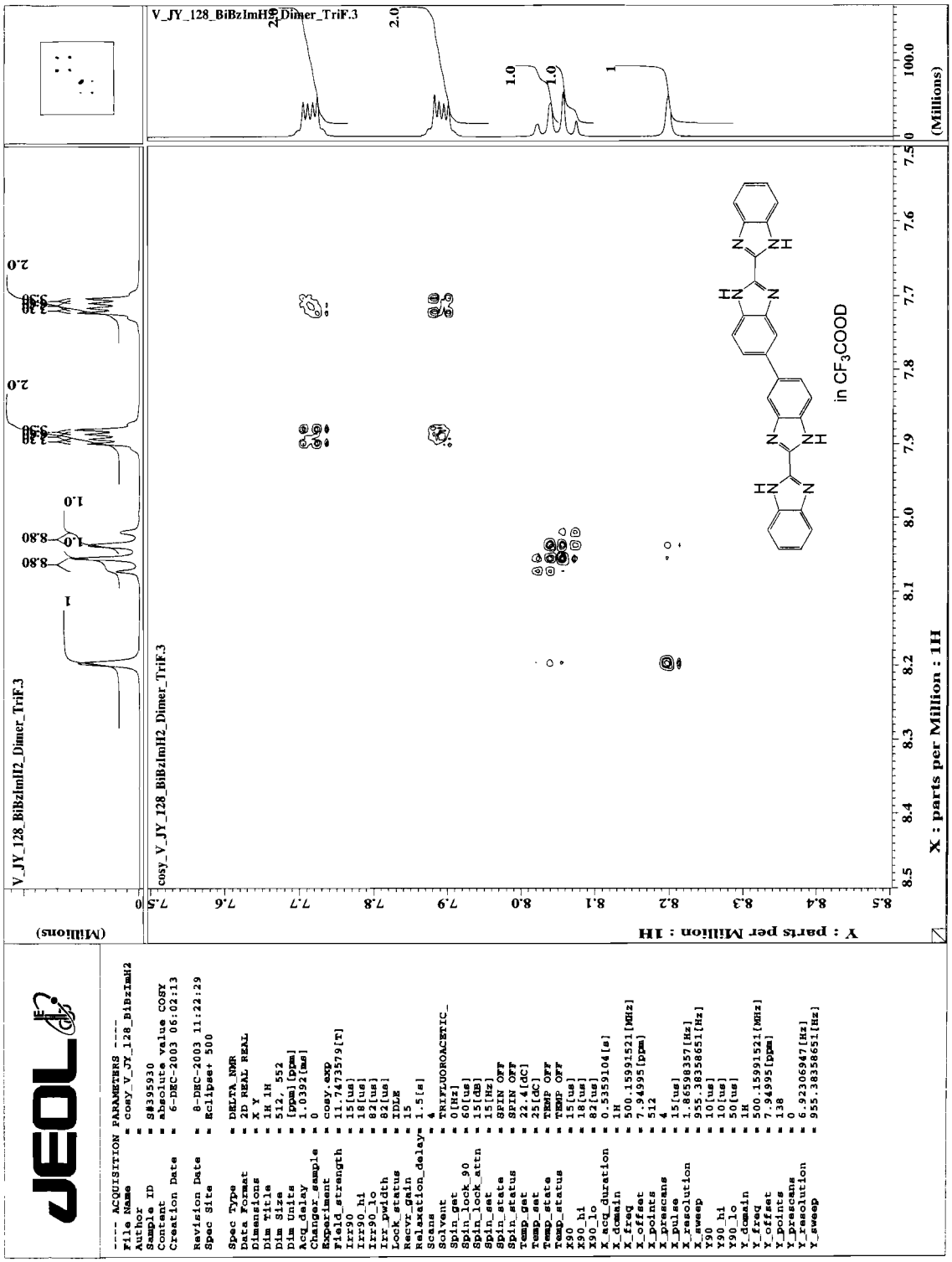
JEOL
V_JY_128_BiBzImH2_Dimer_TriF.3
cosy_V_JY_128_BiBzImH2_Dimer_TriF.3
in CF_3COOD
X : parts per Million : 1H
Y : parts per Million : 1H
(Millions)

```
Filename          = V_JY_128_BiBzImH2_Dim
Experiment        = single_pulse_dec
Sample_id         = S#408656
Solvent           = TRIFLUOROACETIC_
Creation_time     =  6-DEC-2003 15:30:29
Revision_time     = 10-DEC-2003 09:54:39
Current_time      = 25-MAY-2005 21:15:21

Content           = Single Pulse with Bro
Data_format       = 1D COMPLEX
Dim_size          = 65536
Dim_title         = 13C
Dim_units         = [ppm]
Dimensions        = X
Site              = Eclipse+ 500
Spectrometer      = DELTA_NMR

Field_strength    = 11.7473579[T] (500[MH
X_acq_duration    = 2.0840448[s]
X_domain          = 13C
X_freq            = 125.76529768[MHz]
X_offset          = 100[ppm]
X_points          = 65536
X_prescans        = 4
X_resolution      = 0.47983613[Hz]
X_sweep           = 31.44654088[kHz]
Irr_domain        = 1H
Irr_freq          = 500.15991521[MHz]
Irr_offset        = 5[ppm]
Mod_return        = 1
Scans             = 11000

X_90_width        = 14[us]
X_acq_time        = 2.0840448[s]
X_angle           = 30[deg]
X_pulse           = 4.66666667[us]
Initial_wait      = 1[s]
Phase_preset      = 3[us]
Recvr_gain        = 29
Relaxation_delay  = 1[s]
Temp_get          = 23.3[dC]
Unblank_time      = 2[us]
```

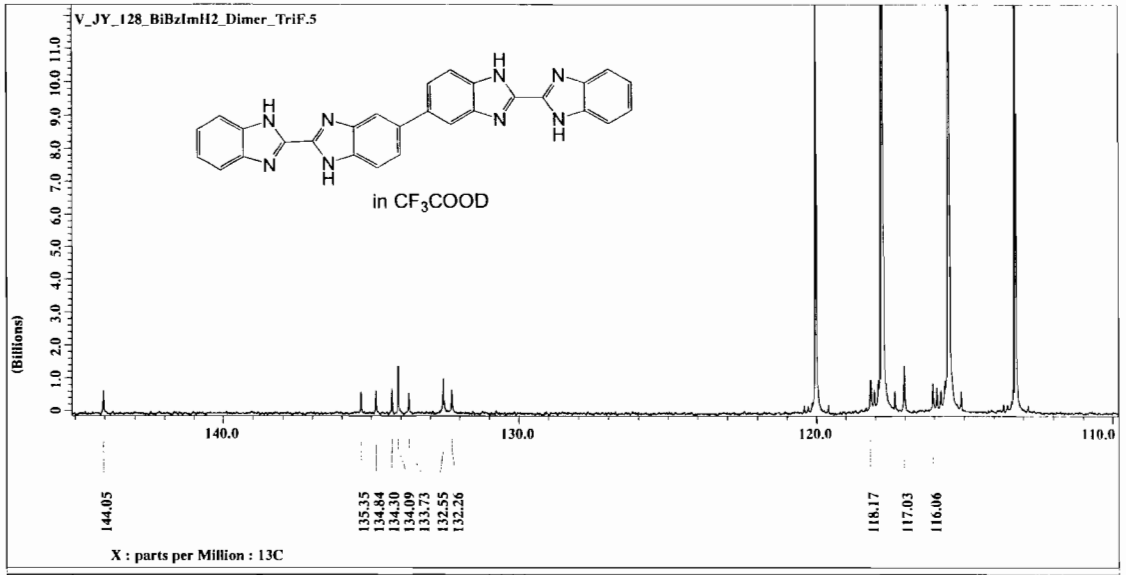

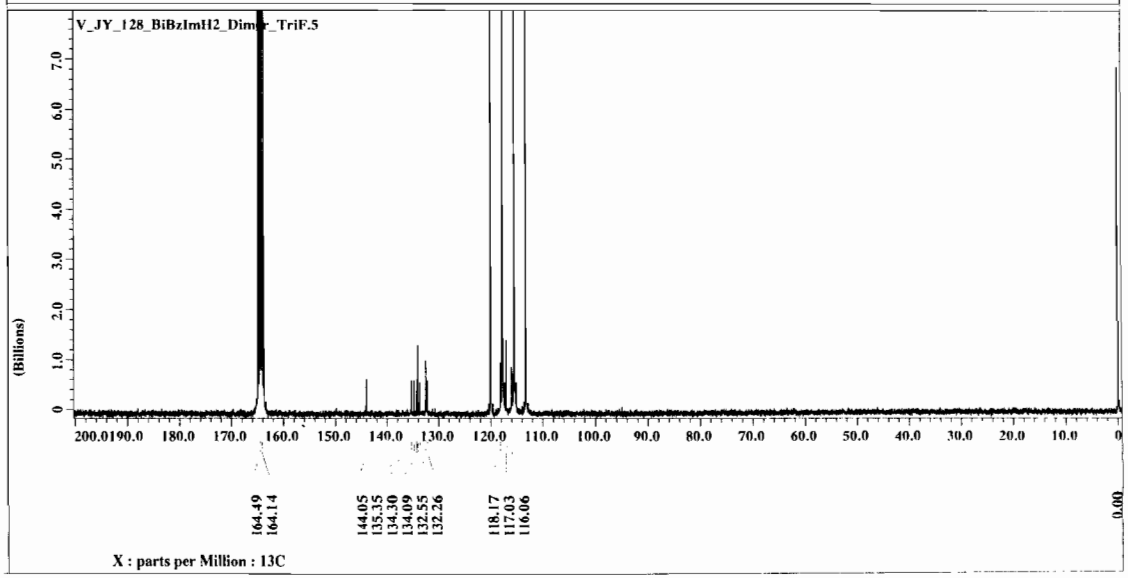

JEOL

Filename	= V_JY_130_BiBzImH2_Dim
Experiment	= single_pulse.exp
Sample_id	= S#827345
Solvent	= DMSO-D6
Creation_time	= 11-DEC-2003 17:49:19
Revision_time	= 25-MAY-2005 21:35:53
Current_time	= 25-MAY-2005 21:36:28
Content	= Single Pulse Experime
Data_format	= 1D COMPLEX
Dim_size	= 16384
Dim_title	= 1H
Dim_units	= [ppm]
Dimensions	= X
Site	= Eclipse+ 500
Spectrometer	= DELTA_NMR
Field_strength	= 11.7473579[T] (500[MH
X_acq_duration	= 1.4876672[s]
X_domain	= 1H
X_freq	= 500.15991521[MHz]
X_offset	= 8[ppm]
X_points	= 16384
X_prescans	= 0
X_resolution	= 0.67219335[Hz]
X_sweep	= 11.01321586[kHz]
Mod_return	= 1
Scans	= 100
X_90_width	= 15[us]
X_acq_time	= 1.4876672[s]
X_angle	= 45[deg]
X_pulse	= 7.5[us]
Initial_wait	= 1[s]
Phase_preset	= 3[us]
Recvr_gain	= 19
Relaxation_delay	= 1[s]
Temp_get	= 21.8[dC]
Unblank_time	= 2[us]

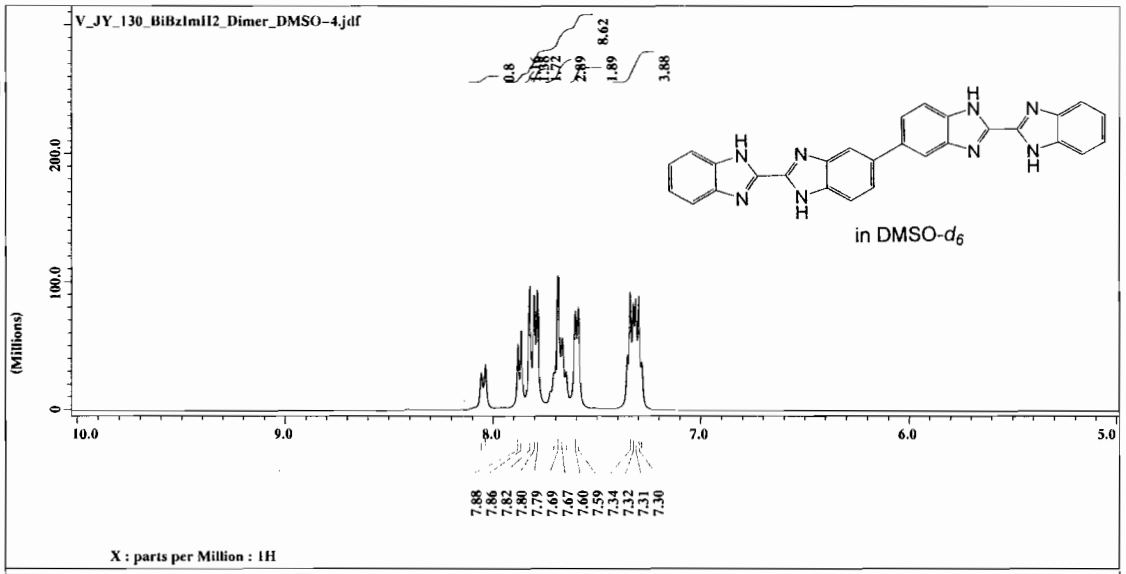

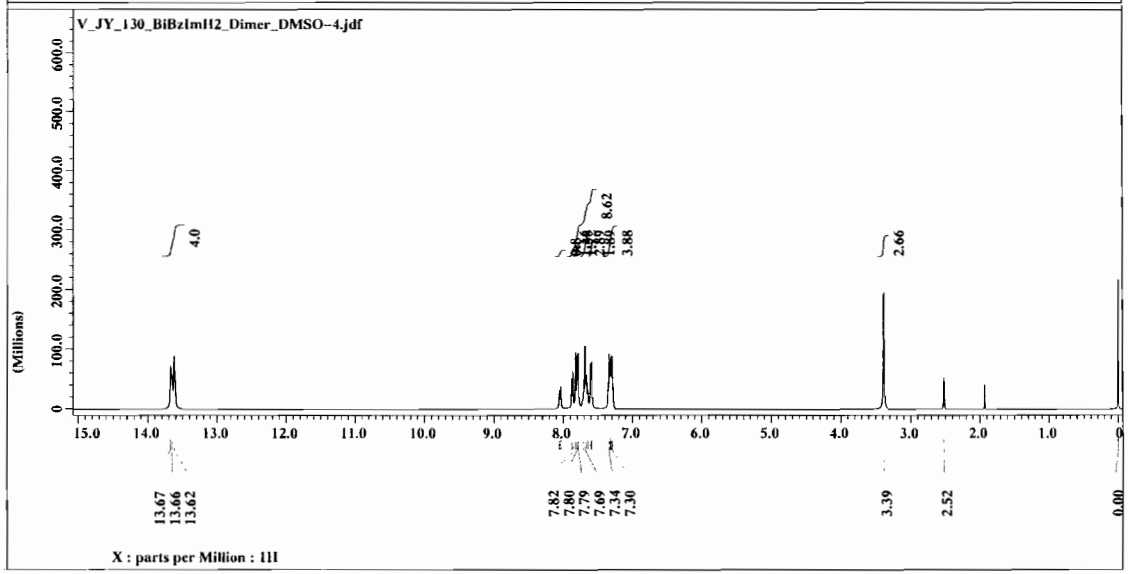

JEOL

```
Filename          = V_JY_130_BiBzImH2_Dim
Experiment        = single_pulse_dec
Sample_id         = S#840177
Solvent           = DMSO-D6
Creation_time     = 11-DEC-2003 20:52:03
Revision_time     = 14-DEC-2003 11:02:34
Current_time      = 25-MAY-2005 21:19:38

Content           = Single Pulse with Bro
Data_format       = 1D COMPLEX
Dim_size          = 32768
Dim_title         = 13C
Dim_units         = [ppm]
Dimensions        = X
Site              = Eclipse+ 500
Spectrometer      = DELTA_NMR

Field_strength    = 11.7473579[T] (500[MH
X_acq_duration    = 1.0420224[s]
X_domain          = 13C
X_freq            = 125.76529768[MHz]
X_offset          = 100[ppm]
X_points          = 32768
X_prescans        = 4
X_resolution      = 0.95967227[Hz]
X_sweep           = 31.44654088[kHz]
Irr_domain        = 1H
Irr_freq          = 500.15991521[MHz]
Irr_offset        = 5[ppm]
Mod_return        = 1
Scans             = 3256

X_90_width        = 14[us]
X_acq_time        = 1.0420224[s]
X_angle           = 30[deg]
X_pulse           = 4.66666667[us]
Initial_wait      = 1[s]
Phase_preset      = 3[us]
Recvr_gain        = 29
Relaxation_delay  = 2[s]
Temp_get          = 22.6[dC]
Unblank_time      = 2[us]
```

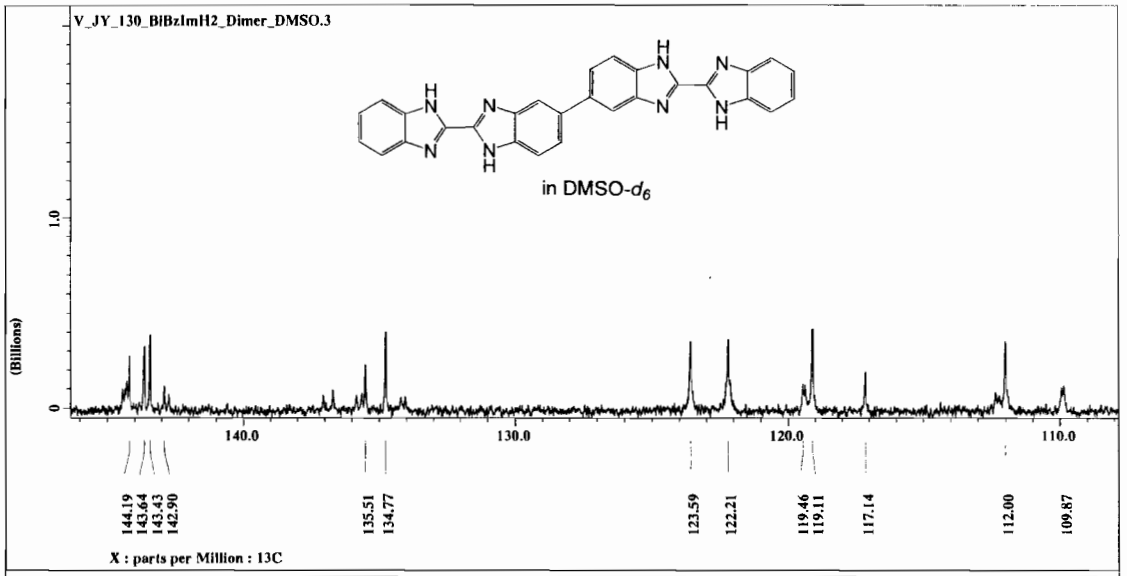

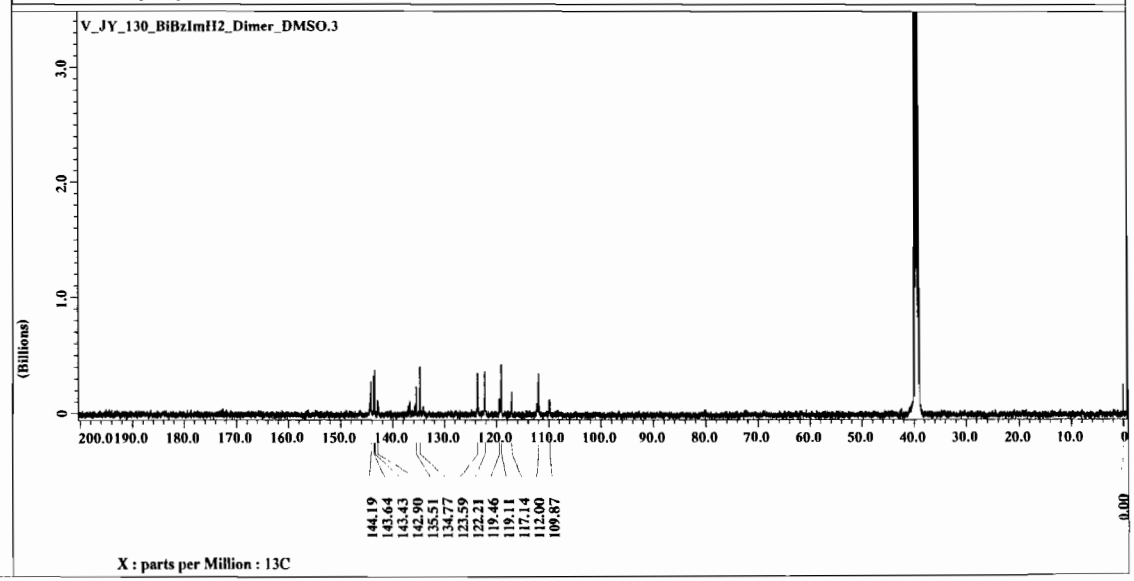

JEOL

```
---- ACQUISITION PARAMETERS ----
File Name          = V_JY_173_DimerBiBzImH2
Author             =
Sample ID          = S#230282
Content            = Single Pulse Experimen
Creation Date      = 22-NOV-2004 02:46:52

Revision Date      = 28-NOV-2004 06:28:05
Spec Site          = Eclipse+ 500

Spec Type          = DELTA_NMR
Data Format        = 1D COMPLEX
Dimensions         = X
Dim Title          = 1H
Dim Size           = 16384
Dim Units          = [ppm]
Acq_delay          = 96.2[us]
Changer_sample     = 0
Experiment         = single_pulse.exp
Field_strength     = 11.7473579[T]
Irr90              = 15[us]
Irr90_hi           = 18[us]
Irr90_lo           = 82[us]
Irr_pwidth         = 82[us]
Lock_status        = IDLE
Recvr_gain         = 14
Relaxation_delay   = 1[s]
Scans              = 28
Solvent            = TRIFLUOROACETIC_
Spin_get           = 16[Hz]
Spin_lock_90       = 60[us]
Spin_lock_attn     = 15[dB]
Spin_set           = 15[Hz]
Spin_state         = SPIN ON
Spin_status        = SPIN ON
Temp_get           = 23.7[dC]
Temp_set           = 25[dC]
Temp_state         = TEMP OFF
Temp_status        = TEMP OFF
X90                = 15[us]
X90_hi             = 18[us]
X90_lo             = 82[us]
X_acq_duration     = 1.6367616[s]
X_domain           = 1H
X_freq             = 500.15991521[MHz]
X_offset           = 8[ppm]
X_points           = 16384
X_prescans         = 0
X_pulse            = 7.5[us]
X_resolution       = 0.61096253[Hz]
X_sweep            = 10.01001001[kHz]
```

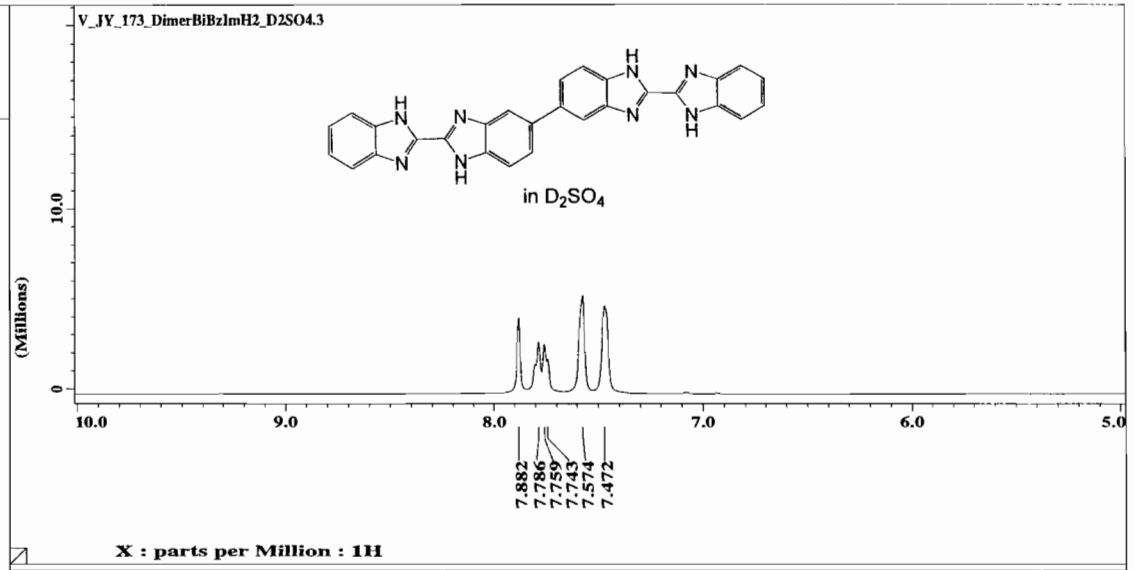

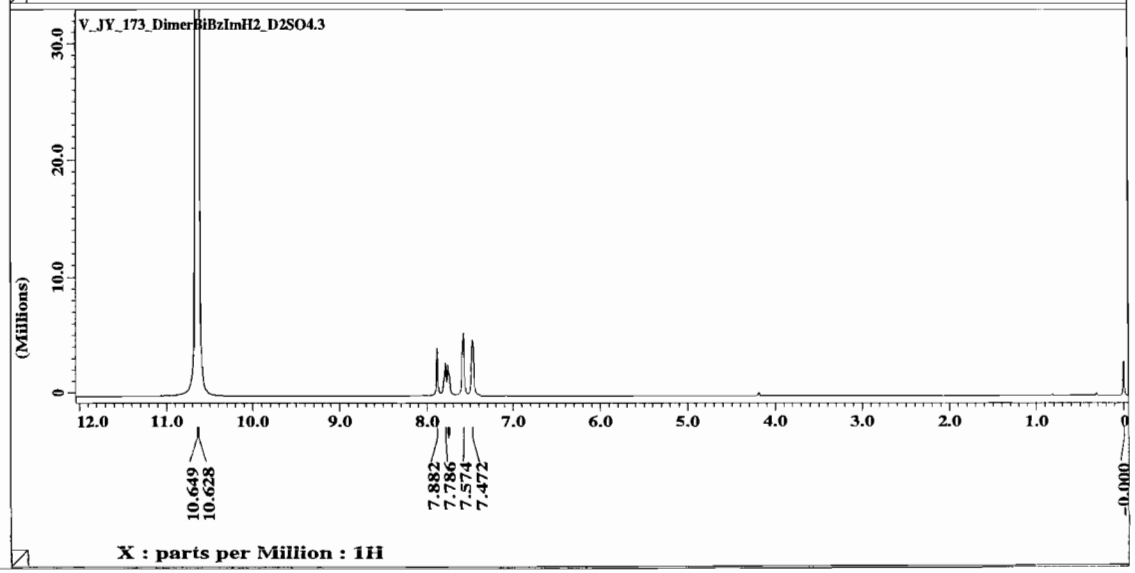

JEOL
---- ACQUISITION PARAMETERS ----
File Name = V_JY_173_BisBiBzImH2_D
Author =
Sample ID = &#032533
Content = Single Pulse with Bros
Creation Date = 28-NOV-2004 20:01:57
Revision Date = 5-DEC-2004 12:52:01
Spec Site = Eclipse+ 500
Spec Type = DELTA_NMR
Data Format = 1D COMPLEX
Dimensions = X
Dim Title = 13C
Dim Size = 65536
Dim Units = [ppm]
Acq_delay = 33.8[us]
Changer_sample = 0
Experiment = single_pulse.dec
Field_strength = 11.7473579[T]
Irr90 = 15[us]
Irr90_hi = 18[us]
Irr90_lo = 82[us]
Irr_domain = 1H
Irr_pwidth = 82[us]
Lock_status = IDLE
Recvr_gain = 29
Relaxation_delay = 2[s]
Scans = 11000
Solvent = TRIFLUOROACETIC_
Spin_get = 14[Hz]
Spin_lock_90 = 60[us]
Spin_lock_attn = 15[dB]
Spin_set = 15[Hz]
Spin_state = SPIN ON
Spin_status = SPIN ON
Temp_get = 24[dC]
Temp_set = 25[dC]
Temp_state = TEMP OFF
Temp_status = TEMP OFF
X90 = 14[us]
X90_hi = 13[us]
X90_lo = 53[us]
X_acq_duration = 2.0840448[s]
X_domain = 13C
X_freq = 125.76529768[MHz]
X_offset = 100[ppm]
X_points = 65536
X_prescans = 4
X_pulse = 4.66666667[us]
X_resolution = 0.47983613[Hz]
X_sweep = 31.44654088[kHz]
V_JY_173_BisBiBzImH2_D2SO4.5
in D_2SO_4
143.067
132.956
132.598
132.472
132.335
132.190
130.496
117.481
116.386
116.280
115.284
115.154
X : parts per Million : 13C
Billions
V_JY_173_BisBiBzImH2_D2SO4.5
143.067
132.956
132.598
132.472
132.335
132.190
130.496
116.386
116.280
115.284
115.154
X : parts per Million : 13C
Billions

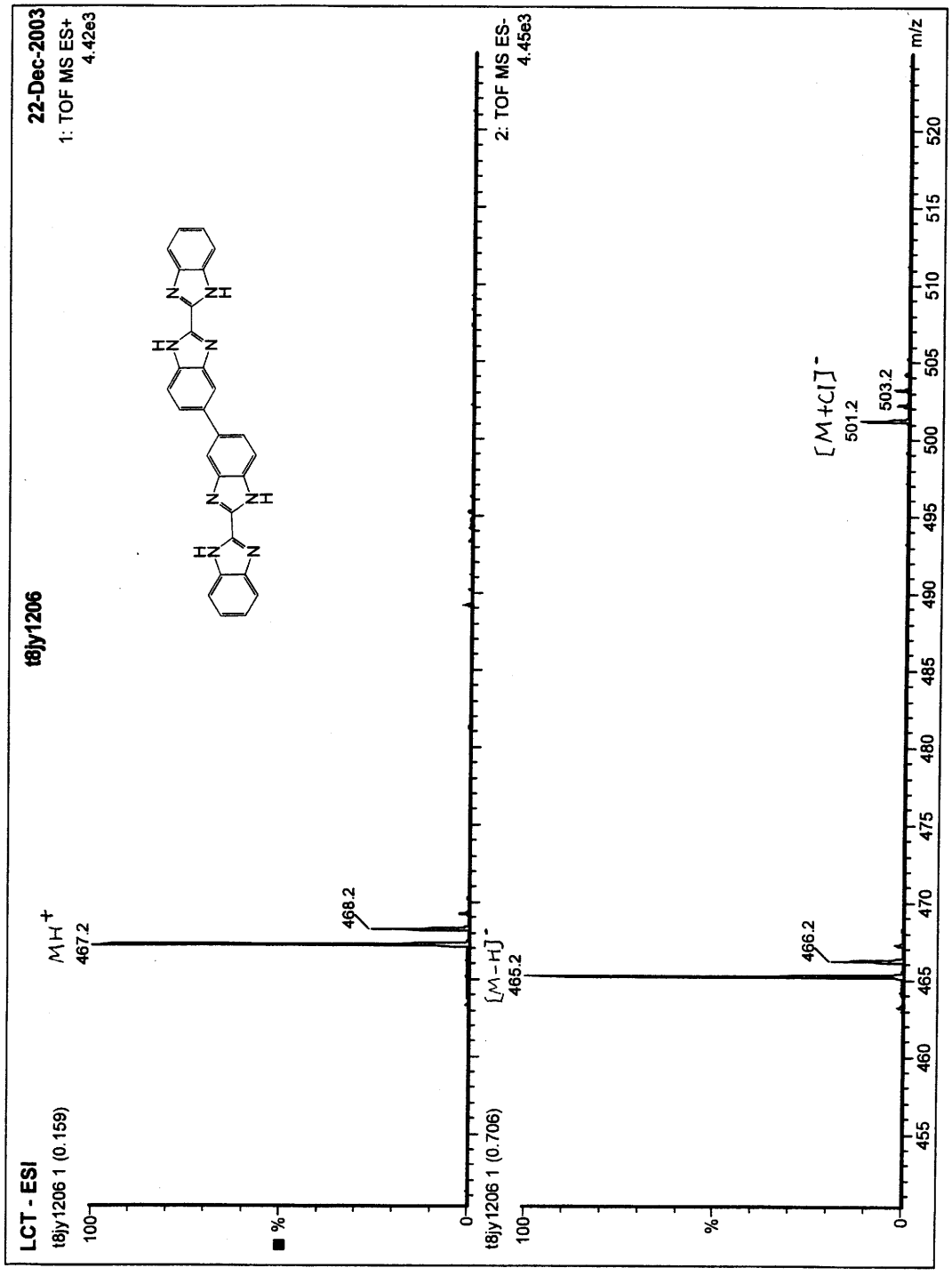
LCT - ESI
t8jy1206 1 (0.159)
22-Dec-2003
t8jy1206
1: TOF MS ES+
4.42e3
MH+
467.2
468.2
2: TOF MS ES-
4.45e3
[M-H]-
465.2
466.2
[M+Cl]-
501.2
503.2
t8jy1206 1 (0.706)
100
%
0
455
460
465
470
475
480
485
490
495
500
505
510
515
520
m/z

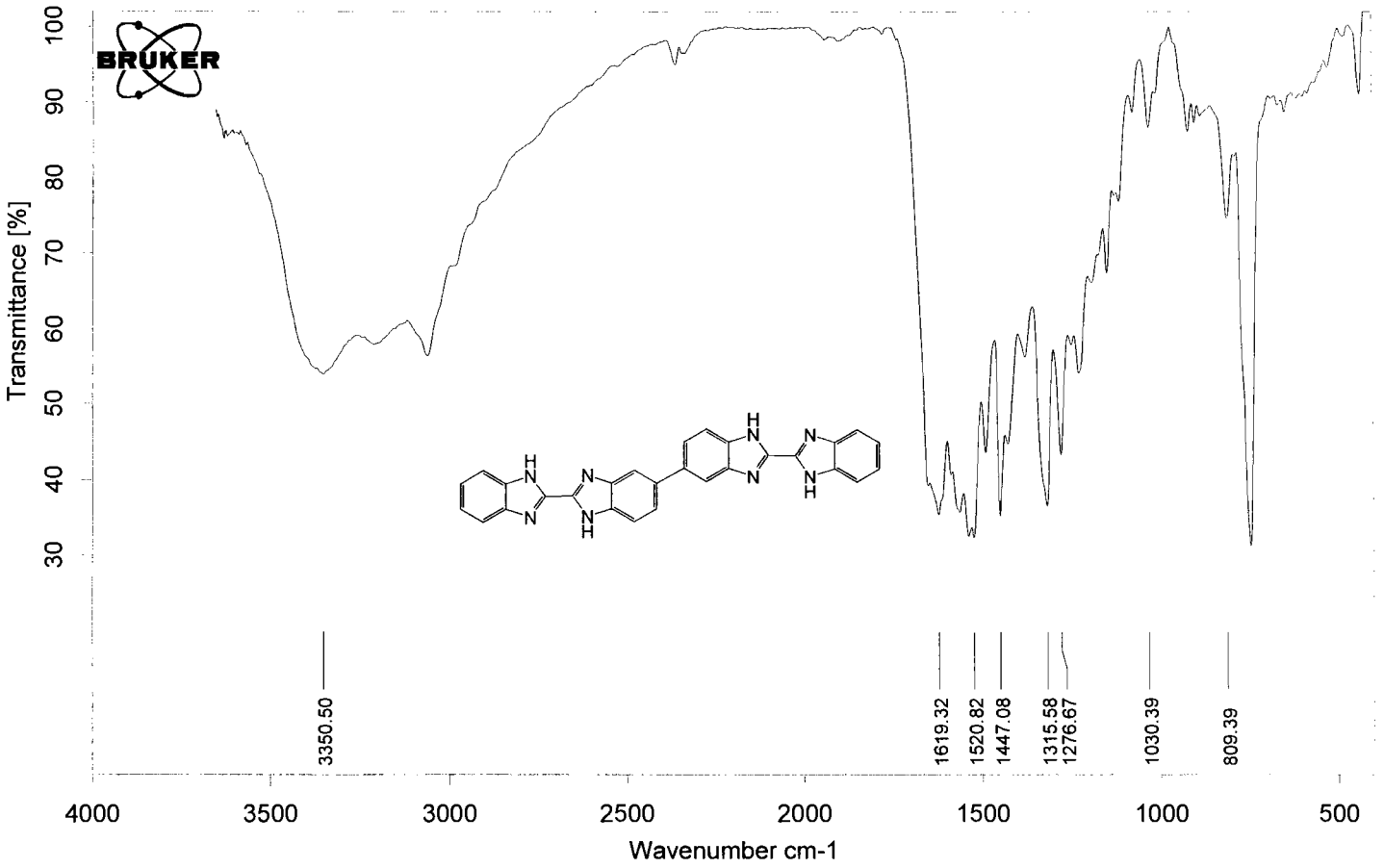

D:\OPUS_NT\DATA\Jun\V_JY_115_BiBzImH2_Dimer_Ethanol.0	V_JY_115_BiBzImH2_Dimer_Ethanol	Solid in KBr	06/12/2003

X-ray Crystallography Data of Bis(2,2′-bibenzimidazole) (14)

Compound	Bis(2,2′-bibenzimidazole) (**14**) with 12 molecules of CF_3COOH
Color/Shape	Yellow block
Crystal Size (mm)	0.277 x 0.398 x 0.402
Formula	$C_{52}H_{30}F_{36}N_8O_{24}$
Formula mass	1834.84
Temperature	-50 ºC
Crystal System	monoclinic
Space Group	$P2_1/c$
Unit cell:	
a (Å)	22.067(4)
b (Å)	19.299(4)
c (Å)	8.537(2)
α (º)	
β (º)	100.13(3)
γ (º)	
Volume ($Å^3$)	3579.0(120)
Z	2
Density (calc.) g/cm^3	1.703
Mu (mm^{-1})	0.19
Diffractometer	Bruker CCD 1000
Radiation/λ	Mo Kα (0.71073 Å)
F(000)	1828
2 θ range	2.8 to 56.7
Reflections collected	43835
Unique reflections	8778
R_{int}	0.0993
Observed reflections	3345
Abs. Corr.	none
Correction Factors	n/a
Refinement Method	Full-matrix least-squares on F^2
Computing	SHELXTL, Version 5
Number of parameters	541
Number of restraints	0
GOF	1.05
Final R ($I > 2\sigma(I)$)	R1 = 0.0755; wR2 = 0.1797
R (all data)	R1 = 0.2197; wR2 = 0.2884
Largest diff.peak/hole	0.63/-0.38
Weights	SHELXTL 0.0944, 7.5859

Atomic coordinates [x 10^4] and equivalent isotropic displacement parameters [$Å^2$ x 10^3]. U(eq) is defined as one third of the trace of the orthogonalized Uij tensor.

	x	y	z	U(eq)
N(1)	1761(2)	4495(2)	5223(4)	33(1)
C(2)	1210(2)	4804(2)	4541(5)	34(1)
C(3)	678(2)	4532(3)	3644(6)	46(1)
C(4)	222(2)	4998(3)	3126(7)	53(2)
C(5)	274(2)	5701(3)	3502(7)	54(2)
C(6)	794(2)	5972(3)	4396(7)	46(1)
C(7)	1269(2)	5505(2)	4926(6)	34(1)
N(8)	1851(2)	5593(2)	5797(5)	36(1)
C(9)	2137(2)	4982(2)	5947(5)	32(1)
C(10)	2758(2)	4866(2)	6779(5)	30(1)
N(11)	3044(2)	4254(2)	6939(4)	32(1)
C(12)	3632(2)	4347(2)	7770(5)	31(1)
C(13)	4106(2)	3893(2)	8250(7)	48(1)
C(14)	4637(2)	4163(2)	9111(7)	44(1)
C(15)	4711(2)	4874(2)	9516(5)	30(1)
C(16)	4227(2)	5322(2)	8990(5)	32(1)
C(17)	3694(2)	5043(2)	8127(5)	30(1)
N(18)	3138(2)	5354(2)	7489(5)	35(1)
O(101)	2317(2)	3226(2)	5499(4)	48(1)
O(102)	1948(2)	2260(2)	4255(5)	53(1)
C(101)	2344(2)	2611(2)	5119(6)	39(1)
C(102)	2949(3)	2240(3)	5804(7)	49(1)
F(101)	3041(2)	1687(2)	4996(5)	83(1)
F(102)	3427(2)	2650(2)	5831(6)	90(1)
F(103)	2949(2)	2039(2)	7274(5)	95(1)
O(201)	2587(2)	6618(2)	7264(5)	49(1)
O(202)	3104(2)	7597(2)	7186(7)	81(2)
C(201)	2634(3)	7254(2)	7195(7)	46(1)
C(202)	2035(3)	7669(3)	7103(8)	58(2)
F(201)	1543(2)	7278(2)	6832(6)	97(2)
F(202)	2029(2)	8010(2)	8458(5)	86(1)
F(203)	1982(2)	8140(2)	5977(6)	102(2)
O(301)	1024(2)	2907(2)	2540(5)	65(1)
O(302)	820(2)	1933(2)	1164(6)	82(2)
C(301)	725(3)	2520(3)	1442(7)	53(2)
C(302)	200(4)	2923(4)	464(9)	74(2)
F(301)	-158(2)	3201(4)	1311(6)	137(2)
F(302)	414(3)	3443(3)	-265(7)	154(3)
F(303)	-121(2)	2560(3)	-644(6)	136(2)
O(401)	1819(2)	4099(2)	9030(5)	62(1)
O(402)	1883(2)	4073(2)	11666(6)	83(2)
C(401)	1806(3)	4363(3)	10423(8)	51(1)
C(402)	1686(3)	5142(3)	10296(8)	58(2)
F(401)	1758(3)	5421(2)	11698(5)	115(2)
F(402)	2089(3)	5457(2)	9584(6)	110(2)

F(403)	1163(3)	5286(3)	9588(11)	207(4)
O(501)	3409(2)	6082(2)	1869(6)	83(2)
O(502)	3050(3)	5818(3)	4083(6)	94(2)
C(501)	3313(3)	5681(3)	3025(8)	60(2)
C(502)	3570(5)	4970(4)	2868(10)	84(2)
F(501)	3346(3)	4692(2)	1438(6)	120(2)
F(502)	3443(4)	4552(2)	3920(7)	175(3)
F(503)	4169(3)	4987(3)	2843(7)	129(2)
O(601)	4050(2)	6853(2)	6724(7)	86(2)
O(602)	4369(3)	7783(3)	5646(9)	128(3)
C(601)	4420(3)	7202(4)	6057(9)	71(2)
C(602)	4956(4)	6774(5)	5762(15)	101(3)
F(601)	4839(3)	6238(5)	5063(15)	258(6)
F(602)	5336(4)	7093(4)	5113(14)	234(5)
F(603)	5286(4)	6571(6)	7067(11)	234(5)

Bond lengths

N(1)-C(9)	1.333(6)	N(1)-C(2)
1.387(6)		
C(2)-C(3)	1.386(7)	C(2)-C(7)
1.394(6)		
C(3)-C(4)	1.366(7)	C(4)-C(5)
1.394(8)		
C(5)-C(6)	1.365(8)	C(6)-C(7)
1.395(7)		
C(7)-N(8)	1.376(6)	N(8)-C(9)
1.333(6)		
C(9)-C(10)	1.444(6)	C(10)-N(18)
1.334(6)		
C(10)-N(11)	1.336(5)	N(11)-C(12)
1.377(6)		
C(12)-C(13)	1.371(6)	C(12)-C(17)
1.379(6)		
C(13)-C(14)	1.371(7)	C(14)-C(15)
1.418(6)		
C(15)-C(16)	1.386(6)	C(15)-C(15)'
1.476(9)		
C(16)-C(17)	1.381(6)	C(17)-N(18)
1.389(6)		
O(101)-C(101)	1.234(5)	O(102)-C(101)
1.241(6)		
C(101)-C(102)	1.537(7)	C(102)-F(101)
1.307(6)		
C(102)-F(103)	1.313(7)	C(102)-F(102)
1.316(6)		
O(201)-C(201)	1.233(6)	O(202)-C(201)
1.232(6)		

C(201)-C(202)	1.537(8)	C(202)-F(203) 1.314(7)
C(202)-F(201)	1.309(7)	C(202)-F(202) 1.333(7)
O(301)-C(301)	1.288(6)	O(302)-C(301) 1.184(7)
C(301)-C(302)	1.518(9)	C(302)-F(301) 1.279(8)
C(302)-F(303)	1.286(8)	C(302)-F(302) 1.311(8)
O(401)-C(401)	1.299(7)	O(402)-C(401) 1.185(7)
C(401)-C(402)	1.526(8)	C(402)-F(403) 1.237(8)
C(402)-F(401)	1.296(7)	C(402)-F(402) 1.311(7)
O(501)-C(501)	1.300(7)	O(502)-C(501) 1.186(7)
C(501)-C(502)	1.500(9)	C(502)-F(502) 1.274(7)
C(502)-F(503)	1.325(10)	C(502)-F(501) 1.345(9)
O(601)-C(601)	1.269(7)	O(602)-C(601) 1.174(8)
C(601)-C(602)	1.499(11)	C(602)-F(601) 1.200(11)
C(602)-F(602)	1.245(10)	C(602)-F(603) 1.280(12)

Bond angles [°]

C(9)-N(1)-C(2)	108.7(4)	C(3)-C(2)-N(1)
131.5(4)		
C(3)-C(2)-C(7)	122.3(4)	N(1)-C(2)-C(7)
106.3(4)		
C(4)-C(3)-C(2)	115.7(5)	C(3)-C(4)-C(5)
122.7(5)		
C(6)-C(5)-C(4)	121.9(5)	C(5)-C(6)-C(7)
116.4(5)		
N(8)-C(7)-C(2)	106.6(4)	N(8)-C(7)-C(6)
132.3(5)		
C(2)-C(7)-C(6)	121.1(5)	C(9)-N(8)-C(7)
109.0(4)		
N(1)-C(9)-N(8)	109.4(4)	N(1)-C(9)-C(10)
125.4(4)		
N(8)-C(9)-C(10)	125.1(4)	N(18)-C(10)-N(11)
109.3(4)		
N(18)-C(10)-C(9)	125.5(4)	N(11)-C(10)-C(9)
125.2(4)		
C(10)-N(11)-C(12)	108.8(4)	C(13)-C(12)-C(17)
121.1(4)		
C(13)-C(12)-N(11)	132.1(4)	C(17)-C(12)-N(11)
106.8(4)		
C(14)-C(13)-C(12)	116.8(4)	C(13)-C(14)-C(15)
123.3(4)		
C(16)-C(15)-C(14)	118.4(4)	C(16)-C(15)-C(15)'
121.2(5)		
C(14)-C(15)-C(15)'	120.4(5)	C(17)-C(16)-C(15)
117.7(4)		
C(12)-C(17)-C(16)	122.7(4)	C(12)-C(17)-N(18)
106.7(4)		
C(16)-C(17)-N(18)	130.6(4)	C(10)-N(18)-C(17)
108.4(4)		
O(101)-C(101)-O(102)	128.2(5)	O(101)-C(101)-C(102)
115.3(4)		
O(102)-C(101)-C(102)	116.5(4)	F(101)-C(102)-F(103)
106.9(5)		
F(101)-C(102)-F(102)	107.5(5)	F(103)-C(102)-F(102)
107.2(5)		
F(101)-C(102)-C(101)	112.7(4)	F(103)-C(102)-C(101)
110.8(5)		
F(102)-C(102)-C(101)	111.6(4)	O(201)-C(201)-O(202)
127.9(5)		
O(201)-C(201)-C(202)	116.1(5)	O(202)-C(201)-C(202)
115.9(4)		
F(203)-C(202)-F(201)	107.8(6)	F(203)-C(202)-F(202)
106.3(5)		
F(201)-C(202)-F(202)	107.7(6)	F(203)-C(202)-C(201)
111.3(5)		
F(201)-C(202)-C(201)	112.8(4)	F(202)-C(202)-C(201)
110.6(5)		

O(302)-C(301)-O(301)	127.9(6)	O(302)-C(301)-C(302) 121.8(6)
O(301)-C(301)-C(302)	110.3(6)	F(301)-C(302)-F(303) 109.2(7)
F(301)-C(302)-F(302)	105.0(8)	F(303)-C(302)-F(302) 105.4(7)
F(301)-C(302)-C(301)	113.1(6)	F(303)-C(302)-C(301) 113.1(7)
F(302)-C(302)-C(301)	110.5(6)	O(402)-C(401)-O(401) 127.7(6)
O(402)-C(401)-C(402)	121.6(6)	O(401)-C(401)-C(402) 110.6(5)
F(403)-C(402)-F(401)	108.1(7)	F(403)-C(402)-F(402) 108.6(7)
F(401)-C(402)-F(402)	104.6(5)	F(403)-C(402)-C(401) 113.0(6)
F(401)-C(402)-C(401)	110.7(5)	F(402)-C(402)-C(401) 111.5(5)
O(502)-C(501)-O(501)	127.6(6)	O(502)-C(501)-C(502) 121.1(6)
O(501)-C(501)-C(502)	111.3(6)	F(502)-C(502)-F(503) 111.7(8)
F(502)-C(502)-F(501)	107.2(7)	F(503)-C(502)-F(501) 101.7(6)
F(502)-C(502)-C(501)	112.6(6)	F(503)-C(502)-C(501) 111.8(7)
F(501)-C(502)-C(501)	111.2(7)	O(602)-C(601)-O(601) 127.3(7)
O(602)-C(601)-C(602)	120.8(7)	O(601)-C(601)-C(602) 111.9(7)
F(601)-C(602)-F(602)	107.9(11)	F(601)-C(602)-F(603) 102.0(11)
F(602)-C(602)-F(603)	102.4(10)	F(601)-C(602)-C(601) 116.8(9)
F(602)-C(602)-C(601)	114.5(9)	F(603)-C(602)-C(601) 111.6(9)

Symmetry transformations used to generate equivalent atoms:

'(x,y,z) → (1-x,1-y,2-z)

Anisotropic displacement parameters

	U11	U22	U33	U23	U13	U12
N(1)	30(2)	27(2)	39(2)	-1(2)	-3(2)	2(2)
C(2)	31(3)	36(3)	33(3)	2(2)	-1(2)	5(2)
C(3)	39(3)	47(3)	46(3)	-5(2)	-8(3)	3(2)
C(4)	34(3)	60(4)	57(4)	3(3)	-12(3)	4(3)
C(5)	35(3)	59(4)	65(4)	16(3)	1(3)	14(3)
C(6)	42(3)	35(3)	59(4)	10(2)	2(3)	10(2)
C(7)	30(3)	36(3)	35(3)	4(2)	0(2)	4(2)
N(8)	33(2)	24(2)	46(2)	1(2)	-2(2)	3(2)
C(9)	29(3)	30(2)	35(3)	3(2)	1(2)	2(2)
C(10)	30(3)	26(2)	34(3)	3(2)	3(2)	1(2)
N(11)	30(2)	24(2)	39(2)	-2(2)	-1(2)	1(2)
C(12)	27(3)	28(2)	36(3)	0(2)	-2(2)	0(2)
C(13)	38(3)	28(3)	70(4)	-11(2)	-11(3)	7(2)
C(14)	33(3)	30(3)	63(4)	-6(2)	-7(3)	11(2)
C(15)	27(2)	29(2)	30(3)	0(2)	0(2)	-1(2)
C(16)	29(3)	28(2)	37(3)	2(2)	1(2)	-1(2)
C(17)	29(3)	28(2)	34(3)	3(2)	6(2)	4(2)
N(18)	30(2)	25(2)	47(2)	0(2)	-3(2)	5(2)
O(101)	46(2)	27(2)	63(2)	-10(2)	-6(2)	2(2)
O(102)	57(2)	35(2)	60(3)	-7(2)	-12(2)	-5(2)
C(101)	44(3)	29(3)	43(3)	-2(2)	4(2)	-4(2)
C(102)	54(4)	38(3)	51(4)	-10(3)	-1(3)	6(3)
F(101)	76(3)	61(2)	109(3)	-34(2)	4(2)	26(2)
F(102)	44(2)	61(2)	155(4)	-9(2)	-5(2)	-2(2)
F(103)	105(3)	115(3)	59(3)	20(2)	3(2)	55(3)
O(201)	48(2)	24(2)	70(3)	0(2)	-2(2)	2(2)
O(202)	58(3)	33(2)	159(5)	-3(3)	32(3)	-7(2)
C(201)	50(3)	28(3)	60(4)	-3(2)	9(3)	3(2)
C(202)	60(4)	33(3)	78(5)	-2(3)	6(3)	1(3)
F(201)	49(2)	61(2)	176(5)	-19(3)	2(2)	3(2)
F(202)	83(3)	77(3)	100(3)	-30(2)	26(2)	16(2)
F(203)	125(4)	63(2)	117(4)	32(2)	15(3)	42(2)
O(301)	63(3)	51(2)	71(3)	-13(2)	-17(2)	-3(2)
O(302)	105(4)	60(3)	76(3)	-14(2)	0(3)	-23(3)
C(301)	59(4)	54(4)	44(3)	-7(3)	5(3)	-21(3)
C(302)	68(5)	93(5)	55(4)	0(4)	-10(4)	-10(4)
F(301)	102(4)	216(6)	83(3)	2(4)	-10(3)	76(4)
F(302)	134(5)	162(5)	139(5)	99(4)	-44(4)	-22(4)
F(303)	99(4)	171(5)	112(4)	-51(4)	-51(3)	-7(3)
O(401)	95(3)	36(2)	55(3)	3(2)	11(2)	1(2)
O(402)	122(4)	71(3)	63(3)	23(2)	33(3)	12(3)
C(401)	55(4)	48(3)	53(4)	7(3)	18(3)	0(3)
C(402)	69(4)	46(3)	60(4)	-5(3)	13(4)	-3(3)
F(401)	218(6)	59(2)	87(3)	-16(2)	77(4)	-23(3)
F(402)	192(5)	49(2)	116(4)	2(2)	96(4)	-14(3)
F(403)	129(5)	81(4)	355(11)	-40(5)	-109(6)	51(3)
O(501)	108(4)	40(2)	115(4)	12(3)	59(3)	12(2)

O(502)	113(4)	101(4)	73(3)	-6(3)	34(3)	39(3)
C(501)	67(4)	52(4)	64(4)	-5(3)	18(4)	6(3)
C(502)	137(8)	49(4)	84(6)	12(4)	69(5)	14(4)
F(501)	218(6)	55(2)	105(4)	-22(2)	80(4)	-20(3)
F(502)	359(10)	75(3)	136(5)	53(3)	164(6)	59(4)
F(503)	141(5)	101(4)	155(5)	23(3)	57(4)	65(3)
O(601)	74(3)	49(3)	145(5)	17(3)	50(3)	3(2)
O(602)	119(5)	63(4)	221(8)	20(4)	78(5)	-5(3)
C(601)	69(5)	54(4)	94(5)	-2(4)	28(4)	-12(4)
C(602)	76(6)	103(7)	130(9)	-6(6)	36(6)	0(5)
F(601)	139(6)	214(8)	429(16)	-209(10)	72(8)	15(6)
F(602)	173(7)	184(7)	398(14)	40(8)	200(9)	14(6)
F(603)	166(7)	349(14)	194(8)	40(8)	53(6)	164(9)

Hydrogen coordinates

	x	y	z	U(eq)
H(1A)	1851(2)	4041(2)	5176(4)	40
H(3A)	637(2)	4047(3)	3401(6)	55
H(4A)	-152(2)	4836(3)	2479(7)	64
H(5A)	-64(2)	6006(3)	3123(7)	65
H(6A)	831(2)	6455(3)	4656(7)	56
H(8A)	2012(2)	5996(2)	6201(5)	43
H(11A)	2880(2)	3848(2)	6559(4)	38
H(13A)	4066(2)	3409(2)	7986(7)	57
H(14A)	4974(2)	3854(2)	9463(7)	53
H(16A)	4258(2)	5809(2)	9220(5)	39
H(18A)	3048(2)	5807(2)	7544(5)	42
H(301)	1409(2)	2713(2)	3210(5)	78
H(401)	1738(2)	3619(2)	8970(5)	75
H(501)	3294(2)	6602(2)	2035(6)	99
H(601)	3760(2)	7107(2)	7441(7)	103

APPENDIX 6

^{1}H, ^{13}C, COSY NMR, AND FTIR SPECTRA OF [(4-(2-(1*H*-Benzo[*d*]imidazol-2-yl)-1*H*-benzo[*d*]imidazol-5-yl)benzene-1,2-diamine)] **15**

JEOL

Filename	= VI_JY_178_2NH2BiBzImH
Experiment	= single_pulse.exp
Sample_id	= S#152426
Solvent	= TRIFLUOROACETIC_
Creation_time	= 12-AUG-2004 01:14:41
Revision_time	= 26-MAY-2005 11:43:19
Current_time	= 26-MAY-2005 11:48:23
Content	= Single Pulse Experime
Data_format	= 1D COMPLEX
Dim_size	= 16384
Dim_title	= 1H
Dim_units	= [ppm]
Dimensions	= X
Site	= Eclipse+ 500
Spectrometer	= DELTA_NMR
Field_strength	= 11.7473579[T] (500[MH
X_acq_duration	= 1.818624[s]
X_domain	= 1H
X_freq	= 500.15991521[MHz]
X_offset	= 7[ppm]
X_points	= 16384
X_prescans	= 0
X_resolution	= 0.54986627[Hz]
X_sweep	= 9.00900901[kHz]
Mod_return	= 1
Scans	= 100
X_90_width	= 15[us]
X_acq_time	= 1.818624[s]
X_angle	= 45[deg]
X_pulse	= 7.5[us]
Initial_wait	= 1[s]
Phase_preset	= 3[us]
Recvr_gain	= 13
Relaxation_delay	= 1[s]
Temp_get	= 24.2[dC]
Unblank_time	= 2[us]

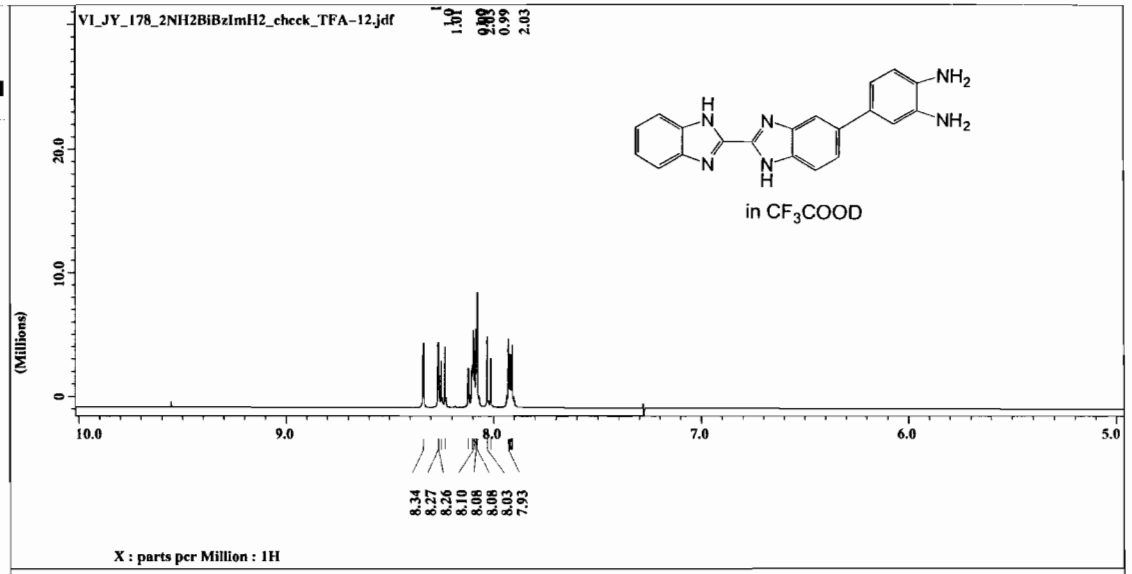

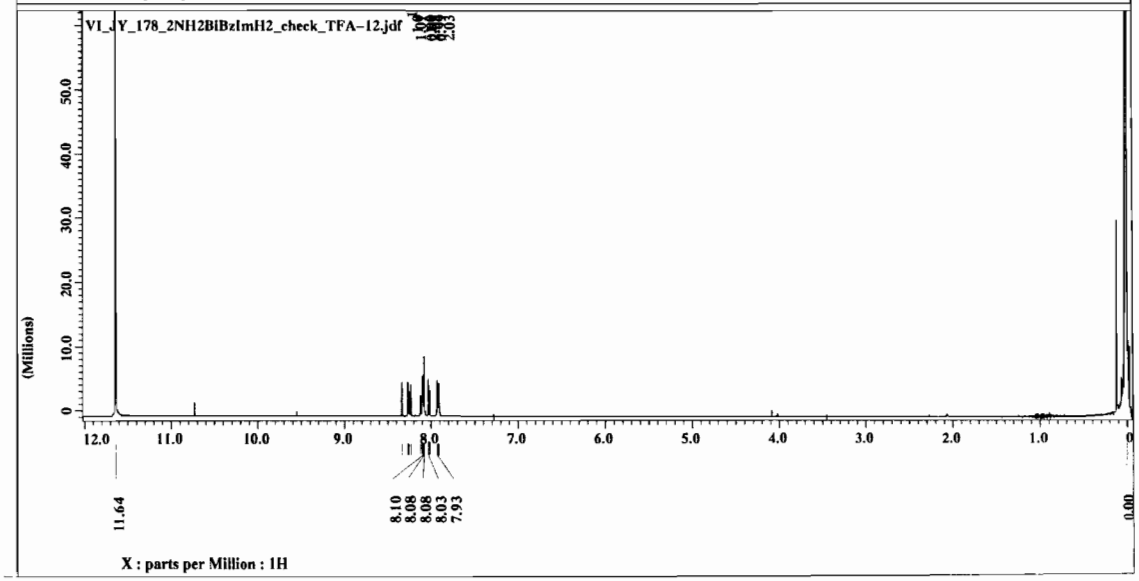

JEOL
Filename = VI_JY_178_2NH2BiBzImH
Experiment = single_pulse.exp
Sample_id = S#152426
Solvent = TRIFLUOROACETIC_
Creation_time = 12-AUG-2004 01:14:41
Revision_time = 26-MAY-2005 11:40:27
Current_time = 26-MAY-2005 11:40:50
Content = Single Pulse Experime
Data_format = 1D COMPLEX
Dim_size = 16384
Dim_title = 1H
Dim_units = [ppm]
Dimensions = X
Site = Eclipse+ 500
Spectrometer = DELTA_NMR
Field_strength = 11.7473579[T] (500[MH
X_acq_duration = 1.818624[s]
X_domain = 1H
X_freq = 500.15991521[MHz]
X_offset = 7[ppm]
X_points = 16384
X_prescans = 0
X_resolution = 0.54986627[Hz]
X_sweep = 9.00900901[kHz]
Mod_return = 1
Scans = 100
X_90_width = 15[us]
X_acq_time = 1.818624[s]
X_angle = 45[deg]
X_pulse = 7.5[us]
Initial_wait = 1[s]
Phase_preset = 3[us]
Recvr_gain = 13
Relaxation_delay = 1[s]
Temp_get = 24.2[dC]
Unblank_time = 2[us]
VI_JY_178_2NH2BiBzImH2_check_TFA-11.jdf
in CF3COOD
NH2
NH2
N
H
N
H
N
H
N
1.65
8.80
8.25
3.30
6.60
3.30
1.65
8.80
3.30
6.60
3.30
1.01
1.0
2.03
0.99
1.0
0.99
2.01
8.34
8.26
8.25
8.24
8.23
8.12
8.11
8.10
8.10
8.09
8.09
8.08
8.03
8.02
8.01
7.93
7.92
7.92
7.91
7.91
7.90
(Millions)
X : parts per Million : 1H

JEOL
---- ACQUISITION PARAMETERS ----
File Name = cosyVI_JY_178_2NH2BiBz
Author =
Sample ID = S#343374
Content = absolute value COSY
Creation Date = 13-AUG-2004 07:28:32
Revision Date = 19-AUG-2004 10:40:41
Spec Site = Eclipse+ 500
Spec Type = DELTA_NMR
Data Format = 2D REAL REAL
Dimensions = X Y
Dim Title = 1H 1H
Dim Size = 512, 884
Dim Units = [ppm] [ppm]
Acq_delay = 4.0742[ms]
Changer_sample = 0
Experiment = cosy.exp
Field_strength = 11.7473579[T]
Irr90 = 15[us]
Irr90_hi = 18[us]
Irr90_lo = 82[us]
Irr_pwidth = 82[us]
Lock_status = OFF
Recvr_gain = 30
Relaxation_delay = 1.5[s]
Scans = 4
Solvent = TRIFLUOROACETIC_
Spin_get = 0[Hz]
Spin_lock_90 = 60[us]
Spin_lock_attn = 15[dB]
Spin_rate = 15[Hz]
Spin_state = SPIN OFF
Spin_status = SPIN OFF
Temp_get = 23.7[dC]
Temp_set = 25.0[dC]
Temp_state = TEMP OFF
Temp_status = TEMP OFF
X90 = 15[us]
X90_hi = 18[us]
X90_lo = 82[us]
X_acq_duration = 2.08983044[s]
X_domain = 1H
X_freq = 500.15991521[MHz]
X_offset = 7.9332[ppm]
X_points = 512
X_prescans = 4
X_pulse = 15[us]
X_resolution = 0.47850773[Hz]
X_sweep = 244.99595757[Hz]
Y90 = 10[us]
Y90_hi = 10[us]
Y90_lo = 50[us]
Y_domain = 1H
Y_freq = 500.15991521[MHz]
Y_offset = 7.9332[ppm]
Y_points = 221
Y_prescans = 0
Y_resolution = 1.10857899[Hz]
Y_sweep = 244.99595757[Hz]
(Millions)
10.0
0
VI_JY_178_2NH2BiBzImH2_check_TFA.8
cosyVI_JY_178_2NH2BiBzImH2_TFA.3
in CF_3COOD
VI_JY_178_2NH2BiBzImH2_check_TFA.7
7.7
7.8
7.9
8.0
8.1
8.2
Y : parts per Million : 1H
8.2
8.1
8.0
7.9
7.8
7.7
X : parts per Million : 1H
0
10.0
(Millions)

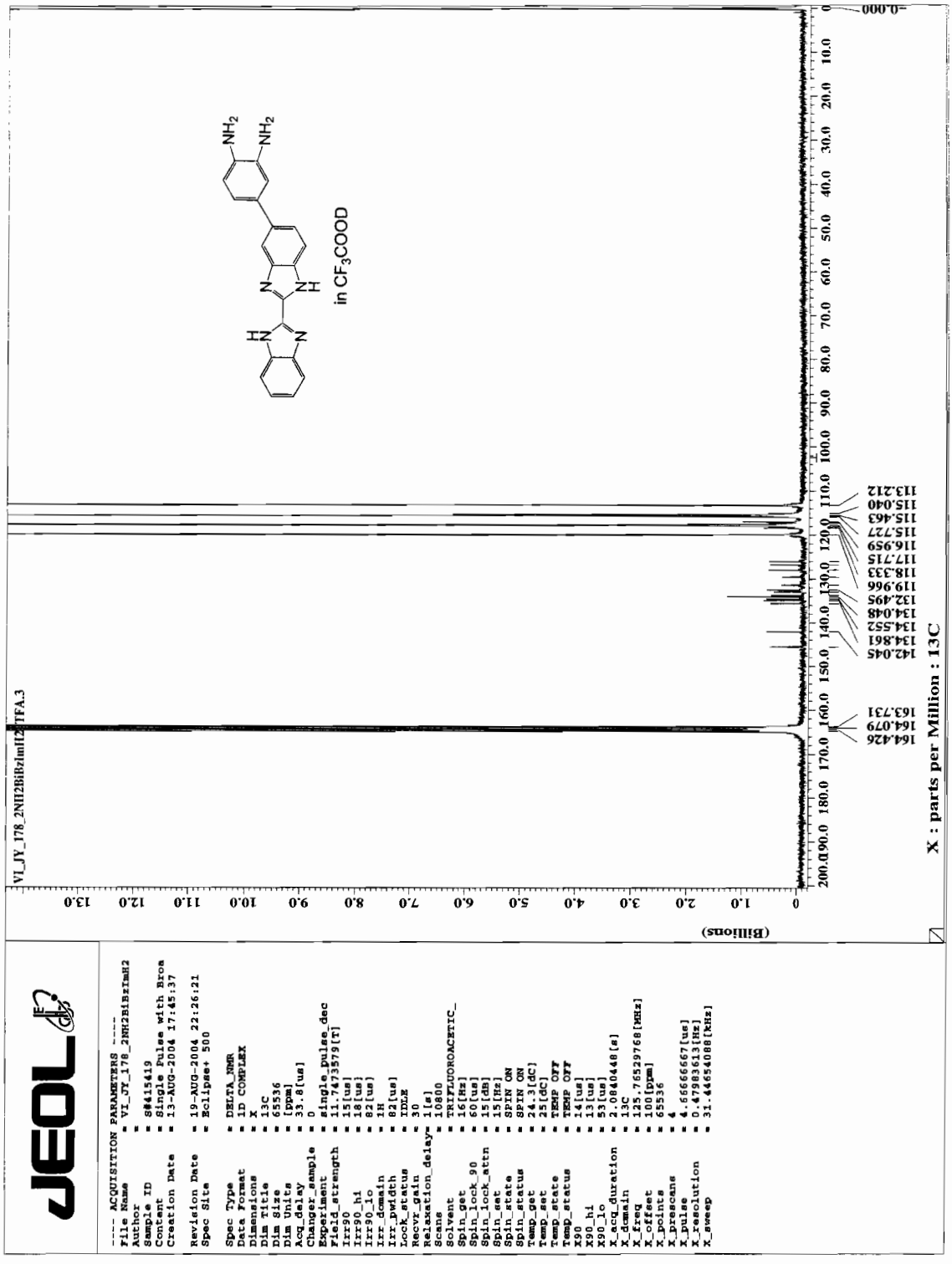
JEOL
---- ACQUISITION PARAMETERS ----
File Name = VI_JY_178_2NH2BiBzImH2
Author =
Sample ID = s#415419
Content = Single Pulse with Broa
Creation Date = 13-AUG-2004 17:45:37
Revision Date = 19-AUG-2004 22:26:21
Spec Site = Eclipse+ 500
Spec Type = DELTA_NMR
Data Format = 1D COMPLEX
Dimensions = X
Dim Title = 13C
Dim Size = 65536
Dim Units = [ppm]
Acq_delay = 33.8[us]
Changer_sample = 0
Experiment = single_pulse_dec
Field_strength = 11.74735791[T]
Irr90 = 15[us]
Irr90_hi = 18[us]
Irr90_lo = 82[us]
Irr_domain = 1H
Irr_pwidth = 82[us]
Lock_status = IDLE
Recvr_gain = 30
Relaxation_delay = 1[s]
Scans = 10800
Solvent = TRIFLUOROACETIC_
Spin_get = 16[Hz]
Spin_lock_90 = 60[us]
Spin_lock_attn = 15[dB]
Spin_set = 15[Hz]
Spin_state = SPIN ON
Spin_status = SPIN ON
Temp_get = 24.3[dC]
Temp_set = 25[dC]
Temp_state = TEMP OFF
Temp_status = TEMP OFF
X90 = 14[us]
X90_hi = 13[us]
X90_lo = 53[us]
X_acq_duration = 2.08404448[s]
X_domain = 13C
X_freq = 125.76529768[MHz]
X_offset = 100[ppm]
X_points = 65536
X_prescans = 4
X_pulse = 4.66666667[us]
X_resolution = 0.47983613[Hz]
X_sweep = 31.44654088[kHz]
VI_JY_178_2NH2BiBzImH2_TFA.3
in CF_3COOD
(Billions)
X : parts per Million : 13C
164.426
164.079
163.731
142.045
134.861
134.552
134.048
132.495
119.966
118.333
117.715
116.959
115.727
115.463
115.040
113.212

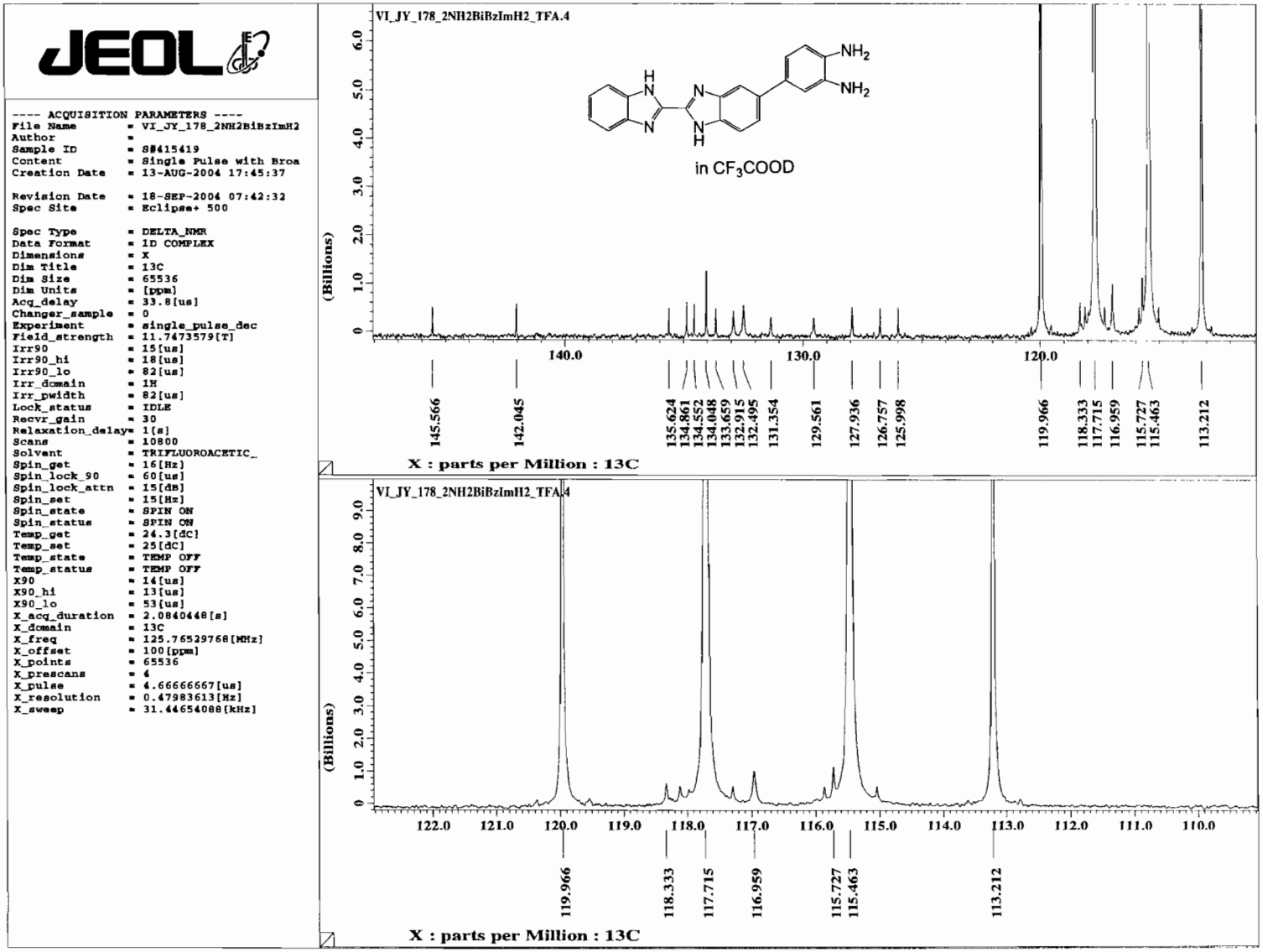
JEOL
---- ACQUISITION PARAMETERS ----
File Name = VI_JY_178_2NH2BiBzImH2
Author =
Sample ID = S#15419
Content = Single Pulse with Broa
Creation Date = 13-AUG-2004 17:45:37
Revision Date = 18-SEP-2004 07:42:32
Spec Site = Eclipse+ 500
Spec Type = DELTA_NMR
Data Format = 1D COMPLEX
Dimensions = X
Dim Title = 13C
Dim Size = 65536
Dim Units = [ppm]
Acq_delay = 33.8[us]
Changer_sample = 0
Experiment = single_pulse_dec
Field_strength = 11.7473579[T]
Irr90 = 15[us]
Irr90_hi = 18[us]
Irr90_lo = 82[us]
Irr_domain = 1H
Irr_pwidth = 82[us]
Lock_status = IDLE
Recvr_gain = 30
Relaxation_delay = 1[s]
Scans = 10800
Solvent = TRIFLUOROACETIC_
Spin_get = 16[Hz]
Spin_lock_90 = 60[us]
Spin_lock_attn = 15[dB]
Spin_set = 15[Hz]
Spin_state = SPIN ON
Spin_status = SPIN ON
Temp_get = 24.3[dC]
Temp_set = 25[dC]
Temp_state = TEMP OFF
Temp_status = TEMP OFF
X90 = 14[us]
X90_hi = 13[us]
X90_lo = 53[us]
X_acq_duration = 2.0840448[s]
X_domain = 13C
X_freq = 125.76529768[MHz]
X_offset = 100[ppm]
X_points = 65536
X_prescans = 4
X_pulse = 4.66666667[us]
X_resolution = 0.47983613[Hz]
X_sweep = 31.44654088[kHz]
VI_JY_178_2NH2BiBzImH2_TFA.4
NH2
NH2
in CF3COOD
(Billions)
145.566
142.045
135.624
134.861
134.552
134.048
133.659
132.915
132.495
131.354
129.561
127.936
126.757
125.998
119.966
118.333
117.715
116.959
115.727
115.463
113.212
X : parts per Million : 13C
VI_JY_178_2NH2BiBzImH2_TFA.4
(Billions)
119.966
118.333
117.715
116.959
115.727
115.463
113.212
X : parts per Million : 13C

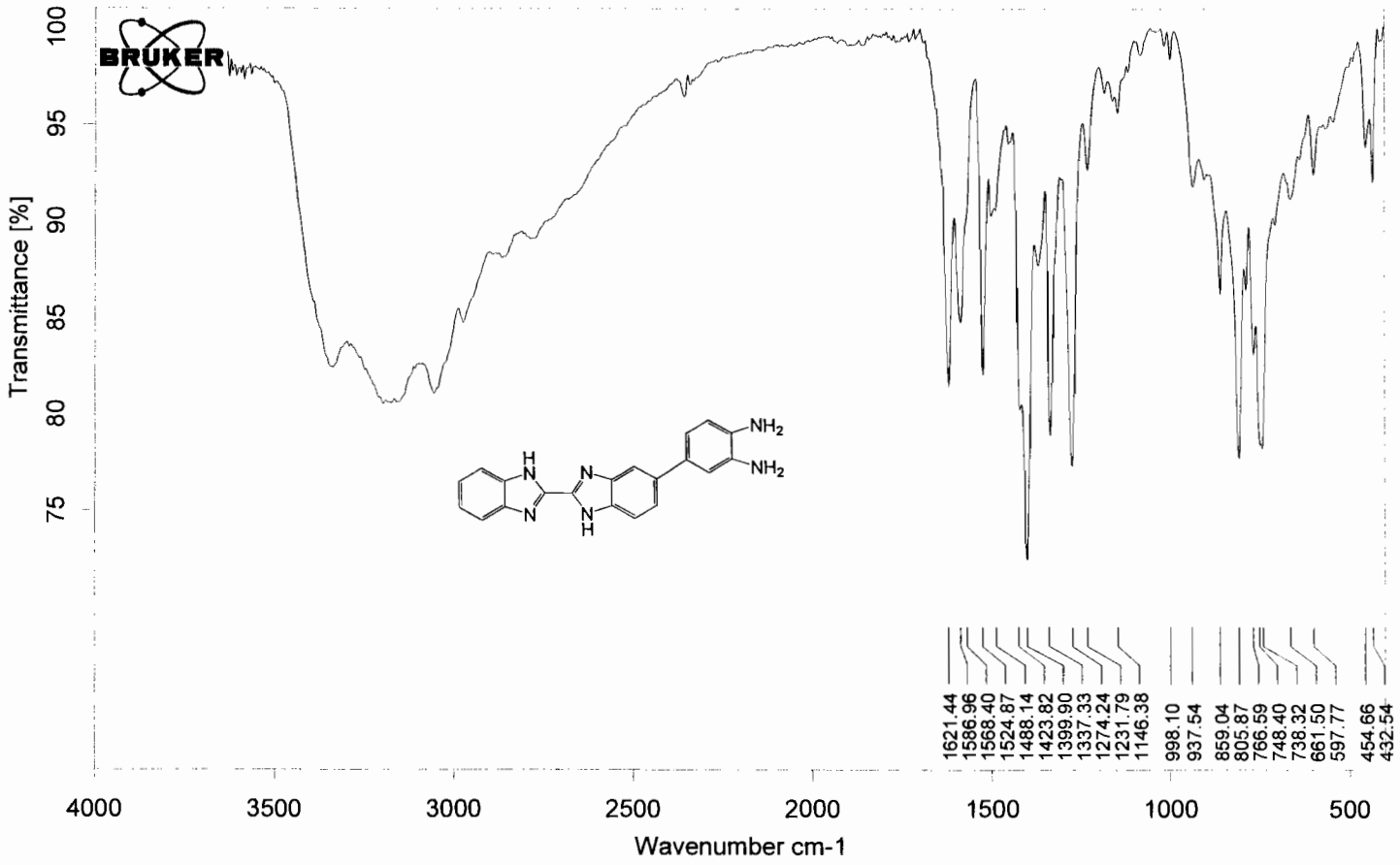

D:\OPUS_NT\DATA\Jun\VI_JY_276_DiamineBiBzImH2.0	VI_JY_276_DiamineBiBzImH2	Solid in KBr	09/11/2004

APPENDIX 7

^{1}H, ^{13}C, COSY NMR, AND FTIR SPECTRA OF

2-(1*H*-Benzo[*d*]imidazol-2-yl)-5-(1*H*-benzo[*d*]imidazol-5-yl)

-1*H*-benzo[*d*]imidazole **16**

```
---- ACQUISITION PARAMETERS ----
File Name          = VI_JY_157_DryRingbypr
Author             =
Sample ID          = S#227886
Content            = Single Pulse Experime
Creation Date      = 21-NOV-2004 02:45:05

Revision Date      =  3-JAN-2005 21:12:12
Spec Site          = Eclipse+ 500

Spec Type          = DELTA_NMR
Data Format        = 1D COMPLEX
Dimensions         = X
Dim Title          = 1H
Dim Size           = 16384
Dim Units          = [ppm]
Field_strength     = 11.7473579[T] (500[MH
X_acq_duration     = 1.6367616[s]
X_domain           = 1H
X_freq             = 500.15991521[MHz]
X_offset           = 8[ppm]
X_points           = 16384
X_prescans         = 0
X_resolution       = 0.61096253[Hz]
X_sweep            = 10.01001001[kHz]
Mod_return         = 1
Scans              = 100

X_90_width         = 15[us]
X_acq_time         = 1.6367616[s]
X_angle            = 45[deg]
X_pulse            = 7.5[us]
Initial_wait       = 1[s]
Phase_preset       = 3[us]
Relaxation_delay   = 1[s]
Unblank_time       = 2[us]
```

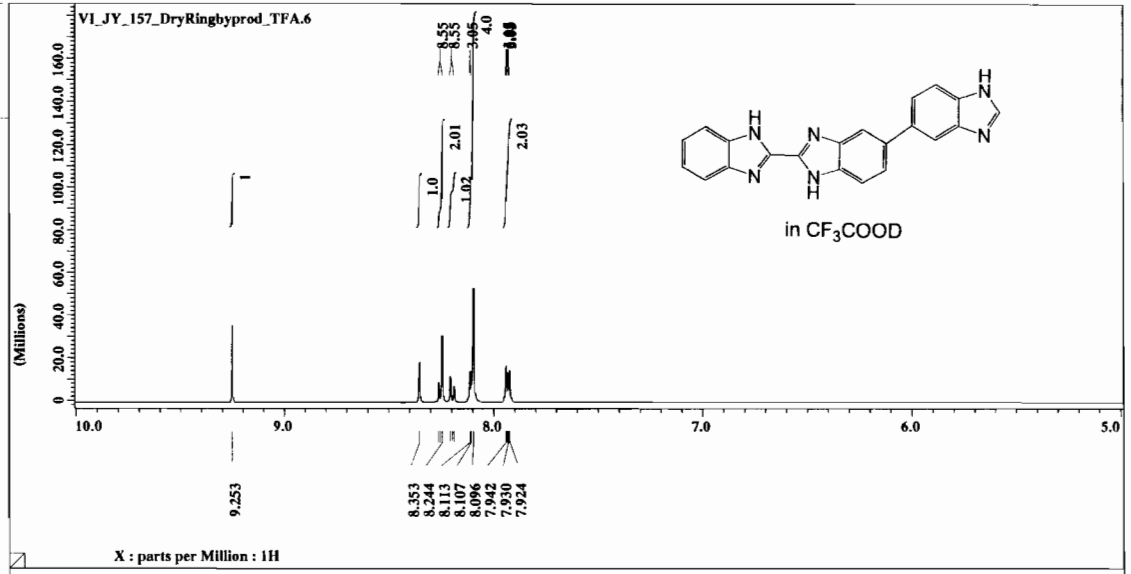

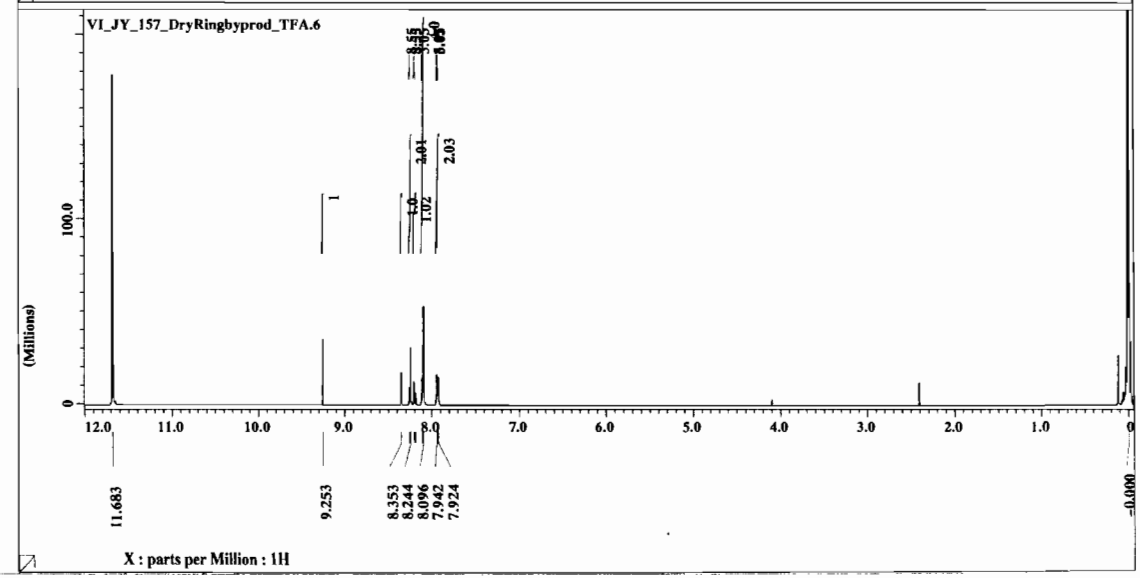

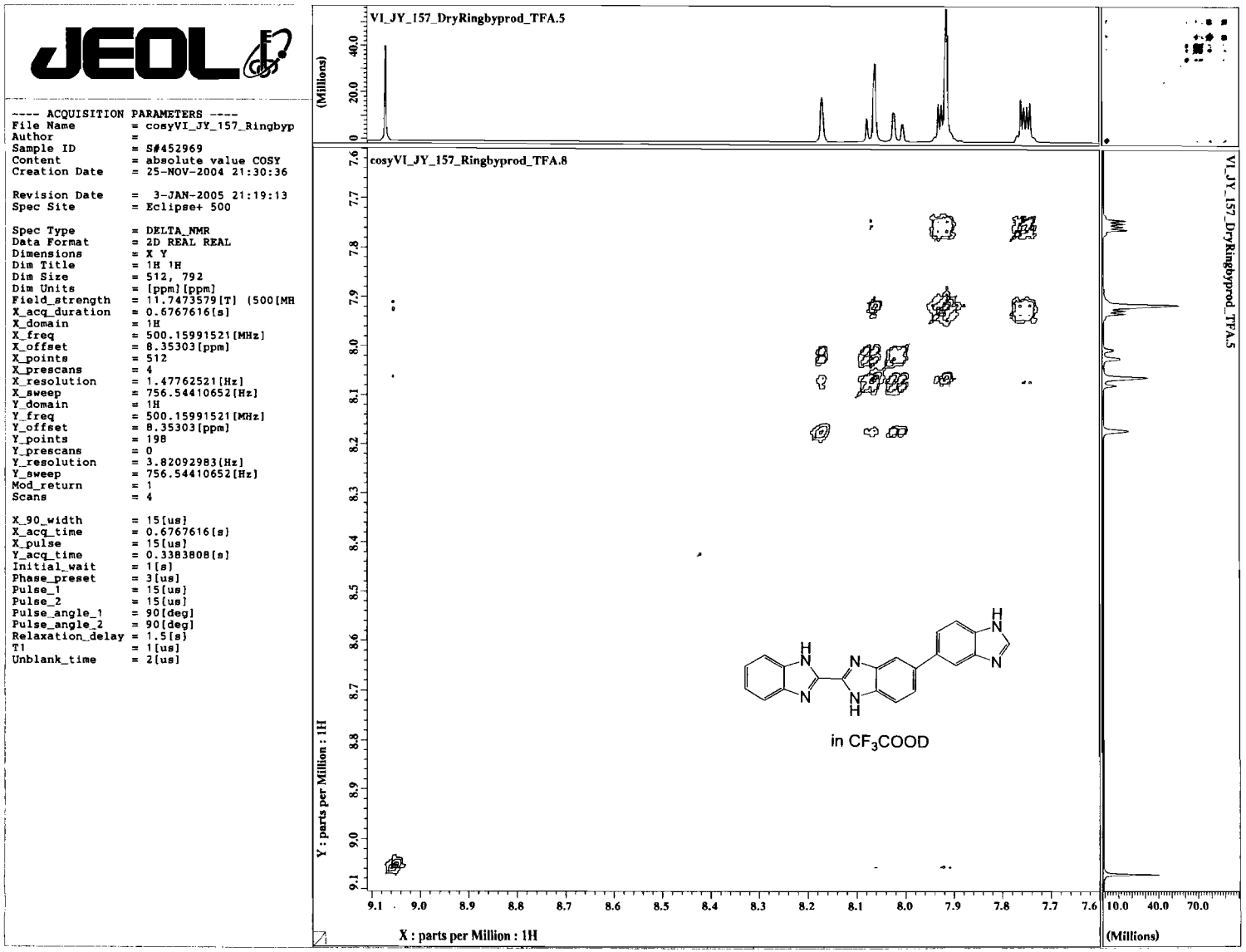
JEOL
---- ACQUISITION PARAMETERS ----
File Name = cosyVI_JY_157_Ringbyp
Author =
Sample ID = S#452969
Content = absolute value COSY
Creation Date = 25-NOV-2004 21:30:36
Revision Date = 3-JAN-2005 21:19:13
Spec Site = Eclipse+ 500
Spec Type = DELTA_NMR
Data Format = 2D REAL REAL
Dimensions = X Y
Dim Title = 1H 1H
Dim Size = 512, 792
Dim Units = [ppm][ppm]
Field_strength = 11.7473579[T] (500[MH
X_acq_duration = 0.6767616[s]
X_domain = 1H
X_freq = 500.15991521[MHz]
X_offset = 8.35303[ppm]
X_points = 512
X_prescans = 4
X_resolution = 1.47762521[Hz]
X_sweep = 756.54410652[Hz]
Y_domain = 1H
Y_freq = 500.15991521[MHz]
Y_offset = 8.35303[ppm]
Y_points = 198
Y_prescans = 0
Y_resolution = 3.82092983[Hz]
Y_sweep = 756.54410652[Hz]
Mod_return = 1
Scans = 4
X_90_width = 15[us]
X_acq_time = 0.6767616[s]
X_pulse = 15[us]
Y_acq_time = 0.3383808[s]
Initial_wait = 1[s]
Phase_preset = 3[us]
Pulse_1 = 15[us]
Pulse_2 = 15[us]
Pulse_angle_1 = 90[deg]
Pulse_angle_2 = 90[deg]
Relaxation_delay = 1.5[s]
T1 = 1[us]
Unblank_time = 2[us]
VI_JY_157_DryRingbyprod_TFA.5
(Millions)
cosyVI_JY_157_Ringbyprod_TFA.8
VI_JY_157_DryRingbyprod_TFA.5
in CF3COOD
Y : parts per Million : 1H
X : parts per Million : 1H
(Millions)

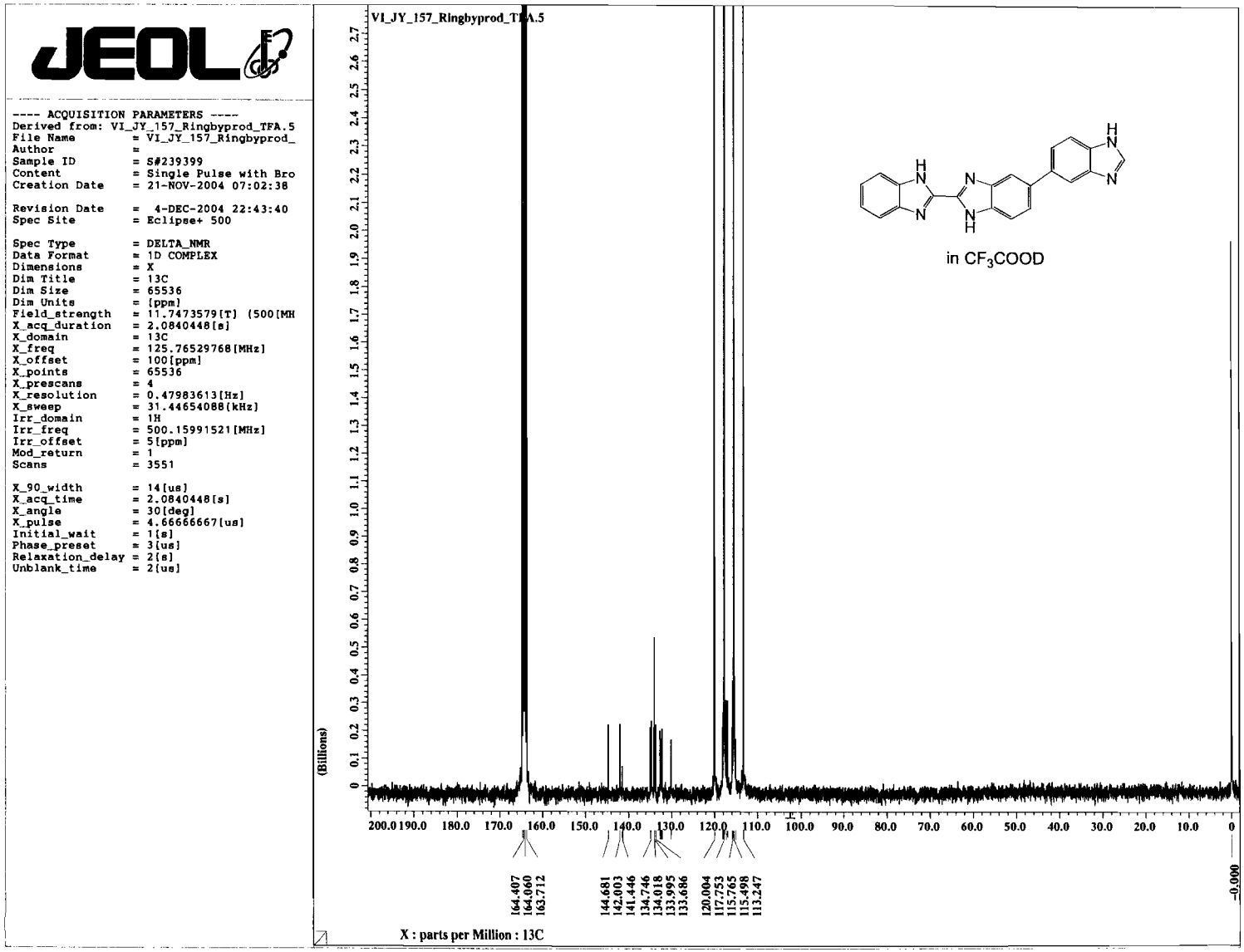
JEOL
---- ACQUISITION PARAMETERS ----
Derived from: VI_JY_157_Ringbyprod_TFA.5
File Name = VI_JY_157_Ringbyprod_
Author =
Sample ID = S#239399
Content = Single Pulse with Bro
Creation Date = 21-NOV-2004 07:02:38
Revision Date = 4-DEC-2004 22:43:40
Spec Site = Eclipse+ 500
Spec Type = DELTA_NMR
Data Format = 1D COMPLEX
Dimensions = X
Dim Title = 13C
Dim Size = 65536
Dim Units = [ppm]
Field_strength = 11.7473579[T] (500[MH
X_acq_duration = 2.0840448[s]
X_domain = 13C
X_freq = 125.76529768[MHz]
X_offset = 100[ppm]
X_points = 65536
X_prescans = 4
X_resolution = 0.47983613[Hz]
X_sweep = 31.44654088[kHz]
Irr_domain = 1H
Irr_freq = 500.15991521[MHz]
Irr_offset = 5[ppm]
Mod_return = 1
Scans = 3551
X_90_width = 14[us]
X_acq_time = 2.0840448[s]
X_angle = 30[deg]
X_pulse = 4.66666667[us]
Initial_wait = 1[s]
Phase_preset = 3[us]
Relaxation_delay = 2[s]
Unblank_time = 2[us]
VI_JY_157_Ringbyprod_TFA.5
(Billions)
in CF3COOD
164.407
164.060
163.712
144.681
142.003
141.446
134.746
134.018
133.995
133.686
120.004
117.753
115.765
115.498
113.247
X : parts per Million : 13C

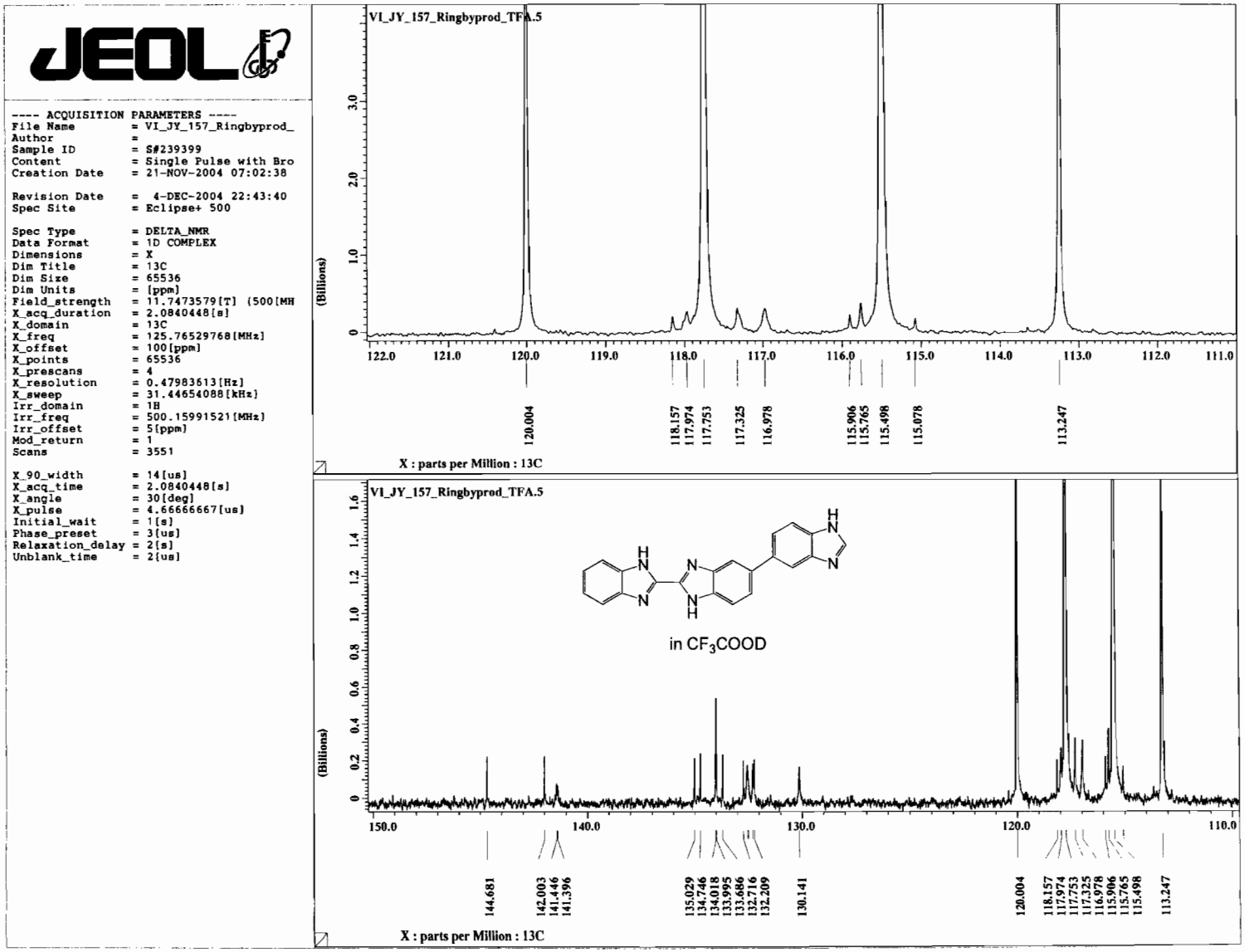
JEOL
---- ACQUISITION PARAMETERS ----
File Name = VI_JY_157_Ringbyprod_
Author =
Sample ID = S#239399
Content = Single Pulse with Bro
Creation Date = 21-NOV-2004 07:02:38
Revision Date = 4-DEC-2004 22:43:40
Spec Site = Eclipse+ 500
Spec Type = DELTA_NMR
Data Format = 1D COMPLEX
Dimensions = X
Dim Title = 13C
Dim Size = 65536
Dim Units = [ppm]
Field_strength = 11.7473579[T] (500[MH
X_acq_duration = 2.0840448[s]
X_domain = 13C
X_freq = 125.76529768[MHz]
X_offset = 100[ppm]
X_points = 65536
X_prescans = 4
X_resolution = 0.47983613[Hz]
X_sweep = 31.44654088[kHz]
Irr_domain = 1H
Irr_freq = 500.15991521[MHz]
Irr_offset = 5[ppm]
Mod_return = 1
Scans = 3551
X_90_width = 14[us]
X_acq_time = 2.0840448[s]
X_angle = 30[deg]
X_pulse = 4.66666667[us]
Initial_wait = 1[s]
Phase_preset = 3[us]
Relaxation_delay = 2[s]
Unblank_time = 2[us]
VI_JY_157_Ringbyprod_TFA.5
(Billions)
X : parts per Million : 13C
120.004
118.157
117.974
117.753
117.325
116.978
115.906
115.765
115.498
115.078
113.247
VI_JY_157_Ringbyprod_TFA.5
in CF3COOD
(Billions)
X : parts per Million : 13C
144.681
142.003
141.446
141.396
135.029
134.746
134.018
133.995
133.686
132.716
132.209
130.141
120.004
118.157
117.974
117.753
117.325
116.978
115.906
115.765
115.498
113.247

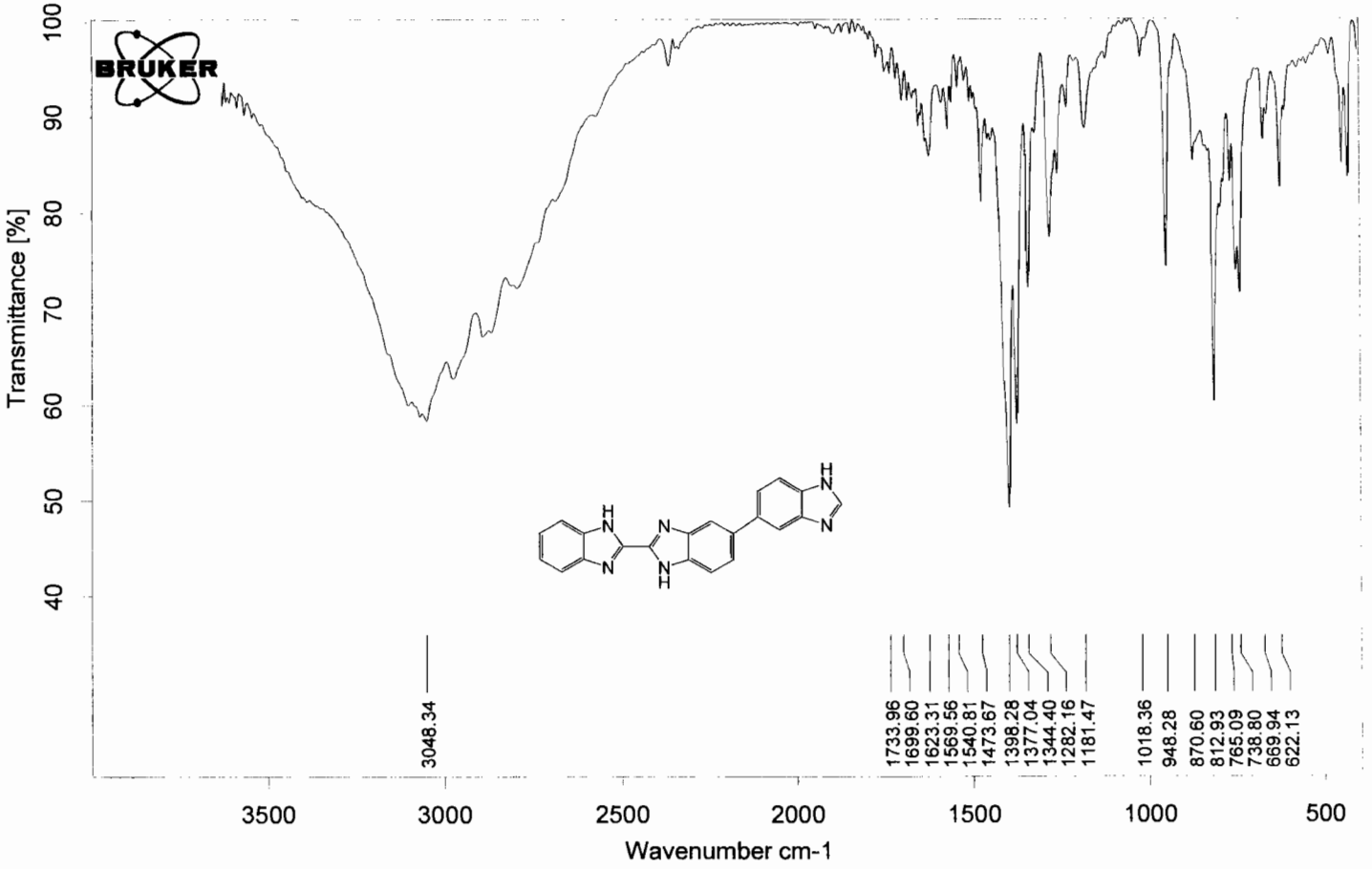

D:\OPUS_NT\DATA\Jun\VI_JY_157_RingClose_ByProduct_2.0	VI_JY_157_RingClose_ByProduct_2	Solid in KBr	02/02/2005

APPENDIX 8

^{1}H, ^{13}C NMR, FTIR, AND ESI MASS SPECTRA OF

Tris(2,2′-bibenzimidazole) **17**

JEOL

```
Filename          = VI_JY_221_Trimer_EG_W
Experiment        = single_pulse.exp
Sample_id         = S#169667
Solvent           = TRIFLUOROACETIC_
Creation time     = 11-AUG-2004 01:44:06
Revision time     = 25-MAY-2005 22:43:00
Current time      = 25-MAY-2005 22:43:00

Content           = Single Pulse Experime
Data format       = 1D COMPLEX
Dim size          = 16384
Dim title         = 1H
Dim units         = [ppm]
Dimensions        = X
Site              = Eclipse+ 500
Spectrometer      = DELTA_NMR

Field strength    = 11.7473579[T] (500[MH
X acq duration    = 1.818624[s]
X domain          = 1H
X freq            = 500.15991521[MHz]
X offset          = 7[ppm]
X points          = 16384
X prescans        = 0
X resolution      = 0.54986627[Hz]
X sweep           = 9.00900901[kHz]
Mod return        = 1
Scans             = 100

X 90 width        = 15[us]
X acq time        = 1.818624[s]
X angle           = 45[deg]
X pulse           = 7.5[us]
Initial wait      = 1[s]
Phase preset      = 3[us]
Recvr gain        = 12
Relaxation delay  = 1[s]
Temp get          = 23.4[dC]
Unblank time      = 2[us]
```

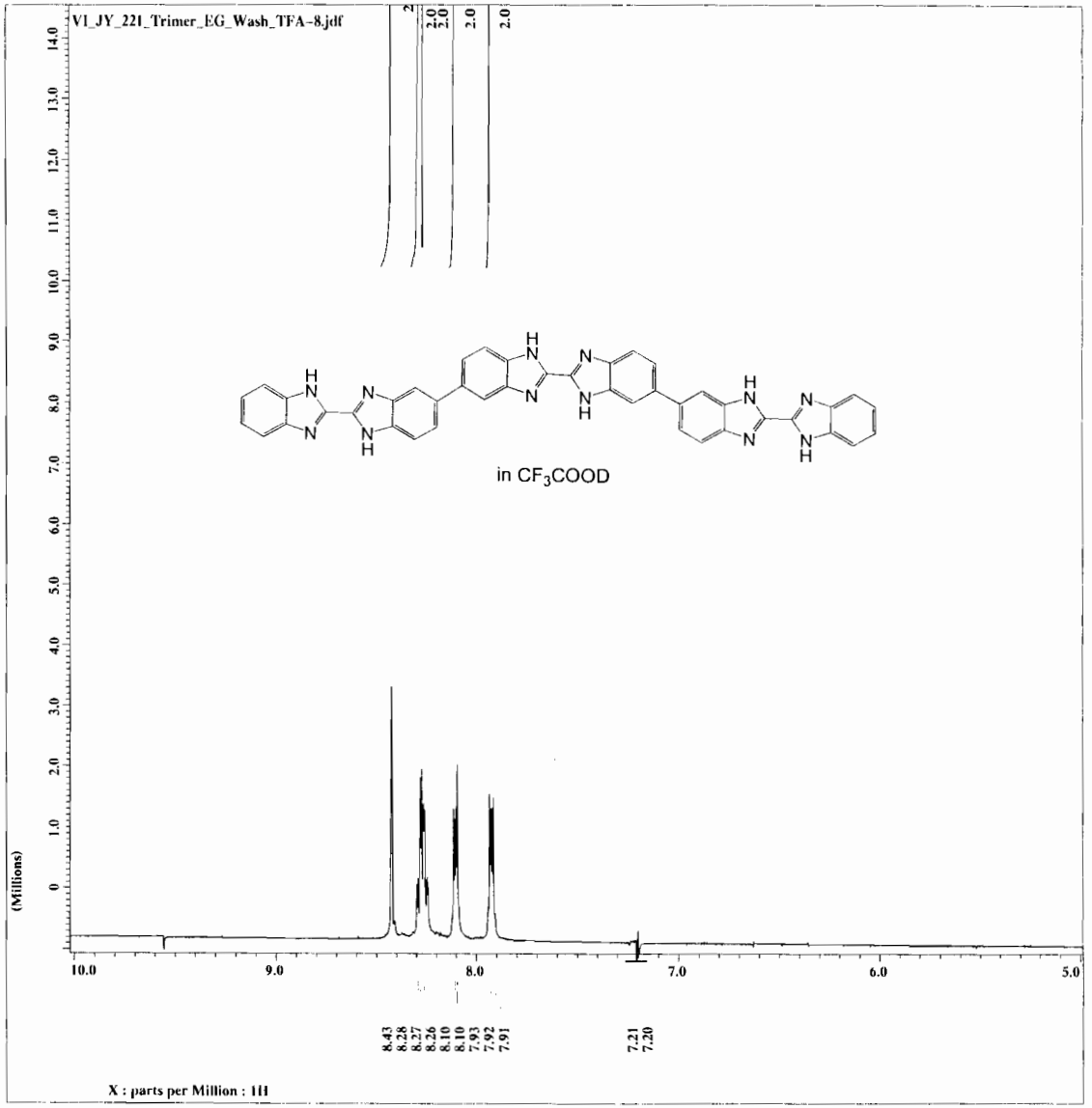

JEOL

```
---- ACQUISITION PARAMETERS ----
File Name          = VI_JY_221_Trimer_EG_Wa
Author             =
Sample ID          = S#169667
Content            = Single Pulse Experimen
Creation Date      = 11-AUG-2004 01:44:06

Revision Date      = 21-SEP-2004 09:19:18
Spec Site          = Eclipse+ 500

Spec Type          = DELTA_NMR
Data Format        = 1D COMPLEX
Dimensions         = X
Dim Title          = 1H
Dim Size           = 16384
Dim Units          = [ppm]
Acq_delay          = 0.1073[ms]
Changer_sample     = 0
Experiment         = single_pulse.exp
Field_strength     = 11.7473579[T]
Irr90              = 15[us]
Irr90_hi           = 18[us]
Irr90_lo           = 82[us]
Irr_pwidth         = 82[us]
Lock_status        = IDLE
Recvr_gain         = 12
Relaxation_delay= 1[s]
Scans              = 100
Solvent            = TRIFLUOROACETIC_
Spin_get           = 16[Hz]
Spin_lock_90       = 60[us]
Spin_lock_attn     = 15[dB]
Spin_set           = 15[Hz]
Spin_state         = SPIN ON
Spin_status        = SPIN ON
Temp_get           = 23.4[dC]
Temp_set           = 25[dC]
Temp_state         = TEMP OFF
Temp_status        = TEMP OFF
X90                = 15[us]
X90_hi             = 18[us]
X90_lo             = 82[us]
X_acq_duration     = 1.818624[s]
X_domain           = 1H
X_freq             = 500.15991521[MHz]
X_offset           = 7[ppm]
X_points           = 16384
X_prescans         = 0
X_pulse            = 7.5[us]
X_resolution       = 0.54986627[Hz]
X_sweep            = 9.00900901[kHz]
```

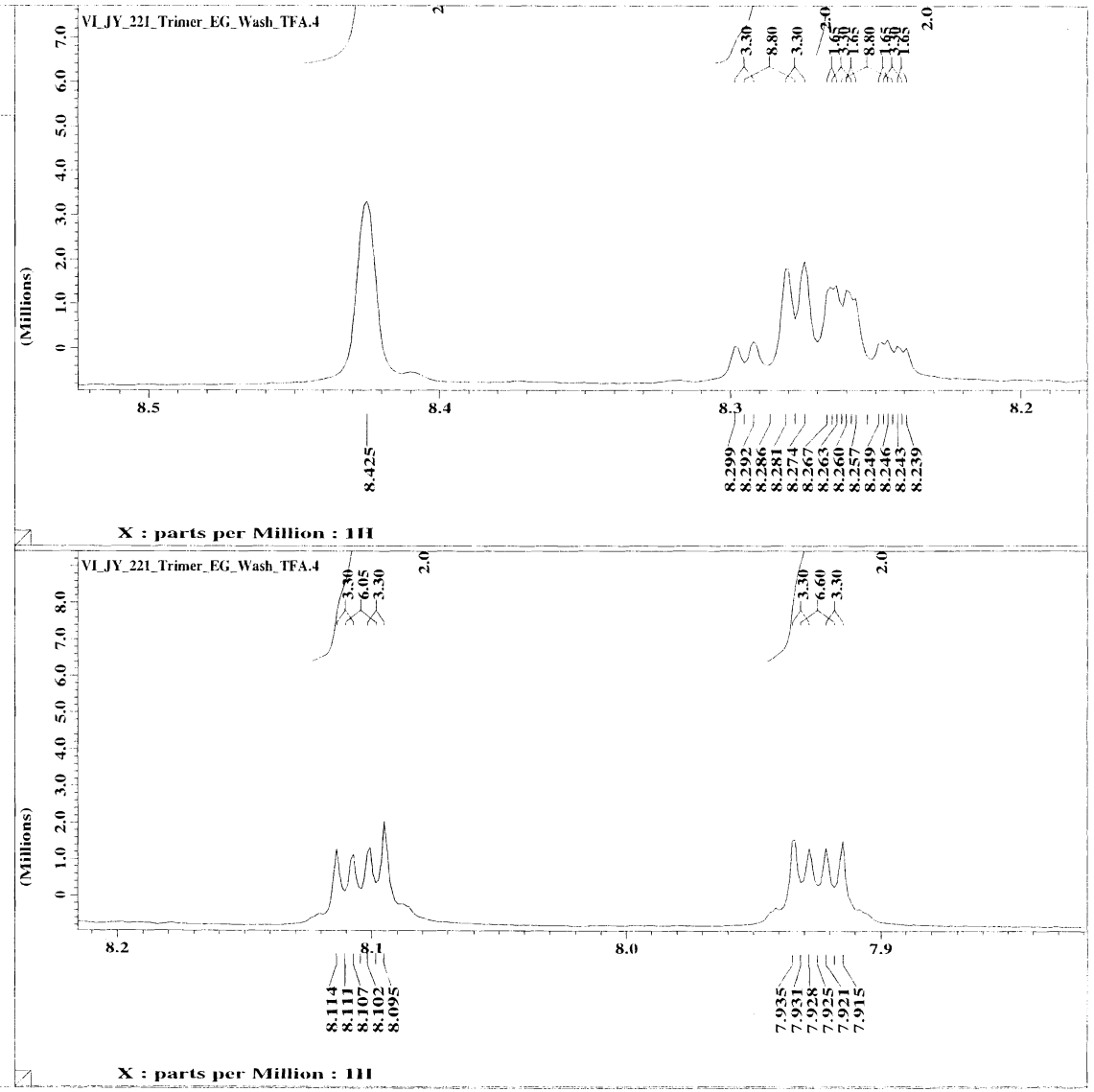

```
Filename          = VI_JY_256_TrimerBFC_D
Experiment        = single_pulse.exp
Sample_id         = S#368237
Solvent           = TRIFLUOROACETIC_
Creation_time     =  6-NOV-2004 06:27:09
Revision_time     = 26-MAY-2005 12:13:08
Current_time      = 26-MAY-2005 12:13:55

Content           = Single Pulse Experime
Data_format       = 1D COMPLEX
Dim_size          = 16384
Dim_title         = 1H
Dim_units         = [ppm]
Dimensions        = X
Site              = Eclipse+ 500
Spectrometer      = DELTA_NMR

Field_strength    = 11.7473579[T] (500[MH
X_acq_duration    = 1.6367616[s]
X_domain          = 1H
X_freq            = 500.15991521[MHz]
X_offset          = 8[ppm]
X_points          = 16384
X_prescans        = 0
X_resolution      = 0.61096253[Hz]
X_sweep           = 10.01001001[kHz]
Mod_return        = 1
Scans             = 35

X_90_width        = 15[us]
X_acq_time        = 1.6367616[s]
X_angle           = 45[deg]
X_pulse           = 7.5[us]
Initial_wait      = 1[s]
Phase_preset      = 3[us]
Recvr_gain        = 11
Relaxation_delay  = 1[s]
Temp_get          = 23.4[dC]
Unblank_time      = 2[us]
```

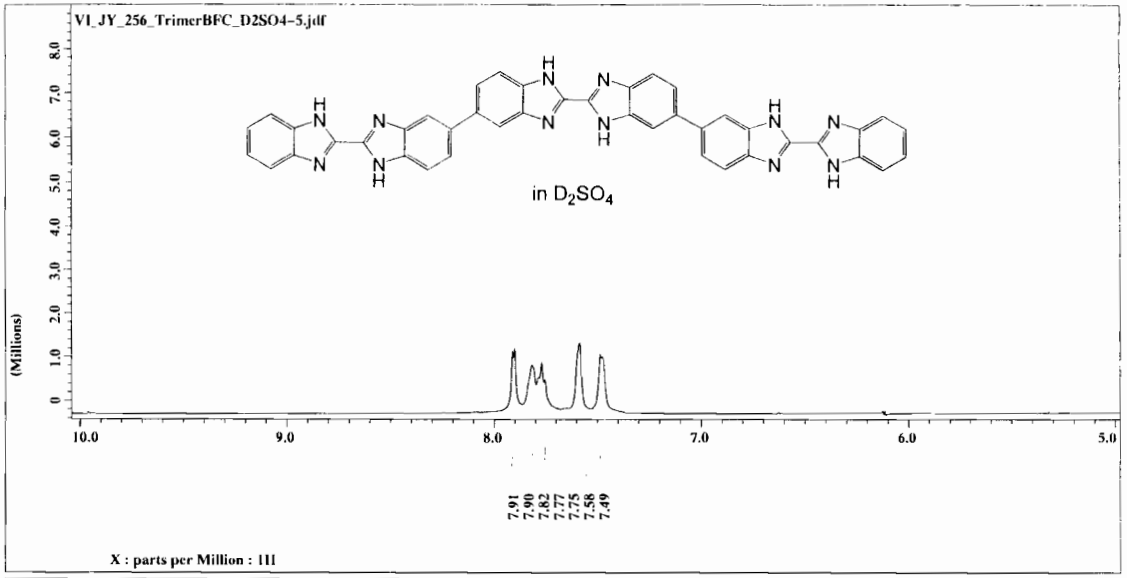

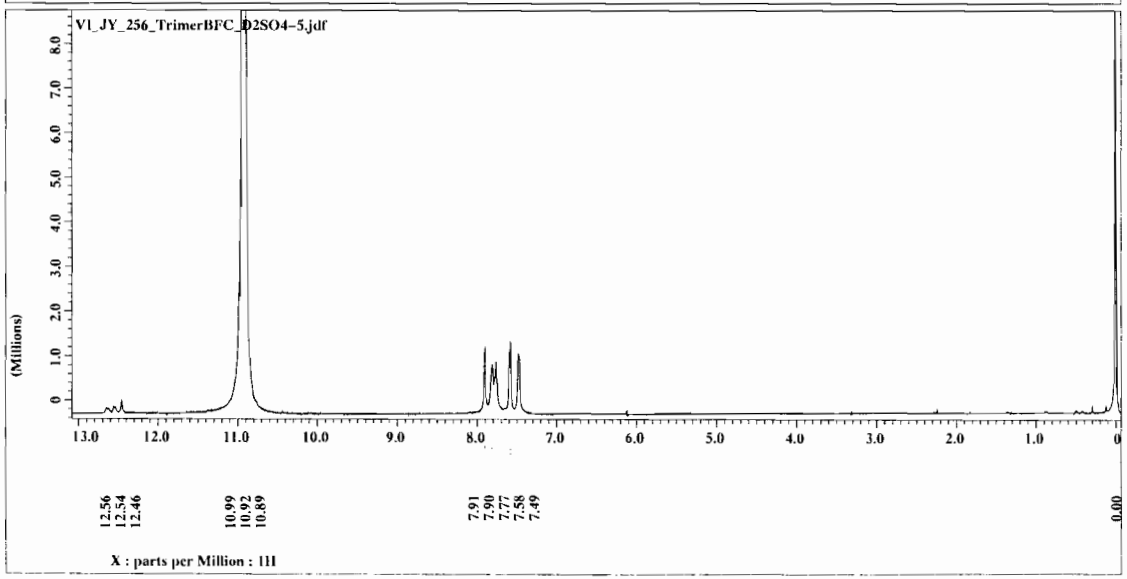

JEOL

```
---- ACQUISITION PARAMETERS ----
File Name          = VI_JY_256_TrimerBiBzIm
Author             =
Sample ID          = S#370225
Content            = Single Pulse with Broa
Creation Date      =  6-NOV-2004 16:39:58

Revision Date      = 13-NOV-2004 05:52:48
Spec Site          = Eclipse+ 500

Spec Type          = DELTA_NMR
Data Format        = 1D COMPLEX
Dimensions         = X
Dim Title          = 13C
Dim Size           = 65536
Dim Units          = [ppm]
Acq_delay          = 33.8[us]
Changer_sample     = 0
Experiment         = single_pulse_dec
Field_strength     = 11.7473579[T]
Irr90              = 15[us]
Irr90_hi           = 18[us]
Irr90_lo           = 82[us]
Irr_domain         = 1H
Irr_pwidth         = 82[us]
Lock_status        = IDLE
Recvr_gain         = 29
Relaxation_delay   = 2[s]
Scans              = 8963
Solvent            = TRIFLUOROACETIC_
Spin_get           = 15[Hz]
Spin_lock_90       = 60[us]
Spin_lock_attn     = 15[dB]
Spin_set           = 15[Hz]
Spin_state         = SPIN ON
Spin_status        = SPIN ON
Temp_get           = 24.6[dC]
Temp_set           = 25[dC]
Temp_state         = TEMP OFF
Temp_status        = TEMP OFF
X90                = 14[us]
X90_hi             = 13[us]
X90_lo             = 53[us]
X_acq_duration     = 2.0840448[s]
X_domain           = 13C
X_freq             = 125.76529768[MHz]
X_offset           = 100[ppm]
X_points           = 65536
X_prescans         = 4
X_pulse            = 4.66666667[us]
X_resolution       = 0.47983613[Hz]
X_sweep            = 31.44654088[kHz]
```

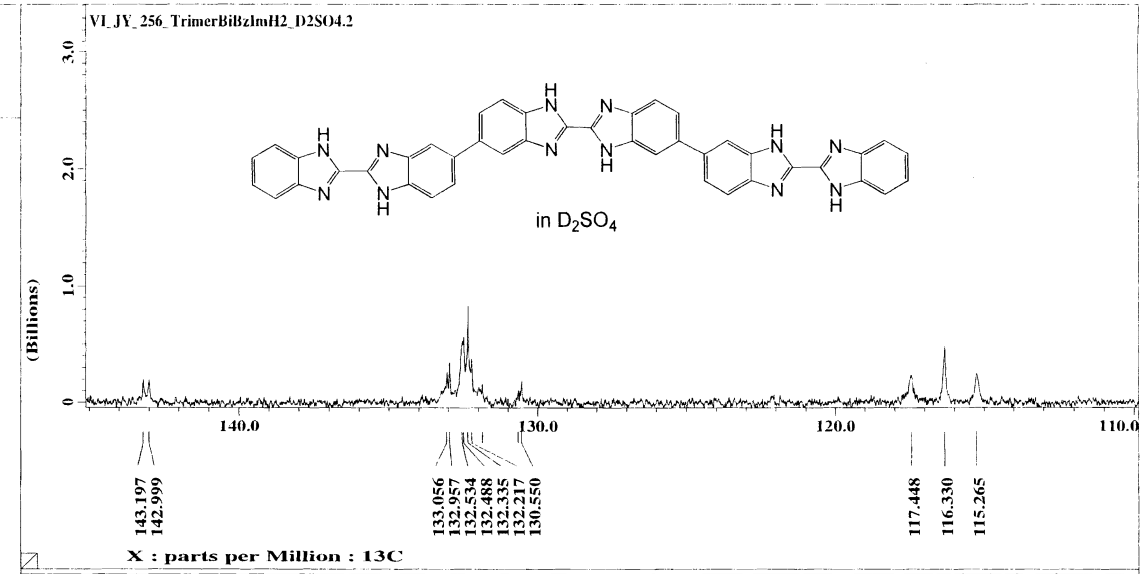

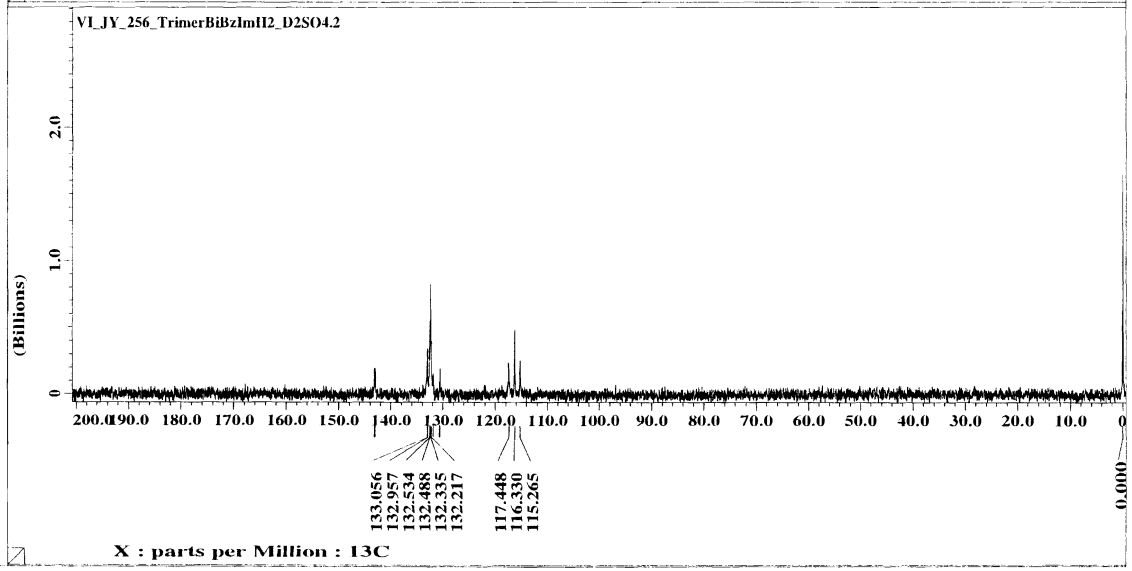

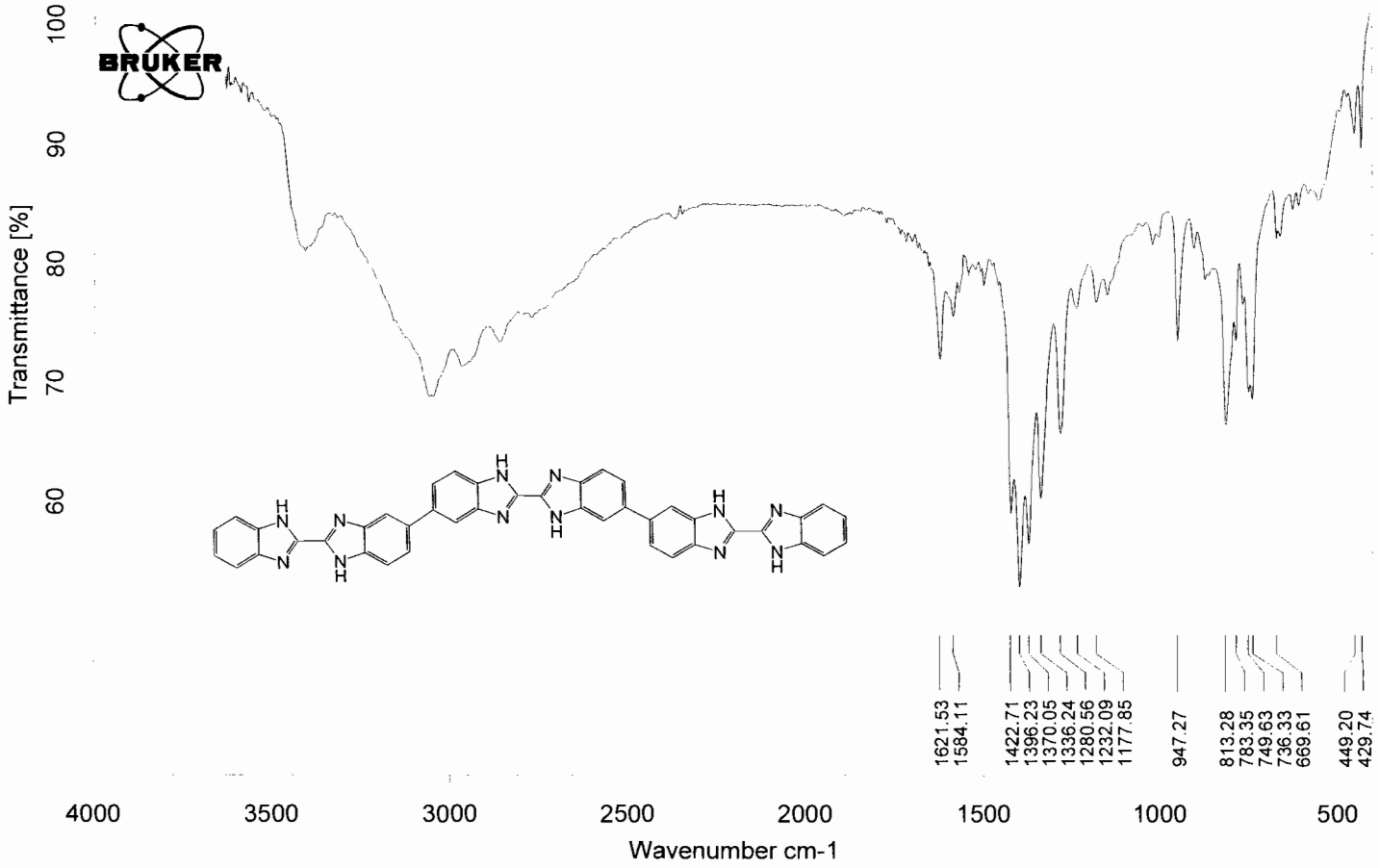

D:\OPUS_NT\DATA\Jun\VI_JY_255_trimer_3.0	VI_JY_255_trimer_3	Solid in KBr	09/11/2004

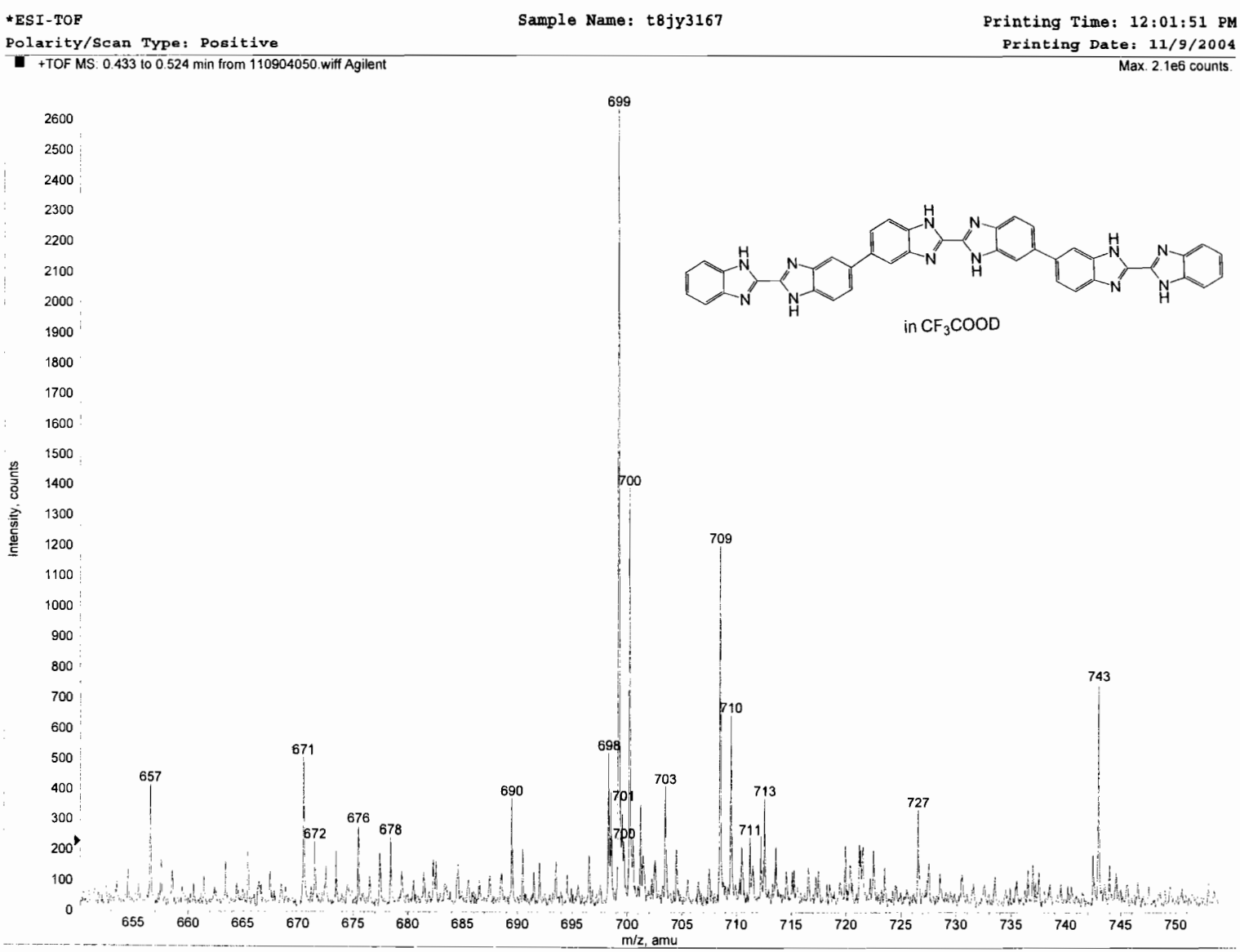
*ESI-TOF
Sample Name: t8jy3167
Printing Time: 12:01:51 PM
Polarity/Scan Type: Positive
Printing Date: 11/9/2004
+TOF MS: 0.433 to 0.524 min from 110904050.wiff Agilent
Max. 2.1e6 counts.
in CF3COOD
Intensity, counts
m/z, amu
699
700
709
710
743
671
698
657
703
690
701
713
727
676
672
678
700
711

APPENDIX 9

^{1}H, ^{13}C NMR, AND FTIR SPECTRA OF

Bis(2-trichloromethylbenzimidazole) **18**

JEOL
Filename = V_JY_196_BisCCl3_TFA-
Experiment = single_pulse.exp
Sample_id = S#172103
Solvent = TRIFLUOROACETIC_
Creation_time = 12-SEP-2004 02:06:33
Revision_time = 25-MAY-2005 23:00:35
Current_time = 25-MAY-2005 23:00:47
Content = Single Pulse Experime
Data_format = 1D COMPLEX
Dim_size = 16384
Dim_title = 1H
Dim_units = [ppm]
Dimensions = X
Site = Eclipse+ 500
Spectrometer = DELTA_NMR
Field_strength = 11.7473579[T] (500[MH
X_acq_duration = 1.818624[s]
X_domain = 1H
X_freq = 500.15991521[MHz]
X_offset = 7[ppm]
X_points = 16384
X_prescans = 0
X_resolution = 0.54986627[Hz]
X_sweep = 9.00900901[kHz]
Mod_return = 1
Scans = 100
X_90_width = 15[us]
X_acq_time = 1.818624[s]
X_angle = 45[deg]
X_pulse = 7.5[us]
Initial_wait = 1[s]
Phase_preset = 3[us]
Recvr_gain = 15
Relaxation_delay = 1[s]
Temp_get = 24.5[dC]
Unblank_time = 2[us]
V_JY_196_BisCCl3_TFA-4.jdf
in CF3COOD
8.25
8.12
X : parts per Million : 1H
V_JY_196_BisCCl3_TFA-4.jdf
11.67
8.25
8.12
0.00
X : parts per Million : 1H
(Millions)

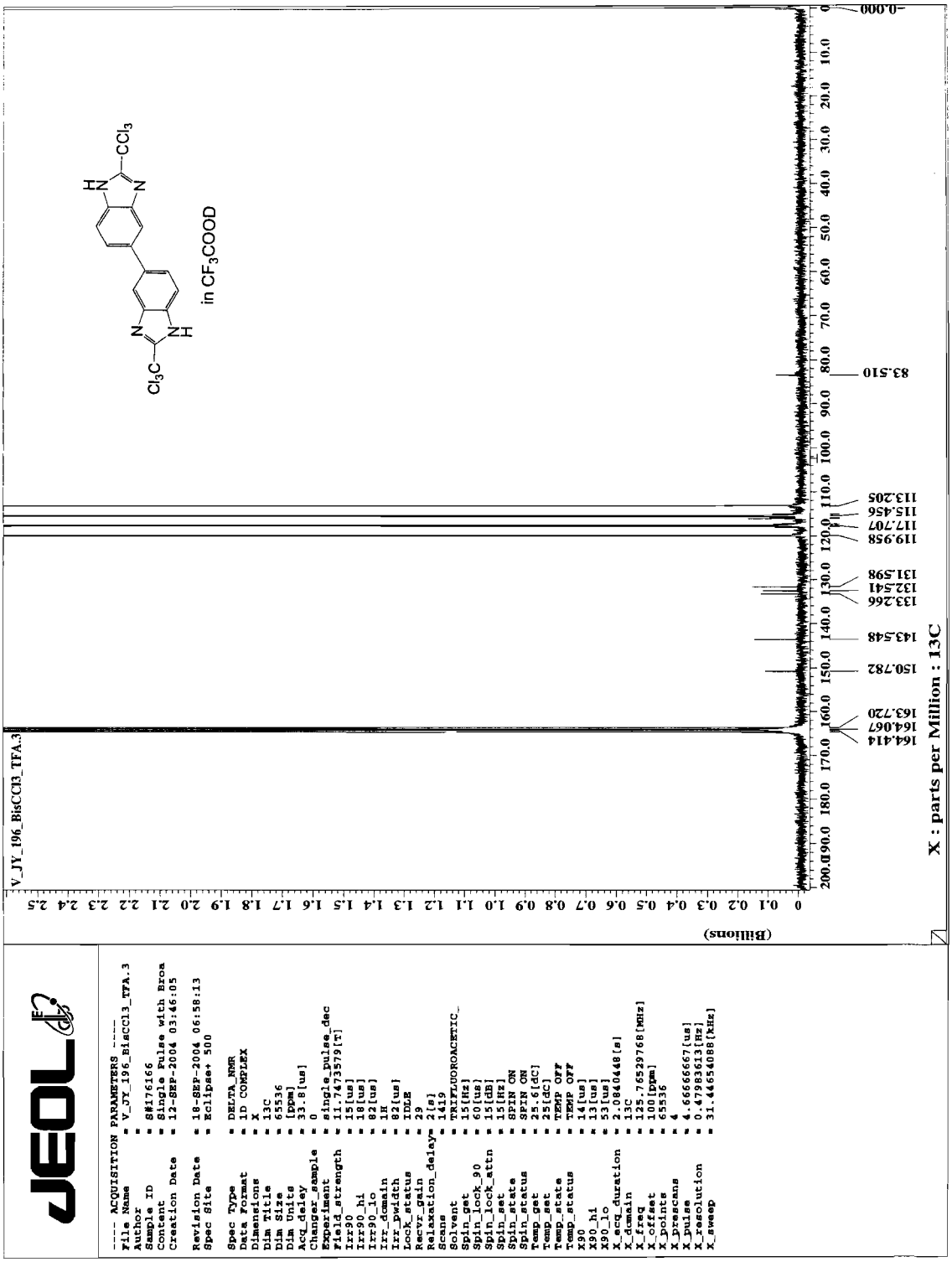
V_JY_196_BisCCl3_TFA.3
in CF3COOD
X : parts per Million : 13C
(Billions)
164.414
164.067
163.720
150.782
143.548
133.266
132.541
131.598
119.958
117.707
115.456
113.205
83.510
-0.000

JEOL

```
---- ACQUISITION PARAMETERS ----
File Name          = V_JY_196_BisCCl3_TFA.4
Author             =
Sample ID          = S#176166
Content            = Single Pulse with Broa
Creation Date      = 12-SEP-2004 03:46:05

Revision Date      = 18-SEP-2004 07:35:13
Spec Site          = Eclipse+ 500

Spec Type          = DELTA_NMR
Data Format        = 1D COMPLEX
Dimensions         = X
Dim Title          = 13C
Dim Size           = 65536
Dim Units          = [ppm]
Acq_delay          = 33.8[us]
Changer_sample     = 0
Experiment         = single_pulse_dec
Field_strength     = 11.7473579[T]
Irr90              = 15[us]
Irr90_hi           = 10[us]
Irr90_lo           = 82[us]
Irr_domain         = 1H
Irr_pwidth         = 82[us]
Lock_status        = IDLE
Recvr_gain         = 29
Relaxation_delay   = 2[s]
Scans              = 1419
Solvent            = TRIFLUOROACETIC_
Spin_get           = 15[Hz]
Spin_lock_90       = 60[us]
Spin_lock_attn     = 15[dB]
Spin_set           = 15[Hz]
Spin_state         = SPIN ON
Spin_status        = SPIN ON
Temp_get           = 25.6[dC]
Temp_set           = 25[dC]
Temp_state         = TEMP OFF
Temp_status        = TEMP OFF
X90                = 14[us]
X90_hi             = 13[us]
X90_lo             = 53[us]
X_acq_duration     = 2.0840448[s]
X_domain           = 13C
X_freq             = 125.76529768[MHz]
X_offset           = 100[ppm]
X_points           = 65536
X_prescans         = 4
X_pulse            = 4.66666667[us]
X_resolution       = 0.47983613[Hz]
X_sweep            = 31.44654088[kHz]
```

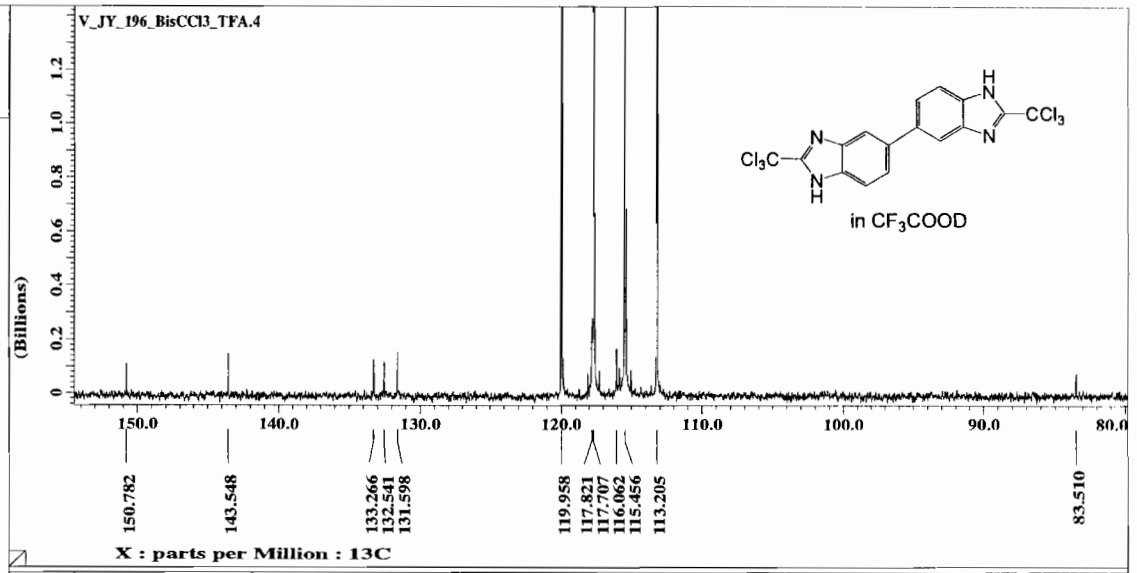

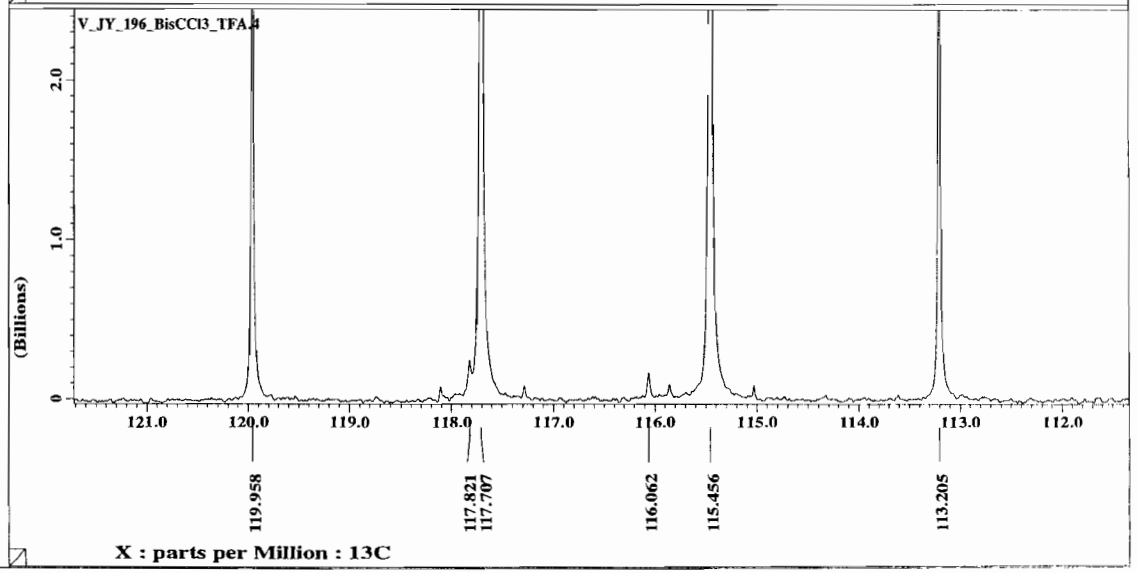

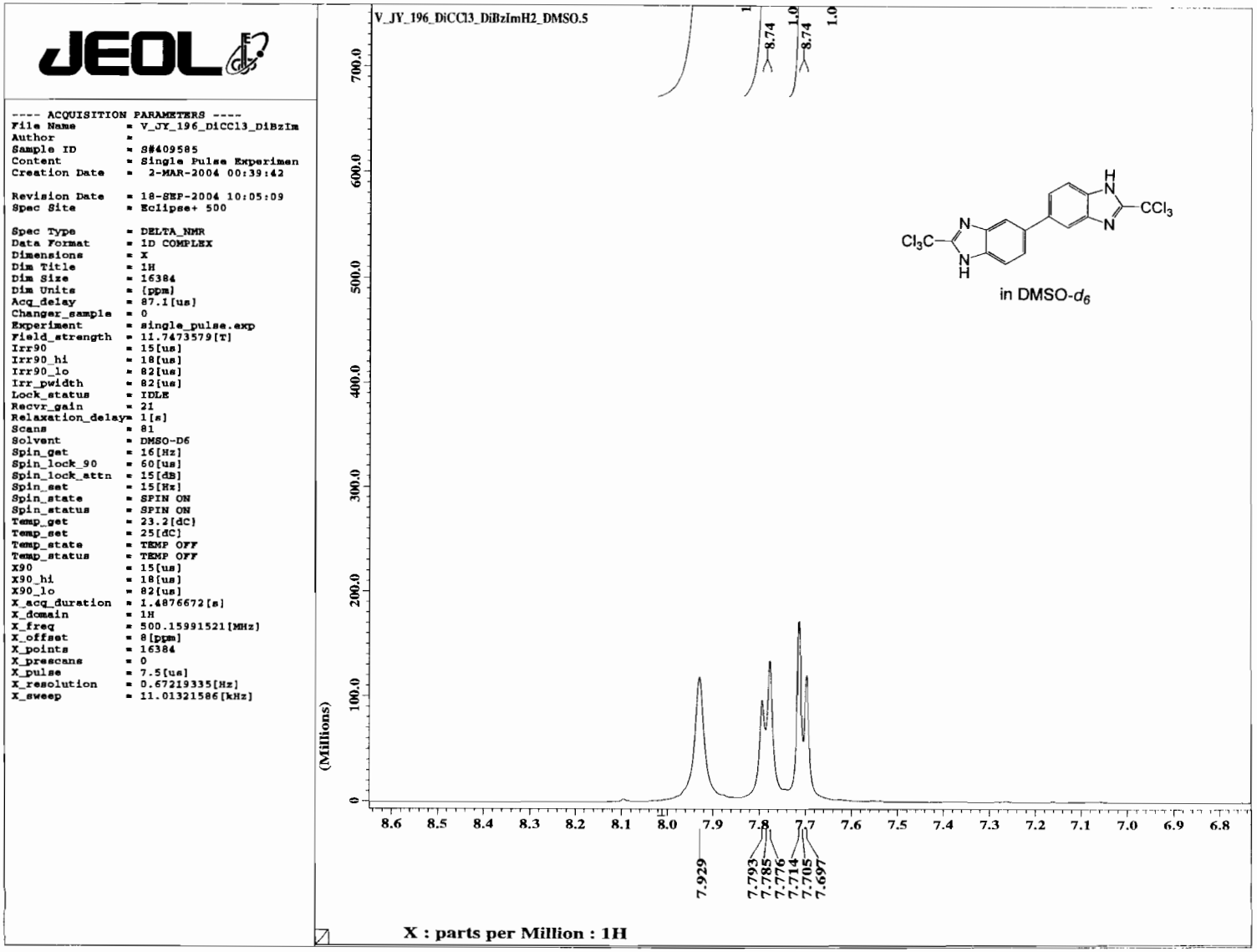
JEOL
---- ACQUISITION PARAMETERS ----
File Name = V_JY_196_DiCCl3_DiBzIm
Author =
Sample ID = S#409585
Content = Single Pulse Experimen
Creation Date = 2-MAR-2004 00:39:42
Revision Date = 18-SEP-2004 10:05:09
Spec Site = Eclipse+ 500
Spec Type = DELTA_NMR
Data Format = 1D COMPLEX
Dimensions = X
Dim Title = 1H
Dim Size = 16384
Dim Units = [ppm]
Acq_delay = 87.1[us]
Changer_sample = 0
Experiment = single_pulse.exp
Field_strength = 11.7473579[T]
Irr90 = 15[us]
Irr90_hi = 18[us]
Irr90_lo = 82[us]
Irr_pwidth = 82[us]
Lock_status = IDLE
Recvr_gain = 21
Relaxation_delay= 1[s]
Scans = 81
Solvent = DMSO-D6
Spin_get = 16[Hz]
Spin_lock_90 = 60[us]
Spin_lock_attn = 15[dB]
Spin_set = 15[Hz]
Spin_state = SPIN ON
Spin_status = SPIN ON
Temp_get = 23.2[dC]
Temp_set = 25[dC]
Temp_state = TEMP OFF
Temp_status = TEMP OFF
X90 = 15[us]
X90_hi = 18[us]
X90_lo = 82[us]
X_acq_duration = 1.4876672[s]
X_domain = 1H
X_freq = 500.15991521[MHz]
X_offset = 8[ppm]
X_points = 16384
X_prescans = 0
X_pulse = 7.5[us]
X_resolution = 0.67219335[Hz]
X_sweep = 11.01321586[kHz]
V_JY_196_DiCCl3_DiBzImH2_DMSO.5
8.74
1.0
8.74
1.0
(Millions)
700.0
600.0
500.0
400.0
300.0
200.0
100.0
0
8.6
8.5
8.4
8.3
8.2
8.1
8.0
7.9
7.8
7.7
7.6
7.5
7.4
7.3
7.2
7.1
7.0
6.9
6.8
7.929
7.793
7.785
7.776
7.714
7.705
7.697
X : parts per Million : 1H
H
N
CCl3
N
Cl3C
N
H
in DMSO-d6

JEOL

```
---- ACQUISITION PARAMETERS ----
File Name          = V_JY_197_BisCCl3_DMSO.
Author             =
Sample ID          = S#351753
Content            = Single Pulse with Brom
Creation Date      = 12-SEP-2004 19:39:11

Revision Date      = 10-SEP-2004 23:33:41
Spec Site          = Eclipse+ 500

Spec Type          = DELTA_NMR
Data Format        = 1D COMPLEX
Dimensions         = X
Dim Title          = 13C
Dim Size           = 32768
Dim Units          = [ppm]
Acq_delay          = 33.8[us]
Changer_sample     = 0
Experiment         = single_pulse_dec
Field_strength     = 11.7473579[T]
Irr90              = 15[us]
Irr90_hi           = 18[us]
Irr90_lo           = 02[us]
Irr_domain         = 1H
Irr_pwidth         = 02[us]
Lock_status        = IDLE
Recvr_gain         = 29
Relaxation_delay   = 4[s]
Scans              = 9000
Solvent            = DMSO-D6
Spin_get           = 14[Hz]
Spin_lock_90       = 60[us]
Spin_lock_attn     = 15[dB]
Spin_set           = 15[Hz]
Spin_state         = SPIN ON
Spin_status        = SPIN ON
Temp_get           = 25.7[dC]
Temp_set           = 25[dC]
Temp_state         = TEMP OFF
Temp_status        = TEMP OFF
X90                = 14[us]
X90_hi             = 13[us]
X90_lo             = 53[us]
X_acq_duration     = 1.0420224[s]
X_domain           = 13C
X_freq             = 125.76529768[MHz]
X_offset           = 100[ppm]
X_points           = 32768
X_prescans         = 4
X_pulse            = 4.66666667[us]
X_resolution       = 0.95967227[Hz]
X_sweep            = 31.44654088[kHz]
```

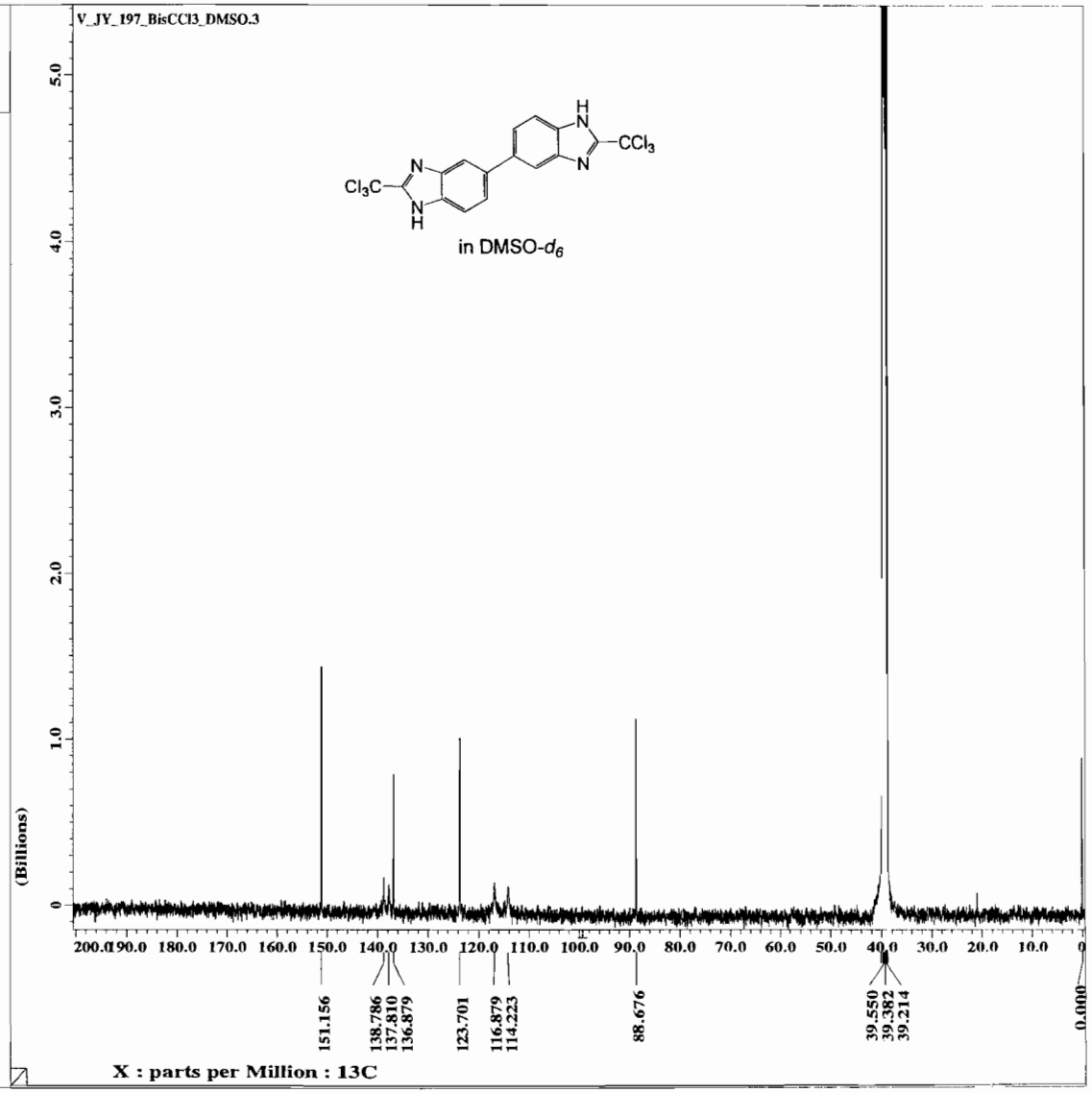

Transmittance [%]
100
95
90
85
80
75
70
65
60
4000
3500
3000
2500
2000
1500
1000
500
Wavenumber cm-1
3427.92
1626.47
1584.25
1507.61
1419.88
1293.41
1280.70
1228.47
1206.23
1163.74
1028.08
1007.98
908.77
876.93
830.53
815.86
776.32
679.26
609.59
514.73
499.45
443.55
422.02
CCl_3
Cl_3C
D:\OPUS_NT\DATA\Jun\V_JY_196_Bis_trichloride_2.1
V_JY_196_Bis_trichloride_2
Solid in KBr
09/11/2004

APPENDIX 10

^{1}H, ^{13}C NMR, FTIR AND ESI MASS SPECTRA OF

Tetra(2,2′-bibenzimidazole) **19**

```
Filename          = VI JY 188 Tetramer Dr
Experiment        = single_pulse.exp
Sample_id         = S#385074
Solvent           = TRIFLUOROACETIC_
Creation time     =  3-SEP-2004 07:56:34
Revision time     = 25-MAY-2005 21:59:13
Current time      = 25-MAY-2005 21:59:25

Content           = Single Pulse Experime
Data_format       = 1D COMPLEX
Dim size          = 16384
Dim_title         = 1H
Dim_units         = [ppm]
Dimensions        = X
Site              = Eclipse+ 500
Spectrometer      = DELTA_NMR

Field strength    = 11.7473579[T] (500[MH
X_acq duration    = 1.818624[s]
X_domain          = 1H
X_freq            = 500.15991521[MHz]
X_offset          = 7[ppm]
X_points          = 16384
X_prescans        = 0
X_resolution      = 0.54986627[Hz]
X_sweep           = 9.00900901[kHz]
Mod return        = 1
Scans             = 100

X_90_width        = 15[us]
X_acq_time        = 1.818624[s]
X_angle           = 45[deg]
X_pulse           = 7.5[us]
Initial_wait      = 1[s]
Phase_preset      = 3[us]
Recvr_gain        = 18
Relaxation_delay  = 1[s]
Temp_get          = 23.8[dC]
Unblank_time      = 2[us]
```

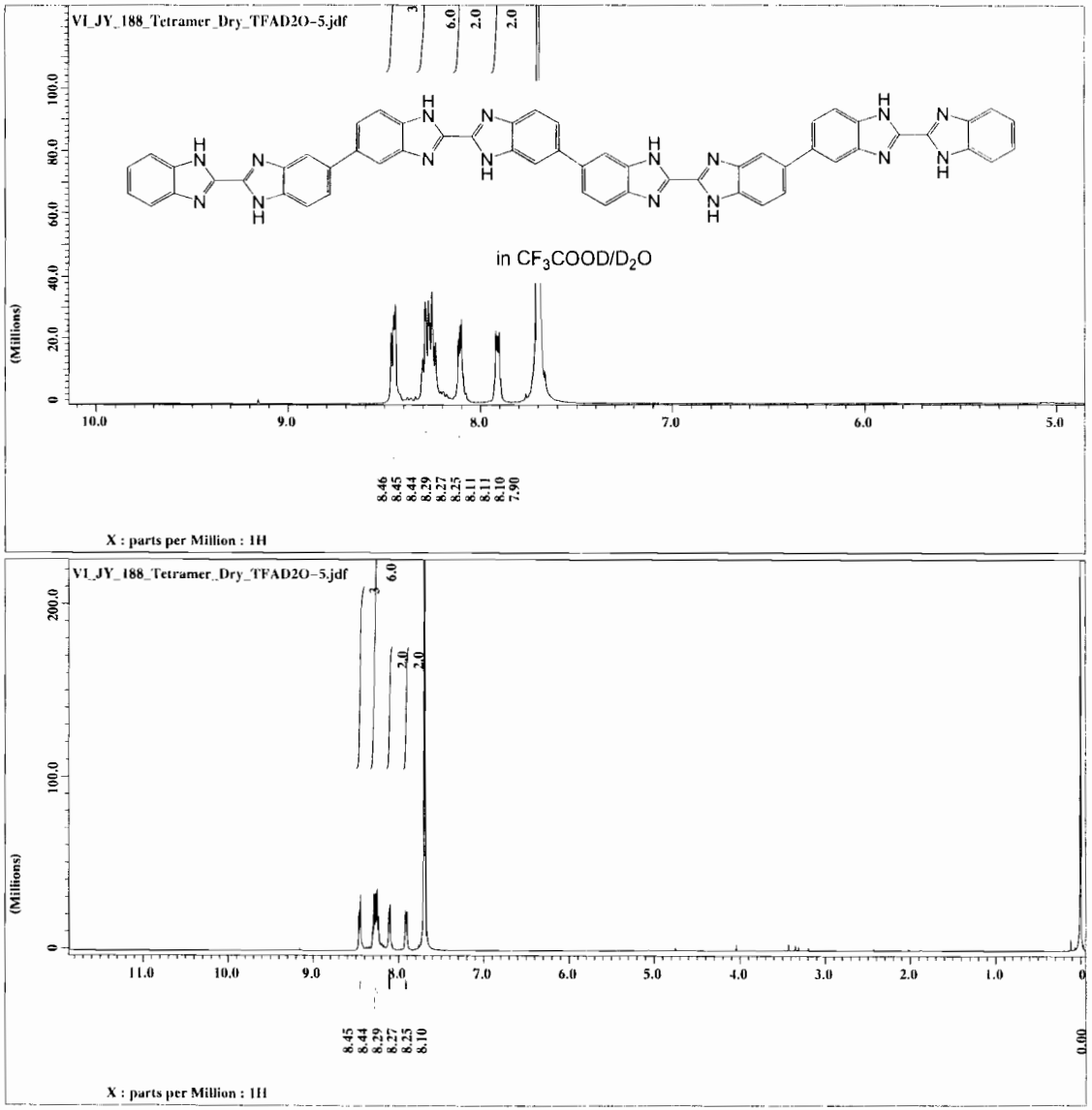

JEOL

```
Filename          = VI JY 188 TetramerBiB
Experiment        = single_pulse_dec
Sample_id         = S#396853
Solvent           = TRIFLUOROACETIC_
Creation_time     =  3-SEP-2004 17:49:27
Revision_time     = 25-MAY-2005 22:03:38
Current_time      = 25-MAY-2005 22:05:00

Content           = Single Pulse with Bro
Data_format       = 1D COMPLEX
Dim_size          = 65536
Dim_title         = 13C
Dim_units         = [ppm]
Dimensions        = X
Site              = Eclipse+ 500
Spectrometer      = DELTA NMR

Field_strength    = 11.7473579[T] (500[MH
X_acq_duration    = 2.0840448[s]
X_domain          = 13C
X_freq            = 125.76529768[MHz]
X_offset          = 100[ppm]
X_points          = 65536
X_prescans        = 4
X_resolution      = 0.47983613[Hz]
X_sweep           = 31.44654088[kHz]
Irr_domain        = 1H
Irr_freq          = 500.15991521[MHz]
Irr_offset        = 5[ppm]
Mod_return        = 1
Scans             = 8478

X_90_width        = 14[us]
X_acq_time        = 2.0840448[s]
X_angle           = 30[deg]
X_pulse           = 4.66666667[us]
Initial_wait      = 1[s]
Phase_preset      = 3[us]
Recvr_gain        = 29
Relaxation_delay  = 2[s]
Temp_get          = 25.2[dC]
Unblank_time      = 2[us]
```

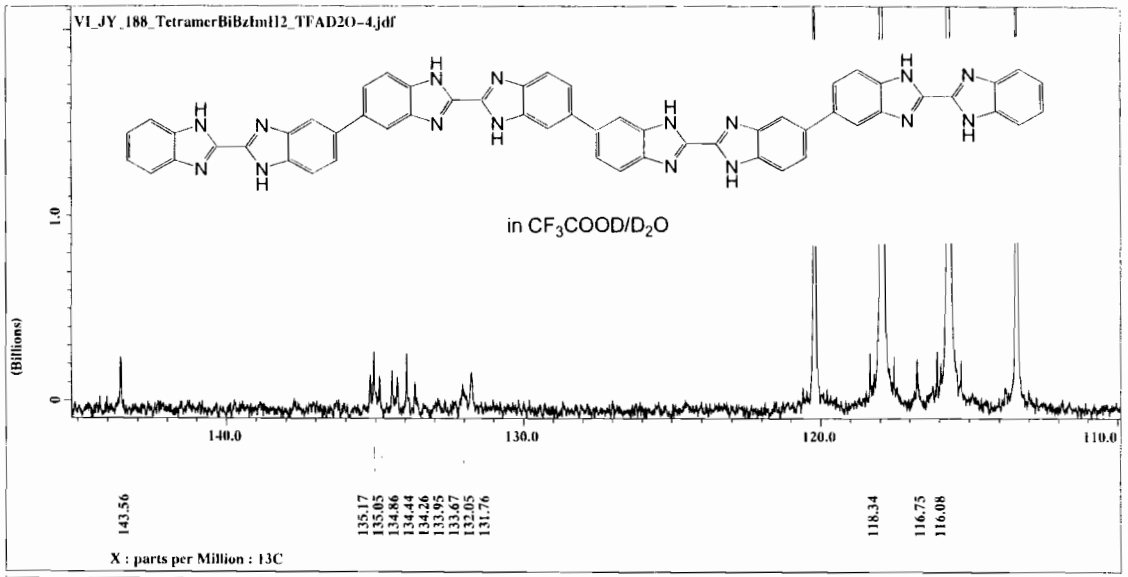

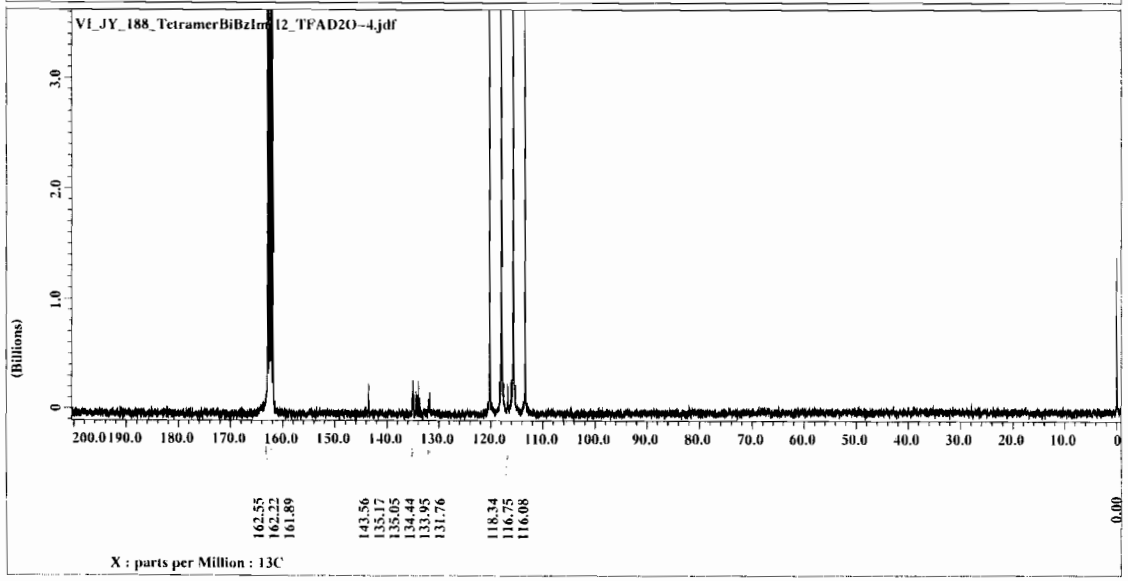

```
Filename          = V1_JY_269_Tetra_D2SO4
Experiment        = single_pulse.exp
Sample_id         = S#104721
Solvent           = TRIFLUOROACETIC_
Creation_time     =  2-NOV-2004 23:12:44
Revision_time     =  9-NOV-2004 03:05:31
Current_time      = 26-MAY-2005 12:18:37

Content           = Single Pulse Experime
Data_format       = 1D COMPLEX
Dim_size          = 16384
Dim_title         = 1H
Dim_units         = [ppm]
Dimensions        = X
Site              = Eclipse+ 500
Spectrometer      = DELTA NMR

Field_strength    = 11.7473579[T] (500[MH
X_acq_duration    = 1.4876672[s]
X_domain          = 1H
X_freq            = 500.15991521[MHz]
X_offset          = 9[ppm]
X_points          = 16384
X_prescans        = 0
X_resolution      = 0.67219335[Hz]
X_sweep           = 11.01321586[kHz]
Mod_return        = 1
Scans             = 212

X_90_width        = 15[us]
X_acq_time        = 1.4876672[s]
X_angle           = 45[deg]
X_pulse           = 7.5[us]
Initial_wait      = 1[s]
Phase_preset      = 3[us]
Recvr_gain        = 20
Relaxation_delay  = 1[s]
Temp_get          = 23.7[dC]
Unblank_time      = 2[us]
```

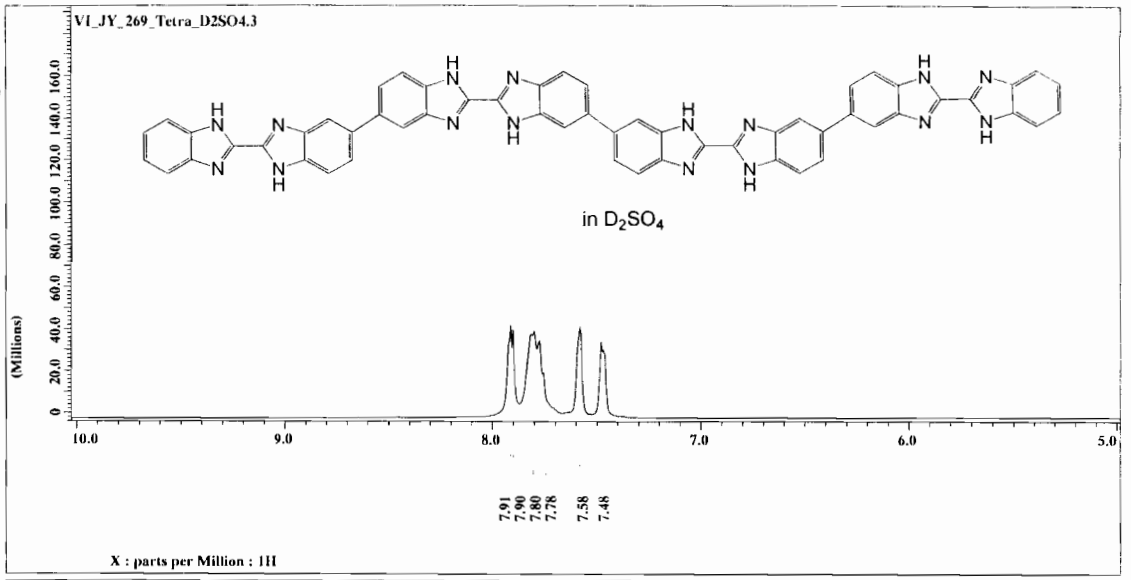

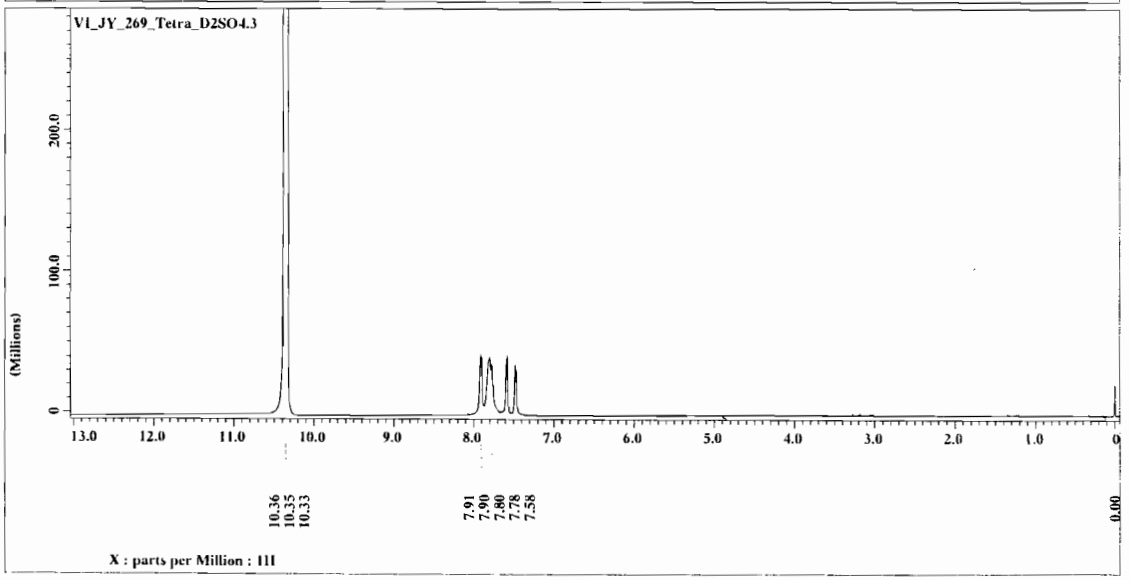

JEOL

```
---- ACQUISITION PARAMETERS ----
File Name          = VI_JY_269_TetraBiBzImH
Author             =
Sample ID          = S#369063
Content            = Single Pulse with Broa
Creation Date      = 20-NOV-2004 18:40:20

Revision Date      = 27-NOV-2004 04:36:23
Spec Site          = Eclipse+ 500

Spec Type          = DELTA_NMR
Data Format        = 1D COMPLEX
Dimensions         = X
Dim Title          = 13C
Dim Size           = 65536
Dim Units          = [ppm]
Acq_delay          = 33.8[us]
Changer_sample     = 0
Experiment         = single_pulse_dec
Field_strength     = 11.7473579[T]
Irr90              = 15[us]
Irr90_hi           = 18[us]
Irr90_lo           = 82[us]
Irr_domain         = 1H
Irr_pwidth         = 82[us]
Lock_status        = IDLE
Recvr_gain         = 29
Relaxation_delay   = 2[s]
Scans              = 10632
Solvent            = TRIFLUOROACETIC_
Spin_get           = 15[Hz]
Spin_lock_90       = 60[us]
Spin_lock_attn     = 15[dB]
Spin_set           = 15[Hz]
Spin_state         = SPIN ON
Spin_status        = SPIN ON
Temp_get           = 24.5[dC]
Temp_set           = 25[dC]
Temp_state         = TEMP OFF
Temp_status        = TEMP OFF
X90                = 14[us]
X90_hi             = 13[us]
X90_lo             = 53[us]
X_acq_duration     = 2.0840448[s]
X_domain           = 13C
X_freq             = 125.76529768[MHz]
X_offset           = 100[ppm]
X_points           = 65536
X_prescans         = 4
X_pulse            = 4.66666667[us]
X_resolution       = 0.47983613[Hz]
X_sweep            = 31.44654088[kHz]
```

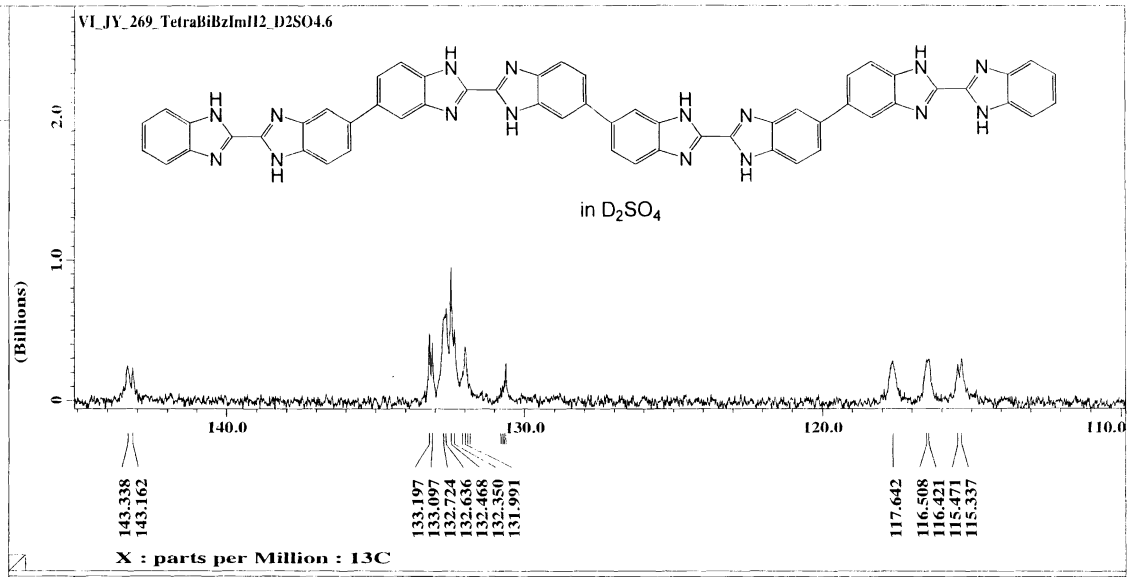

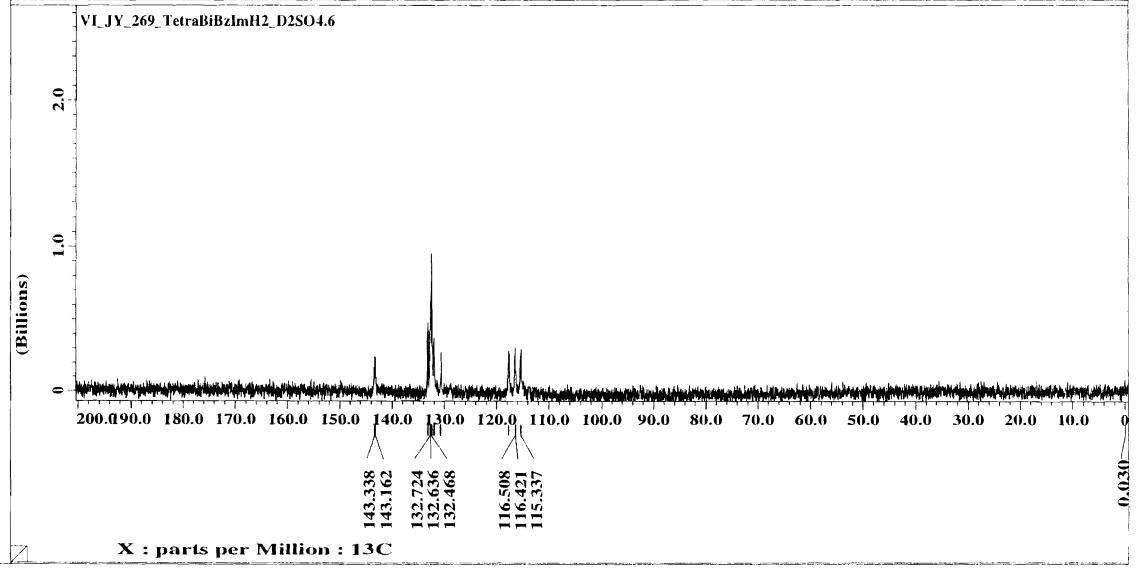

Transmittance [%]
100
95
90
85
80
75
70
65
4000
3500
3000
2500
2000
1500
1000
500
Wavenumber cm-1
1622.26
1585.25
1566.73
1539.18
1496.15
1422.71
1396.55
1372.48
1335.99
1280.74
1177.27
947.10
901.57
871.00
814.02
783.82
749.58
736.60
669.10
657.39
449.86
429.65
D:\OPUS_NT\DATA\Jun\VI_JY_267_tetramer.0
VI_JY_267_tetramer
Solid in KBr
09/11/2004

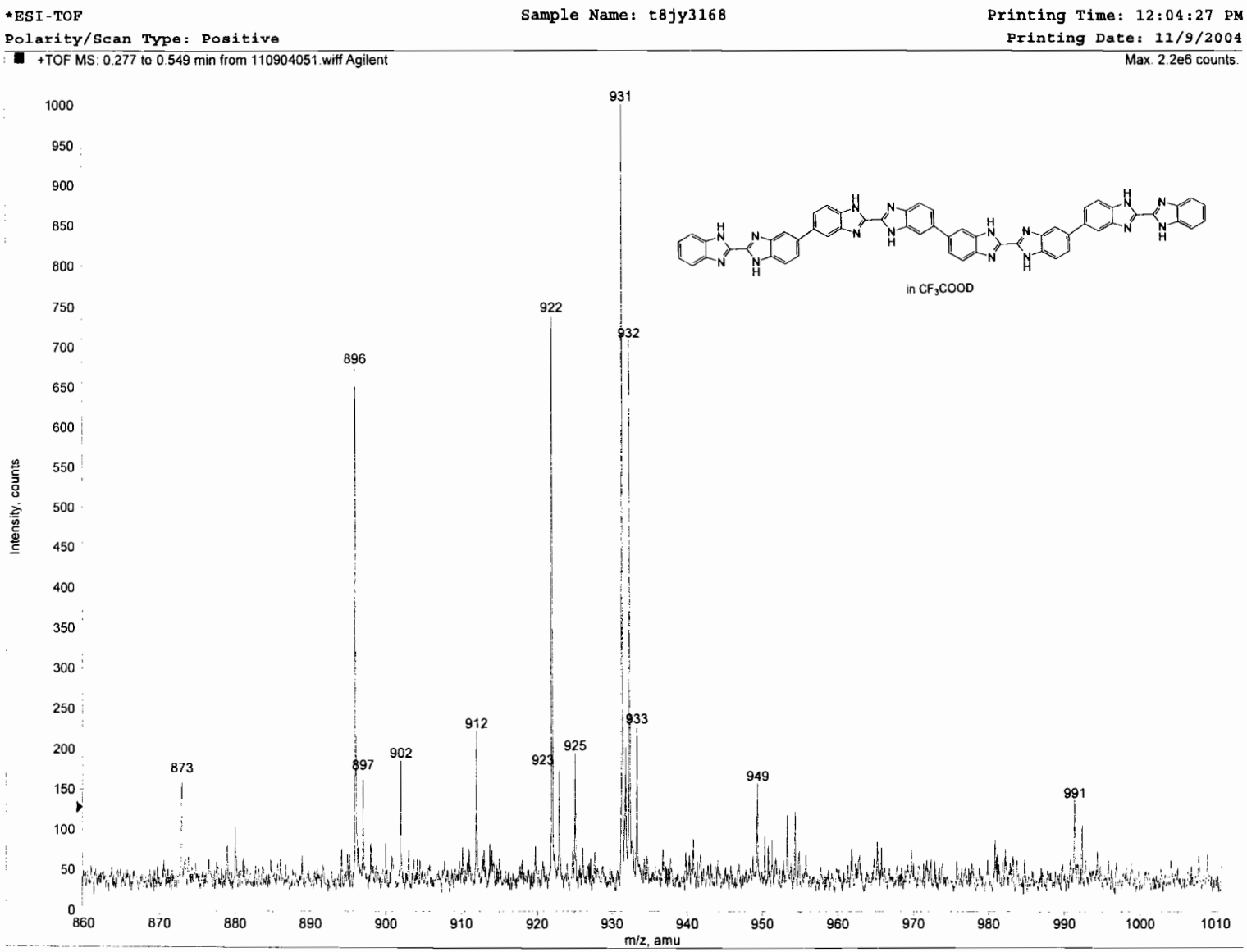
*ESI-TOF
Sample Name: t8jy3168
Printing Time: 12:04:27 PM
Polarity/Scan Type: Positive
Printing Date: 11/9/2004
+TOF MS: 0.277 to 0.549 min from 110904051.wiff Agilent
Max. 2.2e6 counts.
in CF3COOD
Intensity, counts
m/z, amu
931
922
932
896
912
933
902
925
923
897
873
949
991

APPENDIX 11

^{1}H, ^{13}C NMR, AND FTIR SPECTRA OF

Poly(2,2′-bibenzimidazole) **4a**

JEOL

Filename	= VII_JY_150_PolyBiBzIm
Author	= delta
Experiment	= single_pulse.exp
Sample id	= S#783685
Solvent	= TRIFLUOROACETIC_
Creation_time	= 2-JAN-2005 04:14:26
Revision time	= 16-FEB-2005 22:05:48
Current_time	= 26-APR-2005 22:06:31
Content	= Single Pulse Experime
Data_format	= 1D COMPLEX
Dim_size	= 16384
Dim_title	= 1H
Dim_units	= [ppm]
Dimensions	= X
Site	= Eclipse+_500
Spectrometer	= DELTA_NMR
Field strength	= 11.7473579[T] (500[MH
X_acq_duration	= 1.6367616[s]
X_domain	= 1H
X_freq	= 500.15991521[MHz]
X_offset	= 6[ppm]
X_points	= 16384
X_prescans	= 0
X_resolution	= 0.61096253[Hz]
X_sweep	= 10.01001001[kHz]
Clipped	= FALSE
Mod_return	= 1
Scans	= 100
Total_scans	= 100
X_90_width	= 18.5[us]
X_acq_time	= 1.6367616[s]
X_angle	= 45[deg]
X_pulse	= 9.25[us]
Initial_wait	= 1[s]
Phase_preset	= 3[us]
Recvr_gain	= 16
Relaxation_delay	= 1[s]
Temp_get	= 25.8[dC]
Unblank_time	= 2[us]

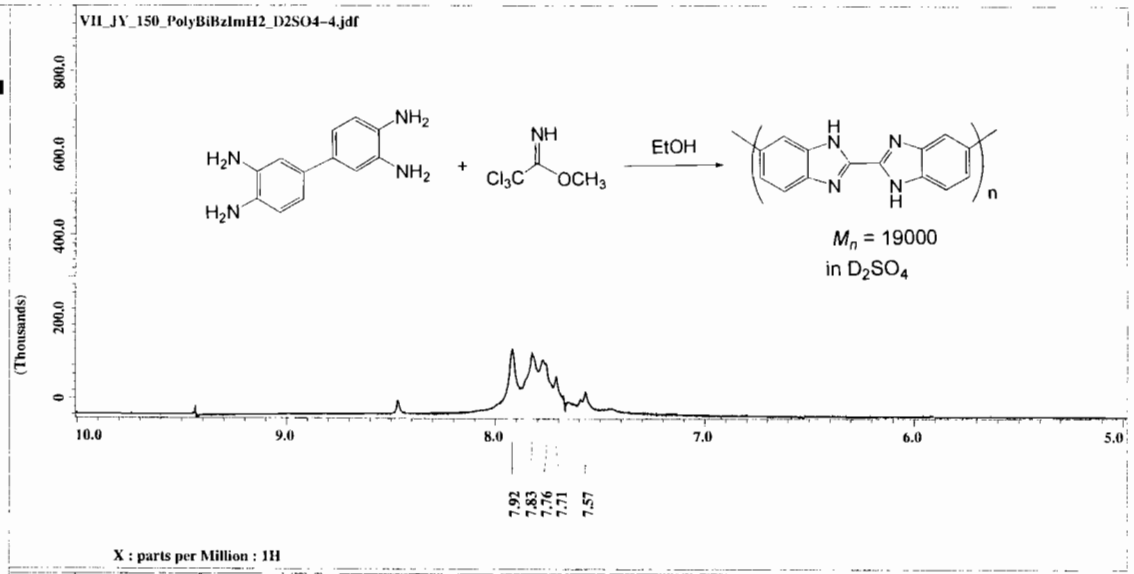

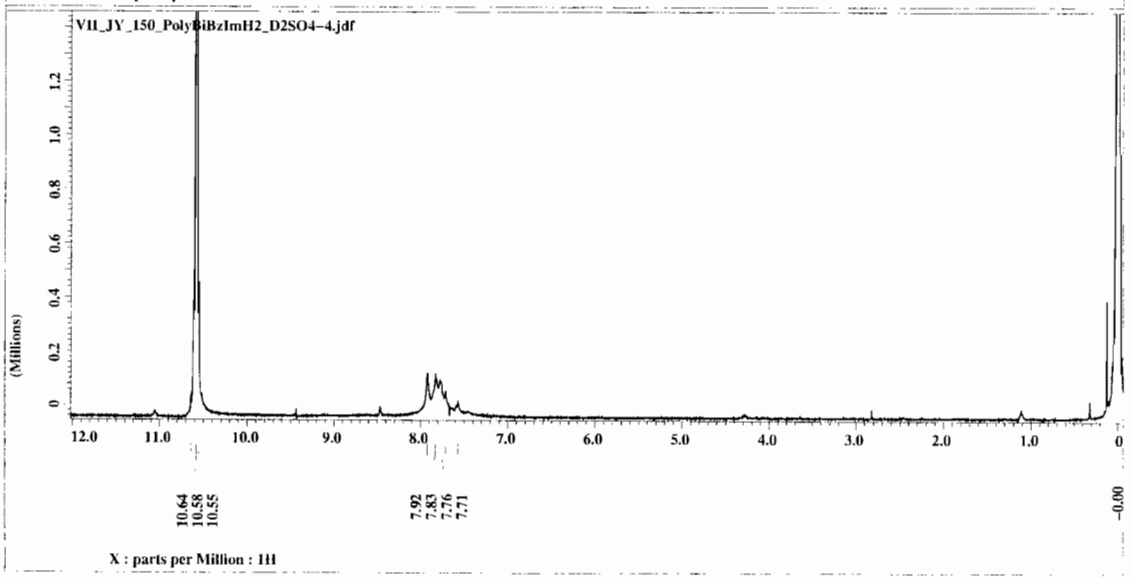

JEOL

Filename	= VII_JY_150_PolyBiBzIm
Author	= delta
Experiment	= single_pulse_dec
Sample_id	= s#745757
Solvent	= TRIFLUOROACETIC_
Creation_time	= 3-JAN-2005 17:30:48
Revision_time	= 8-MAY-2005 12:58:25
Current_time	= 8-MAY-2005 20:31:48
Content	= Single Pulse with Bro
Data_format	= 1D COMPLEX
Dim_size	= 65536
Dim_title	= 13C
Dim_units	= [ppm]
Dimensions	= X
Site	= Eclipse+ 500
Spectrometer	= DELTA_NMR
Field_strength	= 11.7473579[T] (500[MH
X_acq_duration	= 2.0840448[s]
X_domain	= 13C
X_freq	= 125.76529768[MHz]
X_offset	= 100[ppm]
X_points	= 65536
X_prescans	= 4
X_resolution	= 0.47983613[Hz]
X_sweep	= 31.44654088[kHz]
Irr_domain	= 1H
Irr_freq	= 500.15991521[MHz]
Irr_offset	= 5[ppm]
Clipped	= FALSE
Mod_return	= 1
Scans	= 12669
Total_scans	= 12669
X_90_width	= 14.2[us]
X_acq_time	= 2.0840448[s]
X_angle	= 30[deg]
X_pulse	= 4.73333333[us]
Initial_wait	= 1[s]
Phase_preset	= 3[us]
Recvr_gain	= 29
Relaxation_delay	= 2[s]
Temp_get	= 33.5[dC]
Unblank_time	= 2[us]

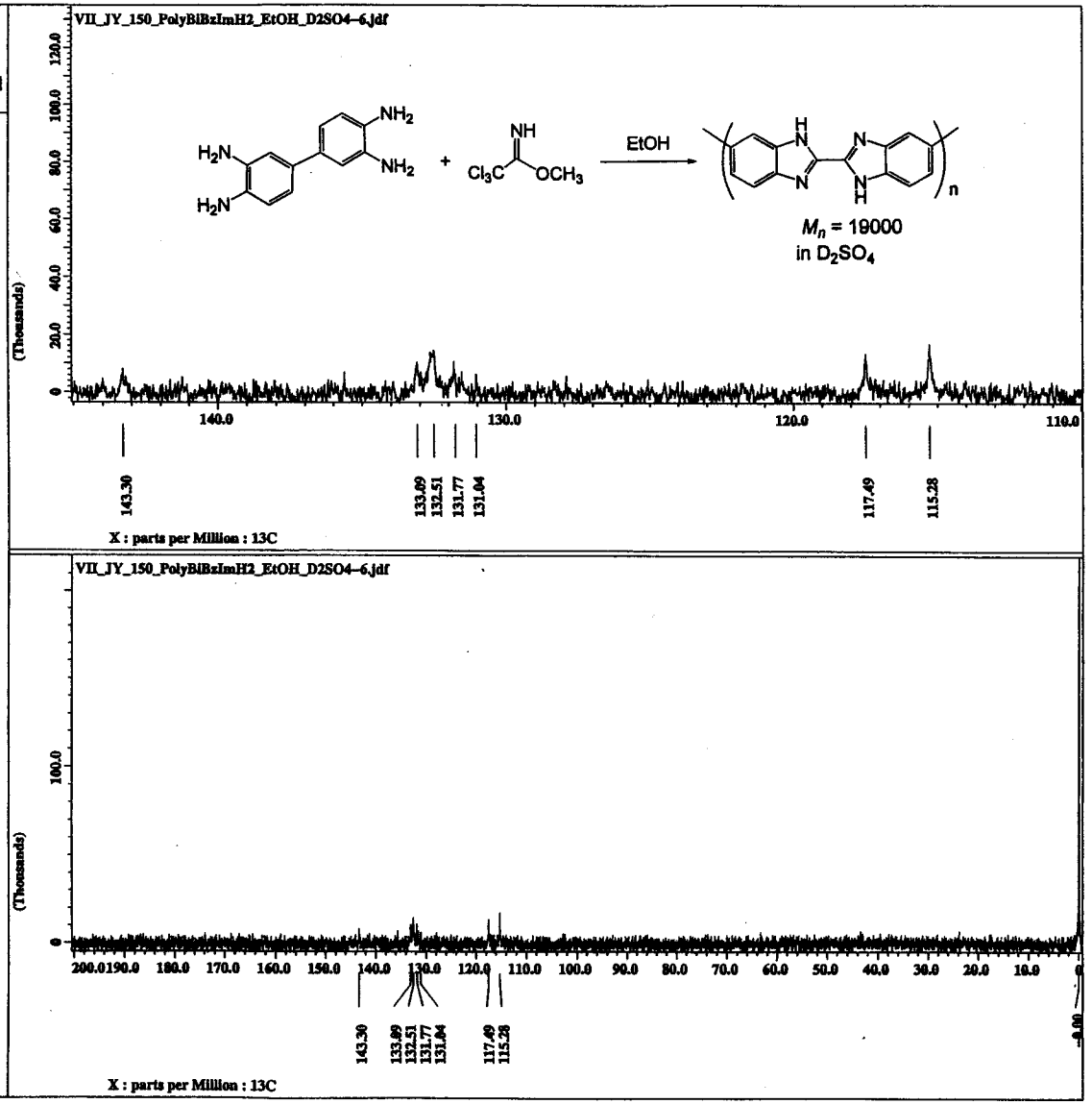

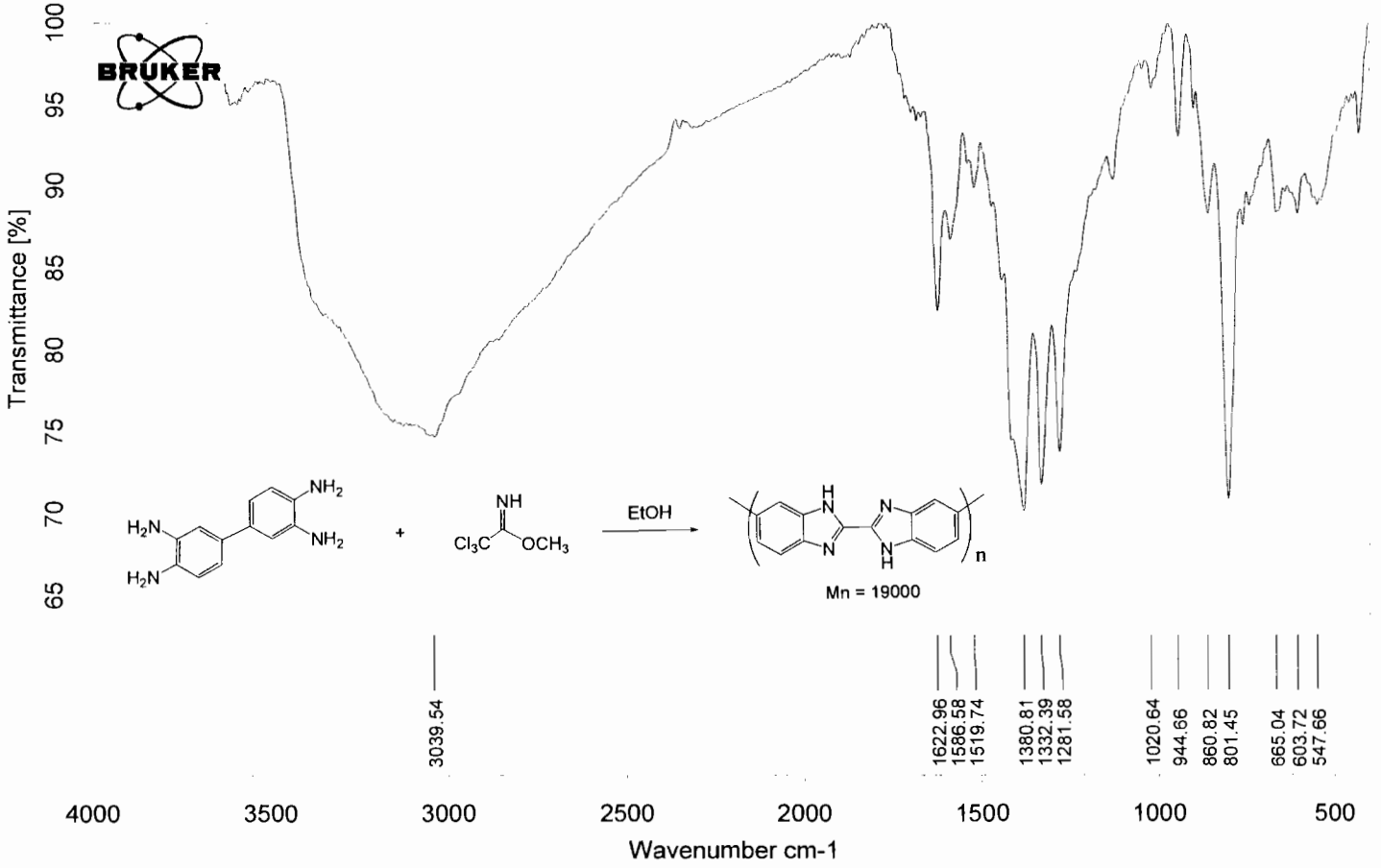

D:\OPUS_NT\DATA\Jun\VII_JY_150_2_PolyBiBzImH2_Acetim.0	VII_JY_150_2_PolyBiBzImH2_Acetim	Solid in KBr	27/05/2005

APPENDIX 12

^{1}H NMR AND FTIR SPECTRA OF

Poly(2,2′-bibenzimidazole) **4b**

JEOL

Filename	= VII_JY_204_PolyBiBzIm
Author	= delta
Experiment	= single_pulse.exp
Sample_id	= S#763185
Solvent	= TRIFLUOROACETIC_
Creation_time	= 6-APR-2005 03:32:21
Revision_time	= 21-MAY-2005 21:22:52
Current_time	= 21-MAY-2005 21:29:19
Content	= Single Pulse Experime
Data_format	= 1D COMPLEX
Dim_size	= 16384
Dim_title	= 1H
Dim_units	= [ppm]
Dimensions	= X
Site	= Eclipse+ 500
Spectrometer	= DELTA_NMR
Field_strength	= 11.7473579[T] (500[MH
X_acq_duration	= 1.6367616[s]
X_domain	= 1H
X_freq	= 500.15991521[MHz]
X_offset	= 8[ppm]
X_points	= 16384
X_prescans	= 0
X_resolution	= 0.61096253[Hz]
X_sweep	= 10.01001001[kHz]
Clipped	= FALSE
Mod_return	= 1
Scans	= 100
Total_scans	= 100
X_90_width	= 18.5[us]
X_acq_time	= 1.6367616[s]
X_angle	= 45[deg]
X_pulse	= 9.25[us]
Initial_wait	= 1[s]
Phase_preset	= 3[us]
Recvr_gain	= 15
Relaxation_delay	= 1[s]
Temp_get	= 25.4[dC]
Unblank_time	= 2[us]

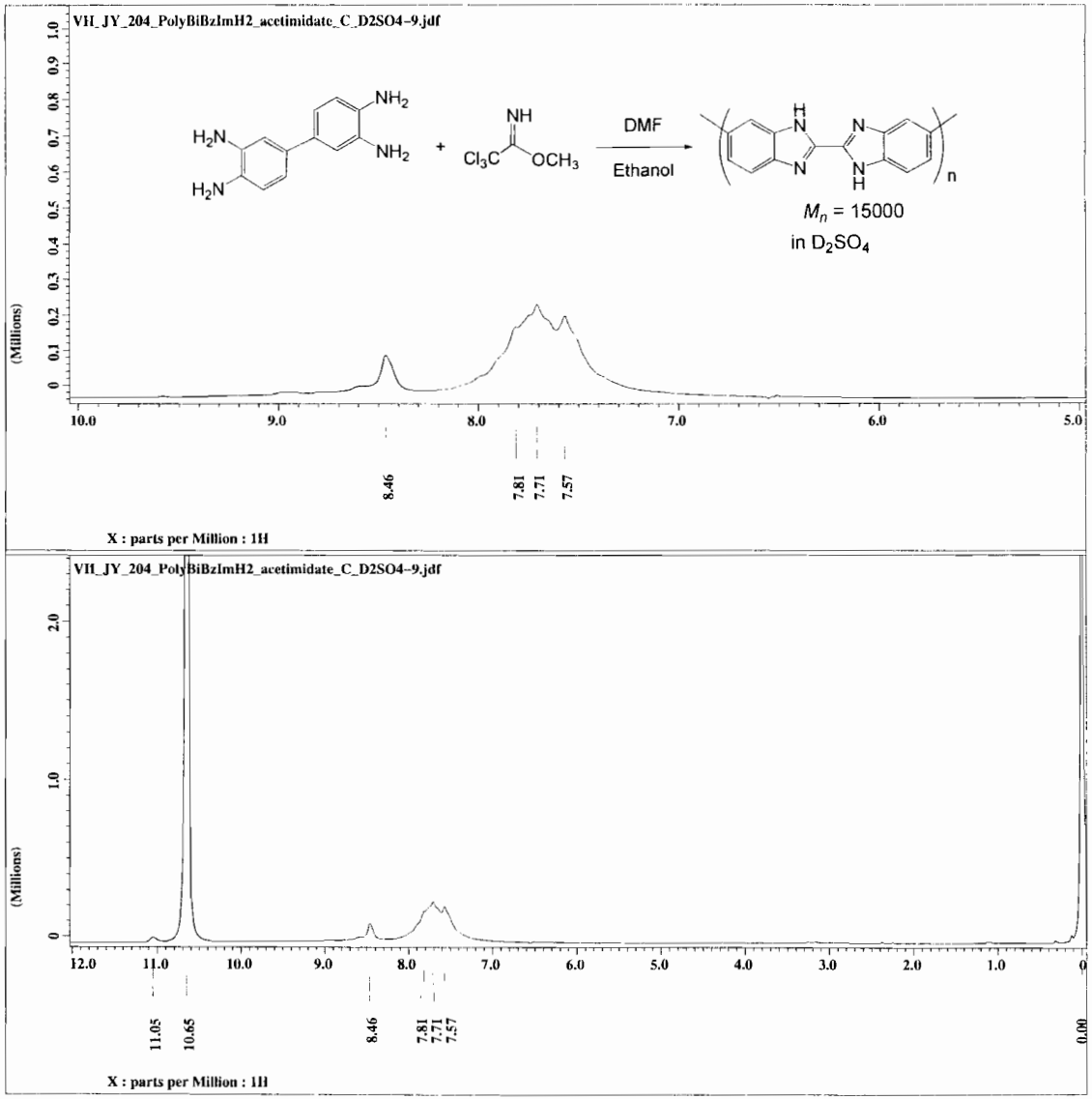

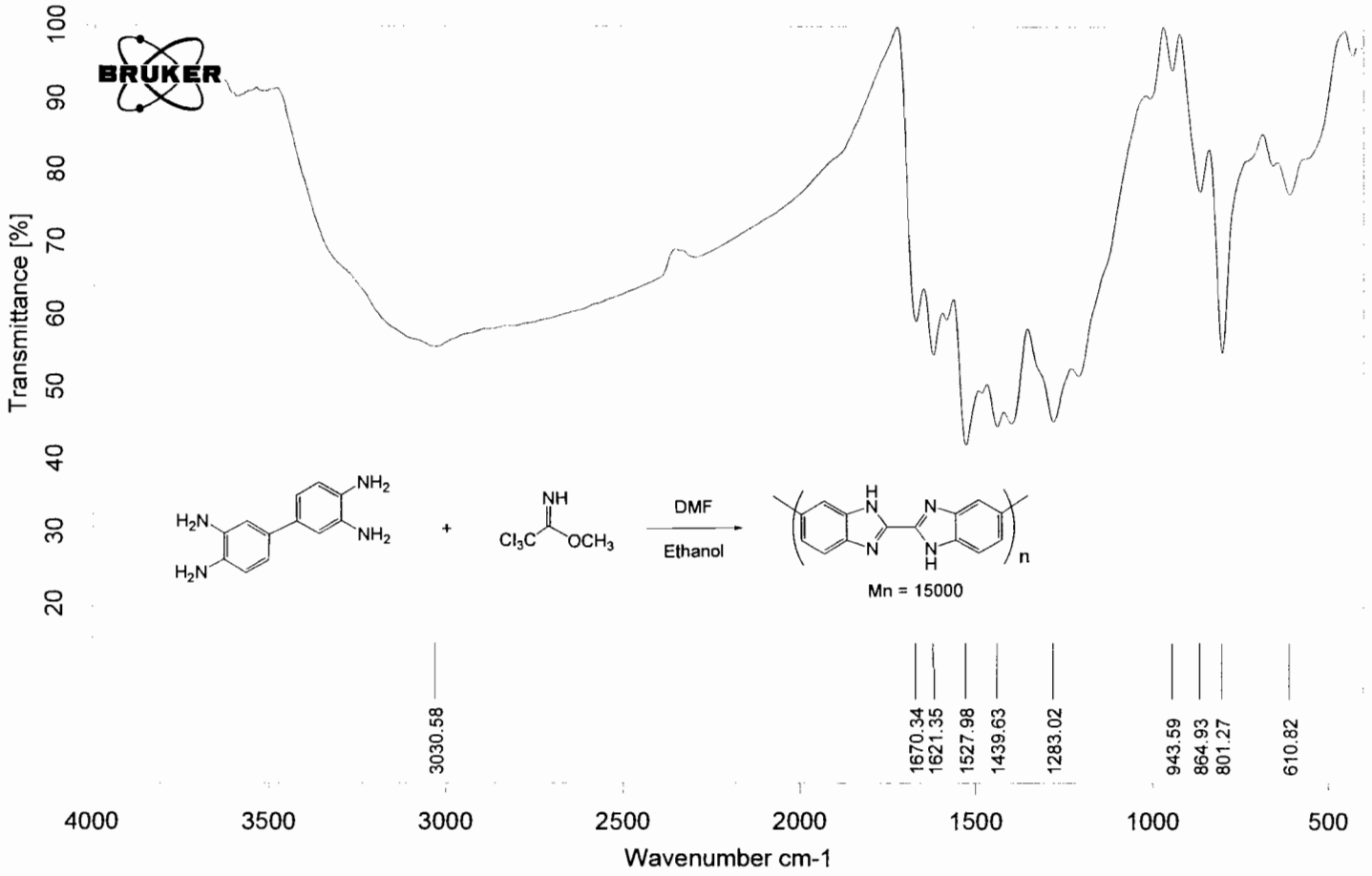

D:\OPUS_NT\DATA\Jun\VII_JY_205_1_PolyBiBzImH2_Acetim.0	VII_JY_205_1_PolyBiBzImH2_Acetim	Solid in KBr	27/05/2005

APPENDIX 13

^{1}H, ^{13}C NMR, AND FTIR SPECTRA OF

Poly(2,2′-bibenzimidazole) **4c**

```
Filename          = VII_JY_213_PolyBiBzIm
Author            = delta
Experiment        = single_pulse.exp
Sample_id         = S#773316
Solvent           = TRIFLUOROACETIC_
Creation_time     =  5-APR-2005 03:48:26
Revision_time     = 20-MAY-2005 21:43:55
Current_time      = 20-MAY-2005 21:59:37

Content           = Single Pulse Experime
Data_format       = 1D COMPLEX
Dim_size          = 16384
Dim_title         = 1H
Dim_units         = [ppm]
Dimensions        = X
Site              = Eclipse+ 500
Spectrometer      = DELTA_NMR

Field_strength    = 11.7473579[T] (500[MH
X_acq_duration    = 1.6367616[s]
X_domain          = 1H
X_freq            = 500.15991521[MHz]
X_offset          = 8[ppm]
X_points          = 16384
X_prescans        = 0
X_resolution      = 0.61096253[Hz]
X_sweep           = 10.01001001[kHz]
Clipped           = FALSE
Mod_return        = 1
Scans             = 100
Total_scans       = 100

X_90_width        = 18.5[us]
X_acq_time        = 1.6367616[s]
X_angle           = 45[deg]
X_pulse           = 9.25[us]
Initial_wait      = 1[s]
Phase_preset      = 3[us]
Recvr_gain        = 11
Relaxation_delay  = 1[s]
Temp_get          = 25.6[dC]
Unblank_time      = 2[us]
```

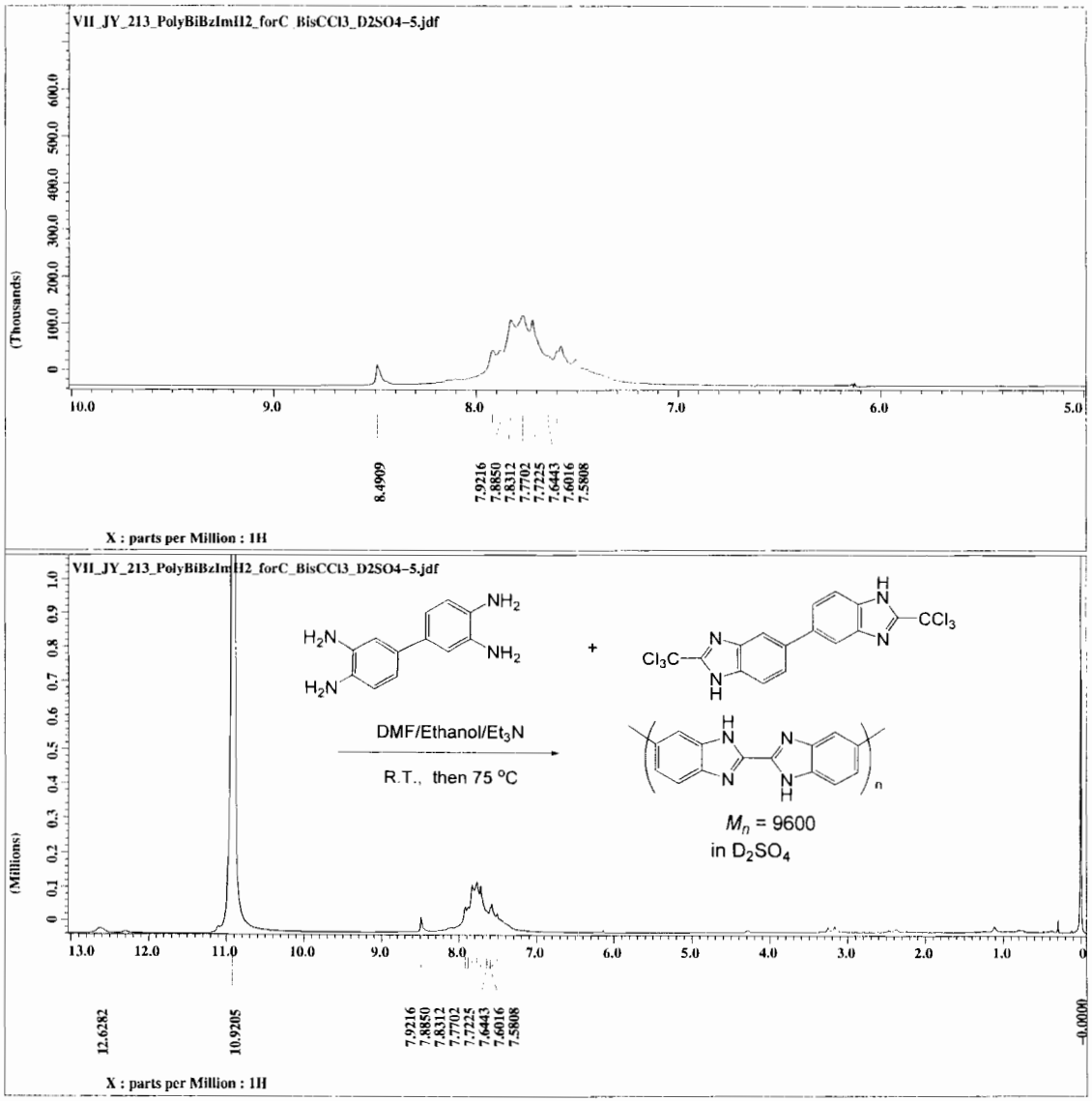

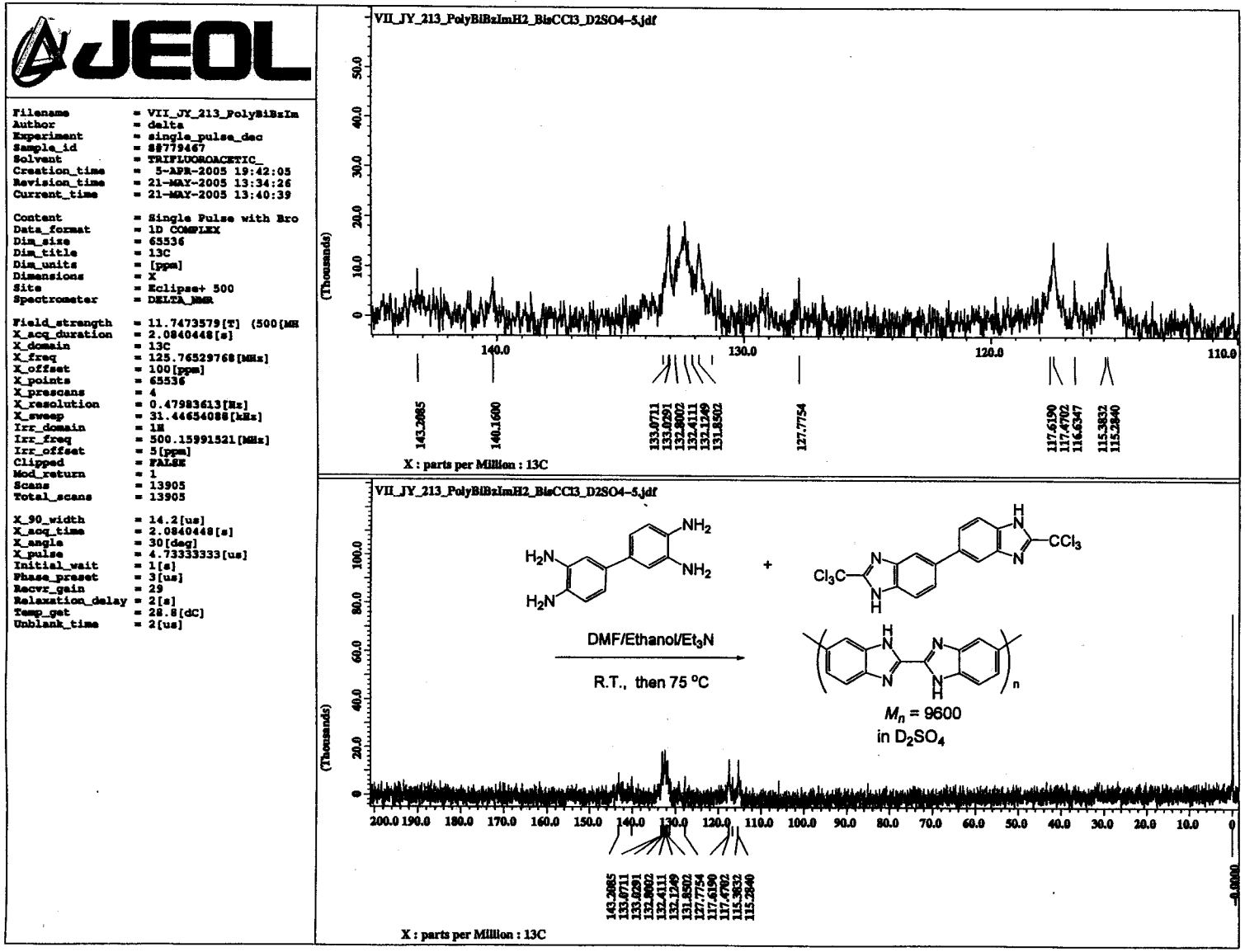
JEOL
Filename = VII_JY_213_PolyBiBzIm
Author = delta
Experiment = single_pulse_dec
Sample_id = ##7794467
Solvent = TRIFLUOROACETIC_
Creation_time = 5-APR-2005 19:42:05
Revision_time = 21-MAY-2005 13:34:26
Current_time = 21-MAY-2005 13:40:39
Content = Single Pulse with Bro
Data_format = 1D COMPLEX
Dim_size = 65536
Dim_title = 13C
Dim_units = [ppm]
Dimensions = X
Site = Eclipse+ 500
Spectrometer = DELTA_NMR
Field_strength = 11.7473579[T] (500[MH
X_acq_duration = 2.0840448[s]
X_domain = 13C
X_freq = 125.76529768[MHz]
X_offset = 100[ppm]
X_points = 65536
X_prescans = 4
X_resolution = 0.47983613[Hz]
X_sweep = 31.44654088[kHz]
Irr_domain = 1H
Irr_freq = 500.15991521[MHz]
Irr_offset = 5[ppm]
Clipped = FALSE
Mod_return = 1
Scans = 13905
Total_scans = 13905
X_90_width = 14.2[us]
X_acq_time = 2.0840448[s]
X_angle = 30[deg]
X_pulse = 4.73333333[us]
Initial_wait = 1[s]
Phase_preset = 3[us]
Recvr_gain = 29
Relaxation_delay = 2[s]
Temp_get = 28.8[dC]
Unblank_time = 2[us]
VII_JY_213_PolyBiBzImH2_BisCCl3_D2SO4-5.jdf
(Thousands)
140.0
130.0
120.0
110.0
143.2085
140.1600
133.0711
133.0291
132.8002
132.4111
132.1249
131.8502
127.7754
117.6190
117.4702
116.6347
115.3832
115.2840
X : parts per Million : 13C
VII_JY_213_PolyBiBzImH2_BisCCl3_D2SO4-5.jdf
NH2
H2N
NH2
H2N
+
Cl3C
CCl3
DMF/Ethanol/Et3N
R.T., then 75 °C
n
Mn = 9600
in D2SO4
(Thousands)
200.0 190.0 180.0 170.0 160.0 150.0 140.0 130.0 120.0 110.0 100.0 90.0 80.0 70.0 60.0 50.0 40.0 30.0 20.0 10.0 0
X : parts per Million : 13C

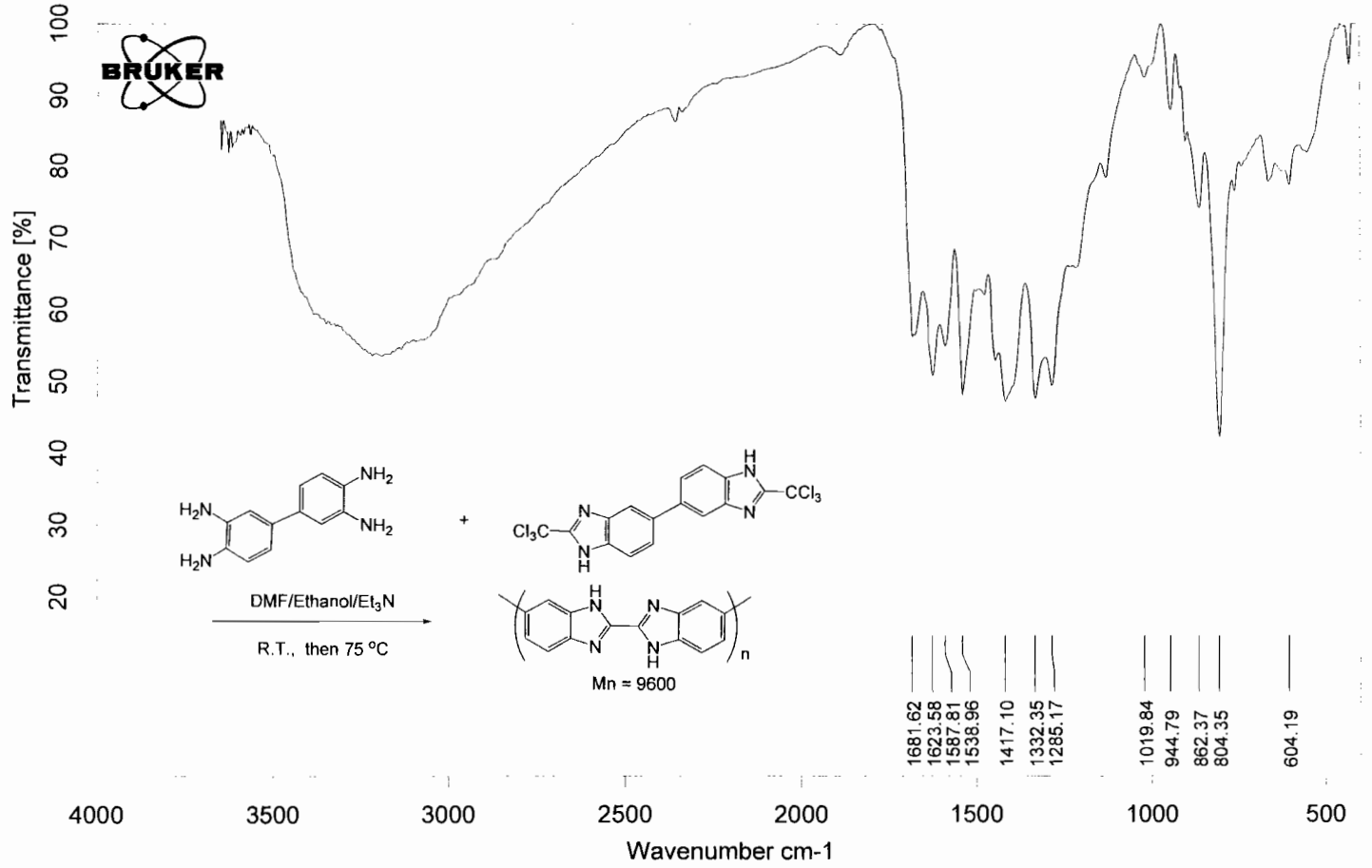

D:\OPUS_NT\DATA\Jun\VII_JY_212_1_PolyBiBzImH2_BisCCl3.0	VII_JY_212_1_PolyBiBzImH2_BisCCl3	Solid in KBr	27/05/2005

APPENDIX 14

^{1}H, ^{13}C NMR, AND FTIR SPECTRA OF

Poly(2,2′-bibenzimidazole) **4d**

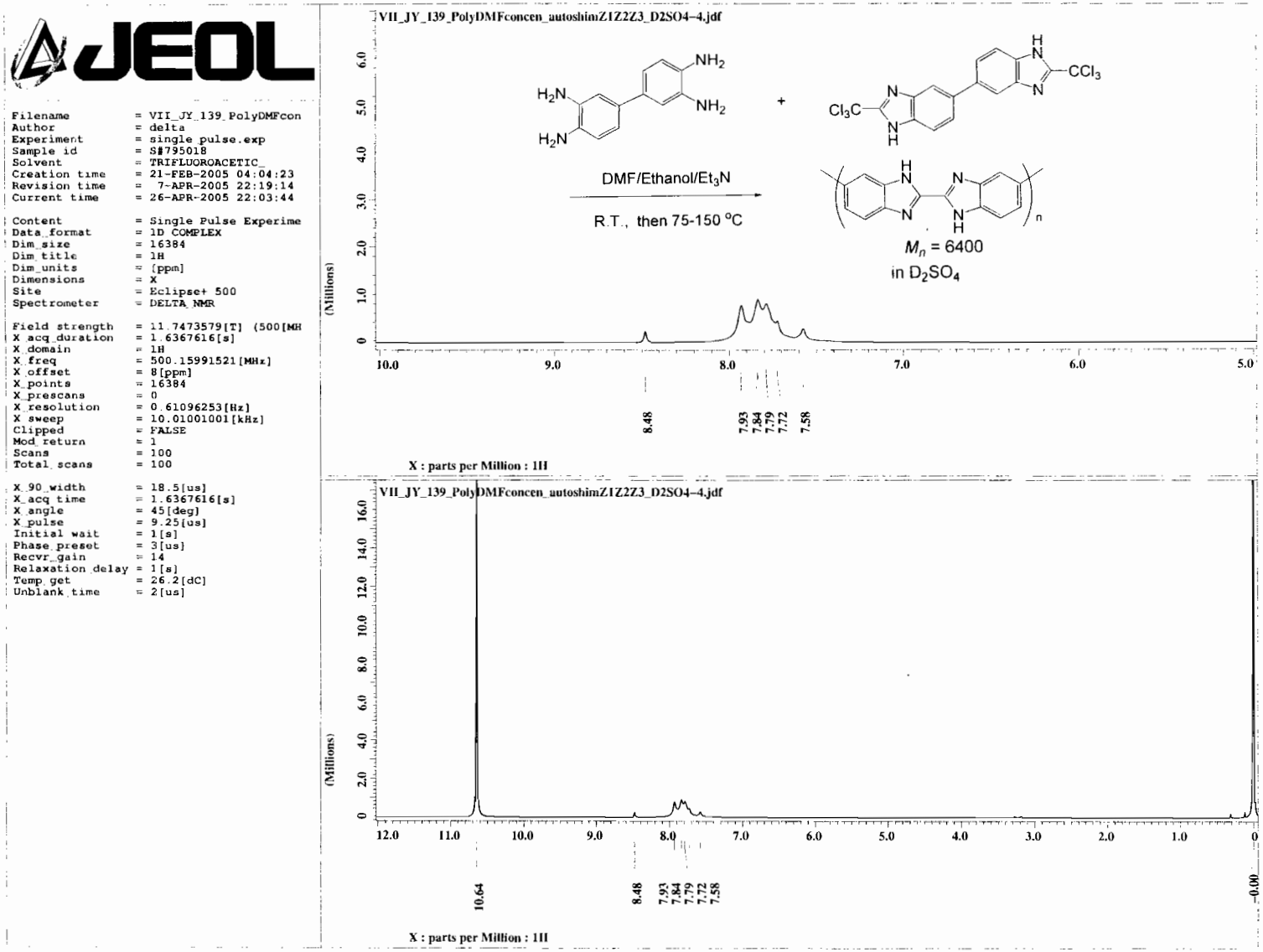
JEOL
Filename = VII_JY_139_PolyDMFcon
Author = delta
Experiment = single_pulse.exp
Sample_id = S#795018
Solvent = TRIFLUOROACETIC_
Creation_time = 21-FEB-2005 04:04:23
Revision_time = 7-APR-2005 22:19:14
Current_time = 26-APR-2005 22:03:44
Content = Single Pulse Experime
Data_format = 1D COMPLEX
Dim_size = 16384
Dim_title = 1H
Dim_units = [ppm]
Dimensions = X
Site = Eclipse+ 500
Spectrometer = DELTA_NMR
Field_strength = 11.7473579[T] (500[MH
X_acq_duration = 1.6367616[s]
X_domain = 1H
X_freq = 500.15991521[MHz]
X_offset = 8[ppm]
X_points = 16384
X_prescans = 0
X_resolution = 0.61096253[Hz]
X_sweep = 10.01001001[kHz]
Clipped = FALSE
Mod_return = 1
Scans = 100
Total_scans = 100
X_90_width = 18.5[us]
X_acq_time = 1.6367616[s]
X_angle = 45[deg]
X_pulse = 9.25[us]
Initial_wait = 1[s]
Phase_preset = 3[us]
Recvr_gain = 14
Relaxation_delay = 1[s]
Temp_get = 26.2[dC]
Unblank_time = 2[us]
VII_JY_139_PolyDMFconcen_autoshimZ1Z2Z3_D2SO4-4.jdf
NH2
H2N
NH2
H2N
+
Cl3C
CCl3
DMF/Ethanol/Et3N
R.T., then 75-150 °C
Mn = 6400
in D2SO4
(Millions)
8.48
7.93
7.84
7.79
7.72
7.58
X : parts per Million : 1H
VII_JY_139_PolyDMFconcen_autoshimZ1Z2Z3_D2SO4-4.jdf
(Millions)
10.64
8.48
7.93
7.84
7.79
7.72
7.58
-0.00
X : parts per Million : 1H

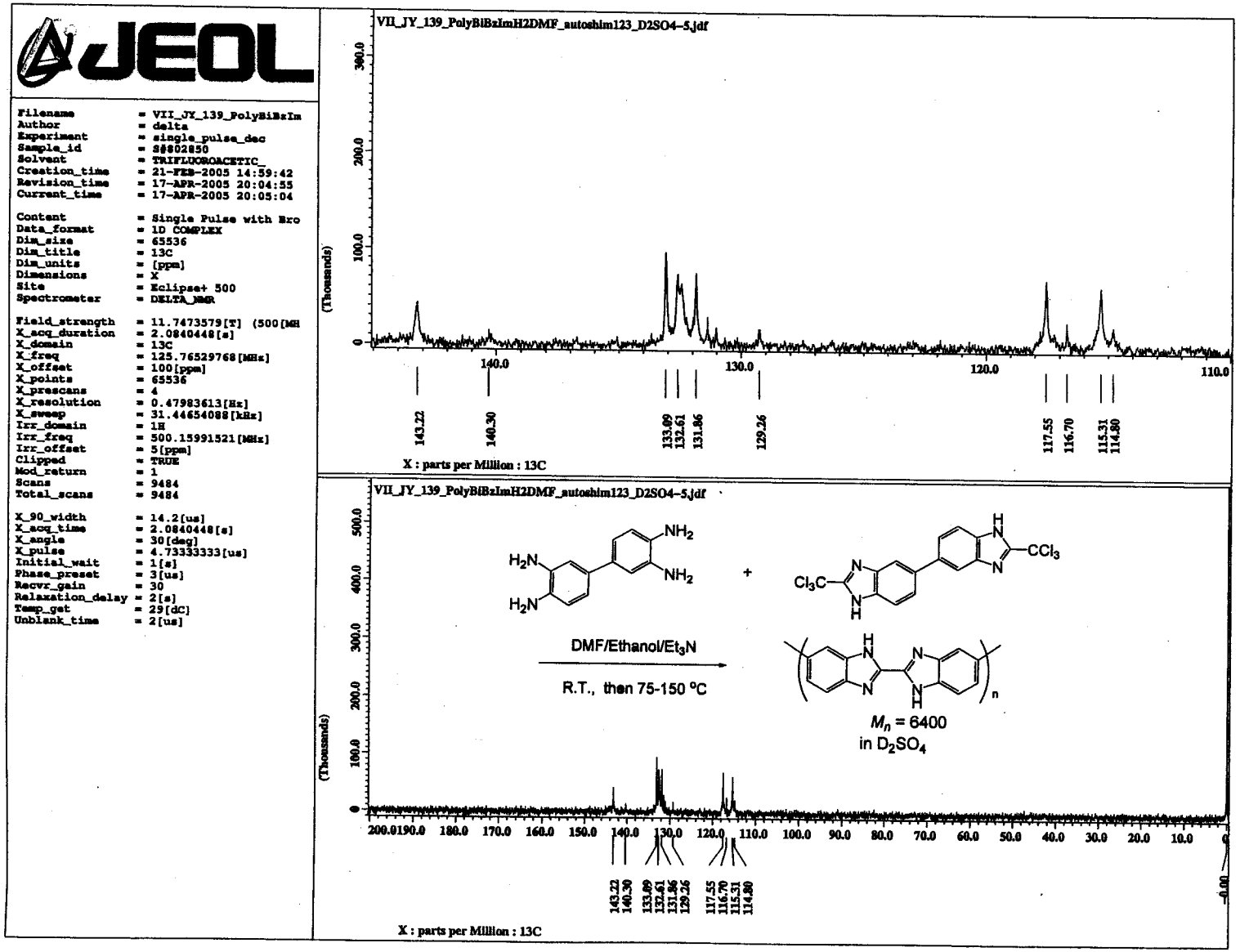
JEOL
Filename = VII_JY_139_PolyBiBzIm
Author = delta
Experiment = single_pulse_dec
Sample_id = S#802850
Solvent = TRIFLUOROACETIC_
Creation_time = 21-FEB-2005 14:59:42
Revision_time = 17-APR-2005 20:04:55
Current_time = 17-APR-2005 20:05:04
Content = Single Pulse with Dro
Data_format = 1D COMPLEX
Dim_size = 65536
Dim_title = 13C
Dim_units = [ppm]
Dimensions = X
Site = Eclipse+ 500
Spectrometer = DELTA_NMR
Field_strength = 11.7473579[T] (500[MH
X_acq_duration = 2.0840448[s]
X_domain = 13C
X_freq = 125.76529768[MHz]
X_offset = 100[ppm]
X_points = 65536
X_prescans = 4
X_resolution = 0.47983613[Hz]
X_sweep = 31.44654088[kHz]
Irr_domain = 1H
Irr_freq = 500.15991521[MHz]
Irr_offset = 5[ppm]
Clipped = TRUE
Mod_return = 1
Scans = 9484
Total_scans = 9484
X_90_width = 14.2[us]
X_acq_time = 2.0840448[s]
X_angle = 30[deg]
X_pulse = 4.73333333[us]
Initial_wait = 1[s]
Phase_preset = 3[us]
Recvr_gain = 30
Relaxation_delay = 2[s]
Temp_get = 29[dC]
Unblank_time = 2[us]
VII_JY_139_PolyBiBzImH2DMF_autoshim123_D2SO4-5.jdf
(Thousands)
300.0
200.0
100.0
0
140.0
130.0
120.0
110.0
143.22
140.30
133.09
132.61
131.86
129.26
117.55
116.70
115.31
114.80
X : parts per Million : 13C
VII_JY_139_PolyBiBzImH2DMF_autoshim123_D2SO4-5.jdf
(Thousands)
500.0
400.0
300.0
200.0
100.0
0
200.0 190.0 180.0 170.0 160.0 150.0 140.0 130.0 120.0 110.0 100.0 90.0 80.0 70.0 60.0 50.0 40.0 30.0 20.0 10.0
143.22
140.30
133.09
132.61
131.86
129.26
117.55
116.70
115.31
114.80
X : parts per Million : 13C
DMF/Ethanol/Et3N
R.T., then 75-150 °C
Mn = 6400
in D2SO4

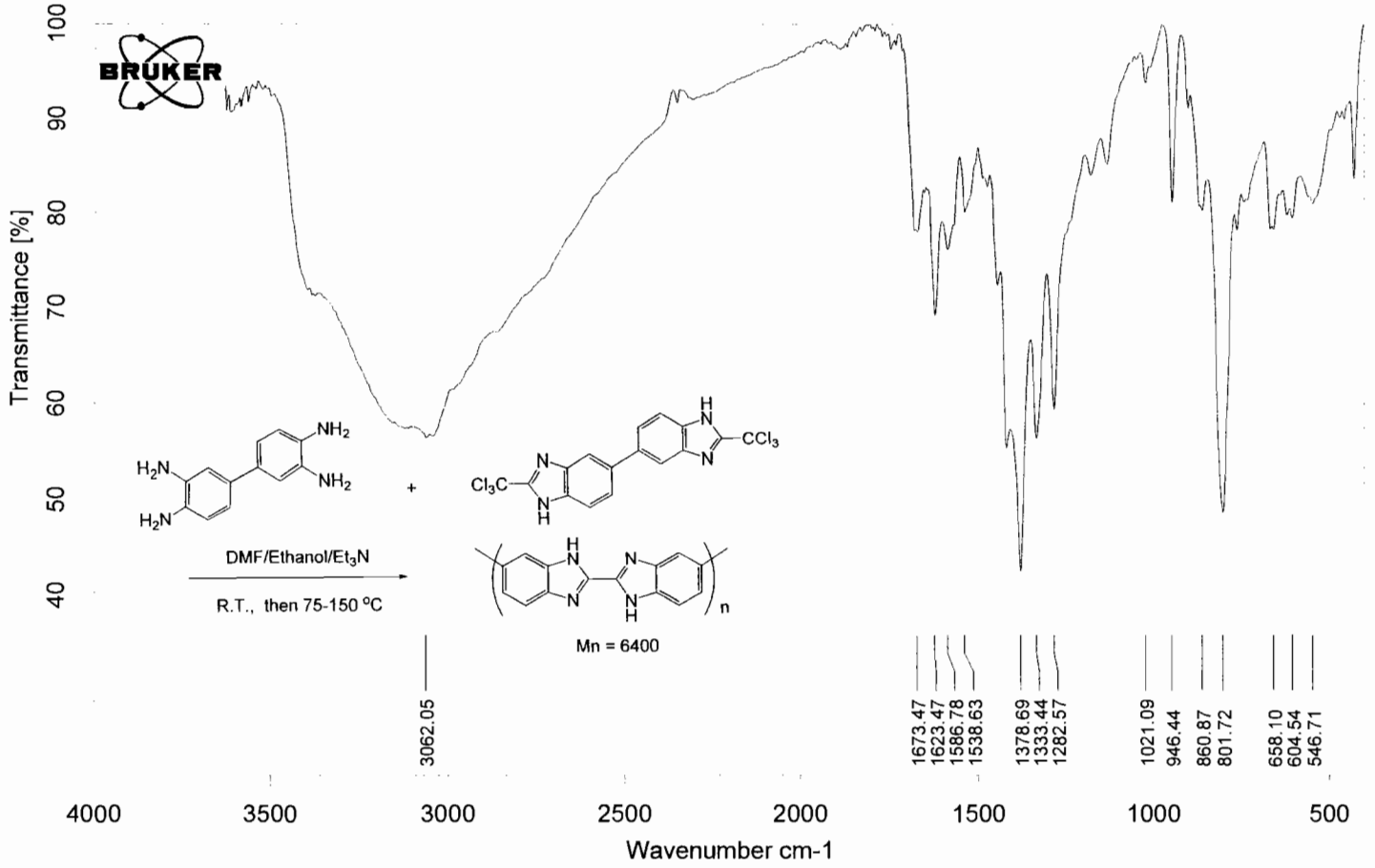

D:\OPUS_NT\DATA\Jun\VII_JY_139_1_PolyBiBzImH2_BisCCl3.0	VII_JY_139_1_PolyBiBzImH2_BisCCl3	Solid in KBr	27/05/2005

APPENDIX 15

^{1}H AND COSY NMR SPECTRA OF

Λ-[Ru(bpy)$_2$(BiBzImH$_2$)](PF$_6$)$_2$ Λ-**20**

```
Filename          = VI_JY_76_Rubpy2BiBzIm
Author            = delta
Experiment        = single_pulse.exp
Sample_id         = S#589513
Solvent           = DMSO-D6
Creation_time     = 14-AUG-2005 17:03:42
Revision_time     = 16-OCT-2005 21:09:08
Current_time      = 16-OCT-2005 21:09:14

Content           = Single Pulse Experime
Data_format       = 1D COMPLEX
Dim_size          = 16384
Dim_title         = 1H
Dim_units         = [ppm]
Dimensions        = X
Site              = Zclipse+ 500
Spectrometer      = DELTA_NMR

Field_strength    = 11.7473579[T] (500[MH
X_acq_duration    = 1.4876672[s]
X_domain          = 1H
X_freq            = 500.15991521[MHz]
X_offset          = 8[ppm]
X_points          = 16384
X_prescans        = 0
X_resolution      = 0.67219335[Hz]
X_sweep           = 11.01321586[kHz]
Clipped           = FALSE
Mod_return        = 1
Scans             = 98
Total_scans       = 98

X_90_width        = 18.5[us]
X_acq_time        = 1.4876672[s]
X_angle           = 45[deg]
X_pulse           = 9.25[us]
Initial_wait      = 1[s]
Phase_preset      = 3[us]
Recvr_gain        = 18
Relaxation_delay  = 1[s]
Temp_get          = 25.6[dC]
Unblank_time      = 2[us]
```

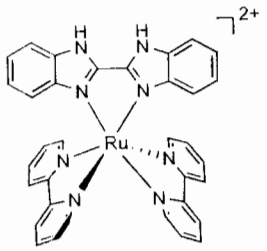

Λ

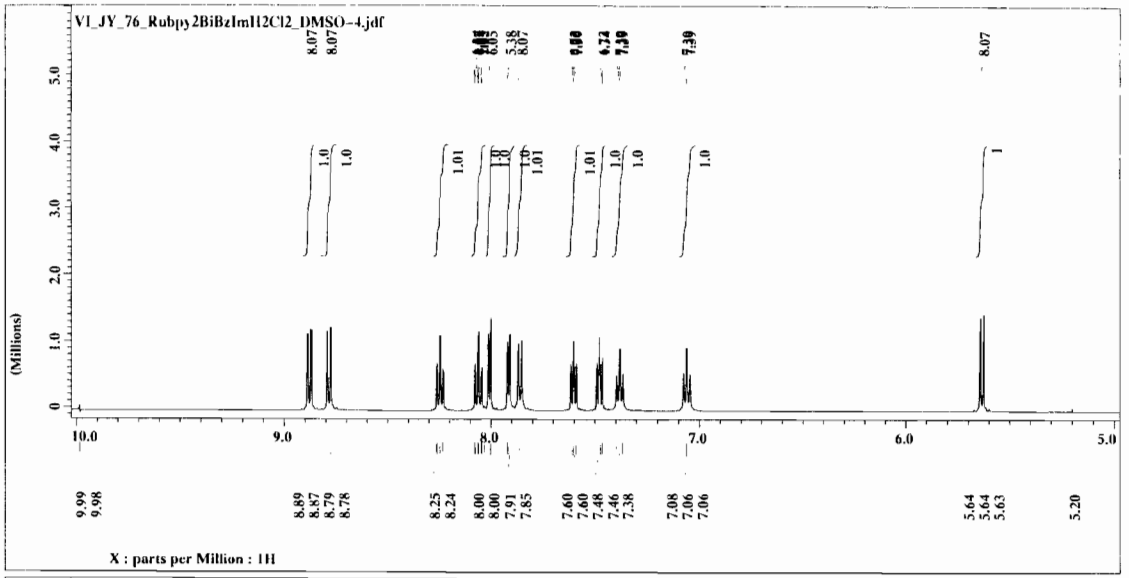

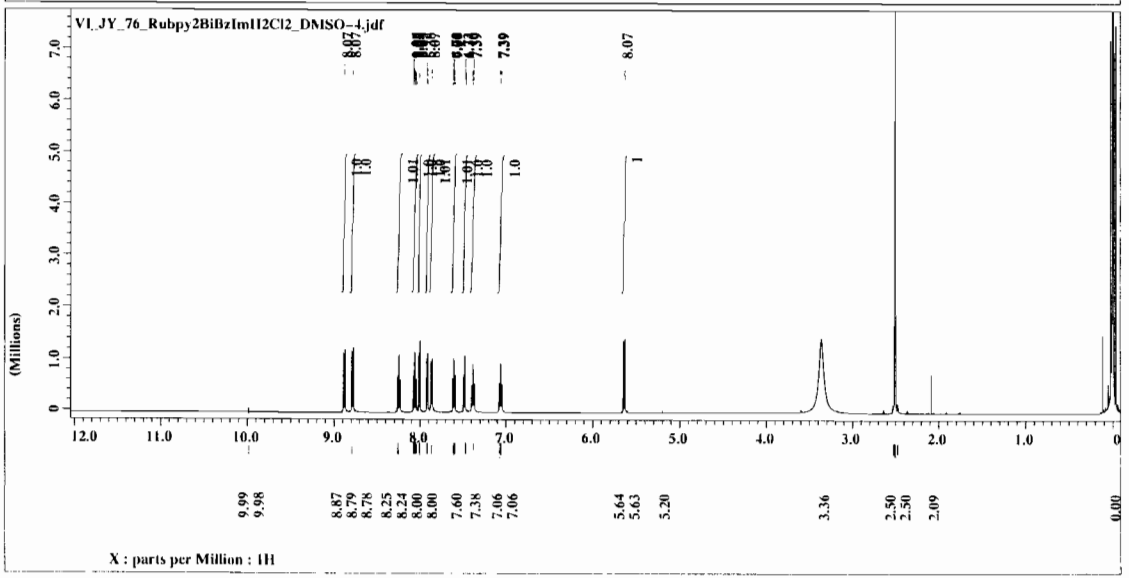

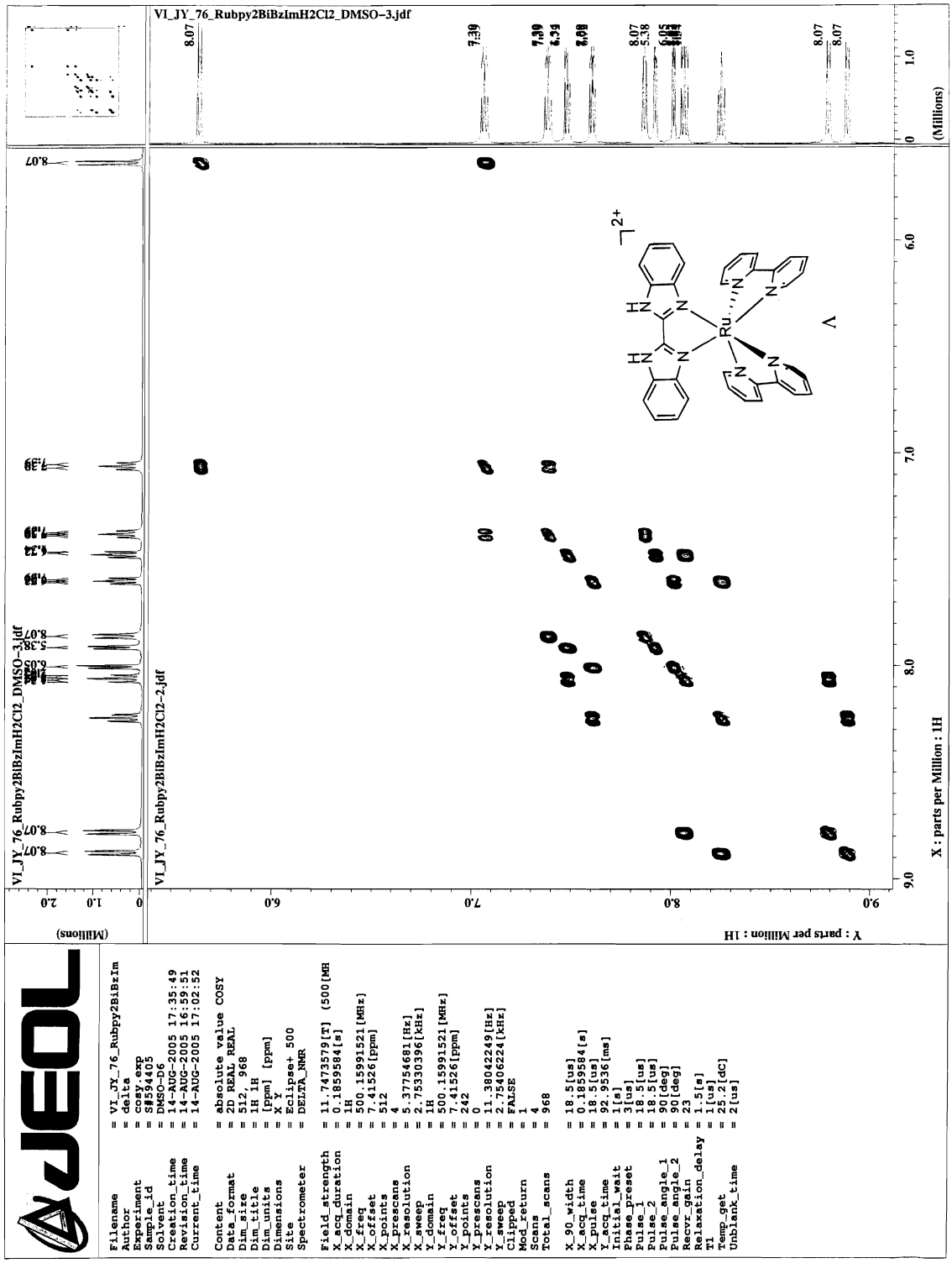
JEOL
Filename = VI_JY_76_Rubpy2BiBzIm
Author = delta
Experiment = cosy.exp
Sample_id = S#594405
Solvent = DMSO-D6
Creation_time = 14-AUG-2005 17:35:49
Revision_time = 14-AUG-2005 16:59:51
Current_time = 14-AUG-2005 17:02:52
Content = absolute value COSY
Data_format = 2D REAL REAL
Dim_size = 512, 968
Dim_title = 1H 1H
Dim_units = [ppm] [ppm]
Dimensions = X Y
Site = Eclipse+ 500
Spectrometer = DELTA_NMR
Field_strength = 11.7473579[T] (500[MH
X_acq_duration = 0.1859584[s]
X_domain = 1H
X_freq = 500.15991521[MHz]
X_offset = 7.41526[ppm]
X_points = 512
X_prescans = 4
X_resolution = 5.37754681[Hz]
X_sweep = 2.75330396[kHz]
Y_domain = 1H
Y_freq = 500.15991521[MHz]
Y_offset = 7.41526[ppm]
Y_points = 242
Y_prescans = 0
Y_resolution = 11.38042249[Hz]
Y_sweep = 2.75406224[kHz]
Clipped = FALSE
Mod_return = 1
Scans = 4
Total_scans = 968
X_90_width = 18.5[us]
X_acq_time = 0.1859584[s]
X_pulse = 18.5[us]
Y_acq_time = 92.9536[ms]
Initial_wait = 1[s]
Phase_preset = 3[us]
Pulse_1 = 18.5[us]
Pulse_2 = 18.5[us]
Pulse_angle_1 = 90[deg]
Pulse_angle_2 = 90[deg]
Recvr_gain = 23
Relaxation_delay = 1.5[s]
T1 = 1[us]
Temp_get = 25.2[dC]
Unblank_time = 2[us]
VI_JY_76_Rubpy2BiBzImH2Cl2_DMSO-3.jdf
VI_JY_76_Rubpy2BiBzImH2Cl2-2.jdf
(Millions)
X : parts per Million : 1H
Y : parts per Million : 1H
2+
Ru
V

APPENDIX 16

^{1}H AND ^{13}C NMR SPECTRA OF

Λ-[$Ru(bpy)_2$(BiBzIm)] Λ-**21**

JEOL

Filename	= V_JY_260_A_Deproton_C
Experiment	= single_pulse.exp
Sample_id	= S#16774
Solvent	= DMSO-D6
Creation_time	= 8-MAR-2004 13:49:49
Revision_time	= 16-OCT-2005 21:03:14
Current_time	= 16-OCT-2005 21:03:22
Content	= Single Pulse Experime
Data_format	= 1D COMPLEX
Dim_size	= 16384
Dim_title	= 1H
Dim_units	= [ppm]
Dimensions	= X
Site	= Eclipse+ 500
Spectrometer	= DELTA_NMR
Field_strength	= 11.7473579[T] (500[MH
X_acq_duration	= 1.4876672[s]
X_domain	= 1H
X_freq	= 500.15991521[MHz]
X_offset	= 8[ppm]
X_points	= 16384
X_prescans	= 0
X_resolution	= 0.67219335[Hz]
X_sweep	= 11.01321586[kHz]
Mod_return	= 1
Scans	= 120
X_90_width	= 15[us]
X_acq_time	= 1.4876672[s]
X_angle	= 45[deg]
X_pulse	= 7.5[us]
Initial_wait	= 1[s]
Phase_preset	= 3[us]
Recvr_gain	= 20
Relaxation_delay	= 1[s]
Temp_get	= 22.9[dC]
Unblank_time	= 2[us]

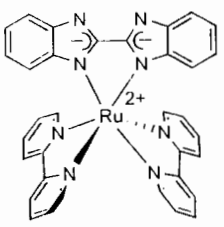

A

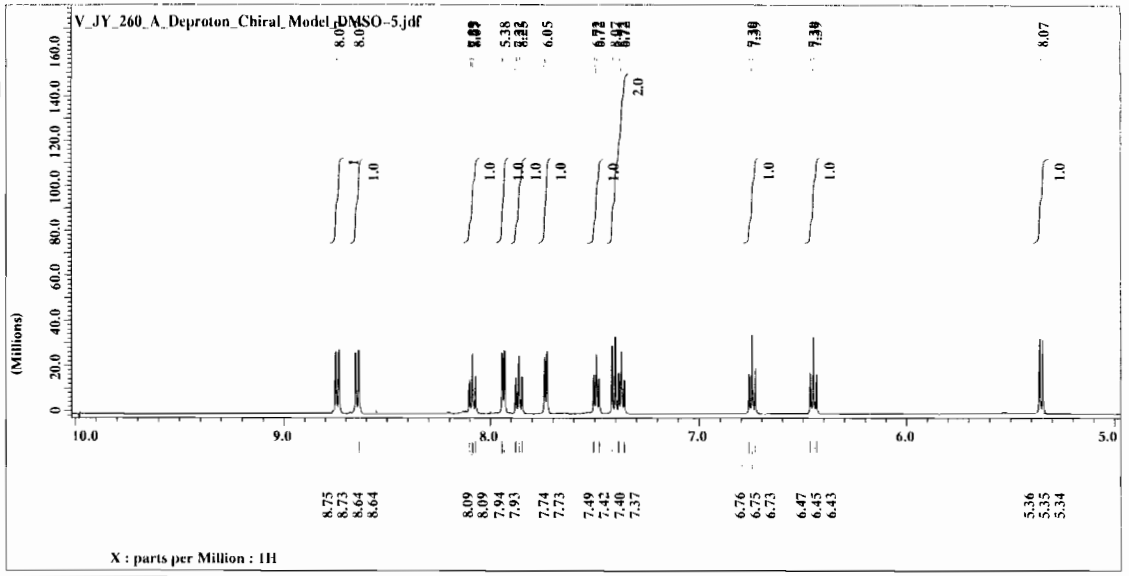

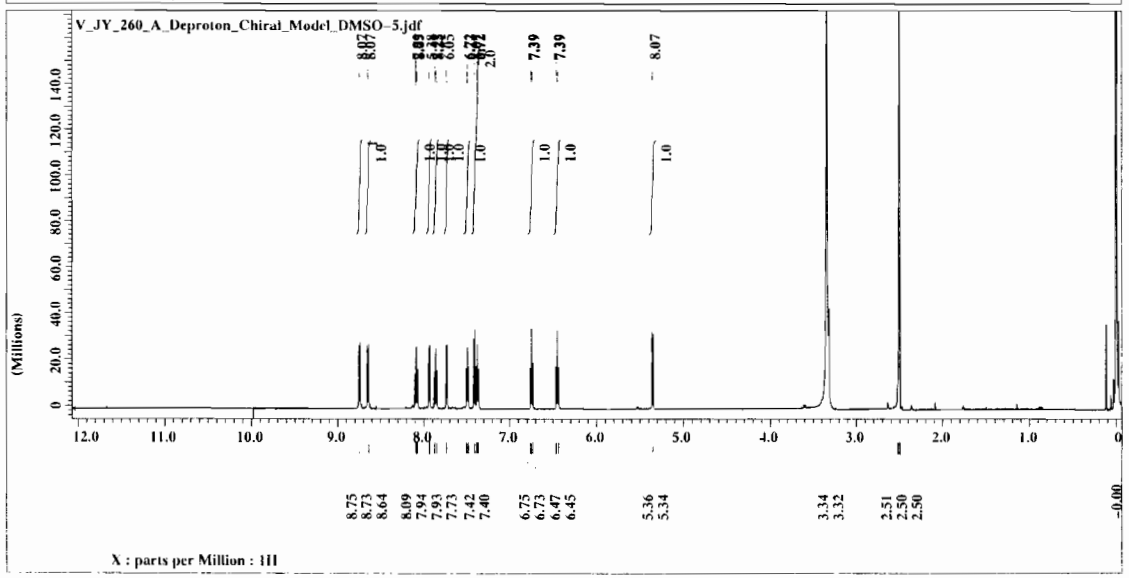

```
Filename          = V_JY_260_A_Deproton_C
Experiment        = single_pulse_dec
Sample_id         = S#359040
Solvent           = DMSO-D6
Creation_time     = 11-MAR-2004 10:11:11
Revision time     = 17-MAR-2004 10:29:34
Current_time      = 16-OCT-2005 21:04:55

Content           = Single Pulse with Bro
Data format       = 1D COMPLEX
Dim_size          = 32768
Dim title         = 13C
Dim_units         = [ppm]
Dimensions        = X
Site              = Eclipse+ 500
Spectrometer      = DELTA NMR

Field strength    = 11.7473579[T] (500[MH
X acq_duration    = 1.0420224[s]
X_domain          = 13C
X_freq            = 125.76529768[MHz]
X offset          = 100[ppm]
X_points          = 32768
X_prescans        = 4
X resolution      = 0.95967227[Hz]
X sweep           = 31.44654088[kHz]
Irr_domain        = 1H
Irr freq          = 500.15991521[MHz]
Irr offset        = 5[ppm]
Mod return        = 1
Scans             = 7771

X_90 width        = 14[us]
X_acq_time        = 1.0420224[s]
X_angle           = 30[deg]
X_pulse           = 4.66666667[us]
Initial_wait      = 1[s]
Phase preset      = 3[us]
Recvr_gain        = 30
Relaxation delay  = 4[s]
Temp_get          = 23.9[dC]
Unblank_time      = 2[us]
```

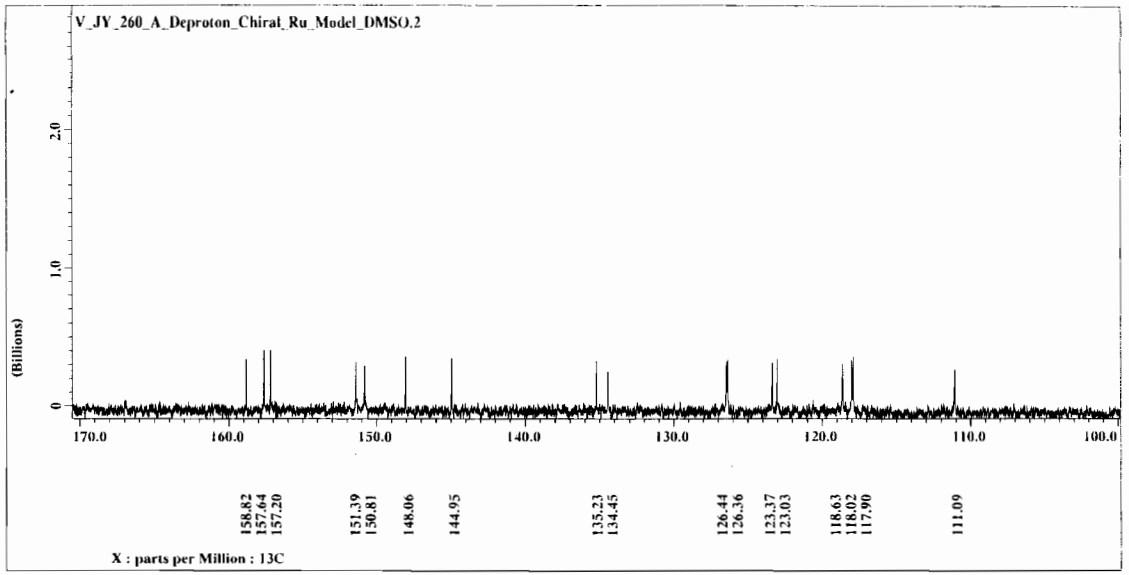

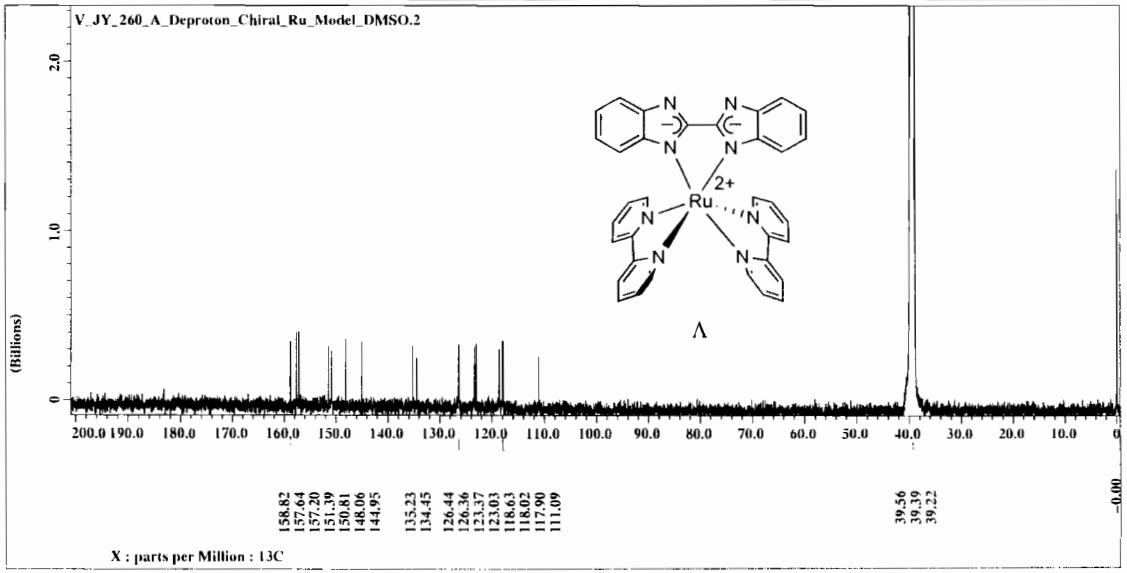

APPENDIX 17

^{1}H, COSY, ^{13}C NMR, ESI-MASS, AND DIFFERENTIAL PULSE VOLTAMMETRY SPECTRA OF

ΛΛ-$[(Ru(bpy)_2)_2(BiBzIm)](PF_6)_2$ ΛΛ-**22**

```
Filename          = V_JY_261_C_byProd_PF6
Experiment        = single_pulse.exp
Sample_id         = S#853611
Solvent           = DMSO-D6
Creation_time     =  8-MAR-2004 13:02:05
Revision_time     = 16-OCT-2005 20:28:25
Current_time      = 16-OCT-2005 20:28:50

Content           = Single Pulse Experime
Data_format       = 1D COMPLEX
Dim_size          = 16384
Dim_title         = 1H
Dim_units         = [ppm]
Dimensions        = X
Site              = Eclipse+ 500
Spectrometer      = DELTA_NMR

Field_strength    = 11.7473579[T] (500[MH
X_acq_duration    = 1.4876672[s]
X_domain          = 1H
X_freq            = 500.15991521[MHz]
X_offset          = 8[ppm]
X_points          = 16384
X_prescans        = 0
X_resolution      = 0.67219335[Hz]
X_sweep           = 11.01321586[kHz]
Mod_return        = 1
Scans             = 60

X_90_width        = 15[us]
X_acq_time        = 1.4876672[s]
X_angle           = 45[deg]
X_pulse           = 7.5[us]
Initial_wait      = 1[s]
Phase_preset      = 3[us]
Recvr_gain        = 19
Relaxation_delay  = 1[s]
Temp_get          = 22.9[dC]
Unblank_time      = 2[us]
```

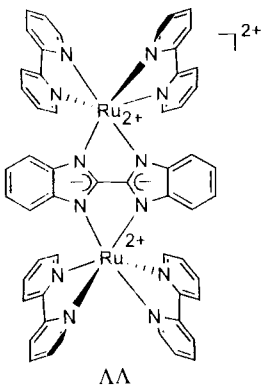

ΛΛ

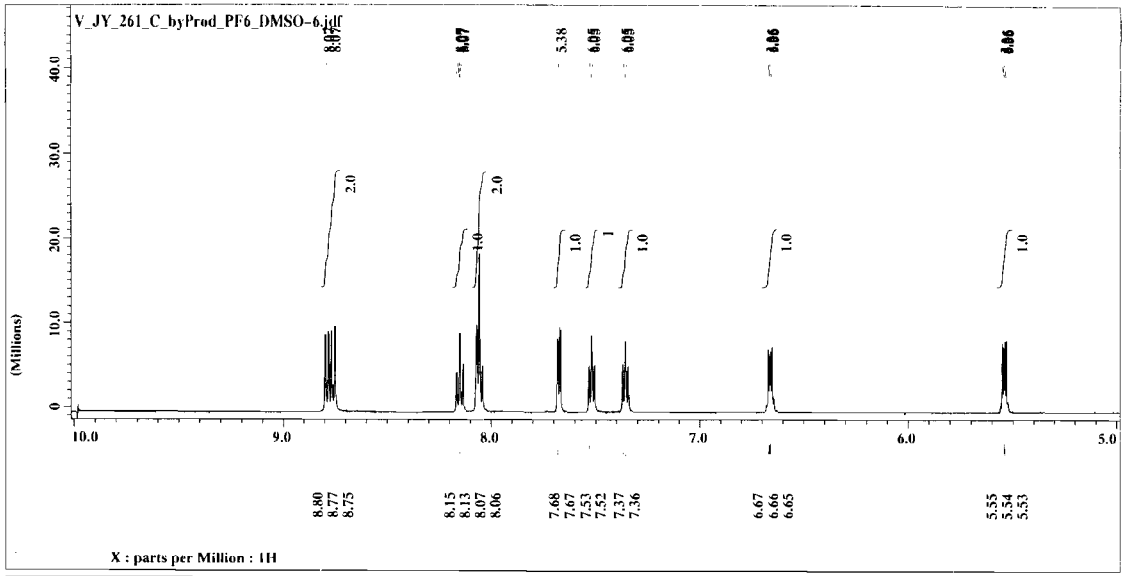

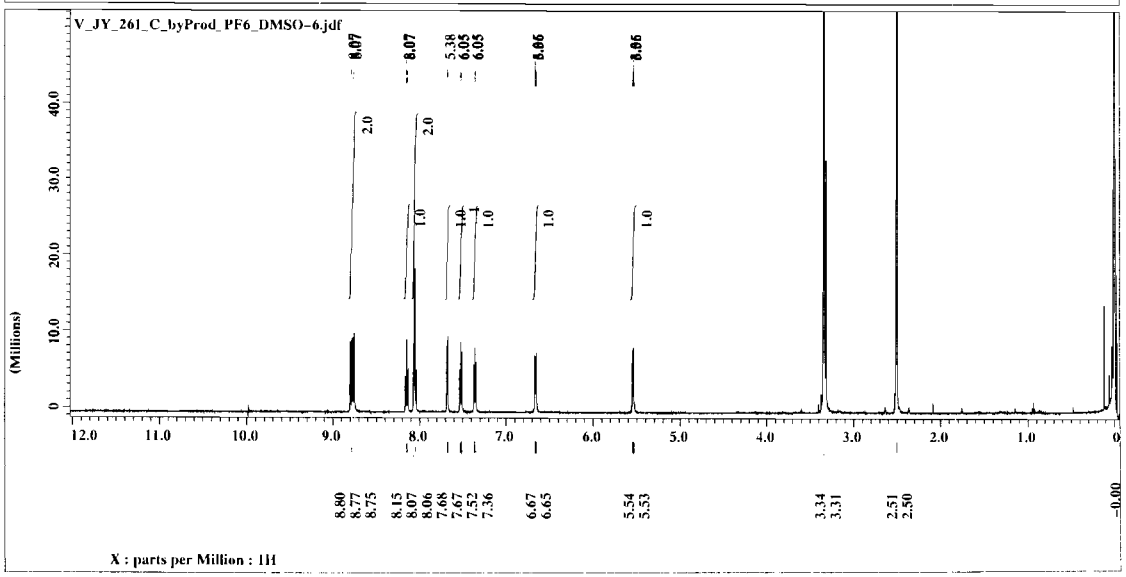

V_JY_261_C_byProd_PF6_DMSO.5
(Millions)
X : parts per Million : 1H
2+
Ru
N
VV
8.797
8.789
8.781
8.766
8.758
8.750
8.07
6.05
7.669
7.675
7.680
7.507
7.513
7.519
7.531
7.345
7.352
7.358
7.370
6.652
6.659
6.661
6.664
6.667
6.671
3.36
8.040
8.056
8.069
8.133
8.141
8.149
8.157
8.165
2.0
1.0

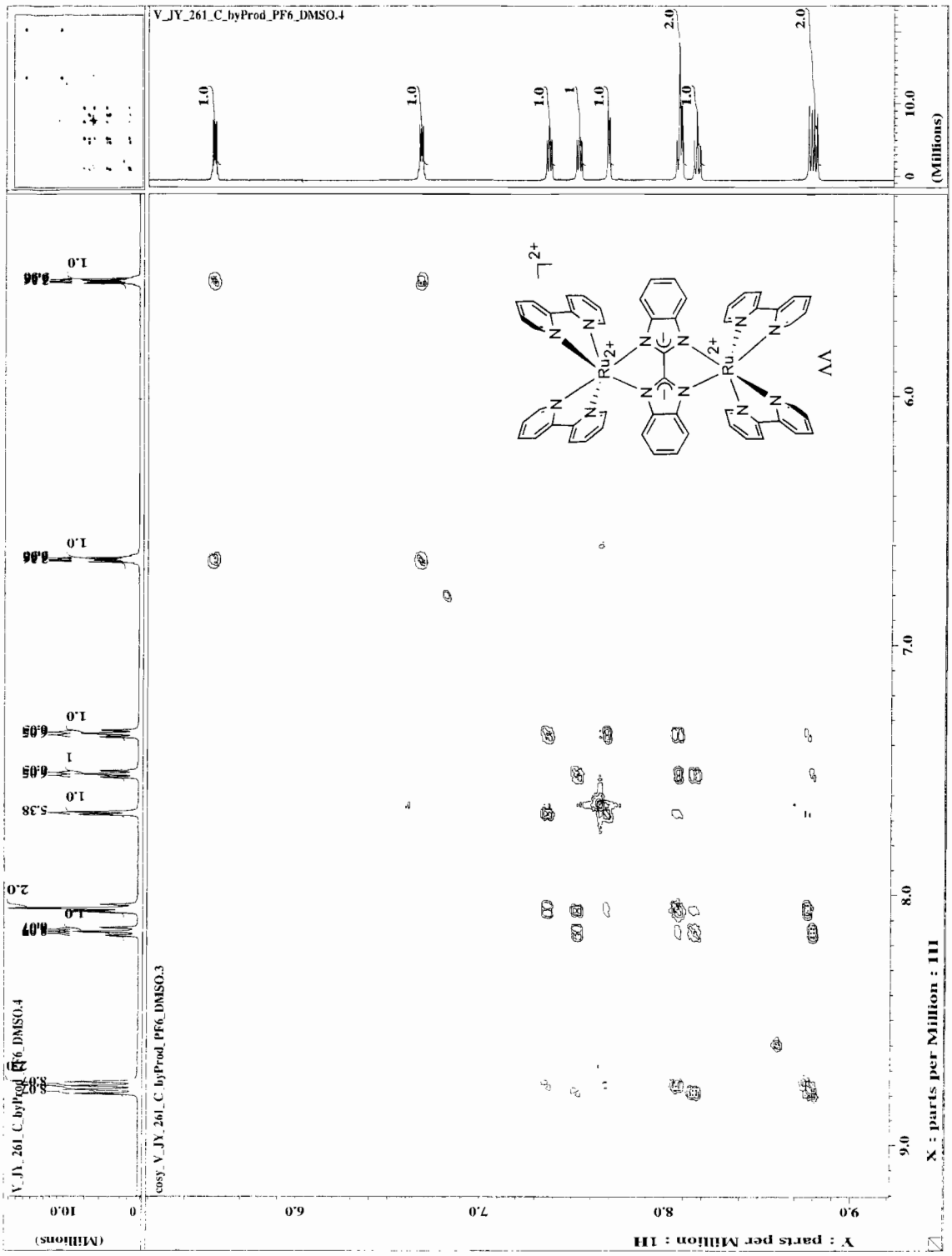
V_JY_261_C_byProd_PF6_DMSO.4
cosy_V_JY_261_C_byProd_PF6_DMSO.3
X : parts per Million : 1H
Y : parts per Million : 1H
(Millions)
VV

JEOL
---- ACQUISITION PARAMETERS ----
File Name = V_JY_261C_byprod__PF6_
Author =
Sample ID = S#361206
Content = Single Pulse with Broa
Creation Date = 10-MAR-2004 10:07:03
Revision Date = 15-MAR-2004 22:10:07
Spec Site = Eclipse+ 500
Spec Type = DELTA_NMR
Data Format = 1D COMPLEX
Dimensions = X
Dim Size = 32768
Dim Title = 13C
Dim Units = [ppm]
Acq_delay = 33.6[us]
Changer_sample = 0
Experiment = single_pulse_dec
Field_strength = 11.747379[T]
Irr90_hi = 15[us]
Irr90_lo = 18[us]
Irr_domain = 1H
Irr_pwidth = 82[us]
Lock_status = IDLE
Recv_gain = 29
Relaxation_delay = 4[s]
Scans = 7686
Solvent = DMSO-D6
Spin_get = 13[Hz]
Spin_lock_90 = 60[us]
Spin_lock_attn = 15[dB]
Spin_set = 15[Hz]
Spin_state = SPIN ON
Spin_status = SPIN ON
Temp_get = 23.8[dC]
Temp_set = 25[dC]
Temp_state = TEMP OFF
Temp_status = TEMP OFF
X90 = 14[us]
X90_hi = 13[us]
X90_lo = 53[us]
X_acq_duration = 1.04202241[s]
X_domain = 13C
X_freq = 125.76529768[MHz]
X_offset = 100[ppm]
X_points = 32768
X_prescans = 4
X_pulse = 4.66666667[us]
X_resolution = 0.95967227[Hz]
X_sweep = 31.44654088[kHz]
V_JY_261C_byprod__PF6_DMSO.3
(Billions)
X : parts per Million : 13C
159.420
157.764
157.566
152.911
150.980
144.929
136.406
136.162
127.165
126.601
123.571
123.518
121.129
113.728
39.565
39.397
39.230
0.000

*MSD-TOF
Polarity/Scan Type: Positive

Sample Name: t8jy3818

Printing Date: 19/03/2004

Printing Time: 11:50:25 AM

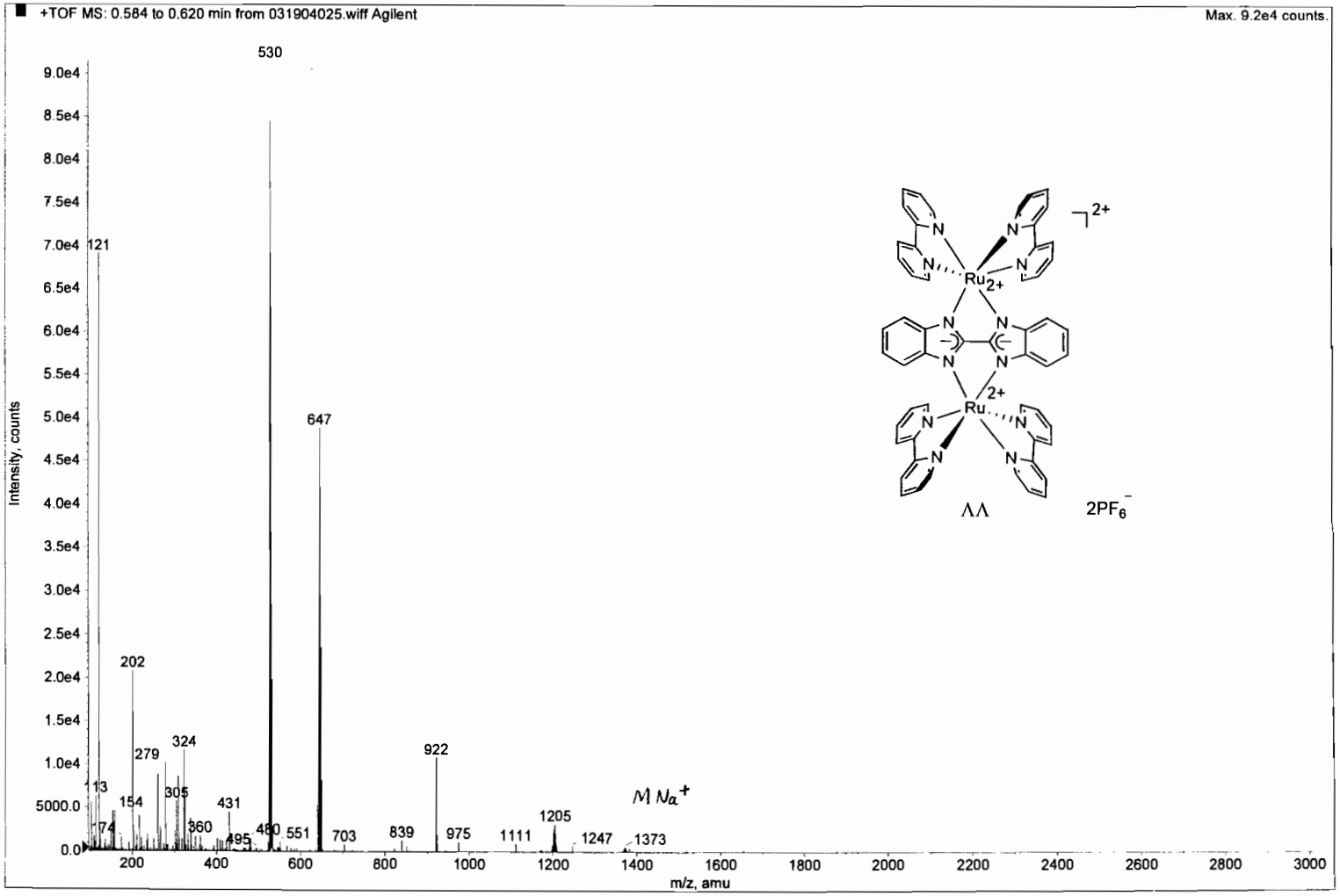

*MSD-TOF
Polarity/Scan Type: Positive

Sample Name: t8jy3818

Printing Date: 19/03/2004

Printing Time: 11:51:21 AM

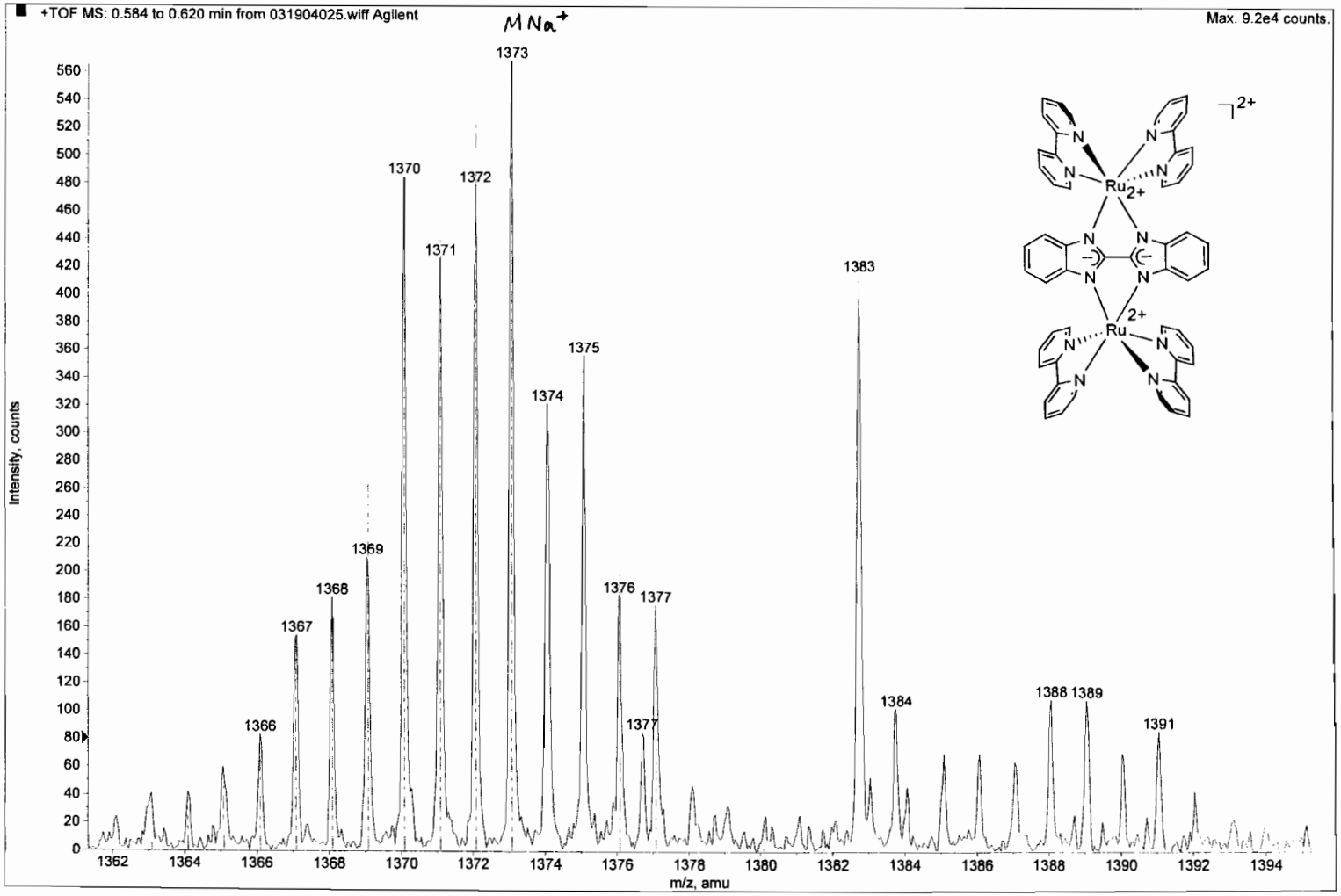

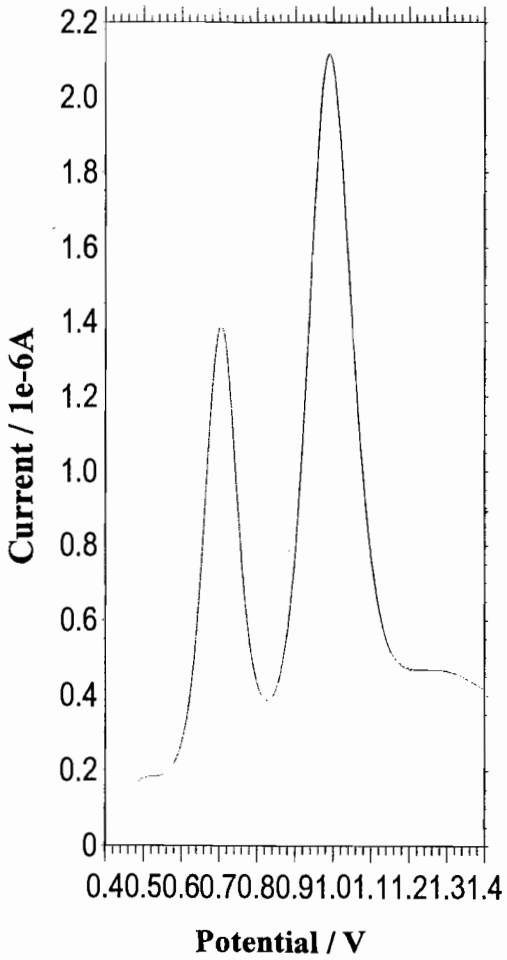

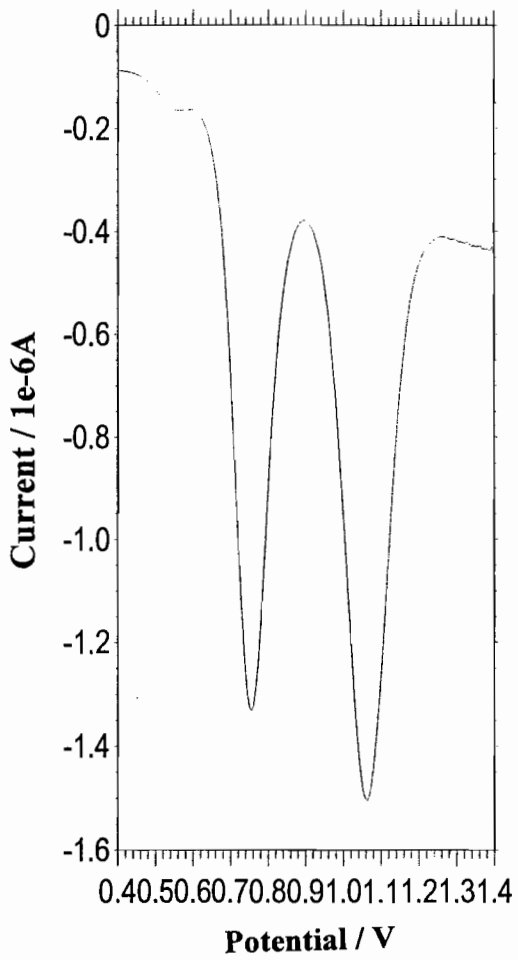

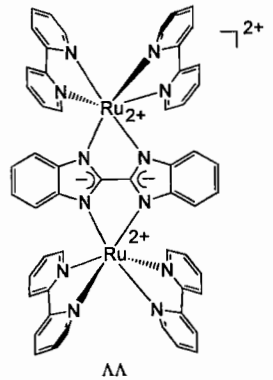

Differential Pulse Voltammetry

APPENDIX 18

^{1}H NMR, DIFFERENTIAL PULSE VOLTAMMETRY

SPECTRA OF $[(Ru(bpy)_2)_2(BiBzIm)](PF_6)_2$ **22**

JEOL

Filename	= VIII JY 53_2RuBiBzImM
Author	= delta
Experiment	= single_pulse.exp
Sample_id	= S#387382
Solvent	= DMSO-D6
Creation time	= 10-AUG-2005 11:21:12
Revision time	= 16-OCT-2005 21:47:41
Current time	= 16-OCT-2005 21:47:51
Content	= Single Pulse Experime
Data_format	= 1D COMPLEX
Dim_size	= 16384
Dim_title	= 1H
Dim_units	= [ppm]
Dimensions	= X
Site	= Eclipse+ 500
Spectrometer	= DELTA NMR
Field strength	= 11.7473579[T] (500[MH
X_acq_duration	= 1.4876672[s]
X_domain	= 1H
X_freq	= 500.15991521[MHz]
X_offset	= 8[ppm]
X_points	= 16384
X_prescans	= 0
X_resolution	= 0.67219335[Hz]
X_sweep	= 11.01321586[kHz]
Clipped	= FALSE
Mod return	= 1
Scans	= 27
Total scans	= 27
X_90_width	= 18.5[us]
X_acq_time	= 1.4876672[s]
X_angle	= 45[deg]
X_pulse	= 9.25[us]
Initial_wait	= 1[s]
Phase_preset	= 3[us]
Recvr_gain	= 19
Relaxation_delay	= 1[s]
Temp_get	= 25.8[dC]
Unblank_time	= 2[us]

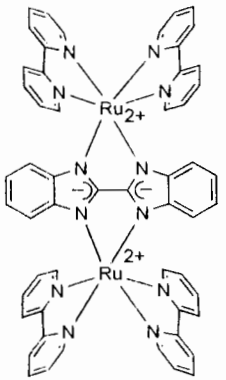

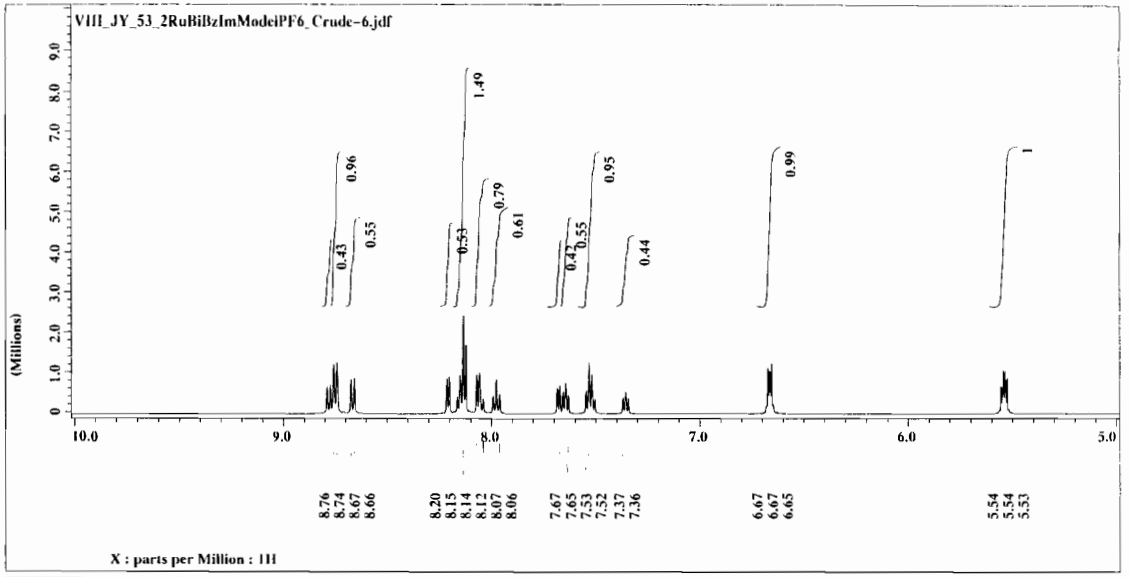

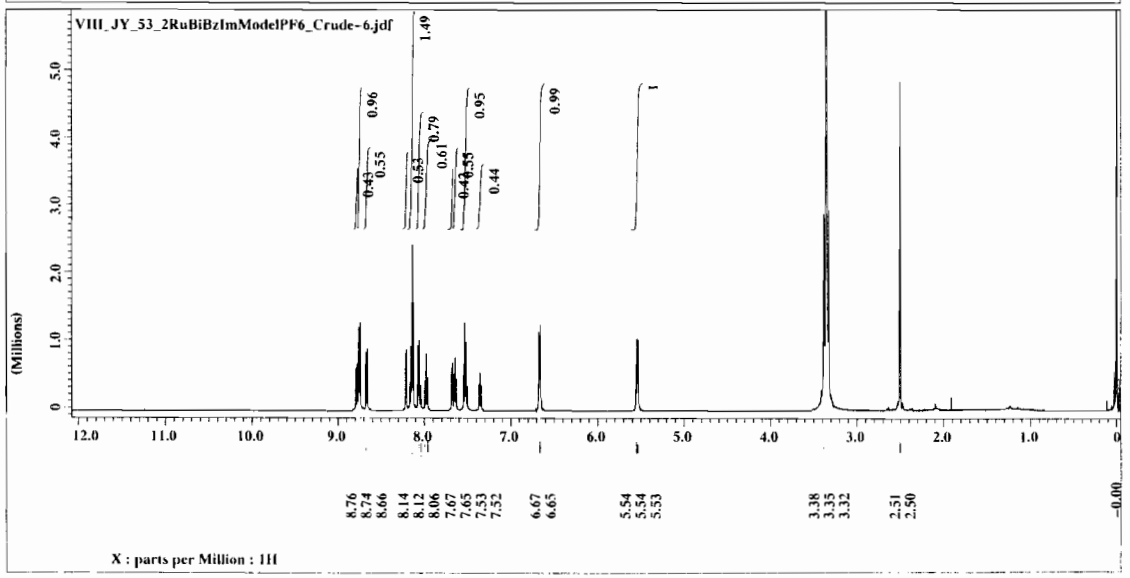

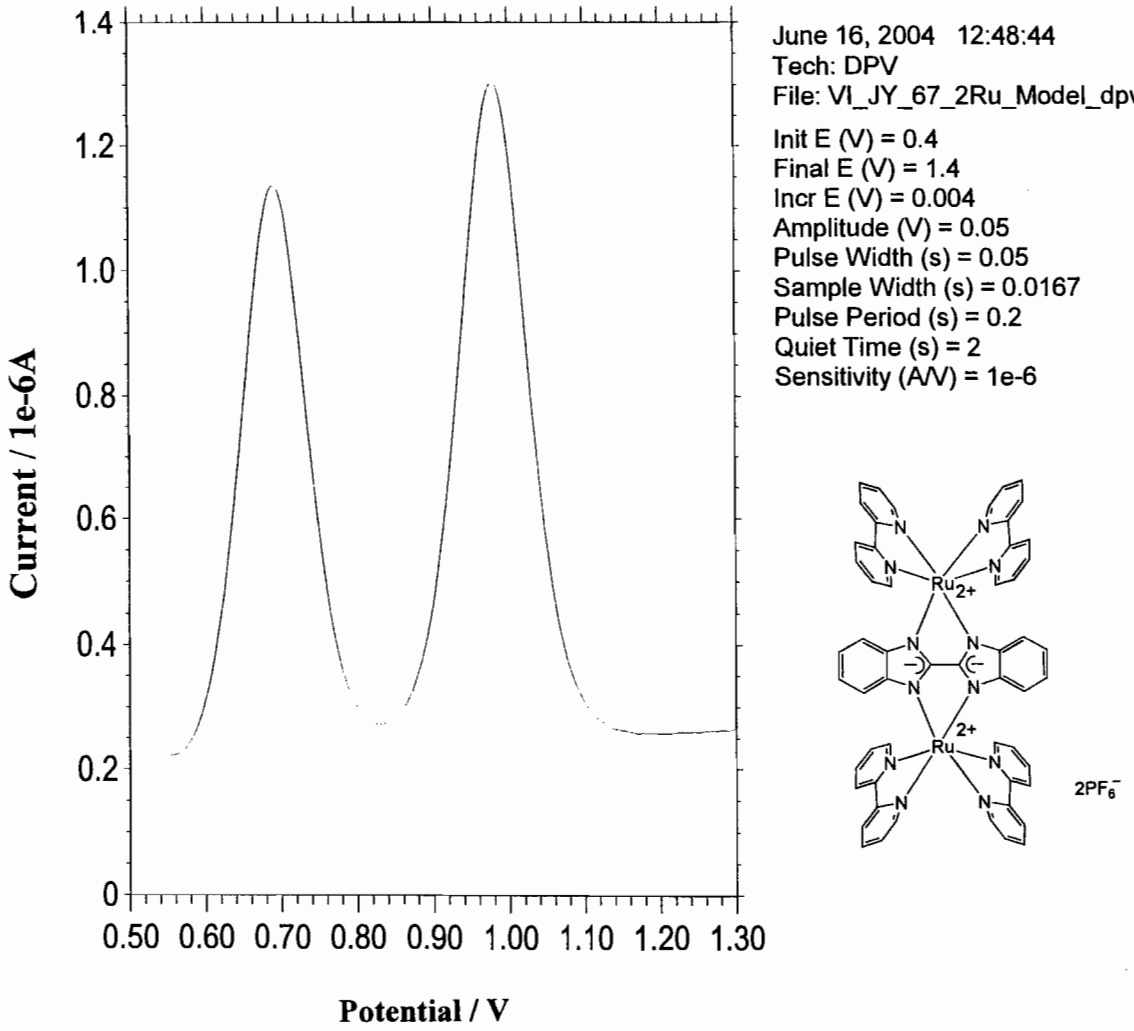

Differential Pulse Voltammetry

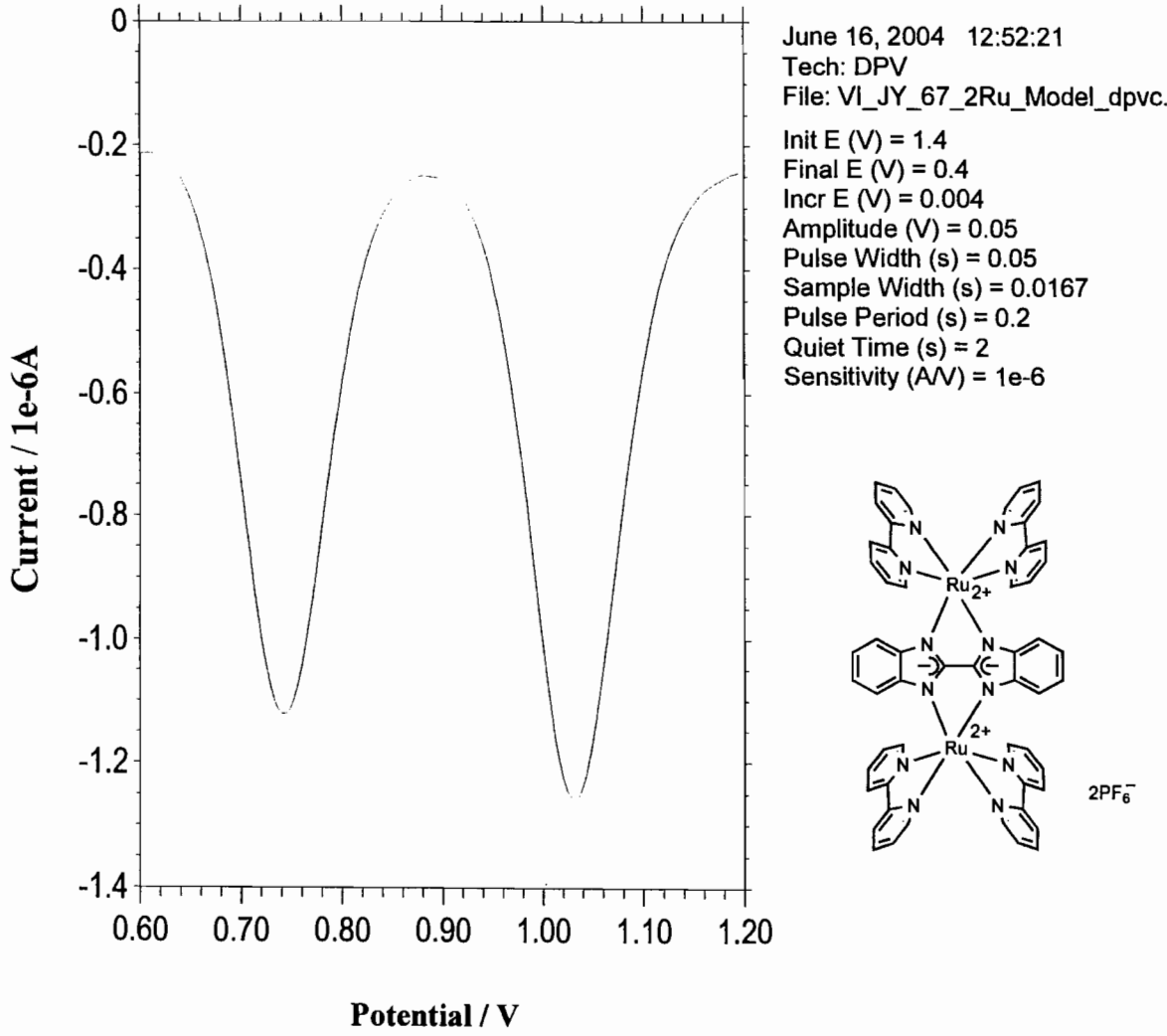

Differential Pulse Voltammetry

APPENDIX 19

^{1}H NMR, MALDI-TOF MASS, AND DIFFERENTIAL PULSE VOLTAMMETRY SPECTRA OF

$[(Ru(bpy)_2)_2(bis(BiBzImH_2))](PF_6)_4$ **23**

```
Filename          = VIII_JY_27_2RuDimerCl
Author            = delta
Experiment        = single_pulse.exp
Sample_id         = S#819097
Solvent           = DMSO-D6
Creation_time     = 18-JUN-2005 22:57:54
Revision_time     = 16-OCT-2005 21:23:33
Current_time      = 16-OCT-2005 21:25:03

Content           = Single Pulse Experime
Data_format       = 1D COMPLEX
Dim_size          = 16384
Dim_title         = 1H
Dim_units         = [ppm]
Dimensions        = X
Site              = Eclipse+ 500
Spectrometer      = DELTA_NMR

Field_strength    = 11.7473579[T] (500[MH
X_acq_duration    = 1.4876672[s]
X_domain          = 1H
X_freq            = 500.15991521[MHz]
X_offset          = 8[ppm]
X_points          = 16384
X_prescans        = 0
X_resolution      = 0.67219335[Hz]
X_sweep           = 11.01321586[kHz]
Clipped           = FALSE
Mod_return        = 1
Scans             = 214
Total_scans       = 214

X_90_width        = 18.5[us]
X_acq_time        = 1.4876672[s]
X_angle           = 45[deg]
X_pulse           = 9.25[us]
Initial_wait      = 1[s]
Phase_preset      = 3[us]
Recvr_gain        = 22
Relaxation_delay  = 1[s]
Temp_get          = 25.7[dC]
Unblank_time      = 2[us]
```

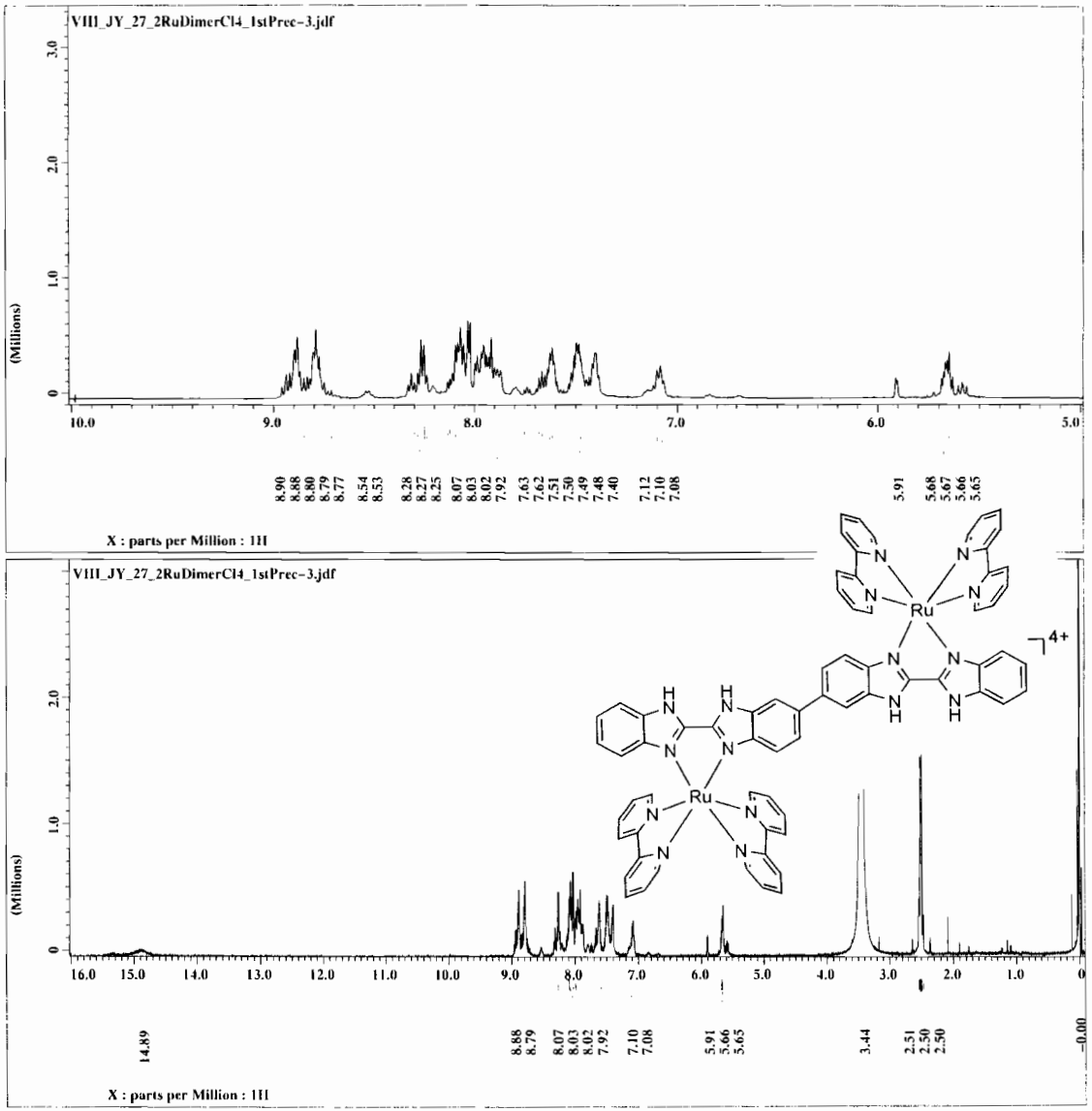

MALDI-TOF REFLECTRON

Original Filename: e:\data\routine\2004\feb\021304\2736.ms
This File # 4 : E:\DATA\ROUTINE\2004\FEB\021304\SMOOTH.MS
Comment:

Method: RDE2000K
Mode: Reflector
Accelerating Voltage: 20000
Grid Voltage: 72.000 %
Guide Wire Voltage: 0.030 %
Delay: 100 ON
Sample: 08

Laser : 1800
Scans Averaged: 55
Pressure: 2.39e-07
Low Mass Gate: OFF
Timed Ion Selector: 180.0 OFF
Negative Ions: OFF
Collected: 2/14/04 4:47 AM

Savitsky-Golay Order = 2 Points = 19

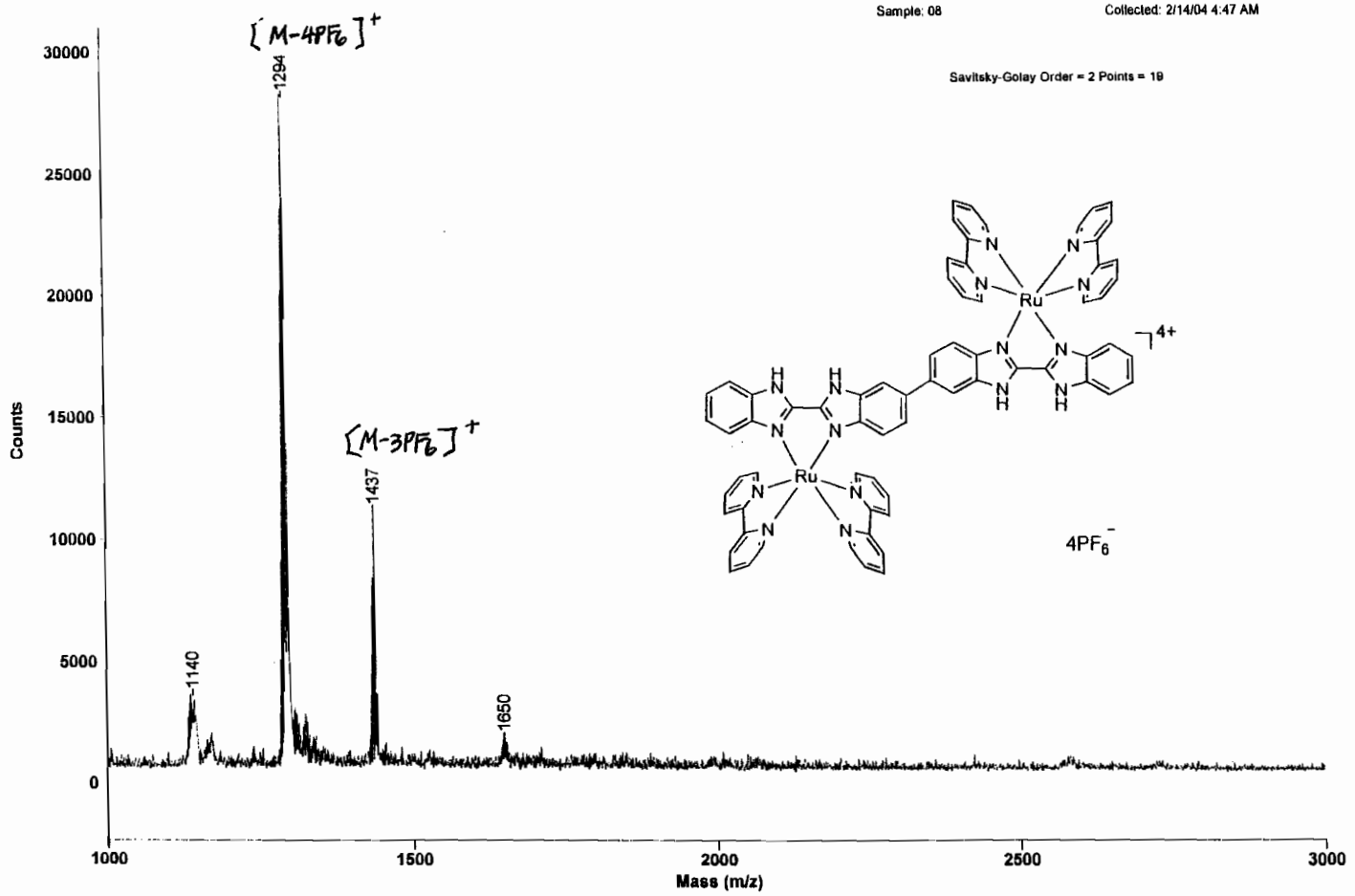

JEOL

Filename	= VI_JY_58_DeprotonDime
Author	= delta
Experiment	= single_pulse.exp
Sample_id	= S#394770
Solvent	= DMSO-D6
Creation_time	= 17-JUN-2005 11:05:30
Revision_time	= 16-OCT-2005 22:04:48
Current_time	= 16-OCT-2005 22:05:21
Content	= Single Pulse Experime
Data_format	= 1D COMPLEX
Dim_size	= 16384
Dim_title	= 1H
Dim_units	= [ppm]
Dimensions	= X
Site	= Eclipse+ 500
Spectrometer	= DELTA_NMR
Field_strength	= 11.7473579[T] (500[MH
X_acq_duration	= 1.4876672[s]
X_domain	= 1H
X_freq	= 500.15991521[MHz]
X_offset	= 8[ppm]
X_points	= 16384
X_prescans	= 0
X_resolution	= 0.67219335[Hz]
X_sweep	= 11.01321586[kHz]
Clipped	= FALSE
Mod_return	= 1
Scans	= 116.0
Total_scans	= 116.0
X_90_width	= 18.5[us]
X_acq_time	= 1.4876672[s]
X_angle	= 45[deg]
X_pulse	= 9.25[us]
Initial_wait	= 1[s]
Phase_preset	= 3[us]
Recvr_gain	= 20
Relaxation_delay	= 1[s]
Temp_get	= 25.7[dC]
Unblank_time	= 2[us]

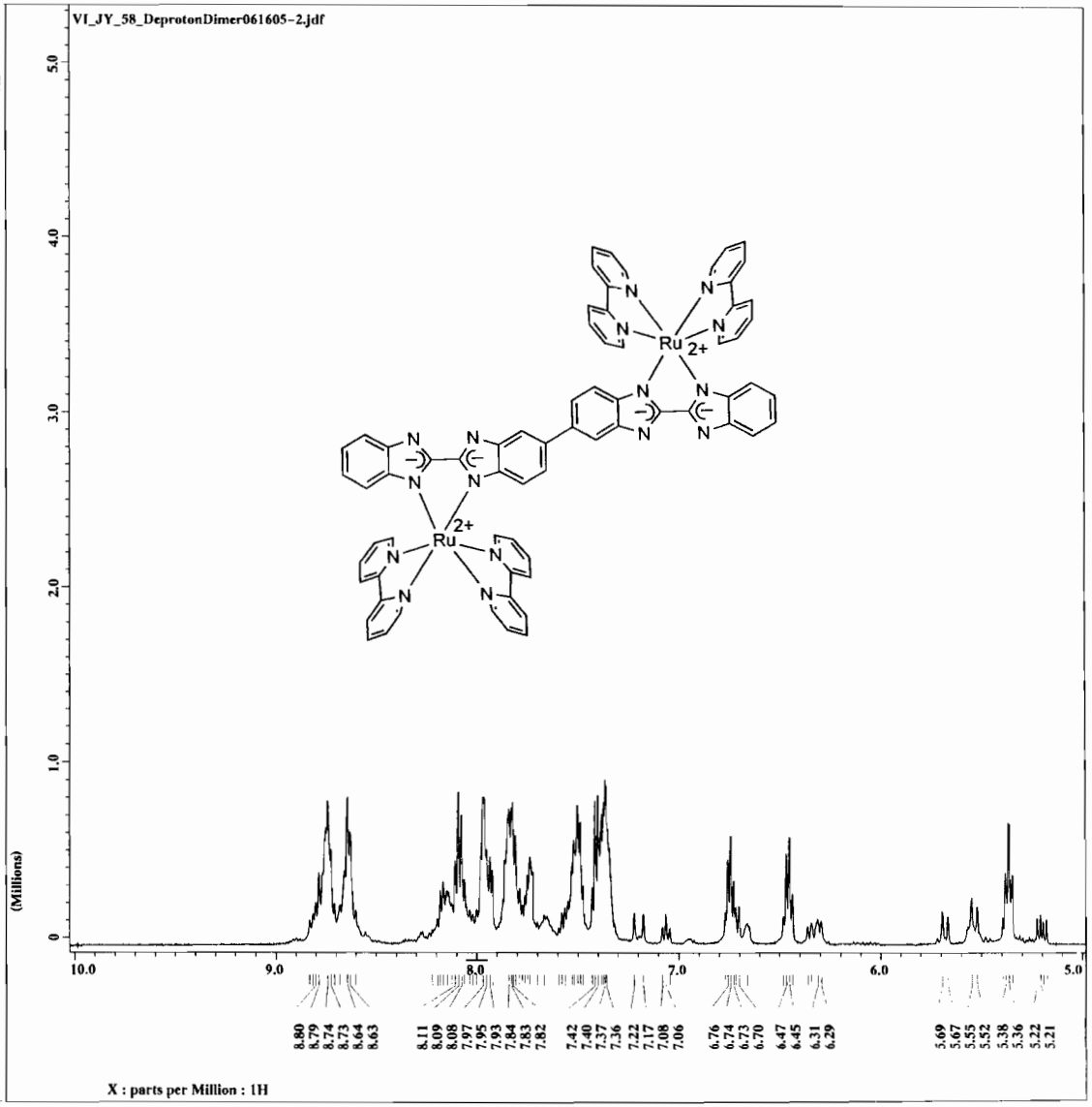

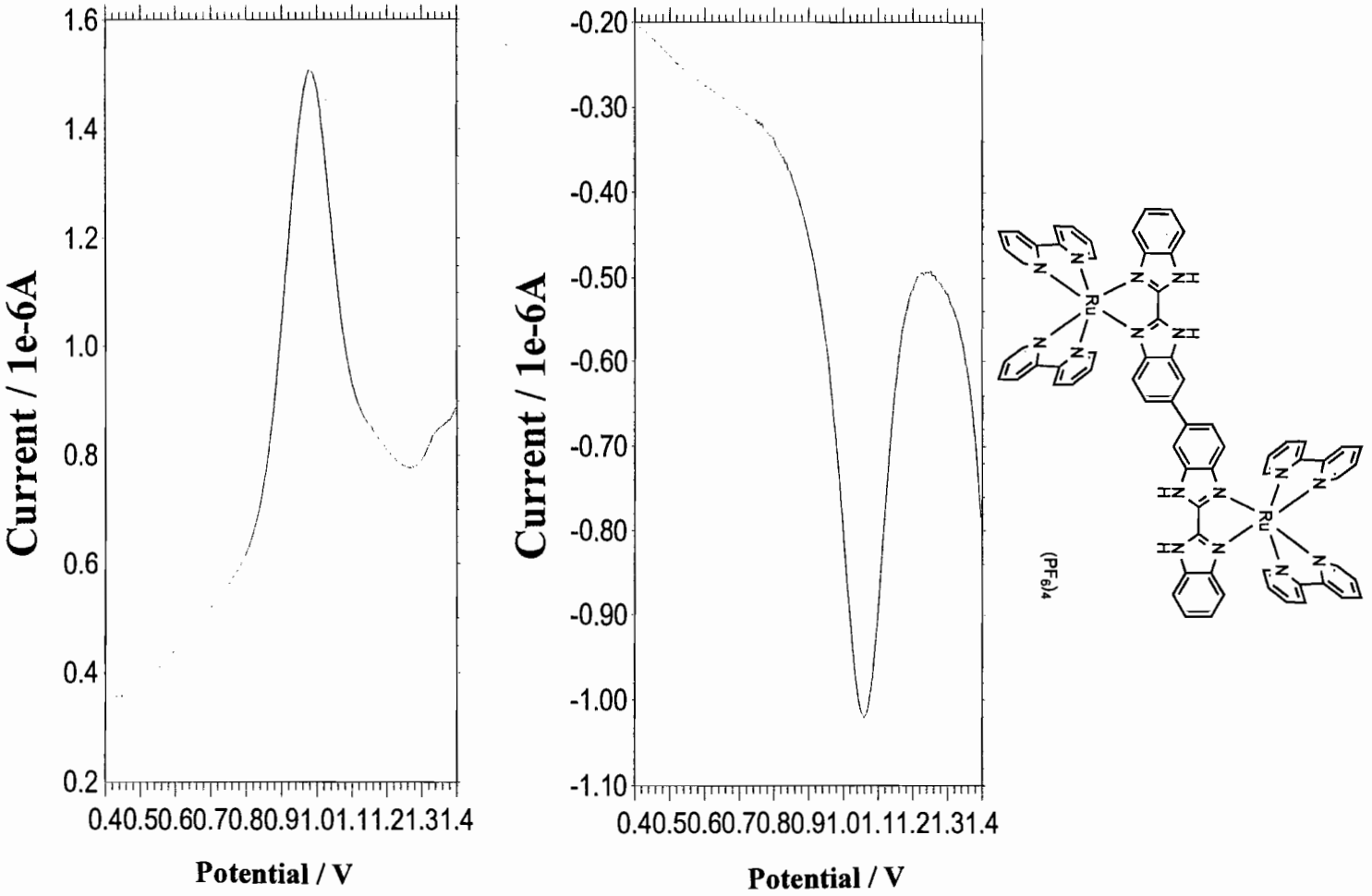

Differential Pulse Voltammetry

APPENDIX 20

^{1}H NMR AND CYCLIC VOLTAMMOGRAM SPECTRA OF

$[(Ru(bpy)_2)_2(bis(BiBzIm))]$ **24**

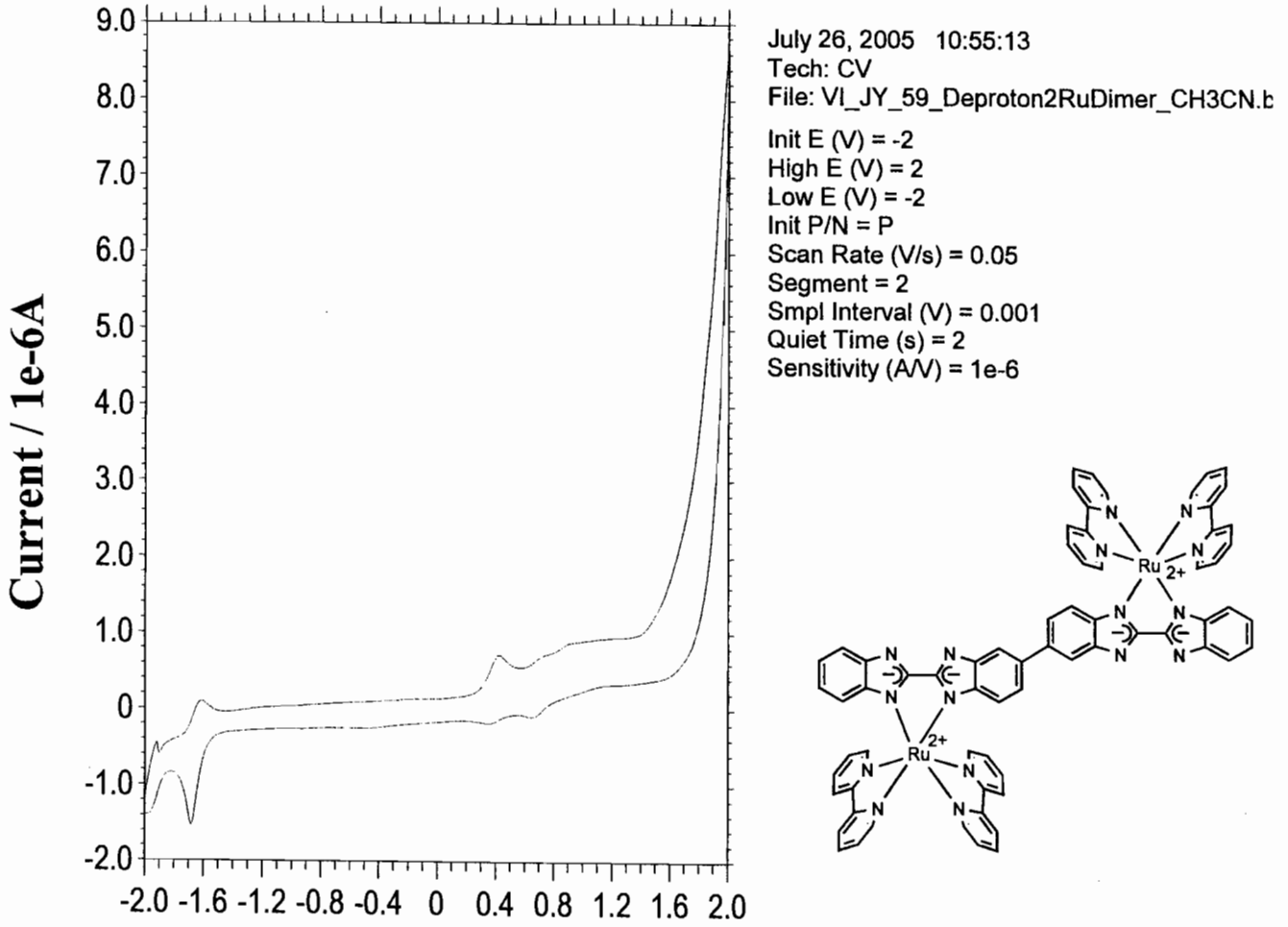

Cyclic Voltammogram

APPENDIX 21

^{1}H NMR, MALDI-TOF MASS AND DIFFERENTIAL PULSE VOLTAMMETRY SPECTRA OF $[(Ru(bpy)_2)_4(bis(BiBzIm))](PF_6)_4$ **25**

```
Filename          = VIII_JY_19_4RuDimerPF
Author            = delta
Experiment        = single_pulse.exp
Sample_id         = S#560506
Solvent           = DMSO-D6
Creation_time     = 23-JUN-2005 15:45:13
Revision_time     = 16-OCT-2005 21:14:48
Current_time      = 16-OCT-2005 21:16:02

Content           = Single Pulse Experime
Data_format       = 1D COMPLEX
Dim_size          = 16384
Dim_title         = 1H
Dim_units         = [ppm]
Dimensions        = X
Site              = Eclipse+ 500
Spectrometer      = DELTA_NMR

Field_strength    = 11.7473579[T] (500[MH
X_acq_duration    = 1.4876672[s]
X_domain          = 1H
X_freq            = 500.15991521[MHz]
X_offset          = 8[ppm]
X_points          = 16384
X_prescans        = 0
X_resolution      = 0.67219335[Hz]
X_sweep           = 11.01321586[kHz]
Clipped           = FALSE
Mod_return        = 1
Scans             = 96
Total_scans       = 96

X_90_width        = 18.5[us]
X_acq_time        = 1.4876672[s]
X_angle           = 45[deg]
X_pulse           = 9.25[us]
Initial_wait      = 1[s]
Phase_preset      = 3[us]
Recvr_gain        = 24
Relaxation_delay  = 1[s]
Temp_get          = 26.1[dC]
Unblank_time      = 2[us]
```

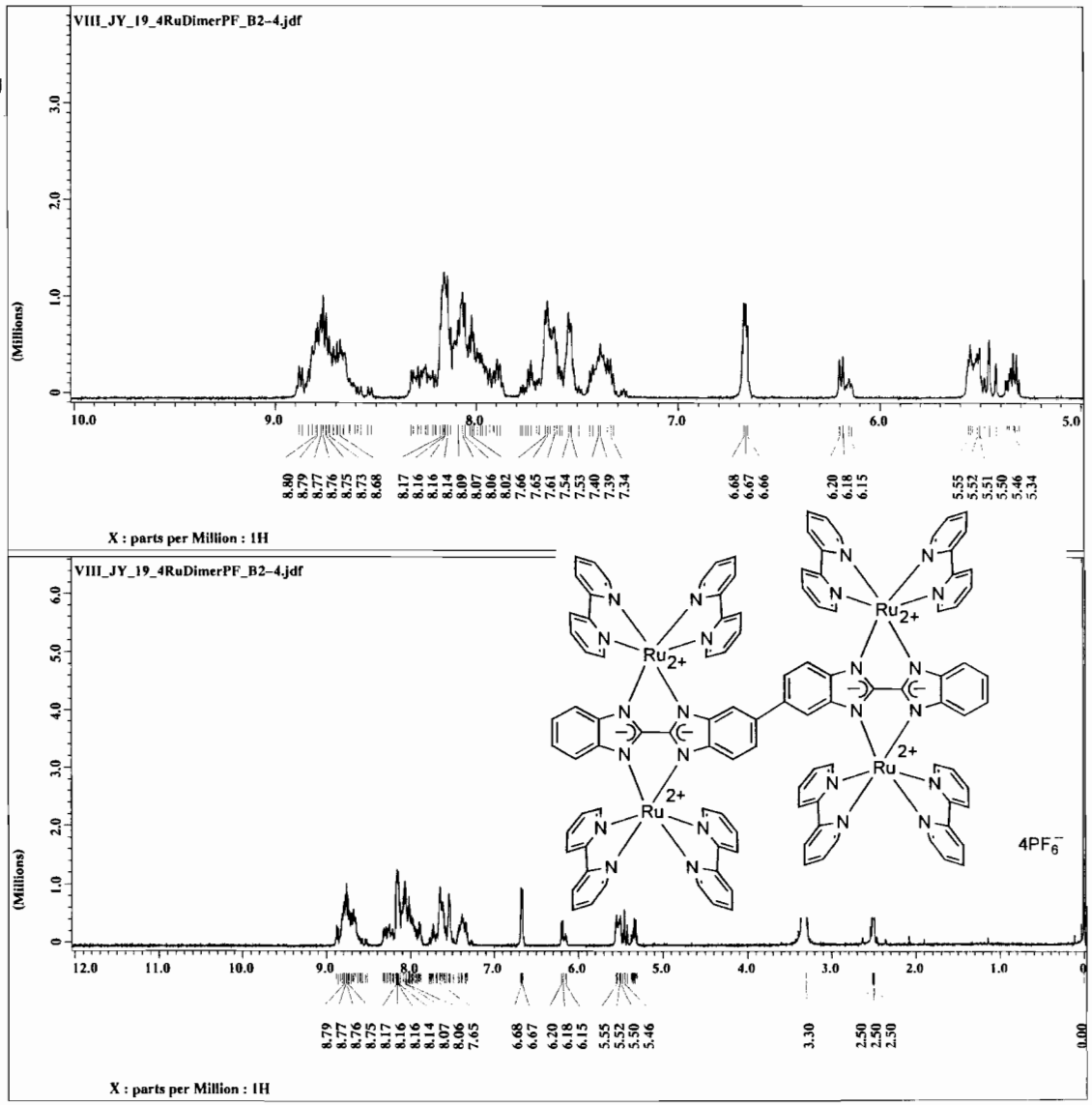

MALDI-TOF REFLECTRON

Original Filename: e:\data\routine\2004\feb\021304\2735.ms

This File # 4 : E:\DATA\ROUTINE\2004\FEB\021304\SMOOTH.MS

Comment:

Method: RDE2000K
Mode: Reflector
Accelerating Voltage: 20000
Grid Voltage: 72.000 %
Guide Wire Voltage: 0.030 %
Delay: 100 ON
Sample: 07

Laser : 1800
Scans Averaged: 126
Pressure: 2.88e-07
Low Mass Gate: OFF
Timed Ion Selector: 180.0 OFF
Negative Ions: OFF
Collected: 2/14/04 4:42 AM

Savitsky-Golay Order = 2 Points = 19

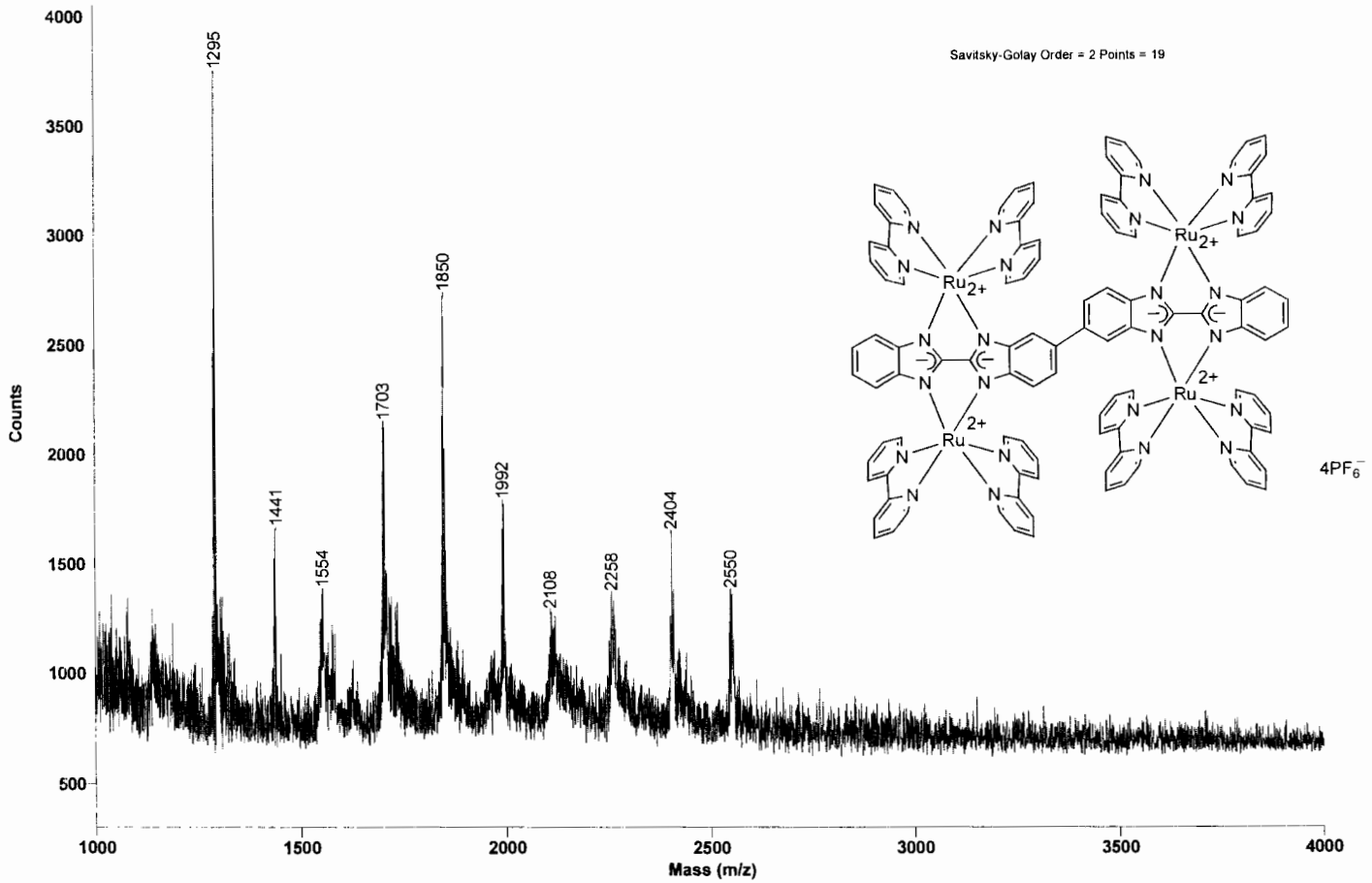

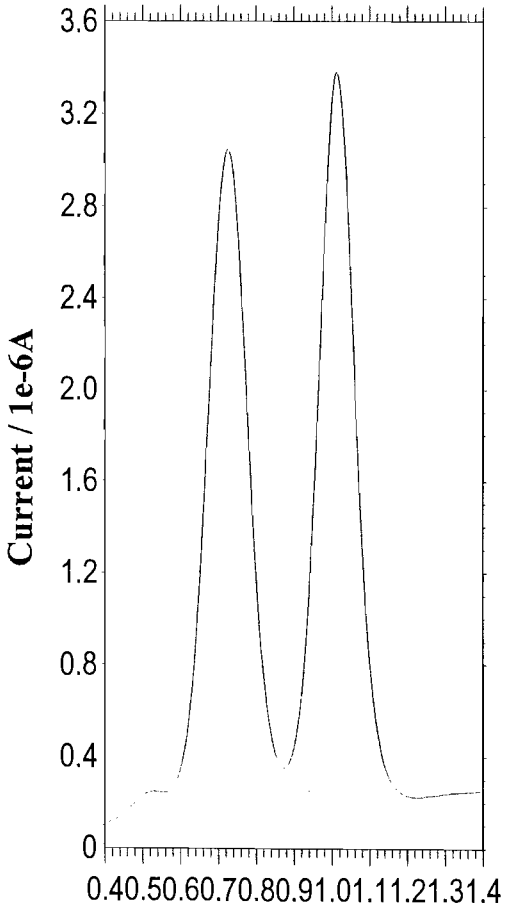

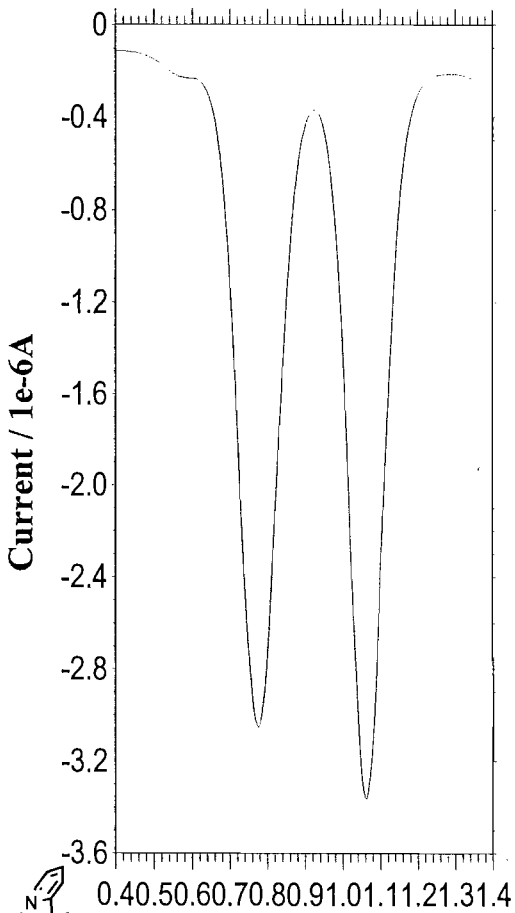

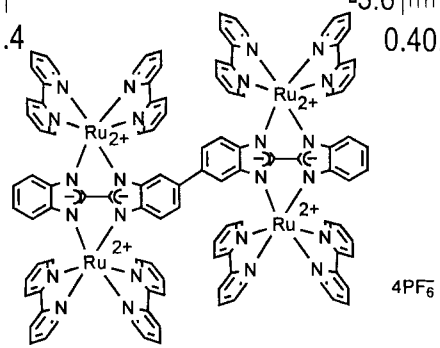

Differential Pulse Voltammetry

APPENDIX 22

^{1}H NMR AND MALDI-TOF MASS SPECTRA OF

Λ_4-[(Ru(bpy)$_2$)$_4$(bis(BiBzIm))](PF$_6$)$_4$ Λ_4-Ru$_4$-**25**

```
Filename          = VIII_JY_67_Chiral4RuD
Author            = delta
Experiment        = single_pulse.exp
Sample_id         = S#599998
Solvent           = DMSO-D6
Creation_time     = 13-SEP-2005 18:10:00
Revision_time     = 16-OCT-2005 21:18:34
Current_time      = 16-OCT-2005 21:20:36

Content           = Single Pulse Experime
Data_format       = 1D COMPLEX
Dim_size          = 16384
Dim_title         = 1H
Dim_units         = [ppm]
Dimensions        = X
Site              = Eclipse+ 500
Spectrometer      = DELTA_NMR

Field_strength    = 11.7473579[T] (500[MH
X_acq_duration    = 1.4876672[s]
X_domain          = 1H
X_freq            = 500.15991521[MHz]
X_offset          = 8[ppm]
X_points          = 16384
X_prescans        = 0
X_resolution      = 0.67219335[Hz]
X_sweep           = 11.01321586[kHz]
Clipped           = FALSE
Mod_return        = 1
Scans             = 883
Total_scans       = 883

X_90_width        = 18.5[us]
X_acq_time        = 1.4876672[s]
X_angle           = 45[deg]
X_pulse           = 9.25[us]
Initial_wait      = 1[s]
Phase_preset      = 3[us]
Recvr_gain        = 15
Relaxation_delay  = 1[s]
Temp_get          = 25.2[dC]
Unblank_time      = 2[us]
```

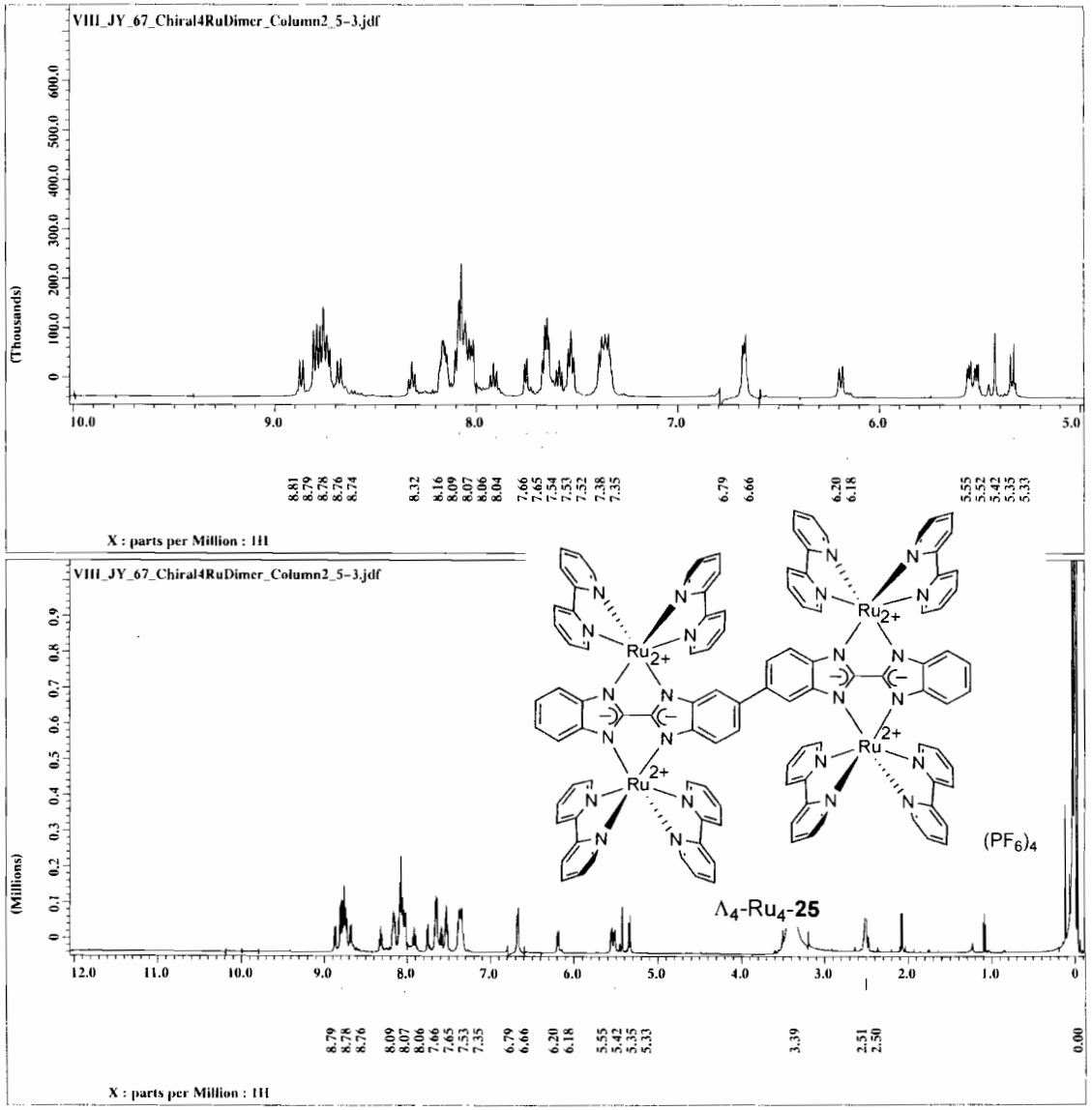

MALDI-TOF REFLECTRON

Original Filename: e:\data\routine\2004\may\050704\5737d.ms

This File # 2 : E:\DATA\ROUTINE\2004\MAY\050704\SMOOTH.MS

Comment:

Method: RDE2000K	Laser : 2400
Mode: Reflector	Scans Averaged: 35
Accelerating Voltage: 20000	Pressure: 5.85e-07
Grid Voltage: 72.000 %	Low Mass Gate: 400.0
Guide Wire Voltage: 0.030 %	Timed Ion Selector: 180.0 OFF
Delay: 100 ON	Negative Ions: OFF
Sample: 05	Collected: 5/8/04 3:11 AM

Savitsky-Golay Order = 2 Points = 19

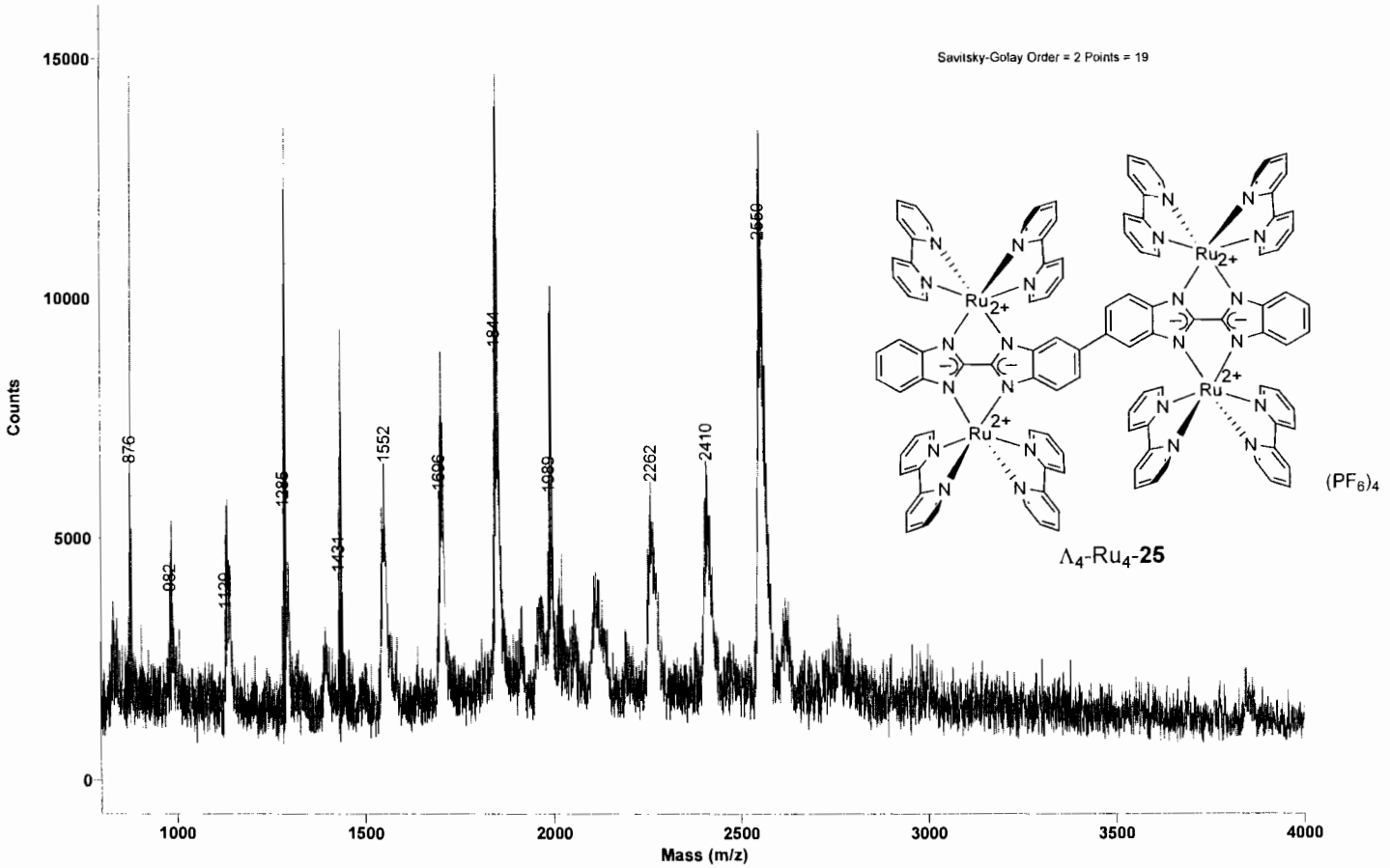

Λ_4-Ru_4-**25**

MALDI-TOF REFLECTRON

Original Filename: e:\data\routine\2004\may\050704\5737d.ms

This File # 2 : E:\DATA\ROUTINE\2004\MAY\050704\SMOOTH.MS

Comment:

Method: RDE2000K
Mode: Reflector
Accelerating Voltage: 20000
Grid Voltage: 72.000 %
Guide Wire Voltage: 0.030 %
Delay: 100 ON
Sample: 05

Laser : 2400
Scans Averaged: 35
Pressure: 5.85e-07
Low Mass Gate: 400.0
Timed Ion Selector: 180.0 OFF
Negative Ions: OFF
Collected: 5/8/04 3:11 AM

Savitsky-Golay Order = 2 Points = 19

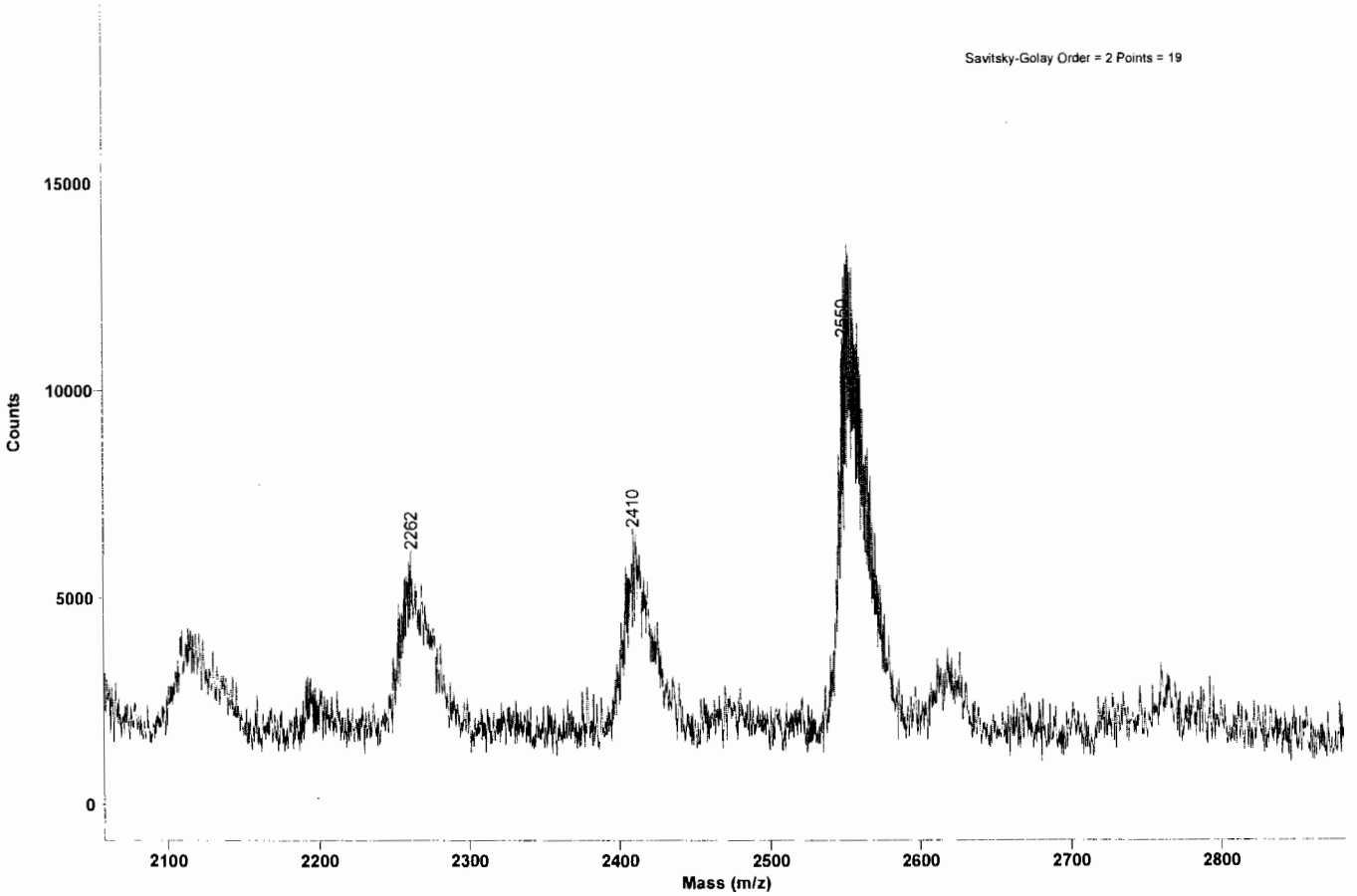

APPENDIX 23

MALDI-TOF MASS SPECTRA AND DIFFERENTIAL PULSE VOLTAMMETRY OF $[(Ru(bpy)_2)_8(tetra(BiBzIm))](PF_6)_8$ **26**

MALDI-TOF REFLECTRON

Savitsky-Golay Order = 2 Points = 19

Method: R2000KH
Mode: Reflector
Accelerating Voltage: 20000
Grid Voltage: 72.000 %
Guide Wire Voltage: 0.030 %

Laser : 2140
Scans Averaged: 202
Pressure: 1.15e-07
Low Mass Gate: 400.0
Timed Ion Selector: 379.0 OFF
Negative Ions: OFF
Collected: 2/10/05 0:34 AM
Delay: 200 ON
Sample: 20

Original Filename: e:\data\routine\2005\feb\020905\5900d.ms

This File # 2 E:\DATA\ROUTINE\2005\FEB\020905\SMOOTH.MS

Comment:

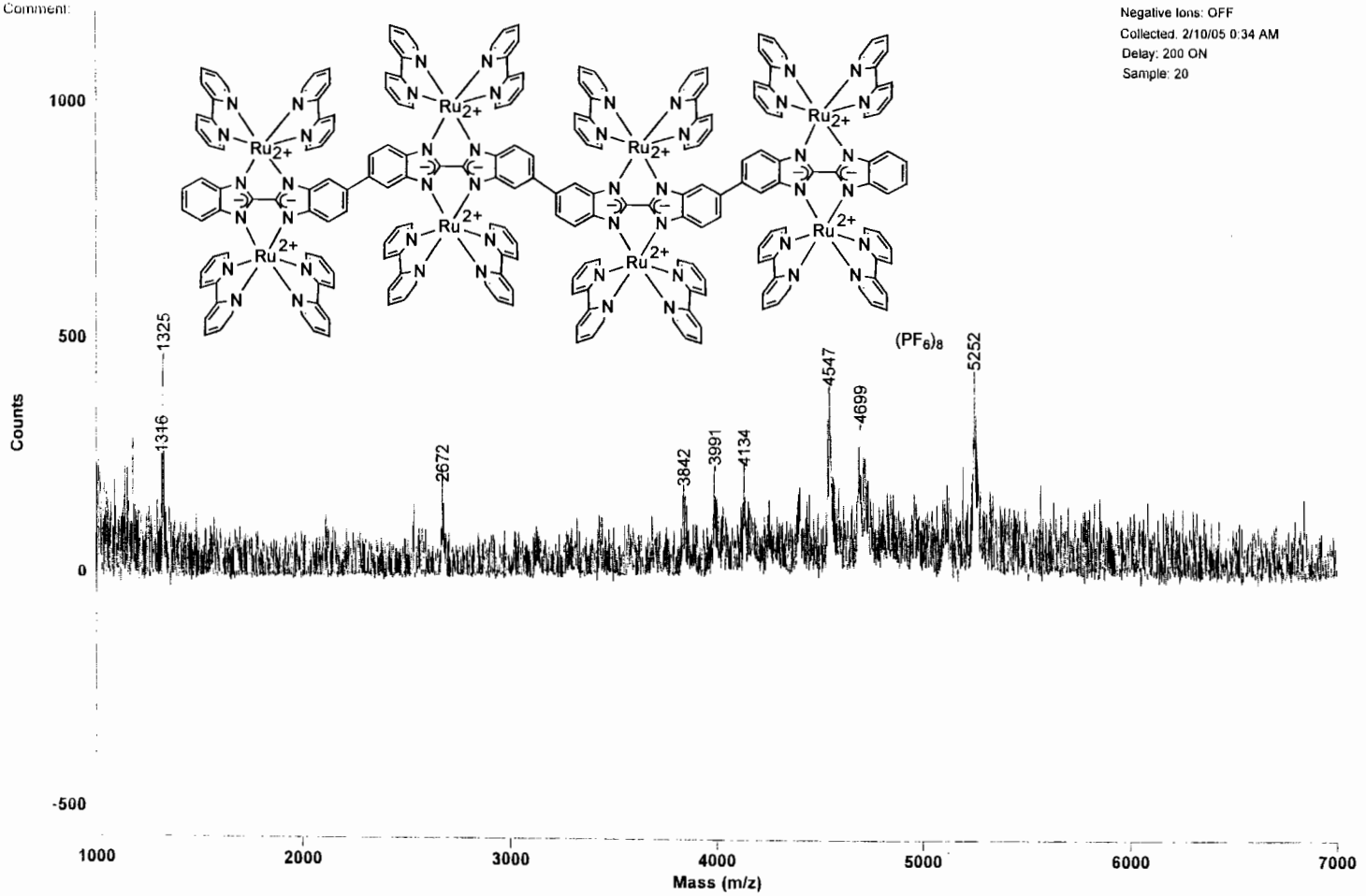

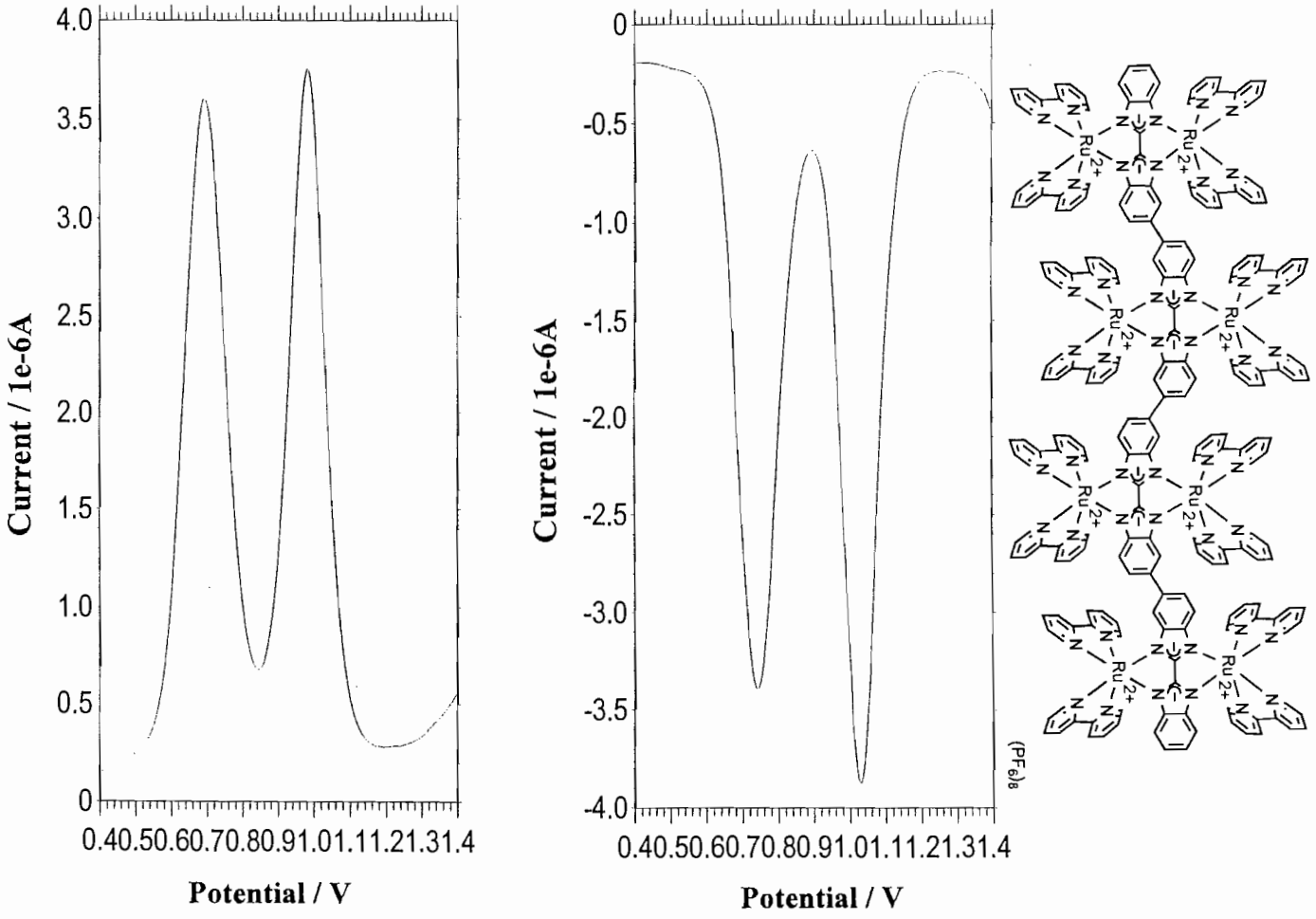

Differential Pulse Voltammetry

APPENDIX 24

MALDI-TOF MASS SPECTRA OF

Λ_8-[(Ru(bpy)$_2$)$_8$(tetra(BiBzIm))](PF$_6$)$_8$ Λ_8-Ru$_8$-**26**

MALDI TOF

Original Filename. d:\data\2005\october\100305\6183d2.ms
This File # 1 : D:\DATA\2005\OCTOBER\100305\SMOOTH.MS
Comment:

Method: PEP
Accelerating Voltage: 20000
Grid Voltage: 93.900 %
Guide Wire Voltage: 0.003 %
Delay: 90 ON
Sample: 26

Laser : 2350
Scans Averaged: 139
Pressure: 6.23e-07
Low Mass Gate: 400.0
Negative Ions. OFF
Collected: 10/4/05 2:07 PM

Savitsky-Golay Order = 2 Points = 19

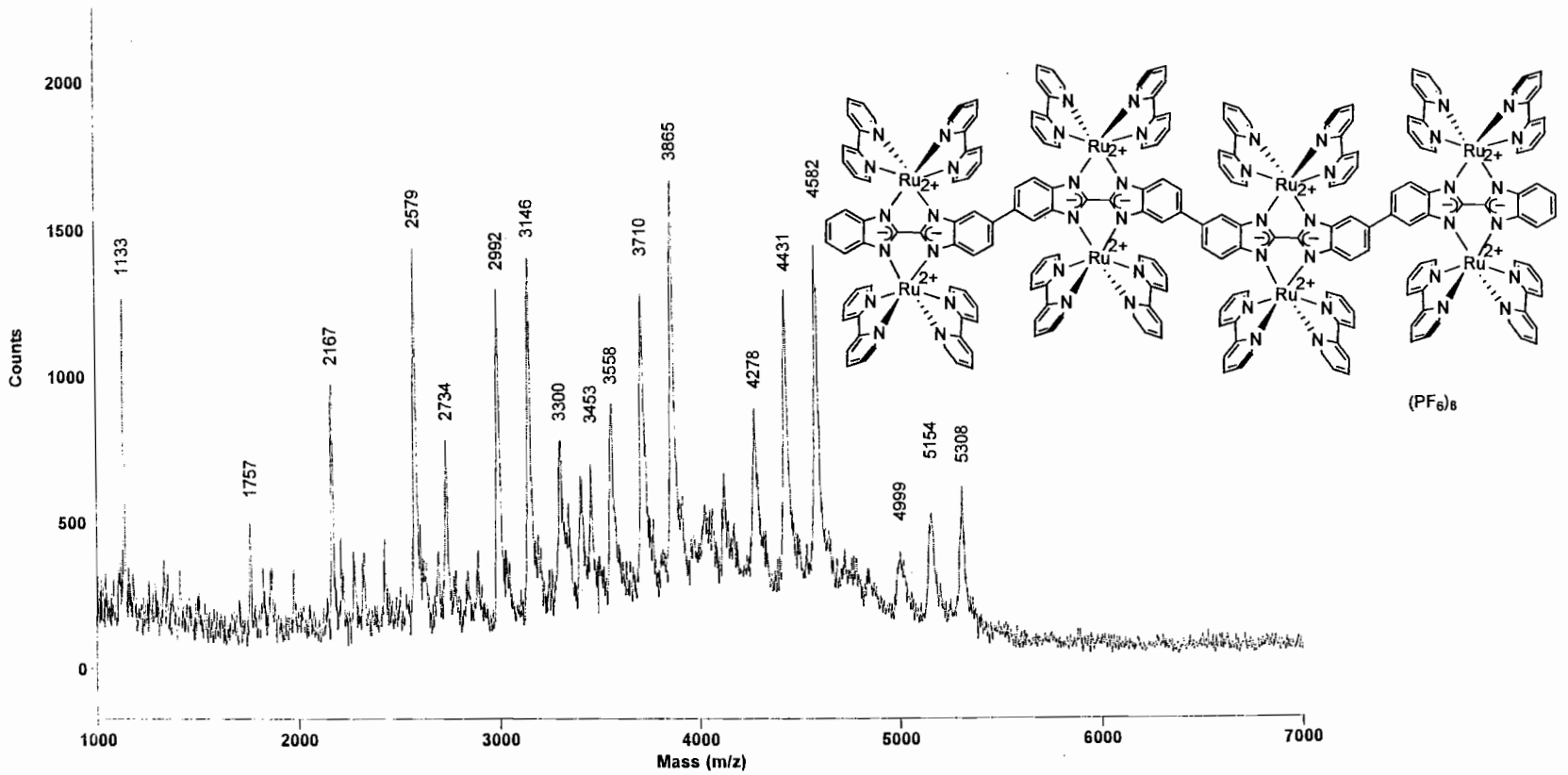

APPENDIX 25

^{1}H AND COSY NMR SPECTRA OF

$[Ru(bpy)_2(py)_2]Cl_2$ **27**

```
Filename          = V_JY_215_Ru(bpy)2(py)
Experiment        = single_pulse.exp
Sample_id         = S#375988
Solvent           = DMSO-D6
Creation_time     =  8-FEB-2004 23:27:49
Revision_time     = 17-OCT-2005 10:53:25
Current_time      = 17-OCT-2005 10:53:43

Content           = Single Pulse Experime
Data_format       = 1D COMPLEX
Dim_size          = 16384
Dim_title         = 1H
Dim_units         = [ppm]
Dimensions        = X
Site              = Eclipse+ 500
Spectrometer      = DELTA NMR

Field_strength    = 11.7473579[T] (500[MH
X_acq_duration    = 1.4876672[s]
X_domain          = 1H
X_freq            = 500.15991521[MHz]
X_offset          = 8[ppm]
X_points          = 16384
X_prescans        = 0
X_resolution      = 0.67219335[Hz]
X_sweep           = 11.01321586[kHz]
Mod_return        = 1
Scans             = 33

X_90_width        = 15[us]
X_acq_time        = 1.4876672[s]
X_angle           = 45[deg]
X_pulse           = 7.5[us]
Initial_wait      = 1[s]
Phase_preset      = 3[us]
Recvr_gain        = 20
Relaxation_delay  = 1[s]
Temp_get          = 21.8[dC]
Unblank_time      = 2[us]
```

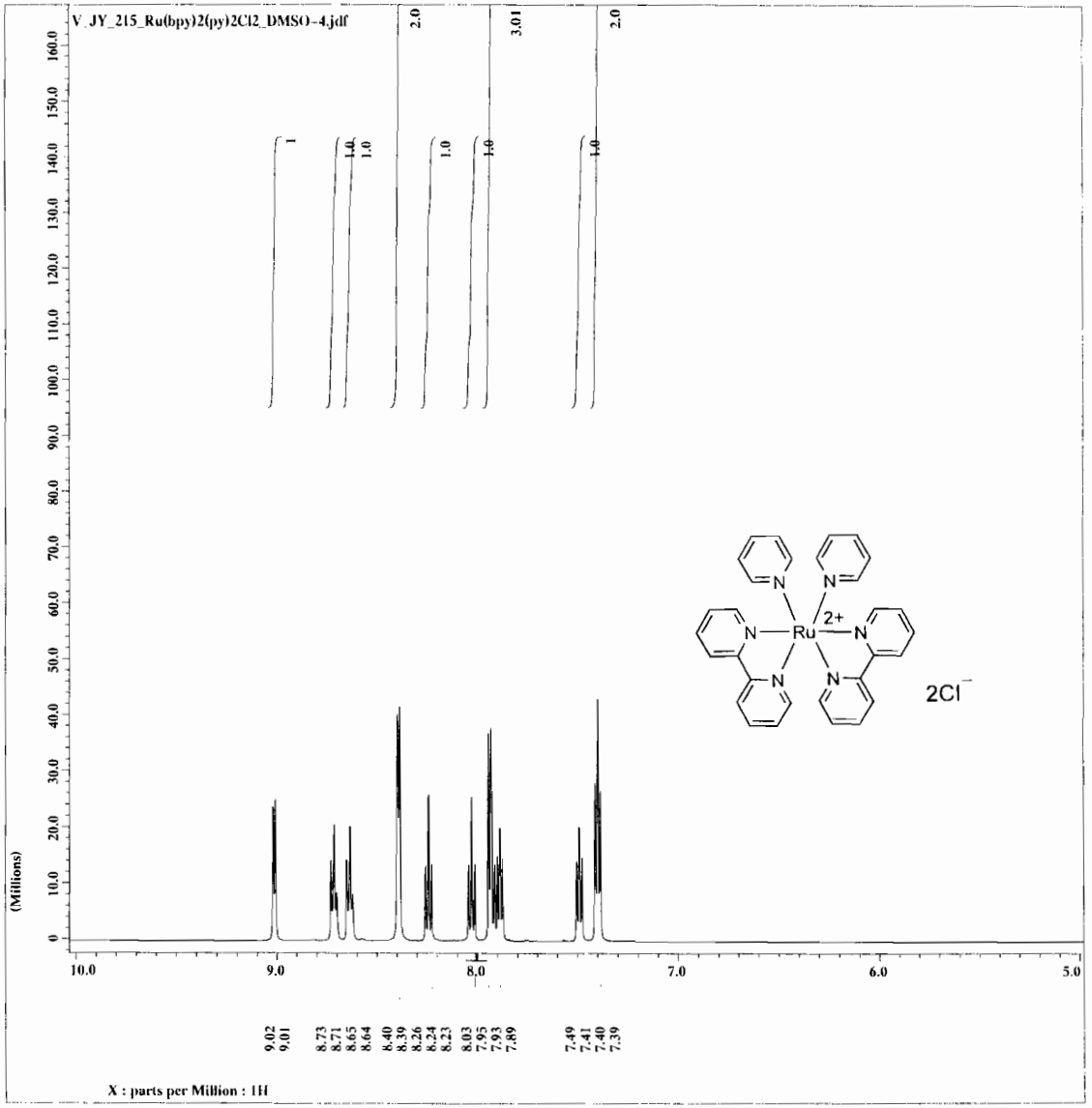

JEOL
---- ACQUISITION PARAMETERS ----
File Name = cosy_V_JY_215_Ru(bpy)2
Author =
Sample ID = S#406541
Content = absolute value COSY
Creation Date = 9-FEB-2004 00:52:31
Revision Date = 15-FEB-2004 11:22:58
Spec Site = Eclipse+ 500
Spec Type = DELTA NMR
Data Format = 2D REAL REAL
Dimensions = X Y
Dim Title = 1H 1H
Dim Size = 512, 1024
Dim Units = [ppm] [ppm]
Acq_delay = 0.8771[ms]
Changer_sample = 0
Experiment = cosy.exp
Field_strength = 11.74735791[T]
Irr90 = 15[us]
Irr90_hi = 18[us]
Irr90_lo = 82[us]
Irr_pwidth = 82[us]
Lock_status = IDLE
Recvr_gain = 15
Relaxation_delay = 1.5[s]
Scans = 4
Solvent = DMSO-D6
Spin_get = 0[Hz]
Spin_lock_90 = 60[us]
Spin_lock_attn = 15[dB]
Spin_set = 15[Hz]
Spin_state = SPIN OFF
Spin_status = SPIN OFF
Temp_get = 21.6[dC]
Temp_set = 25[dC]
Temp_state = TEMP OFF
Temp_status = TEMP OFF
X90 = 15[us]
X90_hi = 18[us]
X90_lo = 82[us]
X_acq_duration = 0.45229152[s]
X_domain = 1H
X_freq = 500.15991521[MHz]
X_offset = 8.20313[ppm]
X_points = 512
X_prescans = 4
X_pulse = 15[us]
X_resolution = 2.20791883[Hz]
X_sweep = 1.13045444[kHz]
Y90 = 10[us]
Y90_hi = 10[us]
Y90_lo = 50[us]
Y_domain = 1H
Y_freq = 500.15991521[MHz]
Y_offset = 8.20313[ppm]
Y_points = 256
Y_prescans = 0
Y_resolution = 4.41583767[Hz]
Y_sweep = 1.13045444[kHz]
V_JY_215_Ru(bpy)2(py)2Cl2_DMSO.4
cosy_V_JY_215_Ru(bpy)2py2Cl2_DMSO.4
V_JY_215_Ru(bpy)2(py)2Cl2_DMSO.4
2Cl⁻
Y : parts per Million : 1H
X : parts per Million : 1H
(Millions)

APPENDIX 26

^{1}H AND ^{13}C NMR SPECTRA OF

Λ-[$Ru(bpy)_2(py)_2$][(−)-*O*,*O*′-dibenzoyl-L-tartrate] **27a**

```
Filename          = V_JY_242_Chiral_Ru(bp
Experiment        = single_pulse.exp
Sample_id         = S#175212
Solvent           = DMSO-D6
Creation_time     =  7-MAR-2004 18:12:39
Revision_time     = 16-OCT-2005 12:29:52
Current_time      = 16-OCT-2005 12:29:59

Content           = Single Pulse Experime
Data_format       = 1D COMPLEX
Dim_size          = 16384
Dim_title         = 1H
Dim_units         = [ppm]
Dimensions        = X
Site              = Eclipse+ 500
Spectrometer      = DELTA_NMR

Field_strength    = 11.7473579[T] (500[MH
X_acq_duration    = 1.4876672[s]
X_domain          = 1H
X_freq            = 500.15991521[MHz]
X_offset          = 8[ppm]
X_points          = 16384
X_prescans        = 0
X_resolution      = 0.67219335[Hz]
X_sweep           = 11.01321586[kHz]
Mod_return        = 1
Scans             = 102

X_90_width        = 15[us]
X_acq_time        = 1.4876672[s]
X_angle           = 45[deg]
X_pulse           = 7.5[us]
Initial_wait      = 1[s]
Phase_preset      = 3[us]
Recvr_gain        = 14
Relaxation delay  = 1[s]
Temp_get          = 22.8[dC]
Unblank_time      = 2[us]
```

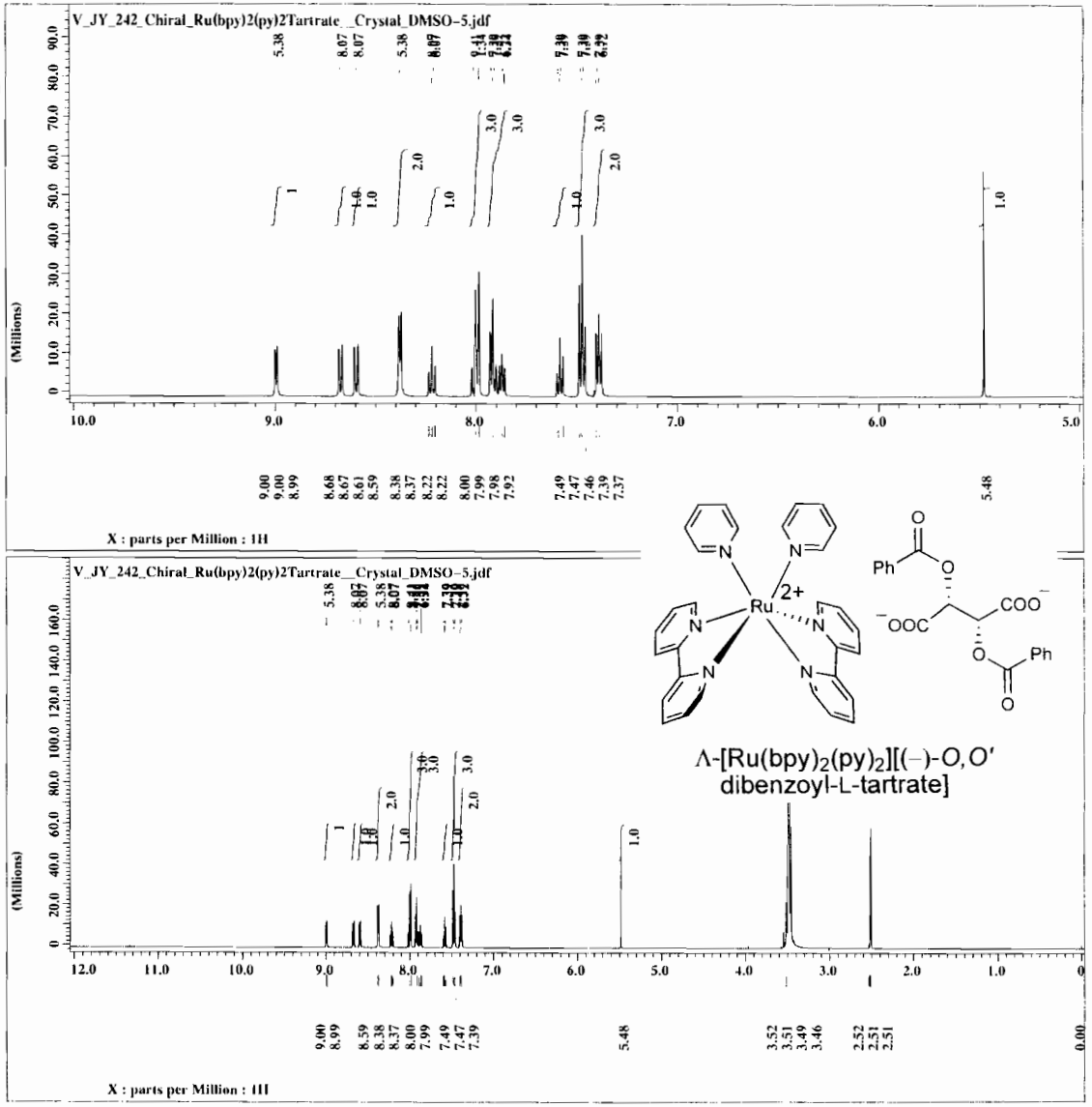

JEOL

```
---- ACQUISITION PARAMETERS ----
File Name        = V_JY_242_Chiral_Ru(bpy
Author           =
Sample ID        = S#185342
Content          = Single Pulse with Broa
Creation Date    =  8-MAR-2004 08:26:58

Revision Date    = 15-MAR-2004 22:25:20
Spec Site        = Eclipse+ 500

Spec Type        = DELTA_NMR
Data Format      = 1D COMPLEX
Dimensions       = X
Dim Title        = 13C
Dim Size         = 32768
Dim Units        = [ppm]
Acq_delay        = 33.8[us]
Changer_sample   = 0
Experiment       = single_pulse_dec
Field_strength   = 11.7473579[T]
Irr90            = 15[us]
Irr90_hi         = 18[us]
Irr90_lo         = 82[us]
Irr_domain       = 1H
Irr_pwidth       = 82[us]
Lock_status      = IDLE
Recvr_gain       = 29
Relaxation_delay= 4[s]
Scans            = 10000
Solvent          = DMSO-D6
Spin_get         = 15[Hz]
Spin_lock_90     = 60[us]
Spin_lock_attn   = 15[dB]
Spin_set         = 15[Hz]
Spin_state       = SPIN ON
Spin_status      = SPIN ON
Temp_get         = 23.5[dC]
Temp_set         = 25[dC]
Temp_state       = TEMP OFF
Temp_status      = TEMP OFF
X90              = 14[us]
X90_hi           = 13[us]
X90_lo           = 53[us]
X_acq_duration   = 1.0420224[s]
X_domain         = 13C
X_freq           = 125.76529768[MHz]
X_offset         = 100[ppm]
X_points         = 32768
X_prescans       = 4
X_pulse          = 4.66666667[us]
X_resolution     = 0.95967227[Hz]
X_sweep          = 31.44654088[kHz]
```

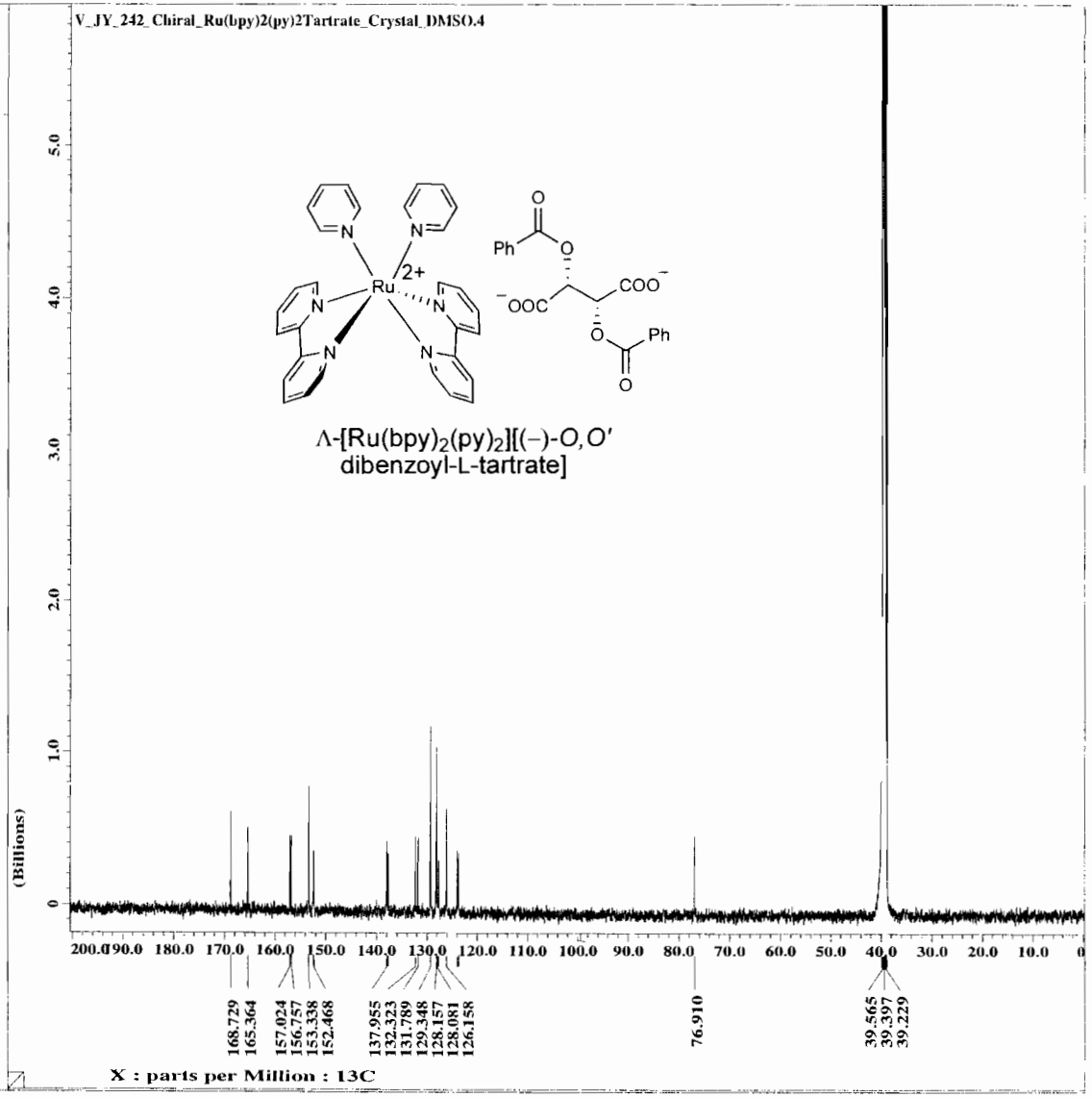

Λ-[Ru(bpy)$_2$(py)$_2$][(−)-*O,O′* dibenzoyl-L-tartrate]

V_JY_242_Chiral_Ru(bpy)2(py)2Tartrate_Crystal_DMSO.4
(Billions)
2.0
1.0
0
Λ-[Ru(bpy)2(py)2][(−)-O,O′
dibenzoyl-L-tartrate]
2+
Ru
N
Ph
O
COO⁻
⁻OOC
169.0
168.0
167.0
166.0
165.0
164.0
163.0
162.0
161.0
160.0
159.0
158.0
157.0
156.0
155.0
154.0
153.0
152.0
168.729
165.364
157.024
156.757
153.338
152.468
152.316
X : parts per Million : 13C
V_JY_242_Chiral_Ru(bpy)2(py)2Tartrate_Crystal_DMSO.4
(Billions)
1.0
0
139.0
138.0
137.0
136.0
135.0
134.0
133.0
132.0
131.0
130.0
129.0
128.0
127.0
126.0
125.0
124.0
123.0
138.039
137.955
137.688
132.323
131.789
129.348
128.157
128.081
127.745
126.158
123.998
123.777
X : parts per Million : 13C

APPENDIX 27

^{1}H NMR SPECTRA OF

[Ru(bpy)$_2$(*R*,*R*-dach)](PF$_6$)$_2$ **30**

JEOL

```
Filename          = VIII_JY_75_Ru(bpy)2(d
Author            = delta
Experiment        = single_pulse.exp
Sample_id         = S#448377
Solvent           = ACETONITRILE-D3
Creation_time     =  4-OCT-2005 13:35:38
Revision_time     = 16-OCT-2005 22:10:30
Current time      = 16-OCT-2005 22:10:33

Content           = Single Pulse Experime
Data_format       = 1D COMPLEX
Dim_size          = 16384
Dim_title         = 1H
Dim_units         = [ppm]
Dimensions        = X
Site              = Eclipse+ 500
Spectrometer      = DELTA_NMR

Field_strength    = 11.7473579[T] (500[MH
X_acq_duration    = 1.4876672[s]
X_domain          = 1H
X_freq            = 500.15991521[MHz]
X_offset          = 8[ppm]
X_points          = 16384
X_prescans        = 0
X_resolution      = 0.67219335[Hz]
X_sweep           = 11.01321586[kHz]
Clipped           = FALSE
Mod_return        = 1
Scans             = 125
Total_scans       = 125

X_90_width        = 18.5[us]
X_acq_time        = 1.4876672[s]
X_angle           = 45[deg]
X_pulse           = 9.25[us]
Initial_wait      = 1[s]
Phase_preset      = 3[us]
Recvr_gain        = 20
Relaxation_delay  = 1[s]
Temp_get          = 25.6[dC]
Unblank_time      = 2[us]
```

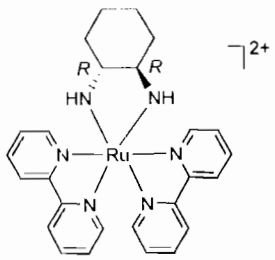

$[Ru(bpy)_2(R,R\text{-dach})]^{2+}$

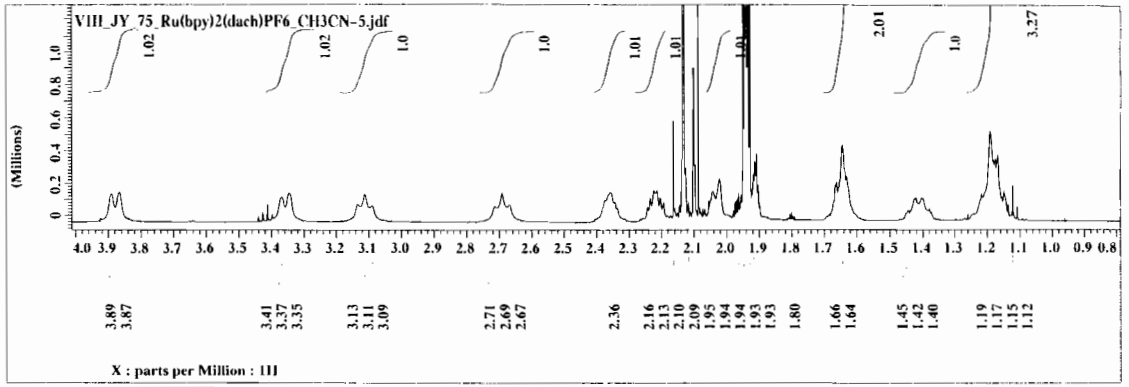

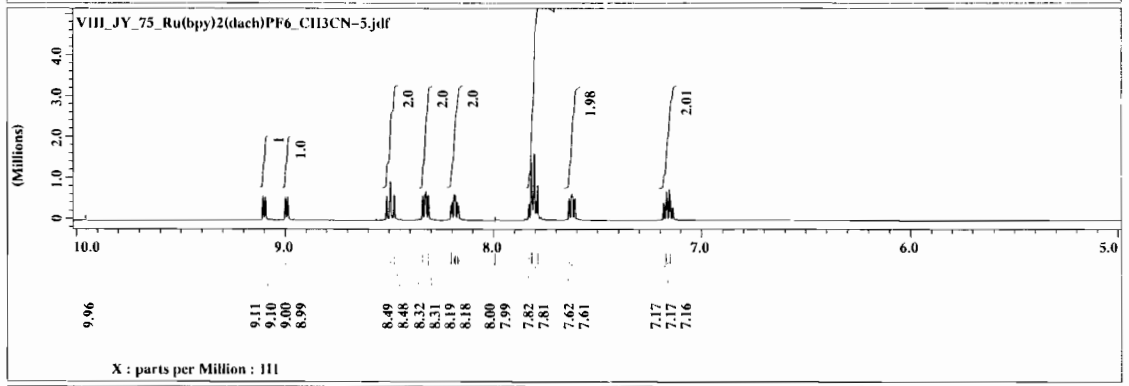

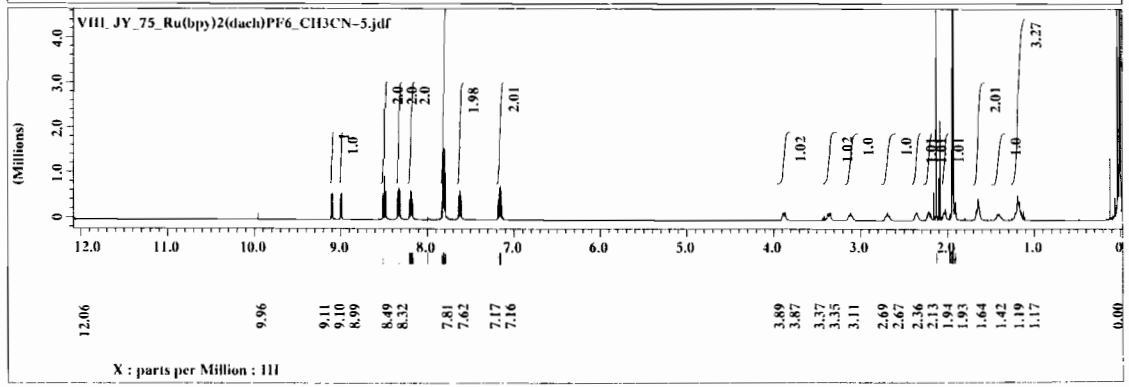

APPENDIX 28

^{1}H NMR SPECTRA OF

Λ-[Ru(bpy)$_2$(*R*,*R*-dach)](PF$_6$)$_2$ **30a**

JEOL

```
Filename          = VIII_JY_79_lamdaRu(bp
Author            = delta
Experiment        = single_pulse.exp
Sample_id         = S#407896
Solvent           = ACETONITRILE-D3
Creation_time     = 17-SEP-2005 12:27:50
Revision_time     = 16-OCT-2005 22:07:51
Current_time      = 16-OCT-2005 22:07:56

Content           = Single Pulse Experime
Data_format       = 1D COMPLEX
Dim_size          = 16384
Dim_title         = 1H
Dim_units         = [ppm]
Dimensions        = X
Site              = Eclipse+ 500
Spectrometer      = DELTA_NMR

Field_strength    = 11.7473579[T] (500[MH
X_acq_duration    = 1.4876672[s]
X_domain          = 1H
X_freq            = 500.15991521[MHz]
X_offset          = 8[ppm]
X_points          = 16384
X_prescans        = 0
X_resolution      = 0.67219335[Hz]
X_sweep           = 11.01321586[kHz]
Clipped           = FALSE
Mod_return        = 1
Scans             = 296
Total_scans       = 296

X_90_width        = 18.5[us]
X_acq_time        = 1.4876672[s]
X_angle           = 45[deg]
X_pulse           = 9.25[us]
Initial_wait      = 1[s]
Phase_preset      = 3[us]
Recvr_gain        = 20
Relaxation_delay  = 1[s]
Temp_get          = 25.9[dC]
Unblank_time      = 2[us]
```

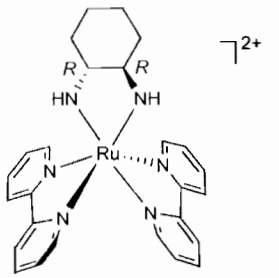

Λ-[Ru(bpy)$_2$(*R*,*R*-dach)]$^{2+}$

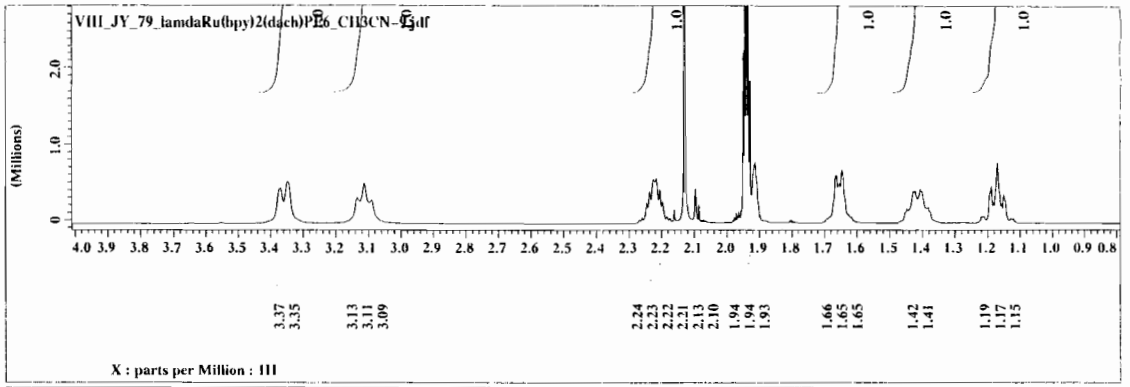

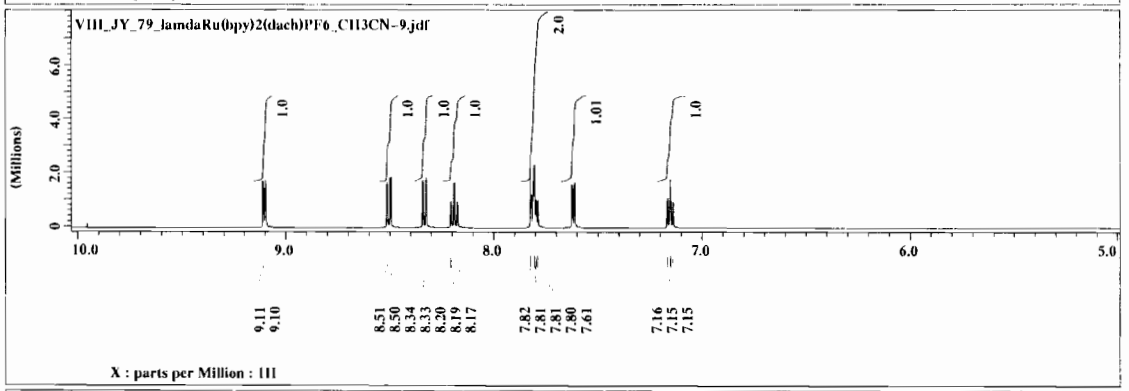

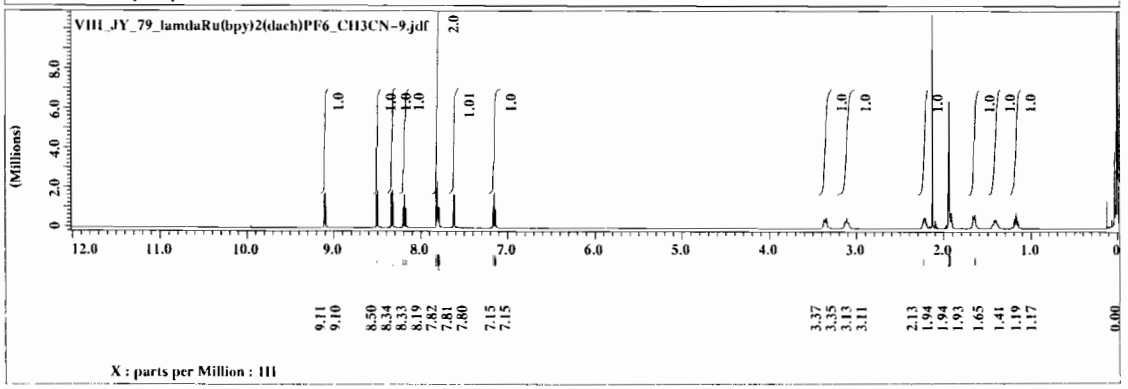

APPENDIX 29

^{1}H NMR SPECTRA OF

(–)-*O*,*O*′-Dibenzoyl-L-tartaric acid

JEOL

```
Filename          = V_JY_203_Dibenzoyl_L_
Experiment        = single pulse.exp
Sample_id         = S#240615
Solvent           = DMSO-D6
Creation_time     =  2-FEB-2004 19:39:13
Revision_time     = 16-OCT-2005 11:30:05
Current_time      = 16-OCT-2005 11:30:35

Content           = Single Pulse Experime
Data_format       = 1D COMPLEX
Dim_size          = 16384
Dim_title         = 1H
Dim_units         = [ppm]
Dimensions        = X
Site              = Eclipse+ 500
Spectrometer      = DELTA_NMR

Field_strength    = 11.7473579[T] (500[MH
X_acq_duration    = 1.4876672[s]
X_domain          = 1H
X_freq            = 500.15991521[MHz]
X_offset          = 8[ppm]
X_points          = 16384
X_prescans        = 0
X_resolution      = 0.67219335[Hz]
X_sweep           = 11.01321586[kHz]
Mod_return        = 1
Scans             = 50

X_90_width        = 15[us]
X_acq_time        = 1.4876672[s]
X_angle           = 45[deg]
X_pulse           = 7.5[us]
Initial_wait      = 1[s]
Phase_preset      = 3[us]
Recvr_gain        = 23
Relaxation_delay  = 1[s]
Temp_get          = 22[dC]
Unblank_time      = 2[us]
```

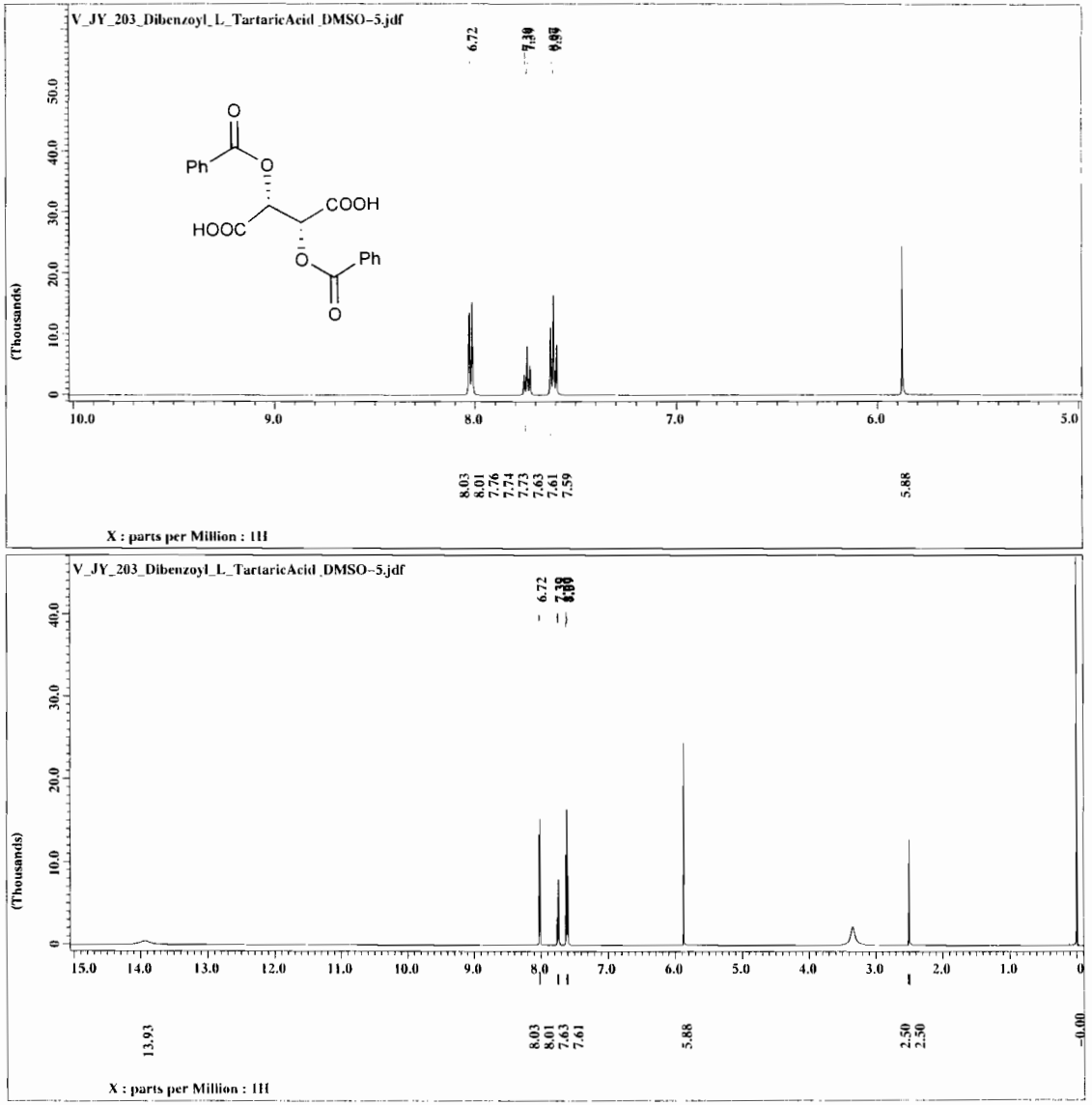

APPENDIX 30

TGA SPECTRA OF Lupasol and crosslinked

lupasol series **33–39**

Sample: LupHighM.W
Size: 3.3430 mg
Method: Ramp

TGA

File: C:...\ll_JY_LupHighMW.001
Operator: Jun
Run Date: 29-Jan-02 18:12

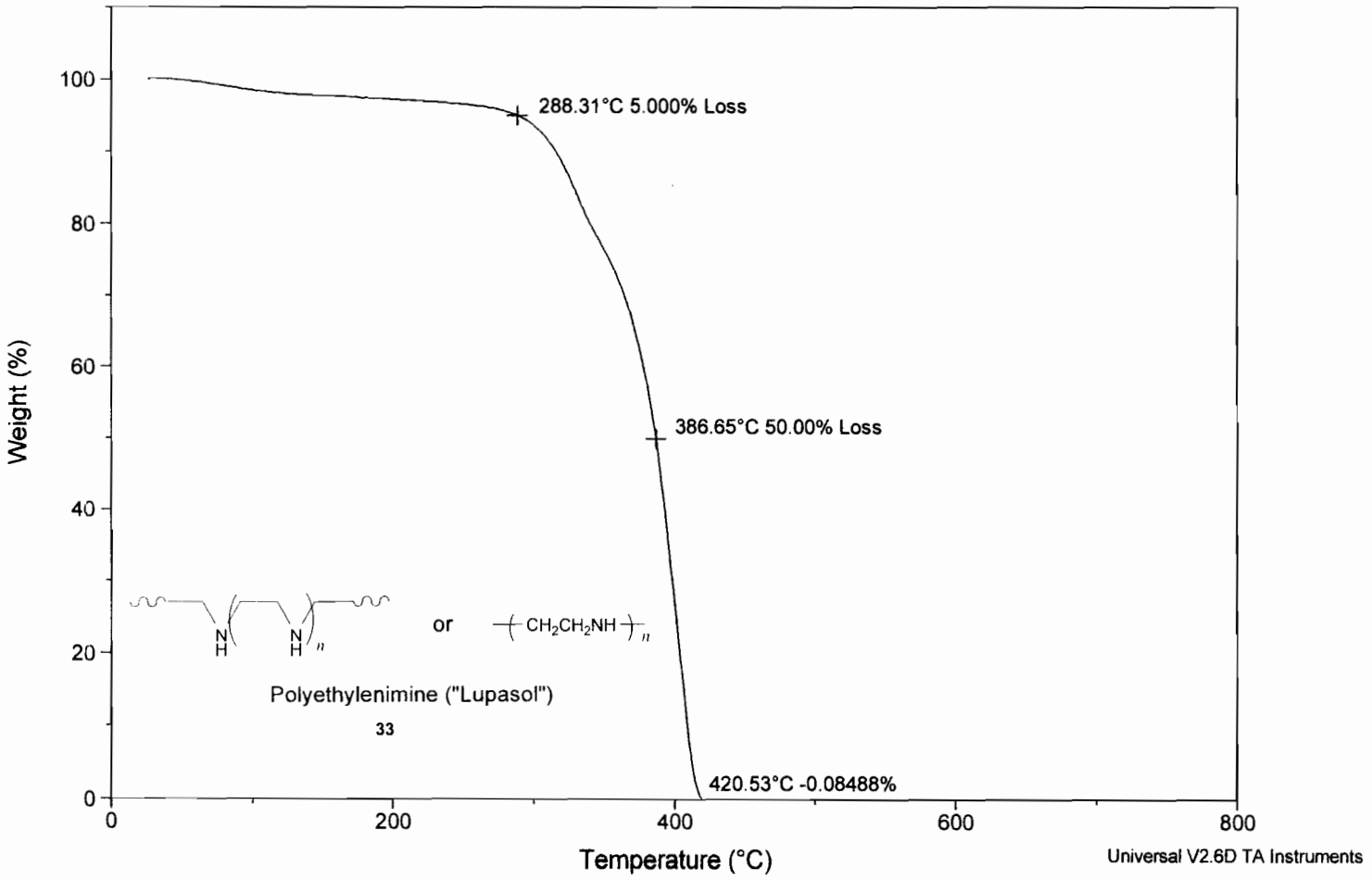

Sample: II_JY_145
Size: 10.7210 mg
Method: Ramp 5°C/min to 800°C
Comment: 5%PD_LUP

TGA

File: C:...\II_JY_145_5%PD_2.001
Operator: Jun
Run Date: 29-Aug-02 16:18

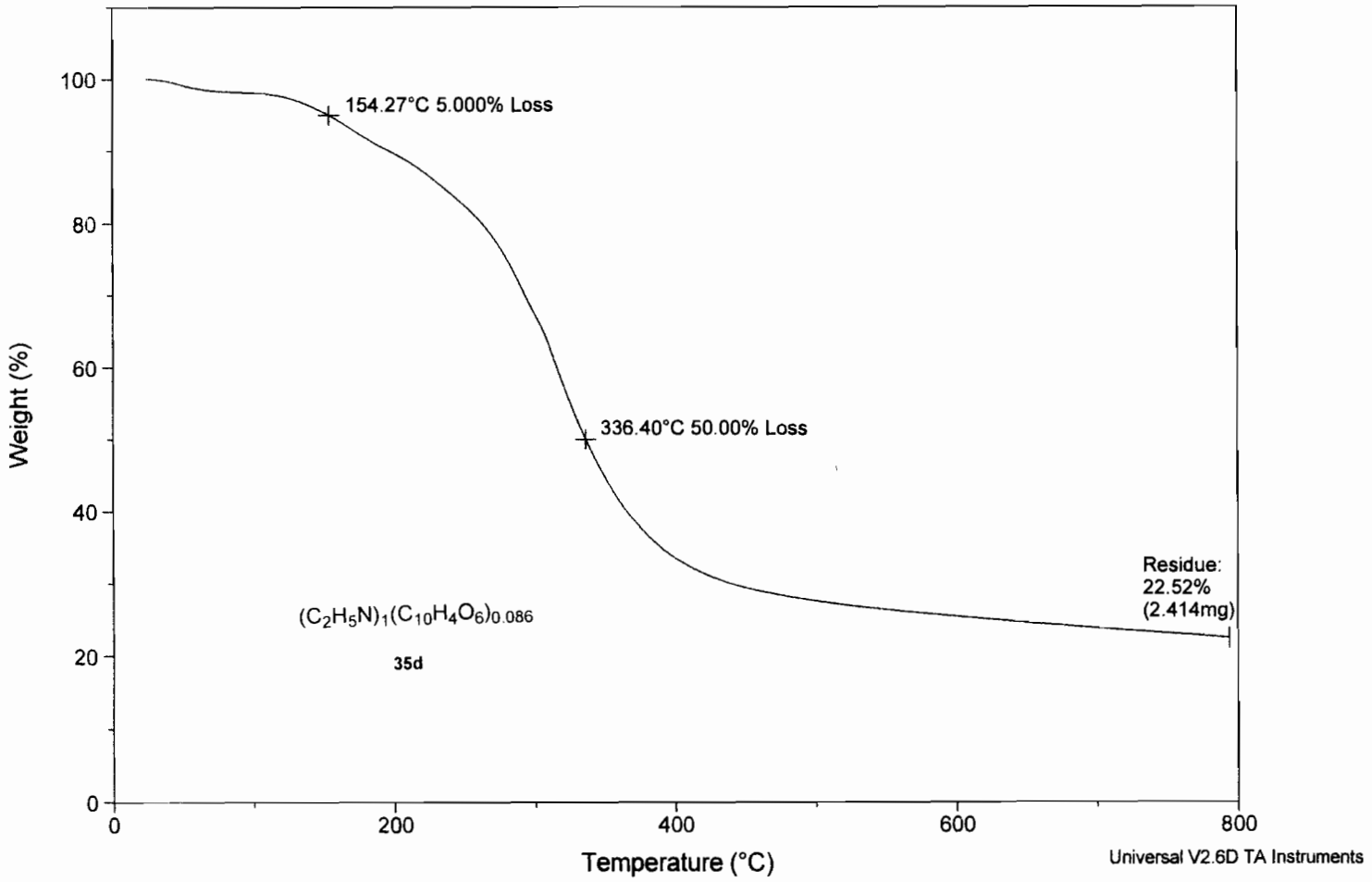

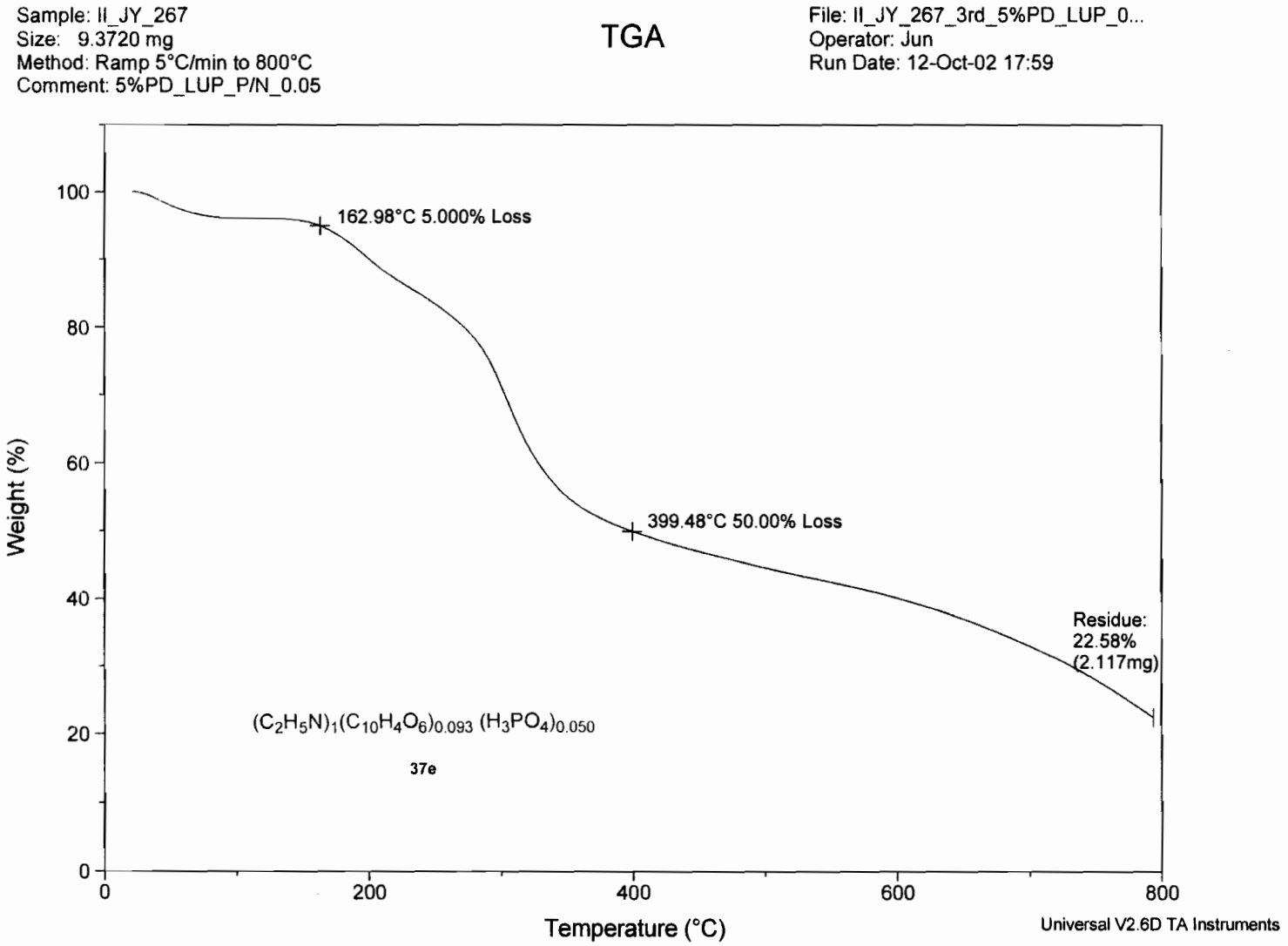
Sample: II_JY_267
Size: 9.3720 mg
Method: Ramp 5°C/min to 800°C
Comment: 5%PD_LUP_P/N_0.05
TGA
File: II_JY_267_3rd_5%PD_LUP_0...
Operator: Jun
Run Date: 12-Oct-02 17:59
162.98°C 5.000% Loss
399.48°C 50.00% Loss
Residue:
22.58%
(2.117mg)
$(C_2H_5N)_1(C_{10}H_4O_6)_{0.093}$ $(H_3PO_4)_{0.050}$
37e
Weight (%)
Temperature (°C)
Universal V2.6D TA Instruments

Sample: III_JY_15
Size: 10.3550 mg
Method: Ramp 5°C/min to 800°C
Comment: 5%PD_LUP_2.13%H3PO4_30min

TGA

File: III_JY_15_5%PD_LUP_2.13%...
Operator: Jun
Run Date: 7-Oct-02 17:39

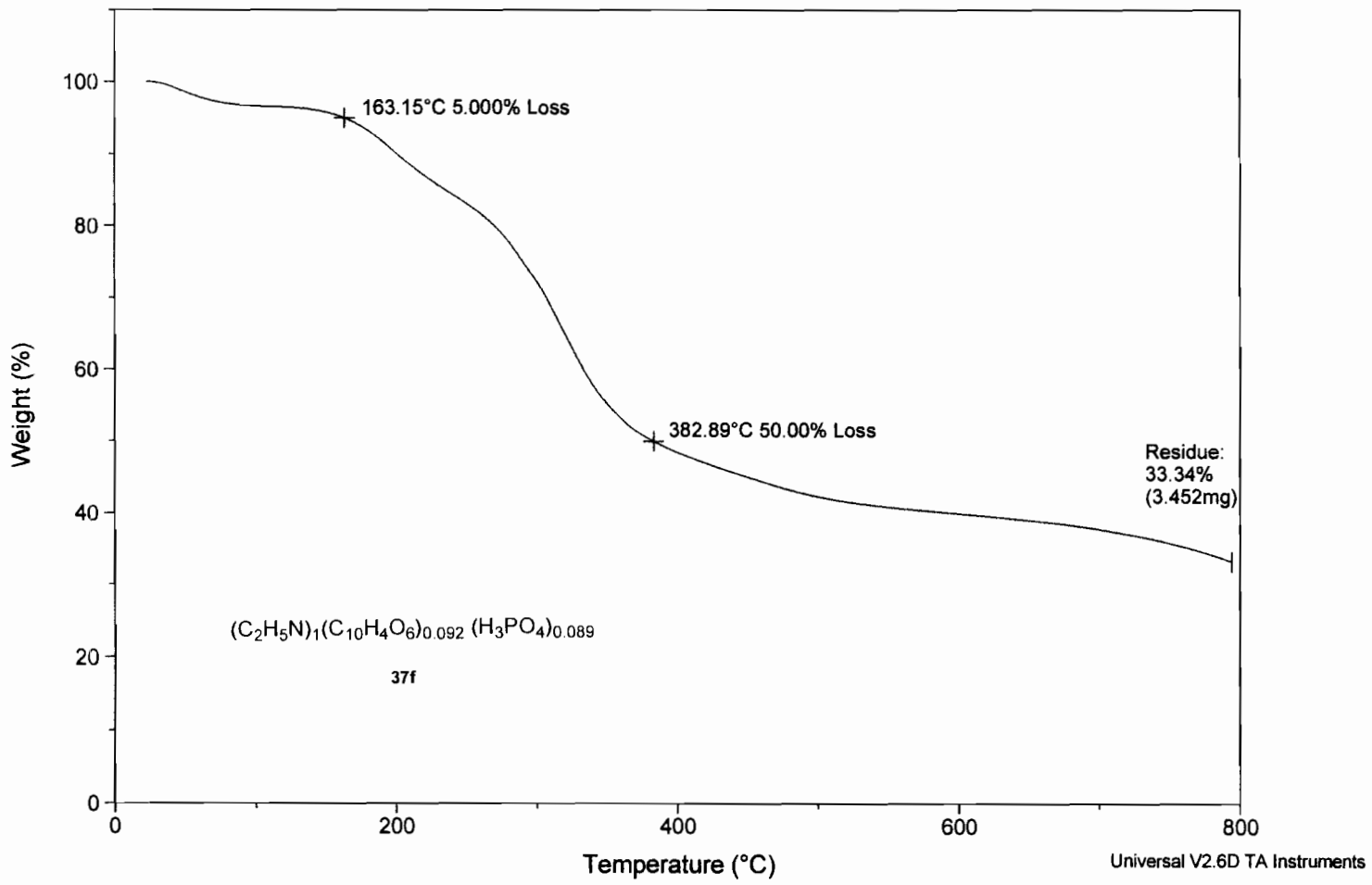

Sample: III_JY_11
Size: 9.3520 mg
Method: Ramp 5°C/min to 800°C
Comment: 5%PD_LUP_4.25%H3PO4_0.5hr

TGA

File: III_JY_11_5%PD_4.25%H3PO...
Operator: Jun
Run Date: 25-Sep-02 17:38

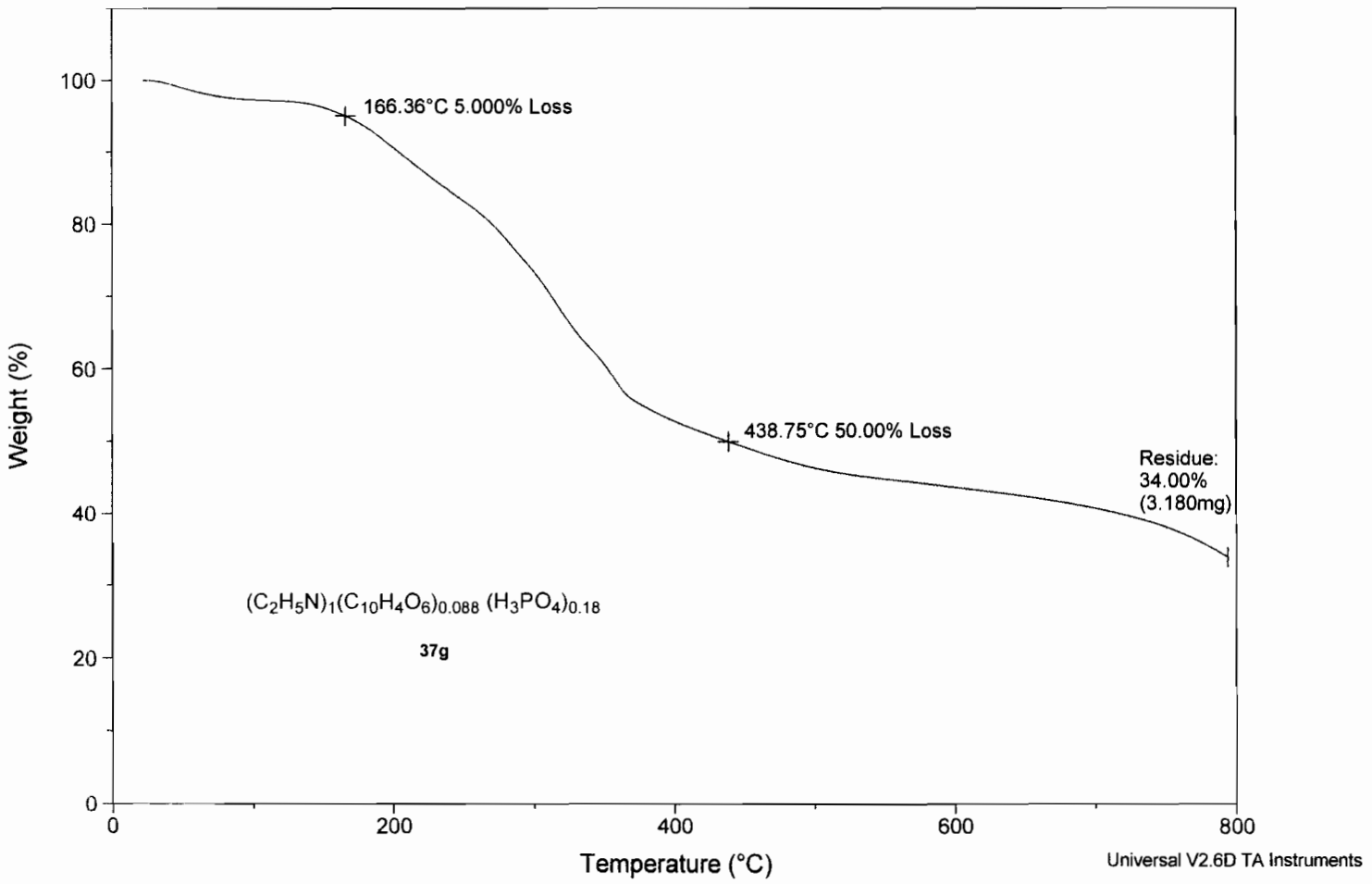

Sample: II_JY_161_Lup_5%PD_P_Dry75°C
Size: 10.2990 mg
Method: Ramp 5°C /min to 800°C
Comment: 8.5%P

TGA

File: C:...\II_JY_161_5%PD_P_Dry75degC.001
Operator: Jun
Run Date: 14-May-2002 18:47
Instrument: 2050 TGA V5.4A

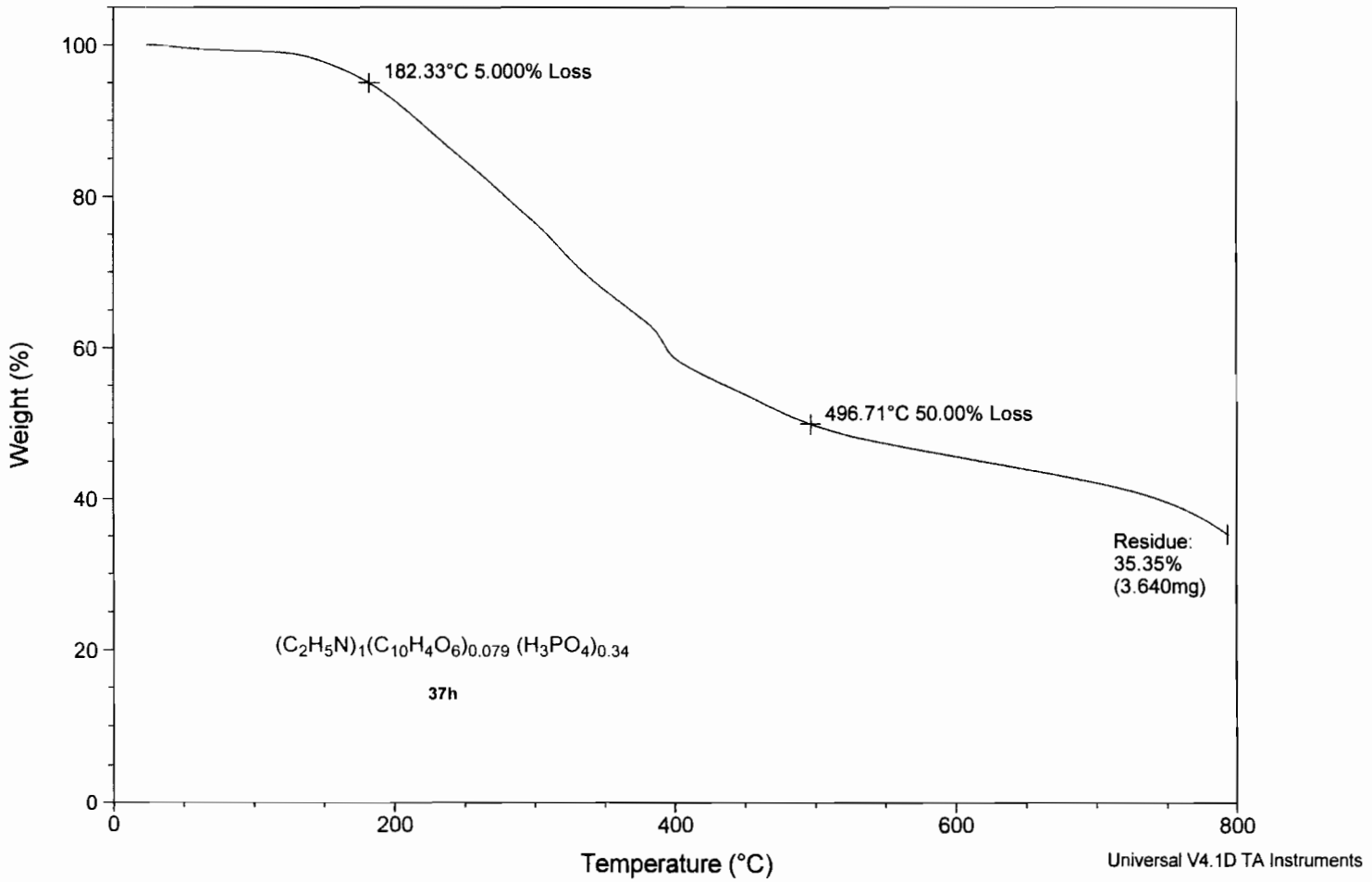

Universal V4.1D TA Instruments

Sample: III_JY_22
Size: 9.2010 mg
Method: Ramp 5°C/min to 800°C
Comment: 5%PD_LUP_12.75%H3PO4_3rd

TGA

File: III_JY_22_5%PD_LUP_12.75...
Operator: Jun
Run Date: 16-Oct-02 11:26

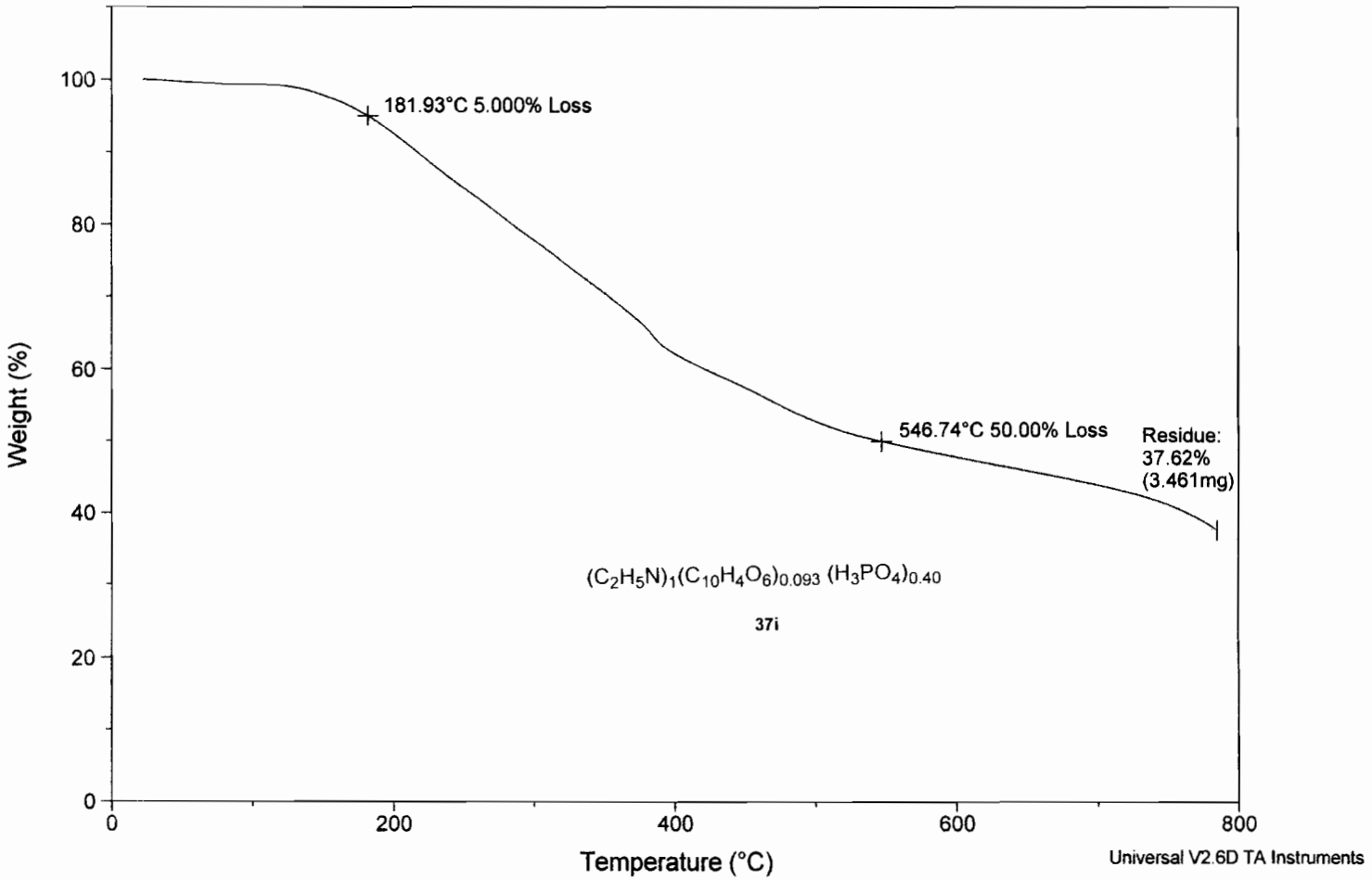

Sample: III_JY_25
Size: 9.8860 mg
Method: Ramp 5°C/min to 800°C
Comment: 5%PD_LUP_17%H3PO4_30min

TGA

File: III_JY_25_5%PD_LUP_17%H3...
Operator: Jun
Run Date: 4-Oct-02 17:50

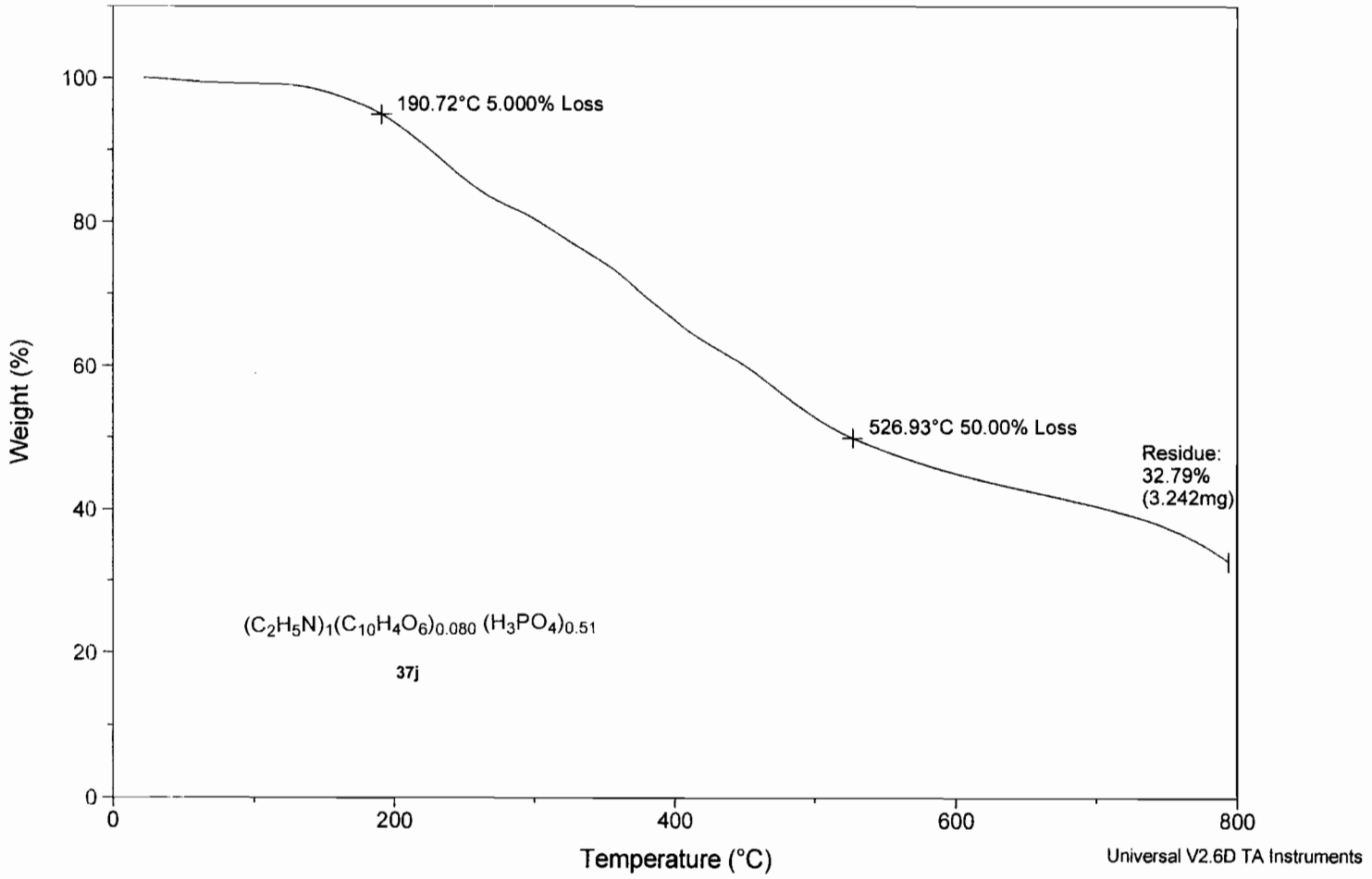

Universal V2.6D TA Instruments

Sample: II_JY_125
Size: 13.6590 mg
Method: Ramp 5degC/min to 800C
Comment:

TGA

File: II_JY_125
Operator: Jun
Run Date: 26-Mar-02 13:43

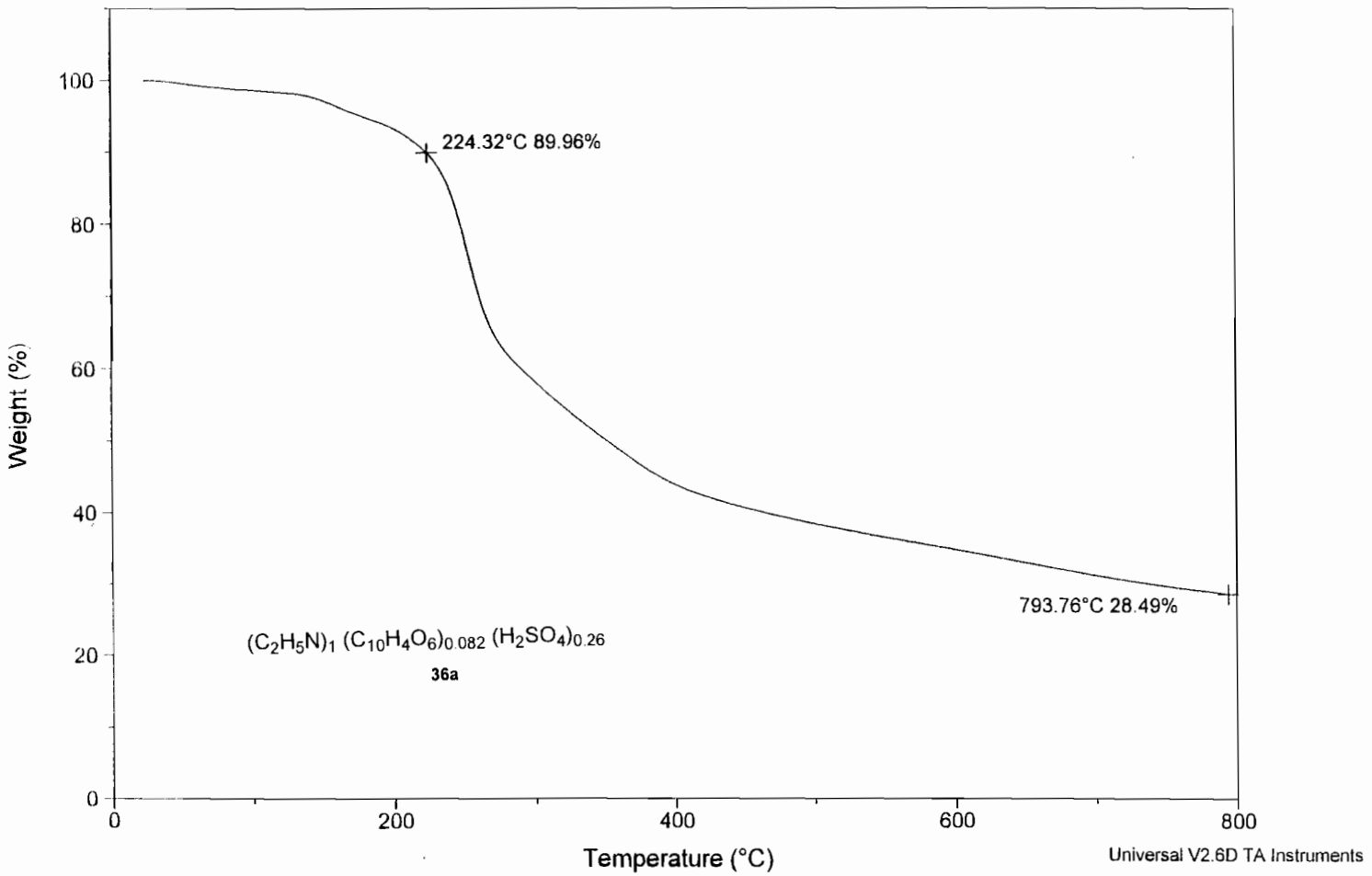

Sample: II_JY_153
Size: 14.0240 mg
Method: Ramp 5°C /min to 800°C
Comment: Lup_5%PD_H2SO4_Dryat75°C

TGA

File: C:...\II_JY_153-5%PD-H2SO4-Dry75degC-2
Operator: Jun
Run Date: 08-May-2002 10:44
Instrument: 2050 TGA V5.4A

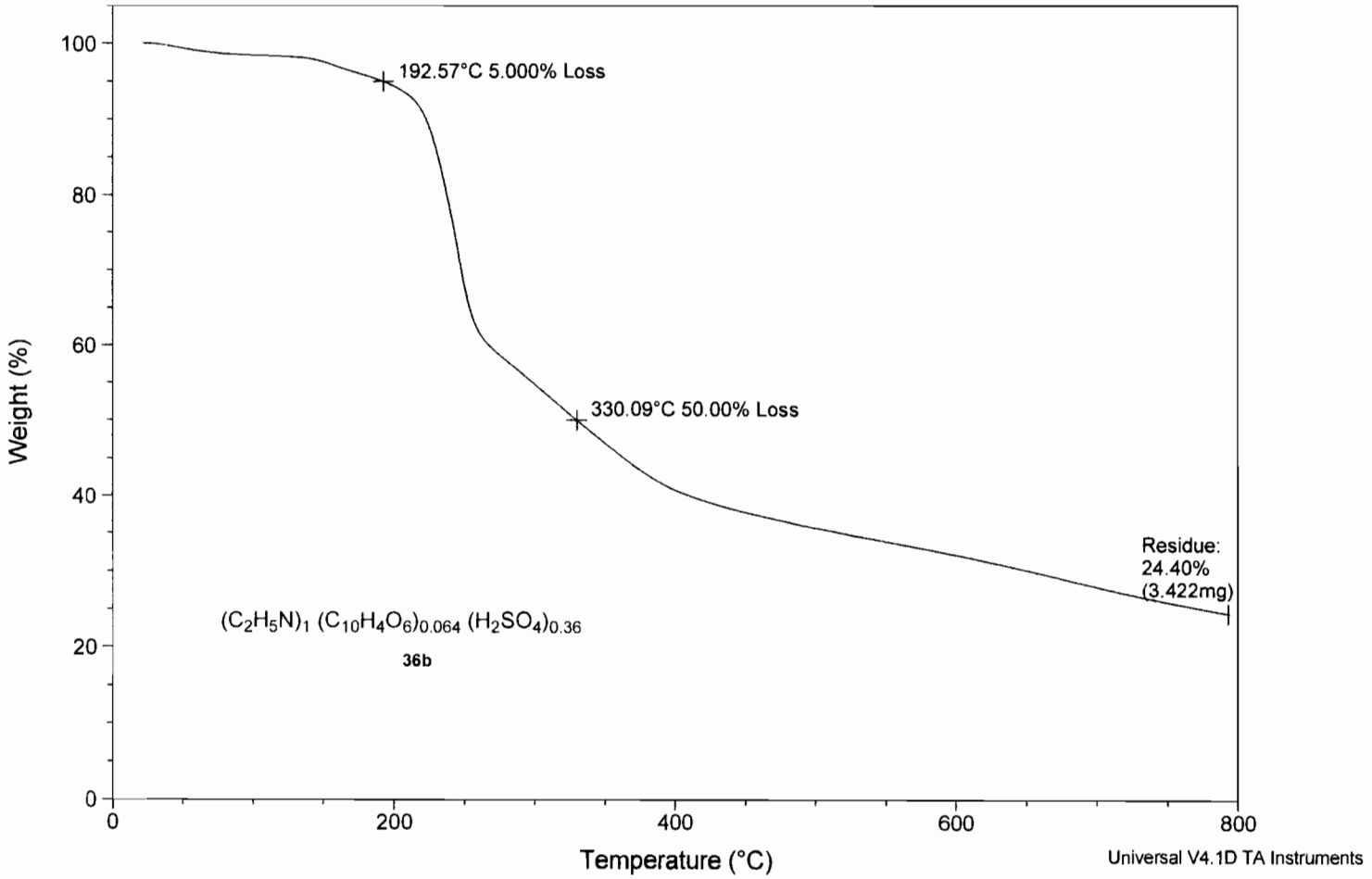

Sample: II_JY_205
Size: 10.3900 mg
Method: Ramp 5°C/min to 800°C
Comment: 10%PD_LUP_10%H2SO4

TGA

File: II_JY_205_10%PD_10%H2SO4...
Operator: Jun
Run Date: 28-Aug-02 10:52

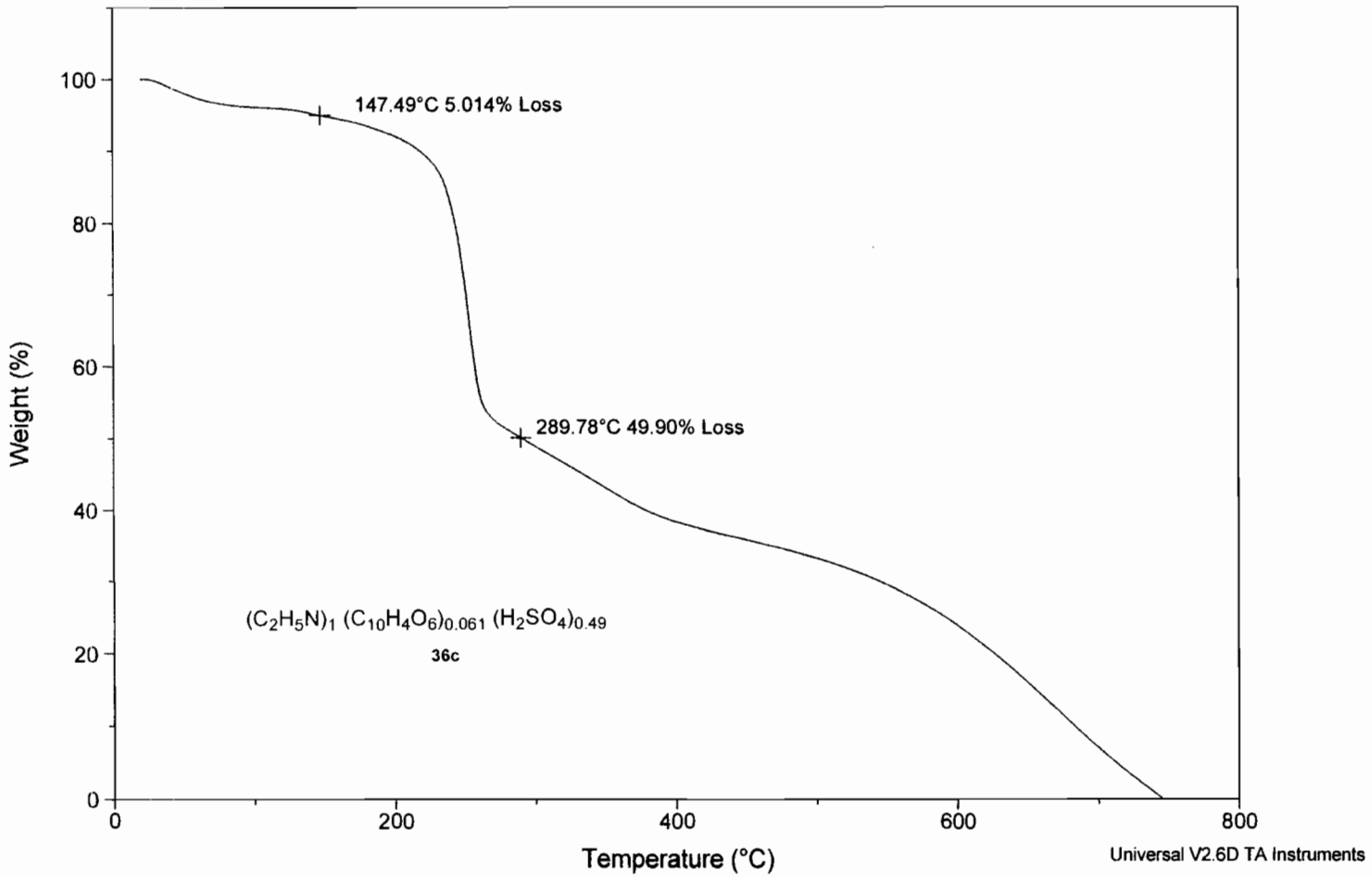

Sample: MDPE Powder
Size: 12.9480 mg
Method: 10.00 °C/min RT to 600°C
Comment: Aldrich 05/02

TGA

File: C:...\MDPE\MDPE powder.001
Operator: Jun
Run Date: 26-Jul-02 16:56

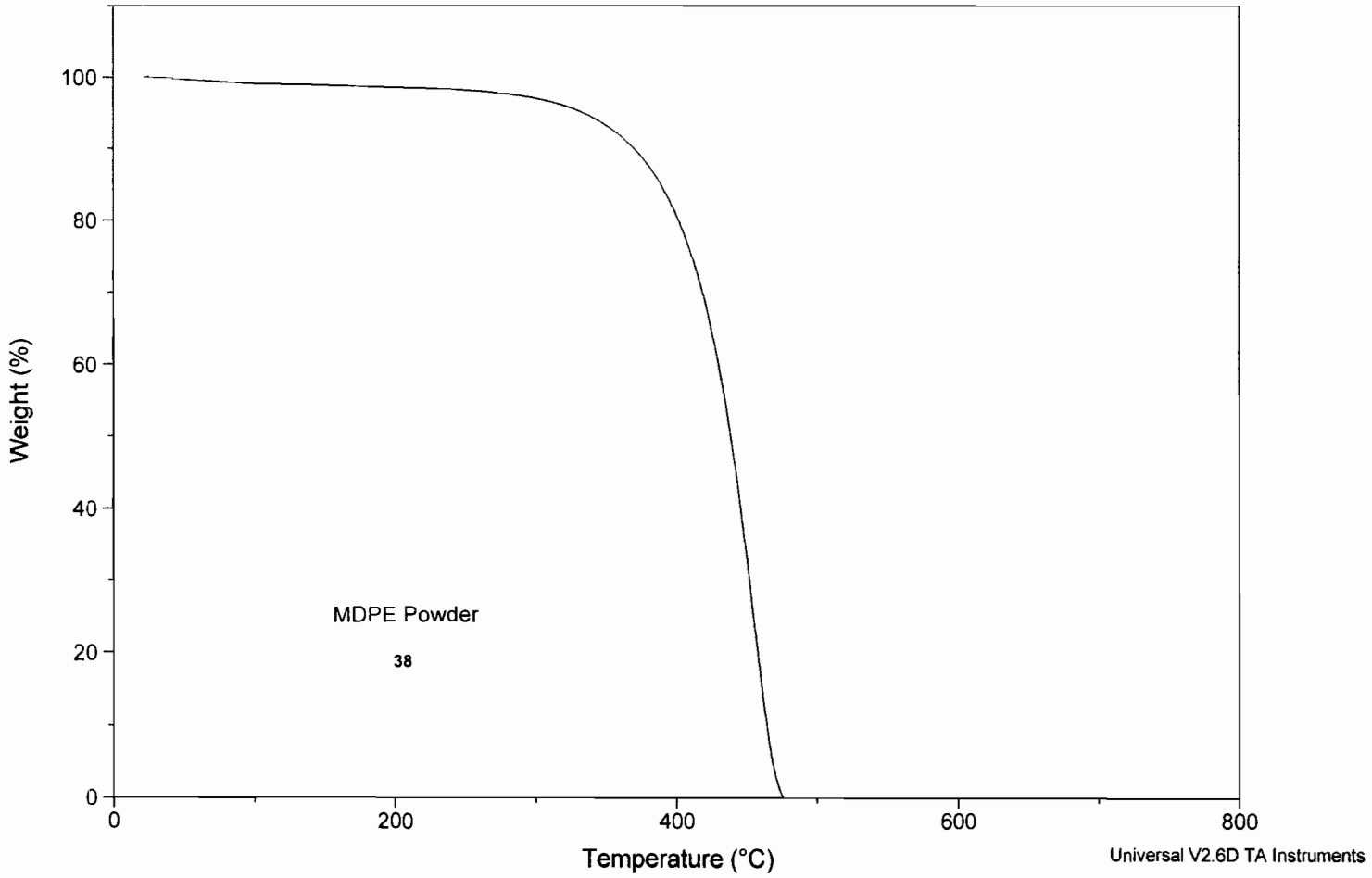

Sample: II_JY_250
Size: 14.0410 mg
Method: Ramp 5°C/min to 800°C
Comment: 54.5%FR_II_JY_151P

TGA

File: C:...\Jun\MDPE\II_JY_250_54.5%FR_JY151P
Operator: Jun
Run Date: 30-Jul-2002 11:49
Instrument: 2050 TGA V5.4A

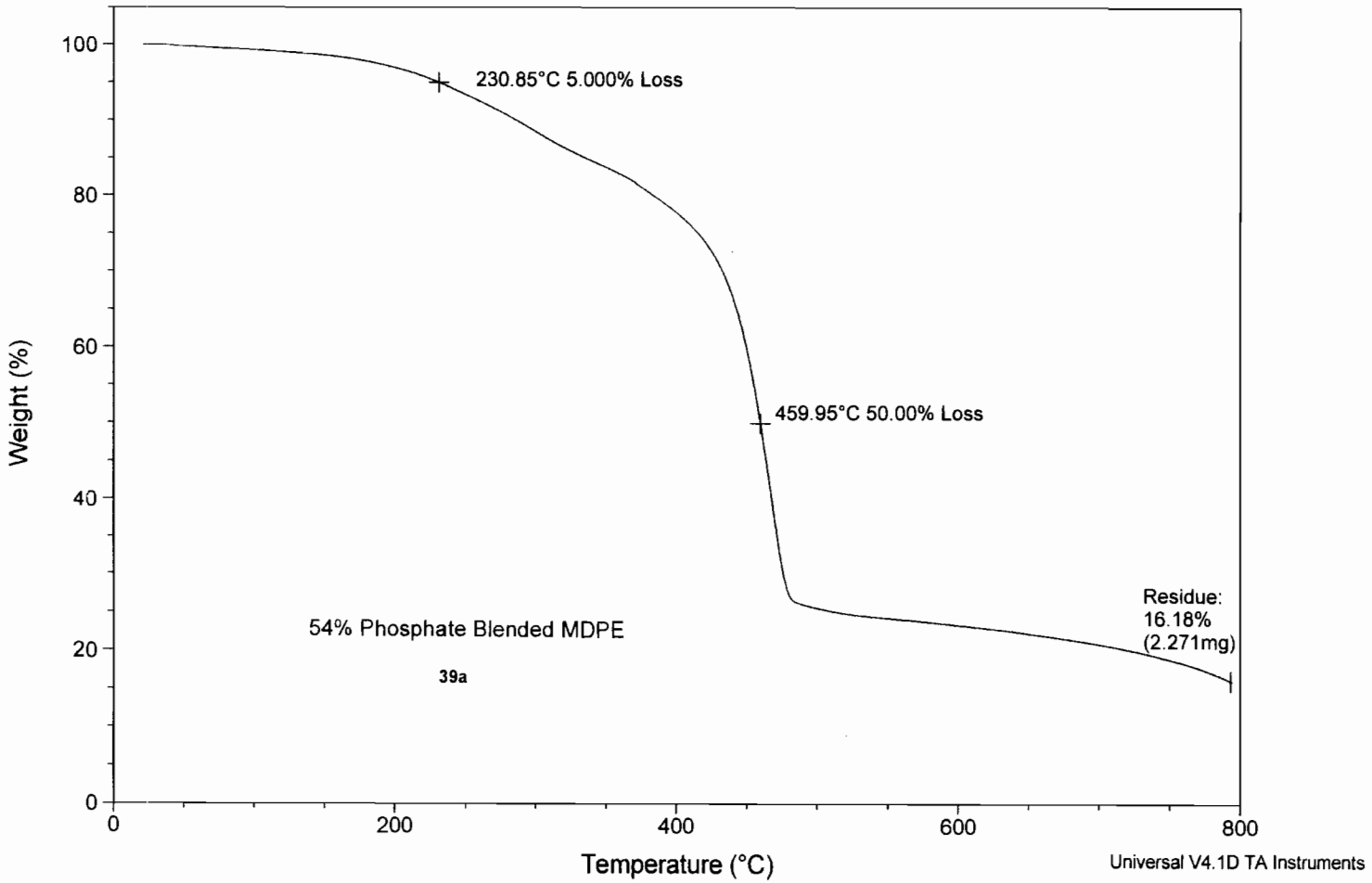

Universal V4.1D TA Instruments

Sample: II_JY_251
Size: 16.4450 mg
Method: Ramp 5°C/min to 800°C
Comment: 61.5%FR_II_JY_151P

TGA

File: C:...\Jun\MDPE\II_JY_251_61.5%FR_JY151P
Operator: Jun
Run Date: 29-Jul-2002 14:03
Instrument: 2050 TGA V5.4A

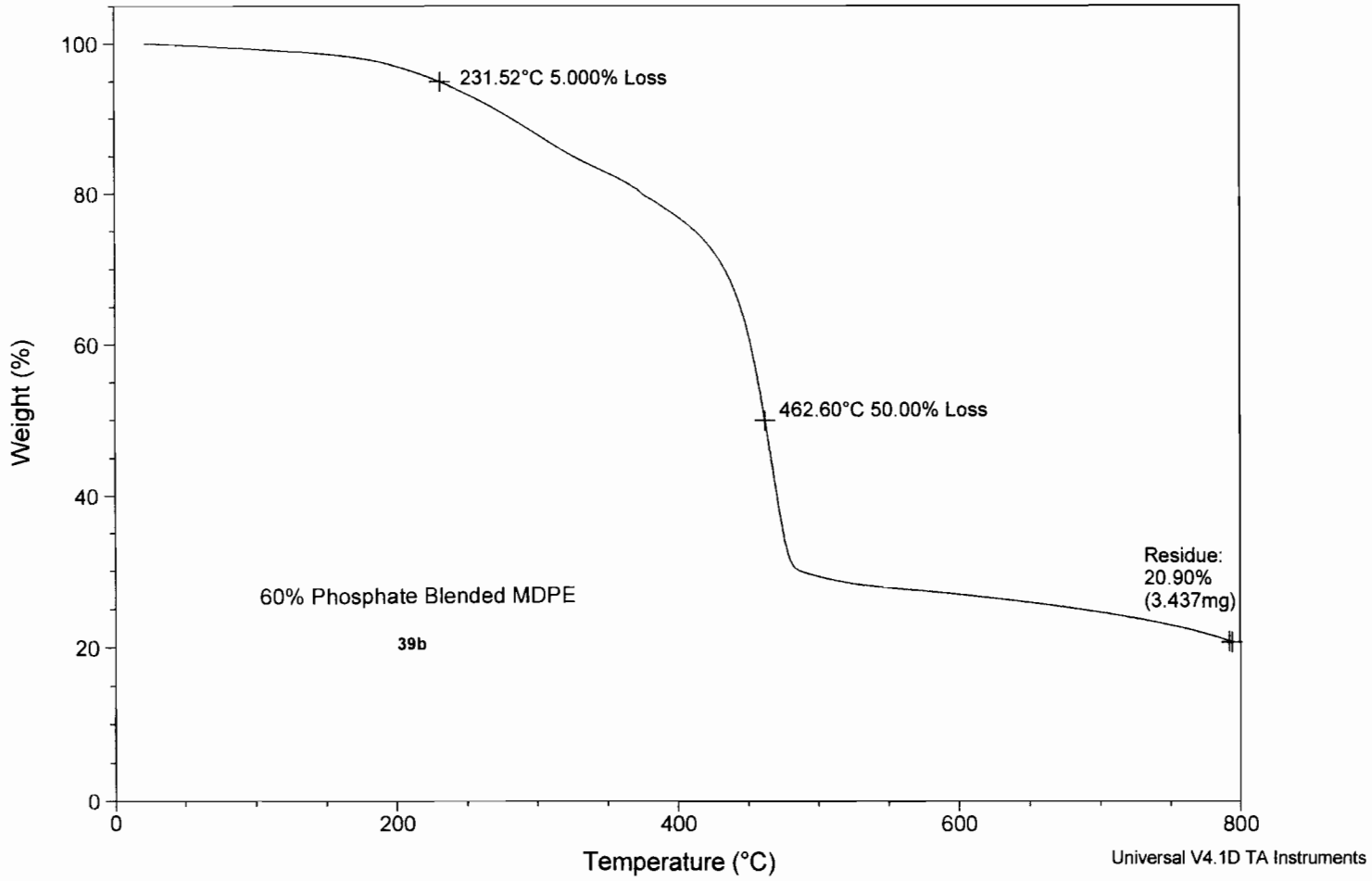

APPENDIX 31

FTIR SPECTRA OF Lupasol and

crosslinked lupasol series **33–37**

Transmittance [%]
100
80
60
40
20
BRUKER
3902.29
3870.16
3853.27
3838.42
3820.30
3801.40
3750.37
3735.13
3711.20
3689.17
3674.54
3648.80
3281.70
3281.70
2939.58
2820.76
2820.76
2339.16
1771.75
1653.15
1599.07
1599.07
1541.47
1458.16
1458.16
1355.15
1296.74
1296.74
1118.82
1118.82
1050.17
920.15
867.55
776.70
776.70
448.51
431.52
421.37
421.37
404.76
404.76
Wavenumber cm-1
4000
3500
3000
2500
2000
1500
1000
500
D:\OPUS_NT\DATA\Jun\Lupasol2.0
Lupasol2
Viscous Liquid
10/11/2002
Polyethylenimine ("Lupasol")
33
or

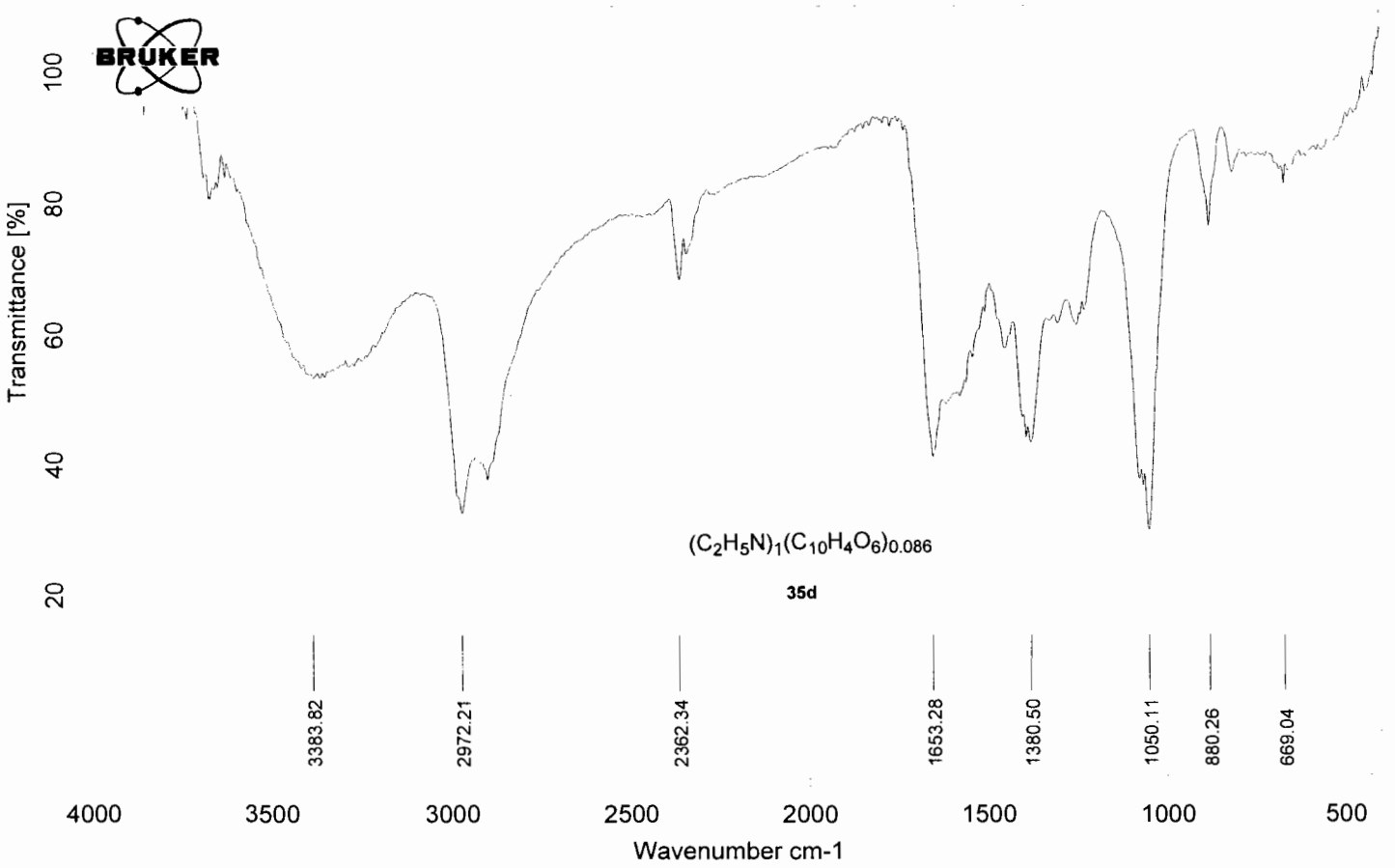

D:\OPUS_NT\DATA\Jun\II_JY_145.0	II_JY_145	Pellet	5%	16/10/2002

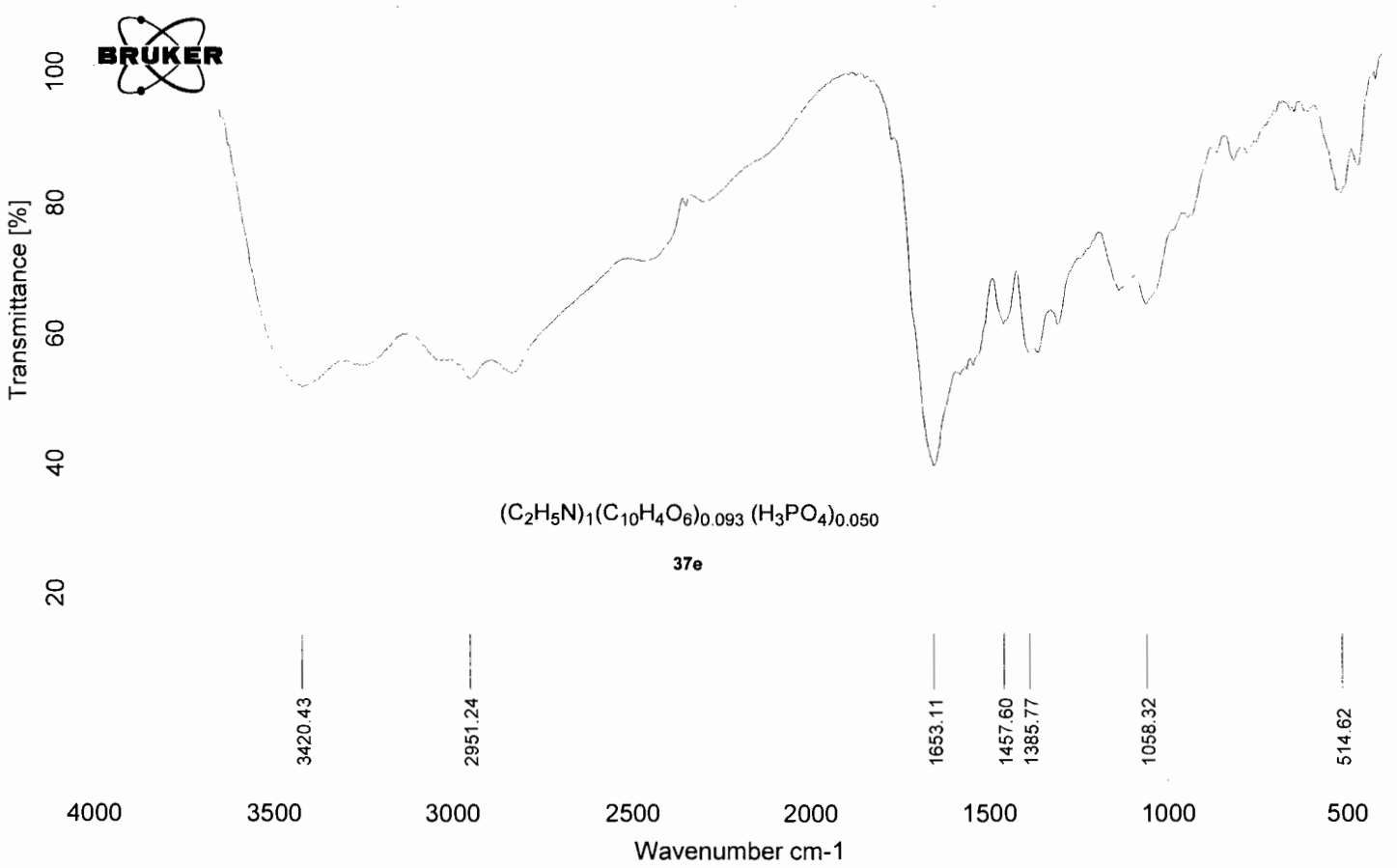

D:\OPUS_NT\DATA\Jun\II_JY_267.1	II_JY_267	Pellet	5%	16/10/2002

Transmittance [%]
0
20
40
60
80
100
4000
3500
3000
2500
2000
1500
1000
500
Wavenumber cm-1
3410.19
2954.52
1653.74
1457.11
1387.56
1057.63
511.70
$(C_2H_5N)_1(C_{10}H_4O_6)_{0.092}(H_3PO_4)_{0.089}$
37f

Transmittance [%]
110
100
90
80
70
60
50
40
4000
3500
3000
2500
2000
1500
1000
500
Wavenumber cm-1
3020.94
1653.06
1395.11
941.86
502.88
$(C_2H_5N)_1(C_{10}H_4O_6)_{0.088}(H_3PO_4)_{0.18}$
37g

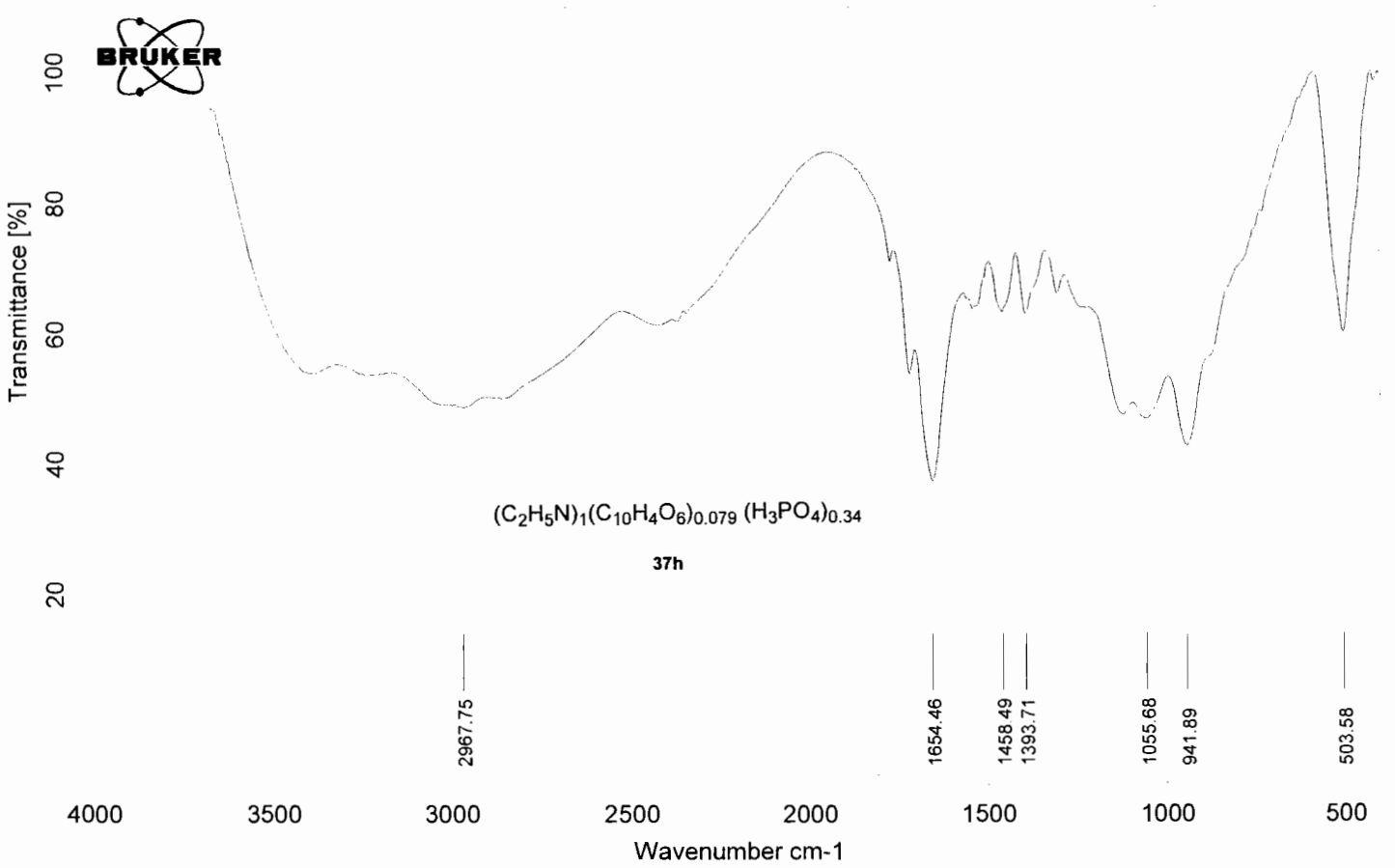

D:\OPUS_NT\DATA\Jun\II_JY_161.1	II_JY_161	Pellet	5% [illegible]	14/10/2002

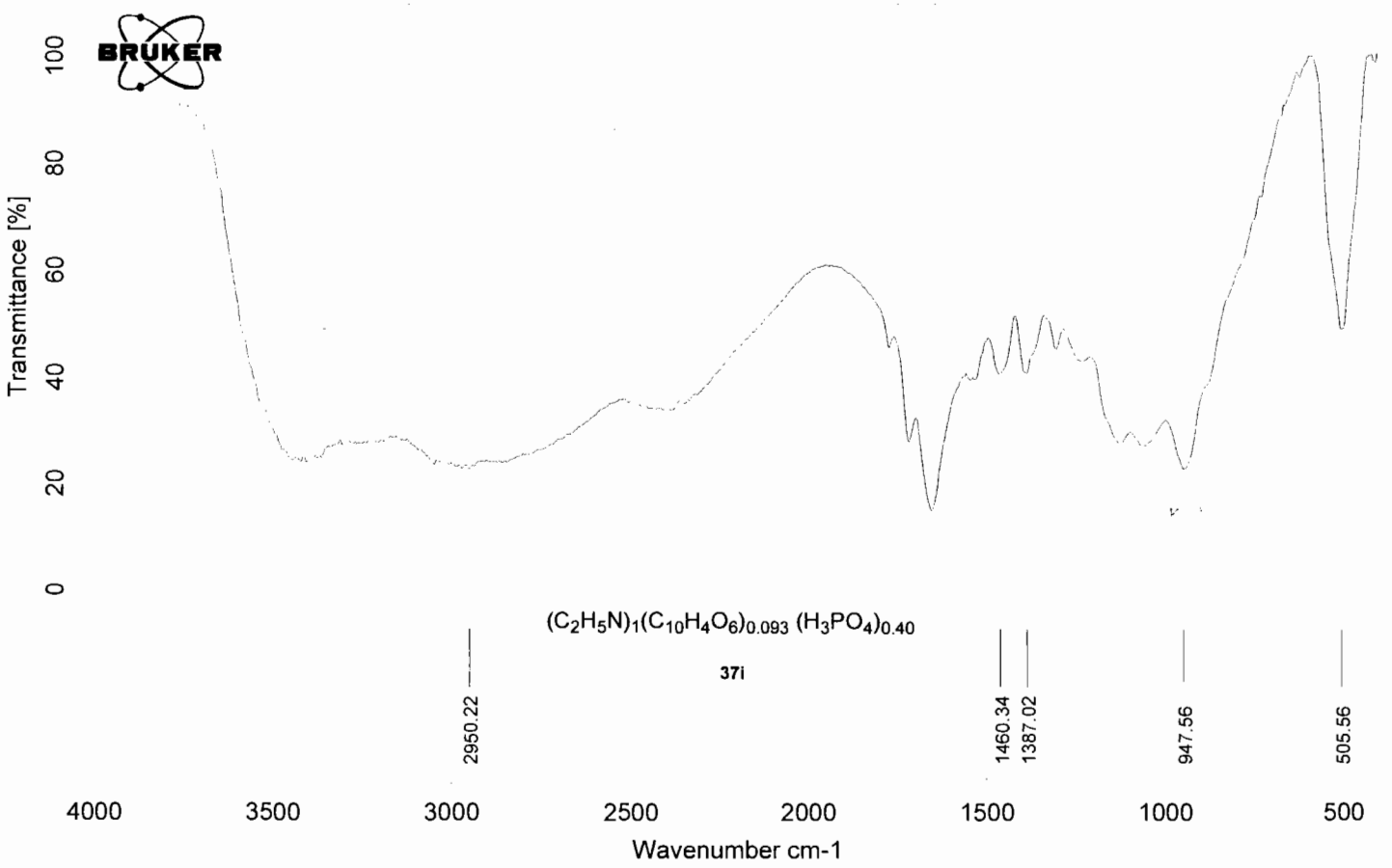
BRUKER
Transmittance [%]
0
20
40
60
80
100
$(C_2H_5N)_1(C_{10}H_4O_6)_{0.093}$ $(H_3PO_4)_{0.40}$
37i
2950.22
1460.34
1387.02
947.56
505.56
4000
3500
3000
2500
2000
1500
1000
500
Wavenumber cm-1

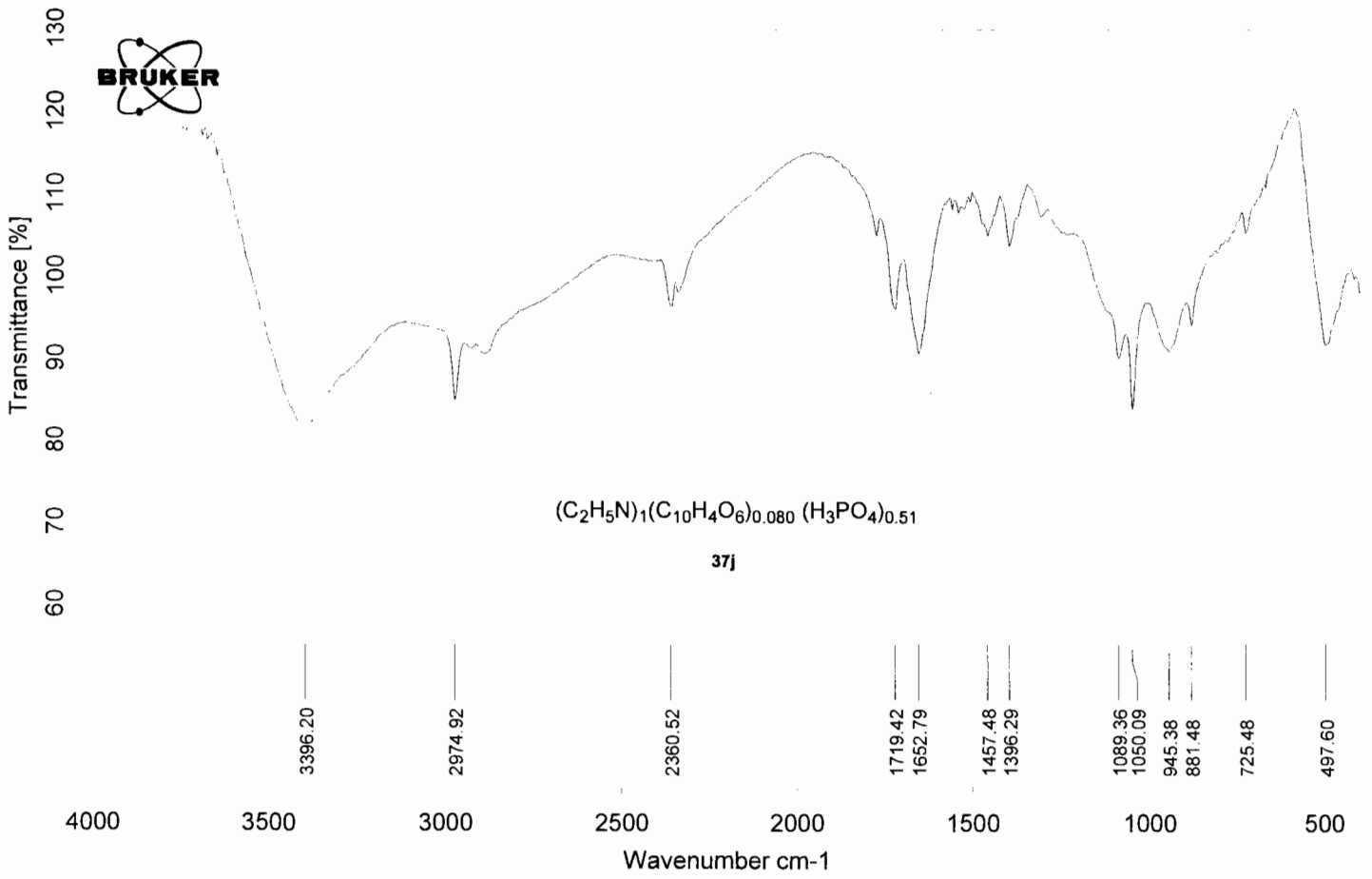

D:\OPUS_NT\DATA\Jun\III_JY_25_Background.0	III_JY_25_Background	Pellet		14/10/2002

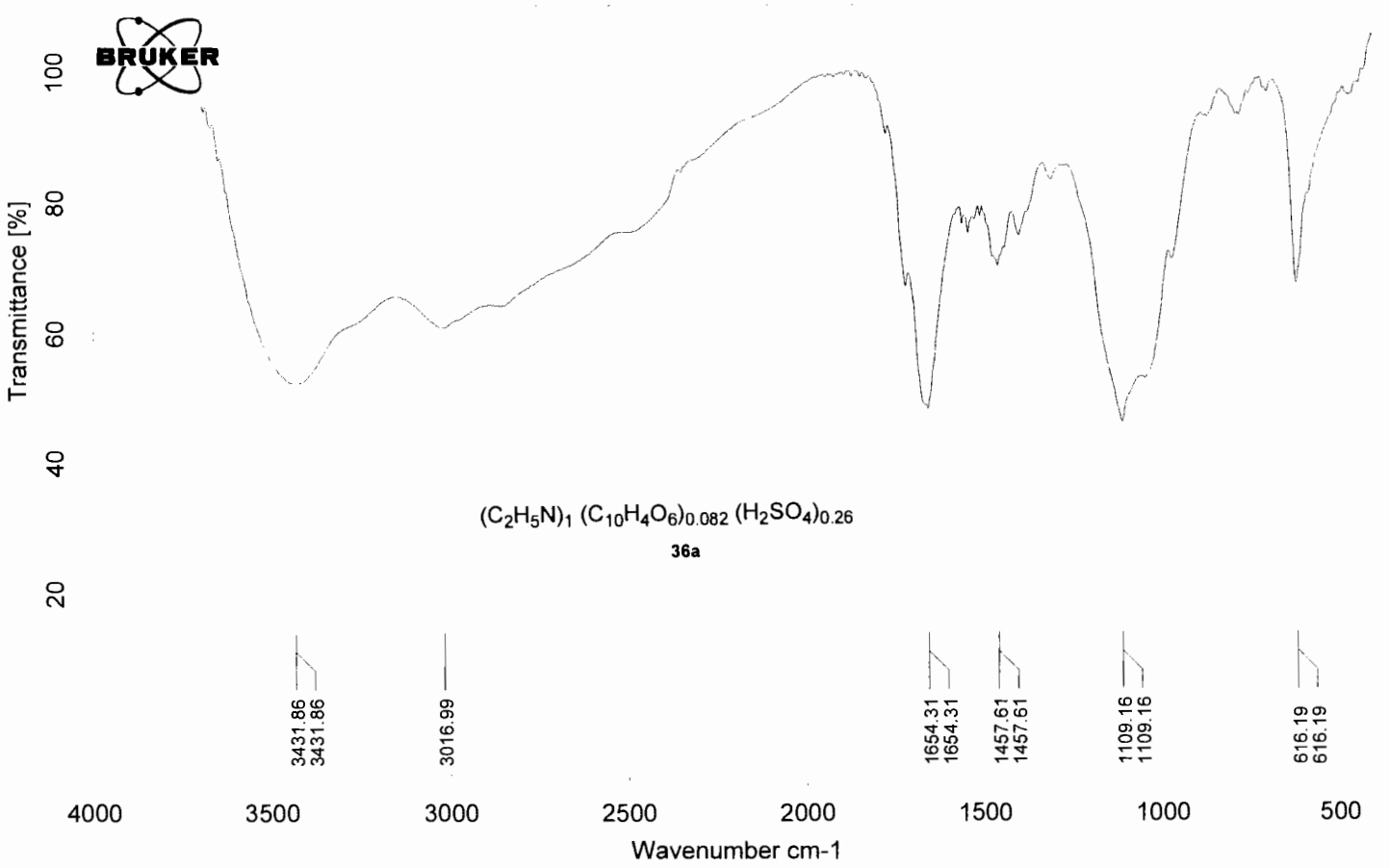
BRUKER
Transmittance [%]
100
80
60
40
20
$(C_2H_5N)_1$ $(C_{10}H_4O_6)_{0.082}$ $(H_2SO_4)_{0.26}$
36a
3431.86
3431.86
3016.99
1654.31
1654.31
1457.61
1457.61
1109.16
1109.16
616.19
616.19
4000
3500
3000
2500
2000
1500
1000
500
Wavenumber cm-1
D:\OPUS_NT\DATA\Jun\II_JY_125.1
II_JY_125
Pellet
5% PBu Dup - S/N 0.26
16/10/2002

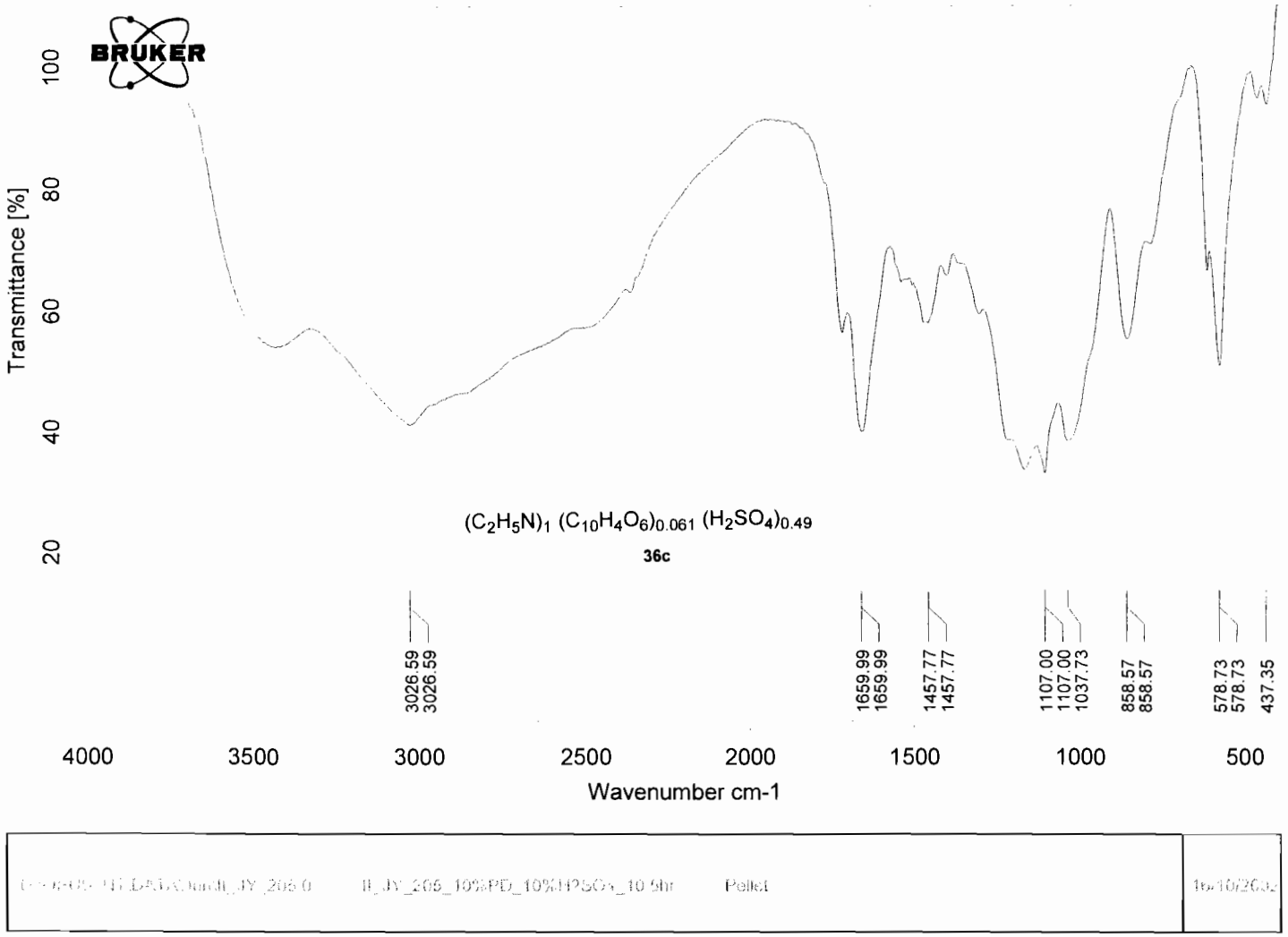
BRUKER
Transmittance [%]
100
80
60
40
20
$(C_2H_5N)_1$ $(C_{10}H_4O_6)_{0.061}$ $(H_2SO_4)_{0.49}$
36c
3026.59
3026.59
1659.99
1659.99
1457.77
1457.77
1107.00
1107.00
1037.73
858.57
858.57
578.73
578.73
437.35
4000
3500
3000
2500
2000
1500
1000
500
Wavenumber cm-1
Pellet

REFERENCES

(1) Holliday, B. J.; Swager, T. M. *Chem. Commun.* **2005**, *1*, 23-36.

(2) Kingsborough, R. P.; Swager, T. M. *Prog. Inorg. Chem.* **1999**, *48*, 123-231.

(3) Liu, Y.; Li, Y.; Schanze, K. S. *J. Photochem. Photobiol., C: Photochem. Rev.* **2002**, *3*, 1-23.

(4) Pickup, P. G. *J. Mater. Chem.* **1999**, *9*, 1641-1653.

(5) Hayashida, N.; Yamamoto, T. *Bull. Chem Soc. Jpn.* **1999**, *72*, 1153-1162.

(6) MacLean, B. J.; Pickup, P. G. *J. Mater. Chem.* **2001**, *11*, 1357-1363.

(7) MacLean, B. J.; Pickup, P. G. *J. Phys. Chem. B* **2002**, *106*, 4658-4662.

(8) Yamamoto, T.; Maruyama, T.; Zhou, Z.-H.; Ito, T.; Fukuda, T.; Yoneda, Y.; Begum, F.; Ikeda, T.; Sasaki, S.; et al. *J. Am. Chem. Soc.* **1994**, *116*, 4832-4845.

(9) Zhu, S. S.; Carroll, P. J.; Swager, T. M. *J. Am. Chem. Soc.* **1996**, *118*, 8713-8714.

(10) Zhu, S. S.; Swager, T. M. *J. Am. Chem. Soc.* **1997**, *119*, 12568-12577.

(11) Cameron, C. G.; Pittman, T. J.; Pickup, P. G. *J. Phys. Chem. B* **2001**, *105*, 8838-8844.

(12) Cameron, C. G.; MacLean, B. J.; Pickup, P. G. *Macromol. Symp.* **2003**, *196*, 165-171.

(13) Buckley, A.; Stuetz, D. E.; Serad, G. A. In *Encyclopedia of Polymer Science and Engineering*; Kroschwitz, J. I., Ed.; Wiley: New York, 1988; Vol. 11, p 572-601.

(14) Haga, M.; Bond, A. M. *Inorg. Chem.* **1991**, *30*, 475-480.

(15) Haga, M.; Matsumura-Inoue, T.; Yamabe, S. *Inorg. Chem.* **1987**, *26*, 4148-4154.

(16) Haga, M.-A. *Inorg. Chim. Acta* **1980**, *45*, L183-L184.

(17) Bond, A. M.; Haga, M. *Inorg. Chem.* **1986**, *25*, 4507-4514.

(18) Haga, M. In *Compr. Coord. Chem. II* 2004; Vol. 1, p 125-134.

(19) Haga, M.; Ano, T.; Kano, K.; Yamabe, S. *Inorg. Chem.* **1991**, *30*, 3843-3849.

(20) Haga, M. A. *Inorg. Chim. Acta* **1983**, *75*, 29-35.

(21) Haga, M.-A.; Ali, M. M.; Koseki, S.; Fujimoto, K.; Yoshimura, A.; Nozaki, K.; Ohno, T.; Nakajima, K.; Stufkens, D. J. *Inorg. Chem.* **1996**, *35*, 3335-3347.

(22) Haga, M.-A.; Ali, M. M.; Arakawa, R. *Angew. Chem. Int. Ed.* **1996**, *35*, 76-78.

(23) Haga, M.-A.; Ali, M. M.; Maegawa, H.; Nozaki, K.; Yoshimura, A.; Ohno, T. *Coord. Chem. Rev.* **1994**, *132*, 99-104.

(24) Haga, M.-A.; Takasugi, T.; Tomie, A.; Ishizuya, M.; Yamada, T.; Hossain, M. D.; Inoue, M. *Dalton Trans.* **2003**, *10*, 2069-2079.

(25) Dudgeon, C. D.; Vogl, O. *J. Polym. Sci., Part A: Polym. Chem.* **1978**, *16*, 1815-1830.

(26) Dudgeon, C. D.; Vogl, O. *J. Polym. Sci., Part A: Polym. Chem.* **1978**, *16*, 1831-1852.

(27) Vogel, H.; Marvel, C. S. *J. Polym. Sci.* **1961**, *50*, 511-539.

(28) Osaheni, J. A.; Jenekhe, S. A. *Macromolecules* **1995**, *28*, 1172-1179.

(29) Tour, J. M. *Chem. Rev.* **1996**, *96*, 537-553.

(30) Yin, J.; Elsenbaumer, R. L. *Polym. Prepr.* (Am. Chem. Soc., Div. Polym. Chem.) **2005**, 46, 636-637.

(31) Yin, J.; Elsenbaumer, R. L. *J. Org. Chem.* **2005**, *70*, 9436-9446.

(32) Babudri, F.; Farinola, G. M.; Naso, F. *J. Mater. Chem.* **2004**, *14*, 11-34.

(33) Fieselmann, B. F.; Hendrickson, D. N.; Stucky, G. D. *Inorg. Chem.* **1978**, *17*, 2078-2083.

(34) Kaupp, G.; Naimi-Jamal, M. R. *Eur. J. Org. Chem.* **2002**, *8*, 1368-1373.

(35) Holan, G.; Samuel, E. L.; Ennis, B. C.; Hinde, R. W. *J. Chem. Soc., C.* **1967**, 20-25.

(36) Holan, G.; Samuel, E. L. *J. Chem. Soc., C.* **1967**, 25-29.

(37) Ennis, B. C.; Holan, G.; Samuel, E. L. *J. Chem. Soc., C.* **1967**, 30-33.

(38) Ennis, B. C.; Holan, G.; Samuel, E. L. *J. Chem. Soc., C.* **1967**, 33-39.

(39) Desaubry, L.; Wermuth, C. G.; Bourguignon, J.-J. *Tetrahedron Lett.* **1995**, *36*, 4249-4252.

(40) Zucco, C.; Dall'Oglio, L.; Salmoria, G. V.; Gallardo, H.; Neves, A.; Rezende, M. C. *J. Phys. Org. Chem.* **1998**, *11*, 411-418.

(41) Huggins, M. L. *J. Am. Chem. Soc.* **1942**, *64*, 2716-2718.

(42) Chen, C. C.; Wang, L. F.; Wang, J. J.; Hsu, T. C.; Chen, C. F. *J. Mater. Sci.* **2002**, *37*, 4109-4115.

(43) Guerra, G.; Choe, S.; Williams, D. J.; Karasz, F. E.; MacKnight, W. J. *Macromolecules* **1988**, *21*, 231-234.

(44) Gieselman, M. B.; Reynolds, J. R. *Macromolecules* **1993**, *26*, 5633-5642.

(45) Balzani, V.; Juris, A.; Venturi, M. *Chem. Rev.* **1996**, *96*, 759-833.

(46) Serroni, S.; Campagna, S.; Puntoriero, F.; Di Pietro, C.; McClenaghan, N. D.; Loiseau, F. *Chem. Soc. Rev.* **2001**, *30*, 367-375.

(47) Kalyanasundaram, K. *Photochemistry of Polypyridine and Porphyrin Complexes*; Academic Press: London, U.K., 1992.

(48) Meyer, T. J. *Acc. Chem. Res.* **1989**, *22*, 163-70.

(49) Crosby, G. A.; Watts, R. J.; Carstens, D. H. W. *Science* **1970**, *170*, 1195-1196.

(50) Balzani, V.; Bolletta, F.; Gandolfi, M. T.; Maestri, M. *Top. Curr. Chem.* **1978**, *75*, 1-64.

(51) De Armond, M. K.; Carlin, C. M. *Coord. Chem. Rev.* **1981**, *36*, 325-355.

(52) Vogler, A. In *Photoinduced Electron Transfer. Part D*; Fox, M. A., Chanon, M., Eds.; Elsevier, Amsterdam, Neth.: New York, 1988, p 179.

(53) Kalyanasundaram, K. *Coord. Chem. Rev.* **1982**, *46*, 159-244.

(54) Horváth, O.; Stevenson, K. L. *Charge Transfer Photochemistry of Coordination Compounds*; VCH: New York, 1993.

(55) Kavarnos, G. J. *Fundamentals of Photoinduced Electron Transfer*; VCH: New York, 1993.

(56) Juris, A.; Balzani, V.; Barigelletti, F.; Campagna, S.; Belser, P.; von Zelewsky, A. *Coord. Chem. Rev.* **1988**, *84*, 85-277.

(57) Vlcek, A. A. *Coord. Chem. Rev.* **1982**, *43*, 39-62.

(58) Dodsworth, E. S.; Vlcek, A. A.; Lever, A. B. P. *Inorg. Chem.* **1994**, *33*, 1045-1049.

(59) Vlcek, A. A.; Dodsworth, E. S.; Pietro, W. J.; Lever, A. B. P. *Inorg. Chem.* **1995**, *34*, 1906-1913.

(60) Roffia, S.; Casadei, R.; Paolucci, F.; Paradisi, C.; Bignozzi, C. A.; Scandola, F. *J. Electroanal. Chem. Interf. Electrochem.* **1991**, *302*, 157-171.

(61) Rillema, D. P.; Sahai, R.; Matthews, P.; Edwards, A. K.; Shaver, R. J.; Morgan, L. *Inorg. Chem.* **1990**, *29*, 167-175.

(62) Rillema, D. P.; Allen, G.; Meyer, T. J.; Conrad, D. *Inorg. Chem.* **1983**, *22*, 1617-1622.

(63) Yin, J.; Elsenbaumer, R. L. *Synth. Met.* **2005**, *154*, 233-236.

(64) Sullivan, B. P.; Salmon, D. J.; Meyer, T. J. *Inorg. Chem.* **1978**, *17*, 3334-3341.

(65) Marmion, M. E.; Takeuchi, K. J. *J. Am. Chem. Soc.* **1988**, *110*, 1472-1480.

(66) Keene, F. R. *Coord. Chem. Rev.* **1998**, *27*, 185-193.

(67) Hua, X.; von Zelewsky, A. *Inorg. Chem.* **1995**, *34*, 5791-5797.

(68) Hua, X.; von Zelewsky, A. *Inorg. Chem.* **1991**, *30*, 3796-3798.

(69) Hua, X., Ph.D. Dissertation, University of Fribourg, Switzerland, 1993.

(70) Hua, X.; Lappin, A. G. *Inorg. Chem.* **1995**, *34*, 992-994.

(71) Kolp, B.; Viebrock, H.; von Zelewsky, A.; Abeln, D. *Inorg. Chem.* **2001**, *40*, 1196-1198.

(72) Morgan, O.; Wang, S.; Bae, S.-A.; Morgan, R. J.; Baker, A. D.; Strekas, T. C.; Engel, R. *J. Chem. Soc., Dalton Trans.* **1997**, 3773-3776.

(73) Rutherford, T. J.; Quagliotto, M. G.; Keene, F. R. *Inorg. Chem.* **1995**, *34*, 3857-3858.

(74) Reitsma, D. A.; Keene, F. R. *J. Chem. Soc., Dalton Trans.* **1993**, *18*, 2859-2860.

(75) Kelso, L. S.; Reitsma, D. A.; Keene, F. R. *Inorg. Chem.* **1996**, *35*, 5144-5153.

(76) Fletcher, N. C.; Keene, F. R.; Viebrock, H.; von Zelewsky, A. *Inorg. Chem.* **1997**, *36*, 1113-1121.

(77) Muerner, H.; Belser, P.; von Zelewsky, A. *J. Am. Chem. Soc.* **1996**, *118*, 7989-7994.

(78) Hiort, C.; Lincoln, P.; Norden, B. *J. Am. Chem. Soc.* **1993**, *115*, 3448-3454.

(79) MacDonnell, F. M.; Bodige, S. *Inorg. Chem.* **1996**, *35*, 5758-5759.

(80) Bodige, S.; Torres, A. S.; Maloney, D. J.; Tate, D.; Kinsel, G.; Walker, A.; MacDonnell, F. M. *J. Am. Chem. Soc.* **1997**, *119*, 10364-10369.

(81) Wärnmark, K.; Thomas, J. A.; Heyke, O.; Lehn, J.-M. *Chem. Commun.* **1996**, *6*, 701-702.

(82) Tzalis, D.; Tor, Y. *J. Am. Chem. Soc.* **1997**, *119*, 852-853.

(83) Bosnich, B.; Dwyer, F. P. *Aust. J. Chem.* **1966**, *19*, 2229-2233.

(84) Bosnich, B. *Inorg. Chem.* **1968**, *7*, 2379-2386.

(85) Bosnich, B. *Inorg. Chem.* **1968**, *7*, 178-180.

(86) Bosnich, B. *Acc. Chem. Res.* **1969**, *2*, 266-273.

(87) Sutker, B. J. In *Polymer Stabilization and Degradation*; Klemchuk, P. P., Ed.; American Chemical Society: Washington D. C., 1985; Vol. II, p 163-190.

(88) Zaikov, G. E.; Lomakin, S. M. *J. Appl. Polym. Sci.* **2002**, *86*, 2449-2462.

(89) Halpern, Y.; Mott, M.; Niswander, R. H. *Ind. Eng. Chem., Prod. Res. & Dev.* **1984**, *23*, 233-238.

(90) Reshetnikov, I. S.; Yablokova, M. Y.; Khalturinskij, N. A. In *Fire Retardancy of Polymers----The Use of Intumescence*; Bras, M. L., Camino, G., Bourbigot, S., Delobel, R., Eds.; The Royal Society of Chemistry: Cambridge, 1998, p 88-103.

(91) Lewin, M. In *Fire Retardancy of Polymers----The Use of Intumescence*; Bras, M. L., Camino, G., Bourbigot, S., Delobel, R., Eds.; The Royal Society of Chemistry: Cambridge, 1998, p 3-32.

(92) Wheeler, J. W.; Zhang, Y.; Tebby, J. C. In *Fire Retardancy of Polymers----The Use of Intumescence*; Bras, M. L., Camino, G., Bourbigot, S., Delobel, R., Eds.; The Royal Society of Chemistry: Cambridge, 1998, p 252-265.

(93) Costa, L.; Catala, J.-M.; et al. In *Fire Retardancy of Polymers----The Use of Intumescence*; Bras, M. L., Camino, G., Bourbigot, S., Delobel, R., Eds.; The Royal Society of Chemistry: Cambridge, 1998, p 76-87.

(94) White, R. H. *Wood Science* **1979**, *12*, 113-121.

(95) Fenimore, C. P. In *Flame-retardant Polymeric Materials*; Lewin, M., Atlas, S. M., Pearce, E. M., Eds.; New York: Plenum: 1975; Vol. 1, p 371-397.

(96) Gandhi, J. S., Master's Thesis, University of Texas at Arlington, 2004.

BIOGRAPHICAL INFORMATION

Jun Yin was born in Guiyang city of China. In July 1995, she received her Bachelor degree of Engineering in Polymer Science and Materials from Sichuan University in Chengdu city, China. During her undergraduate study, she worked with Professor Wen Xu on a research project investigating the effect of mechanical deformation on changes in morphology and physical/chemical properties of high-density polyethylene (HDPE). The results of this project were presented at the 36th IUPAC International Symposium on Macromolecules (8/4/96–8/9/96 in Seoul, Korea) and the paper entitled "A study on morphology and change in properties of HDPE during pan-milling" was published in the conference proceedings.

Upon her graduation in 1995, she joined the Resin Application Research Institute of Beijing Yanshan Petrochemical Group Co. Ltd. (BYPC) in Beijing of China as an application and marketing engineer. BYPC is at present the largest producer of ethylene, plastics, resins, synthetic rubber, basic organic chemical raw materials and synthetic fiber carpet in China. She worked on various R&D projects which were primarily about the development of large-scale and more cost-effective manufacturing processes of synthetic resins for various industrial applications, such as developing better anti-aging, anti-fogging and temperature-keeping properties of low-density polyethylene (LDPE) films used in farms located in various weather zones in China.

She also worked on marketing and sales of BYPC's new and high quality polyethylene and polypropylene products in northeast regions of China.

In 1999, she was granted a full scholarship from the University of Texas at Arlington in Arlington, Texas, and started her Ph.D. program under the guidance of Prof. Ronald L. Elsenbaumer in the Department of Chemistry. Her research topics were in the field of conductive polymers and flame retardants of the polymers. Some of her research results had been published in the following papers: "Efficient Synthesis and Characterization of Novel Bibenzimidazole Oligomers and Polymers as Potential Conjugated Chelating Ligands" *The Journal of Organic Chemistry*, **2005**, *70*, 9436-9446. "Synthesis and Properties of Multi-nuclear Ruthenium (II) Complexes of Bis(2,2'-bibenzimidazole)" *Synthetic Metals,* **2005**, *154*, 233-236. In 2005, she received her Ph.D. degree in Chemistry, and concluded all her research work in her Ph.D. dissertation, entitled: "Oligomeric and Polymeric Bibenzimidazole Based Metal Complexes and Crosslinked Polyethylenimine Based Flame Retardants". She received the Outstanding Research Award at the Department of Chemistry in 2005.

She is affiliated with the American Chemical Society.

In August 2000, she was married to Dr. Yong He, formally from Nanjing city in China. She still keeps her maiden name because of the Chinese tradition. Her primary interest lies in the scientific research in the field of polymer science and materials. She would like to continue her current research work in academic institutions and research laboratories.